THÈSE de DOCTORAT

présentée par :

Lukas Rainer VETH

soutenue le : **28 Septembre 2022**

pour obtenir le grade de : **Docteur de l'université de Strasbourg**

Discipline/ Spécialité : Chimie

Transfer C–H Borylation of Alkenes

THÈSE dirigée par :
Dr DYDIO Pawel   Directeur de thèse, Université de Strasbourg

RAPPORTEURS :
Prof Dr OESTREICH Martin   Rapporteur, Technische Universität Berlin
Dr QUINTARD Adrien   Rapporteur, Université Grenoble Alpes

AUTRES MEMBRES DU JURY :
Dr BELLEMIN-LAPONNAZ Stéphane   Examinateur, Université de Strasbourg

II

Table of Contents

List of abbreviations

2-mphen	2-Methyl-phenanthroline	HRMS	High-resolution mass spectrometry
aam	anthranilamide	KIE	Kinetic isotopic effect
acac	acetylacetone	L	Ligand
Boc	*tert*-Butyloxycarbonyl	LA	Lewis acid
bpy	2,2'-Bipyridine	*m*	Meta
cat	Catecholborane	mac	dimethylacenaphthyl-1 diol
cod	Cycloocta-1,5-diene	Mes	Mesitylene
coe	Cyclooctene	MS	Mass spectroscopy
conv	Conversion	MTBE	Methyl *tert*-butyl ether
Cp*	1,2,3,4,5-Pentamethylcyclo-penta-1,3-diene	NHC	*N*-heterocyclic carbene
CPME	Cyclopentyl methyl ether	NMR	Nuclear magnetic resonance
dan	1,8-diaminonaphthalene	*o*	Ortho
deriv	Derivative	*p*	Para
dFppy	2-(2,4-difluorophenyl)pyridine	Pin	pinacol
DG	Directing group	Pza	pyrazolylaniline
do	Diortho	RDG	Relay directing group
dtbpy	4,4'-Di-*tert*-butyl-2,2'-dipyridyl	rsm	Recovered starting material
eg	Ethylene glycolate	rt	Room temperature
equiv	Equivalent	SI	Supporting information
ESI	Electrospray ionization	*t*	Tert
FID	Flame ionization detector	THF	Tetrahydrofuran
GC	Gas chromatography	TS	Transition state
HPLC	High-performance liquid chromatography		

Résumé

1) Introduction

L'émergence de la catalyse par les métaux de transition a eu un impact transformatif sur les sciences moléculaires au-delà de la synthèse organique. Elle permet de nouvelles transformations chimiques qui ont des applications dans les domaines de la science des matériaux, de la santé, de l'agriculture et des sciences de l'environnement.[1] Un nouveau niveau de complexité peut être obtenu en utilisant la multicatalyse, c'est-à-dire en combinant deux ou plus catalyseurs dans des réactions en un seul pot pour obtenir des transformations encore plus puissantes.[2,3] L'étude du mécanisme de ces transformations catalytiques au niveau moléculaire est de la plus haute importance pour concevoir et développer avec succès de nouveaux systèmes catalytiques ou simplement améliorer des protocoles déjà établis. Cette approche mécanistique permet non seulement de contourner le processus d'optimisation classique et fastidieux par essais et erreurs, mais aussi, et c'est plus important, de mieux comprendre les mécanismes impliqués afin d'exploiter tout le potentiel de ces systèmes catalytiques.

L'objectif de cette thèse est la conception et le développement de réactions de borylation de transfert pour la fonctionnalisation efficace et largement applicable de la matière première alcène à travers une conception rationnelle par des considérations mécanistiques. Bien que plusieurs méthodes aient été établies pour la borylation C–H des alcènes, il n'existe pas de méthode générale applicable à la fois aux alcènes terminaux et internes et présentant une excellente tolérance aux groupes fonctionnels. La borylation C–H par transfert offre la possibilité de débloquer une série de transformations intéressantes pour la synthèse et la dérivatisation tardive de molécules complexes. Cependant, son faible nombre d'antécédents et sa compréhension mécanistique limitée ont entravé le développement de protocoles pratiques. Par conséquent, l'étude du mécanisme des réactions de borylation C–H est d'une grande importance pour cette thèse.

Cette thèse de doctorat se compose de cinq chapitres, qui sont brièvement résumés ci-dessous. Tout d'abord, une revue des tendances récentes dans le domaine des réactions de borylation C–H catalysées par le groupe 9 est fournie (Chapitre 1) comme introduction à la discussion des méthodologies catalytiques associées dans les chapitres suivants de cette thèse.[4] Ensuite, une étude d'une telle réaction - à savoir la borylation C–H de transfert d'alcènes sous catalyse Rh(I) - est décrite. La méthode développée permet la borylation C–H sélective d'alcènes terminaux et internes avec une grande sélectivité et une tolérance aux groupes fonctionnels (Chapitre 2).[5] Une investigation mécanistique approfondie impliquant une série d'expériences catalytiques et stœchiométriques a permis de comprendre le cycle catalytique complet employant une β-élimination de boryle, une étape élémentaire, qui est sans précédent pour la catalyse au Rh, et d'élucider les caractéristiques contrôlant l'activité et

la sélectivité. Par la suite, une autre méthodologie de borylation de transfert a été développée en modifiant le système catalytique et en changeant le catalyseur au Rh(I) pour un catalyseur à l'Ir(I) (chapitre 3). Le protocole résultant offre une tolérance aux groupes fonctionnels, complémentaire à celle du protocole Rh(I), tolérant les fonctions acidiques présentes dans de nombreux motifs d'intérêt pharmaceutique. Ce système a permis d'étendre cette méthode à la fonctionnalisation de molécules bioactives beaucoup plus complexes. Le chapitre suivant décrit la déshomologation d'alcools et d'aldéhydes (allyliques) par multicatalyse séquentielle. La séquence réactionnelle consiste en une (oxydation/)rétro-hydroformylation catalysée par le Rh, suivie d'une étape de borylation par transfert catalysée par l'Ir, développé précédemment, pour accéder à des vinyles boronates qui peuvent être ensuite fonctionnalisés en utilisant des méthodes classiques de la littérature. Dans l'ensemble, le processus séquentiel en un seul pot permet une valorisation rapide, pratique et économe en ressources d'aldéhydes et d'alcools(allyliques) de départ (chapitre 4). Le dernier chapitre de la thèse fournit une perspective sur les défis et les opportunités de cette transformation multicatalytique et leurs futures applications potentielles dans les sciences chimiques (Chapitre 5).[6]

2) Résultats et discussions

2.1 Tendances récentes des réactions de borylation C–H catalysées par les métaux du groupe 9 : Différentes stratégies pour contrôler la sélectivité du sité réactionnel ainsi que la régio et la stéréosélectivité (chapitre 1)

Les composés organoborés continuent de contribuer de manière substantielle aux progrès de la chimie organique grâce à leur rôle croissant à la fois comme intermédiaires de synthèse et comme composés cibles pour la chimie médicinale.[7] Des méthodes particulièrement attrayantes pour leur synthèse sont basées sur la borylation directe des liaisons C–H des produits de départ disponibles car aucune étape de pré-fonctionnalisation n'est nécessaire. Cependant, en raison de la grande abondance de liaisons C–H ayant une réactivité similaire dans les molécules organiques, les protocoles de borylation C–H utiles sur le plan synthétique exigent des stratégies sophistiquées pour obtenir une régio- et stéréosélectivité élevée. À cette fin, des catalyseurs sélectifs à base de métaux de transition ont été développés, les catalyseurs basés sur le groupe 9 étant parmi les plus couramment utilisés. Récemment, une multitude de stratégies diverses ont été développées pour repousser les limites des réactions de borylation C–H en ce qui concerne leur régio- et énantiosélectivité. Ce chapitre donne une vue d'ensemble des approches de la borylation C–H des arènes, des alcènes et des alcanes basées sur des catalyseurs centrés sur le groupe 9, en mettant l'accent sur la littérature récente. Enfin, une perspective est donnée pour évaluer le potentiel futur de ce domaine.[4]

2.2 Borylation C–H de transfert d'alcènes sous catalyse au Rh(I) : Aperçu de la capacité de synthèse, du mécanisme et du contrôle de la sélectivité (Chapitre 2)

La synthèse sélective d'esters vinylboroniques est particulièrement intéressante à étudier en raison de leur grande valeur synthétique et de la présence de motifs alcènes dans divers composés synthétiques et naturels de grande complexité structurelle. Avec l'objectif primordial de formuler une approche qui a le potentiel de répondre aux limitations actuelles de synthèse, nous avons postulé que la borylation par transfert C–H pourrait enrichir la portée des stratégies de borylation des alcènes.
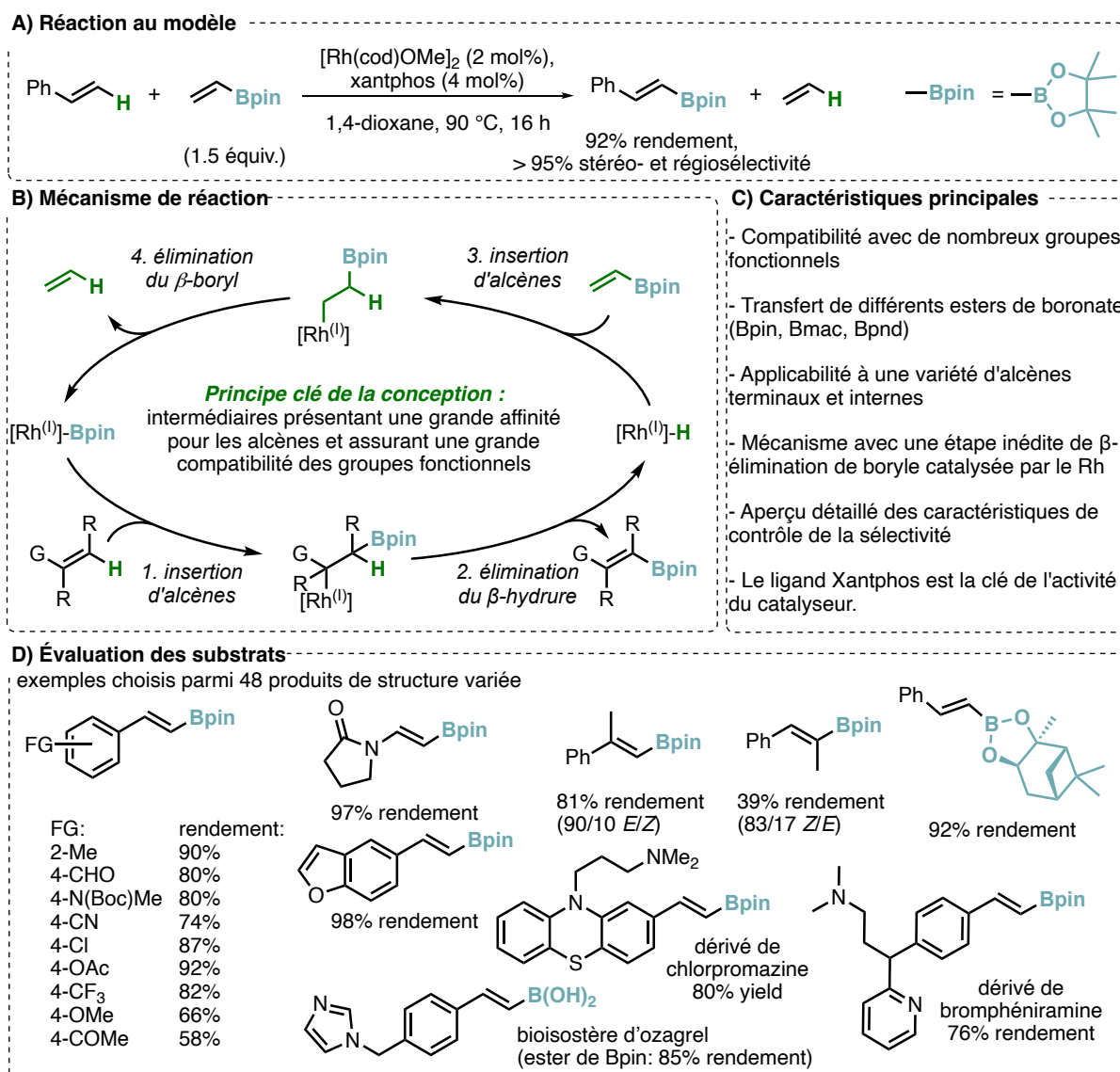

Figure I.1. Borylation C–H par transfert d'alcènes sous catalyse au Rh(I).

Sur la base de considérations mécanistiques, nous avons pensé que les complexes phosphine-Rh(I) seraient des catalyseurs de choix pour un transfert chimiosélectif de groupements borylés. Après évaluation d'une gamme de conditions de réaction, nous avons constaté que la réaction modèle du styrène avec le vinyl bore pinacol (BPin) en présence de [Rh(cod)OMe]$_2$ et de xantphos formait le produit cible avec un rendement de 92% (Figure I.1a), confirmant le succès de la conception de la réaction. Le protocole est compatible avec une large gamme de groupes fonctionnels, y compris des motifs souvent problématiques comme les aldéhydes et

les alcynes, et permet également le transfert d'esters boronates autres qu'un BPin. Elle est en outre applicable aux alcènes et substrats terminaux et internes portant des substituants aux propriétés électroniques et stériques variées, dépassant donc le cadre des protocoles de synthèse jusqu'alors établis. La méthode s'est également avérée efficace dans de le contexte complexe de borylation de composés bioactifs (Figure I.1d). Dans l'ensemble, l'évaluation de 48 exemples démontre une large applicabilité du protocole. Une limitation notable de la méthode est le manque de tolérance des liaisons acidiques.

La clé du développement de la méthodologie a été la compréhension approfondie du mécanisme, à la fois expérimental et computationnel (les études computationnelles ont été réalisées en collaboration avec un collègue de notre groupe). Nous avons pu montrer que la réaction se déroule selon un cycle catalytique impliquant une série d'étapes d'insertion et d'élimination d'alcènes, à partir d'un complexe Rh(I)-boryle ou Rh(I)-hydrure (Figure I.1b). Le point central du cycle est l'étape de β-élimination de boryle, sans précédent mais cruciale. Dans un contexte plus large, ce travail ouvre la voie au développement d'autres réactions d'échange hydrogène contre groupes fonctionnels empruntant des voies similaires.[5]

2.3 Borylation C–H de transfert d'alcènes sous catalyse à l'Iridium (chapitre 3)

La borylation par transfert catalysée par le Rh décrite ci-dessus a permis la fonctionnalisation hautement sélective d'alcènes avec une tolérance fonctionnelle au-delà des méthodes précédemment établies. Cependant, en raison de la réactivité inhérente de l'espèce catalytique Rh, la méthode reste incompatible avec les produits de départ comportant des groupes fonctionnels portant des protons même modérément acides, tels que les carboxyamides primaires et secondaires, les sulfonamides, les urées, les carbamates, les acides carboxyliques, les phénols, les alcools, les NH-indoles ou les NH-amines, et des motifs similaires. Il est important de noter que ces groupes fonctionnels sont généralement impliqués dans la formation d'interactions spécifiques entre les molécules médicamenteuses et leurs cibles biologiques (par le biais de la liaison hydrogène ou d'interactions électrostatiques), et qu'ils sont présents dans une large majorité des produits pharmaceutiques. En fait, 191 des 200 principaux médicaments à petites molécules contiennent au moins un de ces groupes fonctionnels.[8]
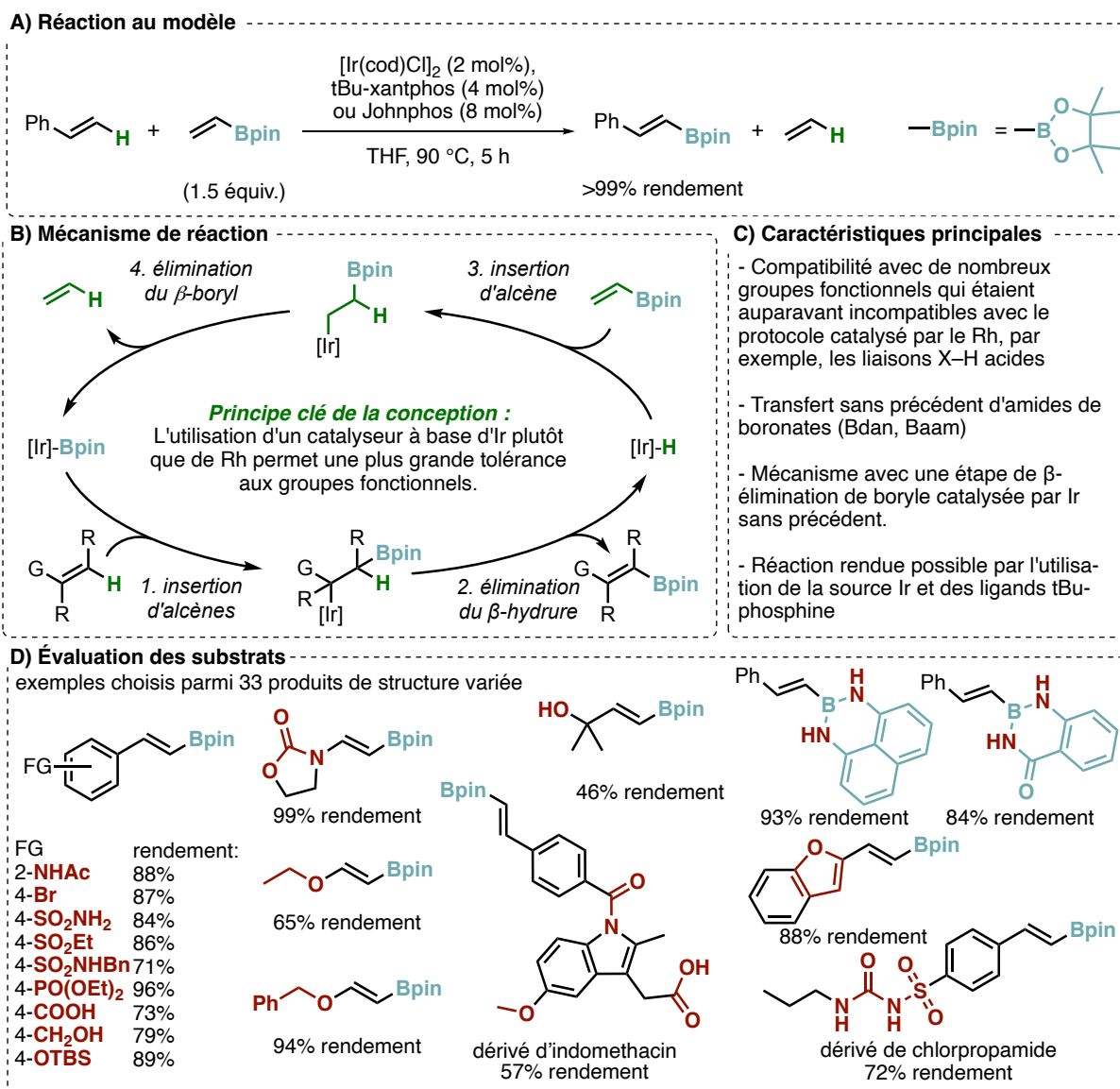
A) Réaction au modèle

Ph⟍⟍H + ⟍Bpin → Ph⟍⟍Bpin + ⟍H

[Ir(cod)Cl]₂ (2 mol%),
tBu-xantphos (4 mol%)
ou Johnphos (8 mol%)

THF, 90 °C, 5 h

(1.5 équiv.)

>99% rendement

—Bpin = —B(O O) (pinacol)

B) Mécanisme de réaction

4. élimination du β-boryl

3. insertion d'alcène

Principe clé de la conception :
L'utilisation d'un catalyseur à base d'Ir plutôt que de Rh permet une plus grande tolérance aux groupes fonctionnels.

1. insertion d'alcènes

2. élimination du β-hydrure

C) Caractéristiques principales

- Compatibilité avec de nombreux groupes fonctionnels qui étaient auparavant incompatibles avec le protocole catalysé par le Rh, par exemple, les liaisons X–H acides

- Transfert sans précédent d'amides de boronates (Bdan, Baam)

- Mécanisme avec une étape de β-élimination de boryle catalysée par Ir sans précédent.

- Réaction rendue possible par l'utilisation de la source Ir et des ligands tBu-phosphine

D) Évaluation des substrats

exemples choisis parmi 33 produits de structure variée

FG | rendement:
2-**NHAc** | 88%
4-**Br** | 87%
4-**SO₂NH₂** | 84%
4-**SO₂Et** | 86%
4-**SO₂NHBn** | 71%
4-**PO(OEt)₂** | 96%
4-**COOH** | 73%
4-**CH₂OH** | 79%
4-**OTBS** | 89%

99% rendement

65% rendement

94% rendement

46% rendement

dérivé d'indomethacin
57% rendement

93% rendement

84% rendement

88% rendement

dérivé de chlorpropamide
72% rendement

Figure I.2. Borylation C–H par transfert d'alcènes sous catalyse à l'Iridium.

En remplaçant le catalyseur au Rh par un catalyseur à l'Ir, inspiré par de nombreux rapports d'autres réactions de borylation C–H catalysées par Ir,[4] cette limitation a été surmontée. En outre, d'autres groupes fonctionnels auparavant incompatibles, tels que les halogénures d'alkyle ou d'aryle, les éthers silyliques et les groupes nitro, ont été bien tolérés. La méthode est également applicable pour la borylation C–H des éthers vinyliques. Une série d'expériences mécanistiques a révélé que la réaction est susceptible de se dérouler par une voie mécanistique similaire à celle en présence de complexes Rh(I), avec des intermédiaires Ir-hydride et Ir-boryle et inclut une étape de β-élimination de boryle sans précédent pour les complexes Ir (Figure I.2b). Nous supposons que le mécanisme réactionnel passant par les intermédiaires Ir(I) plutôt que par les intermédiaires Ir(III), le plus souvent rencontrés, est la clé de la chimiosélectivité, car ces derniers préfèrent généralement les réactions de borylation des liaisons C–H aromatiques plutôt que vinyliques.[9] Cependant, des études supplémentaires sont nécessaires pour révéler le mécanisme détaillé de la réaction.

2.4 Borylation déhomologative d'aldéhydes et d'alcools et leur postfonctionnalisation rendue possible par la multicatalyse (chapitre 4)

Après la liaison C–H, la liaison C–C est la plus répandue et la plus fondamentale dans la synthèse organique. Son clivage peut être rencontré dans de nombreux processus dans la nature, intégré dans des cascades très complexes pour la fragmentation de motifs structurels biologiquement pertinents.[10] Nous nous sommes intéressés aux méthodes de déshomologation, c'est-à-dire aux réactions de clivage C–C dans lesquelles une unité de carbone est retirée du produit de départ, qui opèrent directement sur des groupes fonctionnels communs, tels que les aldéhydes et les alcools, dans des conditions douces garantissant leur applicabilité potentielle à la chimie fine. Nous avons considéré la réactivité unique des complexes de Rh et d'Ir qui permettent l'oxydation des alcools, la rétro-hydroformylation des aldéhydes et la borylation par transfert C–H des alcènes.[5,11,12] La combinaison de ces réactivités permettrait la déshomologation directe des alcools et des aldéhydes en une seule étape de synthèse. De plus, avec la large gamme de réactivité de l'intermédiaire boronate, l'approche peut être directement étendue à une série de fonctionnalisations déshomologatives d'alcools et d'aldéhydes.

Mes travaux ont montré que ces trois activités catalytiques peuvent être combinés et qu'un aldéhyde ou un alcool déshomologué sont libérés *in situ* à partir de l'intermédiaire boronate, validant ainsi le concept de la réaction. Après avoir envisagé différentes approches pour réaliser un tel processus, la catalyse séquentielle s'est avérée capable de le faire (Figure I.3a). L'évaluation du champ d'application montre que la méthode a le potentiel d'être largement applicable (Figure I.3b). En outre, l'introduction réussie de deux réactions de post-fonctionnalisation différentes - à savoir le couplage croisé de Suzuki-Miyaura (Figure I.3d) et l'oxydation - montre le potentiel supplémentaire de la méthode. Cependant, des travaux supplémentaires sont nécessaires pour révéler tout le potentiel de la méthode. Plus précisément, une évaluation plus poussée de l'étendue du substrat et l'application d'un plus grand nombre de réactions de post-fonctionnalisation pourraient élargir l'applicabilité de la méthode à l'avenir. Enfin, une application de la méthode à l'édition du squelette peut être envisagée.
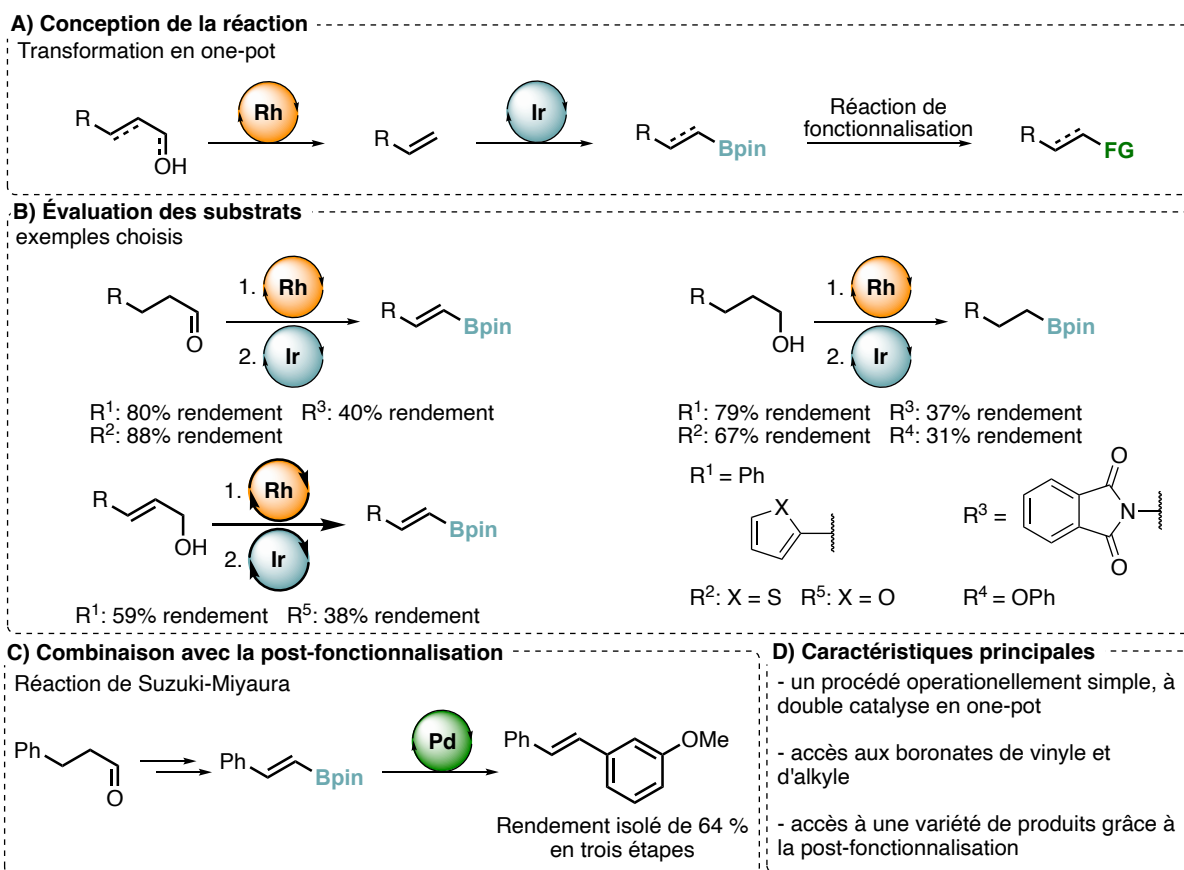
A) Conception de la réaction
Transformation en one-pot

B) Évaluation des substrats
exemples choisis

R^1: 80% rendement   R^3: 40% rendement
R^2: 88% rendement

R^1: 79% rendement   R^3: 37% rendement
R^2: 67% rendement   R^4: 31% rendement

R^1 = Ph

R^1: 59% rendement   R^5: 38% rendement

R^2: X = S   R^5: X = O   R^4 = OPh

C) Combinaison avec la post-fonctionnalisation
Réaction de Suzuki-Miyaura

Rendement isolé de 64 %
en trois étapes

D) Caractéristiques principales
- un procédé operationellement simple, à double catalyse en one-pot

- accès aux boronates de vinyle et d'alkyle

- accès à une variété de produits grâce à la post-fonctionnalisation

Figure I.3. Catalyse séquentielle en one-pot pour la déshomologation des aldéhydes et des alcools dérivés de la biomasse.

2.5 Défis et opportunités de la multicatalyse (chapitre 5)

La multicatalyse est un domaine émergent qui vise à développer des transformations catalytiques efficaces pour convertir rapidement des matières premières relativement simples en produits plus complexes à valeur ajoutée. Dans le cadre des processus multicatalytiques, soit plusieurs catalyseurs exécutent des réactions uniques, soit des séquences précises de réactions catalytiques multiples se déroulent de manière "one-pot". Il est intéressant de noter que les protocoles multicatalytiques permettent non seulement de réaliser des transformations inaccessibles par des approches classiques, mais aussi de réduire considérablement le temps, les déchets et le coût des processus de synthèse, ce qui rend la synthèse organique plus efficace en termes de ressources. Ce chapitre présente une vue d'ensemble des différentes stratégies de multicatalyse qui présentent des défis et des opportunités distincts. Ce domaine global est divisé en trois catégories principales : la catalyse coopérative, la catalyse domino et la catalyse relais. Chaque catégorie est décrite à l'aide d'exemples représentatifs qui mettent en évidence ses caractéristiques. Une attention particulière est accordée à la catalyse à relais, qui est examinée plus en détail dans ses sous-catégories. Enfin, une analyse des systèmes qui intègrent des niveaux de complexité plus élevés et soulignent davantage le potentiel des systèmes multicatalytiques est abordée. Cet article de perspective a été préparé en collaboration avec un collègue (contribution égale) et publié.[6]

3) Conclusion générale

La thèse de doctorat avait pour but de développer, d'étudier et d'appliquer des transformations (multi)catalytiques pour la synthèse de briques moléculaires précieux ayant des applications au-delà de la synthèse organique. Tout au long de la thèse, trois nouvelles méthodes catalysées par les métaux de transition pour la synthèse de tels blocs de construction ont été développées. La borylation C–H des alcènes, catalysée par Rh(I) (chapitre 2), représente une nouvelle méthode pour la fonctionnalisation sélective d'une variété d'alcènes de départ portant une pléthore de groupes fonctionnels. Sur la base du mécanisme étudié, nous avons poursuivi le développement de la borylation C–H des alcènes catalysée par Ir(I) (chapitre 3). Cette transformation peut être considérée comme un progrès important sur la transformation précédente. De façon remarquable, elle tolère une gamme encore plus large de groupes fonctionnels, y compris des fonctions acidiques qui sont très précieuses dans le contexte de la chimie médicinale. Enfin, le concept de borylation par transfert a été incorporé dans un système multicatalytique, dans lequel les alcènes de départ sont générés *in situ* à partir d'aldéhydes ou d'alcools (allyliques). La possibilité supplémentaire de convertir l'intermédiaire boronate *in situ* en d'autres classes de produits déshomologués montre la large applicabilité d'une telle méthode (chapitre 4).

4) Références

(1) Bartholomew, C.H.; Farrauto, R.J. *Fundamentals of Industrial Catalytic Processes*; John Wiley & Sons, Inc.: Hoboken, NJ, USA, 2005. DOI: 10.1002/9780471730071.

(2) Lohr, T.L.; Marks, T.J. Orthogonal Tandem Catalysis. *Nat. Chem.* **2015**, *7*, 477–482. DOI : 10.1038/nchem.2262.

(3) Ambrosini, L.M.; Lambert, T.H. Multicatalysis: Advancing Synthetic Efficiency and Inspiring Discovery. *ChemCatChem* **2010**, 2, 1373. DOI : 10.1002/cctc.200900323.

(4) **Veth, L.;** Grab, H.A.; Dydio, P. Recent Trends in Group 9–catalyzed C–H Borylation Reactions. *Synthesis*, **2022**, *54*, A–Q. DOI : 10.1055/a-1711-5889.

(5) **Veth, L.;** Grab, H.A.; Martinez, S.; Antheaume, C.; Dydio, P. Transfer C–H borylation of alkenes under Rh(I) catalysis: Insight into the synthetic capacity, mechanism, and selectivity control. *Chem Catal.* **2022**, *2*, 1–17. DOI : 10.1016/j.checat.2022.02.008.

(6) Martinez, S.; **Veth, L.;** Lainer, B.; Dydio, P. Challenges and Opportunities in Multicatalysis. *ACS Catal.* **2021**, *11*, 3891 – 3915. DOI : 10.1021/acscatal.0c05725.

(7) Hall, D.G. *Boronic acids : Preparation and Applications in Organic Synthesis and Medicine*; WILEY-VCH Verlag GmbH & Co. KGaA: Weinheim, Germany, 2005. ISBN : 978-3-527-30991-7.

(8) McGrath, N.A.; Brichacek, M.; Njardason, J.T. A Graphical Journey of Innovative Organic Architectures That Have Improved Our Lives. *J. Chem. Educ.* **2010**, *87*, 1348 – 1349. DOI : 10.1021/ed1003806.

(9)   Boller, T.M.; Murphy, J.M.; Hapke, M.; Ishiyama, T.; Miyaura, N.; Hartwig, J.F. Mechanism of the Mild Functionalization of Arenes by Diboron Reagents Catalyzed by Iridium Complexes. Intermediacy and Chemistry of Bipyridine-Ligated Iridium Trisboryl Complexes. *J. Am. Chem. Soc.* **2005**, *127*, 14263 – 14278. DOI : 10.1021/ja053433g.

(10) Chen, F.; Wang, T.; Jiao, N. Recent Advances in Transition‑Metal-Catalyzed Functionalization of Unstrained Carbon–Carbon Bonds. *Chem. Rev.* **2014**, *114*, 8613 – 8661. DOI : 10.1021/cr400628s.

(11) Murphy, S.K.; Park, J.-W.; Lu, A.; Dong, V.M. Rh-catalyzed C–C bond cleavage by transfer hydroformylation. *Science* **2015**, *347*, 56 – 60. DOI : 10.1126/science.1261232.

(12) Wu, X.; Cruz, F.A.; Lu, A.; Dong, V.M. Tandem Catalysis: Transforming Alcohols   to Alkenes by Oxidative Dehydroxymethylation. *J. Am. Chem. Soc.* **2018**, *140*, 10126 – 10130. DOI : 10.1021/jacs.8b06069.

CHAPTER 1

Recent Trends in Group 9 Catalyzed C–H Borylation Reactions: Different Strategies to Control Site-, Regio-, and Stereoselectivity

1.1. Introduction

In the past few decades, new strategies to prepare organoboron compounds have received an increasing interest due to their high value as building blocks in synthetic organic chemistry, for applications in drug discovery and material science, and as target compounds in medicinal chemistry. Numerous methods for their synthesis have been reported, usually requiring pre-functionalized starting materials.[1–4] Modern approaches focus on direct C–H bond borylation as it allows a rapid and atom-economic installation of boryl groups[5–7] and holds the potential to serve as a starting point for the late-stage functionalization of complex bioactive molecules and natural products.[8–10]

However, due to their low reactivity and high abundance, the direct and selective functionalization of C–H bonds poses great challenges to synthetic chemists.[11–15] In the context of borylation reactions, since the pioneering works of Hartwig,[16–18] Smith,[19] and Maleczka[20] for both, sp[3]- and sp[2]-C–H bonds, Rh- and Ir-based catalysts were among the first found to be effective.[21–25] Recently, Co-based catalysts have received increasing attention due to the higher abundance of the metal and its lower cost.[26–29] Besides group 9 centered catalysts, complexes of other metals, such as Pd, Ni, Ru, Fe, and more, have been found to be active as well, but are beyond the scope of this chapter.[30]

1.1.1. Mechanistic considerations

In face of the multitude of developed catalysts for C–H borylation reactions and the different nature of the substrates and utilized reagents, a detailed mechanistic discussion of all cases is beyond the scope of this chapter and a discussion can be found in more specialized review articles.[5,6] In addition, the mechanisms of many catalytic systems have not been studied in detail to date. However, the majority of developed protocols discussed here are based on the combination of an Ir(I) precursor and a bipyridine-based ligand. Such a highly effective and widely applied combination was initially introduced by Ishiyama, Miyaura, and Hartwig,[23] who also studied the underlying mechanism of the reaction (Scheme 1.1).[31] Based on the results of a set of stochiometric and catalytic experiments and kinetic data, the catalytic cycle depicted in Scheme 1.1 was proposed. The suggested mechanism commences with the 16-electron complex **1** that is formed *in situ*. This species undergoes a rate-limiting and selectivity-determining C–H bond cleavage either via oxidative addition or σ-bond metathesis. Both possibilities lead to the formation of the product and the bis(boryl)hydrido complex **3** that regenerates the tris(boryl) complex **1** upon reaction with B_2pin_2. While these studies shed light on the key intermediate, i.e., the tris(boryl) complex **1**, whose involvement in the mechanism has been sometimes questioned,[31] the exact nature of the remaining elementary steps remains to be established.
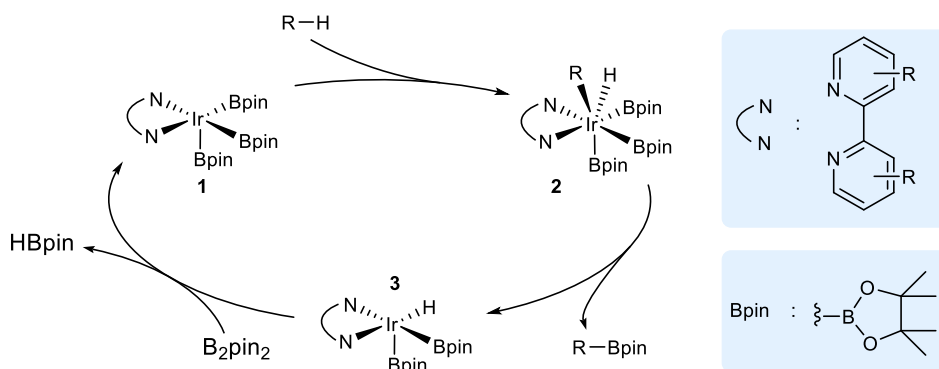
Scheme 1.1. Postulated mechanism for the C–H borylation of arenes using Ir/bpy as catalyst.

## 1.1.2. Selectivity Issues in C–H Borylation

In case of the most thoroughly studied and highly efficient iridium-based catalysts bearing a bipyridine ligand, the regioselectivity of the C–H borylation reaction is usually controlled by steric effects imposed by the starting material. Typically, the most sterically accessible C–H bonds are functionalized. When multiple C–H bonds are equally accessible, with no clear electronical bias, the reaction leads to the formation of a mixture of products. Apart from a few specific exceptions (cf. Section 1.2.4), the borylation does not occur readily in the *ortho*-position to another sizable substituent.[5] Therefore, for instance, the reaction of 1,4-dichlorobenzene is considerably more sluggish (24 h reaction time, 53% yield) than 1,3-dichlorobenzene (2 h reaction time, 84%) under standard Ir(I)/dtbpy conditions (Scheme 1.2).[24] On the other hand, 1-chloro-2-methoxybenzene forms a 60:40 mixture of regioisomers under similar conditions, as electronics contribute only minorly to the selectivity.[32]

Similarly unselective are reactions for monosubstituted arenes, such as toluene,[23] or when multiple aryl rings are present in the starting material.[33] Analogous selectivity issues are encountered in the borylation of sp^3-C–H bonds. For example, borylation of 2-methylheptane under Rh catalysis yields a 5:1 mixture of regioisomers.[21] Due to these limitations, sophisticated ligands and catalysts have been engineered over the years that interact in different modes of action with starting materials to promote the reaction and control its selectivity precisely.
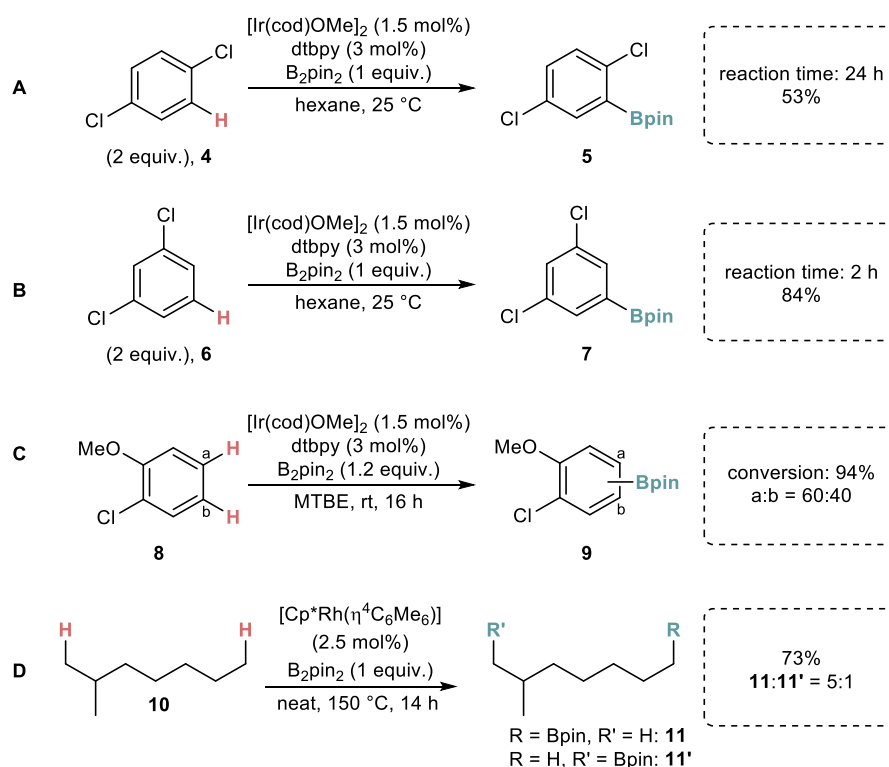
Scheme 1.2. Examples for group 9 catalyzed C–H borylation reactions; sluggish reaction of aromatic substrates with 1,4-substitution pattern (**A**); high reactivity and selectivity for 1,3-substitution pattern (**B**); low selectivity in case of 1,2-disubstitution (**C**); moderate site-selectivity for Rh-catalyzed sp^3-C–H borylation (**D**).

1.1.3. Different Modes of Action Employing Directing Group Strategies in C–H Borylation

Among different modes of action to control the selectivity through directing group strategies, three different scenarios can be distinguished: chelate-, relay-, and outer-sphere-directed metalation (Scheme 1.3).[34] In the first case, chelate-direction, the substrate bears a Lewis basic group which coordinates to the metal center prior to C–H bond cleavage. Therefore, in this approach ligands are applied that are capable of creating a vacant site at the metal center for the coordination of the starting material to be feasible.[34] Consequently, the commonly used bipyridine-based ligands are usually unsuitable.[35] Instead, this type of ligand can be used in relay-type approaches, where the vacant site crucial for the coordination of the substrate to the metal center is created through the reaction of the directing group with one of the boryl ligands. In their seminal work, Hartwig and co-workers utilized benzyl hydrosilanes that react with one boryl ligand in the tris(boryl)complex **1** to form HBpin and a silyl ligand coordinated to the metal center.[36] In the course of the reaction, the hydrosilane is re-formed by reductive elimination with simultaneous regeneration of complex **1**. In the third approach, the outer-sphere mode, the directing group does not coordinate to the metal directly, but interacts with its ligand sphere, e.g., a bipyridine or boryl group, making an additional vacant site for the substrate obsolete. Seminal work for this approach was described by Singleton, Maleczka, and Smith.[35]
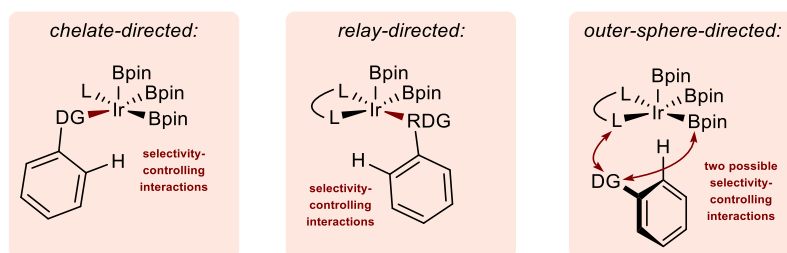
Scheme 1.3. Different modes of action underlying directing group strategies in C–H borylation.

1.1.4. Scope and Aim of this Chapter

This chapter provides an overview of different approaches in the field of C–H borylation reactions mediated by group 9 metal based catalysts that target the control of the activity and the selectivity of the reaction. Instead of presenting an exhaustive overview[6,30,37–46] selected examples are discussed with the main focus on recent studies, typically reported after 2017, and aims to give credit to different contributors to the field. The chapter covers the C–H borylation of arenes, alkenes, and alkanes,[47] but does not cover reactions of heteroarenes that have recently been reviewed extensively elsewhere.[48–51]

It should be noted that the terms 'regioselectivity' and 'site-selectivity' are used inconsequently in the literature, often with interchangeable definitions. In this chapter, the term regioselectivity is used for the selective reaction at one position within a functional group, e.g., *meta*- versus *para*-position within a single aromatic ring, while the term site-selectivity is used for the selectivity of one functional group over another, e.g., one aromatic ring preferentially over another one.[52]

1.2. Trends in C–H Borylation Reactions

Given the versatile modes of actions underlying modern approaches toward selective C–H borylation, this chapter is divided into seven sub-sections focusing on different catalytic key features that control the catalytic activity or selectivity. The overview begins with photo-induced catalysis and continues with transfer borylation chemistry, approaches based on Lewis acid-base interactions, followed by an overview of recent achievements based on directed metalation. The subsequent sections focus on undirected reactions in case of which the selectivity is determined by the inherent electronic or steric properties of the substrates, followed by protocols relying on both attractive and repulsive electrostatic interactions. The final section deals with selectivity imposed by hydrogen bonding between the starting material and a carefully designed catalyst equipped with a binding unit. The chapter concludes with a summary and an outlook providing potential future directions in C–H borylations reactions and underscoring remaining challenges that should be addressed in the future to unlock the full potential of the field.

1.2.1. Photoinduced Catalysis

Photoinduced transition metal catalysis has gained increasing attention recently due to the unusual modulation of oxidation states under mild reaction conditions.[53–56] Baslé and co-workers reported the first regioselective visible-light-induced C–H borylation directed by 2-

pyridyl groups (Scheme 1.4A).[57] The reaction is catalyzed by NHC-Rh^I complex **14** and allows the borylation of a range of substrates with substantial functional group tolerance under mild reaction conditions. Preliminary mechanistic studies revealed that the NHC-Rh^I complex absorbs the visible light, enabling the oxidative addition of the *ortho*-C–H bond to form a cyclometalated Rh^{III}-hydride intermediate. It is further proposed that this intermediate reacts with B$_2$pin$_2$ to form HBpin and the corresponding Rh^{III}-boryl species. The product is then formed upon reductive elimination.

In 2021, Tanaka and co-workers reported the related photoinduced C–H borylation catalyzed by Rh^{III}-cyclopentadienyl complex **17** (Scheme 1.4B).[58] However, in contrast to the previous study by Baslé, the photoinduction is required to reduce the metal after the addition of the C–H bond to form a Rh^{II}-ate complex that facilitates the ligand exchange with B$_2$pin$_2$. Key to enhanced yields was the use of [Ir(dFppy)$_3$] as photoredox catalyst. In contrast to the previous work, the method is applicable to substrates with pyrazoles as directing groups but has a lower functional group tolerance.
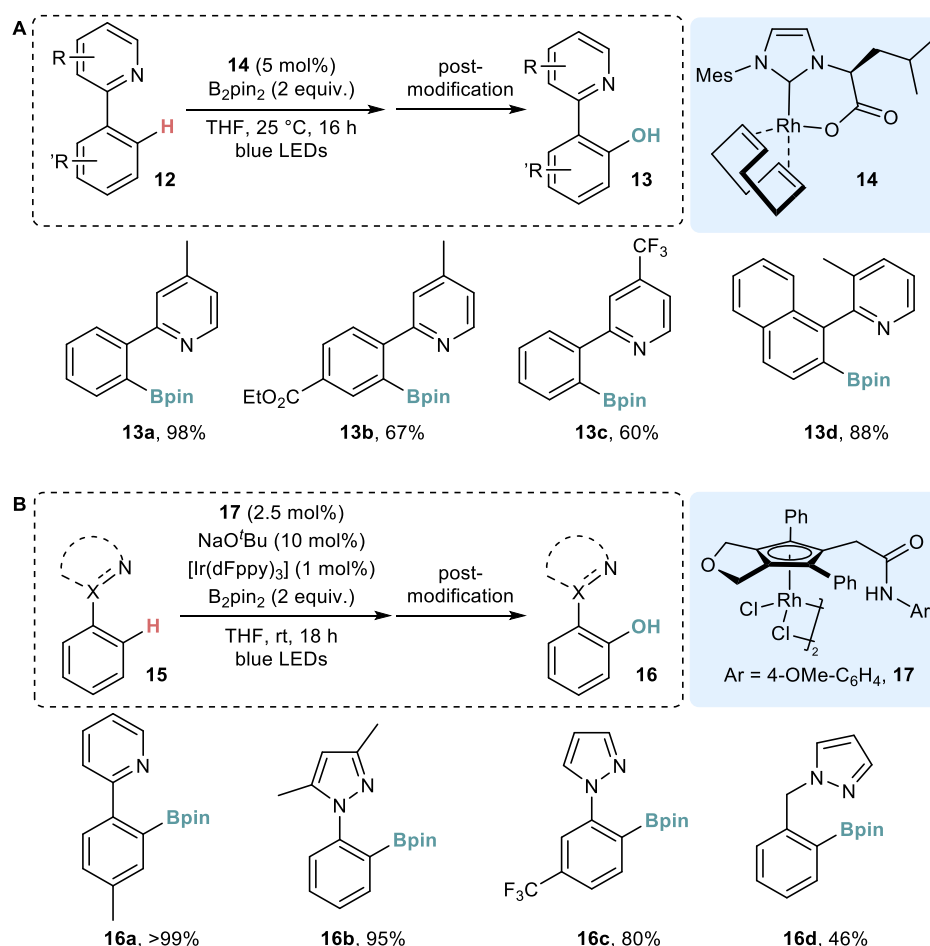
Scheme 1.4. Visible-light-induced Rh-catalyzed methods for the *ortho*-selective C–H borylation of arenes by Baslé (**A**) and Tanaka (**B**).

1.2.2. C–H Borylation of Alkenes

C–H Borylation reactions of alkenes generally lead to the formation of alkenylboronates.[3] The synthesis of (*E*)-alkenylboronates from alkenes has been described using different

approaches, the most studied being dehydrogenative borylation, initially described by Masuda and co-workers using a Rh(I) complex.[59–62] Despite the elegance of established protocols, a truly general approach toward alkenylboronates still remains elusive, as each protocol is unsuitable for certain types of substrates due to catalyst inhibition or impeding side reactions. The most recent contributions to this field are the core of this thesis and are described in chapter 2 and 3.

1.2.3. Lewis Acid Mediated C–H Borylation

Lewis acids (LA) and combinations of LA with transition metals have been widely used to achieve highly selective transformations[63–65] and have recently also been applied to C–H borylation reactions.

Nakao and co-workers reported two different strategies for the *para*- and *meta*-selective[66,67] C–H borylation of benzamides by using a combination of iridium and aluminum catalysis (Scheme 1.5).[68,69] The *para*-selective reaction was realized by cooperative iridium/aluminum catalysis (Scheme 1.5A).[69] The Lewis basic benzamide moiety of the substrate is coordinated by the LA catalyst making the substrate more reactive due to charge transfer. Because of the steric repulsion between the iridium and LA catalyst, the *ortho*- and *meta*-positions are blocked, thereby the reaction occurs selectively at the *para*-position.
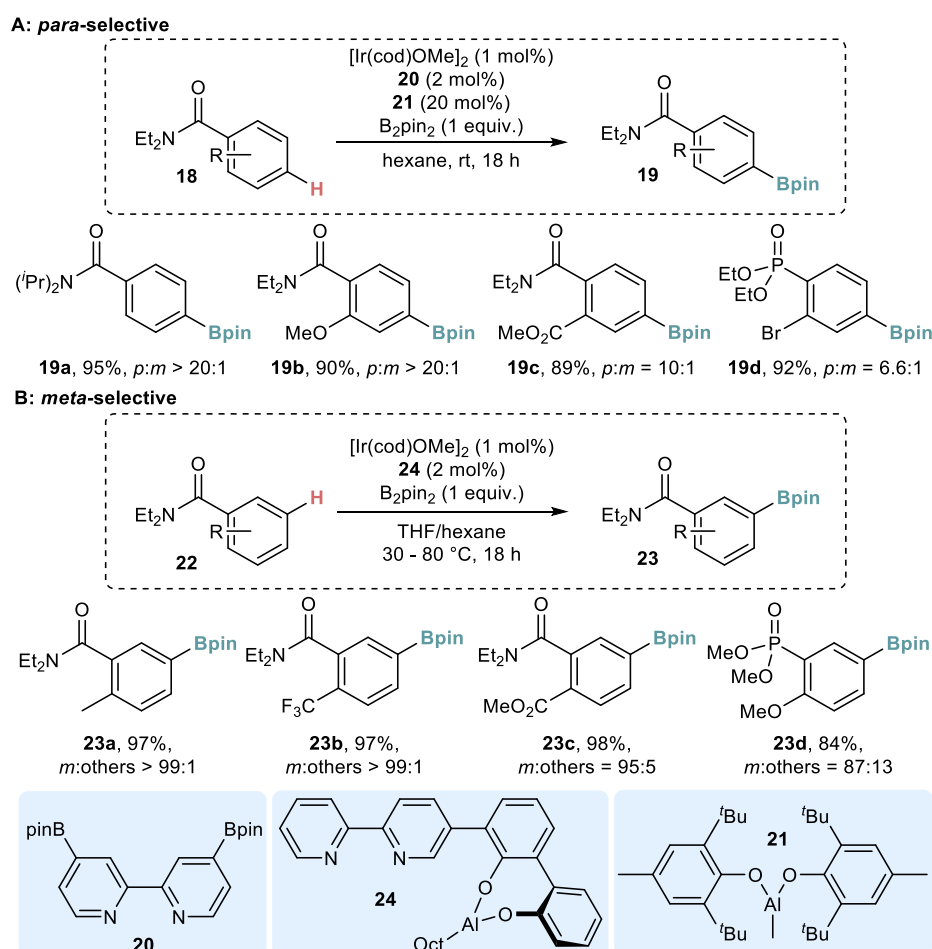
Scheme 1.5. Ir/Al-catalysis enables the (A) *para*- and (B) *meta*-selective C–H borylation of benzamides by interaction of the Lewis acid with a Lewis basic group of the substrate by Nakao.

The *meta*-selective reactions were catalyzed by a single bifunctional Ir/LA catalyst (Scheme 1.5B).[68] A ligand containing a Lewis acidic Al moiety that binds to the Lewis basic benzamide substrate, analogously to the previous publication, was used. In this case, the Lewis acid–Lewis base interaction places the iridium catalyst in the suitable position to activate the *meta*-C–H bond.

Both above-described methods have a broad functional group tolerance and remain selective in the presence of other Lewis basic groups. It was shown for both methods that phosphonates can be used as directing groups instead of amides as well. Related reports combining LA and Ir catalysts for the regioselective C–H borylation of arenes have also been reported by other groups.[70–73]

Suzuki, Yamashita, and Nakamura reported the α-C–H borylation of triethylamine with an Ir complex bearing an aluminabenzene ligand (Scheme 1.6).[74] The aluminum atom of the ligand acts as a LA as indicated by the formation of a Lewis acid–base complex with 4-(dimethylamino)pyridine. The α-site-selectivity is presumably achieved thanks to the Lewis acid–base interactions between the Al site of the catalyst and the nitrogen atom of the starting material. Unfortunately, similar substrates such as tripropylamine and *N,N*-dimethylbenzyl-amine did not show a similar reactivity and instead underwent either linear borylation or *ortho*-selective borylation of the phenyl ring, respectively.
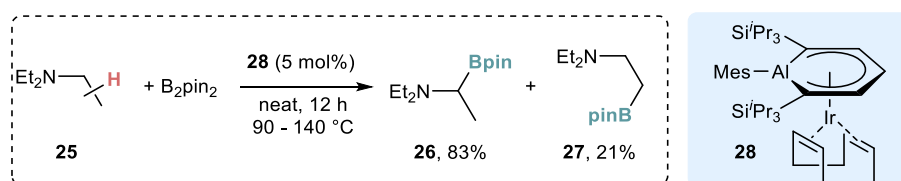
Scheme 1.6. An aluminabenzene-Ir-complex catalyzes the α-C–H-borylation of triethylamine via the formation of a Lewis acid-base-complex by Suzuki and Yamashita.

The interactions between a potassium quinolate and aromatic esters and amides have been efficiently instrumentalized by Chattopadhyay and co-workers to dictate the regioselectivity for either *para*- or *meta*-selective C–H borylation of benzoate esters or benzamides, respectively (Scheme 1.7).[71,72] By engineering the bifunctional 'L-shaped' ligand **31** bearing a bipyridine and a quinolone moiety (which is converted *in situ* into the corresponding potassium quinolate), both substrates react via an organized transition state where either the *meta*- or *para*-C–H bond of the substrate is directed toward the metal center. The different regioselectivity for ester (*para*) and amide (*meta*) substrates is postulated to result from a different structural distortion of the latter in the key transition state when compared to the ester transition state which is caused by the substantial steric bulk of the substituents at the amide nitrogen atom of the former.
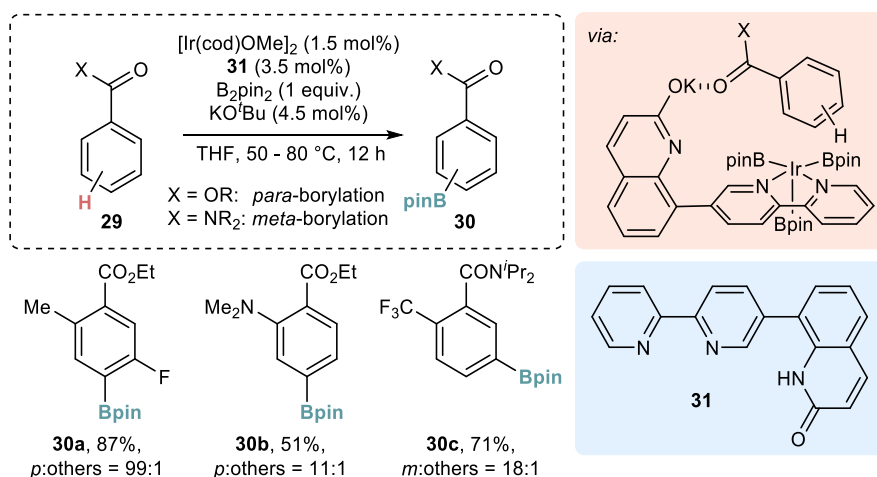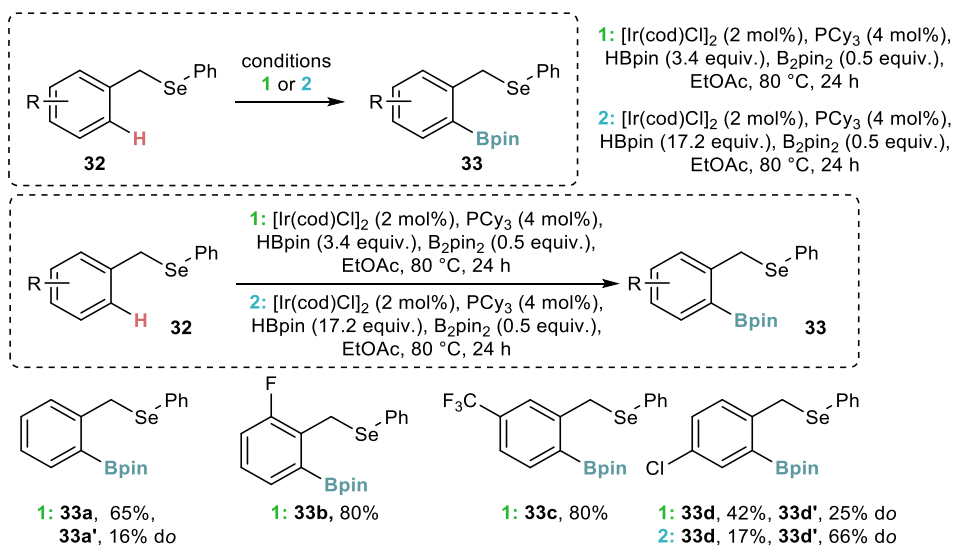
Scheme 1.7. *para*- or *meta*-Selective C–H borylation of benzoates and benzamides enabled by a weak interaction between ligand and substrate developed by Chattopadhyay.

1.2.4. Directed Metalation

A common strategy to obtain regioselective functionalization reactions is the introduction of a directing group (DG). A DG is a moiety incorporated into the starting material, which can coordinate to the metal center. Upon coordination, the catalyst is positioned next to the target C–H bond, thereby controlling the regioselectivity of the reaction. Many strategies have been developed and reviewed for the regioselective C–H borylation using different types of DGs,[34,75–79] most commonly to achieve *ortho*-selectivity. Included here is a short discussion of recent contributions to this field.

1.2.4.1. *ortho*-Selective, Selenium-Directed

The first *ortho*-C–H borylation directed by a selenium-substituent was reported by Zhou and co-workers (Scheme 1.8).[80] The Ir-catalyzed reaction converted benzyl selenide derivatives into the corresponding borylated products. Reactions of substrates bearing *ortho*- or *meta*-substituents afforded mainly monoborylated products. In turn, the reaction of *para*-substituted substrates led to the formation of mixtures of mono- and diborylated products. The latter were formed more selectively when a large excess of HBpin reagent was used.

Scheme 1.8. Ir-catalyzed *ortho*-selective, selenium-directed C–H borylation of arenes by Zhou.

1.2.4.2. *ortho*-Selective, Sulfur-Directed

Yamanaka, Kuninobu, and co-workers reported the Ir-catalyzed *ortho*-selective C–H borylation of thioanisole derivatives (Scheme 1.9).[81] Key to the directing effect is the use of the appropriately substituted bipyridine-type ligand **36**. DFT calculations (performed for dtbpy-Ir(Beg)$_3$ and bpy-Ir(Beg)$_3$, eg = ethylene glycolate) indicated that the regioselectivity originates from a hydrogen bond between the C–H bond of the SCH$_3$ group of the substrate and an oxygen atom of the boryl ligand. The method is applicable to substrates bearing substituents in the *ortho*-, *meta*-, and *para*- positions. Benzyl methyl sulfide underwent *ortho*-borylation with high selectivity as well.
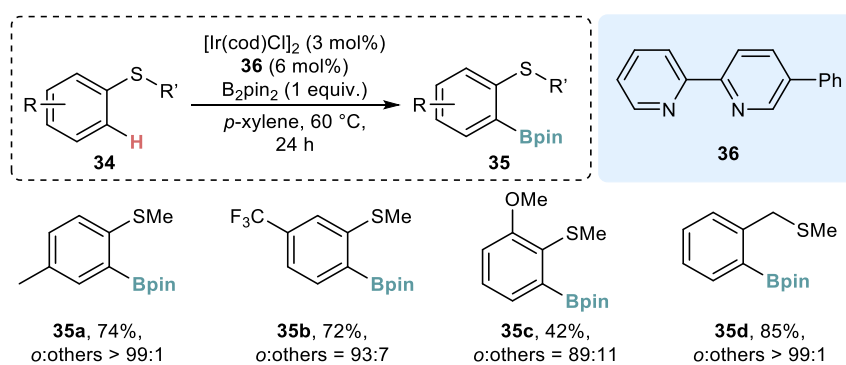
Scheme 1.9. Ir-catalyzed *ortho*-selective, sulfur-directed C–H borylation of arenes by Yamanaka and Kuninobu.

1.2.4.3. *ortho*-Selective, Phosphorus-Directed

In 2019, Shi and co-workers reported the first Rh-catalyzed P^{III}-directed *ortho*-selective C–H borylation (scheme 10A).[82] The operationally simple method allows the functionalization of triaryl-, alkyldiaryl-, and dialkylarylphosphines in high yields. To facilitate their purification, the products were converted to the corresponding borane complexes. Although the functional group tolerance is limited, the method simplifies the synthetic route to access these *ortho*-borylated phosphine products. A similar method based on a Ru-catalyst was also reported by Takaya in 2019.[83]

In 2020, shortly after the work of Shi and co-workers, Clarke, Watson, and co-workers reported phosphonate-directed *ortho*-C–H borylation (Scheme 1.10B).[84] The reaction is catalyzed by a simple Ir-catalyst and possesses, in comparison to previous methods, a broad functional group tolerance (e.g., esters and amines). Further, it is more tolerant with respect to the substitution pattern of the substrates, i.e., (multiple) substitutions in *ortho*-, *meta*-, and *para*-positions are well tolerated. The method provides a useful synthetic shortcut compared to established methods.[75,85]
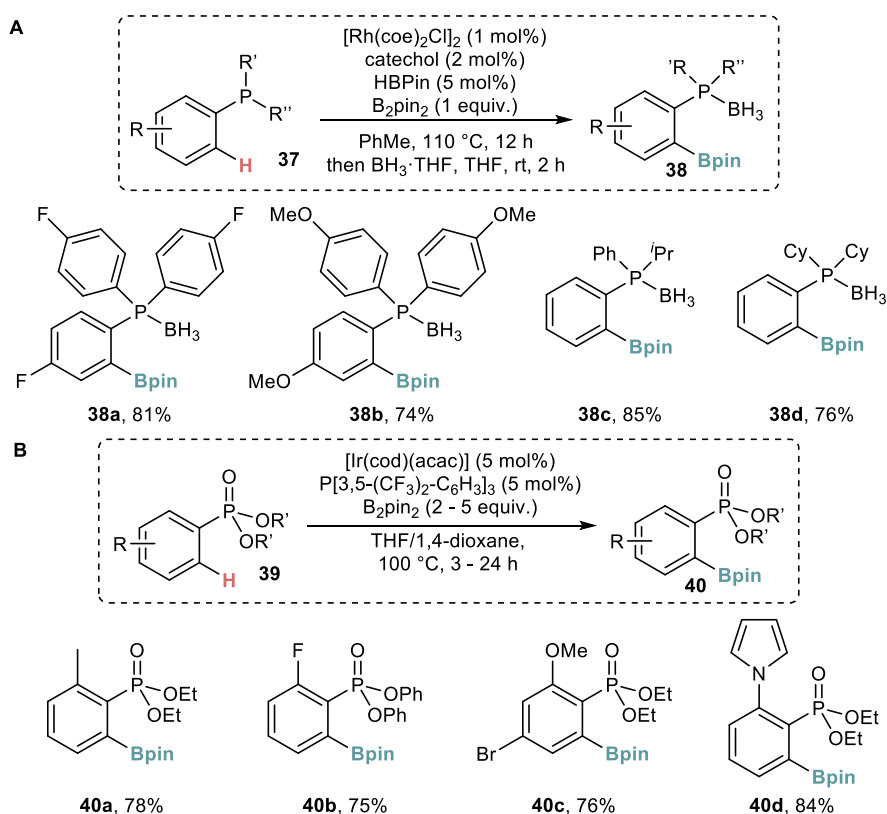
Scheme 1.10. Rh- and Ir-catalyzed *ortho*-selective, phosphorus-directed C–H borylations of arenes by Shi (**A**) and Clarke and Watson (**B**).

1.2.4.4. *ortho*-Selective, Ester- and Amide-Directed

Li, Jiao, and co-workers recently reported the Ir-catalyzed *ortho*-selective C–H borylation of (hetero)arenecarboxylate esters and arylamides (Scheme 1.11).[86] Although not the first report for the C–H borylation of such compounds,[87–89] this method is the first C–H borylation reaction utilizing a *S*-containing ligand. The newly developed *Si,S*-chelating ligand **43** is easy to prepare and enables the reaction to proceed with high yields and regioselectivity. Different esters as well as dimethylamides can be used as directing groups.
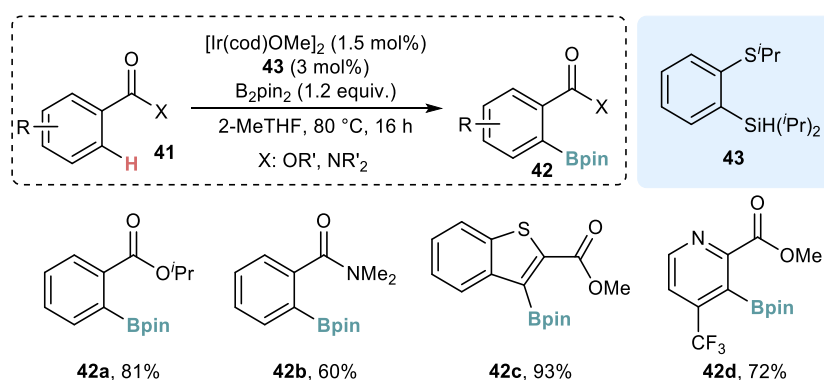
Scheme 1.11. Ir-catalyzed *ortho*-selective, ester- and amide-directed C–H borylation of arenes by Li and Jiao.

1.2.4.5. *ortho*-Selective, Nitrogen-Directed

Despite their well-established reactivity in the C–H borylation of alkanes,[21,90] Cp*Rh[III] complexes have been used once for the C–H borylation of arenes so far.[91] Baslé and co-workers reported the pyridine-directed *ortho*-C–H borylation catalyzed by the readily prepared (NHC)Cp*Rh[III] catalyst **46** (Scheme 1.12A).[92] Both electron-donating and electron-withdrawing substituents are well tolerated, although only in the *para*-position. Any substituent in *ortho*- or *meta*-position led to diminished yields. Further, it was demonstrated that the same complex can be used for the C–H borylation of *n*-octane at elevated temperatures.

Xu and co-workers reported the *ortho*-selective C–H borylation of 2-benzylpyridines in the presence of simple [Ir(cod)OMe]$_2$ (Scheme 1.12B).[93] The reaction occurs at room temperature in high yields and excellent regioselectivity, albeit with a rather moderate functional group tolerance. From a practicality point of view, it is worth noting that previous methods offering such selectivity required the use of specialized ligands[94–96] highlighting the advancement offered by this work. Further, ^{11}B NMR spectroscopy indicated a coordination between the nitrogen and the boron atoms in most cases of the products. A method for the similar *ortho*-selective C–H borylation of 8-arylquinolines was reported in 2021 by Chattopadhyay and co-workers.[97]

It is worth noting that amines have also been used as additives to construct imines *in situ* that act as traceless directing groups for the *ortho*- and *meta*-selective C–H borylation of benzaldehydes.[98]
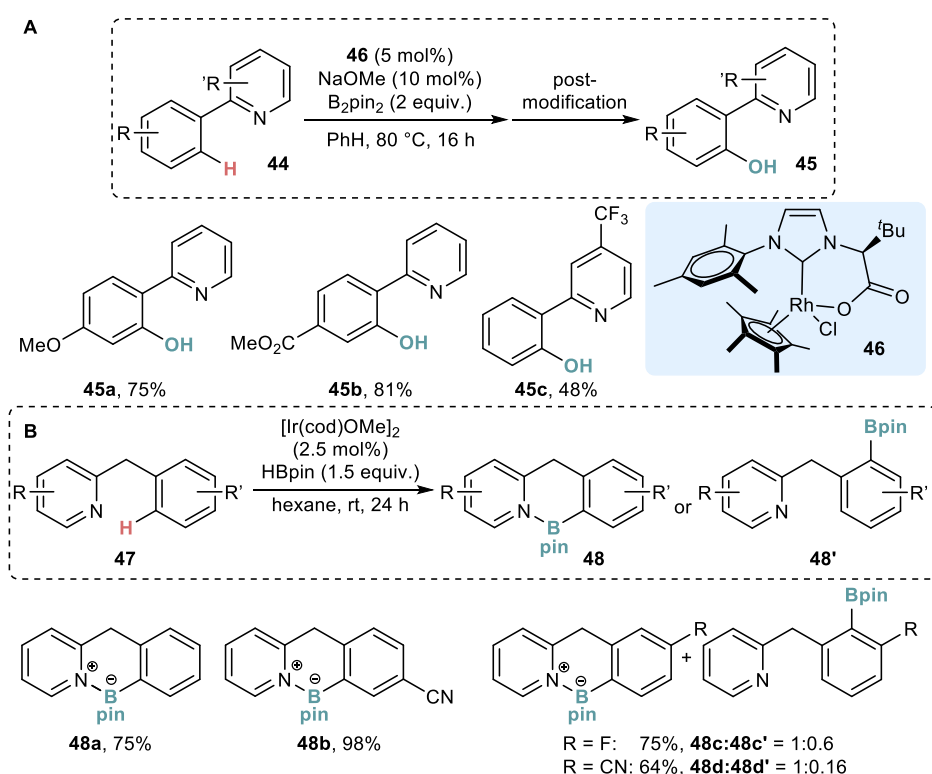
Scheme 1.12. Rh- and Ir-catalyzed *ortho*-selective, pyridine-directed C–H borylations of arenes by Baslé (A) and Xu (B).

1.2.4.6. *ortho*-Selective C–H Borylation of Substrates bearing Diverse Directing Groups

While most of the *ortho*-selective borylation reactions demand a specific combination of a directing group and a catalyst, Chattopadhyay and co-workers developed the thienylpyridine ligand **51**, which promotes a powerful, yet highly selective Ir-catalyzed C–H borylation reaction suitable for a remarkable range of directing groups (Scheme 1.13).[99] In addition, the protocol tolerates diverse functional groups with no discrimination toward the substituents positioned within the arene ring. Mechanistically, the thienylpyridine serves as a bidentate ligand, and the reaction proceeds via an $Ir^{III/V}$ catalytic cycle. It is worth noting that this catalyst proved effective also when utilized under air, when the air-stable complex $[Ir(cod)(Cl)]_2$ was used as a pre-catalyst.
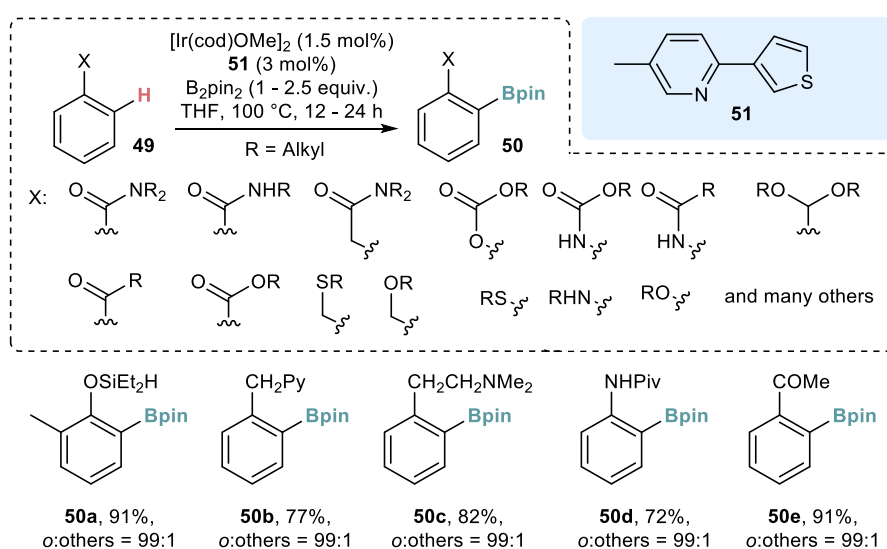
Scheme 1.13. Ir-catalyzed *ortho*-selective C–H borylation of arenes enabled by a thienylpyridine ligand: scope of directing groups by Chattopadhyay.

1.2.4.7. Pyridine- and Pyrimidine-Directed sp³-C–H Borylation

An Ir-complex of the thienylpyridine ligand **51** also enables a selective borylation reaction of aliphatic C–H bonds (Scheme 1.14).[99] Although the corresponding products are obtained in moderate yields, the method displays a high site-selectivity with only one isomer formed and offers synthetically useful chemoselectivities.
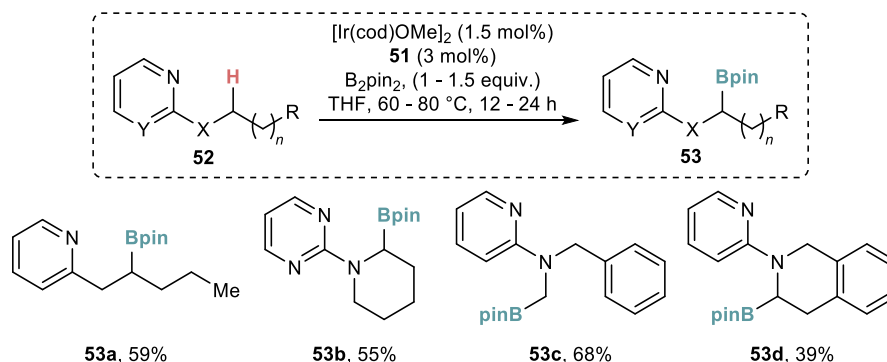
Scheme 1.14. Ir-catalyzed C–H borylation of alkanes enabled by a thienylpyridine ligand by Chattopadhyay.

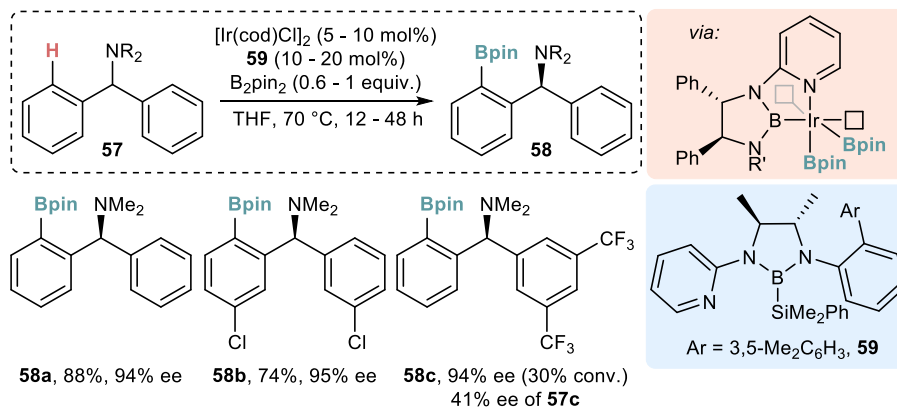## 1.2.4.8. Relay-Directed Enantioselective C–H Borylation

Soon after the first enantioselective C–H borylation was reported with a Pd catalyst in 2017,[100] the groups of Hartwig and Shi realized the relay-directed C–H borylation of diaryl-methylsilanes with a combination of an iridium source and the chiral quinolyl-oxazoline ligand **56** (Scheme 1.15).[101] An extensive ligand screening revealed that a C1-symmetric dinitrogen ligand is required to obtain even traces of product and the enantioselectivity could be improved by fusion of an indane skeleton to the oxazoline ring rather than varying the steric and electronic properties of the nitrogen heterocycles. A number of substrates underwent enantioselective borylation revealing a moderate functional group tolerance. Due to the presence of both a C–Si and C–B bond, the products offer the possibility to undergo a plethora of post-functionalization reactions.
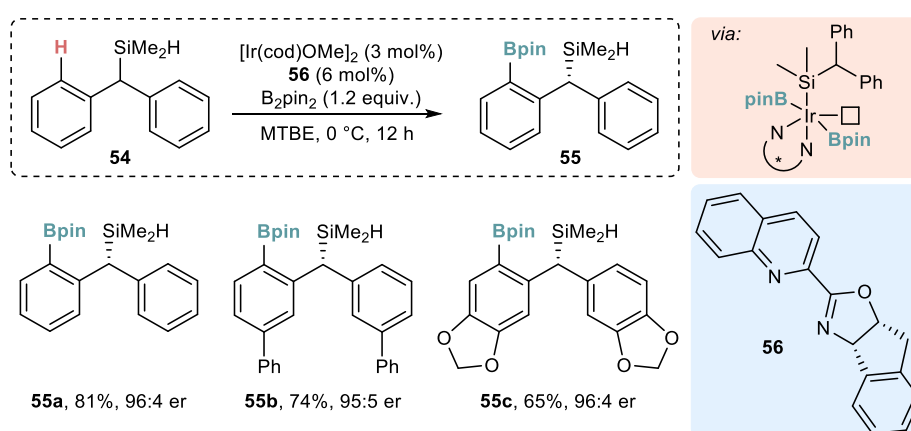
Scheme 1.15. Relay-directed enantioselective C–H borylation of diarylmethylsilanes by Hartwig and Shi.

1.2.4.9. Chelate-Directed Enantioselective C–H Borylation

Xu and co-workers also reported an iridium-catalyzed method for the borylation of diarylmethylamines (Scheme 1.16),[102] that is chelate-directed.[35] The method employs a chiral bidentate boryl ligand **59** (for the use of similar ligands, see Scheme 1.18). The method allows the desymmetrization of prochiral substrates in high yields, excellent enantioselectivities, and with a broad functional group tolerance. Furthermore, for the first time, racemic diarylmethylamines underwent kinetic resolution with excellent enantioselectivity. Other groups reported methods that extend the scope of substrates and functional group tolerance for the presented enantioselective C–H borylation reactions.[103,104]

Scheme 1.16. Chelate-directed enantioselective C–H borylation of diarylmethylamines by Xu.

1.2.4.10. peri-Borylation

Using a similar approach as in the enantioselective C–H borylation of diarylmethylsilanes (Scheme 1.15), Hartwig and co-workers reported the first relay-directed Ir-catalyzed peri-borylation of fused polycyclic arenes (Scheme 1.17).[105] The reaction occurs under mild conditions and different arenes can be used as substrates. Compared to established methods, this protocol offers a much broader functional group tolerance and excellent regioselectivity.
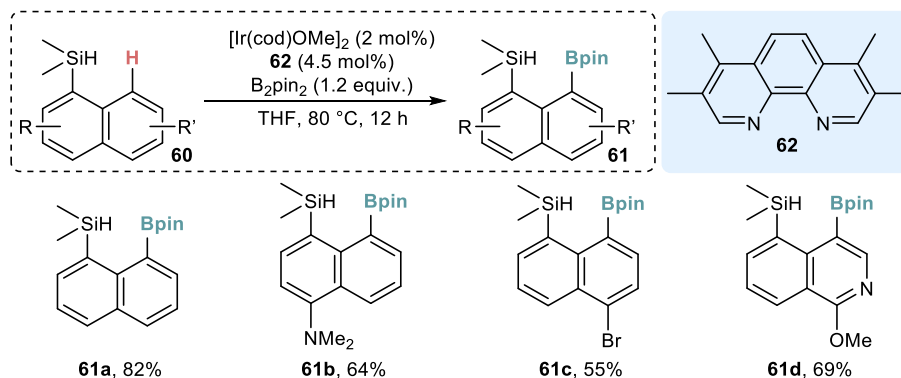
Scheme 1.17. Ir-catalyzed peri-selective, silyl-directed C–H borylation of fused polycyclic arenes by Hartwig.

1.2.4.11. Enantioselective C–H Borylation of Alkanes

Enantioselective C–H borylation of alkanes represents a great challenge since it requires at the same time the discrimination between different methylene groups and the discrimination between two enantiotopic C–H bonds. The Xu group developed a new class of bidentate chiral boryl ligands that were initially used for the C–H borylation of diarylmethylamines (cf. Scheme 1.16). Using a similar approach, the enantioselective and β-selective borylation of cyclopropanecarboxamides[106] (Scheme 1.18A), α-selective borylation of azacycles[107] (Scheme 1.18B), β-selective borylation of pyrazoles[108] (Scheme 1.18C), and β-selective borylation of acyclic amides were achieved[109] (Scheme 1.18D). For a detailed insight into the mechanistic design, the reader is referred to another short review article dealing with these reactions.[110]
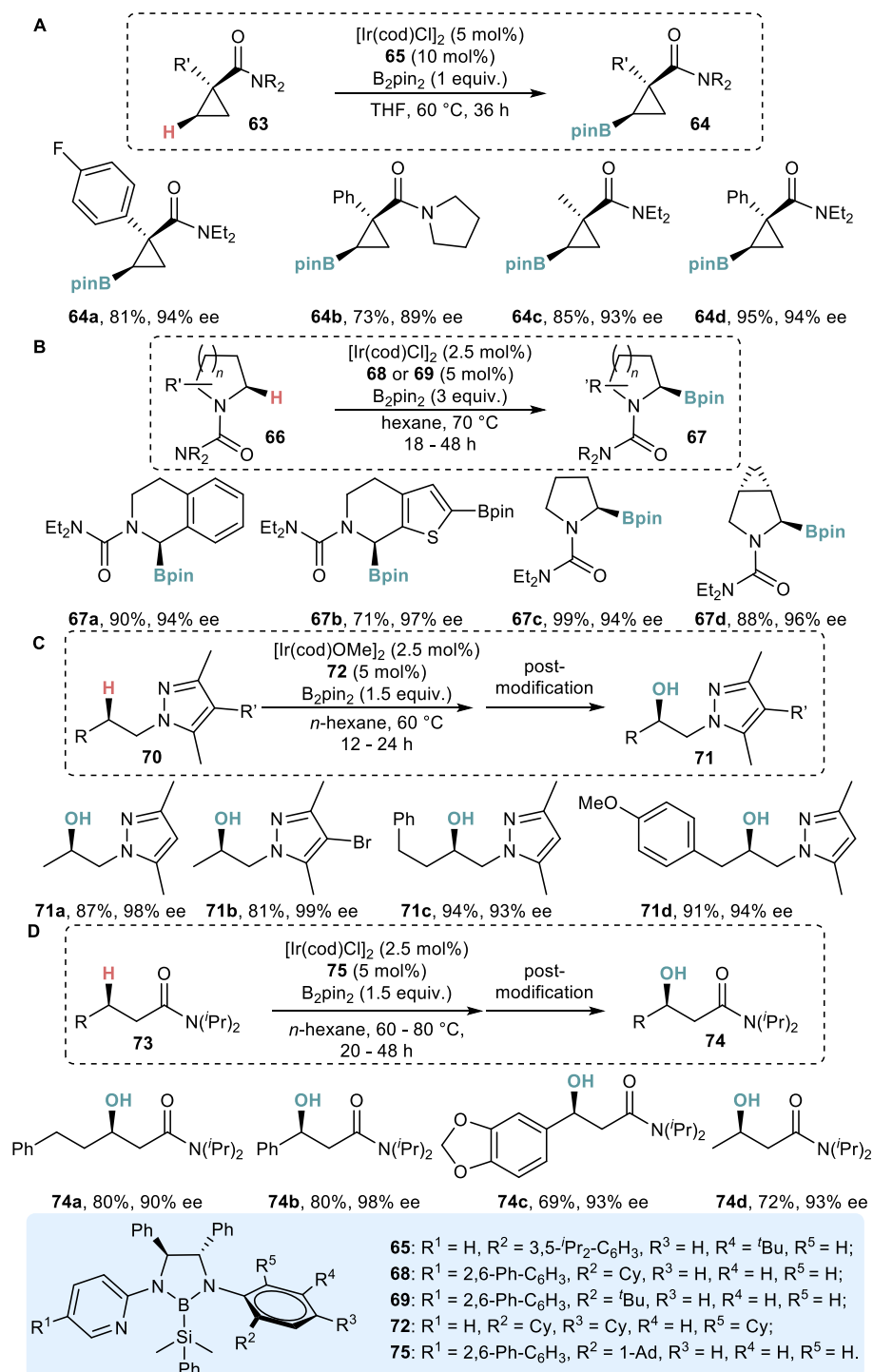
Scheme 1.18. Enantioselective C–H borylation of different alkanes enabled by a newly developed class of bidentate chiral boryl ligands by Xu.

1.2.4.12. Boryl-Directed C–H Borylation

Suginome and co-workers reported the boryl-directed C–H borylation of alkanes using an Ir-catalyst and a temporary pyrazolylaniline (Pza) derived boryl-directing group (Scheme 1.19).[111] The Pza group can be installed in one step starting from the corresponding boronic acids. Generally, the reaction is selective for the functionalization in the α-position; however, β-, and γ-C–H bonds can react as well. Depending on the amount of catalyst and B₂pin₂,

multiple C–H bonds at the same carbon atom can be borylated. The Pza group can be converted into a Bpin group *in situ* to obtain valuable polyborylated products.[112,113]

Scheme 1.19. Boryl-directed Ir-catalyzed C–H borylation by Suginome.
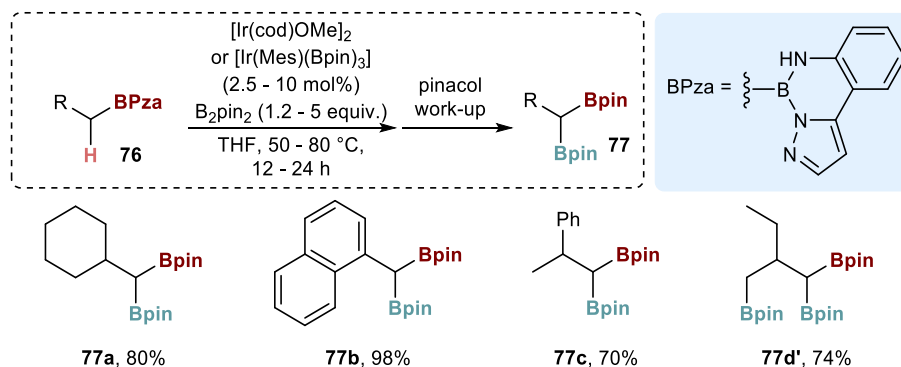
1.2.5. Miscellaneous C–H Borylation Reactions

The reactions discussed in this section are undirected reactions, i.e., the substrate does not contain a DG. The selectivity is determined by the differentiation of the C–H bonds in the substrate, through either steric repulsion or relative C–H bond activation energies, or any combination thereof.

1.2.5.1. *ortho*-Selective C–H Borylation

The Ir-catalyzed *ortho*-selective C–H borylation of fluoroarenes has been previously reported.[114–118] Ilies and co-workers developed a new approach based on the design of a novel terpyridine-derived ligand (Scheme 1.20).[119] The method tolerates a wide range of functional groups, such as esters, ethers, or halides, and occurs with a high regioselectivity. Interestingly, mechanistic investigations suggested that the ligand is likely to undergo cyclometalation to generate an unusual *N,N,C*- instead of *N,N,N*-iridium complex. Further, the complex may form a borylated ligand.

Scheme 1.20. Ir-catalyzed *ortho*-selective C–H borylation of fluoroarenes by Ilies.
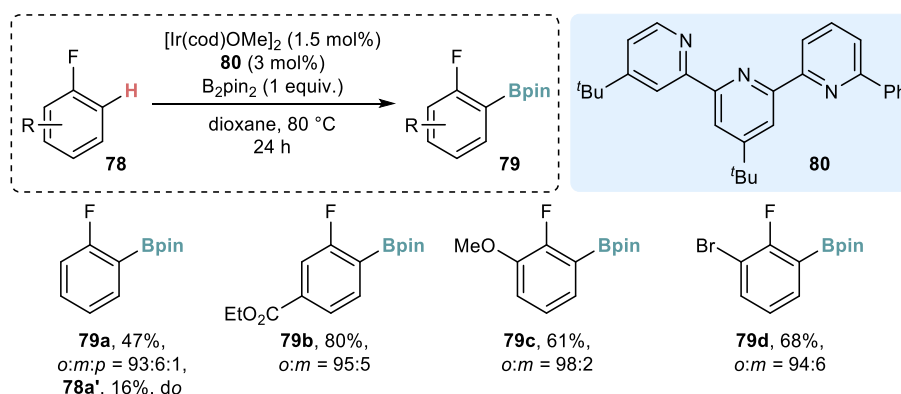
### 1.2.5.2. C–H Borylation of Primary Alkanes

Great progress has recently been made for the C–H borylation of primary sp^3-C–H bonds. Although selective methods for their reaction were reported earlier, these methods required harsh reaction conditions, the substrate was used as solvent, and the reactions offered a

rather low atom economy in terms of the B_2pin_2 reagent.[21,120–124] One of the first to report a more efficient Ir-catalyzed C–H borylation of primary alkanes were Schley and co-workers in 2020 (Scheme 1.21).[125] The reaction was performed under neat conditions and proceeded with excellent selectivity for primary alkanes with yields of up to 199% with respect to B_2pin_2 thus enhancing the atom economy compared to prior methods. The high reactivity of the catalyst is enabled by the appropriate dipyridylarylmethane ligand **83**. Furthermore, the high reactivity also allows for the C–H borylation of starting materials under non-neat conditions in cyclohexane as a solvent using a higher catalyst loading and longer reaction times. Under solvent conditions, the functional group tolerance is enhanced but yields are lower and range from 44% to 134% with respect to B_2pin_2.
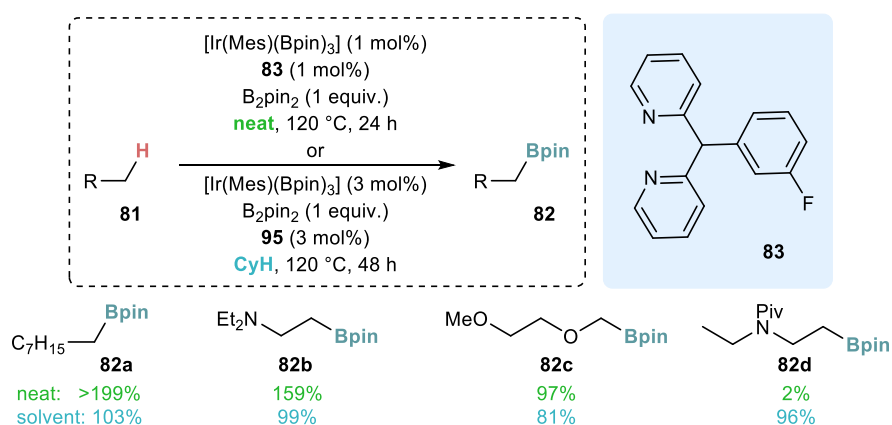
Scheme 1.21. Highly efficient Ir-catalyzed C–H borylation of alkanes by Schley; yields are based on the boron reagent B_2pin_2.

Also in 2020, Hartwig and co-workers reported the first alkyl C–H borylation with the substrate as the limiting reagent (Scheme 1.22).[126] The reaction is selective toward primary C–H bonds for many substrates. Saturated heterocycles can be also functionalized at secondary C–H bonds in the β-position with respect to the heteroatom. Key to the method development was the choice of the 2-methylphenanthroline (2-mphen) ligand **86** that enhances the reactivity of the catalyst by almost two orders of magnitude compared to other bipyridine and phenanthroline ligands. Preliminary mechanistic studies revealed that the high reactivity likely originates from a modification of the 2-mphen at the methyl group to generate the active catalyst. The high selectivity for primary C–H bonds is likely to result from a selective oxidative addition of the primary C–H bond rather than from a C–B bond formation as previously reported.[127] The selectivity toward the β-position in heterocycles has been discussed in previous reports.[5,123,128]
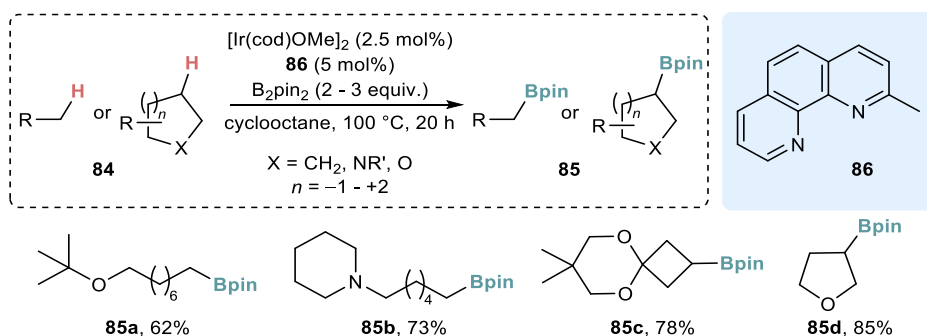
Scheme 1.22. Ir-catalyzed C–H borylation of alkanes with substrates as limiting reagents by Hartwig.

1.2.5.3. C–H Borylation of Aromatic C–H Bonds According to Inherent Electronic Differences in Bond Energies

While most *para-* or *meta*-selective borylation reactions of aromatic C–H bonds utilize designed catalyst-substrate interactions, Chirik and co-workers pursued a different approach where they applied a cobalt complex bearing a PNP-pincer ligand which borylates arenes selectively according to their intrinsic electronic properties. In their previous studies, high *ortho*-to-fluorine selectivity was observed.[27,114,117,129–131] In 2021, they investigated the use of other substrate classes under the developed conditions and found benzoates and arylboronate esters to undergo borylation with remarkable *para*-selectivities (Scheme 1.23).[132] A combination of kinetic experiments, KIE and *in situ* NMR analysis, revealed that in case of the benzoate substrates the regioselectivity does not result from a difference in the rates of the oxidative addition to the C–H bond, but from a kinetically controlled oxidative addition of HBpin on the interconverting intermediates after C–H activation in the *meta-* and *para*-position, thereby leading preferably to the *para*-substituted product in a Curtin–Hammett scenario. In contrast, the same set of experiments revealed that in case of arylboronate esters as starting materials the selectivity originates from a kinetically controlled oxidative addition to the C–H bond in the *para*-position.
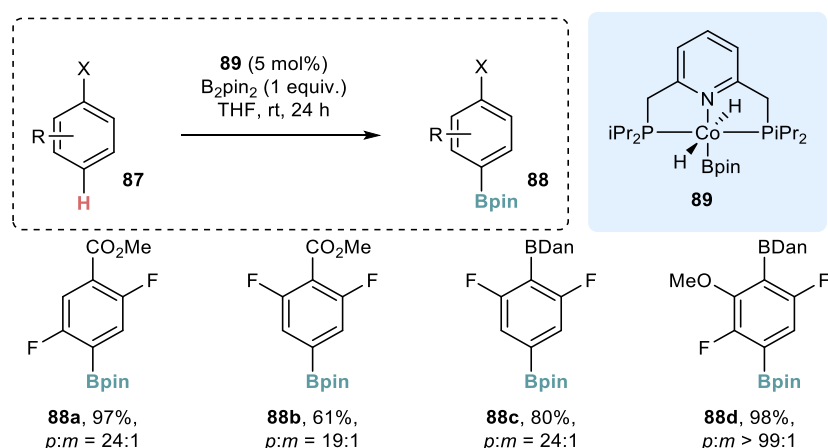

Scheme 1.23. Co-catalyzed *para*-selective C–H borylation according to intrinsic reactivity of benzoates and arylboronate esters by Chirik.

Because of its high versatility with respect to post-functionalization, a selective C–H borylation of complex molecules is of high interest for drug discovery since it enables the rapid construction of libraries with diverse functionality. In this context, Itami and co-workers

reported the Ir-catalyzed highly C3-selective C–H borylation of strychnine, which is among the most famous natural products and displays a high degree of structural complexity (Scheme 1.24A).[133] The molecule contains a tertiary amine, amide, alkene, ether, and indoline moieties with six asymmetric carbon atoms. The correct choice of ligand, in combination with an iridium source, enables the C3-selective borylation of strychnine with moderate selectivity (C3:C2, 73:27), which is driven by steric effects. The double bond between C21–C22 isomerizes to the C20–C21 position,[134] but all stereocenters and functional groups are maintained. The synthetic versatility was further shown by post-functionalization reactions.

Further, the C–H borylation methodology enables the regioselective functionalization of unsymmetrically 1,2- and 1,3-disubstituted benzenes and other arenes with a high functional group tolerance and regioselectivities (Scheme 1.24B). In general, the least sterically hindered position is functionalized, likely driven by the relatively large size of the ligand of the catalyst. Earlier, the same group reported a similar strategy, exclusively relying on steric repulsion, for the *para*-selective C–H borylation of benzene derivatives.[135]
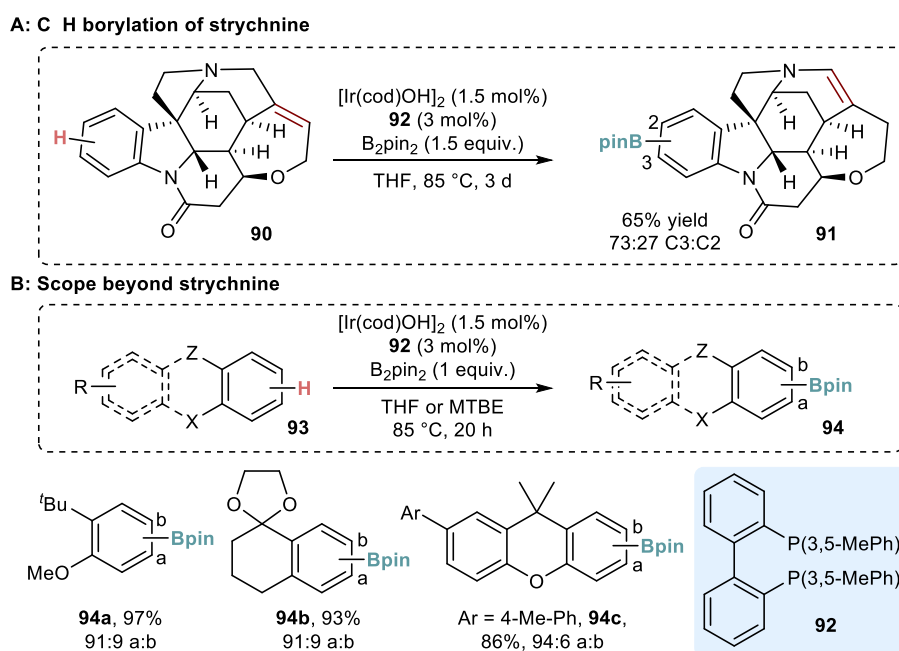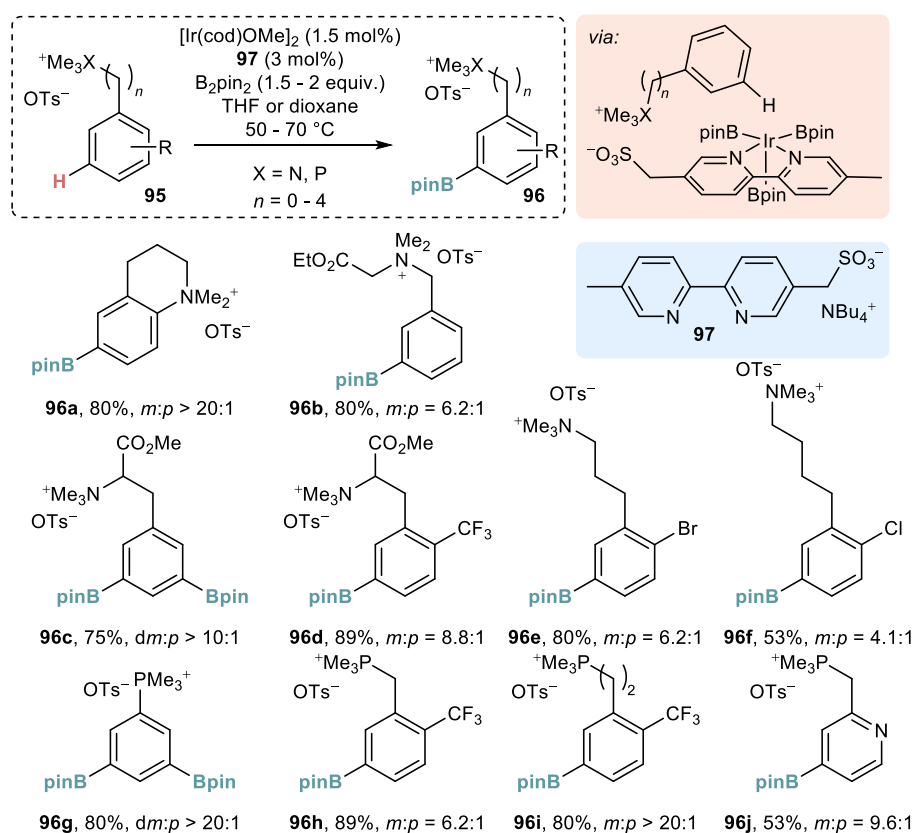

Scheme 1.24. C3-Selective C–H borylation of strychnine and scope beyond by Itami.

1.2.6. Electrostatic Interactions

1.2.6.1. Ion Pairing

While pairing chiral ions to achieve enantioselectivity represents an established concept,[136–138] the utilization of ion-pairing to control regioselectivity has evolved to be a versatile tool within recent years. The first work in the field of borylation chemistry was published by the Phipps group in 2016 who developed the anionic sulfonate-substituted bipyridine ligand **97** that can be combined with a range of ionic substrates in regioselective iridium-catalyzed borylation reactions. Initial studies revealed that this ligand can effectively guide both anilinium and benzylammonium salts with the *meta*-C–H bond pointing toward the metal center, thereby leading to high *meta*-over-*para*-selectivities (Scheme 1.25).[139] Although the use of ion-pairing as the regioselectivity-determining principle is generally attributed to be

challenging due to the lack of directionality of this interaction, even substrates bearing a flexible carbon chain, i.e., quaternized phenethylamines, 3-phenylpropylamines, and a 4-phenylbutylamine,[140] were selectively functionalized in the *meta*-position. Albeit the generally remarkably high *meta*-selectivity, the selectivity is less pronounced for phenethyl substrates when compared to a protocol based on more directed hydrogen bonding.[141] In addition, the method is restricted to electron-poor aryl rings narrowing the overall synthetic utility. It is worth noting that substrates bearing a small or no substituent in the *ortho*-position tend to give the diborylated product. In 2019, Phipps and co-workers reported that phosphonium salts were equally suitable for *meta*-selective borylation, but with a moderate functional group tolerance, using the same catalytic system (Scheme 1.25).[142]

Scheme 1.25. Attractive ion-pairing-based *meta*-selective C–H borylation of ammonium and phosphonium substrates by Phipps.

While methods for the C–H borylation in the *ortho*-position are common and few methods for *meta*-selective borylation have recently been reported, *para*-selective borylation procedures remain scarcely described in the literature.[143] Approaches based on ion-pairing were independently described by the Phipps group[144] and the joint Smith and Maleczka groups (Scheme 1.26).[145] The anionic substrates are paired with a tetrabutylammonium cation which imposes the steric bulk blocking the *meta*-position of the substrate. This strategy is in contrast to previously described *meta*-selective borylation reactions, which relied on an attractive ion-pairing (cf. Scheme 1.25). A combination of iridium methoxide precursor and an appropriate bipyridine ligand effectively borylates a set of substrates with high *para*-selectivity. Although these methods are adequate for different substrate classes, at least one substituent in the

ortho- or *meta*-position is required as the bulky cation is only capable of blocking one of the two *meta*-positions. It is worth noting that the sulfate or sulfamate group, which needs to be introduced in an additional pre-functionalization step, was shown to be cleavable in all cases. While the protocol of the Phipps group is applicable to three additional substrate classes, the protocol of Smith and Maleczka tends to give higher *para*-over-*meta*-selectivities. Furthermore, the latter is suitable for electron-rich substrates that reacted rather sluggishly under the conditions of the former.
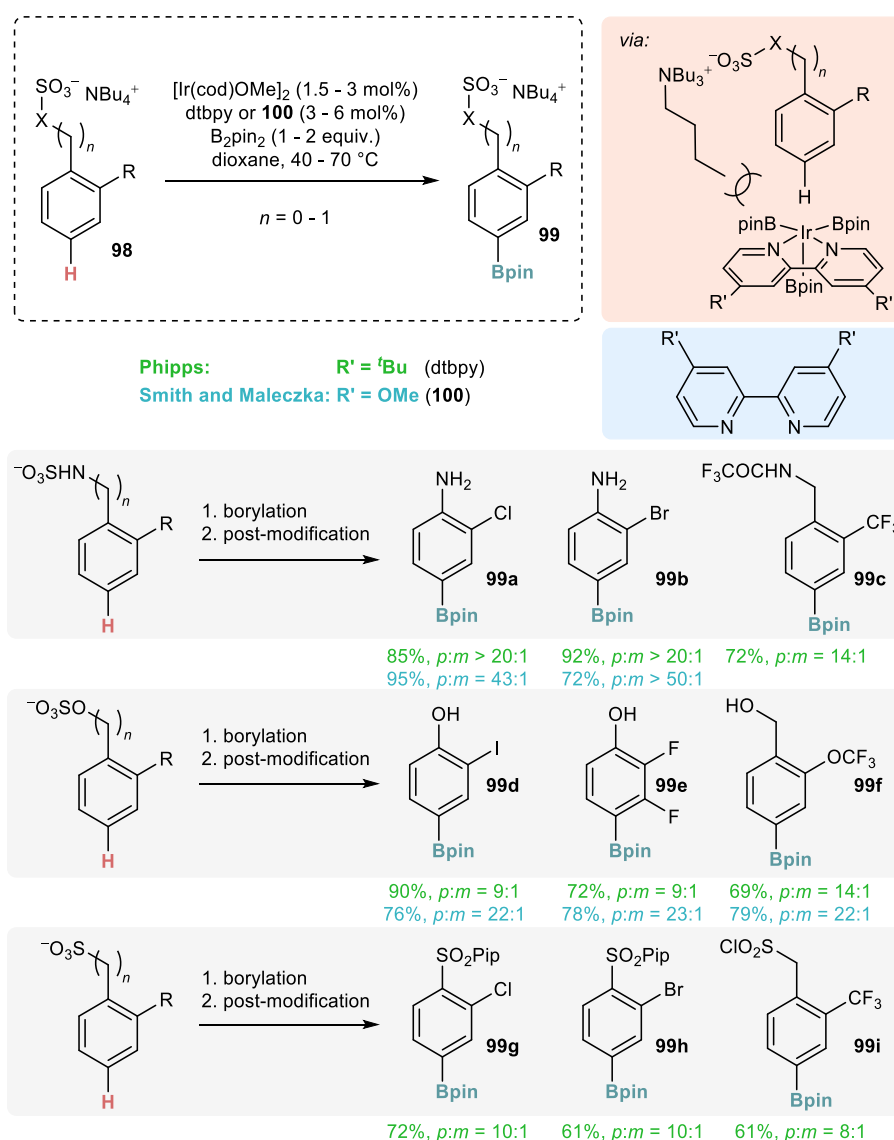
Scheme 1.26. Repulsive ion-pairing-based *para*-selective C–H borylation of sulfamate, sulfate, and sulfonate substrates by Phipps and Smith and Maleczka.

1.2.6.2. Other Electrostatic Interactions

Singleton, Smith, and Maleczka studied the dependance of the regioselectivity in the iridium-catalyzed C–H borylation of phenols on the nature of the borylation reagent (Scheme 1.27).[146] While their protocol gave significant *ortho*-selectivity only for substrates bearing relatively large substituents in the *para*-position using B_2pin_2 as the borylation reagent, it was shown that a change to B_2eg_2 led to a significant improvement in regioselectivity. Based on DFT

calculations, it was proposed that the observed selectivity originates from an electrostatic interaction between the bipyridine ligand and the oxygen atom within the glycolate ring temporarily attached to the phenolic hydroxy group. Later, this borylation agent was also key to substantially broaden the scope of anilines[147] suitable for *ortho*-selective C–H borylation (Scheme 1.27). The same strategy was further used for the functionalization of (*R*)-BINOL.[148,149] It should be noted that, according to DFT calculations, substrates lacking a substituent at the aniline nitrogen atom go through a transition state different to the one depicted in Scheme 1.27, where an additional hydrogen bond between the N–H and Ir-coordinated Beg is responsible for the *ortho*-selectivity. For substrates lacking the N–H hydrogen atom, a transition state based on electrostatic interactions analogous to the corresponding one for phenols was identified.
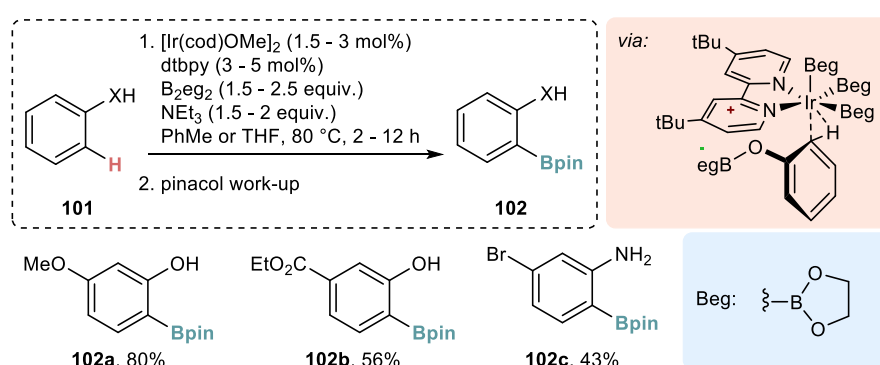
Scheme 1.27. B_2eg_2-enabled direct *ortho*-selective C–H borylation of phenols and anilines by Singleton, Smith, and Maleczka.

Building on the selectivity-determining electrostatic interactions between Beg and the bipyridine ligand (cf. Scheme 1.27), Chattopadhyay and co-workers anticipated that similar interactions could be also established between a substrate and the ligand if the ligand was sufficiently electron-poor. While indeed bipyridines with electron-withdrawing substituents effectively interacted with sulfonate-substituted anilines resulting in their *meta*-selective C–H borylation, electron-poor phenanthroline proved to be ideally suited to interact with a broad range of different sulfamates and amides (Scheme 1.28).[150] Even 1,4-disubstituted arenes, such as the 4-*t*Bu-substituted substrate **103d**, which are considered to be challenging for *meta*-selective borylation due to the steric shielding,[22] were converted into the borylated products, e.g. **104d**, in a highly selective manner. Sulfamates derived from benzylamines are applicable to the protocol, though their regioselectivity largely depends on the electronics of the arene. From a standpoint of atom-economy, it can be considered advantageous that, in contrast to earlier works by Smith and Maleczka, no transesterification from Beg to Bpin is necessary.
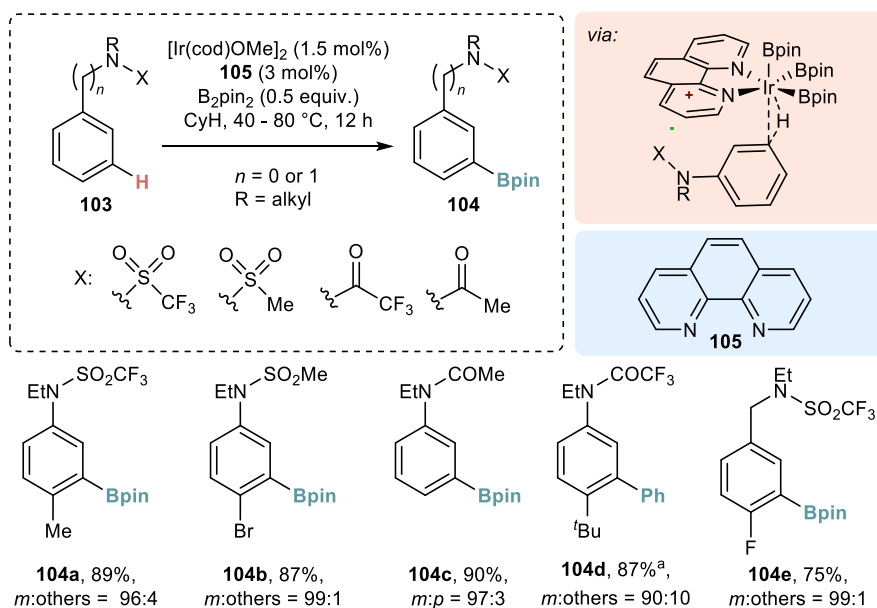
Scheme 1.28. *meta*-Selective C–H borylation of aromatic and benzylic sulfamates and amides enabled by electrostatic interactions of substrate and ligand by Chattopadhyay. a Yield after post-functionalization.

1.2.7. Hydrogen Bonding

Kuninobu, Kanai, and co-workers reported the Ir-catalyzed *meta*-selective C–H borylation of tertiary benzamides using hydrogen bonding interactions to control regioselectivity (Scheme 1.29).[151] Key to the transformation was the development of the bipyridine-derived ligand **108** that contains a precisely positioned urea moiety. Hydrogen bonding between the urea moiety and the carbonyl group of the amide group (a hydrogen acceptor) of the starting material places the iridium center close to the *meta*-C–H bond, which is then selectively functionalized. The method tolerates common functional groups in the *ortho*- and/or *meta*-position and is applicable to substrates containing different tertiary amides as a DG. In addition to amides, phosphonates can also act as a DG.
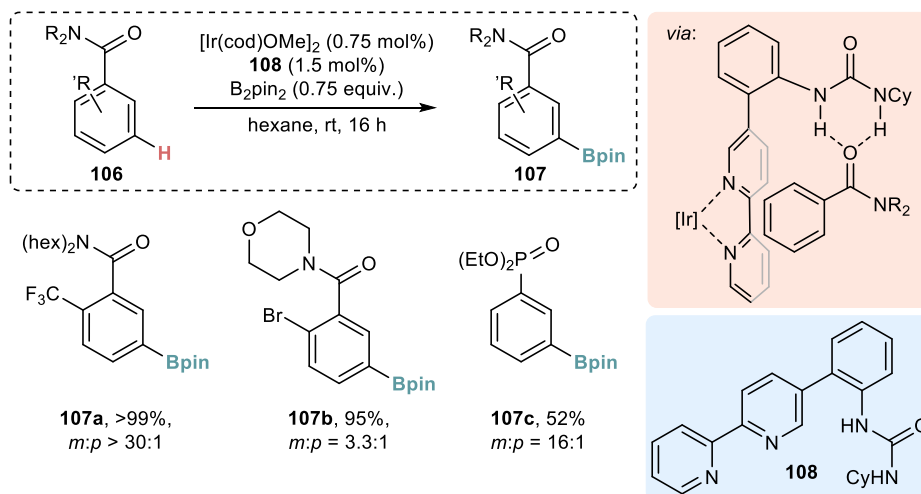

Scheme 1.29. Ir-catalyzed hydrogen-bonding directed *meta*-selective C–H borylation of arenes with amide and phosphonate directing groups by Kuninobu and Kanai.

Based on their previous work (Scheme 1.29), Kuninobu and co-workers later reported that urea-containing ligands also accelerate the *meta*-selective C–H borylation of benzamides.[152] By introducing substituents to the ligand described in their earlier work, the acceleration could be further enhanced. In addition, a functional group specificity (amide vs. ester) and substrate specificity for starting materials bearing different amide groups were achieved.
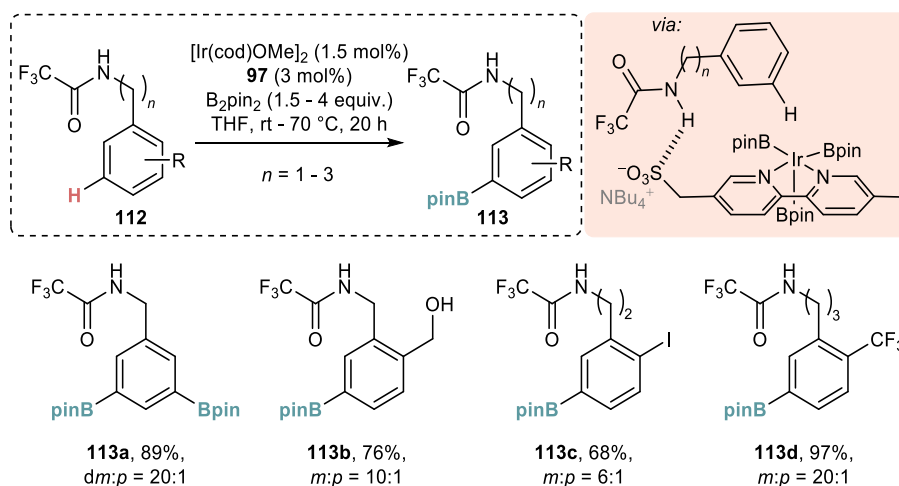
Further, the *meta*-selective C–H borylation could be combined with post-functionalization reactions in a one-pot fashion. This approach enables direct *meta*-selective C–H functionalization reactions of benzamides without isolation of the intermediary boryl compounds and is of great synthetic value.[153]

A bifunctional ligand for the iridium-catalyzed *ortho*-selective installation of Bpin into secondary benzamides was designed by Reek and co-workers (Scheme 1.30).[154] The ligand **111** contains a 2,2'-bipyridine moiety for the coordination of the metal center and an amide-substituted indole for the pre-organization of the substrate guaranteeing a high activity and regioselectivity through a total of three hydrogen bonds.
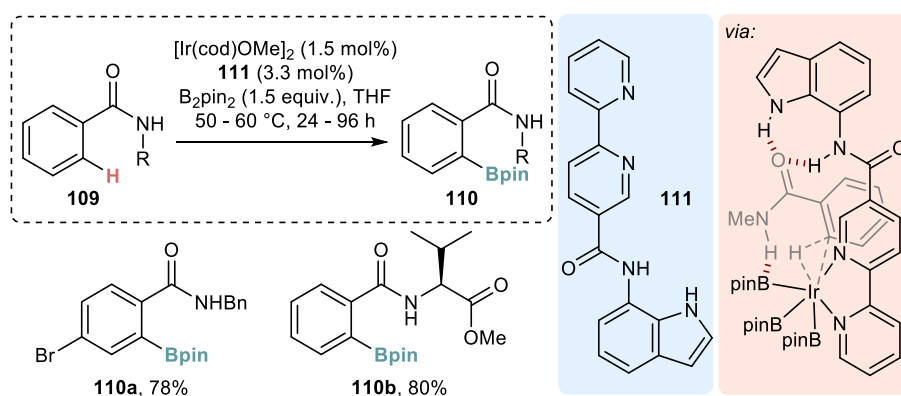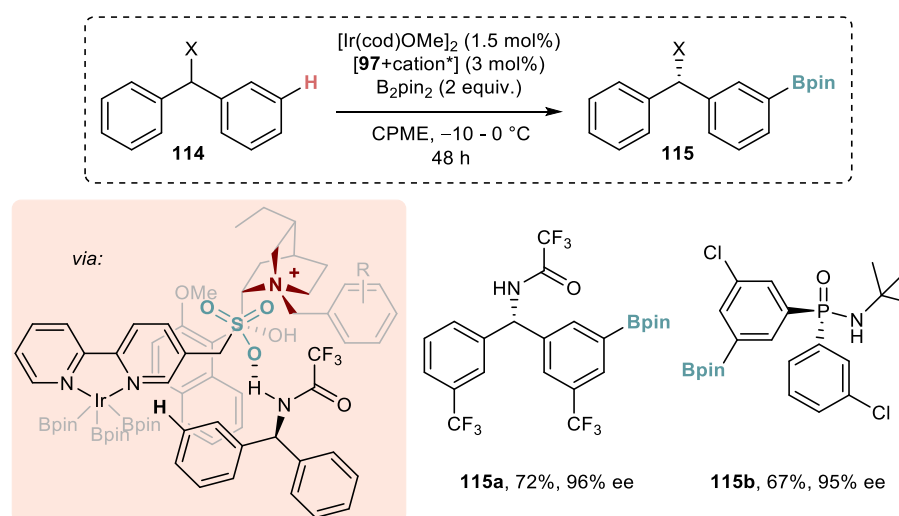

Scheme 1.30. *ortho*-Selective C–H borylation of aromatic amides enabled by hydrogen bonding by Reek.

The bipyridine-derived ligand **97** bearing a sulfonate tag, which was initially designed to ion-pair with cationic substrates (cf. Scheme 1.25), was used by the Phipps group to act as an efficient hydrogen-bond acceptor interacting with N-benzylamides (or their homologues) enabling their iridium-catalyzed *meta*-selective C–H borylation (Scheme 1.31).[141] Notably, unless a sufficiently large *ortho*-substituent is present in the starting material, the reaction forms diborylated products.

Scheme 1.31. *meta*-Selective C–H borylation enabled by a hydrogen bond between the substrate and the anionic ligand **97** by Phipps.

In 2020, exchanging the achiral counterion of ligand **97** for a chiral dihydroquinine-derived one enabled the Ir-catalyzed C–H borylation of benzhydrylamides and diarylphosphinamides in high yields and enantioselectivity (Scheme 1.32).[155] Conceptually, the hydrogen bond between substrate and anionic ligand assures an organized approach of the substrate towards the metal center, while the chiral counterion ensures a chiral environment resulting in a high differentiation of the two enantiotopic aryl substituents within the substrate.

Scheme 1.32. Enantioselective C–H borylation by combination of ion-pairing with hydrogen bonding by Phipps.

1.3. Conclusion and Outlook

As outlined in this chapter, group 9 catalyzed C–H borylation reactions continue to be a subject of rapid development. In recent years, a large body of research has focused on the development of site-selective reactions driven by precise non-covalent catalyst-substrate interactions, which complement initial methods in case of which regioselectivity was driven by steric interactions, hence functionalizing the most accessible C–H bonds. Therefore, synthetically useful borylation reactions were restricted to 1,3- and 1,2,3-substituted arenes as starting materials. Nowadays, a broad repertoire of protocols is available for the installation

of boryl groups in the *ortho*-position to a variety of directing groups. While this field can be considered well developed, the *meta-* and *para*-selective arene C–H borylation still lacks general approaches, because existing methods are restricted to specific substrate classes. Nevertheless, sophisticated concepts have been reported and further development toward a broader applicability might be expected. The very recent report on remote steric control for undirected *meta*-selective C-H borylation of arenes by Asako, Illies, and coworkers is a noteworthy step in this direction.[156] Importantly, some of the concepts originally designed for regioselective arene borylation have been shown to be transferable to the site-selective borylation of aliphatic substrates and more research in this direction with potential applications in enantioselective catalysis is of high demand. In case of the C–H borylation of alkenes, two new methods have been developed recently that are the first examples of group 9 catalyzed transfer borylations and are the subject of the discussion in chapters 2 and 3. In contrast, methods for the direct functionalization of alkenes with α- or *Z*-selectivity remain elusive. In addition, most of the protocols introduced in recent years still require the use of precious iridium and rhodium, while methods relying on cobalt are, despite its substantial natural abundance, scarcely described in the literature.

1.4. Aim and Outline of this Thesis

The aim of this thesis is the design and development of transfer borylation reactions for the efficient and widely applicable functionalization of alkene starting materials through a rational design by mechanistic considerations. Although several methods are established for the C–H borylation of alkenes, no general method that is applicable to both terminal and internal alkenes and displays an excellent functional group tolerance is available. Transfer C–H borylation bears the potential to unlock a range of attractive transformations for the synthesis and late-stage derivatization of complex molecules. However, its scarce precedence and previously limited mechanistic understanding hindered the development of practical protocols. Therefore, studying the mechanism of the C–H borylation reactions is of high importance for this thesis. In a broader context, this thesis sets the stage for the development of a range of other hydrogen-for-functional group exchange reactions undergoing similar pathways.

This PhD thesis consists of five chapters, which are briefly summarized below. First, a review of the recent trends in the field of group 9 catalyzed C–H borylation reactions is provided (this chapter) as an introduction to the discussion of related catalytic methodologies in the subsequent chapters of this thesis. Thereafter, a study of such a reaction – namely the transfer C–H borylation of alkenes under Rh(I)-catalysis – is described. The developed method enables the selective C–H borylation of terminal and internal alkenes with high selectivity and excellent functional group tolerance (Chapter 2). A thorough mechanistic investigation involving a series of catalytic and stoichiometric experiments gives insight into the full catalytic cycle employing a β-boryl elimination, an elementary step, which is unprecedented for Rh-catalysis, and elucidated the features controlling the activity and the selectivity. Subsequently, another transfer borylation methodology was developed by modifying the catalytic system

and exchanging the Rh(I)-catalyst for an Ir-catalyst (Chapter 3). The resulting protocol provides a broad functional group tolerance beyond that of the Rh(I) protocol, including the tolerance of acidic X–H bonds present in many pharmaceutically valuable motives. This feature enhanced the application of the method in late-stage functionalization settings of more complex bioactive molecules. In the next chapter, the borylative dehomologation of (allylic and aliphatic) alcohols and aldehydes through sequential multicatalysis is described. The reaction sequence consists of a Rh-catalyzed (oxidation or isomerization and) retro-hydroformylation followed by the formerly developed Ir-catalyzed transfer borylation protocol to access vinyl boronate motives that can be further functionalized using established literature methods. Overall, the sequential one-pot process enables a fast, convenient, and resource-saving dehomologative derivatization of aldehydes and (allylic) alcohols (Chapter 4). The last chapter of the thesis provides a perspective on the challenges and opportunities of such multicatalytic transformation and their future potential applications in chemical sciences (Chapter 5).

1.5. References

(1)   Chow, W. K.; Yuen, O. Y.; Choy, P. Y.; So, C. M.; Lau, C. P.; Wong, W. T.; Kwong, F. Y. A Decade Advancement of Transition Metal-Catalyzed Borylation of Aryl Halides and Sulfonates. *RSC Adv.* **2013**, *3* (31), 12518–12539. https://doi.org/10.1039/c3ra22905j.

(2)   Murata, M. Transition-Metal-Catalyzed Borylation of Organic Halides with Hydroboranes. *Heterocycles* **2012**, *85* (8), 1795–1819. https://doi.org/10.3987/REV-12-736.

(3)   Carreras, J.; Caballero, A.; Pérez, P. J. Alkenyl Boronates: Synthesis and Applications. *Chem. - Asian J.* **2019**, *14* (3), 329–343. https://doi.org/10.1002/asia.201801559.

(4)   Molander, G. A.; Sandrock, D. L. Potassium Trifluoroborate Salts as Convenient, Stable Reagents for Difficult Alkyl Transfers. *Curr. Opin. Drug Discov. Devel.* **2009**, *12* (6), 811–823.

(5)   Hartwig, J. F. Regioselectivity of the Borylation of Alkanes and Arenes. *Chem. Soc. Rev.* **2011**, *40* (4), 1992–2002. https://doi.org/10.1039/c0cs00156b.

(6)   Mkhalid, I. A. I.; Barnard, J. H.; Marder, T. B.; Murphy, J. M.; Hartwig, J. F. C-H Activation for the Construction of C-B Bonds. *Chem. Rev.* **2010**, *110* (2), 890–931. https://doi.org/10.1021/cr900206p.

(7)   Hartwig, J. F.; Larsen, M. A. Undirected, Homogeneous C-H Bond Functionalization: Challenges and Opportunities. *ACS Cent. Sci.* **2016**, *2* (5), 281–292. https://doi.org/10.1021/acscentsci.6b00032.

(8)   Hartwig, J. F. Borylation and Silylation of C?H Bonds: A Platform for Diverse C?H Bond Functionalizations. *Acc. Chem. Res.* **2012**, *45* (6), 865–873. https://doi.org/10.1021/ar200206a.

(9)   Fyfe, J. W. B.; Watson, A. J. B. Recent Developments in Organoboron Chemistry: Old Dogs, New Tricks. *Chem* **2017**, *3* (1), 31–55. https://doi.org/10.1016/j.chempr.2017.05.008.

(10)   Fernández, E.; Whiting, A. Synthesis and Application of Organoboron Compounds. In *Topics in Organometallic Chemistry*; Springer: Cham, 2015.

(11)   Woźniak, Ł.; Tan, J. F.; Nguyen, Q. H.; Madron Du Vigné, A.; Smal, V.; Cao, Y. X.; Cramer, N. Catalytic Enantioselective Functionalizations of C-H Bonds by Chiral Iridium Complexes. *Chem. Rev.* **2020**, *120* (18), 10516–10543. https://doi.org/10.1021/acs.chemrev.0c00559.

(12)   Baccalini, A.; Vergura, S.; Dolui, P.; Zanoni, G.; Maiti, D. Recent Advances in Cobalt-Catalysed C-H Functionalizations. *Org. Biomol. Chem.* **2019**, *17* (48), 10119–10141. https://doi.org/10.1039/c9ob01994d.

(13)   Achar, T. K.; Maiti, S.; Jana, S.; Maiti, D. Transition Metal Catalyzed Enantioselective C(Sp2)-H Bond Functionalization. *ACS Catal.* **2020**, *10* (23), 13748–13793. https://doi.org/10.1021/acscatal.0c03743.

(14)   Baudoin, O. Multiple Catalytic C–H Bond Functionalization for Natural Product Synthesis. *Angew. Chem. Int. Ed.* **2020**, *59* (41), 17798–17809. https://doi.org/10.1002/anie.202001224.

(15)   Liao, G.; Zhang, T.; Lin, Z. K.; Shi, B. F. Transition Metal-Catalyzed Enantioselective C–H Functionalization via Chiral Transient Directing Group Strategies. *Angew. Chem. Int. Ed.* **2020**, *59* (45), 19773–19786. https://doi.org/10.1002/anie.202008437.

(16)   Waltz, K. M.; He, X.; Muhoro, C.; Hartwig, J. F. Hydrocarbon Functionalization by Transition Metal Boryls. *J. Am. Chem. Soc.* **1995**, *4* (11), 11357–11358. https://doi.org/10.1021/ja00150a041.

(17)   Waltz, K. M.; Hartwig, J. F. Selective Functionalization of Alkanes by Transition-Metal Boryl Complexes. *Science* **1997**, *277* (5323), 211–213. https://doi.org/10.1126/science.277.5323.211.

(18)   Chen, H.; Hartwig, J. F. Catalytic, Regiospecific End-Functionalization of Alkanes: Rhenium-Catalyzed Borylation under Photochemical Conditions. *Angew. Chem. Int. Ed.* **1999**, *38* (22), 3391–3393. https://doi.org/10.1002/(SICI)1521-3773(19991115)38:22<3391::AID-ANIE3391>3.0.CO;2-N.

(19)   Iverson, C. N.; Smith, M. R. Stoichiometric and Catalytic B-C Bond Formation from Unactivated Hydrocarbons and Boranes. *J. Am. Chem. Soc.* **1999**, *121*, 7696–7697. https://doi.org/10.1021/ja991258w.

(20)   Cho, J. Y.; Tse, M. K.; Holmes, D.; Maleczka, R. E.; Smith, M. R. Remarkably Selective Iridium Catalysts for the Elaboration of Aromatic C-H Bonds. *Science* **2002**, *295* (5553), 305–308. https://doi.org/10.1126/science.1067074.

(21)   Chen, H.; Schlecht, S.; Semple, T. C.; Hartwig, J. F. Thermal, Catalytic, Regiospecific Functionalization of Alkanes. *Science* **2000**, *287*

(5460), 1995–1997. https://doi.org/10.1126/science.287.5460.1995.

(22) Yang, J. Transition Metal Catalyzed Meta-C-H Functionalization of Aromatic Compounds. *Org. Biomol. Chem.* **2015**, *13* (7), 1930–1941. https://doi.org/10.1039/c4ob02171a.

(23) Ishiyama, T.; Takagi, J.; Ishida, K.; Miyaura, N.; Anastasi, N. R.; Hartwig, J. F. Mild Iridium-Catalyzed Borylation of Arenes. High Turnover Numbers, Room Temperature Reactions, and Isolation of a Potential Intermediate. *J. Am. Chem. Soc.* **2002**, *124* (3), 390–391. https://doi.org/10.1021/ja0173019.

(24) Ishiyama, T.; Takagi, J.; Hartwig, J. F.; Miyaura, N. A Stoichiometric Aromatic C?H Borylation Catalyzed by Iridium(i)/2,2'-Bipyridine Complexes at Room Temperature. *Angew. Chem. Int. Ed.* **2002**, *41*, 3056–3058.

(25) Cho, J. Y.; Iverson, C. N.; Smith, M. R. Steric and Chelate Directing Effects in Aromatic Borylation [3]. *J. Am. Chem. Soc.* **2000**, *122* (51), 12868–12869. https://doi.org/10.1021/ja0013069.

(26) Su, B.; Cao, Z. C.; Shi, Z. J. Exploration of Earth-Abundant Transition Metals (Fe, Co, and Ni) as Catalysts in Unreactive Chemical Bond Activations. *Acc. Chem. Res.* **2015**, *48* (3), 886–896. https://doi.org/10.1021/ar500345f.

(27) Obligacion, J. V.; Semproni, S. P.; Chirik, P. J. Cobalt-Catalyzed C–H Borylation. *J. Am. Chem. Soc.* **2014**, *136*, 4133–4136. https://doi.org/10.1021/ja500712z.

(28) Moselage, M.; Li, J.; Ackermann, L. Cobalt-Catalyzed C-H Activation. *ACS Catal.* **2016**, *6* (2), 498–525. https://doi.org/10.1021/acscatal.5b02344.

(29) Gandeepan, P.; Müller, T.; Zell, D.; Cera, G.; Warratz, S.; Ackermann, L. 3d Transition Metals for C-H Activation. *Chem. Rev.* **2019**, *119* (4), 2192–2452. https://doi.org/10.1021/acs.chemrev.8b00507.

(30) Xu, L.; Wang, G.; Zhang, S.; Wang, H.; Wang, L.; Liu, L.; Jiao, J.; Li, P. Recent Advances in Catalytic C–H Borylation Reactions. *Tetrahedron* **2017**, *73* (51), 7123–7157. https://doi.org/10.1016/j.tet.2017.11.005.

(31) Boller, T. M.; Murphy, J. M.; Hapke, M.; Ishiyama, T.; Miyaura, N.; Hartwig, J. F. Mechanism of the Mild Functionalization of Arenes by Diboron Reagents Catalyzed by Iridium Complexes. Intermediacy and Chemistry of Bipyridine-Ligated Iridium Trisboryl Complexes. *J. Am. Chem. Soc.* **2005**, *127* (41), 14263–14278. https://doi.org/10.1021/ja053433g.

(32) Tajuddin, H.; Harrisson, P.; Bitterlich, B.; Collings, J. C.; Sim, N.; Batsanov, A. S.; Cheung, M. S.; Kawamorita, S.; Maxwell, A. C.; Shukla, L.; Morris, J.; Lin, Z.; Marder, T. B.; Steel, P. G. Iridium-Catalyzed C-H Borylation of Quinolines and Unsymmetrical 1,2-Disubstituted Benzenes: Insights into Steric and Electronic Effects on Selectivity. *Chem. Sci.* **2012**, *3* (12), 3505–3515. https://doi.org/10.1039/c2sc20776a.

(33) Kruse, T.; Hansen, M. K.; Münzel, M. W. B.; Thogersen, H.; Sauerberg, P.; Rasmussen, J. E.; Behrens, C.; Hoeg-Jensen, T.; Balsanek, V.; Drob-Nakova, Z.; Droz, L.; Havranek, M.; Kotek, V.; Stengl, M.; Snajdr, I.; Vanova, H. Glucose-Sensitive Albumin-Binding Derivatives. **2019**.

(34) Ros, A.; Fernández, R.; Lassaletta, J. M. Functional Group Directed C-H Borylation. *Chem. Soc. Rev.* **2014**, *43* (10), 3229–3243. https://doi.org/10.1039/c3cs60418g.

(35) Roosen, P. C.; Kallepalli, V. A.; Chattopadhyay, B.; Singleton, D. A.; Maleczka, R. E.; Smith, M. R. Outer-Sphere Direction in Iridium C-H Borylation. *J. Am. Chem. Soc.* **2012**, *134* (28), 11350–11353. https://doi.org/10.1021/ja303443m.

(36) Boebel, T. A.; Hartwig, J. F. Silyl-Directed, Iridium-Catalyzed Ortho-Borylation of Arenes. A One-Pot Ortho-Borylation of Phenols, Arylamines, and Alkylarenes. *J. Am. Chem. Soc.* **2008**, *130* (24), 7534–7535. https://doi.org/10.1021/ja8015878.

(37) Reyes, R.; Sawamura, M. An Introductory Overview of C–H Bond Activation/ Functionalization Chemistry with Focus on Catalytic C(Sp3)–H Bond Borylation. *Kimika* **2021**, *32* (1), 70–109. https://doi.org/10.26534/kimika.v32i1.70-109.

(38) Rej, S.; Das, A.; Chatani, N. Strategic Evolution in Transition Metal-Catalyzed Directed C–H Bond Activation and Future Directions. *Coord. Chem. Rev.* **2021**, *431*, 213683–213683. https://doi.org/10.1016/j.ccr.2020.213683.

(39) Dutta, U.; Maiti, S.; Bhattacharya, T.; Maiti, D. Arene Diversification through Distal C(Sp2)-H Functionalization. *Science* **2021**, *372* (6543). https://doi.org/10.1126/science.abd5992.

(40) Neeve, E. C.; Geier, S. J.; Mkhalid, I. A. I.; Westcott, S. A.; Marder, T. B. Diboron(4) Compounds: From Structural Curiosity to Synthetic Workhorse. *Chem. Rev.* **2016**, *116* (16), 9091–9161. https://doi.org/10.1021/acs.chemrev.6b00193.

(41) Meng, G.; Lam, N. Y. S.; Lucas, E. L.; Saint-Denis, T. G.; Verma, P.; Chekshin, N.; Yu, J. Q. Achieving Site-Selectivity for C-H Activation Processes Based on Distance and Geometry: A Carpenter's Approach. *J. Am. Chem. Soc.* **2020**, *142* (24), 10571–10591. https://doi.org/10.1021/jacs.0c04074.

(42) Niu, B.; Yang, K.; Lawrence, B.; Ge, H. Transient Ligand-Enabled Transition Metal-Catalyzed C–H Functionalization. *ChemSusChem* **2019**, *12* (13), 2955–2969. https://doi.org/10.1002/cssc.201900151.

(43) Trouvé, J.; Gramage-Doria, R. Beyond Hydrogen Bonding: Recent Trends of Outer Sphere Interactions in Transition Metal Catalysis. *Chem. Soc. Rev.* **2021**, *50* (5), 3565–3584. https://doi.org/10.1039/d0cs01339k.

(44) Kuninobu, Y.; Torigoe, T. Recent Progress of Transition Metal-Catalysed Regioselective C-H Transformations Based on Noncovalent Interactions. *Org. Biomol. Chem.* **2020**, *18* (22), 4126–4134. https://doi.org/10.1039/d0ob00703j.

(45) Davis, H. J.; Phipps, R. J. Harnessing Non-Covalent Interactions to Exert Control over Regioselectivity and Site-Selectivity in Catalytic Reactions. *Chem. Sci.* **2017**, *8* (2), 864–877. https://doi.org/10.1039/C6SC04157D.

(46) Kuroda, Y.; Nakao, Y. Catalyst-Enabled Site-Selectivity in the Iridium-Catalyzed CH Borylation of Arenes. *Chem. Lett.* **2019**, *48* (9), 1092–1100. https://doi.org/10.1246/cl.190372.

(47) Pell, C. J.; Ozerov, O. V. Synthesis and Rh-Catalyzed Reductive Cyclization of 1,6-Enynes and 1,6-Diynes Containing Alkynylboronate Termini. *J. Organomet. Chem.* **2020**, *912*, 121143–121154. https://doi.org/10.1016/j.jorganchem.2020.121143.

(48) Wright, J. S.; Scott, P. J. H.; Steel, P. G. Iridium-Catalysed C–H Borylation of Heteroarenes: Balancing Steric and Electronic Regiocontrol. *Angew. Chem. Int. Ed.* **2021**, *60* (6), 2796–2821. https://doi.org/10.1002/anie.202001520.

(49) Primas, N.; Bouillon, A.; Rault, S. Recent Progress in the Synthesis of Five-Membered Heterocycle Boronic Acids and Esters. *Tetrahedron* **2010**, *66* (41), 8121–8136. https://doi.org/10.1016/j.tet.2010.08.001.

(50) Trouvé, J.; Zardi, P.; Al-Shehimy, S.; Roisnel, T.; Gramage-Doria, R. Enzyme-like Supramolecular Iridium Catalysis Enabling C–H Bond Borylation of Pyridines with Meta-Selectivity. *Angew. Chem. Int. Ed.* **2021**, *60* (33), 18006–18013. https://doi.org/10.1002/anie.202101997.

(51) Larsen, M. A.; Hartwig, J. F. Iridium-Catalyzed C-H Borylation of Heteroarenes: Scope, Regioselectivity, Application to Late-Stage Functionalization, and Mechanism. *J. Am. Chem. Soc.* **2014**, *136* (11), 4287–4299. https://doi.org/10.1021/ja412563e.

(52) Huang, Z.; Dong, G. Site-Selectivity Control in Organic Reactions: A Quest to Differentiate Reactivity among the Same Kind of Functional Groups. *Acc. Chem. Res.* **2017**, *50* (3), 465–471. https://doi.org/10.1021/acs.accounts.6b00476.

(53) Cheng, W. M.; Shang, R. Transition Metal-Catalyzed Organic Reactions under Visible Light: Recent Developments and Future Perspectives. *ACS Catal.* **2020**, *10* (16), 9170–9196. https://doi.org/10.1021/acscatal.0c01979.

(54) Revathi, L.; Ravindar, L.; Fang, W. Y.; Rakesh, K. P.; Qin, H. L. Visible Light-Induced C–H Bond Functionalization: A Critical Review.

30

Adv. Synth. Catal. **2018**, *360* (24), 4652–4698. https://doi.org/10.1002/adsc.201800736.

(55) Tian, Y. M.; Guo, X. N.; Braunschweig, H.; Radius, U.; Marder, T. B. Photoinduced Borylation for the Synthesis of Organoboron Compounds. *Chem. Rev.* **2021**, *121* (7), 3561–3597. https://doi.org/10.1021/acs.chemrev.0c01236.

(56) Pak, K.; Cheung, S.; Sarkar, S.; Gevorgyan, V. Visible Light-Induced Transition Metal Catalysis. *Chem. Rev.* **2021**. https://doi.org/10.1021/acs.chemrev.1c00403.

(57) Thongpaen, J.; Manguin, R.; Dorcet, V.; Vives, T.; Duhayon, C.; Mauduit, M.; Baslé, O. Visible Light Induced Rhodium(I)-Catalyzed C–H Borylation. *Angew. Chem. Int. Ed.* **2019**, *58* (43), 15244–15248. https://doi.org/10.1002/anie.201905924.

(58) Tanaka, J.; Nagashima, Y.; Araujo Dias, A. J.; Tanaka, K. Photo-Induced Ortho-C-H Borylation of Arenes through in Situ Generation of Rhodium(II) Ate Complexes. *J. Am. Chem. Soc.* **2021**, *143* (30), 11325–11331. https://doi.org/10.1021/jacs.1c05859.

(59) Murata, M.; Watanabe, S.; Masuda, Y. Rhodium-Catalyzed Dehydrogenative Coupling Reaction of Vinylarenes with Pinacolborane to Vinylboronates. *Tetrahedron Lett.* **1999**, *40* (13), 2585–2588. https://doi.org/10.1016/S0040-4039(99)00253-1.

(60) Wang, C.; Wu, C.; Ge, S. Iron-Catalyzed E-Selective Dehydrogenative Borylation of Vinylarenes with Pinacolborane. *ACS Catal.* **2016**, *6* (11), 7585–7589. https://doi.org/10.1021/acscatal.6b02654.

(61) Mazzacano, T. J.; Mankad, N. P. Dehydrogenative Borylation and Silylation of Styrenes Catalyzed by Copper-Carbenes. *ACS Catal.* **2017**, *7* (1), 146–149. https://doi.org/10.1021/acscatal.6b02594.

(62) Shi, X.; Li, S.; Wu, L. H2-Acceptorless Dehydrogenative Boration and Transfer Boration of Alkenes Enabled by Zirconium Catalyst. *Angew. Chem. Int. Ed.* **2019**, *58* (45), 16167–16171. https://doi.org/10.1002/anie.201908931.

(63) Sasmal, S.; Dutta, U.; Lahiri, G. K.; Maiti, D. Transition Metals and Transition Metals/Lewis Acid Cooperative Catalysis for Directing Group Assisted Para-CH Functionalization. *Chem. Lett.* **2020**, *49* (11), 1406–1420. https://doi.org/10.1246/CL.200500.

(64) Bouhadir, G.; Bourissou, D. Complexes of Ambiphilic Ligands: Reactivity and Catalytic Applications. *Chem. Soc. Rev.* **2016**, *45* (4), 1065–1079. https://doi.org/10.1039/c5cs00697j.

(65) Kanai, M.; Kato, N.; Ichikawa, E.; Shibasaki, M. Power of Cooperativity: Lewis Acid-Lewis Base Bifunctional Asymmetric Catalysis. *Synlett* **2005**, No. 10, 1491–1508. https://doi.org/10.1055/s-2005-869831.

(66) Mihai, M. T.; Genov, G. R.; Phipps, R. J. Access to the Meta Position of Arenes through Transition Metal Catalysed C-H Bond Functionalisation: A Focus on Metals Other than Palladium. *Chem. Soc. Rev.* **2018**, *47* (1), 149–171. https://doi.org/10.1039/c7cs00637c.

(67) Ali, R.; Siddiqui, R. Recent Developments in Remote Meta-C–H Bond Functionalizations. *Adv. Synth. Catal.* **2021**, *363* (5), 1290–1316. https://doi.org/10.1002/adsc.202001053.

(68) Yang, L.; Uemura, N.; Nakao, Y. Meta-Selective C-H Borylation of Benzamides and Pyridines by an Iridium-Lewis Acid Bifunctional Catalyst. *J. Am. Chem. Soc.* **2019**, *141* (19), 7972–7979. https://doi.org/10.1021/jacs.9b03138.

(69) Yang, L.; Semba, K.; Nakao, Y. Para-Selective C–H Borylation of (Hetero)Arenes by Cooperative Iridium/Aluminum Catalysis. *Angew. Chem. Int. Ed.* **2017**, *56* (17), 4853–4857. https://doi.org/10.1002/anie.201701238.

(70) Li, H. L.; Kuninobu, Y.; Kanai, M. Lewis Acid–Base Interaction-Controlled Ortho-Selective C–H Borylation of Aryl Sulfides. *Angew. Chem. Int. Ed.* **2017**, *56* (6), 1495–1499. https://doi.org/10.1002/anie.201610041.

(71) Hoque, M. E.; Bisht, R.; Haldar, C.; Chattopadhyay, B. Noncovalent Interactions in Ir-Catalyzed C-H Activation: L-Shaped Ligand for Para-Selective Borylation of Aromatic Esters. *J. Am. Chem. Soc.* **2017**, *139* (23), 7745–7748. https://doi.org/10.1021/jacs.7b04490.

(72) Bisht, R.; Hoque, M. E.; Chattopadhyay, B. Amide Effects in C–H Activation: Noncovalent Interactions with L-Shaped Ligand for Meta Borylation of Aromatic Amides. *Angew. Chem. Int. Ed.* **2018**, *57* (48), 15762–15766. https://doi.org/10.1002/anie.201809929.

(73) Bisht, R.; Chattopadhyay, B. Formal Ir-Catalyzed Ligand-Enabled Ortho and Meta Borylation of Aromatic Aldehydes via in Situ-Generated Imines. *J. Am. Chem. Soc.* **2016**, *138* (1), 84–87. https://doi.org/10.1021/jacs.5b11683.

(74) Nakamura, T.; Suzuki, K.; Yamashita, M. Aluminabenzene-Rh and -Ir Complexes: Synthesis, Structure, and Application toward Catalytic C-H Borylation. *J. Am. Chem. Soc.* **2017**, *139* (49), 17763–17766. https://doi.org/10.1021/jacs.7b11127.

(75) Auth, M. R.; McGarry, K. A.; Clark, T. B. Phosphorus-Directed C–H Borylation. *Adv. Synth. Catal.* **2021**, 2354–2365. https://doi.org/10.1002/adsc.202100173.

(76) Haldar, C.; Emdadul Hoque, M.; Bisht, R.; Chattopadhyay, B. Concept of Ir-Catalyzed C–H Bond Activation/Borylation by Noncovalent Interaction. *Tetrahedron Lett.* **2018**, *59* (14), 1269–1277. https://doi.org/10.1016/j.tetlet.2018.01.098.

(77) Sambiagio, C.; Schönbauer, D.; Blieck, R.; Dao-Huy, T.; Pototschnig, G.; Schaaf, P.; Wiesinger, T.; Zia, M. F.; Wencel-Delord, J.; Besset, T.; Maes, B. U. W.; Schnürch, M. A Comprehensive Overview of Directing Groups Applied in Metal-Catalysed C-H Functionalisation Chemistry. *Chem. Soc. Rev.* **2018**, *47* (17), 6603–6743. https://doi.org/10.1039/c8cs00201k.

(78) Lapuh, M. I.; Mazeh, S.; Besset, T. Chiral Transient Directing Groups in Transition-Metal-Catalyzed Enantioselective C–H Bond Functionalization. *ACS Catal.* **2020**, *10* (21), 12898–12919. https://doi.org/10.1021/acscatal.0c03317.

(79) Zheng, Q.; Liu, C. F.; Chen, J.; Rao, G. W. C–H Functionalization of Aromatic Amides. *Adv. Synth. Catal.* **2020**, *362* (7), 1406–1446. https://doi.org/10.1002/adsc.201901158.

(80) Tang, J.; Singh, T.; Li, X.; Liu, L.; Zhou, T. Selenium-Directed Ortho-C-H Borylation by Iridium Catalysis. *J. Org. Chem.* **2020**, *85* (18), 11959–11967. https://doi.org/10.1021/acs.joc.0c01559.

(81) Zeng, J.; Naito, M.; Torigoe, T.; Yamanaka, M.; Kuninobu, Y. Iridium-Catalyzed Ortho-C-H Borylation of Thioanisole Derivatives Using Bipyridine-Type Ligand. *Org. Lett.* **2020**, *22* (9), 3485–3489. https://doi.org/10.1021/acs.orglett.0c00946.

(82) Wen, J.; Wang, D.; Qian, J.; Wang, D.; Zhu, C.; Zhao, Y.; Shi, Z. Rhodium-Catalyzed P III -Directed Ortho-C–H Borylation of Arylphosphines. *Angew. Chem. Int. Ed.* **2019**, *58* (7), 2078–2082. https://doi.org/10.1002/anie.201813452.

(83) Fukuda, K.; Iwasawa, N.; Takaya, J. Ruthenium-Catalyzed Ortho C–H Borylation of Arylphosphines. *Angew. Chem. Int. Ed.* **2019**, *58* (9), 2850–2853. https://doi.org/10.1002/anie.201813278.

(84) Xu, F.; Duke, O. M.; Rojas, D.; Eichelberger, H. M.; Kim, R. S.; Clark, T. B.; Watson, D. A. Arylphosphonate-Directed Ortho C-H Borylation: Rapid Entry into Highly-Substituted Phosphoarenes. *J. Am. Chem. Soc.* **2020**, *142* (28), 11988–11992. https://doi.org/10.1021/jacs.0c04159.

(85) Doherty, S.; Knight, J. G.; Ward, N. A. B.; Perry, D. O.; Bittner, D. M.; Probert, M. R.; Westcott, S. A. Palladium-Catalyzed Suzuki-Miyaura Cross-Couplings with 2-Diethylphosphonato-Substituted Aryl-and Naphthylboronate Esters as the Nucleophilic Partner: A Complementary Approach to the Synthesis of Biaryl Monophosphonates. *Organometallics* **2014**, *33* (19), 5209–5219. https://doi.org/10.1021/om500520z.

(86) Jiao, J.; Nie, W.; Song, P.; Li, P. A New Air-Stable Si,S-Chelating Ligand for Ir-Catalyzed Directed: Ortho C-H Borylation. *Org. Biomol. Chem.* **2021**, *19* (2), 355–359. https://doi.org/10.1039/d0ob02335c.

(87) Ishiyama, T.; Isou, H.; Kikuchi, T.; Miyaura, N. Ortho-C-H Borylation of Benzoate Esters with Bis(Pinacolato)Diboron Catalyzed by Iridium-Phosphine Complexes. *Chem. Commun.* **2010**, *46* (1), 159–161. https://doi.org/10.1039/b910298a.

(88) Kawamorita, S.; Ohmiya, H.; Hara, K.; Fukuoka, A.; Sawamura, M. Directed Ortho Borylation of Functionalized Arenes Catalyzed by a Silica-Supported Compact Phosphine-Iridium System. *J. Am. Chem. Soc.* **2009**, *131* (14), 5058–5059. https://doi.org/10.1021/ja9008419.

(89) Ghaffari, B.; Preshlock, S. M.; Plattner, D. L.; Staples, R. J.; Maligres, P. E.; Krska, S. W.; Maleczka, R. E.; Smith, M. R. Silyl Phosphorus and Nitrogen Donor Chelates for Homogeneous Ortho Borylation Catalysis. *J. Am. Chem. Soc.* **2014**, *136* (41), 14345–14348. https://doi.org/10.1021/ja506229s.

(90) Cook, A. K.; Schimler, S. D.; Matzger, A. J.; Sanford, M. S. Catalyst-Controlled Selectivity in the C-H Borylation of Methane and Ethane. *Science* **2016**, *351* (6280), 1421–1424. https://doi.org/10.1126/science.aad9289.

(91) Jiang, Q.; Duan-Mu, D.; Zhong, W.; Chen, H.; Yan, H. Amino-Directed RhIII-Catalyzed C-H Activation Leading to One-Pot Synthesis of N-H Carbazoles. *Chem. - Eur. J.* **2013**, *19* (6), 1903–1907. https://doi.org/10.1002/chem.201203856.

(92) Thongpaen, J.; Schmid, T. E.; Toupet, L.; Dorcet, V.; Mauduit, M.; Baslé, O. Directed: Ortho C-H Borylation Catalyzed Using Cp∗Rh(Iii)-NHC Complexes. *Chem. Commun.* **2018**, *54* (59), 8202–8205. https://doi.org/10.1039/c8cc03144d.

(93) Yang, Y.; Gao, Q.; Xu, S. Ligand-Free Iridium-Catalyzed Dehydrogenative Ortho C−H Borylation of Benzyl-2-Pyridines at Room Temperature. *Adv. Synth. Catal.* **2019**, *361* (4), 858–862. https://doi.org/10.1002/adsc.201801292.

(94) Wang, G.; Liu, L.; Wang, H.; Ding, Y. S.; Zhou, J.; Mao, S.; Li, P. N,B-Bidentate Boryl Ligand-Supported Iridium Catalyst for Efficient Functional-Group-Directed C-H Borylation. *J. Am. Chem. Soc.* **2017**, *139* (1), 91–94. https://doi.org/10.1021/jacs.6b11867.

(95) Ros, A.; Estepa, B.; López-Rodríguez, R.; Álvarez, E.; Fernández, R.; Lassaletta, J. M. Use of Hemilabile N,N Ligands in Nitrogen-Directed Iridium-Catalyzed Borylations of Arenes. *Angew. Chem. Int. Ed.* **2011**, *50* (49), 11724–11728. https://doi.org/10.1002/anie.201104544.

(96) Kawamorita, S.; Miyazaki, T.; Ohmiya, H.; Iwai, T.; Sawamura, M. Rh-Catalyzed Ortho -Selective C-H Borylation of N-Functionalized Arenes with Silica-Supported Bridgehead Monophosphine Ligands. *J. Am. Chem. Soc.* **2011**, *133* (48), 19310–19313. https://doi.org/10.1021/ja208364a.

(97) Hassan, M. M. M.; Hoque, M. E.; Dey, S.; Guria, S.; Roy, B.; Chattopadhyay, B. Iridium-Catalyzed Site-Selective Borylation of 8-Arylquinolines. *Synthesis* **2021**, *53*, 3333–3342. https://doi.org/10.1055/a-1506-3884.

(98) Bisht, R.; Chattopadhyay, B. Ortho - And Meta -Selective C-H Activation and Borylation of Aromatic Aldehydes via in Situ Generated Imines. *Synlett* **2016**, *27* (14), 2043–2050. https://doi.org/10.1055/s-0035-1562236.

(99) Hoque, M. E.; Hassan, M. M. M.; Chattopadhyay, B. Remarkably Efficient Iridium Catalysts for Directed C(Sp2)-H and C(Sp3)-H Borylation of Diverse Classes of Substrates. *J. Am. Chem. Soc.* **2021**, *143* (13), 5022–5037. https://doi.org/10.1021/jacs.0c13415.

(100) He, J.; Shao, Q.; Wu, Q.; Yu, J. Q. Pd(II)-Catalyzed Enantioselective C(Sp3)-H Borylation. *J. Am. Chem. Soc.* **2017**, *139* (9), 3344–3347. https://doi.org/10.1021/jacs.6b13389.

(101) Su, B.; Zhou, T. G.; Xu, P. L.; Shi, Z. J.; Hartwig, J. F. Enantioselective Borylation of Aromatic C−H Bonds with Chiral Dinitrogen Ligands. *Angew. Chem. Int. Ed.* **2017**, *56* (25), 7205–7208. https://doi.org/10.1002/anie.201702628.

(102) Zou, X.; Zhao, H.; Li, Y.; Gao, Q.; Ke, Z.; Xu, S. Chiral Bidentate Boryl Ligand Enabled Iridium-Catalyzed Asymmetric C(Sp2)-H Borylation of Diarylmethylamines. *J. Am. Chem. Soc.* **2019**, *141* (13), 5334–5342. https://doi.org/10.1021/jacs.8b13756.

(103) Park, D.; Baek, D.; Lee, C. W.; Ryu, H.; Park, S.; Han, W.; Hong, S. Enantioselective C(Sp2)–H Borylation of Diarylmethylsilanes Catalyzed by Chiral Pyridine-Dihydroisoquinoline Iridium Complexes. *Tetrahedron* **2021**, *79*, 131811–131811. https://doi.org/10.1016/j.tet.2020.131811.

(104) Song, P.; Hu, L.; Yu, T.; Jiao, J.; He, Y.; Xu, L.; Li, P. Development of a Tunable Chiral Pyridine Ligand Unit for Enantioselective Iridium-Catalyzed C-H Borylation. *ACS Catal.* **2021**, *11* (12), 7339–7349. https://doi.org/10.1021/acscatal.1c01671.

(105) Su, B.; Hartwig, J. F. Iridium-Catalyzed, Silyl-Directed, Peri-Borylation of C−H Bonds in Fused Polycyclic Arenes and Heteroarenes. *Angew. Chem. Int. Ed.* **2018**, *57* (32), 10163–10167. https://doi.org/10.1002/anie.201805086.

(106) Shi, Y.; Gao, Q.; Xu, S. Chiral Bidentate Boryl Ligand Enabled Iridium-Catalyzed Enantioselective C(Sp3)-H Borylation of Cyclopropanes. *J. Am. Chem. Soc.* **2019**, *141* (27), 10599–10604. https://doi.org/10.1021/jacs.9b04549.

(107) Chen, L.; Yang, Y.; Liu, L.; Gao, Q.; Xu, S. Iridium-Catalyzed Enantioselective α-C(Sp3)-H Borylation of Azacycles. *J. Am. Chem. Soc.* **2020**, *142* (28), 12062–12068. https://doi.org/10.1021/jacs.0c06756.

(108) Du, R.; Liu, L.; Xu, S. Iridium-Catalyzed Regio- and Enantioselective Borylation of Unbiased Methylene C(Sp3)−H Bonds at the Position β to a Nitrogen Center. *Angew. Chem. Int. Ed.* **2021**, *60* (11), 5843–5847. https://doi.org/10.1002/anie.202016009.

(109) Yang, Y.; Chen, L.; Xu, S. Iridium-Catalyzed Enantioselective Unbiased Methylene C(Sp3)–H Borylation of Acyclic Amides. *Angew. Chem. Int. Ed.* **2021**, *60* (7), 3524–3528. https://doi.org/10.1002/anie.202013568.

(110) Shi, Y.; Gao, Q.; Xu, S. Iridium-Catalyzed Asymmetric C-H Borylation Enabled by Chiral Bidentate Boryl Ligands. *Synlett* **2019**, *30* (19), 2107–2112. https://doi.org/10.1055/s-0039-1690225.

(111) Yamamoto, T.; Ishibashi, A.; Suginome, M. Boryl-Directed, Ir-Catalyzed C(Sp3)-H Borylation of Alkylboronic Acids Leading to Site-Selective Synthesis of Polyborylalkanes. *Org. Lett.* **2019**, *21* (16), 6235–6240. https://doi.org/10.1021/acs.orglett.9b02112.

(112) Shimizu, M.; Hiyama, T. Polyborylated Reagents for Modern Organic Synthesis. *Proc. Jpn. Acad. Ser. B Phys. Biol. Sci.* **2008**, *84* (3), 75–85. https://doi.org/10.2183/pjab.84.75.

(113) Nallagonda, R.; Padala, K.; Masarwa, A. Gem -Diborylalkanes: Recent Advances in Their Preparation, Transformation and Application. *Org. Biomol. Chem.* **2018**, *16* (7), 1050–1064. https://doi.org/10.1039/c7ob02978k.

(114) Obligacion, J. V.; Bezdek, M. J.; Chirik, P. J. C(Sp2)-H Borylation of Fluorinated Arenes Using an Air-Stable Cobalt Precatalyst: Electronically Enhanced Site Selectivity Enables Synthetic Opportunities. *J. Am. Chem. Soc.* **2017**, *139* (7), 2825–2832. https://doi.org/10.1021/jacs.6b13346.

(115) Robbins, D. W.; Hartwig, J. F. A C-H Borylation Approach to Suzuki-Miyaura Coupling of Typically Unstable 2-Heteroaryl and Polyfluorophenyl Boronates. *Org. Lett.* **2012**, *14* (16), 4266–4269. https://doi.org/10.1021/ol301570t.

(116) Jayasundara, C. R. K.; Unold, J. M.; Oppenheimer, J.; Smith, M. R.; Maleczka, R. E. A Catalytic Borylation/Dehalogenation Route to o -Fluoro Arylboronates. *Org. Lett.* **2014**, *16* (23), 6072–6075. https://doi.org/10.1021/ol5028738.

(117) Pabst, T. P.; Obligacion, J. V.; Rochette, É.; Pappas, I.; Chirik, P. J. Cobalt-Catalyzed Borylation of Fluorinated Arenes: Thermodynamic Control of C(Sp2)-H Oxidative Addition Results in Ortho-to-Fluorine Selectivity. *J. Am. Chem. Soc.* **2019**, *141* (38), 15378–15389. https://doi.org/10.1021/jacs.9b07984.

(118) Miller, S. L.; Chotana, G. A.; Fritz, J. A.; Chattopadhyay, B.; Maleczka, R. E.; Smith, M. R. C-H Borylation Catalysts That Distinguish between Similarly Sized Substituents like Fluorine and Hydrogen. *Org. Lett.* **2019**, *21* (16), 6388–6392. https://doi.org/10.1021/acs.orglett.9b02299.

(119) Kuleshova, O.; Asako, S.; Ilies, L. Ligand-Enabled, Iridium-Catalyzed Ortho-Borylation of Fluoroarenes. *ACS Catal.* **2021**, *11* (10), 5968–5973. https://doi.org/10.1021/acscatal.1c01206.

(120) Liskey, C. W.; Hartwig, J. F. Iridium-Catalyzed Borylation of Secondary C-H Bonds in Cyclic Ethers. *J. Am. Chem. Soc.* **2012**, *134* (30),

12422–12425. https://doi.org/10.1021/ja305596v.

(121) Ohmura, T.; Torigoe, T.; Suginome, M. Iridium-Catalysed Borylation of Sterically Hindered C(Sp3)-H Bonds: Remarkable Rate Acceleration by a Catalytic Amount of Potassium Tert-Butoxide. *Chem. Commun.* **2014**, *50* (48), 6333–6336. https://doi.org/10.1039/c4cc01262c.

(122) Lawrence, J. D.; Takahashi, M.; Bae, C.; Hartwig, J. F. Regiospecific Functionalization of Methyl C-H Bonds of Alkyl Groups in Reagents with Heteroatom Functionality. *J. Am. Chem. Soc.* **2004**, *126* (47), 15334–15335. https://doi.org/10.1021/ja044933x.

(123) Li, Q.; Liskey, C. W.; Hartwig, J. F. Regioselective Borylation of the C−H Bonds in Alkylamines and Alkyl Ethers. Observation and Origin of High Reactivity of Primary C−H Bonds Beta to Nitrogen and Oxygen. *J. Am. Chem. Soc.* **2014**, *136*, 8755–8765. https://doi.org/10.1021/ja503676d.

(124) Ohmura, T.; Torigoe, T.; Suginome, M. Functionalization of Tetraorganosilanes and Permethyloligosilanes at a Methyl Group on Silicon via Iridium-Catalyzed C(Sp3)-H Borylation. *Organometallics* **2013**, *32* (21), 6170–6173. https://doi.org/10.1021/om400900z.

(125) Jones, M. R.; Fast, C. D.; Schley, N. D. Iridium-Catalyzed Sp3 C-H Borylation in Hydrocarbon Solvent Enabled by 2,2'-Dipyridylarylmethane Ligands. *J. Am. Chem. Soc.* **2020**, *142* (14), 6488–6492. https://doi.org/10.1021/jacs.0c00524.

(126) Oeschger, R.; Su, B.; Yu, I.; Ehinger, C.; Romero, E.; He, S.; Hartwig, J. Diverse Functionalization of Strong Alkyl C–H Bonds by Undirected Borylation. *Science* **2020**, *368* (6492), 736–741. https://doi.org/10.1126/science.aba6146.

(127) Wei, C. S.; Jiménez-Hoyos, C. A.; Videa, M. F.; Hartwig, J. F.; Hall, M. B. Origins of the Selectivity for Borylation of Primary over Secondary C-H Bonds Catalyzed by Cp-Rhodium Complexes. *J. Am. Chem. Soc.* **2010**, *132* (9), 3078–3091. https://doi.org/10.1021/ja909453g.

(128) Zhong, R. L.; Sakaki, S. Sp3 C-H Borylation Catalyzed by Iridium(III) Triboryl Complex: Comprehensive Theoretical Study of Reactivity, Regioselectivity, and Prediction of Excellent Ligand. *J. Am. Chem. Soc.* **2019**, *141* (25), 9854–9866. https://doi.org/10.1021/jacs.9b01767.

(129) Léonard, N. G.; Bezdek, M. J.; Chirik, P. J. Cobalt-Catalyzed C(Sp2)-H Borylation with an Air-Stable, Readily Prepared Terpyridine Cobalt(II) Bis(Acetate) Precatalyst. *Organometallics* **2017**, *36* (1), 142–150. https://doi.org/10.1021/acs.organomet.6b00630.

(130) Obligacion, J. V.; Semproni, S. P.; Pappas, I.; Chirik, P. J. Cobalt-Catalyzed C(Sp2)-H Borylation: Mechanistic Insights Inspire Catalyst Design. *J. Am. Chem. Soc.* **2016**, *138* (33), 10645–10653. https://doi.org/10.1021/jacs.6b06144.

(131) Palmer, W. N.; Obligacion, J. V.; Pappas, I.; Chirik, P. J. Cobalt-Catalyzed Benzylic Borylation: Enabling Polyborylation and Functionalization of Remote, Unactivated C(Sp3)-H Bonds. *J. Am. Chem. Soc.* **2016**, *138* (3), 766–769. https://doi.org/10.1021/jacs.5b12249.

(132) Pabst, T. P.; Quach, L.; MacMillan, K. T.; Chirik, P. J. Mechanistic Origins of Regioselectivity in Cobalt-Catalyzed C(Sp2)-H Borylation of Benzoate Esters and Arylboronate Esters. *Chem* **2021**, *7* (1), 237–254. https://doi.org/10.1016/j.chempr.2020.11.017.

(133) Saito, Y.; Yamanoue, K.; Segawa, Y.; Itami, K. Selective Transformation of Strychnine and 1,2-Disubstituted Benzenes by C–H Borylation. *Chem* **2020**, *6* (4), 985–993. https://doi.org/10.1016/j.chempr.2020.02.004.

(134) Chakravarti, R. N.; Robinson, R. 16. Strychnine and Brucine. Part XLVI. The Preparation of Neostrychnine and Neobrucine. *J. Chem. Soc.* **1947**, 78–80. https://doi.org/10.1039/JR9470000078.

(135) Saito, Y.; Segawa, Y.; Itami, K. Para -C-H Borylation of Benzene Derivatives by a Bulky Iridium Catalyst. *J. Am. Chem. Soc.* **2015**, *137* (15), 5193–5198. https://doi.org/10.1021/jacs.5b02052.

(136) Brak, K.; Jacobsen, E. N. Asymmetric Ion-Pairing Catalysis. *Angew. Chem. Int. Ed.* **2013**, *52* (2), 534–561. https://doi.org/10.1002/anie.201205449.

(137) Ooi, T.; Maruoka, K. Recent Advances in Asymmetric Phase-Transfer Catalysis. *Angew. Chem. Int. Ed.* **2007**, *46* (23), 4222–4266. https://doi.org/10.1002/anie.200601737.

(138) Shirakawa, S.; Maruoka, K. Recent Developments in Asymmetric Phase-Transfer Reactions. *Angew. Chem. Int. Ed.* **2013**, *52* (16), 4312–4348. https://doi.org/10.1002/anie.201206835.

(139) Davis, H. J.; Mihai, M. T.; Phipps, R. J. Ion Pair-Directed Regiocontrol in Transition-Metal Catalysis: A Meta-Selective C-H Borylation of Aromatic Quaternary Ammonium Salts. *J. Am. Chem. Soc.* **2016**, *138* (39), 12759–12762. https://doi.org/10.1021/jacs.6b08164.

(140) Mihai, M. T.; Davis, H. J.; Genov, G. R.; Phipps, R. J. Ion Pair-Directed C-H Activation on Flexible Ammonium Salts: Meta-Selective Borylation of Quaternized Phenethylamines and Phenylpropylamines. *ACS Catal.* **2018**, *8* (5), 3764–3769. https://doi.org/10.1021/acscatal.8b00423.

(141) Davis, H. J.; Genov, G. R.; Phipps, R. J. Meta-Selective C−H Borylation of Benzylamine-, Phenethylamine-, and Phenylpropylamine-Derived Amides Enabled by a Single Anionic Ligand. *Angew. Chem. Int. Ed.* **2017**, *56* (43), 13351–13355. https://doi.org/10.1002/anie.201708967.

(142) Lee, B.; Mihai, M. T.; Stojalnikova, V.; Phipps, R. J. Ion-Pair-Directed Borylation of Aromatic Phosphonium Salts. *J. Org. Chem.* **2019**, *84* (20), 13124–13134. https://doi.org/10.1021/acs.joc.9b00878.

(143) Dey, A.; Maity, S.; Maiti, D. Reaching the South: Metal-Catalyzed Transformation of the Aromatic: Para -Position. *Chem. Commun.* **2016**, *52* (84), 12398–12414. https://doi.org/10.1039/c6cc05235e.

(144) Mihai, M. T.; Williams, B. D.; Phipps, R. J. Para-Selective C-H Borylation of Common Arene Building Blocks Enabled by Ion-Pairing with a Bulky Countercation. *J. Am. Chem. Soc.* **2019**, *141* (39), 15477–15482. https://doi.org/10.1021/jacs.9b07267.

(145) Montero Bastidas, J. R.; Oleskey, T. J.; Miller, S. L.; Smith, M. R.; Maleczka, R. E. Para-Selective, Iridium-Catalyzed C-H Borylations of Sulfated Phenols, Benzyl Alcohols, and Anilines Directed by Ion-Pair Electrostatic Interactions. *J. Am. Chem. Soc.* **2019**, *141* (39), 15483–15487. https://doi.org/10.1021/jacs.9b08464.

(146) Chattopadhyay, B.; Dannatt, J. E.; Andujar-De Sanctis, I. L.; Gore, K. A.; Maleczka, R. E.; Singleton, D. A.; Smith, M. R. Ir-Catalyzed Ortho-Borylation of Phenols Directed by Substrate-Ligand Electrostatic Interactions: A Combined Experimental/in Silico Strategy for Optimizing Weak Interactions. *J. Am. Chem. Soc.* **2017**, *139* (23), 7864–7871. https://doi.org/10.1021/jacs.7b02232.

(147) Smith, M. R.; Bisht, R.; Haldar, C.; Pandey, G.; Dannatt, J. E.; Ghaffari, B.; Maleczka, R. E.; Chattopadhyay, B. Achieving High Ortho Selectivity in Aniline C-H Borylations by Modifying Boron Substituents. *ACS Catal.* **2018**, *8* (7), 6216–6223. https://doi.org/10.1021/acscatal.8b00641.

(148) Preshlock, S. M.; Plattner, D. L.; Maligres, P. E.; Krska, S. W.; Maleczka, R. E.; Smith, M. R. A Traceless Directing Group for C - H Borylation. *Angew. Chem. Int. Ed.* **2013**, *52* (49), 12915–12919. https://doi.org/10.1002/anie.201306511.

(149) Bisht, R.; Chaturvedi, J.; Pandey, G.; Chattopadhyay, B. Double-Fold Ortho and Remote C-H Bond Activation/Borylation of BINOL: A Unified Strategy for Arylation of BINOL. *Org. Lett.* **2019**, *21* (16), 6476–6480. https://doi.org/10.1021/acs.orglett.9b02347.

(150) Chaturvedi, J.; Haldar, C.; Bisht, R.; Pandey, G.; Chattopadhyay, B. Meta Selective C-H Borylation of Sterically Biased and Unbiased Substrates Directed by Electrostatic Interaction. *J. Am. Chem. Soc.* **2021**, *143* (20), 7604–7611. https://doi.org/10.1021/jacs.1c01770.

(151) Kuninobu, Y.; Ida, H.; Nishi, M.; Kanai, M. A Meta-Selective C-H Borylation Directed by a Secondary Interaction between Ligand and

Substrate. *Nat. Chem.* **2015**, *7* (9), 712–717. https://doi.org/10.1038/nchem.2322.

(152)   Lu, X.; Yoshigoe, Y.; Ida, H.; Nishi, M.; Kanai, M.; Kuninobu, Y. Hydrogen Bond-Accelerated Meta-Selective C-H Borylation of Aromatic Compounds and Expression of Functional Group and Substrate Specificities. *ACS Catal.* **2019**, *9* (3), 1705–1709. https://doi.org/10.1021/acscatal.8b05005.

(153)   Wang, J.; Torigoe, T.; Kuninobu, Y. Hydrogen-Bond-Controlled Formal Meta-Selective C-H Transformations and Regioselective Synthesis of Multisubstituted Aromatic Compounds. *Org. Lett.* **2019**, *21* (5), 1342–1346. https://doi.org/10.1021/acs.orglett.9b00030.

(154)   Bai, S. T.; Bheeter, C. B.; Reek, J. N. H. Hydrogen Bond Directed Ortho-Selective C–H Borylation of Secondary Aromatic Amides. *Angew. Chem. Int. Ed.* **2019**, *58* (37), 13039–13043. https://doi.org/10.1002/anie.201907366.

(155)   Genov, G. R.; Douthwaite, J. L.; Lahdenperä, A. S. K.; Gibson, D. C.; Phipps, R. J. Enantioselective Remote C-H Activation Directed by a Chiral Cation. *Science* **2020**, *367* (6483), 1246–1251. https://doi.org/10.1126/science.aba1120.

(156)   Ramadoss, B.; Jin, Y.; Asako, S.; Ilies, L. Remote Steric Control for Undirected *Meta* -Selective C–H Activation of Arenes. *Science* **2022**, *375* (6581), 658–663. https://doi.org/10.1126/science.abm7599.

CHAPTER 2

Transfer C–H Borylation of Alkenes under Rh(I)-Catalysis: Insight into the Synthetic Capacity, Mechanism & Selectivity-Control

2.1 Introduction

Given the pharmacophoric properties of boronic acid derivatives[1–3] as well as the multitude of methods to convert a C–B bond into a C–C or C–X bond,[4–7] the ability to install a boronic ester group by a selective functionalization of one of the C–H bonds in available starting materials is highly appealing for both modular synthesis of functional materials and late-stage functionalization of complex molecules.[8] While the borylation of aromatic and aliphatic C–H bonds has been extensively studied,[9–14] the direct borylation of vinylic C–H bonds remains underdeveloped with no general method being available, despite the presence of these motifs in various synthetic and natural compounds (Figure 2.1a).[15–17] In that context, alkene cross-metathesis employing a simple vinyl boronate ester as a reagent[18–22] enables formal C–H bond borylation of terminal alkenes under mild conditions and with high atom-economy (Figure 2.1b); thereby the strategy has found numerous applications in fine-chemical synthesis.[23–27] However, when the initial carbon skeleton is to be maintained, the approach is unsuitable for the borylation of substrates bearing internal alkenes, e.g., many (macrocyclic) natural products. In contrast, the boryl-Heck[28–30] and dehydrogenative[31–44] protocols were reported to be applicable to the C–H borylation of terminal and internal alkene starting materials. Still, the synthetic utility of these reactions is often limited. In the case of the boryl-Heck reaction, the use of ClBcat or BrBcat as the borylation reagent leads to the inevitable incompatibility with many nucleophilic functional groups, including soft nucleophiles, such as enolizable ketones or esters, in addition to amines or alcohols. Also, the involvement of multiple reagents and a post-synthetic transesterification of unstable Bcat products further diminishes the atom-economy of the protocol. In turn, dehydrogenative borylation methods often suffer from competitive hydrogenation and hydroboration side-reactions. In addition, these processes involve high-valent metal-hydride intermediates, which need to be either quenched by a sacrificial reagent or undergo an extrusion of dihydrogen. Therefore, starting materials bearing functional groups of high reactivity toward such metal-hydrides are inherently incompatible.

Functional group transfer catalysis[45] that would mediate the exchange of hydrogen for a boryl group between starting materials could enrich the scope of strategies for C–H bond borylation by being applicable to both terminal and internal alkene starting materials, while at the same time employing a benign reagent as a boryl group donor, ensuring a tolerance toward a broad range of functional groups and high atom-economy of the process (Figure 2.1c).[46] Although, Marciniec[47,48] and Wu[44] reported a boryl group transfer between boryl group donors and alkenes in the presence of [RuHCl(CO)(PCy$_3$)$_2$] or [Cp$_2$ZrH$_2$], the reported scopes of these methods remain restricted to simple monosubstituted alkenes, such as styrene and its derivatives bearing a limited range of functional groups (i.e., halogens, alkyl, and alkoxy substituents).[44,47,49–51] For instance, no examples of starting materials containing an internal double bond or bearing other common functional groups, such as alkynes, aldehydes, ketones, amides, or any heterocycles, were reported to be productive, and thus these methods found no practical applications in fine-chemical synthesis so far. Further, limited mechanistic insight

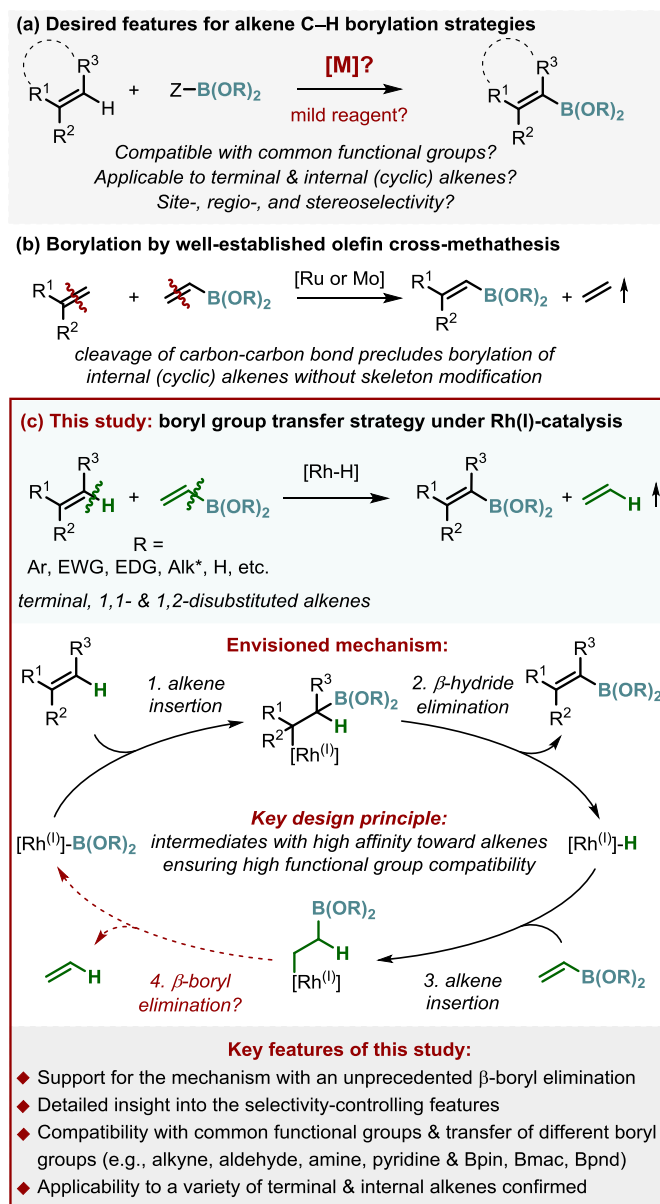into the boryl group transfer catalysis hinders rational development of these protocols toward synthetic applications.[52]

Figure 2.1. Context of this work. (a) C–H borylation of alkenes with appealing features for fine-chemical synthesis, (b) state of the art – alkene cross-metathesis, (c) transfer borylation reaction under Rh(I)-catalysis – summary of this work. * When thermodynamically favored, the isomerization of the double bond across an alkyl group is detrimental for the reaction.

We hypothesized that phosphine-Rh(I)-complexes would be the catalysts of choice for a chemoselective boryl group transfer that would occur in a proposed catalytic cycle involving a series of alkene insertion and β-elimination steps, as shown in Figure 2.1c. Our reasoning was as follows: (i) In stoichiometric experiments, a Rh(I)-boryl complex reacted with styrene to form Rh(I)-hydride and styryl boronate ester,[53] indicating the feasibility of two elementary steps of the proposed catalytic cycle (steps 1,2). In turn, (ii) Rh(I)-hydrides are known to react selectively with alkenes to form Rh(I)-alkyl species tolerating a broad range of functional groups (step 3).[54–57] (iii) Although the final elementary step, the β-boryl elimination, (step 4),

is unreported for Rh-complexes, microscopic reversibility for the reverse step, i.e., an alkene insertion into a Rh(I)-B bond,[53,58] supported its feasibility.[59–61] (iv) Lastly, the engagement of only low-valent Rh(I)-intermediates obviates otherwise impeding side-reactions based on reductive elimination reactivity of high-valent complexes, such as competitive hydroboration or hydrogenation. The chemoselectivity of the alkene insertion into a Rh(I)–B bond remained an open question.[62–67]

Here we report our studies establishing the development, mechanism, and key features of transfer C–H borylation of alkenes under Rh(I)-catalysis. The method proved to be applicable not only to terminal but also to so far challenging internal alkene starting materials and compatible with a broad range of functional groups, including motifs that are typically problematic using established approaches. A series of experimental mechanistic studies, corroborated by DFT calculations, provided insight into the details of the catalytic cycle that introduces the thus far unreported yet relatively fast β-boryl elimination step engaging the Rh(I)-(β-borylalkyl) intermediate. Further, the studies revealed the rate and selectivity determining aspects of the reaction. The studies set the stage for developing new valuable hydrogen-for-functional group exchange transformations for fine-chemical synthesis.

2.2. Results and Discussion

2.2.1. Catalyst formulation

We commenced our studies by evaluating the feasibility of the devised reactivity in a model reaction of styrene **1a** with vinyl boronate pinacol ester **2** forming product **3a**. To identify a suitable catalyst, we considered precursors that could form the prospective species that operate in the catalytic cycle, i.e., either a Rh(I)-hydride or a Rh(I)-boryl complex (Figure 2.1c). We selected phosphine-Rh(I)-alkoxide complexes, which were reported to form coordinatively unsaturated Rh(I)-hydride species through migratory insertion of an olefin into the Rh–O bond and subsequent β-hydride elimination.[68,69]

Upon evaluation of a range of complexes of different phosphine ligands and conditions (Table 2.1, sections 2.4.2.1. – 2.4.2.6.), we found that the model reaction of **1a** with **2** (1.5 equiv) in the presence of [Rh(cod)OMe]$_2$ and xantphos formed product **3a** in 92% NMR yield (81% yield of isolated material; entry 1), confirming the successful reaction design. Importantly, no other isomers of the product were observed. It should be noted that, because this isodesmic reaction is merely exergonic (DG^o = -0.57 kcal/mol),[70] the release of the gaseous ethene by-product is a driving force of the reaction. The formation of ethene was confirmed by *in situ* NMR spectroscopy.[70]

Table 2.1. Evaluation of reaction conditions
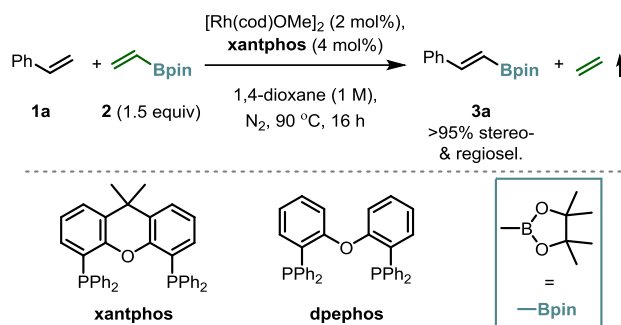
entry	variations from standard conditions	yield (%)[a]
1	none	92 (81)[b]
2	[Rh(cod)Cl]$_2$ as precursor[c]	<2
3	[Rh(cod)Cl]$_2$ + NaOMe as precursor[c]	92
4	[Rh(cod)Cl]$_2$ + NaOtBu as precursor[c]	92
5	no [Rh(cod)OMe]$_2$	<2
6	no xantphos	18
7	**dpephos** instead of **xantphos**	<2
8	1/2 cat. loading	<2
9	1/2 cat. loading + 5 mol% B$_2$pin$_2$	92
10	1/8 cat. loading + 1.2 mol% B$_2$pin$_2$	81

[a] Yield determined by ^{1}H NMR analysis of the reaction mixture with an internal standard; [b] yield of isolated material by a column chromatography purification; [c] instead of [Rh(cod)OMe]$_2$; 1 : 1 ratio of Rh to sodium alkoxide. For reactions with other phosphine ligands and reaction conditions, see section 2.4.2.

The phosphine-Rh(I)-alkoxide complex is key to the catalytic activity, as confirmed in a series of control experiments (Table 2.1). No reaction was observed with [Rh(cod)Cl]$_2$ in place of [Rh(cod)OMe]$_2$ (entry 2). However, the catalytic activity was recovered when [Rh(cod)Cl]$_2$ was used with a variety of alkoxide salts (entries 3-4 and Table 2.2) that formed the rhodium(I)-alkoxide complexes *in situ*. No reaction occurred in the absence of the rhodium precursor (entry 5), but low activity of the rhodium(I)-alkoxide precursor was maintained in the absence of any phosphine ligand (18% yield, entry 6).
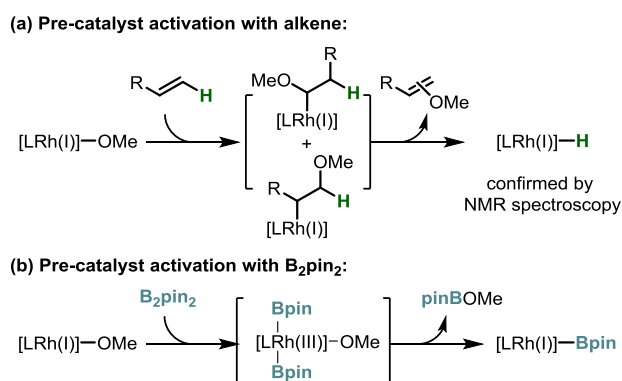
Scheme 2.1. Different modes of pre-catalyst activation

The formation of a catalytic Rh(I)-hydride species via migratory insertion of an alkene into the Rh(I)-alkoxide bond and β-hydride elimination was confirmed in stochiometric NMR experiments (Scheme 2.1a); however, the process is not quantitative. As judged by the characteristic hydride signal at -12.4 ppm in the ^{1}H NMR spectrum, up to 16% of a Rh-hydride species was formed after 2 h at 22 °C in the stoichiometric reactions of alkene **1a** with xantphos-Rh(I)-alkoxide containing either the MeO or tBuO ligand (see section 2.4.3.5.). No increase of the yield of the Rh-hydride was observed upon further reaction at this or elevated temperatures, but a mixture of other unidentified complexes was formed as judged by ^{31}P NMR spectroscopy.[70]

We found that catalytic amounts of B$_2$pin$_2$ are beneficial for the rate of the catalytic reaction (Figure 2.24). Most likely, the addition of B$_2$pin$_2$ enables an alternative pathway of the pre-catalyst activation by the facile formation of the other catalytic intermediate of the cycle, i.e. the Rh(I)-Bpin complex, in a sequence of oxidative addition of B$_2$pin$_2$ and reductive elimination of MeOBpin (Scheme 2.1b).[71] Noteworthy, a control catalytic reaction of **1a** with a stoichiometric amount of B$_2$pin$_2$ in the absence of vinyl Bpin **2** formed only trace of product **3a**, in line with B$_2$pin$_2$ acting as a pre-catalyst activator rather than an alternative stochiometric boryl group donor. Most importantly, the use of co-catalytic amounts of B$_2$pin$_2$ additive enables to lower the catalyst loading substantially (Table 2.1, entries 1 and 8-10, and section 2.4.2.7.).

2.2.2. Synthetic Capacity

With the established conditions in hand, we evaluated the reaction with respect to its functional group compatibility, its applicability to sterically and electronically varied olefines, including natural products and bioactive materials, as well as its ability to transfer different boryl groups (Figure 2.2). We established the following:

- The method is compatible with a broad variety of functional groups (**1b-1q**) and heteroaromatic moieties (**1r-1u**). Particularly noteworthy is the compatibility with aldehydes **1b**, alkynes **1p**, **1q**, amines **1c**, **1d**, and pyridines **1r**, **1s**, which are often problematic in borylation protocols,[15] due to either their ability to inhibit the catalyst or their intrinsic incompatibility with reagents (e.g., HBpin) or catalytic intermediates (e.g., Ru(II)- or Rh(III)-hydrides). We found that although acidic NH, OH, or CH groups are problematic (Figure 2.47), they can be effectivly protected, as observed in experiments with alkenes **1d**, **1k**, **1l**, and **1q**. It is worth noting that in initial reactions of alkynes **1p** or **1q** with donor **2**, a competitive ene-yne coupling was observed;[72,73] however, the use of vinyl (*E*)-1,2-bisboronate **4** in place of donor **2** prevented these side-reactions. *Inter se*, alkene **1v** that contains an alkyl-benzyl alkyne moiety reacted to form boryl derivative **3v** bearing a (non-borylated) 1,3-diene motif, revealing the alkyne-isomerization activity[74] of this Rh-catalyst as well as a high selectivity of the catalyst towards terminal mono alkenes over dienes.

- The method is applicable to a range of olefins bearing electronically (**1w**-**1aa**) and sterically (e.g., **1ab**) varied double bonds and different substitution patterns, including 1,1- and 1,2-disubstituted alkenes **1ac**-**1an**. It is noteworthy that the borylation of enamides like **1x**-**1aa** have been thus far rather underdeveloped, with only a single substrate being borylated in a synthetically useful yield.[37,38,47,75] In reactions of starting materials **1ab-1an**, the presence of co-catalytic B_2pin_2 was essential for the efficient catalytic activity; presumably alkenes **1ab-1an** are not able to activate the pre-catalyst efficiently due to their hindered insertion into the Rh–O bond. In case of 1,1-disubstituted alkenes, the stereoselectivity of the reaction seems to be controlled by steric effects. Unsymmetric alkenes **1ag-1aj** bearing two aryl rings of similar size, that is, phenyl rings with varied substituents in (remote) *para*- or *meta*-positions, reacted to form close to equimolar mixtures of stereoisomeric products irrespectively of the electronic effects. On the other hand, alkenes **1ac**, **1ae**, and **1ak** bearing one phenyl and one methyl, trifluoromethyl, or 2-thiophene ring furnished one isomer of the product preferentially with a synthetically useful stereoselectivity (77 to 90%). Similarly, 1,2-disubstituted alkenes **1al-1n** reacted with a substantial stereoselectivity (77 to >95%); however, the electronic effect on the selectivity was pronounced. While both (*E*)- and (*Z*)-β-methylstyrene **1al** reacted to form the same stereoisomer of **3al** with 83% selectivity (39% yield), (*E*)-methylisoeugenol **1am** furnished **3am** with excellent selectivity (>95%), with only traces of the other isomer. It should be noted that internal aliphatic alkenes, such as cyclooctene, alkenes that tend to isomerize to internal or trisubstituted alkenes, such as 1-octene or α-ethylstyrene, or alkenes bearing highly congested double bonds, such as α-tert-butylstyrene, failed to form the target products in substantial amounts, establishing the current limitations of the method (for details, see section 2.4.6.).
- The method is applicable to transfer different boronate ester groups, including Bmac (**3ao**), or the chiral α-pinene-based Bpnd group (**3ap**), providing an easy access to boronic acid derivatives of varied reactivity for tailored synthetic applications.[76–79] It is also worth noting that the method employs only simple readily available reagents and is easily scalable (1.1 g of **3aq** (76% yield) furnished using just 0.24 mol% of [Rh(cod)OMe]$_2$).
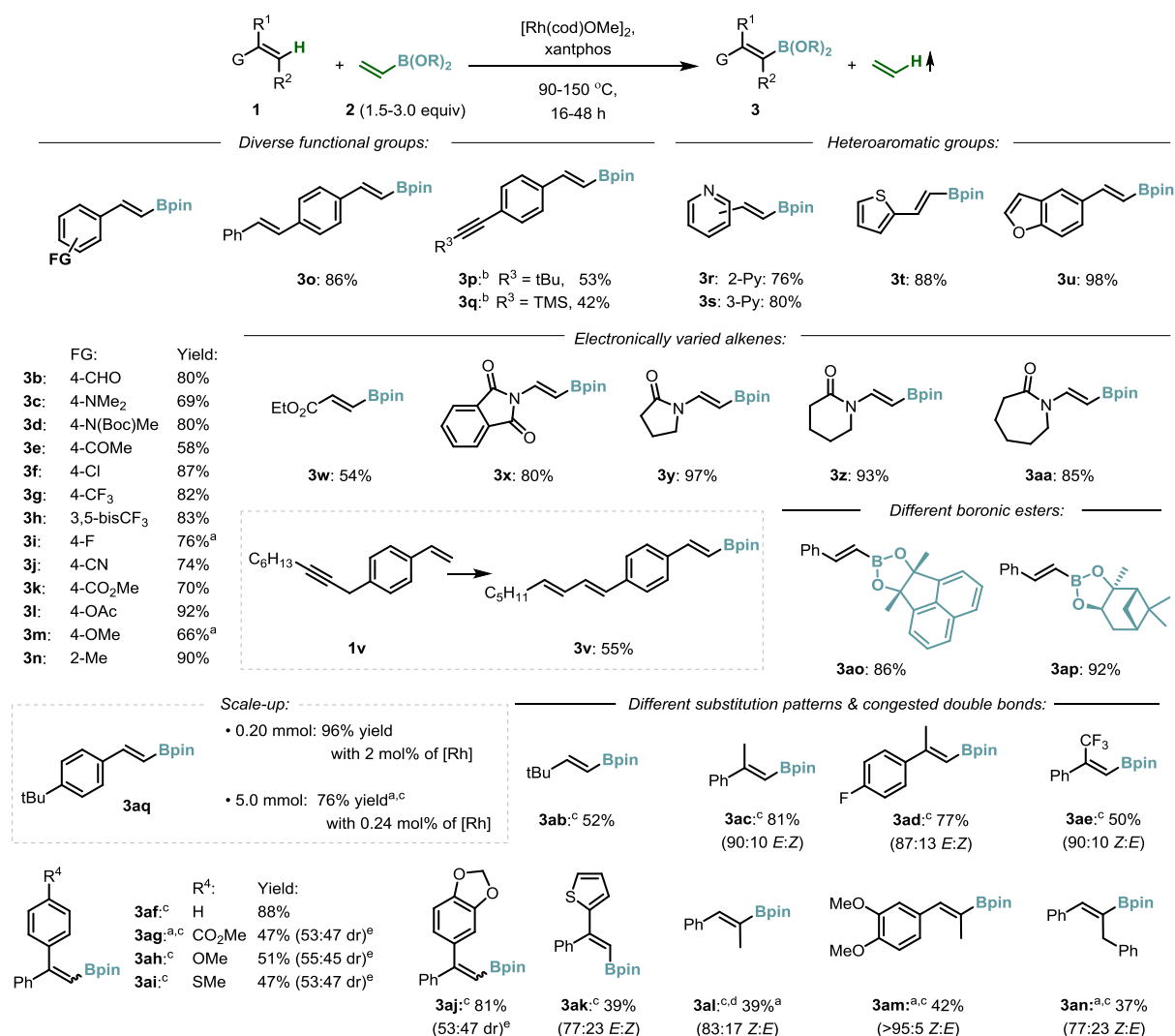
Figure 2.2. Compatibility of the method with different functional groups, heteroaromatic motifs, electronically and sterically varied terminal and internal alkenes, and different boronic esters. For an overview of the reaction conditions, including the comparison between the analytical yields determined by ^{1}H NMR analysis of the reaction mixture with an internal standard and the yields of isolated materials, see section 2.4.6. Because vinylboronic esters tend to partially decompose during chromatography on silica gel,[28,80,81] the analytical yields are reported here to indicate the actual reaction performance; for all experimental details, and product characterization, sections 2.4.5. – 2.4.7.; [a] isolated yield; [b] **4** (1.0 equiv) instead of **2**; [c] B₂pin₂ as an additive; [d] starting from *cis*-**1al**, starting from *trans*-**1al**: 38% isolated yield (83:17 *Z:E*); [e] dr, diastereomeric ratio between (*E*)- and (*Z*)-products; major stereoisomer was not assigned.

- Typical motifs of drug molecules with multiple strongly coordinating *N*- or *S*-sites that could chelate to the metal center and hence impede the reaction, often represent a significant challenge in transition metal catalysis (Figure 2.3). Nonetheless, we observed that derivatives of antihistamine Brompheniramine **1ar**, antipsychotic Chlorpromazine **1as**, and agonist of retinoid receptor CD3254 **3au** underwent transfer borylation efficiently, establishing a powerful entry point for the synthesis of large libraries of such bioactive molecules. Additionally, boronic acids are bioisosteres of carboxylic acids that find diverse applications in pharmacology.[1–3] In this context, the protocol proved effective in the concise synthesis of the boronic acid bioisostere of antiplatelet drug Ozagrel **5** through its Bpin ester **3at.**

- Complex natural products of macrocyclic structure are particularly challenging. Gratifyingly, our protocol furnished boryl derivative **3av** of Zearalenol, a nonsteroidal mycoestrogen found in *Fusarium spp*. Albeit the product was formed in modest yield, this example demonstrates the unique synthetic capacity of the transfer borylation strategy for the late-stage functionalization of complex substrates.

3ar[b]: Brompheniramine deriv.   **3as**: Chlorpromazine deriv.   **5**: Ozagrel bioisostere[c]
76%[a]   80%   (**3at**: Bpin ester: 85%)

3au: CD3254 deriv.   **3av**:[b,d] Zearalenol deriv.
89%   11% (33% rsm)
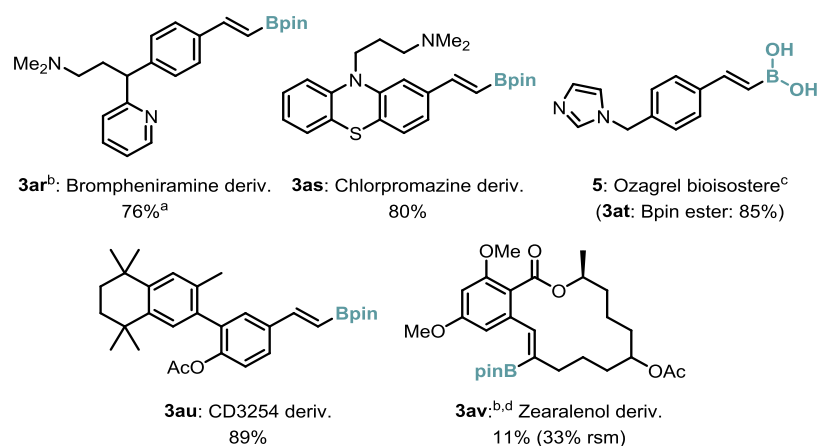
Figure 2.3. Compatibility of the method with polyfunctionalized bioactive compounds. [a] isolated yield; [b] B₂pin₂ as an additive; [c] The ester **3at** was readily hydrolyzed to the boronic acid **5** (68% yield);[70] [d] the catalyst solution was added portion-wise (in total 8.75 mol% of Rh-precursor);[70] deriv, derivative, rsm, recovered starting material.

2.2.3. Experimental mechanistic studies

Having established the boryl group transfer between alkenes under phosphine-Rh(I)-alkoxide catalysis and its broad applicability with an excellent functional group tolerance, open questions arose regarding the mechanistic aspects of the reaction that could assist further rational development of the method. In particular, we wondered whether the reaction occurred in the proposed catalytic cycle involving Rh(I)-hydride and Rh(I)-boryl intermediates with the Rh(I)-(β-borylalkyl) intermediates engaging in the so far unreported β-boryl elimination step (see Figure 2.1c) or whether an alternative mechanism involving a Rh-alkoxide mediated C(sp²)−H bond activation was operating.[82–84] The origin of the excellent regio- and stereoselectivity remained to be solved as well. To shed light on the above questions, we performed a series of experimental studies, which we further corroborated by DFT calculations.

Probing Alternative Catalytic Cycles. Stereochemical considerations for the formation of the product involving either a sequence of alkene insertion into a Rh−B bond and β-hydride elimination or a direct C-H activation implied different fate of the olefinic hydrogen atoms of alkene **1a** depending on the mechanism of the reaction (paths I-II, Figure 2.4a). Furthermore, because the earlier mechanism operates through the formation of a Rh−H species, this pathway might also lead to a proton scrambling throughout different positions of the alkene starting materials, depending on selectivity, rates, and reversibility of alkene insertion steps (paths III-IV, Figure 2.4a). To differentiate between these scenarios, we performed catalytic experiments with deuterium-labeled starting materials (Figure 2.4b). The reaction of (*E*)-β-

deuteriostyrene **1a**-β-*d* furnished product **3a** that partially retained deuterium labeling, which was scrambled between both vinylic C−H bonds (reaction 1). This outcome of **3a** maintaining some deuterium is inconsistent with the mechanism involving a direct C−H bond activation by the Rh(I)-alkoxide species (path II, Figure 2.4a), but it is consistent with the mechanism involving an alkene insertion into the Rh(I)−Bpin followed with a β-hydride elimination to form the product and a Rh-hydride (path I). In this reaction, the deuterium scrambling results most likely from a fast and reversible alkene insertion into the Rh-H bond (paths III-IV). In fact, both (*E*)- or (*Z*)-β-deuteriostyrene **1a**-β-*d* reacted with **2** forming product **3a** with similar content and relative distribution of deuterium at the α- and β-sites (reactions 1-2). Furthermore, *in situ* NMR spectroscopy and GC-MS analysis of the reaction of styrene-d_8 **1a**-d_8 with **2** revealed the extensive hydrogen/deuterium scrambling not only throughout the α- and β-sites of product **3a**, but also between both alkene starting materials **1a**-d_8 and **2** occurring already early in the process (reactions 3-4). This result indicates that the reversible insertions into the Rh−H/Rh−D bonds are faster than the actual transfer of the boryl group. We also found that the product re-enters the cycle during the catalytic reaction. Compound **3t**, the analogue of **3a** bearing a different aryl ring, added to the reaction of **1a**-d_8 and **2** as a 'spectator' underwent partial deuterium incorporation into its α- and β-positions, implying its reversible insertion into the Rh−H/Rh−D bond occurring also early in the process (3 h; reaction 5). Lastly, utilizing compound **3a** as the boryl group donor instead of vinyl boronate **2** in the reaction of 4-chlorostyrene **1f**, we observed the formation of **3f**, 4-chloro analogue of **3a**, and styrene **1a** (reaction 6), indicating the reversibility of all steps of the catalytic cycle. It should be noted that these experiments confirmed the reversibility of all steps in the catalytic cycle forming **3a**, i.e., (*E*)-product; however, the relative rates between the steps (e.g., alkene insertion into the Rh-B versus β-boryl elimination) as well as the feasibility of the catalytic cycle forming alternative products, i.e., (*Z*)- and α-isomers, had yet to be investigated.
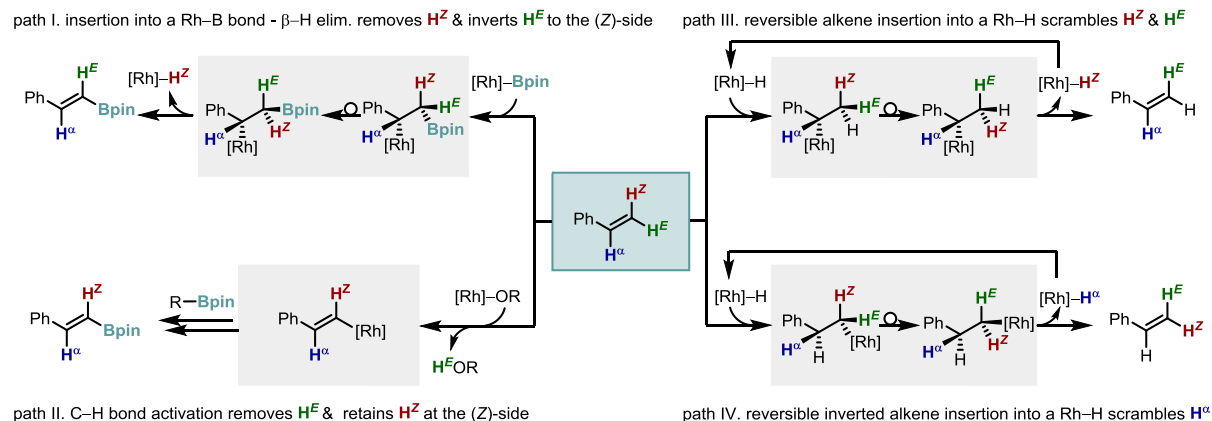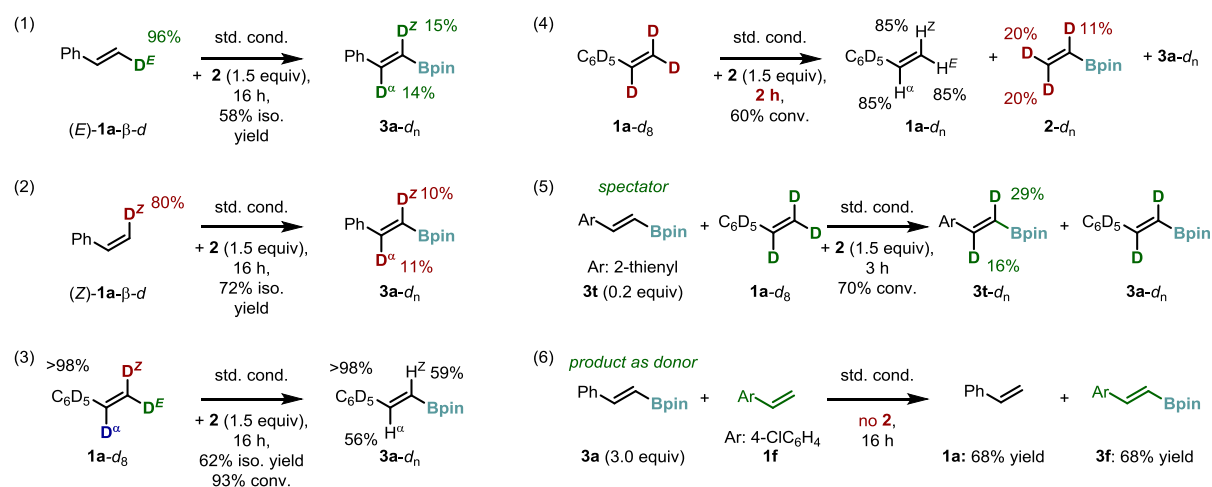
Figure 2.4. Mechanistic experiments probing the prospective catalytic cycle for the boryl group transfer. (1-2): Partial deuterium retaining in **3a** in the reaction of (*E*)-**1a**-β-*d* is consistent with the mechanism involving alkene insertion into a Rh−B bond & β-hydride elimination sequence; (1-4): H/D scrambling between starting materials indicates fast & reversible alkene insertion into the Rh−H intermediate; (5): Deuterium incorporation into **3t** indicates that the product re-enters the cycle; (6): Boryl group transfer between **3a** and **1f** indicates that the reaction is reversible. For standard conditions, see Table 2.1; for further details, see section 2.4.3.2.

Insight into the Rate Limiting Step. With the observed fast hydrogen/deuterium scrambling (Figure 2.4b), we considered that both the insertion of alkenes into the Rh(I)-hydride and β-hydride elimination must be fast, and hence the overall rate of the reaction is limited by either the alkene insertion into the Rh(I)-boryl intermediate or the β-boryl elimination step (Figure 2.1c). To differentiate between these scenarios, we studied the reactivity of the independently prepared Rh(I)-boryl intermediate, **LRhBpin** (Figure 2.5).[70,71] First, we found that **LRhBpin** reacted with alkene **1a** to form product **3a** gradually in time, implying a rather slow alkene insertion into the Rh−B bond (Figure 2.5a). In turn, we observed that **LRhBpin** is catalytically active in the model reaction, with similar rates of the formation of **3a** early in the reaction, i.e., before the first catalytic turnover, and later in the reaction, i.e., after the first catalytic turnover (Figure 2.5b). Most importantly, the formation of **3a** before the first turnover involves only the insertion of alkene into the Rh−B bond of *starting* **LRhBpin** (and the fast β-hydride elimination), while the formation of **3a** in the later phase of the reaction requires all steps of the cycle, including the β-boryl elimination step. Thus, similar rates in the different

phases of the reaction indicate that the alkene insertion into the Rh–B bond is slower than the β-boryl elimination, and hence is most likely the rate-limiting step of the catalytic process.

(a) Reactivity of Rh(I)-Bpin intermediate with an alkene

LRh(I)—**Bpin**   +   Ph ⟍⟍   →   Ph ⟍⟍ **Bpin**

thf-d_8/thf

LRhBpin
(1 equiv)

1a
(>10 equiv)

3a

L = xantphos

conditions	yield
22 °C, 16 h:	50%
45 °C, 5 h:	74%

(b) Catalytic activity of Rh(I)-Bpin intermediate

LRh(I)—**Bpin**
(6.7 mol%)

Ph ⟍⟍   +   ⟍⟍ **Bpin**   →   Ph ⟍⟍ **Bpin**

thf-d_8/thf
45 °C

1a (1 equiv)   **2** (1.2 equiv)   **3a**

phase (time):	TOF/ h^{-1}	TON
< 1st turnover (5 h):	0.09(1)	0.44
> 1st turnover (16 h):	0.09(1)	1.52
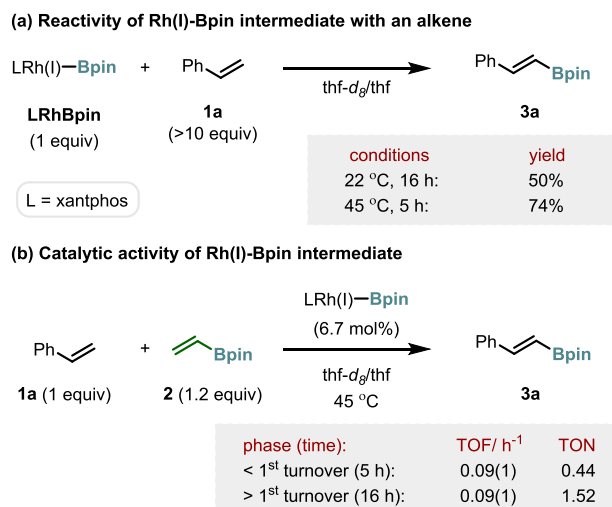
Figure 2.5. Reactivity of independently prepared xantphos-Rh(I)-Bpin intermediate. **LRhBpin** reacts with **1a** rather slowly and is catalytically active under similar conditions; the formation of **3a** with similar rates in the different phases of the catalytic reaction suggests that the alkene insertion is rate-liming. TOF, turnover frequency; TON, turnover number; for full experimental details, see sections 2.4.3.6. and 2.4.3.7.

Probing Stereo- and Regiocontrol of the Reaction. Because product **3a** is more stable than isomers (Z)-**3a** and (α)-**3a** (0.0 vs. +4.2 and +5.0 kcal/mol, respectively),[70] the stereo- and regioselectivity of the reaction might be either under thermodynamic control, that is, when the formation of different isomers of the product is similarly fast, but isomers quickly interconvert to form the product of the lowest energy, or under kinetic control, that is, when the formation of one isomer is much faster than that of the other isomers. To shed light on these scenarios, we studied the reactivity of independently prepared isomers (Z)-**3a** and (α)-**3a** under catalytic conditions. We observed that stereoisomer (Z)-**3a** underwent fast conversion to (E)-isomer **3a**, when present as a spectator of a catalytic reaction of substrate **1aq** under otherwise standard conditions (Figure 2.6, reaction 1). This observation indicates that stereoselectivity might be indeed thermodynamically controlled.[28,35] However, the quick formation of (Z)-**3a** along with **3a** would need to be confirmed to exclude the possibility of kinetic control operating, where the reaction forms **3a** much faster than (Z)-**3a**. In contrast, in an analogous experiment, the α-regioisomer of **3a**, (α)-**3a** was rather reluctant to the isomerization: only 11% of (α)-**3a** converted to **3a** after 3 h, while at the same time the (β-selective) catalytic reaction was nearly finished (84% yield of **3m**; Figure 2.6, reaction 2). This experiment clearly showed that the formation of (E)-isomer is much faster than the formation of the α-isomer, in line with kinetic control of the regioselectivity. Overall, the conversions of (Z)-**3a** and (α)-**3a** to **3a** indicate that both prospective products of the reaction can enter the catalytic cycle, and hence, due to the principle of microscopic reversibility, they could be formed in the reaction as well. However, the slower conversion of the α-isomer to the (E)-isomer compared to the rate of the actual catalytic formation of the (E)-isomer implies that the regioselectivity of the reaction is kinetically controlled, a rather unusual feature in functional group transfer catalysis.[85] Most importantly, because the kinetic control depends

on the catalyst, the data suggest the feasibility of accessing different isomers using different catalysts.
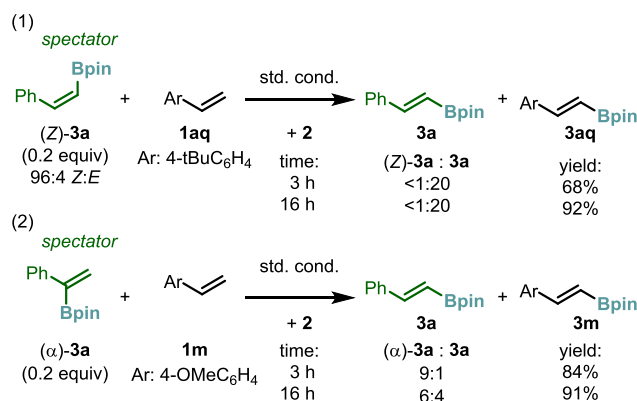
Figure 2.6. Mechanistic experiments probing the pathways toward formation of stereo- and regioisomeric products. (1): Fast isomerization of (Z)-**3a** to **3a** indicates that the stereoselectivity of the reaction might be thermodynamically controlled or kinetically controlled at the β-hydride elimination step. (2): As the isomerization of (α)-**3a** to **3a** is slower than the catalytic reaction, the regioselectivity is controlled kinetically. For standard conditions, see Table 2.1; for details, see section 2.4.3.2.

2.2.4. Computational mechanistic studies

The experimental mechanistic findings were corroborated by DFT calculations performed at the M06-L/def2-TZVP$_{(SMD,1,4-dioxane)}$//M06-L/def2-SVP level of theory. The computed free energy surfaces for the formation of **3a**, (Z)-**3a** and (α)-**3a** (Figure 2.7) demonstrated the feasibility of the initially considered catalytic cycle (Figure 2.1c) and further supported the alkene insertion into the Rh–B bond as the rate-limiting step of the reaction. Importantly, our computations not only support that the regioselectivity is kinetically controlled but also suggested that the stereoselectivity is also under kinetic control. Additionally, we provided a detailed analysis on the unprecedented β-boryl elimination process (section 4.3 of the SI), as well as an insight into the preferential P-P coordination mode of xantphos during the reaction (not part of this thesis).[86]

Specifically, the initial xantphos-Rh(I)-hydride complex coordinated by boryl group donor **2**, **LRhH**(η^2-**2**) is predicted to readily form the Rh(I)-boryl intermediate, **LRhBpin**(η^2-ethene) in an exergonic process (DG$_{rel}$ = -6.0 kcal/mol) through an alkene insertion (via transition state 1, **TS-1**) – β-boryl elimination (**TS-2**) sequence with a low free energy barrier of +5.6 kcal/mol. Noteworthy, the oxygen atom of the xantphos ligand does not interact with the metal center during the process, while such an interaction was found to be important in other Rh-catalyzed reactions.[67] Parallel calculations indicate that such a pathway would lead to a significantly higher free energy barrier (DG$_{rel}$ = +10.5 kcal/mol vs +5.6 kcal/mol).[86] Therefore, the activity of the **xantphos**-Rh(I) complex originates most likely from the distinct wide bite angle of the ligand rather than the presence of the oxygen atom. In accordance, no activity was observed for the analogous complex bearing flexible **dpephos** (cf. Table 2.1).
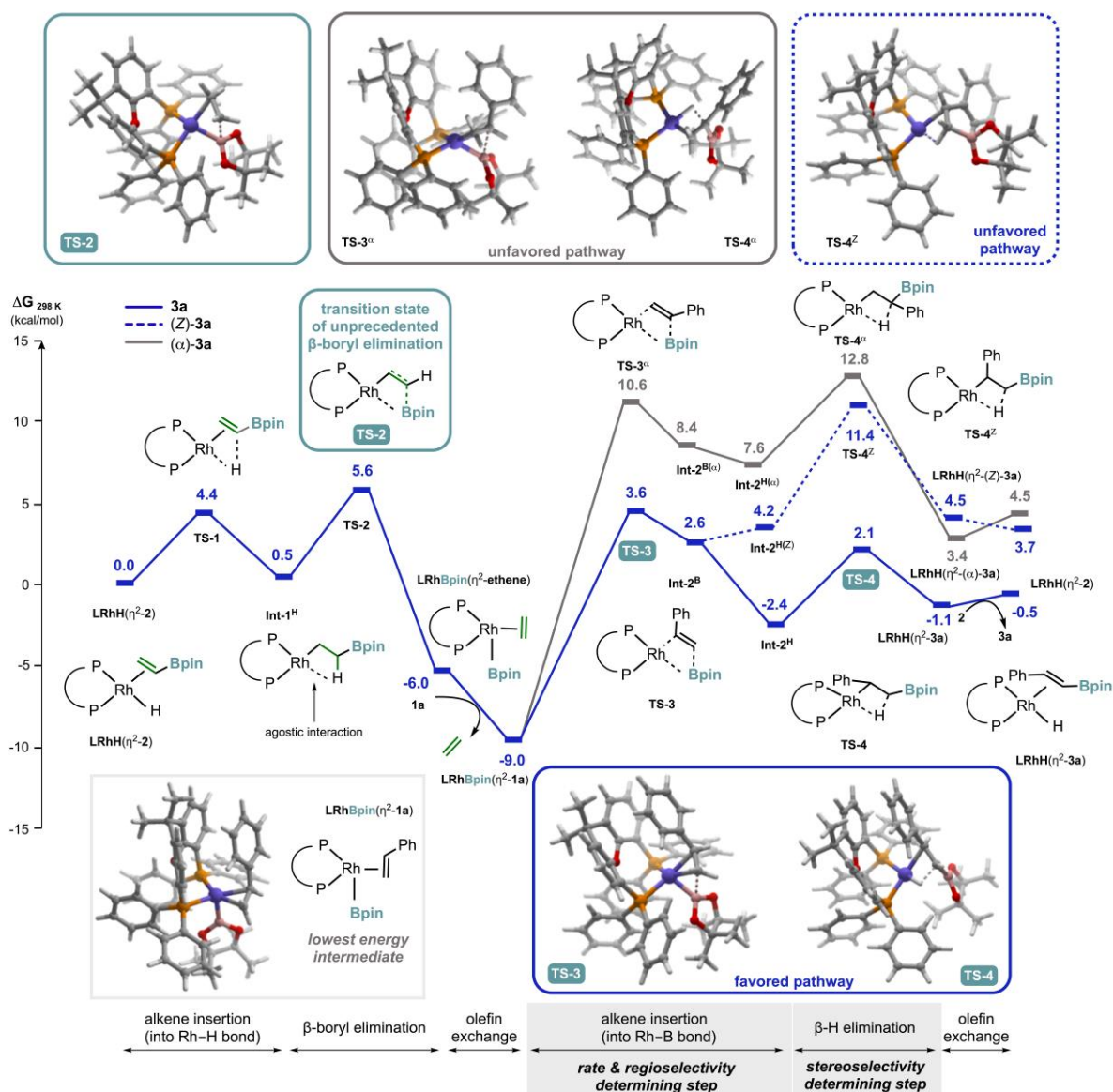
Figure 2.7. DFT investigation of the free energy surfaces for the reaction pathways leading to products **3a**, (*Z*)-**3a**, or (α)-**3a**. Calculations have been performed at the M06-L/def2-TZVP(SMD)//M06-L/def2-SVP level of theory in 1,4-dioxane as solvent (SMD solvation model); SMD, solvation model based on density; Int, intermediate, TS, transition state. For full discussions, structures of all transition states and intermediates, and further details, see the SI of the published article.[86]

The borylation of **1a** with the thus-formed **LRhBpin**(η^2-ethene) intermediate embarks upon a ligand exchange to form **LRhBpin**(η^2-**1a**) (along with the extrusion of ethene), which is the lowest energy intermediate of the catalytic cycle (DG$_{rel}$ = -9.0 kcal/mol).[86] The subsequent alkene insertion into its Rh(I)−B bond is predicted to be rate-limiting with the free energy barrier of +12.6 kcal/mol (**TS-3**). The following β-hydride elimination to form product **3a** through **TS-4** proceeds with a low barrier (+4.5 kcal/mol). Product **3a** is released from **LRhH**(η^2-**3a**) upon the ligand exchange with another molecule of **2**, closing the catalytic cycle. Notably, the alternative β-hydride elimination step toward the formation of stereoisomeric product (*Z*)-**3a** involves a significantly higher energy barrier (**TS-4**^{Z}), even greater than that for

49

the alkene insertion into the Rh–B bond (**TS-3**), accounting for the overall barrier of +20.4 kcal/mol (from **LRhBpin**(h^2-**1a**); dotted blue line in Figure 2.7), in line with kinetic control of the stereoselectivity. Further, the reaction pathway toward the formation of regioisomeric product (α)-**3a** involves higher energy transition states for both alkene insertion (**TS-3ª**) and β-hydride elimination (**TS-4ª**) with the overall barrier of +21.8 kcal/mol (grey line in Figure 2.7), in line with kinetic control of the regioselectivity. Noteworthy, computations also predict that both (*Z*)-**3a** and (α)-**3a** can enter the catalytic cycle with energy barriers of +6.9 and +9.4 kcal/mol, respectively. These results correlate well with the observed interconversions of (*Z*)-**3a** and (α)-**3a** to product **3a**, which were found to be fast and slow in comparison to the rate of the actual catalytic reaction, respectively (cf. Figure 2.6). Overall, although isomer **3a** is thermodynamically more stable than (Z)-**3a** and α-**3a**, the calculations suggest that its formation is kinetically controlled.

It is worth mentioning that a stepwise analysis of the β-boryl elimination process revealed that prior to the transition state, there is an intermediate engaging an interaction between boron and Rh atoms, which leads to the C–B bond weakening and its elongation prior to the bond breaking event, and hence facilitating this unprecedented elementary reaction. For full discussions, including all higher-energy pathways, further details, and structures of all transition states and intermediates, see section the SI of the published article.[86]

2.2.5. Summarized Mechanistic Proposal

Based on the collected data we propose that Rh(I)-catalyzed transfer borylation of alkenes occurs as shown in Figure 2.8. The key mechanistic features are:

1. The Rh(I)-alkoxide pre-catalyst enters the catalytic cycle either through the alkene insertion into the Rh–O bond – β-hydride elimination sequence forming the catalytic Rh-hydride species (path a) or through its reaction with co-catalytic B_2pin_2 additive to form the catalytic Rh(I)-boryl complex along with pinBOMe under B_2pin_2-based activation (path b).

2. In the catalytic cycle, the Rh(I)-hydride intermediate with coordinated Bpin-donor **2**, **LRhH**(η^2-**2**), reacts readily to form the Rh(I)-boryl species, **LRhBpin**(η^2-ethene), through an alkene insertion into the Rh–H bond – β-boryl elimination sequence (steps I-II).

3. **LRhBpin**(η^2-**1**), formed upon olefin exchange of ethene for starting material **1**, is the lowest energy intermediate of the catalytic cycle (step III), which is in equilibrium engaging other alkenes in the mixture (step III'). The complex undergoes rate-limiting regioselective alkene insertion (step IV), followed by a fast and stereoselective β-hydride elimination (step V), and the release of product **3** through an olefin exchange, which completes the cycle (step VI).

4. The relatively low free energy barriers for all steps of the catalytic cycle forming the (*E*)-isomer of the product have two main consequences: First, many elementary steps are reversible, which can lead to isomerization and scrambling processes (through steps I' and IV'). Second, the free energy surface for the overall transformation is

relatively flat, which is essential for effective catalysis in isodesmic processes with a limited energetic driving force. However, the study shows that a catalyst might impose high energy barriers (e.g., competitive steps IV' or V') for the formation of different isomers of the products, creating the prospects for the kinetic control of selectivity in functional group transfer catalysis.[85]
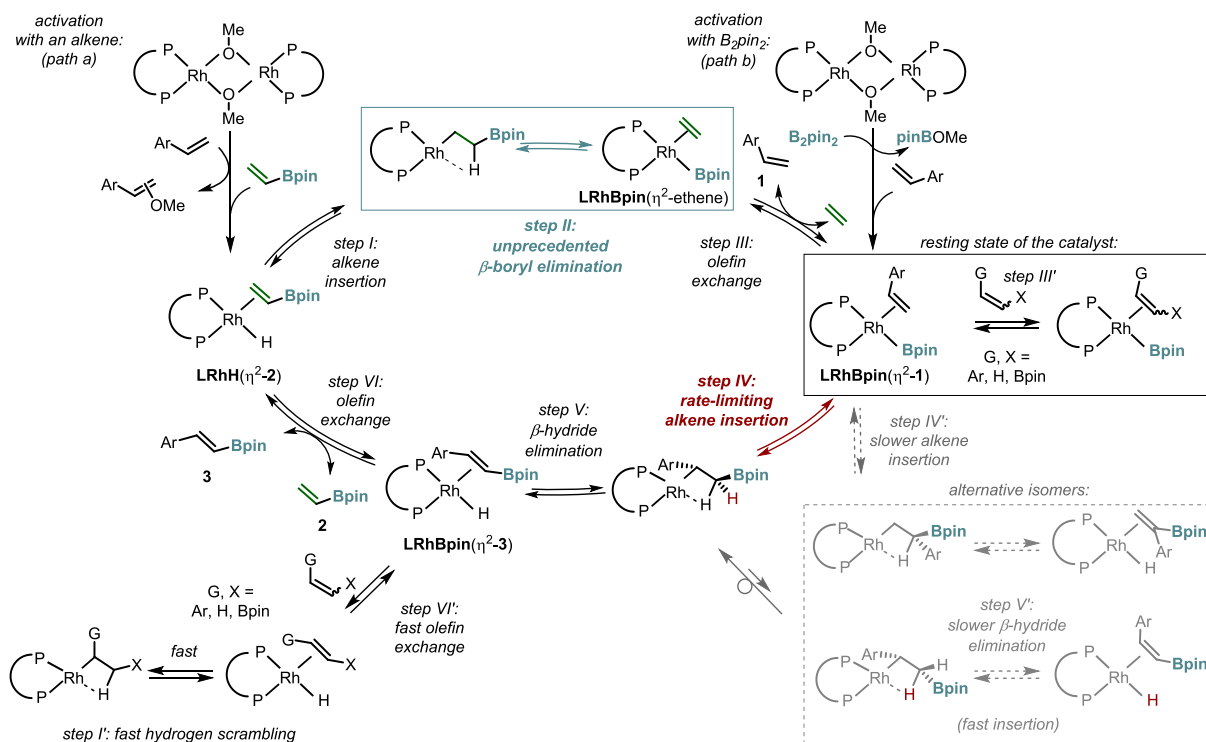
Figure 2.8. Full proposal of the mechanism of Rh(I)-catalyzed transfer borylation of alkenes.

2.3. Conclusions

In conclusion, the herein disclosed Rh(I)-catalyzed boryl group transfer reaction proved to be applicable not only to simple alkenes but also to more complex settings of polyfunctionalized molecules with multiple groups that could inhibit the catalyst. Therefore, such reactivity together with an excellent functional group tolerance indicates its possible applicability to late-stage modifications of complex fine chemicals. Further, the mechanistic studies provided insight into the features controlling the selectivity setting the stage for the development of methods to access different regio- and stereoisomers of the products by C–H borylation; a feature that remains elusive with current strategies.

The studies revealed that an uncommon β-boryl elimination step engaged in the reaction is notably easy, especially in contrast to the well-documented reverse step – an alkene insertion into a Rh–B bond. Considering the number of known alkene insertion elementary reactions into different metal-heteroatom bonds, the mechanistic approach carries the potential for the development of other hydrogen-functional group exchange reactions of high value to organic synthesis. The research to uncover the full capacity of the strategy continues in our laboratories.

2.4. Experimental details

2.4.1. Experimental methods

Unless stated otherwise, all reactions and manipulations were conducted on the laboratory bench or in a well-ventilated fume hood in air with reagent grade solvents. Reactions under inert gas atmosphere were carried out in oven-dried glassware in a nitrogen-filled glove box or by standard Schlenk techniques under nitrogen. Unless noted otherwise, all reagents and solvents were purchased from commercial suppliers and used without further purification. [Rh(COD)OMe]$_2$ was synthesized according to a literature procedure.[87] For experiments under inert gas atmosphere, dried and degassed solvents were purchased from commercial suppliers, stored in a nitrogen-filled glove box and used as received. Column chromatography was carried out with the aid of a CombiFlash EZ Prep Chromatography System with integrated ELSD using the RediSep Rf (Gold) Silica Gel Disposable Flash columns. TLC was carried out on Merck Kieselgel F254 plates. TLC visualization was carried out with ultraviolet light (254 nm), followed by staining with a 1% aqueous KMnO$_4$ solution. NMR spectra were acquired on the 400 MHz (Bruker 400 MHz NMR UltraShield Magnet, Console Avance III, equipped by a standard probe BBFO ^{1}H-X inverse 5 mm (with ^{31}P < X < ^{15}N)) or 500 MHz (Bruker 500 MHz NMR Ascend Magnet, Console Avance Neo equipped by a Cryo-Probe Prodigy ^{1}H-X 5 mm (with ^{31}P < X < ^{15}N) with a 24-positions auto-sampler) instruments at the Institute of Science and Supramolecular Engineering (ISIS). NMR spectra were processed using the MestReNova 14.1 software. Chemical shifts are reported in parts per million (ppm) and referenced to residual solvent peaks or tetramethylsilane (TMS). Coupling constants are reported in hertz (Hz). GC-FID analysis was obtained on a Shimadzu GC-2010 Plus instrument equipped with a SH-Rxi-5MS column (25 m x 0.20 mm ID x 0.33 mm film) connected to a FID detector. GC-MS analysis was obtained on a Shimadzu QP2020 (EI) instrument equipped with a SH-Rxi-5MS column (25 m x 0.20 mm ID x 0.33 mm film). GC-FID and NMR yields were calculated using dodecane, 1,3,5-trimethoxybenzene, mesitylene or isochroman as the internal standards. GC-FID yields were corrected for response factors for all compounds. High-resolution electrospray ionization mass spectra (HR-ESI-MS) were obtained at the Analytical Facility of the Department of Chemistry, University of Strasbourg or at the Institute of Science and Supramolecular Engineering using a ThermoFisher Orbitrap Exactive Plus with Extend Mass Range(source HESI II) with a Vanquish PDA (VF-XX) detector. Preparative HPLC was carried out with an Agilent semi-preparative HPLC system equipped with: a 1260 Infinity II Binary pump, a 1260 Infinity II Variable Wavelength Detector equipped with a 3 mm preparative cell, a 1290 Infinity II Preparative Open-Bed Sampler/Collector with a 20 mL injection loop, and an Agilent 5 Prep C18 50*21.2 mm column 5 μm particle size.

2.4.2. Evaluation of reaction parameters
2.4.2.1. Evaluation of different rhodium pre-catalysts and additives
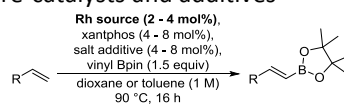
Entry	R =	Rh source	Salt additive	Yield %
1[a]	Ph	[Rh(COD)OMe]$_2$	-	92
2[a]	Ph	[Rh(COD)Cl]$_2$	-	n.d.
3[a]	Ph	[Rh(COD)Cl]$_2$	NaOMe	92
4[a]	Ph	[Rh(COD)Cl]$_2$	KOMe	92
5[a]	Ph	[Rh(COD)Cl]$_2$	NaOEt	92
6[a]	Ph	[Rh(COD)Cl]$_2$	NaOtBu	92
7[a]	Ph	[Rh(COD)Cl]$_2$	NaF	n.d.
8[b]	Ph	[RhCp*Cl$_2$]$_2$	NaOMe	n.d.
9[c]	Ph	[RhCp*Cl$_2$]$_2$	NaOMe	n.d.
10[a,e]	Ph	[Rh(xantphos)Cl]$_2$	NaOtBu + B$_2$pin$_2$	93
11[d]	CO$_2$Et	[Rh(COD)OMe]$_2$	-	54
12[d]	CO$_2$Et	[Rh(C$_2$H$_4$)$_2$Cl]$_2$	AgBF$_4$	n.d.
13[d]	CO$_2$Et	[Rh(COD)(MeCN)$_2$]BF$_4$	-	n.d.
14[d]	CO$_2$Et	[Rh(COD)$_2$]SbF$_6$	-	n.d.

Table 2.2. Evaluation of different rhodium pre-catalysts and additives.

a) Conditions: 0.2 mmol of styrene, 0.3 mmol vinyl Bpin, 2 mol% Rh source, 4 mol% xantphos, 4 mol% of salt additive, dioxane (200 μL, 1 M), 90 °C, 16 h. Yields were determined by analysis of ^{1}H NMR spectra using 1,3,5-trimethoxybenzene as an internal standard. b) Conditions: 0.2 mmol of styrene, 0.3 mmol vinyl Bpin, 4 mol% [RhCp*Cl$_2$]$_2$, 8 mol% xantphos, 16 mol% of NaOMe, dioxane (200 μL, 1 M), 90 °C, 16 h. Yields were determined by analysis of ^{1}H NMR spectra using 1,3,5-trimethoxybenzene as an internal standard. n.d.: not detected. c) Conditions: 0.2 mmol of styrene, 0.3 mmol vinyl Bpin, 4 mol% [RhCp*Cl$_2$]$_2$, 8 mol% xantphos, 16 mol% of NaOMe, toluene (200 μL, 1 M), 90 °C, 16 h. Yields were determined by analysis of ^{1}H NMR spectra using 1,3,5-trimethoxybenzene as an internal standard. n.d.: not detected. d) Conditions: 0.2 mmol of ethyl acrylate, 0.6 mmol vinyl Bpin, 8 mol% Rh source (4 mol% for dimeric Rh source), 8 mol% xantphos, 8 mol% of salt additive, toluene (200 μL, 1 M), 110 °C, 24 h. Yields were determined by analysis of ^{1}H NMR spectra using 1,3,5-trimethoxybenzene as an internal standard. e) Additional B$_2$pin$_2$ (5 mol%) was used.

2.4.2.2. Evaluation of solvents
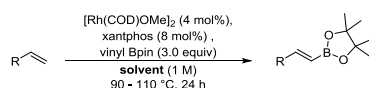
Entry	R =	Solvent	Yield %
1[a]	Ph	Dioxane	92
2[a]	Ph	THF	92
3[a]	Ph	Toluene	64
4[b]	CO_2Et	Dioxane	42
5[b]	CO_2Et	Toluene	46
6[c]	CO_2Et	Toluene	54
7[b]	CO_2Et	THF	28
8[b]	CO_2Et	DCM	n.d.
9[b]	CO_2Et	Benzene	29
10[b]	CO_2Et	Acetonitrile	n.d.
11[b]	CO_2Et	Hexane	46
12[b]	CO_2Et	$PhCF_3$	35
13[b]	CO_2Et	HFIP	n.d.
14[c]	CO_2Et	Decalin	44
15[c]	CO_2Et	p-Xylene	36
16[c]	CO_2Et	Heptane	52

Table 2.3. Evaluation of solvents.

a) Conditions: 0.2 mmol of styrene, 0.3 mmol vinyl Bpin, 2 mol% [Rh(COD)OMe]$_2$, 4 mol% xantphos, solvent (200 µL, 1 M), 90 °C, 16 h. Yields were determined by analysis of ^{1}H NMR spectra using 1,3,5-trimethoxybenzene as an internal standard. b) Conditions: 0.2 mmol of ethyl acrylate, 0.6 mmol vinyl Bpin, 4 mol% [Rh(COD)OMe]$_2$, 8 mol% xantphos, solvent (200 µL, 1 M), 90 °C, 24 h. Yields were determined by analysis of ^{1}H NMR spectra using 1,3,5-trimethoxybenzene as an internal standard. c) Conditions: 0.2 mmol of ethyl acrylate, 0.6 mmol vinyl Bpin, 4 mol% [Rh(COD)OMe]$_2$, 8 mol% xantphos, solvent (200 µL, 1 M), 110 °C, 24 h. Yields were determined by analysis of ^{1}H NMR spectra using 1,3,5-trimethoxybenzene as an internal standard. n.d.: not detected.

2.4.2.3. Evaluation of ligands
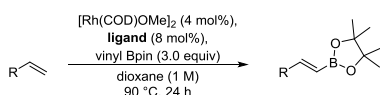
Entry	R =	Ligand	Yield %
1[a]	Ph	L$_1$	92
2[a]	Ph	L$_3$	n.d.
3[a]	Ph	L$_4$	n.d.
4[a]	Ph	L$_5$	n.d.
8[b]	CO_2Et	L$_1$	42
9[b]	CO_2Et	L$_2$	35
10[b]	CO_2Et	L$_3$	n.d.
11[b]	CO_2Et	L$_4$	trace
12[b]	CO_2Et	L$_5$	n.d.
13[b]	CO_2Et	L$_6$	n.d.
14[b]	CO_2Et	L$_7$	trace
15[b]	CO_2Et	L$_8$	trace
16[b]	CO_2Et	L$_9$	trace

Table 2.4. Evaluation of ligands

a) Conditions: 0.2 mmol of styrene, 0.3 mmol vinyl Bpin, 2 mol% [Rh(COD)OMe]$_2$, 4 mol% xantphos, solvent (200 µL, 1 M), 90 °C, 16 h. Yields were determined by analysis of ^{1}H NMR spectra using 1,3,5-trimethoxybenzene as an internal standard. b) Conditions: 0.2 mmol of ethyl acrylate, 0.6 mmol vinyl Bpin, 4 mol% [Rh(COD)OMe]2, 8 mol% xantphos, dioxane (200 µL, 1 M), 90 °C, 24 h. Yields were determined by analysis of ^{1}H NMR spectra using 1,3,5-trimethoxybenzene as an internal standard. n.d.: not detected.

2.4.2.4. Evaluation of temperature
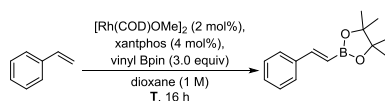
Entry	Temperature	Yield %
1[a]	25 °C	n.d.
2[a]	50 °C	n.d.
3[a]	70 °C	31
4[a]	80 °C	93
5[a]	90 °C	95

Table 2.5. Evaluation of temperature.

a) Conditions: 0.2 mmol of styrene, 0.6 mmol vinyl Bpin, 2 mol% [Rh(COD)OMe]2, 4 mol% xantphos, dioxane (200 μL, 1 M), indicated temperature, 16 h. Yields were determined by analysis of ^{1}H NMR spectra using 1,3,5-trimethoxybenzene as an internal standard. n.d.: not detected.

2.4.2.5. Evaluation of catalyst loading
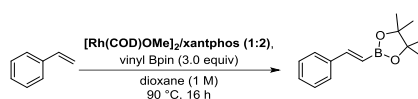
Entry	Catalyst/ligand loading	Yield %
1[a]	4 mol% / 8 mol%	94
2[a]	3 mol% / 6 mol%	94
3[a]	2 mol% / 4 mol%	95
4[a]	1.5 mol% / 3 mol%	Up to 92[b]
5[a]	1 mol% / 2 mol%	n.d.

Table 2.6. Evaluation of catalyst loading.

a) Conditions: 0.2 mmol of styrene, 0.6 mmol vinyl Bpin, [Rh(COD)OMe]2/xantphos (1:2 ratio), dioxane (200 μL, 1 M), 90 °C, 16 h. Yields were determined by analysis of ^{1}H NMR spectra using 1,3,5-trimethoxybenzene as an internal standard. b) The yields obtained with 1.5 mol% catalyst loading were barely reproducible. Therefore, 2 mol% catalyst loading were chosen for any further studies. n.d.: not detected.

2.4.2.6. Evaluation of vinyl Bpin loading
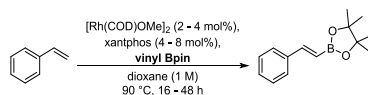
Entry	Vinyl Bpin loading	Yield %
1[a]	5.0 equiv	93
2[a]	4.0 equiv	95
3[a]	3.0 equiv	93
5[b]	2.5 equiv	94
6[b]	2.0 equiv	94
7[a]	2.0 equiv	88
8[b]	1.5 equiv	92

Table 2.7. Evaluation of vinyl Bpin loading.

a) Conditions: 0.2 mmol of styrene, vinyl Bpin, [Rh(COD)OMe]2 (4 mol%), xantphos (8 mol%), dioxane (200 μL, 1 M), 90 °C, 48 h. Yields were determined by analysis of ^{1}H NMR spectra using 1,3,5-trimethoxybenzene as an internal standard. b) Conditions: 0.2 mmol of styrene, vinyl Bpin, [Rh(COD)OMe]2 (2 mol%), xantphos (4 mol%), dioxane (200 μL, 1 M), 90 °C, 16 h. Yields were determined by analysis of ^{1}H NMR spectra using 1,3,5-trimethoxybenzene as an internal standard.

2.4.2.7. Evaluation of catalyst loading with B_2pin_2
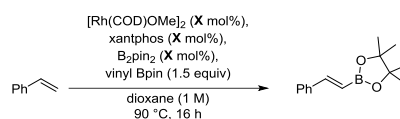
Entry	[Rh(COD)OMe]₂	Xantphos	B₂pin₂	Yield	TON
1ᵃ	1.96 mol%	3.92 mol%	9.80 mol%	101%	26
2ᵃ	1.00 mol%	2.00 mol%	5.00 mol%	92%	46
3ᵃ	0.475 mol%	0.950 mol%	2.38 mol%	84%	88
4ᵃ	0.240 mol%	0.480 mol%	1.20 mol%	81%	169
5ᵃ	0.0954 mol%	0.191 mol%	0.477 mol%	36%	188
6ᵃ	0.0475 mol%	0.0950 mol%	0.238 mol%	traces	/

Table 2.8. Evaluation of catalyst loading with B_2pin_2.

a) Scale: 0.2 mmol of styrene, 0.3 mmol vinyl Bpin. Yields were determined by analysis of ^{1}H NMR spectra using 0.25 equiv of 1,3,5-trimethoxybenzene as an internal standard.

2.4.2.8. Evaluation of catalyst pre-activation with B_2pin_2
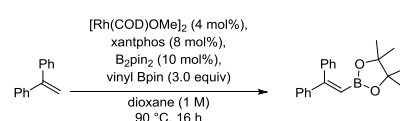
Entry	Time of pre-activation	Yield
1ᵃ,ᵇ	none	23%
2ᵃ	15 min	25%
3ᵃ	1 h	10%
4ᵃ	5 h 20 min	traces

Table 2.9. Evaluation of catalyst pre-activation with B_2pin_2.

a) [Rh(COD)OMe]2, xantphos, B2pin2 and dioxane (100 μL) were allowed to stir at 80 °C for the indicated time, before 1,1-diphenylethylene (0.2 mmol), vinyl Bpin (0.3 mmol), dioxane (100 μL) were added and room temperature. Afterwards, the mixture was allowed to stir for 16 h at 90 °C. Yields were determined by analysis of ^{1}H NMR spectra using 0.25 equiv of 1,3,5-trimethoxybenzene as an internal standard. b)The reaction mixture was allowed to stir for 22.5 h instead of 16 h at 90 °C.

2.4.2.9. Evaluation of reaction conditions for 1,1-disubstituted substrates
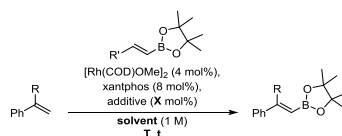
Entry	R =	Additive [equiv]	R', [equiv]	Solvent	Temperature [°C]	Time [h]	d.r. (E)/(Z)	Yield
1ᵃ	Ph	/	H (3.0)	dioxane	90	16	/	n.d.
2ᵃ	Ph	/	-"-	o-xylene	150	48	/	5%
3ᵃ	Ph	4-tert-butylstyrene (0.10)	-"-	dioxane	-"-	16	/	23%
4ᵃ	Ph	-"-	-"-	-"-	-"-	48	/	22%
5ᵃ	Ph	(EtO)₂P(O)OH (0.20)	-"-	-"-	90	16.5	/	traces
6ᵃ	Ph	B₂pin₂ (0.10)	-"-	-"-	-"-	16	/	23%
7ᵃ	Ph	-"-	-"-	-"-	110	-"-	/	48%
8ᵃ	Ph	-"-	-"-	-"-	150	-"-	/	63%
9ᵃ	Ph	-"-	-"-	PhMe	150	-"-	/	72%
10ᵃ	Ph	-"-	-"-	o-xylene	-"-	-"-	/	64%
11ᵃ	Ph	-"-	H (2.0)	dioxane	-"-	-"-	/	88%
12ᵃ	**Ph**	**B₂pin₂ (0.10)**	**tBu (2.0)**	**-"-**	**-"-**	**-"-**	**/**	**94%**
13ᵃ	Me	(EtO)₂P(O)OH (0.20)	H (3.0)	-"-	90	16.5	/	traces
14ᵃ	Me	B₂pin₂ (0.10)	-"-	-"-	-"-	16	93/7	68%
15ᵃ	Me	-"-	-"-	-"-	110	-"-	91/9	70%
16ᵃ	**Me**	**-"-**	**-"-**	**-"-**	**150**	**-"-**	**90/10**	**81%**
17ᵃ	Me	-"-	-"-	PhMe	-"-	-"-	96/4	53%
18ᵃ	Me	-"-	-"-	o-xylene	-"-	-"-	98/2	56%
19ᵃ	Me	-"-	H (2.0)	dioxane	-"-	-"-	90/10	52%
20ᵃ	Me	-"-	tBu (2.0)	-"-	-"-	-"-	90/10	63%

Table 2.10. Evaluation of reaction conditions for 1,1-disubstituted substrates.

a) Scale: typically 0.2 mmol of substrate. Yields were determined by analysis of ^{1}H NMR spectra using 0.25 equiv of 1,3,5-trimethoxybenzene as an internal standard.

2.4.3. Mechanistic Investigations

2.4.3.1. Preparation of mono-deuterated styrenes and product (*Z*)-**3a**

trimethyl(phenylethynyl)silane SI1
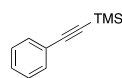
The compound was prepared according to a modified literature procedure.[88] Under a nitrogen atmosphere, to a solution of phenylacetylene (5.5 mL, 5.1 g, 50.0 mmol, 1.0 equiv) in dry THF (50 mL) at -78 °C, *n*-BuLi (1.6 M in hexanes, 34.4 mL, 55.0 mmol, 1.1 equiv) was added dropwise over the course of 20 min. After stirring at -78 °C for 30 min, trimethylsilyl chloride (7.6 mL, 6.5 g, 60.0 mmol, 1.2 equiv) was added over the course of 15 min. After stirring at -78 °C for 50 min, the reaction mixture was allowed to warm to room temperature and allowed to stir at this temperature for 2 h. Upon quenching with sat. aqueous NH₄Cl solution (40 mL) at 0 °C, the phases were separated, and the aqueous phase was washed with diethyl ether (2 x 60 mL). The combined organic phases were washed with brine (40 mL) and dried over Na₂SO₄. After filtration, the volatiles of the filtrate were removed under reduced pressure to give the title compound (8.5 g, 4.9 mmol, 98%) as a colorless oil. The NMR data match previously reported data for the title product.[88]

¹H NMR (400 MHz, CDCl₃) δ 7.53 – 7.42 (m, 2H), 7.33 – 7.27 (m, 3H), 0.25 (s, 9H).

The following compounds were prepared according to a literature procedure:[89]

(*Z*)-trimethyl(2-phenylvinyl-1-*d*)silane (*Z*)-SI2
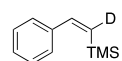
Under a nitrogen atmosphere, to an oven-dried round-bottom flask under a nitrogen-atmosphere were added dry THF (1.75 mL) and dibal-H (1 M in hexanes, 10 mL, 10.0 mmol, 2.0 equiv). The reaction mixture was cooled down to 0 °C and trimethyl(phenylethynyl)silane (**SI1**, 979 μL, 871 mg, 5.0 mmol, 1.0 equiv) was added dropwise. The mixture was allowed to stir at 55 °C for 23 h. The reaction was quenched upon dropwise addition of D₂O (180 μL, 200 mg, 10.0 mmol, 2.0 equiv) at 0 °C. The mixture was allowed to stir at room temperature for 1 h. The mixture was transferred to a separatory funnel after which a sat. solution of Rochelle's salt (20 mL) and sat. aqueous NH₄Cl solution (20 mL) were added. The phases were separated. The aqueous phase was washed with diethyl ether (3 x 20 mL) and the combined organic phases were dried over Na₂SO₄. After filtration, the volatiles of the filtrate were removed under reduced pressure to give the title compound (789 mg, 4.4 mmol, 89%, 96% D) as a colorless oil which was used in the next step without further purification.

¹H NMR (400 MHz, CDCl₃) δ 7.37 – 7.15 (m, 6H), 0.03 (s, 9H).

trans*-styrene-(β)-*d* (*E*)-1a-β-*d
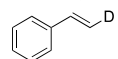
To (*Z*)-trimethyl(2-phenylvinyl-1-*d*)silane ((*Z*)-**SI2**, 1.05 g, 6.0 mmol, 1.0 equiv), TBAF (1 M in THF, 9 mL, 9.0 mmol, 1.5 equiv) was added under a nitrogen atmosphere. The mixture was allowed to stir at 60 °C for 18 h. After cooling to room temperature, water was added. The phases were separated. The aqueous phase was washed with diethyl ether (3 x 25 mL). The combined organic phases were dried over Na₂SO₄ and the volatiles were carefully removed under reduced pressure. The resulting yellow oil was subjected to Kugelrohr distillation to isolate the title compound (299.0 mg, 2.8 mmol, 47% yield, 98:2 *E*:*Z*, 96% D, purity by GC-FID analysis: 96%) as a light yellow liquid. The NMR data match previously reported data for the title product.[89]

¹H NMR (500 MHz, CDCl₃) δ 7.49 – 7.37 (m, 2H), 7.32 (t, *J* = 7.5 Hz, 2H), 7.27 – 7.21 (m, 1H), 6.78 – 6.64 (m, 1H), 5.77 – 5.68 (m, 1H).

(*E*)-trimethyl(2-phenylvinyl-1-*d*)silane (*E*)-SI2
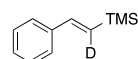
To an oven-dried round-bottom flask under a nitrogen-atmosphere was added dibal-H (1 M in hexanes, 10 mL, 10.0 mmol, 2.0 equiv). Trimethyl(phenylethynyl)silane (**SI1**, 979 μL, 871 mg, 5.0 mmol, 1.0 equiv) was added dropwise at 0 °C. The reaction mixture was allowed to stir at 55 °C for 23 h. The reaction was quenched upon dropwise addition of D₂O (180 μL, 200 mg, 10.0 mmol, 2.0 equiv) at 0 °C. The mixture was allowed to stir at room temperature for 1 h. The mixture was transferred to a separatory funnel after which a sat. solution of Rochelle's salt (20 mL) and sat. aqueous NH₄Cl solution (20 mL) were added. The phases were separated. The aqueous phase was washed with diethyl ether (3 x 20 mL) and the combined organic phases were dried over Na₂SO₄. After filtration, the volatiles of the filtrate were removed under reduced pressure to give the title compound (832 mg, 4.7 mmol, 94%, 80% D) as a yellowish oil which was used in the next step without further purification.

¹H NMR (400 MHz, CDCl₃) δ 7.48 – 7.38 (m, 2H), 7.36 – 7.27 (m, 3H), 6.89 – 6.83 (m, 1H), 0.16 (s, 9H).

cis*-styrene-(β)-*d* (*Z*)-1a-β-*d

To (*E*)-trimethyl(2-phenylvinyl-1-*d*)silane ((*E*)-**SI2**, 850 mg, 4.8 mmol, 1.0 equiv), TBAF (1 M in THF, 7.2 mL, 7.2 mmol, 1.5 equiv) was added under a nitrogen atmosphere. The mixture was allowed to stir at 75 °C for 18 h. After cooling to room temperature, water was added. The phases were separated. The aqueous fraction was washed with diethyl ether (3 x 25 mL). The combined organic phases were dried over Na₂SO₄. After filtration, the volatiles from the filtrate were carefully removed under reduced pressure. The resulting yellow oil was subjected to Kugelrohr distillation to isolate the title compound (202.3 mg, 1.9 mmol, 40%, 96:4 *Z*:*E*, 80% D, purity by GC-FID analysis: 87%) as a light pink liquid. The NMR data match previously reported data for the title product.[89]

¹H NMR (500 MHz, CDCl₃) δ 7.41 (dd, *J* = 7.0, 1.5 Hz, 2H), 7.32 (td, *J* = 6.8, 1.8 Hz, 2H), 7.29 – 7.11 (m, 1H), 6.79 – 6.59 (m, 1H), 5.26 – 5.19 (m, 1H).

**(*Z*)-4,4,5,5-tetramethyl-2-styryl-1,3,2-dioxaborolane (*Z*)-3a**
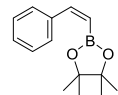
The compound was prepared in accordance to a modified literature procedure.[90] [Rh(cod)Cl]₂ (9.6 mg, 19.5 μmol, 0.01 equiv), triisopropylphosphine (22.4 μL, 18.8 mg, 117 μmol, 0.06 equiv), triethylamine (1.36 mL, 988 mg, 9.77 mmol, 5.0 equiv), HBpin (250 mg, 283 μL, 1.95 mmol, 1.0 equiv) in cyclohexane (5.9 mL) were allowed to stir at room temperature for 30 minutes under a nitrogen atmosphere. A solution of phenylacetylene (257 μL, 239 mg, 2.34 mmol, 1.2 equiv) in cyclohexane (1.0 mL) was added, and the resulting mixture was allowed to stir for 4 h at room temperature. The reaction was quenched by addition of MeOH (3 mL). The reaction mixture was filtered over celite (Et₂O, 100 mL). The filtrate was concentrated under reduced pressure, and the residue was subjected to column chromatography (silica, 5% EtOAc in petroleum ether) to isolate the title compound (94:6 = *Z*:*E*, 145 mg, 631 μmol, 32%) as a brown oil. The NMR data match previously reported data for the title product.[91]

¹H NMR (500 MHz, CDCl₃) δ 7.57 – 7.52 (m, 2H), 7.34 – 7.25 (m, 3H), 7.22 (d, *J* = 14.9 Hz, 1H), 5.60 (d, *J* = 14.9 Hz, 1H), 1.30 (s, 12H).

2.4.3.2. Experiments with isotope-labeled starting materials or potential products

The experiments described below are shown in **Figure 2.4b** in the main text.
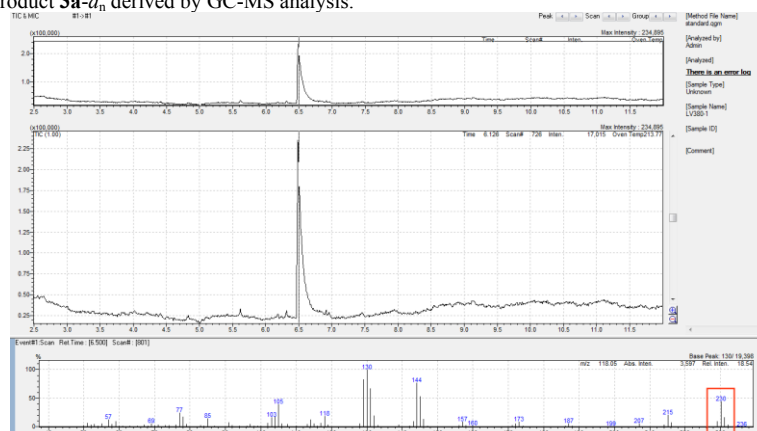(1)
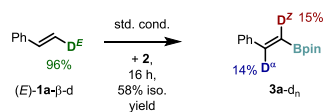
The experiment was performed according to general procedure 1 by reaction of *trans*-styrene-(β)-*d* (21.0 mg, 200 μmol) with vinyl Bpin (46.2 mg, 300 μmol) and the product was isolated by column chromatography (silica gel, 0 – 4.6% MTBE in petroleum ether) to give a colorless oil (26.7 mg, 116 μmol, 58%).
¹H NMR (CDCl₃, 500 MHz):

Figure 2.9: Partial deuterium retaining in **3a** in the reaction of (*E*)-**1a**-β-*d* detected by ¹H-NMR spectroscopy.
Isotopomeric cluster of product **3a**-*d*ₙ derived by GC-MS analysis:

For comparison, the isotopomeric cluster of non-deuterated product **3a** derived by GC-MS analysis:
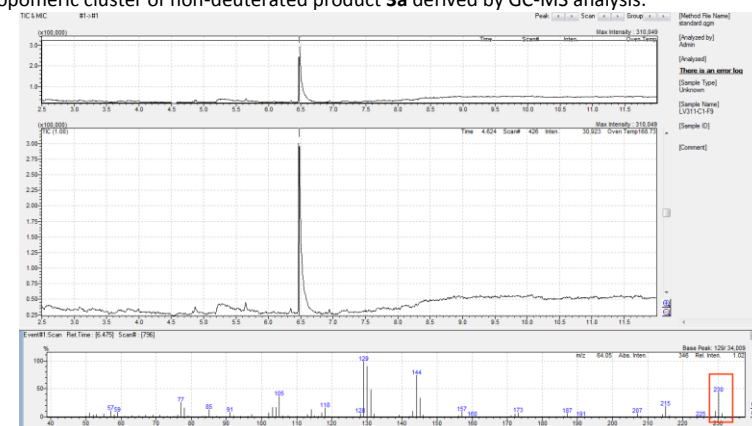
Figure 2.10: Partial deuterium retaining in **3a** in the reaction of (*E*)-**1a**-β-*d* detected by GC-MS analysis.

(2)
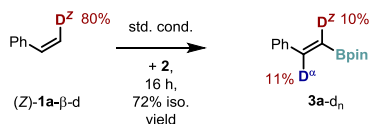
The experiment was performed according to general procedure 1 by reaction of *cis*-styrene-(β)-*d* (21.0 mg, 200 μmol) with vinyl Bpin (46.2 mg, 300 μmol) and the product was isolated by column chromatography (silica gel, 0 – 5.2% MTBE in petroleum ether) to give a colorless oil (33.1 mg, 144 μmol, 72%).

¹H NMR (CDCl₃, 500 MHz):
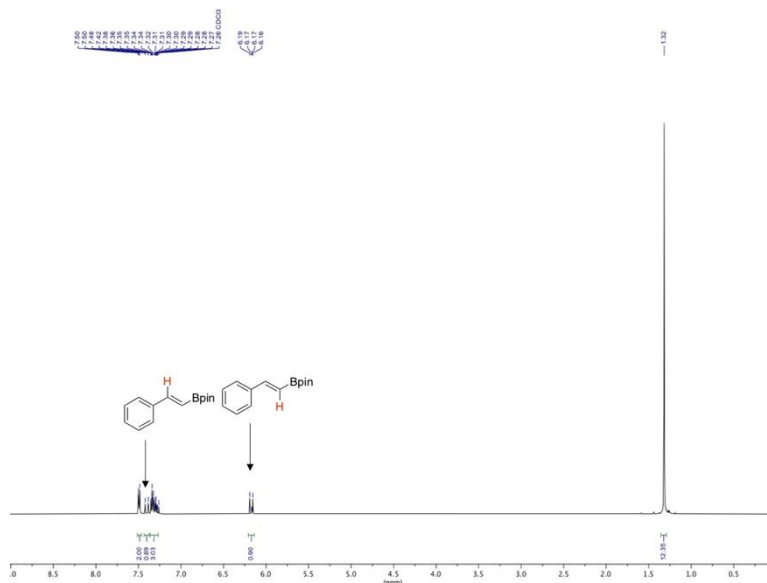
Figure 2.11: Partial deuterium retaining in **3a** in the reaction of (*Z*)-**1a**-β-*d* detected by ¹H-NMR spectroscopy.
*Isotopomeric cluster of product **3a-dₙ** derived by GC-MS analysis:*
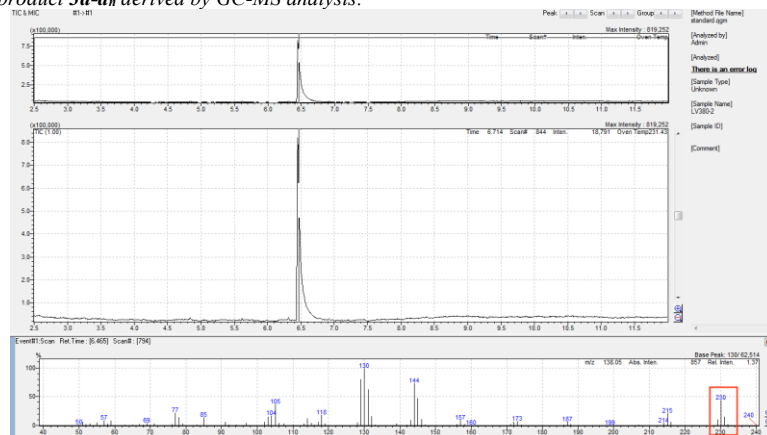
Figure 2.12: Partial deuterium retaining in **3a** in the reaction of (*Z*)-**1a**-β-*d* detected by GC-MS analysis.
For a comparison to non-deuterated product **3a**, see section (1).

(3)
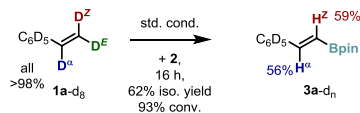
The experiment was performed according to general procedure 1 by reaction of styrene-*d₈* (22.4 mg, 200 μmol) and vinyl Bpin (46.2 mg, 300 μmol) and the product was isolated by column chromatography (silica gel, 0 – 6% MTBE in petroleum ether) to give a red oil (30.1 mg, 124 μmol, 62%).

A second reaction was performed with mesitylene (6.9 μL, 6.0 mg, 50 μmol, 0.25 equiv) as an internal standard and a GC-FID analysis of the crude reaction mixture was performed.

The ¹H NMR of the isolated product shows the deuterium incorporation in the olefinic protons.

¹H NMR (CDCl₃, 500 MHz):
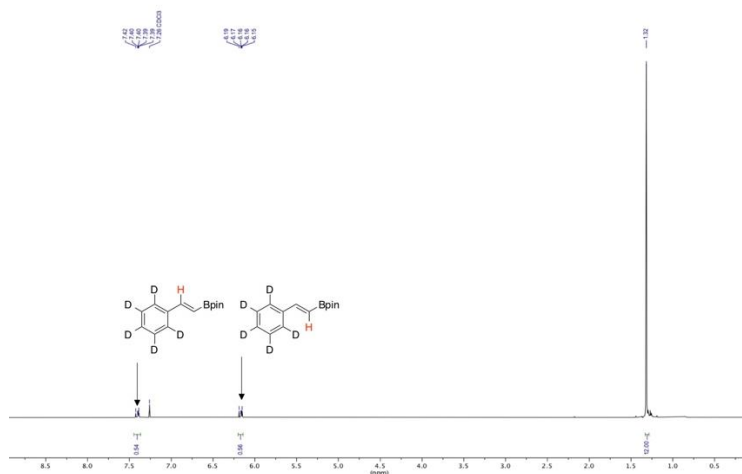
Figure 2.13: Partial deuterium retaining in **3a** in the reaction of **1a**-d_8 detected by ¹H-NMR spectroscopy.
The conversion of styrene (93%) was determined by GC-FID analysis using a calibration for styrene with mesitylene as an internal standard.
Isotopomeric cluster of product **3a**-d_n derived by GC-MS analysis:
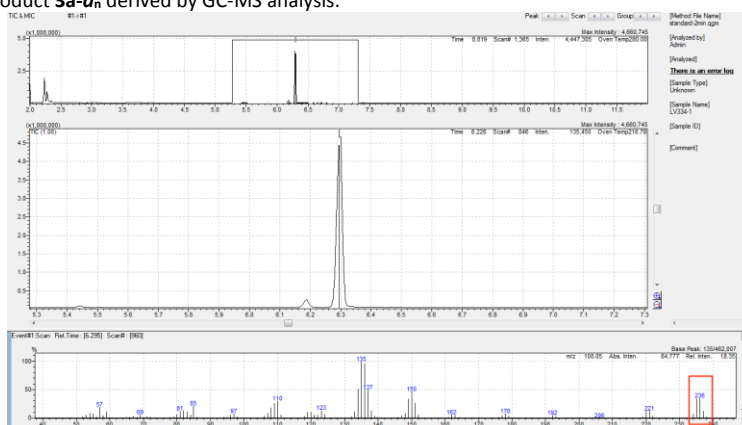
Figure 2.14: Partial deuterium retaining in **3a** in the reaction of **1a**-d_8 detected by GC-MS analysis.
For a comparison to non-deuterated product **3a**, see section (1).

 (4)
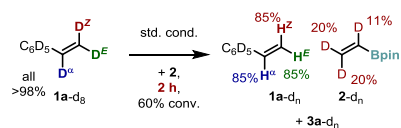
In a nitrogen-filled glove box, a 10 mL screw-cap vial equipped with a Teflon-coated magnetic stirring bar was charged with [Rh(COD)OMe]₂ (3.9 mg, 8 μmol, 2 mol%), xantphos (9.3 mg, 16 μmol, 4 mol%), dioxane (400 μL), benzene-d_6 (40 μL), vinyl Bpin (92.4 mg, 600 μmol, 1.5 equiv), styrene-d_8 (44.9 mg, 400 μmol, 1.0 equiv) and mesitylene (13.8 μL, 12.0 mg, 100 μmol, 0.25 equiv). The vial was sealed with a cap, removed from the glove box, placed in a pre-heated aluminum block, and allowed to stir (800 rpm) at 90 °C for 2 h. Upon cooling to room temperature, the reaction mixture was subjected to GC-FID and NMR analysis.

¹H NMR (1,4-dioxane, C₆D₆, 500 MHz) – full spectrum:
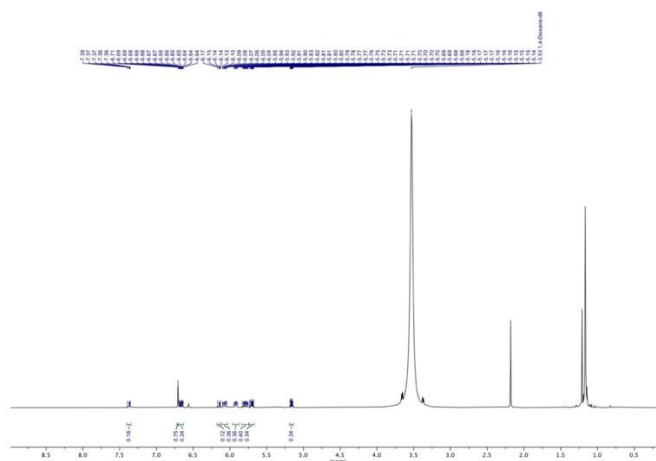
Figure 2.15: Partial deuterium retaining in **3a** and deuterium incorporation into **2** in the reaction of **1a**-d_8 detected by ¹H NMR spectroscopy.

¹H NMR (1,4-dioxane, C₆D₆, 500 MHz) – zoom:
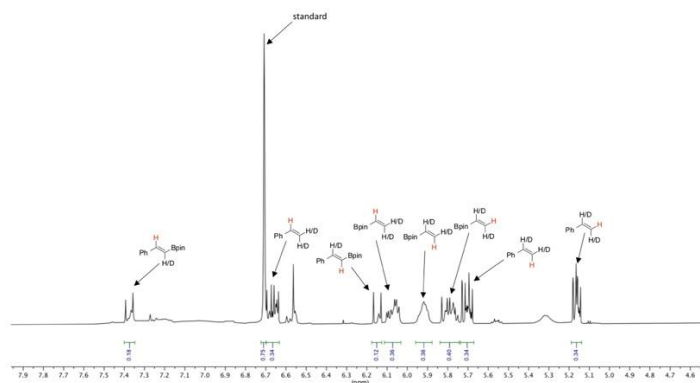
Figure 2.16: Partial deuterium retaining in **3a** and deuterium incorporation into **2** in the reaction of **1a**-d_8 detected by ¹H NMR spectroscopy.

The conversion of styrene (60%) and vinyl Bpin (55%) was determined by GC-FID analysis using a calibration for styrene and vinyl Bpin with mesitylene as an internal standard. Together with the integrals shown in the ¹H NMR spectra, the H/D ratio for the indicated positions was calculated.

Isotopomeric cluster of **1a**-d_n derived by GC-MS analysis:
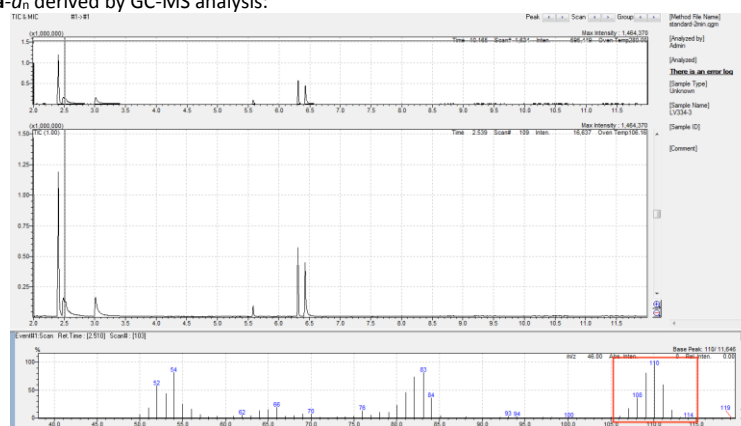
For comparison, the isotopomeric cluster of deuterated styrene-d_8 **1a**-d_8 derived by GC-MS analysis:
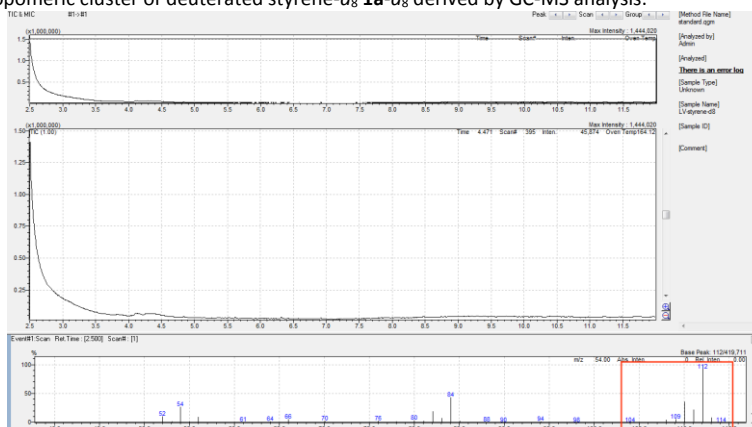
For comparison, isotopomeric cluster of non-deuterated styrene **1a** derived by GC-MS analysis:

Isotopomeric cluster of **2-d_n** derived by GC-MS analysis:
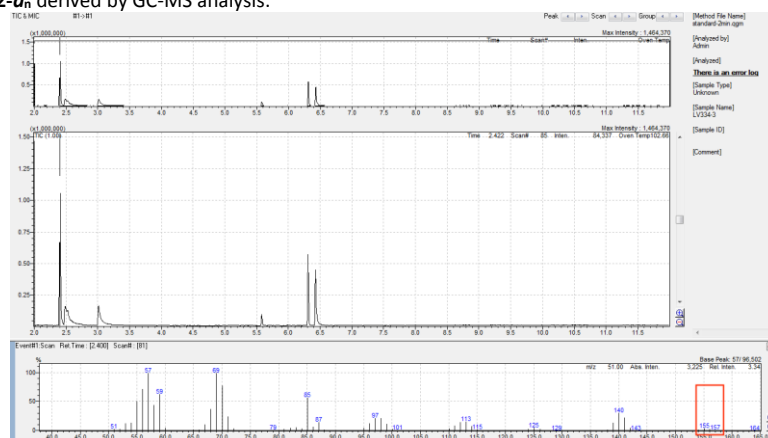
For comparison, the isotopomeric cluster of non-deuterated **2** derived by GC-MS analysis:
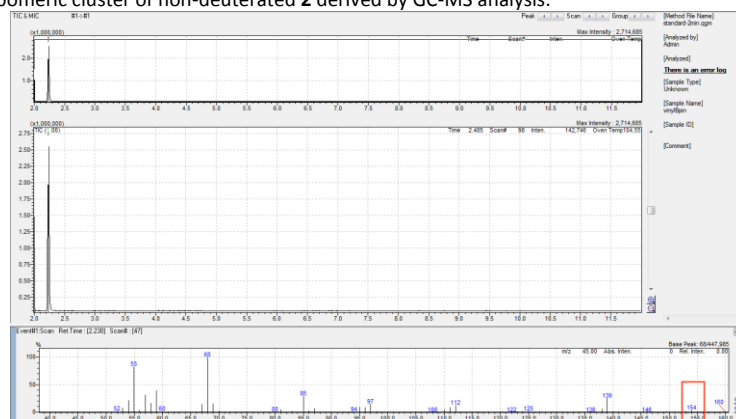
Figure 2.17: Partial deuterium retaining in **3a** and deuterium incorporation into **2** in the reaction of **1a**-d_8 detected by GC-MS analysis. *(5)*
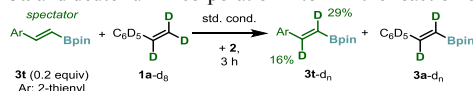
In a nitrogen-filled glove box, styrene-d_8 (22.4 mg, 200 µmol, 1.0 equiv) was added to a mixture of (*E*)-4,4,5,5-tetramethyl-2-(2-(thiophen-2-yl)vinyl)-1,3,2-dioxaborolane (**3t**, 9.2 mg, 40.0 µmol, 0.20 equiv) xantphos (4.6 mg, 8.00 µmol, 0.04 equiv), [Rh(COD)OMe]₂ (1.9 mg, 4.00 µmol, 0.02 equiv), and vinyl Bpin (46.2 mg, 300 µmol, 1.5 equiv) in dioxane (200 µL) in a 10 mL screw-cap vial equipped with a Teflon-coated magnetic stirring. The vial was sealed with a cap, removed from the glove box, placed in a pre-heated aluminum block and allowed to stir (800 rpm) at 90 °C for 3 h. Upon cooling to room temperature, a standard solution (100 µL of 0.5 M mesitylene in chloroform) and CDCl₃ (400 µL) were added to the reaction mixture. An aliquot was taken and submitted to GC-FID revealing the conversion of styrene-d_8 to be 70%. The solvent of the crude product was removed, and the residue was subjected to column chromatography (silica, 0 – 10% MTBE in petroleum ether) to yield a mixture of the partially deuterated spectator **3t**-d_n and partially deuterated product **3a**-d_n (28.1 mg, pale yellow oil).

¹H NMR (CDCl$_3$/CHCl$_3$/dioxane, 400 MHz):
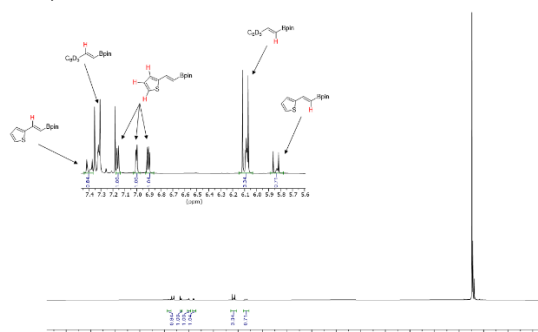
Figure 2.18: Partial deuterium incorporation in spectator **3t** in the reaction of **1a**-d_8 detected by ¹H-NMR spectroscopy.
Isotopomeric cluster of product **3t** derived by GC-MS analysis:
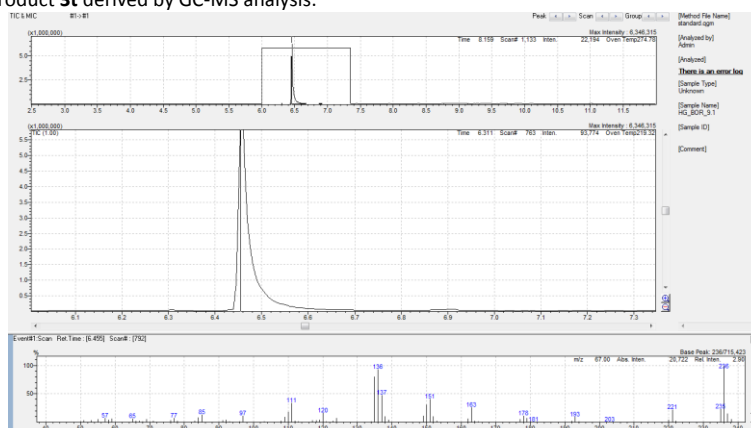
Isotopomeric cluster of spectator **3t**-d_n after the reaction derived by GC-MS analysis:
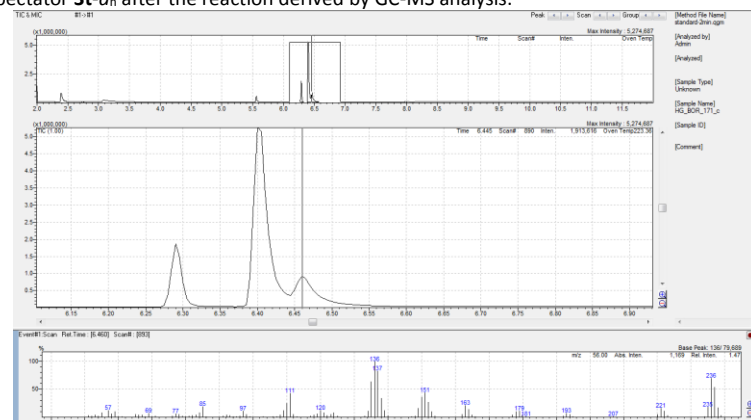
Figure 2.19: Partial deuterium incorporation in spectator **3t** in the reaction of **1a**-d_8 detected by GC-MS analysis. When product **3k** (0.2 equiv) was added as a spectator in an analogous way, deuterium incorporation was also confirmed with GC-MS analysis:
Isotopomeric cluster of product **3k** derived by GC-MS analysis:
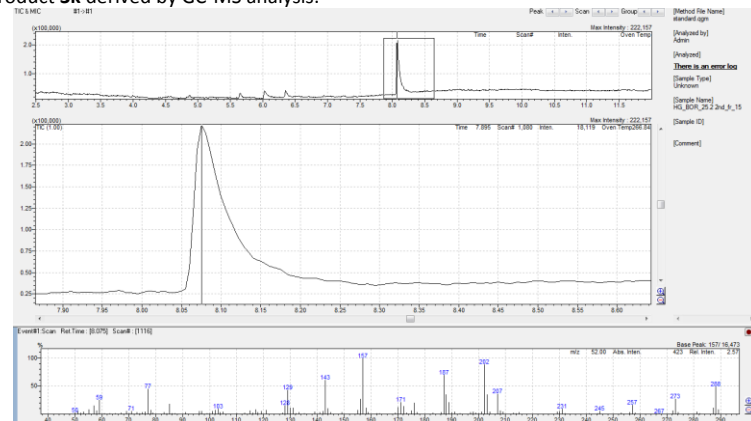
Isotopomeric cluster of spectator **3k**-*d*ₙ after the reaction derived by GC-MS analysis:
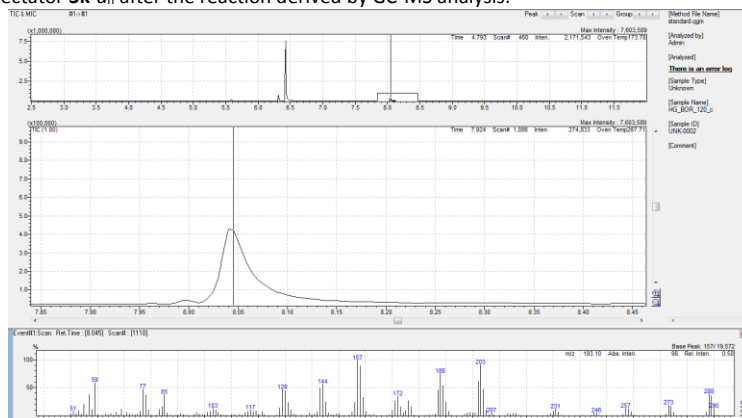
Figure 2.20: Partial deuterium incorporation in spectator **3k** in the reaction of **1a**-*d*₈ detected by GC-MS analysis.

(6)
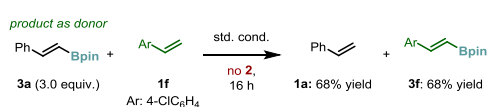
The experiment was performed according to general procedure 2 by reaction of *p*-chlorostyrene (**1f**, 27.7 mg, 200 µmol) and *trans*-2-phenylvinyl Bpin (**3a**, 138.1 mg, 600 µmol). Upon cooling to room temperature, a standard solution (100 µL of 0.5 M 1,3,5-trimethoxybenzene in chloroform) and CDCl₃ (400 µL) were added to the reaction mixture. The yield was determined by the ratio the integrals of the internal standard's aromatic signal and an isolated product's signal in a ¹H NMR experiment.

¹H NMR (CDCl₃, CHCl₃, 1,4-dioxane, 400 MHz):
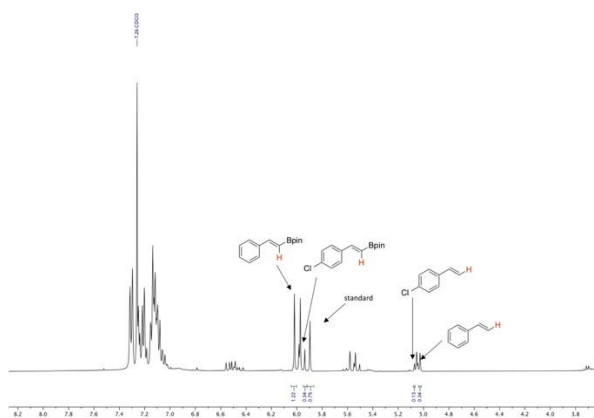
Figure 2.21: ¹H-NMR of reaction (6) after 16 h.

The experiments described below are shown in the manuscript in **Figure 2.6** in the main text.
(1)
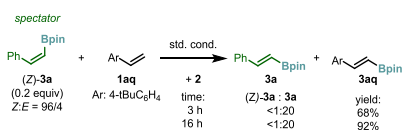
In a nitrogen-filled glove box, 4-*tert*-butylstyrene (32.1 mg, 200 µmol, 1.0 equiv) was added to a mixture of (*Z*)-4,4,5,5-tetramethyl-2-styryl-1,3,2-dioxaborolane ((*Z*)-**3a**, 9.2 mg, 40.0 µmol, 0.20 equiv), xantphos (4.6 mg, 8.00 µmol, 0.04 equiv), [Rh(COD)OMe]₂ (1.9 mg, 4.00 µmol, 0.02 equiv), and vinyl Bpin (46.2 mg, 300 µmol, 1.5 equiv) in dioxane (200 µL) in a 10 mL screw-cap vial equipped with a Teflon-coated magnetic stirring. The vial was sealed with a cap, removed from the glove box, placed in a pre-heated aluminum block and allowed to stir (800 rpm) at 90 °C for 3 or 16 h. Upon cooling to room temperature, a standard solution (100 µL of 0.5 M 1,3,5-trimethoxybenzene in chloroform) and CDCl₃ (400 µL) were added to the reaction mixture. The yield was determined by the ratio the integrals of the internal standard's aromatic signal and a product's signal in a ¹H NMR experiment (see below).

63

After 3 h: **¹H NMR** (CDCl₃/CHCl₃/dioxane, 400 MHz):

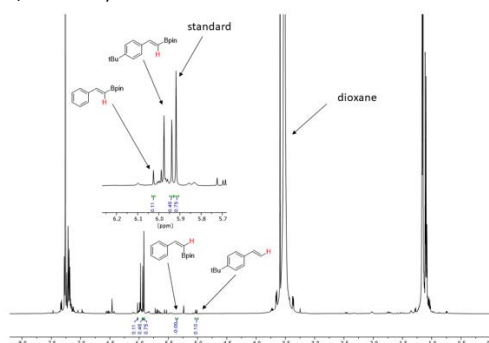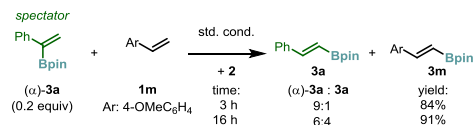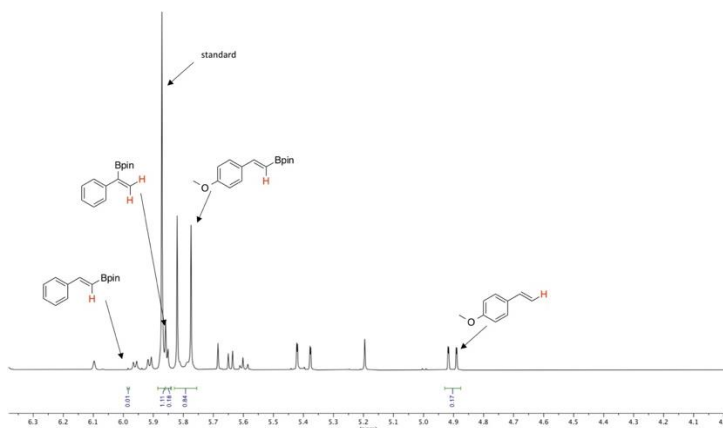After 16 h: **¹H NMR** (CDCl₃/CHCl₃/dioxane, 500 MHz)

Figure 2.22: ¹H-NMR of reaction (7) after 3 h (top) and 16 h (bottom).

(2)

In a nitrogen-filled glove box, a 10 mL screw-cap vial equipped with a Teflon-coated magnetic stirring bar was charged with [Rh(COD)OMe]₂ (1.9 mg, 4 μmol, 2 mol%), xantphos (4.6 mg, 8 μmol, 4 mol%), 1,4-dioxane (200 μL), vinyl Bpin (46.2 mg, 300 μmol, 1.5 equiv), *p*-methoxystyrene (26.8 mg, 200 μmol, 1.0 equiv) and 1-phenylvinyl Bpin (9.2 mg, 40 μmol, 0.2 equiv). The vial was sealed with a cap, removed from the glove box, placed in a pre-heated aluminum block and allowed to stir (800 rpm) at 90 °C for 3 or 16 h. Upon cooling to room temperature, a standard solution (100 μL of 0.5 M 1,3,5-trimethoxybenzene in chloroform) and CDCl₃ (400 μL) were added to the reaction mixture. The yield was determined by the ratio the integrals of the internal standard's aromatic signal and a product's signal in a ¹H NMR experiment (see below).

After 3 h: **¹H NMR** (CDCl₃/CHCl₃/1,4-dioxane, 400 MHz):

After 16 h: **¹H NMR** (CDCl₃/CHCl₃/1,4-dioxane, 500 MHz):
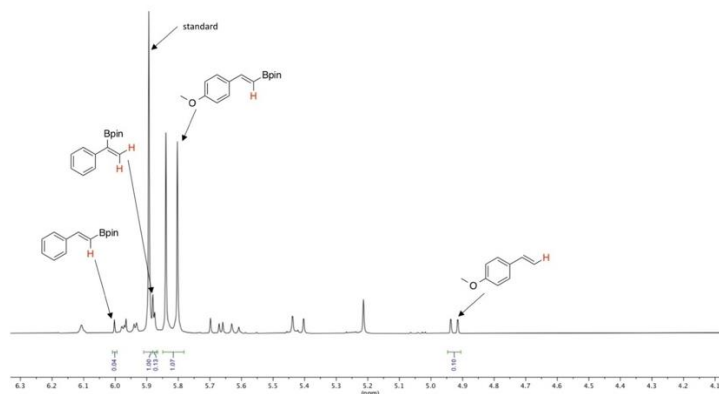
Figure 2.23: ^{1}H NMR of reaction (8) after 3 h (top) and 16 h (bottom).

2.4.3.3. Kinetic experiments

Without B_2pin_2:
In a nitrogen-filled glove box, a 4 mL screw-cap vial was charged with [Rh(COD)OMe]$_2$ (3.9 mg, 8 μmol, 2 mol%), xantphos (9.3 mg, 16 μmol, 4 mol%), 1,4-dioxane (400 μL), benzene-d_6 (60 μL), vinyl Bpin (92.4 mg, 600 μmol, 1.5 equiv), styrene (41.7 mg, 400 μmol, 1.0 equiv), and mesitylene (13.8 μL, 12.0 mg, 100 μmol, 0.25 equiv). The reaction mixture was transferred to a J. Young NMR tube with a pipette, sealed with a cap and removed from the glove box. The NMR tube was then placed in a NMR spectrometer, heated to 76.1 °C, and the progress of the reaction was followed by measuring ^{1}H NMR spectra for 16 h.

With B_2pin_2:
In a nitrogen-filled glove box, a 4 mL screw-cap vial was charged with [Rh(COD)OMe]$_2$ (3.9 mg, 8 μmol, 2 mol%), xantphos (9.3 mg, 16 μmol, 4 mol%), B_2pin_2 (5.1 mg, 20 μmol, 5 mol%), 1,4-dioxane (400 μL), benzene-d_6 (60 μL), vinyl Bpin (92.4 mg, 600 μmol, 1.5 equiv), styrene (41.7 mg, 400 μmol, 1.0 equiv) and mesitylene (13.8 μL, 12.0 mg, 100 μmol, 0.25 equiv). The reaction mixture was transferred in a J. Young NMR tube with a pipette, sealed with a cap and removed from the glove box. The NMR tube was then placed in a NMR spectrometer, heated to 76.1 °C and the progress of the reaction was followed by measuring ^{1}H NMR spectra for 16 h.
The conversion of starting materials and yield of products were determined by the ratio of the integrals of the internal standard's aromatic signal (s, 6.64 ppm) and olefinic signals of starting materials (styrene: dd, 4.98 ppm, vinyl Bpin: m, 5.78 – 5.68 ppm), (*E*)-1,2-bis(4,4,5,5-tetramethyl-1,3,2-dioxaborolan-2-yl)ethene (s, 6.40 ppm) and product (d, 5.96 ppm). The results of the kinetic experiments are depicted in Figure 2.3 and discussed in the manuscript.
Discussion:
As shown in Figure 2.24, the presence of co-catalytic B_2pin_2 is beneficial for the activity of the catalyst in the model reaction. Following the reaction both with and without B_2pin_2 in time using in situ ^{1}H NMR spectroscopy revealed that the reaction in the presence of small amounts of B_2pin_2 occurred with over 2-fold higher rate than the analogous reaction in its absence. Most likely, the reason for the increased rate is the higher level of pre-catalyst activation by B_2pin_2. Interestingly, in the initial phase of the reaction, the boryl group transfer occurred largely to form vinyl (*E*)-1,2-bisboronate **4**, which was followed by the phase of the formation of product **3a** and the consumption of **4**.
It should be noted that a control experiment showed that B_2pin_2 cannot be used as the borylation reagent instead of vinyl Bpin. In the experiment using a stoichiometric amount of B_2pin_2 instead of vinyl Bpin **2**, only traces of the product were formed.
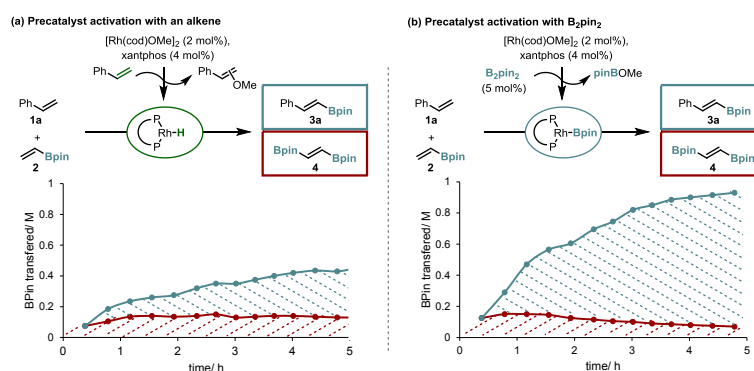

Figure 2.24: Evaluation of an alternative precatalyst activation – influence of catalytic amounts of B_2pin_2.

2.4.3.4. Formation of ethylene under reaction reactions

In a nitrogen-filled glove box, a 4 mL screw-cap vial was charged with [Rh(COD)OMe]$_2$ (3.9 mg, 8 μmol, 2 mol%), xantphos (9.3 mg, 16 μmol, 4 mol%), 1,4-dioxane (400 μL), toluene-d_8 (400 μL), vinyl Bpin (92.4 mg, 600 μmol, 1.5 equiv) and styrene (41.7 mg, 400 μmol, 1.0 equiv). The reaction mixture was transferred to a J. Young NMR tube with a pipette, sealed with a cap and removed from the glove box. The NMR tube was then placed in a pre-heated aluminum block and heated at 90 °C for 16 h. Subsequently, the reaction mixture was allowed to cool down and a ^{1}H NMR spectrum was measured.
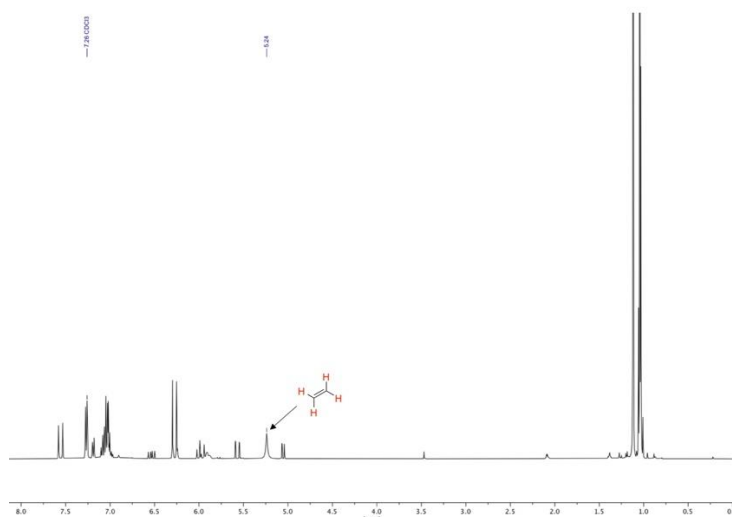**^{1}H NMR** (1,4-dioxane/toluene-d_8, 400 MHz):

Figure 2.25: Formation of ethylene as detected by ^{1}H-NMR spectroscopy.

As shown in Figure 2.25, the formation of ethylene in a standard reaction can be confirmed by the broad singlet at 5.24 ppm, in accordance to the literature.[92] A quantification cannot be conducted because of the headspace of the J. Young NMR tube.

2.4.3.5. Formation of Rh–H

In a nitrogen-filled glove box, a 4 mL screw-cap vial was charged with [RhCl(C$_2$H$_4$)]$_2$ (1.6 mg, 4 μmol, 0.5 equiv), xantphos (4.6 mg, 8 μmol, 1.0 equiv), PCy$_3$ (2.2 mg, 8 μmol, 1.0 equiv), NaOMe (0.4 mg, 8 μmol, 1.0 equiv) or NaOtBu (0.8 mg, 8 μmol, 1.0 equiv), toluene-d_8 (375 μL), alkene (8 μmol, 1.0 equiv), and isochroman (0.50 μL, 0.5 mg, 4 μmol, 0.5 equiv) as an internal standard. The reaction mixture was transferred to a J. Young NMR tube with a pipette, sealed with a cap and removed from the glove box. The NMR tube was then kept at the indicated temperature, and it was occasionally transferred to a NMR spectrometer to collect the NMR data.
^{1}**H NMR** (toluene-d_8, 500 MHz):
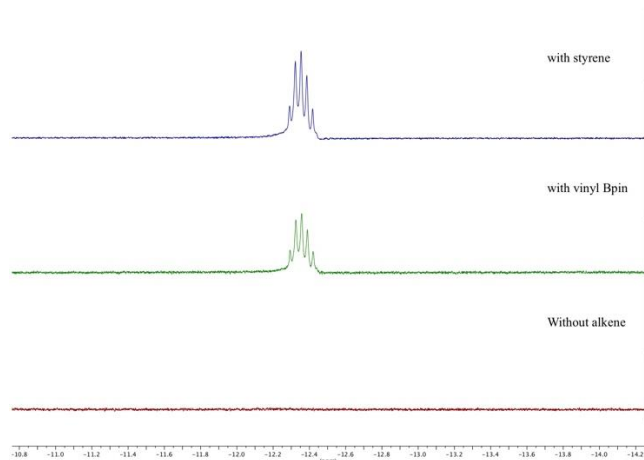
Figure 2.26: Formation of [Rh]–H species as detected by ^{1}H-NMR spectroscopy.

As judged by the appearance of a characteristic quintet hydride signal (quint, -12.35 ppm, J = 15.5 Hz) in the ^{1}H NMR spectra, the formation of Rh-hydride complexes is rather fast (<2 h at room temperature), but the process requires the presence of an alkene. Figure 2.26 contains representative ^{1}H NMR spectra of three analogues reactions with either styrene (top) or vinyl Bpin (middle) as an alkene additive, or without any alkene additive (bottom) in experiments at room temperature after 2 h. A Rh-hydride signal is observed only in experiments with an alkene present, albeit different yields are observed for different alkenes (styrene: 16%, vinyl Bpin: 7%). Also, no further conversion was observed upon longer reaction time or at higher temperatures. These results are consistent with the formation of a Rh-hydride species through an (intermolecular) alkene insertion-b-hydride elimination sequence, as reported by Hartwig et al for an intramolecular reaction.[93] In turn, lack of formation of the hydrides in the experiments with Rh-methoxide complex (in the absence of any alkene) suggests that an alternative mechanism involving the direct b-hydride elimination from the methoxy ligand is not operational under these conditions.
Noteworthy, additional PCy$_3$ ligand is required in order to stabilize the hydride complex, in agreement with the studies by Hartwig et al.[93]; no hydride signals were observed in analogous experiments in its absence. Unfortunately, the exact structure of the Rh-hydride complex remains unclear. We were unable to isolate or characterize the complex in situ, due to the low yield of the hydride formation as well as the presence of multiple products (as judged by ^{31}P NMR data). However, the ^{1}H-^{31}P HMBC experiment shows the coupling of the hydride signal to one phosphine signal at 17.4 ppm (d, J = 134.4 Hz, Figure 2.27). In turn, the ^{1}H{^{31}P} NMR spectrum shows a singlet for the hydride signal (Figure 2.28, top), suggesting both low rhodium-hydride coupling (J < 2 Hz) and coupling of the hydride with 4 equivalent phosphines. The coupling pattern would be consistent with a dimeric rhodium-hydride species[94]; however, formation of other complexes containing both xantphos and PCy$_3$ ligands cannot be excluded.
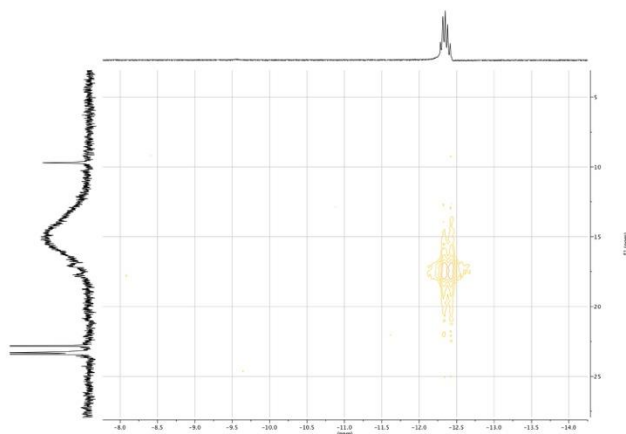
66

¹H-³¹P HMBC (toluene-d_8, 500 MHz):

Figure 2.27: ¹H-³¹P HMBC experiment shows the coupling of the hydride signal to a doublet at 17.4 ppm.

¹H and ¹H{³¹P} NMR spectra (toluene-d_8, 500 MHz):

Figure 2.28: Formation of Rh–H as detected by ³¹P-decoupled ¹H NMR spectroscopy in the reaction with styrene.

³¹P{¹H} NMR spectrum (toluene-d_8, 202 MHz):
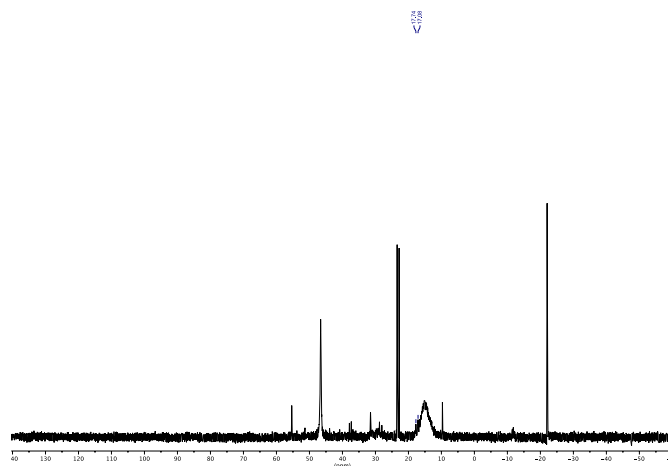
Figure 2.29: ³¹P{¹H} NMR spectrum of the reaction with styrene.

2.4.3.6. Independent Synthesis of xantphos-Rh(I)-Bpin

[Rh(xantphos)Cl]₂ SI3

The compound was prepared in accordance to a literature procedure.[93] In a nitrogen-filled glove box, [Rh(ethylene)Cl]₂ (30.0 mg, 77.1 µmol, 1.0 equiv), xantphos (89.3 mg, 154 µmol, 2.0 equiv), and THF (1.7 mL) were allowed to stir at room temperature for 23 h. The reaction mixture was concentrated to ca. 0.2 mL under reduced pressure. Et₂O (3 mL) was added. The resulting precipitate was collected by filtration, washed with Et₂O (7 mL), and dried under reduced pressure to yield a red-brown powder (61.2 mg), which was used without further purification.

For the measurement of the ³¹P{¹H} NMR spectrum, an aliquot of the product and a spatula tip of KPF₆ (as an internal standard) were dissolved in a mixture of THF-d_8/THF (1/4, 0.5 mL) (the complex dissolves only to a limited extent). Analogous spectrum was recorded in the absence of KPF₆ excluding its interference with the complex.

³¹P{¹H} NMR (162 MHz, THF-*d₈*/THF) δ 19.3 (d, *J* = 133.9 Hz).
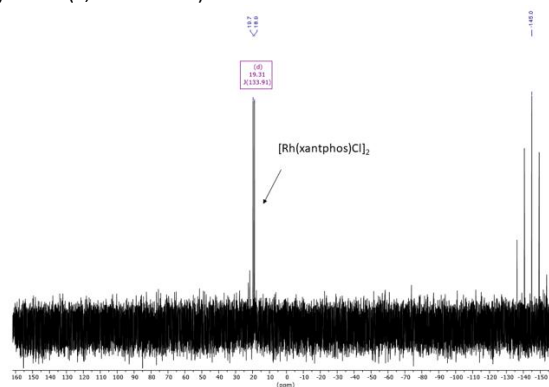
General comments on the synthesis of xantphos-Rh(I)-Bpin

Initial attempts targeting the synthesis of xantphos-Rh(I)-Bpin through the reaction of vinyl Bpin with xantphos-Rh-hydride complex prepared according to the procedure of Hartwig and co-workers[93] (without additional PPh₃ or PCy₃ ligand) or according to the procedure reported by Esteruelas and co-workers[95] for related complexes led to a complex mixture of unidentified products. Therefore, an alternative pathway through the reaction of Rh(I)-alkoxide with B₂pin₂ was devised:[96,97]
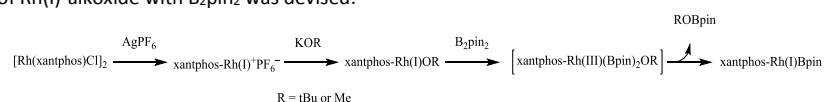
Figure 2.30: Formation of xantphos-Rh(I)-Bpin via sequential ligand exchange.

The NMR analysis and the HRMS analysis confirmed the formation of xantphos-Rh(I)-Bpin complex in the presented sequence through the transient formation of xantphos-Rh(III)(Bpin)₂OR (see below). Reductive elimination of ROBpin from the xantphos-Rh(III)(Bpin)₂OR complex was found to occur fast (<5 min at 45 °C to 1 h at room temperature, depending on the exact reaction conditions; typically transient xantphos-Rh(III)(Bpin)₂OR was not observed). However, it should be stressed out that xantphos-Rh(I)-Bpin was highly unstable so that we were unable to isolate the complex. Therefore, a series of experiments was performed to prepare and study the reactivity of xantphos-Rh(I)-Bpin complex *in situ*.

Of note, the reaction of [Rh(xantphos)Cl]₂ with AgPF₆ in THF led to a complex mixture of unidentified products, implying low stability of cationic [xantphos-Rh(I)]PF₆ complex, presumably due to its reactivity towards the C-H bond activation.[98] However, the analogous reaction in the presence of an alkoxide ligand donor (e.g., MeONa or tBuONa) led to clean conversion to the Rh(I)-alkoxide complex. Therefore, the exchange of chloride ligand for an alkoxy ligand was performed *in situ*, as described in experimental procedures below.

It should be also noted that the synthesis of xantphos-Rh(I)-Bpin proved to be sensitive even to minor changes in the procedure or the conditions, especially temperature. The reproducibility of its synthesis was improved when the solutions of B₂pin₂, KOtBu, and AgPF₆ were added in the order described in the below described representative experiment 2 (compared to experiment 1). In general, it was crucial to verify the clean formation of xantphos-Rh(I)-Bpin with NMR spectroscopy before studying its reactivity in stochiometric experiments described in section 6.6.

Below four representative experiments are described, which were used to establish the method for the *in situ* synthesis of xantphos-Rh(I)-Bpin.

Experiment 1: Synthesis of xantphos-Rh(I)-Bpin with sequential formation of xantphos-Rh(I)OtBu followed by its subsequent reaction with B₂pin₂

In a nitrogen-filled glove box, to a J-Young NMR tube charged with [Rh(xantphos)Cl]₂ (**SI3**, 6.0 mg, 4.18 μmol, 1.0 equiv), a solution of KOtBu (939 μg, 8.37 μmol, 2.0 equiv) in THF (0.1 mL), a solution of AgPF₆ (2.12 mg, 8.37 μmol, 2.0 equiv) in THF (0.1 mL), THF (0.1 mL), and THF-*d₈* (0.2 mL) were added sequentially. The NMR tube was sealed, and the reaction progress was monitored with NMR spectroscopy.

A new species was formed that was assigned to xantphos-Rh(I)-OtBu. (An analogous procedure using NaOMe and AgBF₄ led to the formation of a similar complex (~33 ppm, *J* = 200.3 Hz)).

³¹P{¹H} NMR (162 MHz, THF-*d₈*/THF) after 20 minutes:

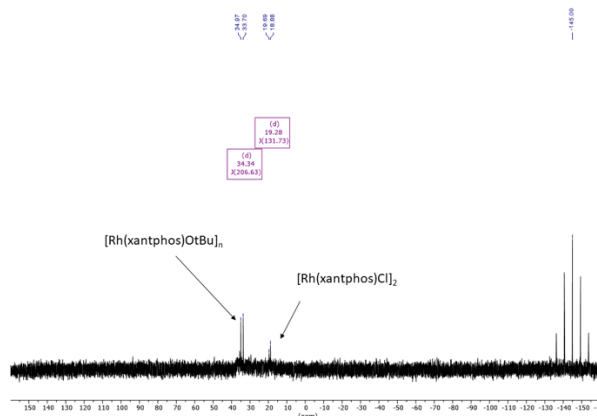**Figure 2.31:** ³¹P NMR spectrum of reaction of [Rh(xantphos)Cl]₂ with KOtBu and AgPF₆.

To this reaction mixture, a solution of B₂pin₂ (2.13 mg, 8.37 µmol, 2.0 equiv) in a mixture of THF (0.1 mL) and THF-d_8 (0.1 mL) was added (in a nitrogen filled glove box) and the reaction progress was monitored with NMR spectroscopy.

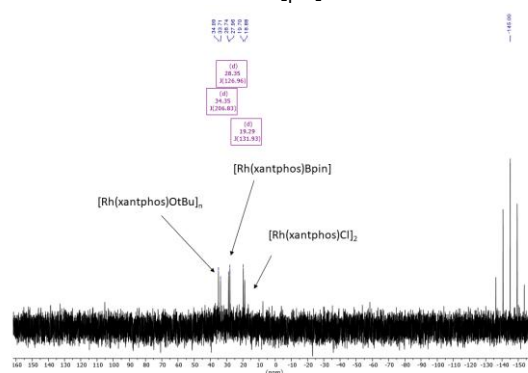**³¹P{¹H} NMR** (162 MHz, THF-d_8/THF) 11 minutes after the addition of B₂pin₂:

Figure 2.32: ³¹P NMR spectrum of reaction of [Rh(xantphos)Cl]₂ with KOtBu, AgPF₆ and B₂pin₂.

¹¹B NMR (128 MHz, THF-d_8/THF) 21 minutes after the addition of B₂pin₂:

Two signals are assigned to B₂pin₂ (31.7 ppm, literature:[99] 30.7 ppm in THF-d_8) and tBuOBPin (23.2 ppm, literature:[100] 21.4 ppm in THF-d_8).
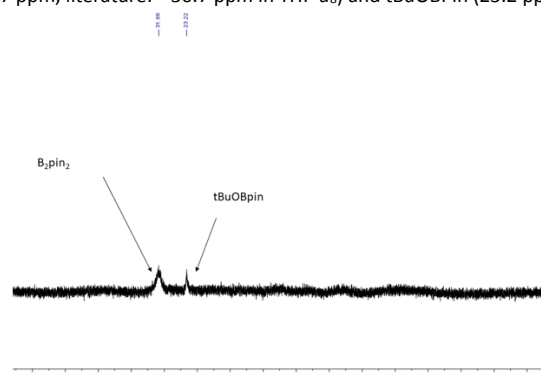

Figure 2.33: ¹¹B NMR spectrum of reaction of [Rh(xantphos)Cl]₂ with KOtBu, AgPF₆ and B₂pin₂.

¹¹B NMR (128 MHz, THF-d_8/THF) 43 minutes after the addition of B₂pin₂:

After 43 minutes, the signal of B₂pin₂ (31.7 ppm) almost vanished, while the signal of tBuOBPin (23.3 ppm) increased in intensity. The signal of xantphos-Rh(I)-Bpin complex could not be unambiguously assigned. The corresponding signals in the ¹¹B NMR spectra for related Rh(I)-Bpin complexes are typically relatively broad[101] and occur typically at 30-40 ppm.[102,103] The signal at 22.0 ppm (appearing at the shoulder of the signal of tBuOBPin) cannot be unambiguously assigned, but could correspond to B₂pin₃, a common decomposition product.[101]
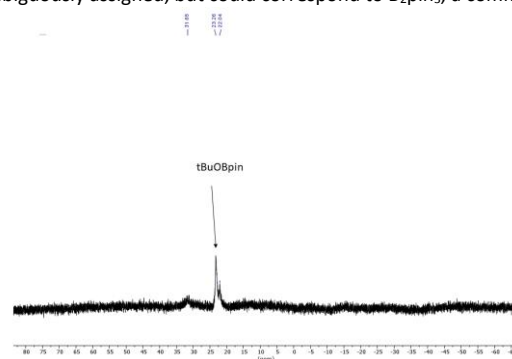

Figure 2.34: ¹¹B NMR spectrum of reaction of [Rh(xantphos)Cl]₂ with KOtBu, AgPF₆ and B₂pin₂.

³¹P{¹H} NMR (162 MHz, THF-d_8/THF) 53 minutes after the addition of B₂pin₂:

The signals of the corresponding *tert*-butoxide and chloride complexes vanished while only one signal remained that was tentatively assigned to the xantphos-Rh(I)-Bpin (see experiment 2 and chapter 6.6).
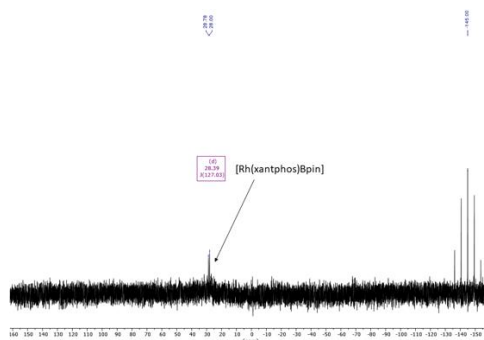
Figure 2.35: ^{31}P NMR spectrum of reaction of [Rh(xantphos)Cl]$_2$ with KOtBu, AgPF$_6$ and B$_2$pin$_2$.

Experiment 2: Direct synthesis of xantphos-Rh(I)-Bpin

In a nitrogen-filled glove box, to a J-Young NMR tube charged with [Rh(xantphos)Cl]$_2$ (**SI3**, 6.2 mg, 4.32 µmol, 1.0 equiv), a solution of B$_2$pin$_2$ (2.20 mg, 8.65 µmol, 2.0 equiv) in THF (124 µL), a solution of KOtBu (970 µg, 8.65 µmol, 2.0 equiv) in THF (124 µL), a solution of AgPF$_6$ (2.19 mg, 8.65 µmol, 2.0 equiv) in THF (124 µL), and THF-d_8 (200 µL) were added sequentially. The NMR tube was sealed, and the reaction progress was monitored with NMR spectroscopy.

The ^{31}P NMR data showed the initial formation of xantphos-Rh(III)(Bpin)$_2$(OtBu), which in time converted to xantphos-Rh(I)-Bpin (the presence of xantphos-Rh(III)(Bpin)$_2$(OtBu) and xantphos-Rh(I)-Bpin complexes as well their conversion in time was further supported by the HRMS analysis in the analogous experiments shown below – experiments 3 and 4.).

^{31}**P{^{1}H} NMR** (162 MHz, THF-d_8/THF) 5 minutes of reaction time at room temperature:
The ^{31}P NMR spectrum shows a major species (28.9 ppm, d, J = 127.4 Hz), which was assigned to xantphos-Rh(III)(Bpin)$_2$(OtBu), and a minor species, which was assigned to be [Rh(xantphos)Bpin] (28.4 ppm, d, J = 127.1 Hz) in experiment 1.
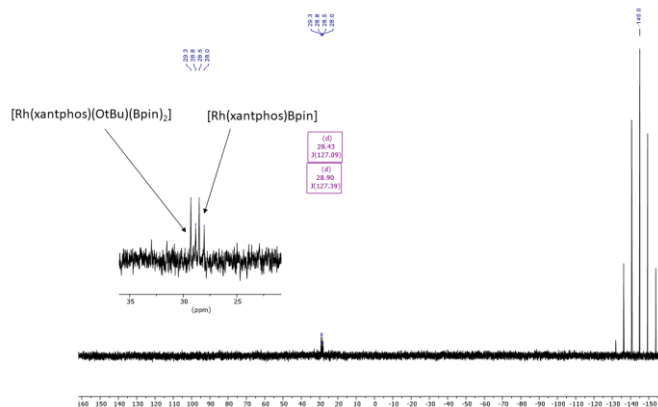

Figure 2.36: ^{31}P NMR spectrum of reaction of [Rh(xantphos)Cl]$_2$ with KOtBu, AgPF$_6$ and B$_2$pin$_2$.
^{31}**P{^{1}H} NMR** (162 MHz, THF-d_8/THF) 20 minutes of reaction time at room temperature:
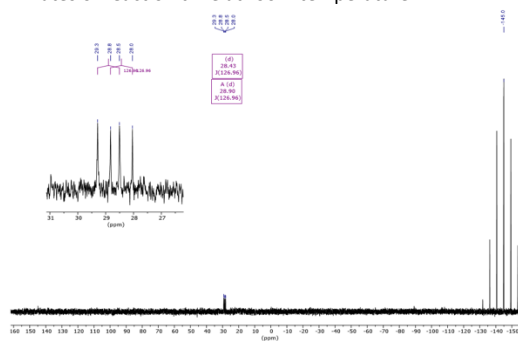
Figure 2.37: ^{31}P NMR spectrum of reaction of [Rh(xantphos)Cl]$_2$ with KOtBu, AgPF$_6$ and B$_2$pin$_2$.

³¹P{¹H} NMR (162 MHz, THF-*d₈*/THF) 40 minutes of reaction time at room temperature:
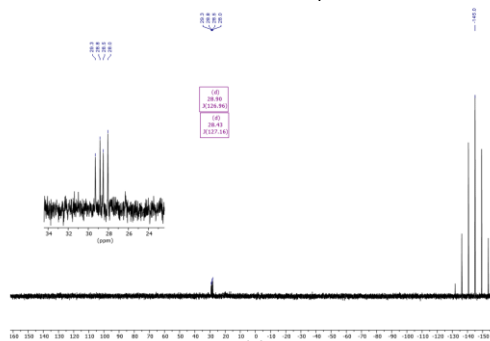
Figure 2.38: ³¹P NMR spectrum of reaction of [Rh(xantphos)Cl]₂ with KOtBu, AgPF₆ and B₂pin₂.

³¹P{¹H} NMR (162 MHz, THF-*d₈*/THF, 319 K) 48 minutes of reaction time at room temperature + 12 minutes at 45 °C:
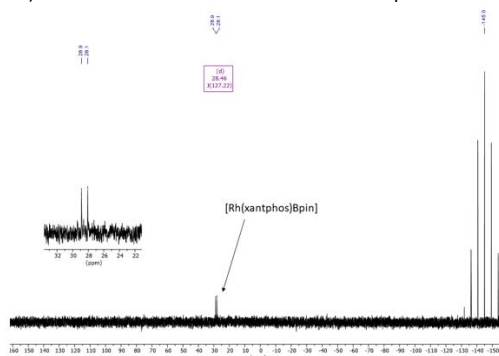
Figure 2.37: ³¹P NMR spectrum of reaction of [Rh(xantphos)Cl]₂ with KOtBu, AgPF₆ and B₂pin₂.

Experiment 3: Formation of xantphos-Rh(III)(Bpin)₂(OtBu) and xantphos-Rh(I)-Bpin in a short reaction time

The experiment was set up in analogy to experiment 2, but on a scale of 1.3 mg [Rh(xantphos)Cl]₂ (**SI3**, 907 nmol). Approximately 2 minutes after addition of the last reagent, an aliquot of this reaction was diluted in dry MeCN (1 mL) and the sample was stored on ice before it was analyzed by high resolution ESI mass spectroscopy.

Three distinguished Rh-species, that is, [Rh(III)(xantphos)(Bpin)₂]⁺, {[Rh(I)(xantphos)(Bpin)]H}⁺, and [Rh(I)(xantphos)]⁺, were detected in the mass spectrum:

Mass spectrum - zoom into the m/z = 550-1000 region:
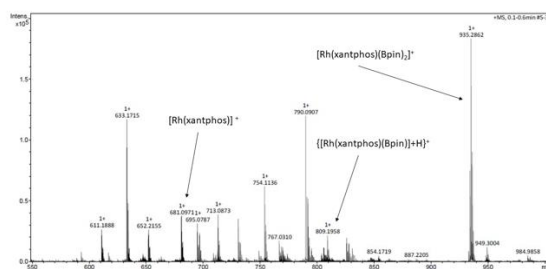
Full range mass spectrum:

Found and simulated signals of isotopomeric cluster of the molecular ion [Rh(xantphos)(Bpin)$_2$]$^+$:

Figure 2.40: High resolution mass spectra of the reaction of [Rh(xantphos)Cl]$_2$ with KOtBu, AgPF$_6$ and B$_2$pin$_2$.
For found and simulated signals of isotopomeric clusters of the molecular ions {[Rh(xantphos)(Bpin)]H}$^+$ and [Rh(xantphos)]$^+$, see experiment 4 where these where more pronounced than in experiment 4.

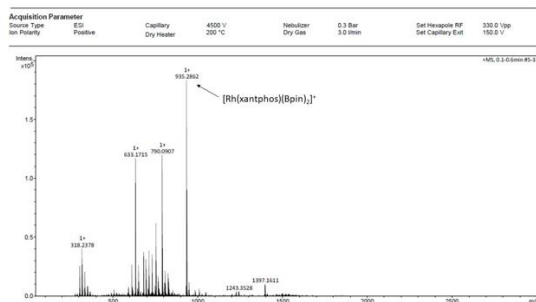*Experiment 4: Synthesis of xantphos-Rh(III)(Bpin)$_2$(OtBu) and xantphos-Rh(I)-Bpin – a longer reaction time*
The experiment was set up in analogy to experiment 2, but on a scale of 4.4 mg [Rh(xantphos)Cl]$_2$ (**SI3**, 907 nmol). Additionally, the mixture was heated at 45 °C for ca. 10 minutes, before an aliquot of this reaction was diluted in dry MeCN (1 mL) and the sample was analyzed by high resolution ESI mass spectroscopy.

In this experiment, the same three Rh-species, that is, [Rh(III)(xantphos)(Bpin)$_2$]$^+$, {[Rh(I)(xantphos)(Bpin)]H}$^+$, and [Rh(I)(xantphos)]$^+$, were detected in the mass spectrum. However, the relative abundance of {[Rh(I)(xantphos)(Bpin)]H}$^+$ versus [Rh(III)(xantphos)(Bpin)$_2$]$^+$ increased in time, in agreement with the formation of {[Rh(I)(xantphos)(Bpin)]H}$^+$ from [Rh(III)(xantphos)(Bpin)$_2$]$^+$ in time. It is worth noting that due to the different abilities of different complexes to ionize in the ESI-MS mode, the ratio of the abundances of the signals of different complexes in the mass spectra does not reflect the absolute ratio between their concentrations in the solution. Therefore, the ratio should be treated relatively.
Mass spectrum - zoom into the m/z = 550-1000 region:
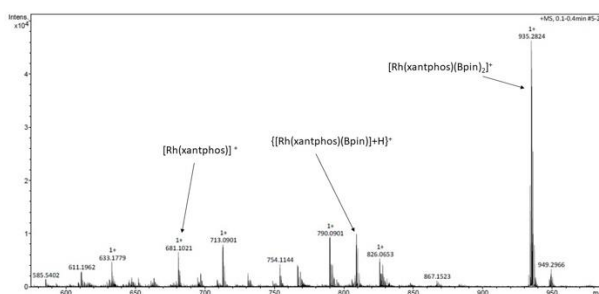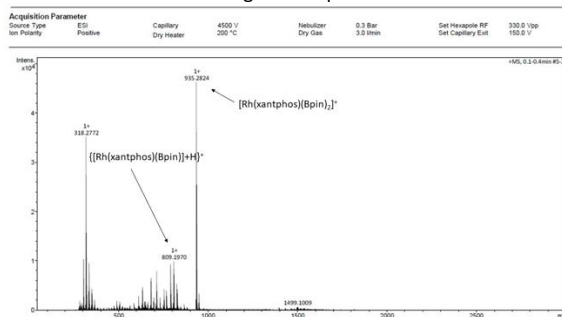
Full range mass spectrum:

Found and simulated signals of isotopomeric cluster of the molecular ion {[Rh(xantphos)(Bpin)]H}$^+$:

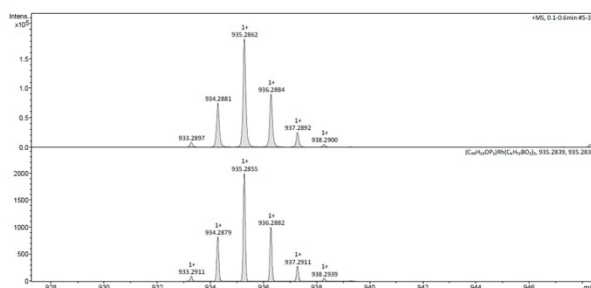Found and simulated signals of isotopomeric cluster of the molecular ion [Rh(xantphos)] $^+$:

Figure 2.41: High resolution mass spectra of the reaction of [Rh(xantphos)Cl]$_2$ with KOtBu, AgPF$_6$ and B$_2$pin$_2$.
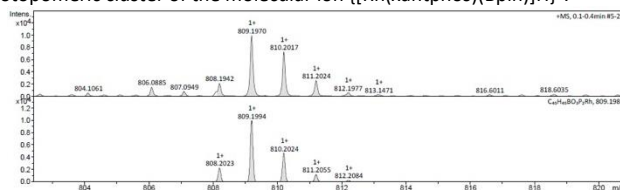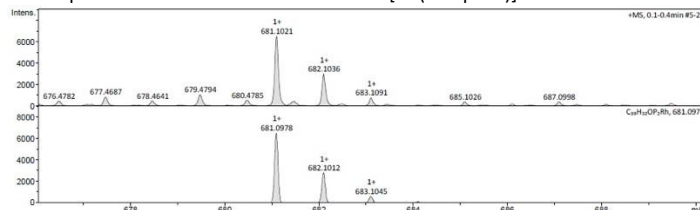
2.4.3.7. Reactivity of independently prepared xantphos-Rh(I)-Bpin

Reactivity of xantphos-Rh(I)-Bpin at room temperature towards styrene
In a nitrogen-filled glovebox, to a J. Young tube charged with [Rh(xantphos)Cl]$_2$ (**SI3**, 5.0 mg, 3.49 µmol, 1.0 equiv), a solution of B$_2$pin$_2$ (1.77 mg, 6.97 µmol, 2.0 equiv) in THF (100 µL), a solution of KOtBu (783 µg, 6.97 µmol, 2.0 equiv) in THF (100 µL), a solution of AgPF$_6$ (1.76 mg, 6.97 µmol, 2.0 equiv) in THF (100 µL), and THF-d_8 (200 µL) were added sequentially. The NMR tube was sealed and after typically 5-60 min at room temperature the clean formation of [Rh(xantphos)Bpin] was observed with ^{31}P NMR spectroscopy (28.4 ppm, d, J = 127.1 Hz).* Subsequently, a solution of styrene (7.26 mg, 7.99 µL, 69.7 µmol, 10.0 equiv) in THF (100 µL), a solution of isochroman (234 µg, 219 nL, 1.74 µL, 0.25 eq.) in THF (100 µL) as an internal standard, and THF (150 µL) were added. The NMR tube was sealed again, and the reaction was monitored at room temperature with NMR spectroscopy.
*If other species were present, the sample was discarded, and the synthesis of xantphos-Rh(I)-Bpin was repeated.

^{1}H NMR (400 MHz, THF-d_8/THF) after 16 h 15 min of reaction time:

Figure 2.42: ^{1}H NMR spectrum of the reaction of independently prepared xantphos-Rh-Bpin and styrene at rt.
Progression of ^{31}P and ^{1}H NMR spectroscopy in time:
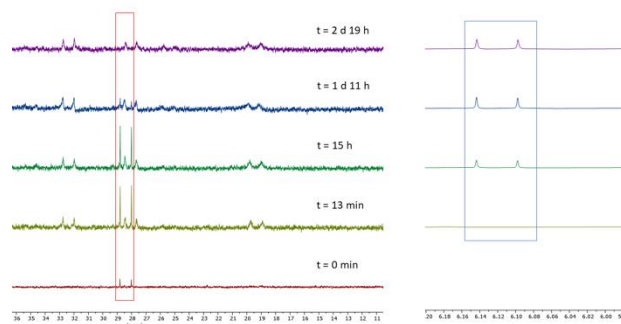
Figure 2.43: ^{1}H NMR and ^{31}P spectra of the reaction of independently prepared xantphos-Rh-Bpin and styrene over time at rt.

In this experiment, the formation of product **3a** was observed to be paralleled by a consumption of the [Rh(xantphos)Bpin] (28.4 ppm, J = 127 Hz), indicating its reactivity towards an insertion of styrene in accordance with our assignment in the ^{31}P NMR spectra as well as our mechanistic proposal.

Reactivity of xantphos-Rh(I)-Bpin at 45 °C towards styrene
To [Rh(xantphos)Cl]$_2$ (5.0 mg, 3.49 µmol, 1.0 equiv) in a J. Young tube were added sequentially a solution of B$_2$pin$_2$ (1.77 mg, 6.97 µmol, 2.0 equiv) in THF (100 µL), a solution of KOtBu (783 µg, 6.97 µmol, 2.0 equiv) in THF (100 µL), a solution of AgPF$_6$
 (1.76 mg, 6.97 µmol, 2.0 equiv) in THF (100 µL), and THF-d_8 (150 µL) in a nitrogen-filled glove box. The NMR tube was sealed and after typically 5-60 min at room temperature the clean formation of [Rh(xantphos)Bpin] was confirmed with ^{31}P NMR spectroscopy (28.4 ppm, d, J = 127.1 Hz).* Subsequently, a solution of styrene (10.9 mg, 12.0 µL, 105 µmol, 15.0 equiv) in THF (150 µL), a solution of isochroman (234 µg, 219 nL, 1.74 µmoL, 0.25 eq.) in THF (100 µL) as an internal standard, and THF (200 µL) were added. The NMR tube was sealed again, and the reaction was monitored at 45 °C via NMR spectroscopy.
*If other species were present, the sample was discarded, and the synthesis of xantphos-Rh(I)-Bpin was repeated.

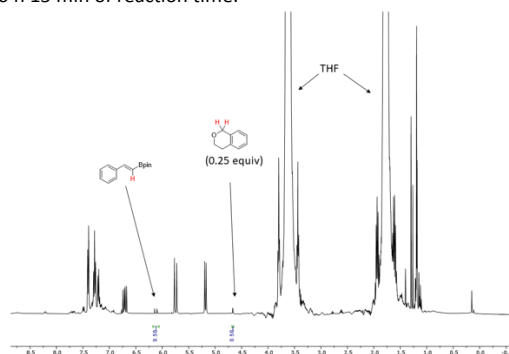**¹H NMR** (400 MHz, THF-*d₈*/THF, 318 K) after 5 h 14 min of reaction time:
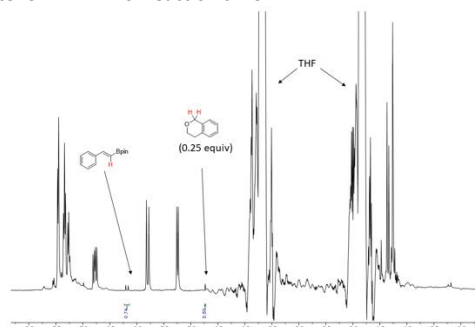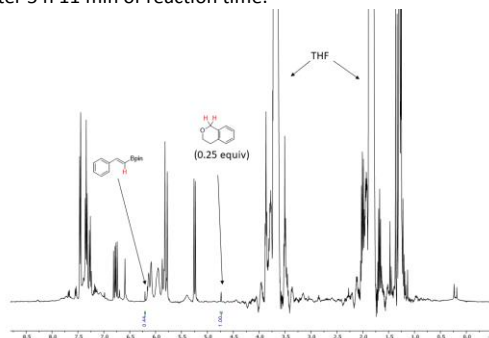

Figure 2.44: ¹H NMR spectrum of the reaction of independently prepared xantphos-Rh-Bpin and styrene at 45 °C.

Reactivity of xantphos-Rh(I)-Bpin at 45 °C under catalytic conditions
To [Rh(xantphos)Cl]₂ (**SI3**, 5.5 mg, 3.84 µmol, 1.0 equiv) in a J. Young tube were added sequentially a solution of B₂pin₂ (1.95 mg, 7.67 µmol, 2.0 equiv) in THF (110 µL), a solution of KOtBu (861 µg, 7.67 µmol, 2.0 equiv) in THF (110 µL), a solution of AgPF₆ (1.94 mg, 7.67 µmol, 2.0 equiv) in THF (110 µL), and THF-*d₈* (165 µL) in a nitrogen-filled glove box. The NMR tube was sealed, heated at 45 °C for 10 minutes, and after typically 5-60 min at room temperature the clean formation of [Rh(xantphos)Bpin] was confirmed with ³¹P NMR spectroscopy (28.4 ppm, d, *J* = 127.1 Hz).*Subsequently, a solution of styrene (12.0 mg, 13.2 µL, 115 µmol, 15.0 equiv) in THF (110 µL), a solution of isochroman (257 µg, 241 nL, 1.92 µmoL, 0.25 eq.) in THF (110 µL) as an internal standard, and THF-*d₈* (165 µL) were added. The NMR tube was sealed again, and the reaction was monitored at 45 °C via NMR spectroscopy.
**If other species were present, the sample was discarded, and the synthesis of xantphos-Rh(I)-Bpin was repeated.*

¹H NMR (400 MHz, THF-*d₈*/THF, 318 K) after 5 h 11 min of reaction time:

¹H NMR (400 MHz, THF-*d₈*/THF, 318 K) after 16 h 20 min of reaction time:
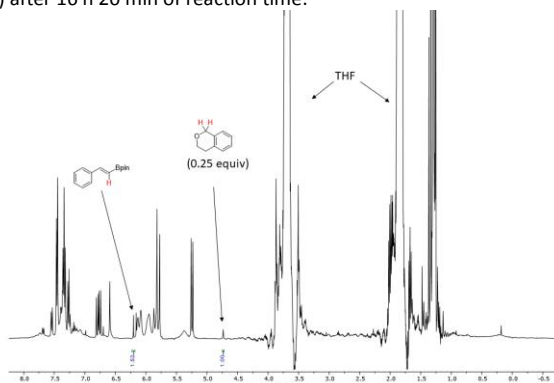
Figure 2.45: ¹H NMR spectrum of the reaction of independently prepared xantphos-Rh-Bpin, styrene and vinyl Bpin at 45 °C.

The nature of the product was further confirmed in similar one-timepoint experiments, where the same doublet was observed in the ¹H NMR spectra, while the GC-MS analysis of the crude reactions revealed the presence of product **3a**.

2.4.4. Preparation and characterization of starting materials

2.4.4.1. Preparation and characterization of alkene substrates

4-vinylbenzaldehyde 1b
The compound was prepared in accordance to a literature procedure.[104] Under a nitrogen atmosphere, *n*-BuLi (2.84 mL, 1.6 M in *n*-hexane, 4.55 mmol, 1.11 equiv) was added to a solution of 4-bromostyrene (536 µL, 750 mg, 4.10 mmol, 1.0 equiv) in THF (15 mL) at −78 °C in a dropwise manner. After allowing to stir for 2 h at this temperature, DMF (350 µL, 332 mg, 4.55 mmol, 1.11 equiv) was added in a dropwise manner. The resulting solution was allowed to stir for 30 min at this temperature. The
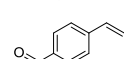
reaction mixture was allowed to warm to room temperature. NH$_4$Cl solution (30 mL) was added. The fractions were separated, and the aqueous fraction was washed with CH$_2$Cl$_2$ (3 × 30 mL). The combined organic fractions were dried over Na$_2$SO$_4$, filtered, and the volatiles of the filtrate were removed under reduced pressure. The residue was subjected to column chromatography (silica gel, 0-7% MTBE in petroleum ether) to isolate the title compound (378 mg, 2.86 mmol, 70%) as a yellow liquid. The NMR data match previously reported data for the title product.[104]

¹H NMR (500 MHz, CDCl$_3$) δ 9.99 (s, 1H), 7.88 – 7.81 (m, 2H), 7.58 – 7.53 (m, 2H), 6.78 (dd, *J* = 17.6, 10.9 Hz, 1H), 5.92 (d, *J* = 17.5 Hz, 1H), 5.44 (d, *J* = 10.8 Hz, 1H).

N,N-dimethyl-4-vinylaniline 1c
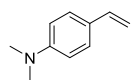
The compound was prepared according to a modified literature procedure.[105] To a solution of methyltriphenylphosphonium bromide (982 mg, 2.8 mmol, 1.1 equiv) in anhydrous THF (10 mL), n-BuLi (1.7 mL, 1.6 M in hexanes, 2.8 mmol, 1.1 equiv) was added dropwise at 0 °C under a N$_2$ atmosphere. The solution was allowed to stir at room temperature for 1.5 h. Then, a solution of dimethylaminobenzaldehyde (373 mg, 2.5 mmol, 1.0 equiv) in anhydrous THF (5 mL) was added dropwise to the mixture kept at 0 °C. The reaction mixture was allowed to stir for 16 h at room temperature. The reaction was quenched by addition of saturated aqueous NH$_4$Cl (15 mL) solution. The organic phase was separated. The aqueous phase was washed with EtOAc (3 × 20 mL). The combined organic fractions were washed with brine (40 mL) and dried over Na$_2$SO$_4$. After filtration, the volatiles of the filtrate were removed under reduced pressure and the residue was subjected to column chromatography (silica gel, 10% EtOAc in petroleum ether) to isolate the title product as a colorless oil (311 mg, 2.1 mmol, 84%). The NMR data match previously reported data for the title product.[105]

¹H NMR (500 MHz, CDCl$_3$) δ 7.36 – 7.28 (m, 2H), 6.71 – 6.67 (m, 2H), 6.64 (dd, *J* = 17.6, 10.9 Hz, 1H), 5.54 (d, *J* = 17.5 Hz, 1H), 5.02 (d, *J* = 9.6 Hz, 1H), 2.96 (s, 6H).

tert-butyl (4-vinylphenyl)carbamate SI4

The compound was prepared in accordance to a literature procedure.[106] A solution of 4-aminostyrene (258 mg, 254 µL, 2.17 mmol, 1.0 eq.) and di-*tert*-butyl dicarbonate (995 µL, 945 mg, 2.17 mmol, 1.0 eq.) in CH$_2$Cl$_2$ (1.55 mL) was allowed to stir at room temperature for 30 h under a nitrogen atmosphere. CH$_2$Cl$_2$ (10 mL) was added, and the organic fraction was washed with 1 M HCl (10 mL). The aqueous fraction was washed with CH$_2$Cl$_2$ (2 × 10 mL). The combined organic fractions were washed with brine (10 mL), dried over Na$_2$SO$_4$. After filtration, the volatiles from the filtrate were removed under reduced pressure. The residue was subjected twice to column chromatography (silica, 0-10% EtOAc in petroleum ether; silica, 0-7% Et$_2$O in petroleum ether). Imidazole (443 mg, 6.51 mmol, 3.0 eq.) was added to a solution of the crude product in CH$_2$Cl$_2$ (22 mL) and the resulting solution was allowed to stir for 4.5 h at room temperature. The subsequent work-up was performed according to a literature procedure:[107] The volatiles were removed under reduced pressure. CH$_2$Cl$_2$ (20 mL) was added. The organic fraction was washed with 1 M HCl (2 × 10 mL) and water (10 mL), dried over Na$_2$SO$_4$ and filtrated. All volatiles of the filtrate were removed under reduced pressure and the residue was subjected twice to column chromatography (2 ×, silica, 0-20%, Et$_2$O in petroleum ether) to isolate the title product (204 mg, 928 µmol, 43%) as a colorless solid. The NMR data match previously reported data for the title product.[108]

¹H NMR (500 MHz, CDCl$_3$) δ 7.37 – 7.29 (m, 4H), 6.65 (dd, *J* = 17.6, 10.9 Hz, 1H), 6.47 (s, 1H), 5.65 (dd, *J* = 17.6, 1.0 Hz, 1H), 5.16 (dd, *J* = 10.9, 0.9 Hz, 1H), 1.52 (s, 9H);

¹³C{¹H} NMR (126 MHz, CDCl$_3$) δ 152.6, 137.9, 136.2, 132.5, 126.9, 118.4, 112.4, 80.6, 28.4.

tert-butyl methyl(4-vinylphenyl)carbamate 1d
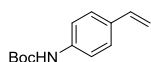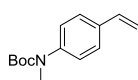
The compound was prepared in accordance to a literature procedure.[109] Under a nitrogen atmosphere, a solution of amine **SI4** (105 mg, 478 µmol, 1.0 equiv) in DMF (0.96 mL) was added to a mixture of NaH (28.7 mg, 60% dispersion in mineral oil, 717 µmol, 1.50 equiv) in DMF (1.45 mL). After addition of MeI (149 µL, 339 mg, 2.39 mmol, 5.0 equiv), the reaction mixture was allowed to stir 15.5 h at room temperature. NH$_4$Cl solution (50 mL) was added, and the mixture washed with ethyl acetate (2 × 5 mL). The combined organic fractions were washed with water (2 × 10 mL) and brine (10 mL), dried over Na$_2$SO$_4$ and filtered. The volatiles of the filtrate were removed under reduced pressure. The residue was subjected to column chromatography (silica gel, 0-5% MTBE in petroleum ether) to isolate the title compound (90.7 mg, 389 µmol, 81%) as a colorless oil. The NMR data match previously reported data for the title product.[110]

¹H NMR (400 MHz, CDCl$_3$) δ 7.40 – 7.32 (m, 2H), 7.22 – 7.15 (m, 2H), 6.69 (dd, *J* = 17.6, 10.9 Hz, 1H), 5.70 (dd, *J* = 17.6, 0.9 Hz, 1H), 5.22 (dd, *J* = 10.9, 0.9 Hz, 1H), 3.25 (s, 3H), 1.45 (s, 9H).

1-(4-vinylphenyl)ethanone 1e
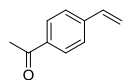
The compound was prepared according to a modified literature procedure.[111] In a sealed vial under a nitrogen atmosphere, a solution of potassium vinyltrifluoroborate (268 mg, 2.0 mmol, 1.0 equiv), PdCl$_2$ (7.1 mg, 0.04 mmol, 2 mol%), PPh$_3$ (31.5 mg, 0.12 mmol, 6 mol%), Cs$_2$CO$_3$ (1.95 g, 6.0 mmol, 3.0 equiv), and 4-iodoacetophenone (492 mg, 2.0 mmol, 1.0 equiv) in THF/H$_2$O (9:1, 4 mL) was allowed to stir at 85 °C for 22 h. The reaction mixture was allowed to cool to room temperature, diluted with H$_2$O (6 mL), and then washed with DCM (3 x 20 mL). The combined organic fractions were dried over Na$_2$SO$_4$. After filtration, the volatiles of the filtrate were removed under reduced pressure. The residue was subjected to column chromatography (silica gel, 0 – 10% EtOAc in petroleum ether) to isolate the title product as a pale yellow solid (210 mg, 1.4 mmol, 72%). The NMR data match previously reported data for the title product.[112]

¹H NMR (500 MHz, CDCl$_3$) δ 7.97 – 7.85 (m, 2H), 7.51 – 7.45 (m, 2H), 6.76 (dd, *J* = 17.6, 10.9 Hz, 1H), 5.88 (d, *J* = 17.5 Hz, 1H), 5.40 (d, *J* = 10.8 Hz, 1H), 2.60 (s, 3H).

(*E*)-1-styryl-4-vinylbenzene 1o
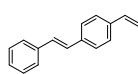
The compound was prepared according to a modified literature procedure.[113] Under a nitrogen atmosphere, to a solution of 4-bromostyrene (366 mg, 2.0 mmol, 1.0 equiv), potassium tert-butoxide (673 mg, 6.0 mmol, 3.0 equiv), and ethanol (18.4 mg, 0.4 mmol, 0.2 equiv) in DMF (5 mL), styrene (1.04 g, 10.0 mmol, 5.0 equiv) was added. The reaction mixture was allowed to stir at 80 °C for 2 h, when GC/MS analysis indicated full conversion of the arylhalide. The reaction mixture was allowed to cool to room temperature. The reaction was quenched by the addition of H$_2$O. The reaction mixture was washed with diethyl ether (3 x 10 mL). The combined organic phases were dried over Na$_2$SO$_4$. After filtration, the volatiles of the filtrate were removed under reduced pressure. The residue was subjected to column chromatography (silica gel, 100% petroleum ether) to isolate the title product as a white solid (41.3 mg, 0.20 mmol, 10%). The NMR data match previously reported data for the title product.[113]

¹H NMR (500 MHz, CDCl$_3$) δ 7.57 – 7.47 (m, 4H), 7.47 – 7.34 (m, 4H), 7.34 – 7.21 (m, 1H), 7.11 (d, *J* = 1.4 Hz, 2H), 6.73 (dd, *J* = 17.6, 10.9 Hz, 1H), 5.78 (d, *J* = 17.7 Hz, 1H), 5.26 (d, *J* = 10.8 Hz, 1H).

1-(3,3-dimethylbut-1-yn-1-yl)-4-vinylbenzene 1p
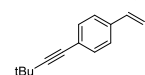
The compound was prepared in analogy to a literature procedure.[114] 4-Bromostyrene (350 mg, 250 µL, 1.91 mmol, 1.0 equiv) was added to a suspension of [(PPh$_3$)$_2$PdCl$_2$] (26.8 mg, 38.2 µmol, 0.02 equiv) and 3,3-dimethyl-1-butyne (509 µL, 339 mg, 4.13 mmol, 2.16 equiv) in triethylamine (7.7 mL). The resulting suspension was allowed to stir for 5 min at 50 °C in the dark under a nitrogen atmosphere. Copper(I)-iodide (5.7 mg, 29.8 µmol, 0.02 eq.) was added at room temperature and the resulting suspension was allowed to stir for 22.5 h at 50 °C. The suspension was filtered over celite (Et$_2$O, 50 mL) and the volatiles from the filtrate were removed under reduced pressure. The residue was subjected to column chromatography (silica, *n*-heptane) to isolate the title compound (190 mg, 1.03 mmol, 54%) as a colorless oil.

^{1}H NMR (500 MHz, CDCl$_3$) δ 7.37 – 7.28 (m, 4H), 6.68 (dd, *J* = 17.6, 10.9 Hz, 1H), 5.73 (dd, *J* = 17.6, 0.5 Hz, 1H), 5.25 (dd, *J* = 10.9, 0.6 Hz, 1H), 1.32 (s, 9H);

^{13}C{^{1}H} NMR (126 MHz, CDCl$_3$) δ 136.7, 136.5, 131.8, 126.1, 123.6, 114.3, 99.4, 79.1, 31.2, 28.1.

HRMS (ESI) m/z calcd. for C$_{14}$H$_{17}$ ([M+H]$^+$): 185.1325; found: 185.1321.

trimethyl((4-vinylphenyl)ethynyl)silane 1q

The compound was prepared in accordance to a literature procedure.[114] 4-Bromostyrene (300 mg, 214 µL, 1.64 mmol, 1.0 equiv) was added to a suspension of [(PPh$_3$)$_2$PdCl$_2$] (23.0 mg, 32.8 µmol, 0.02 equiv) and trimethylsilylacetylene (491 µL, 348 mg, 3.54 mmol, 2.16 equiv) in triethylamine (6.6 mL). The resulting suspension was allowed to stir for 5 min at 50 °C in the dark under a nitrogen atmosphere. Copper(I)-iodide (4.9 mg, 25.6 µmol, 0.02 eq.) was added at room temperature and the resulting suspension was allowed to stir for 20.5 h at 50 °C. The suspension was filtered over celite (Et$_2$O, 30 mL) and the volatiles from the filtrate were removed under reduced pressure. The residue was subjected to column chromatography (silica, *n*-heptane) to isolate the title compound (231 mg, 1.15 mmol, 70%) as a slightly yellow liquid. The NMR data match previously reported data for the title product.[114]

^{1}H NMR (500 MHz, CDCl$_3$) δ 7.45 – 7.39 (m, 2H), 7.37 – 7.31 (m, 2H), 6.68 (dd, *J* = 17.6, 10.9 Hz, 1H), 5.76 (dd, *J* = 17.6, 0.7 Hz, 1H), 5.29 (dd, *J* = 10.8, 0.8 Hz, 1H), 0.25 (s, 9H).
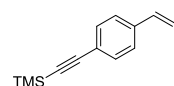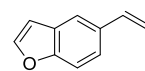
5-vinylbenzofuran 1u

The compound was prepared in accordance to a literature procedure.[105] Under a nitrogen atmosphere, *n*-BuLi (4.70 mL, 1.6 M in *n*-hexane, 7.53 mmol, 1.10 equiv) was added to a suspension of methyltriphosphonium bromide (2.69 g, 7.53 mmol, 1.10 equiv) in THF (27 mL) at 0 °C. The resulting suspension was allowed to stir for 2.5 h at room temperature. A solution of benzofuran-5-carbaldehyde (1.00 g, 6.84 mmol, 1.0 equiv) in THF (6.8 mL) was added in a dropwise manner at 0 °C. The reaction mixture was allowed to stir for 19 h at room temperature. NH$_4$Cl solution (50 mL) was added. The mixture was washed with ethyl acetate (3 × 50 mL). The combined organic fractions were washed with brine (50 mL) and dried over Na$_2$SO$_4$. After filtration, the volatiles from the filtrate were removed under reduced pressure. The residue was subjected to column chromatography (silica gel, 0-1% Et$_2$O in petroleum ether) to isolate the title compound (684 mg, 4.74 mmol, 69%) as a colorless liquid. The NMR data match previously reported data for the title product.[115]

^{1}H NMR (500 MHz, CDCl$_3$) δ 7.62 (d, *J* = 1.2 Hz, 1H)*, 7.61 (d, *J* = 2.2 Hz, 1H)*, 7.46 (d, *J* = 8.5 Hz, 1H), 7.40 (dd, *J* = 8.5, 1.8 Hz, 1H), 6.82 (dd, *J* = 17.5, 10.9 Hz, 1H), 6.75 (dd, *J* = 2.2, 0.9 Hz, 1H), 5.73 (d, *J* = 17.5 Hz, 1H), 5.22 (d, *J* = 11.0 Hz, 1H);

* Signals overlap.

Preparation of 1-(non-2-yn-1-yl)-4-vinylbenzene 1v
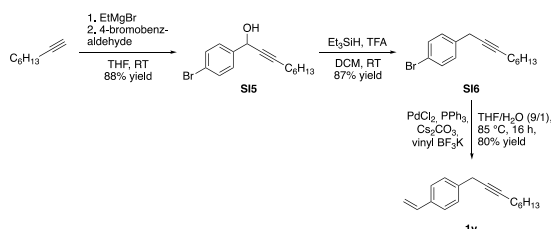
1-(4-bromophenyl)non-2-yn-1-ol SI5
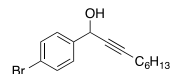
Under a nitrogen atmosphere, to a round-bottom flask containing 1-octyne (1.35 g, 1.8 mL, 12.2 mmol, 1.6 equiv) in dry THF (30 mL), ethylmagnesium bromide (3.0 M solution in Et$_2$O, 3.0 mL, 9.0 mmol, 1.2 equiv) was added. The reaction mixture was allowed to stir at room temperature for 2 h. Subsequently, a solution of *p*-bromobenzaldehyde (1.39 g, 7.5 mL mmol, 1.0 equiv) in dry THF (6 mL) was added. The reaction mixture was allowed to stir at room temperature for 3 h. The reaction was quenched with saturated aqueous NH$_4$Cl solution (30 mL). The reaction mixture was washed with Et$_2$O (3 x 30 mL). The combined organic fractions were dried over Na$_2$SO$_4$. After filtration, the volatiles of the filtrate were removed under reduced pressure. The residue was subjected to column chromatography (silica gel, 0 – 10% EtOAc in petroleum ether) to isolate the title product as a colourless oil (1.95 g, 6.6 mmol, 88%).

^{1}H NMR (400 MHz, CDCl$_3$) δ 7.54 – 7.46 (m, 2H), 7.46 – 7.37 (m, 2H), 5.40 (s, 1H), 2.26 (td, *J* = 7.1, 2.1 Hz, 2H), 2.17 (s, 1H), 1.67 – 1.48 (m, 2H), 1.46 – 1.21 (m, 6H), 0.89 (t, *J* = 6.9 Hz, 3H);

^{13}C{^{1}H} NMR (101 MHz, CDCl$_3$) δ 140.4, 131.7, 128.5, 122.3, 88.3, 79.6, 64.3, 31.4, 28.7, 28.6, 22.7, 18.9, 14.2.

HRMS (ESI) m/z calcd. for C$_{15}$H$_{20}$^{79}BrO ([M+H]$^+$): 295.0692; found: 295.0685;

m/z calcd. for C$_{15}$H$_{20}$^{81}BrO ([M+H]$^+$): 297.0672; found: 295.0665.

1-bromo-4-(non-2-yn-1-yl)benzene SI6
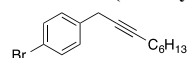
The compound was prepared according to a modified literature procedure.[116] To a solution of 1-(4-bromophenyl)non-2-yn-1-ol (**SI5**, 1.88 g, 6.4 mmol, 1.0 equiv) and triethylsilane (1.48 g, 2.0 mL, 12.8 mmol, 2.0 equiv) in DCM (40 mL), trifluoroacetic acid (6.55 g, 4.4 mL, 57.4 mmol, 9.0 equiv) was added. The reaction mixture was allowed to stir at room temperature for 2 h, followed by the addition of saturated aqueous NH$_4$Cl (50 mL) solution. The mixture was washed with DCM (3 x 40 mL). The combined organic fractions were dried over Na$_2$SO$_4$. After filtration, the volatiles of the filtrate were removed under reduced pressure. The residue was subjected to column chromatography (silica gel, 100% petroleum ether) to isolate the title product as a yellow oil (1.54 g, 5.5 mmol, 87%).

¹H NMR (400 MHz, CDCl₃) δ 7.46 – 7.38 (m, 2H), 7.25 – 7.16 (m, 2H), 3.52 (t, *J* = 2.6 Hz, 2H), 2.21 (tt, *J* = 7.1, 2.4 Hz, 2H), 1.51 (dd, *J* = 13.9, 8.3 Hz, 2H), 1.45 – 1.16 (m, 6H), 0.90 (t, *J* = 7.0 Hz, 3H);
¹³C{¹H} NMR (101 MHz, CDCl₃) δ 136.8, 131.6, 129.8, 120.3, 83.4, 77.0, 31.5, 29.1, 28.7, 24.8, 22.7, 19.0, 14.2;
HRMS (ESI) m/z calcd. for C₁₅H₂₀⁷⁹Br ([M+H]⁺): 279.0743; found: 279.0749;
m/z calcd. for C₁₅H₂₀⁸¹Br ([M+H]⁺): 281.0722; found: 281.0728.

1-(non-2-yn-1-yl)-4-vinylbenzene 1v
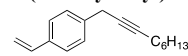
The compound was prepared according to a modified literature procedure.[111] In a sealed vial under a nitrogen atmosphere, a solution of potassium vinyltrifluoroborate (402 mg, 3.0 mmol, 1.0 equiv), PdCl₂ (10.6 mg, 0.06 mmol, 2 mol%), PPh₃ (47.2 mg, 0.18 mmol, 6 mol%), Cs₂CO₃ (2.93 g, 9.0 mmol, 3.0 equiv), and 1-bromo-4-(non-2-yn-1-yl)benzene (838 mg, 3.0 mmol, 1.0 equiv) in THF/H₂O (9:1, 6 mL) was allowed to stir at 85 °C for 16 h. The reaction mixture was allowed to cool to room temperature, diluted with H₂O (20 mL), and washed with DCM (3 x 30 mL). The combined organic fractions were dried over Na₂SO₄. After filtration, the volatiles of the filtrate were removed under reduced pressure. The residue was subjected to column chromatography (silica gel, 100% petroleum ether) to isolate the title product as a yellow solid (545 mg, 2.4 mmol, 80%).
¹H NMR (500 MHz, CDCl₃) δ 7.36 (d, *J* = 8.3 Hz, 2H), 7.31 (d, *J* = 8.0 Hz, 2H), 6.71 (dd, *J* = 17.6, 10.9 Hz, 1H), 5.72 (dd, *J* = 17.6, 1.0 Hz, 1H), 5.21 (dd, *J* = 10.9, 1.0 Hz, 1H), 3.57 (t, *J* = 2.5 Hz, 2H), 2.22 (tt, *J* = 7.1, 2.5 Hz, 2H), 1.61 – 1.47 (m, 2H), 1.46 – 1.19 (m, 6H), 0.90 (t, *J* = 6.9 Hz, 3H);
¹³C{¹H} NMR (126 MHz, CDCl₃) δ 137.4, 136.7, 136.0, 128.1, 126.4, 113.5, 82.9, 77.5, 31.5, 29.1, 28.7, 25.1, 22.7, 19.0, 14.2;
HRMS (ESI) m/z calcd. for C₁₇H₂₃ ([M+H]⁺): 227.1794; found: 227.1795.

N-vinyl-d-valerolactam 1z

A mixture of d-valerolactam (297.4 mg, 3.0 mmol, 1.0 equiv.), CuI (28.6 mg, 0.15 mmol, 5 mol%), *N,N'*-dimethylethylenediamine (26.4 mg, 0.30 mmol, 10 mol%), K₂CO₃ (829.2 mg, 6.0 mmol, 2.0 equiv.) and vinyl bromide (1M in THF, 6 mL, 6.0 mmol, 2.0 equiv.) was allowed to stir for 16 h at 80 °C under a nitrogen atmosphere. The reaction mixture was filtered over celite and the volatiles were removed under reduced pressure. The residue was subjected to column chromatography (silica gel, 50% EtOAc in petroleum ether) to isolate the title compound (106.2 mg, 0.85 mmol, 28%) as a white solid. The NMR data match previously reported data for the title product.[117]
**¹H NMR (400 MHz, CDCl₃)** δ 7.61 (dd, J = 16.3, 9.4 Hz, 2H), 4.67 – 4.03 (m, 2H), 3.39 (t, J = 6.2 Hz, 2H), 2.49 (t, J = 6.6 Hz, 2H), 1.94 – 1.85 (m, 2H), 1.84 – 1.76 (m, 2H).

General procedure for the synthesis of 1,1-diarylstyrenes

The compounds were prepared according to a literature procedure.[118] Under a nitrogen atmosphere, a mixture of a-bromostyrene (1.0 equiv.), an arylboronic acid (1.3 equiv.), and Pd(PPh₃)₄ (5 mol%), K₃PO₄ (3.0 equiv.) in THF (0.2 M) was allowed to stir for 16 h at 80 °C. The reaction mixture was filtered over celite and the volatiles were removed under reduced pressure. The residue was subjected to column chromatography to isolate the title compound.

methyl 4-(1-phenylvinyl)benzoate 1ag
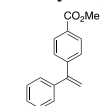
The compound was prepared according to general procedure for the synthesis of 1,1-diarylstyrenes by reaction of a-bromostyrene (366.1 mg, 2.0 mmol) and 4-methoxycarbonylphenylboronic acid (515 mg, 2.6 mmol) and was isolated by column chromatography (silica gel, 0-20 % EtOAc in petroleum ether) to give a colorless oil (352 mg, 1.48 mmol, 74%). The NMR data match previously reported data for the title product.[119]
¹H NMR (500 MHz, CDCl₃) δ 8.04 – 7.97 (m, 2H), 7.44 – 7.39 (m, 2H), 7.39 – 7.29 (m, 5H), 5.55 (d, J = 1.0 Hz, 1H), 5.54 (d, J = 1.1 Hz, 1H), 3.93 (s, 3H).

1-methoxy-4-(1-phenylvinyl)benzene 1ah
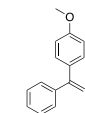
The compound was prepared according to general procedure for the synthesis of 1,1-diarylstyrenes by reaction of a-bromostyrene (366.1 mg, 2.0 mmol) and 4-methoxyphenylboronic acid (395 mg, 2.6 mmol) and was isolated by column chromatography (silica gel, 0-30 % EtOAc in petroleum ether) to give a pale yellow solid (91.8 mg, 0.44 mmol, 22%). The NMR data match previously reported data for the title product.[120]
¹H NMR (400 MHz, CDCl₃) δ 7.36 – 7.26 (m, 7H), 6.90 – 6.84 (m, 2H), 5.40 (d, J = 1.3 Hz, 1H), 5.36 (d, J = 1.2 Hz, 1H), 3.83 (s, 3H).

methyl(4-(1-phenylvinyl)phenyl)sulfane 1ai
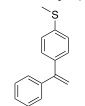
The compound was prepared according to general procedure for the synthesis of 1,1-diarylstyrenes by reaction of a-bromostyrene (366.1 mg, 2.0 mmol) and 4-(methylthio)benzeneboronic acid (437 mg, 2.6 mmol) and was isolated by column chromatography (silica gel, 0-10 % EtOAc in petroleum ether) to give a colorless solid (283.6 mg, 1.25 mmol, 63%). The NMR data match previously reported data for the title product.[120]
¹H NMR (400 MHz, CDCl₃) δ 7.35 – 7.32 (m, 5H), 7.29 – 7.25 (m, 2H), 7.24 – 7.20 (m, 2H), 5.45 (d, J = 1.2 Hz, 1H), 5.42 (d, J = 1.2 Hz, 1H), 2.51 (s, 3H).

5-(1-phenylvinyl)benzo[d][1,3]dioxole 1aj
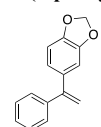
The compound was prepared according to general procedure for the synthesis of 1,1-diarylstyrenes by reaction of a-bromostyrene (366.1 mg, 2.0 mmol) and 3,4-(methylenedioxy)benzeneboronic acid (431 mg, 2.6 mmol) and was isolated by column chromatography (silica gel, 0-5 % EtOAc in petroleum ether) to give a yellow oil (264.2 mg, 1.18 mmol, 59%). The NMR data match previously reported data for the title product.[120]
¹H NMR (500 MHz, CDCl₃) δ 7.37 – 7.28 (m, 5H), 6.86 – 6.80 (m, 2H), 6.77 (d, J = 8.0 Hz, 1H), 5.97 (s, 2H), 5.39 (d, J = 1.2 Hz, 1H), 5.36 (d, J = 1.3 Hz, 1H).

2-(1-phenylvinyl)thiophene 1ak
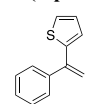
The compound was prepared according to general procedure for the synthesis of 1,1-diarylstyrenes by reaction of a-bromostyrene (366.1 mg, 2.0 mmol) and thiophene-2-boronic acid (332.7 mg, 2.6 mmol) and was isolated by column chromatography (silica gel, 100% petroleum ether) to give a yellow oil (262 mg, 1.41 mmol, 70%). The NMR data match previously reported data for the title product.[119]
¹H NMR (400 MHz, CDCl₃) δ 7.54 – 7.41 (m, 2H), 7.39 – 7.35 (m, 3H), 7.29 – 7.19 (m, 1H), 6.98 (dd, *J* = 5.1, 3.6 Hz, 1H), 6.92 (dd, *J* = 3.6, 1.1 Hz, 1H), 5.59 (s, 1H), 5.25 (s, 1H).

(E)-prop-1-ene-1,3-diyldibenzene 1an

Ph⁓⁓Ph The compound was prepared according to a modified literature procedure.[121] Under a nitrogen atmosphere, a mixture of cinnamyl alcohol (335.5 mg, 2.5 mmol, 1.0 equiv.), phenylboronic acid (365.8 mg, 3.0 mmol, 1.2 equiv.), and Pd(PPh$_3$)$_4$ (28.9 mg, 25 µmol, 1 mol%) in THF (6 mL) was allowed to stir for 16 h at 80 °C. The reaction mixture was filtered over celite and the volatiles were removed under reduced pressure. The residue was subjected to column chromatography (silica gel, 100% petroleum ether) to isolate the title compound (375.0 mg, 1.93 mmol, 77%) as a colorless oil. The NMR data match previously reported data for the title product.[121]

^{1}H NMR (400 MHz, CDCl$_3$) δ 7.42 – 7.35 (m, 2H), 7.34 – 7.28 (m, 4H), 7.27 – 7.18 (m, 4H), 6.47 (d, J = 15.9 Hz, 1H), 6.37 (dt, J = 15.8, 6.6 Hz, 1H), 3.56 (d, J = 6.6 Hz, 2H).

N,N-dimethyl-3-(pyridin-2-yl)-3-(4-vinylphenyl)propan-1-amine 1ar
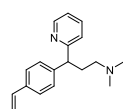
A mixture of brompheniramine maleate (500 mg, 1.15 mmol, 1.0 equiv), K$_2$CO$_3$ (635 mg, 4.59 mmol, 4.0 equiv), Pd(OAc)$_2$ (12.9 mg, 57.4 mg, 0.05 equiv), SPhos (47.2 mg, 115 µmol, 0.10 equiv), and potassium vinyltrifluoroborate (308 mg, 2.30 mmol, 2.0 equiv), in water (820 µL) and dioxane (4.9 mL) was allowed to stir for 17 h at 90 °C under a nitrogen atmosphere. The reaction mixture was filtered over celite (EtOAc, 40 mL). The filtrate was washed with water (15 mL). The aqueous fraction was washed with EtOAc (2 × 10 mL). The combined organic fractions were washed with brine (20 mL), dried over Na$_2$SO$_4$. After filtration, the volatiles from the filtrate were removed under reduced pressure and the residue was subjected to column chromatography (silica gel, 0-10% of MeOH/NEt$_3$ (10/1) in CH$_2$Cl$_2$) to isolate the title compound (249 mg, 936 µmol, 82%) as a brown oil.

^{1}H NMR (400 MHz, CDCl$_3$) δ 8.56 (d, J = 4.5 Hz, 1H), 7.55 (t, J = 7.6 Hz, 1H), 7.36 – 7.27 (m, 4H), 7.16 (d, J = 7.9 Hz, 1H), 7.08 (dd, J = 7.5, 4.8 Hz, 1H), 6.67 (dd, J = 17.6, 10.9 Hz, 1H), 5.69 (d, J = 17.6 Hz, 1H), 5.19 (d, J = 10.9 Hz, 1H), 4.13 (t, J = 6.9 Hz, 1H), 2.51 – 2.36 (m, 1H), 2.28 – 2.19 (m, 3H)*, 2.21 (s, 6H)*;

* Signals overlap.

^{13}C{^{1}H} NMR (126 MHz, CDCl$_3$) δ 163.8, 149. 5, 143.5, 136.8, 136.5, 136.1, 128.4, 126.5, 123.0, 121.4, 113. 5, 58.0, 51.3, 45.6, 32.9;

HRMS (ESI) m/z calcd. for C$_{18}$H$_{23}$N$_2$ ([M+H]$^+$): 267.1856; found: 267.1850.

N,N-dimethyl-3-(2-vinyl-10H-phenothiazin-10-yl)propan-1-amine 1as
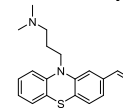
The compound was prepared according to a modified literature procedure.[122] In a sealed vial under a nitrogen atmosphere, a mixture of chlorpromazine hydrochloride (1.07 g, 3.0 mmol, 1.0 equiv), potassium vinyltrifluoroborate (482 mg, 3.6 mmol, 1.2 equiv), K$_2$CO$_3$ (1.24 g, 9.0 mmol, 3.0 equiv), Pd(OAc)$_2$ (33.7 mg, 0.15 mmol, 5 mol%), and SPhos (123 mg, 0.3 mmol, 10 mol%) in dioxane/H$_2$O (6:1, 14 mL) was allowed to stir at 90 °C for 2.5 h. The reaction mixture was allowed to cool to room temperature, followed by the addition of potassium vinyltrifluoroborate (321 mg, 2.4 mmol, 0.8 equiv), K$_2$CO$_3$ (414 mg, 3.0 mmol, 1.0 equiv), Pd(OAc)$_2$ (16.8 mg, 0.075 mmol, 2.5 mol%), and SPhos (61.6 mg, 0.15 mmol, 5 mol%) a nitrogen atmosphere (glove box). The vial was sealed and allowed to stir at 90 °C for 16 h. The reaction mixture was allowed to cool to room temperature and passed through a plug of celite (eluent: ethyl acetate). The phases were separated. The aqueous phase was washed with ethyl acetate (2 x 20 mL). The combined organic phases were washed with brine and dried over Na$_2$SO$_4$. After filtration, the volatiles of the filtrate were removed under reduced pressure and the residue was subjected to column chromatography (silica gel, 9% Et$_3$N in EtOAc) to isolate the title product as a brown oil (671 mg, 2.16 mmol, 72%). The NMR data match previously reported data for the title product.[122]

^{1}H NMR (500 MHz, CDCl$_3$) δ 7.17 – 7.11 (m, 2H), 7.08 (d, J = 7.8 Hz, 1H), 6.97 (dd, J = 7.9, 1.8 Hz, 1H), 6.93 – 6.86 (m, 3H), 6.65 (dd, J = 17.5, 10.8 Hz, 1H), 5.70 (d, J = 17.5 Hz, 1H), 5.22 (d, J = 10.8 Hz, 1H), 3.96 – 3.91 (m, 2H), 2.41 (t, J = 7.0 Hz, 2H), 2.21 (s, 6H), 1.96 (p, J = 7.0 Hz, 2H).

1-(4-vinylbenzyl)-1 H-imidazole 1at
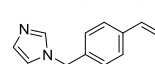
The compound was prepared according to a modified literature procedure.[123] Under a nitrogen atmosphere, to a suspension of imidazole (1.36 g, 20.0 mmol, 4.0 equiv) in acetonitrile (8 mL), NaHCO$_3$ (525 mg, 6.25 mmol, 1.25 equiv) and 1-(chloromethyl)-4-vinylbenzene (techn. 90%, 848 mg, 5.0 mmol, 1.0 equiv) were added. The reaction mixture was allowed to stir at 50 °C for 17 h. The volatiles were removed under reduced pressure to the residue. Water (15 mL) was added to the residue. The mixture was washed with diethyl ether (3 x 20 mL). The combined organic fractions were washed subsequently washed with HCl (1.2 M, 3 x 20 mL). The combined aqueous fractions were titrated with the aqueous solution of NaOH (1.3 M) until pH 7-8 was reached. The resulting aqueous mixture was washed with diethyl ether (3 x 40 mL). The combined organic fractions were dried over Na$_2$SO$_4$. After filtration, the volatiles of the filtrate were removed under reduced pressure to isolate the title product as a yellow oil (593 mg, 3.2 mmol, 64%). The NMR data match previously reported data for the title product.[123]

^{1}H NMR (500 MHz, CDCl$_3$) δ 7.54 (s, 1H), 7.42 – 7.35 (m, 2H), 7.24 – 7.03 (m, 3H), 6.89 (t, J = 1.3 Hz, 1H), 6.69 (dd, J = 17.6, 10.9 Hz, 1H), 5.75 (d, J = 17.6 Hz, 1H), 5.27 (d, J = 10.9 Hz, 1H), 5.09 (s, 2H).

Preparation of 2-(3,5,5,8,8-pentamethyl-5,6,7,8-tetrahydronaphthalen-2-yl)-4-vinylphenyl acetate 1au
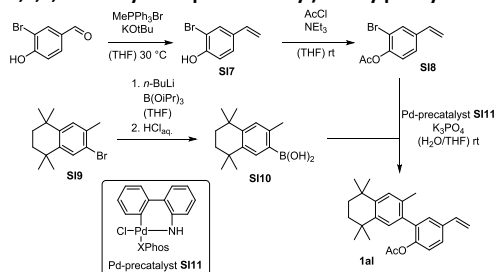
2-bromo-4-vinylphenol SI7
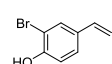
The compound was prepared in accordance to a modified literature procedure.[124] A mixture of 3-bromo-4-hydroxybenzaldehyde (1.00 g, 4.97 mol, 1.0 equiv), KOtBu (1.28 g, 11.4 mmol, 2.30 equiv) and methyltriphenylphosphonium bromide (4.09 g, 11.4 mmol, 2.3 equiv) in THF (14 mL) was allowed to stir for 17 h at 30 °C under a nitrogen atmosphere. After addition of water (50 mL), the aqueous fraction was adjusted to pH = 7 with aqueous (1 M HCl), and washed with Et$_2$O (3 × 50 mL). The combined organic fractions were washed with brine (50 mL), dried over Na$_2$SO$_4$. After filtration, n-pentane (100 mL) and celite were added to the filtrate, and the volatiles were carefully removed under reduced pressure (minimal pressure: 650 mbar). The residue was subjected to column chromatography (silica, 0 – 100% Et$_2$O in n-pentane) with careful removal of the solvent under reduced pressure (minimal

pressure: 700 mbar, then under a stream of N_2) to isolate the title compound (656 mg, 3.30 mmol, 66%) as a pale yellow solid. The NMR data match previously reported data for the title product.[125]

¹H NMR (400 MHz, CDCl₃) δ 7.52 (d, *J* = 2.1 Hz, 1H), 7.30 – 7.25 (m, 1H), 6.98 (d, *J* = 8.4 Hz, 1H), 6.58 (dd, k = 17.5, 10.9 Hz, 1H), 5.61 (dd, *J* = 17.5, 0.7 Hz, 1H), 5.48 (s, 1H), 5.17 (dd, *J* = 10.9, 0.7 Hz, 1H);

¹³C{¹H} NMR (101 MHz, CDCl₃) δ 152.0, 135.1, 132.2, 129.8, 127.2, 116.2, 113.2, 110.6.

2-bromo-4-vinylphenyl acetate SI8
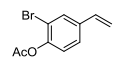
Under a nitrogen atmosphere, to a solution of phenol **SI7** (505 mg, 2.54 mmol, 1.0 equiv) in THF (8.5 mL), NEt₃ (530 µL, 385 mg, 3.81 mmol, 1.5 equiv) and AcCl (272 µL, 299 mg, 3.81 mmol, 1.5 equiv) were added sequentially. The resulting suspension was allowed to stir at room temperature for 21 h. The volatiles were removed under reduced pressure and the residue was subjected to column chromatography (silica, 0-10% MTBE in petroleum ether) to isolate the title compound (592 mg, 2.45 mmol, 97%) as a colorless oil.

¹H NMR (400 MHz, CDCl₃) δ 7.64 (d, *J* = 2.0 Hz, 1H), 7.35 (ddd, *J* = 8.4, 2.1, 0.5 Hz, 1H), 7.08 (d, *J* = 8.3 Hz, 1H), 6.64 (dd, *J* = 17.7, 11.0 Hz, 1H), 5.72 (dd, *J* = 17.6, 0.6 Hz, 1H), 5.30 (dd, *J* = 10.9, 0.6 Hz, 1H), 2.35 (s, 3H);

¹³C{¹H} NMR (126 MHz, CDCl₃) δ 168.8, 147.7, 137.4, 134.8, 131.0, 126.4, 123.8, 116.5, 115.7, 20.9.

HRMS (ESI) m/z calcd. for $C_{10}H_{10}{}^{79}BrO_2$ ([M+H]⁺): 240.9859; found: 240.9856;

m/z calcd. for $C_{10}H_{10}{}^{81}BrO_2$ ([M+H]⁺): 242.9839; found: 240.9837.

(3,5,5,8,8-pentamethyl-5,6,7,8-tetrahydronaphthalen-2-yl)boronic acid SI10

The compound was prepared in accordance to a literature procedure.[126] Under a nitrogen atmosphere, a solution of bromide **SI9** (200 mg, 711 µmol, 1.0 equiv) in THF (0.53 mL) was added over five minutes to a solution of *n*-BuLi (1.6 M in *n*-hexane, 0.53 mL, 853 µmol, 1.2 equiv) in THF (2.0 mL) at −78 °C. The mixture was allowed to stir for 10 min at this temperature. A solution of triisopropyl borate (328 µL, 268 mg, 1.42 mmol, 2.0 equiv) in THF (0.66 mL) was added. The mixture was allowed to stir for 1 h at this temperature. The mixture was allowed to warm to room temperature and was allowed to stir for 2 h. Aqueous HCl (3 M, 2.3 mL) was added, and the mixture was allowed to stir for 2 h at room temperature. Water (20 mL) was added. The aqueous fraction was washed with EtOAc (3 × 20 mL). The combined organic fractions were dried over Na₂SO₄, filtered, and the volatiles from the filtrate were removed under reduced pressure. The residue was dissolved in a small amount of CH₂Cl₂ and filtered through a short plug of silica. The silica plug was washed with a mixture of *n*-pentane and EtOAc (4/1, 500 mL). The volatiles of the filtrate were removed under reduced pressure to isolate the title compound (130 mg, 528 µmol, 74%) as a colorless solid, which was used in the next step without further purification. The NMR data match previously reported data for the title product.[127]

¹H NMR (400 MHz, CDCl₃) δ 8.28 (s, 1H), 7.21 (s, 1H), 2.81 (s, 3H), 1.72 (s, 4H), 1.34 (s, 6H), 1.32 (s, 6H).

2-(3,5,5,8,8-pentamethyl-5,6,7,8-tetrahydronaphthalen-2-yl)-4-vinylphenyl acetate 1au

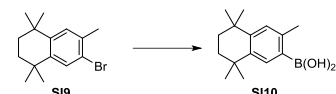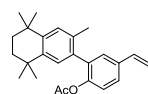Under a nitrogen atmosphere, to a solution of boronic acid **SI10** (421 mg, 1.71 mmol, 1.5 equiv), aryl bromide **SI8** (275 mg, 1.14 mmol, 1.0 equiv), and pre-catalyst **SI11**[128] (26.9 mg, 34.2 µmol, 0.03 equiv) in THF (2.3 mL) at room temperature, a degassed solution of K₃PO₄ (484 mg, 2.28 mmol, 2.0 equiv) in water (4.6 mL) was added. The mixture was allowed to stir at this temperature for 17 h. Water (10 mL) and Et₂O (10 mL) were added. After separation of the organic fraction, the aqueous fraction was washed with Et₂O (2 × 10 mL). The combined organic fractions were washed with brine (10 mL) and dried over Na₂SO₄. After filtration, the volatiles of the filtrate were removed under reduced pressure. The residue was subjected to column chromatography (silica, 0-5% acetone in petroleum ether) to isolate the title compound (264 mg, 728 µmol, 64%) as a colorless resin.

¹H NMR (500 MHz, CDCl₃) δ 7.40 (dd, *J* = 8.3, 2.2 Hz, 1H), 7.36 (d, *J* = 2.1 Hz, 1H), 7.16 (s, 1H), 7.09 (d, *J* = 8.3 Hz, 1H), 7.06 (s, 1H), 6.72 (dd, *J* = 17.6, 10.9 Hz, 1H), 5.71 (d, *J* = 17.6 Hz, 1H), 5.25 (d, *J* = 10.9 Hz, 1H), 2.12 (s, 3H), 1.91 (s, 3H), 1.69 (s, 4H), 1.30 (s, 6H), 1.24 (s, 6H);

¹³C{¹H} NMR (126 MHz, CDCl₃) δ 169.6, 148.2, 144.4, 141.9, 136.1, 135.5, 135.2, 134.0, 133.1, 129.3, 128.1, 128.0, 126.1, 122.7, 114.3, 35.3, 35.3, 34.1, 34.0, 32.0 (br, 2 × C), 20.7, 19.8;

HRMS (ESI) m/z calcd. for $C_{25}H_{31}O_2$ ([M+H]⁺): 363.2319; found: 363.2330.

Preparation of zearalenol derivative 1av
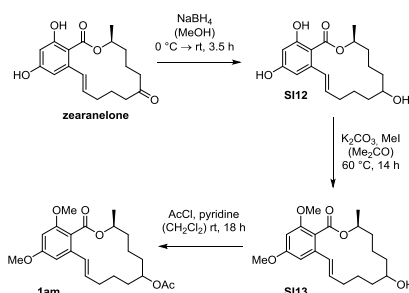
a/b-zearanelol SI12
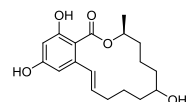
The compound was prepared in accordance to a modified literature procedure.[129] To a solution of zearanelone (80.0 mg, 251 µmol, 1.0 equiv) in MeOH (1.3 mL) allowed to stir at 0 °C, NaBH₄ (42.8 mg, 1.13 mmol, 4.50 equiv) was added portionwise. The mixture was allowed to stir at room temperature for 3.5 h. Water (20 mL) was added and the pH was adjusted to pH = 7 using 1 M HCl. The aqueous fraction was washed with EtOAc (4 × 10 mL). The combined organic fractions were washed with brine (20 mL) and dried over Na₂SO₄. After filtration, the volatiles of the filtrate were removed under reduced pressure to isolate the title compound (71.5 mg, 223 µmol, 89%, dr α/β = 31/69; (3S,7R)/(3S,7S)) as a colorless solid. The NMR data match previously reported data for the title product.[130]

¹H NMR (500 MHz, (CD₃)₂CO) δ 12.20 (s, 1H α), 11.04 (s, 1H β), 9.26 − 8.95 (m, 1H α + 1H β), 7.17 (d, *J* = 15.3 Hz, 1H α), 6.86 (d, *J* = 15.5 Hz, 1H β), 6.54 (d, *J* = 2.4 Hz, 1H β), 6.46 (d, *J* = 2.5 Hz, 1H α), 6.30 (d, *J* = 2.6 Hz, 1H α), 6.29 (d, *J* = 2.4 Hz, 1H β), 5.98 (ddd, *J* = 15.6, 8.4, 6.0 Hz, 1H β), 5.78 − 5.68 (m, 1H α), 5.14 − 5.06 (m, 1H β), 5.01 − 4.92 (m, 1H α), 3.82 − 3.69 (m, 1H α + 1H β), 3.48 − 3.35 (m, 1H α + 1H β), 2.37 − 2.21 (m, 2H α + 2H β), 1.95 − 1.88 (m, 2H α + 1H β), 1.81 − 1.41 (m, 7H α + 8H β), 1.40 (d, *J* = 6.1 Hz, 3H α), 1.35 (d, *J* = 6.3 Hz, 3H β), 1.32 − 1.24 (m, 1H β), 1.14 − 1.09 (m, 1H α).

a/b-2,4-dimethoxy zearanelol SI13
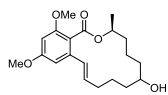
The compound was prepared in accordance to a modified literature procedure.[129] To a solution of zearanelol (50.0 mg, 156 µmol, α/β = 35/65, 1.0 equiv) in acetone (223 µL), K$_2$CO$_3$ (216 µg, 1.56 mmol, 10.0 equiv) and iodomethane (97.2 µL, 222 µg, 1.56 mmol, 10.0 equiv) were added sequentially. The mixture was allowed to stir at 60 °C for 14 h. Water (5 mL) and brine (5 mL) were added. The aqueous fraction was washed with EtOAc (4 × 5 mL). The combined organic fractions were washed with brine (10 mL) and dried over Na$_2$SO$_4$. After filtration, the volatiles of the filtrate were removed under reduced pressure. The residue was subjected to column chromatography (silica, 0-100% EtOAc in petroleum ether) to isolate the title compound (40.3 mg, 116 µmol, 74%, dr α/β = 36/64; (3S,7R)/(3S,7S)) as a colorless resin. The NMR data match previously reported data for the title product.[129]

¹H NMR (400 MHz, CDCl$_3$) δ 6.60 (d, *J* = 2.2 Hz, 1H β), 6.55 (d, *J* = 2.2 Hz, 1H α), 6.48 (d, *J* = 16.0 Hz, 1H α), 6.39 (d, *J* = 15.8 Hz, 1H β), 6.36 − 6.34 (m, 1H α + 1H β), 6.21 (dt, *J* = 16.0, 5.9 Hz, 1H α), 6.08 (ddd, *J* = 15.8, 9.1, 4.8 Hz, 1H β), 5.42 − 5.31 (m, 1H β), 5.27 − 5.17 (m, 1H α), 3.82 (s, 3H β), 3.81 (s, 3H α), 3.79 − 3.78 (m, 3H α + 3H β), 3.77 − 3.59 (m, 1H α + 1H β), 2.42 − 2.09 (m, 2H α + 2H β), 1.86 − 1.17 (m, 10H α + 10H β)[*+], 1.34 (d, *J* = 6.4 Hz, 3H α)[+], 1.30 (d, *J* = 6.4 Hz, 3H β)[*].

[+*] Signals overlap.

2,4-dimethoxy-6'-acetoxy a/b-zearanelol 1av
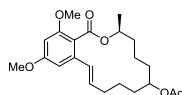
The compound was prepared in accordance to a modified literature procedure.[129] To a solution of 2,4-dimethoxy zearanelol (**SI13**, 584 mg, 1.68 mmol, α/β = 34/66, 1.0 equiv) in CH$_2$Cl$_2$ (16.8 mL), pyridine (675 µL, 663 µg, 8.38 mmol, 5.0 equiv) and AcCl (299 µL, 329 mg, 4.19 mmol, 2.5 equiv) were added sequentially. The mixture was allowed to stir at room temperature for 18 h. An aqueous solution of NaHCO$_3$ (40 mL) was added, and the aqueous fraction was washed with EtOAc (3 × 30 mL). The combined organic fractions were washed with CuSO$_4$ solution (50 mL). The CuSO$_4$ solution was washed with EtOAc (15 mL). The combined organic fractions were washed with brine (50 mL) and dried over Na$_2$SO$_4$. After filtration, the volatiles of the filtrate were removed under reduced pressure. The residue was subjected to column chromatography (silica, 25-50% EtOAc in petroleum ether) to isolate the title compound (656 mg, 1.68 µmol, quant., dr α/β = 34/66; (3S,7R)/(3S,7S)) as a slightly yellow resin. Diastereoisomers α/β were assigned by analogy to compounds **SI12** and **SI13**.

¹H NMR (500 MHz, CDCl$_3$) δ 6.60 (d, *J* = 2.1 Hz, 1H β), 6.56 (d, *J* = 2.3 Hz, 1H α), 6.49 (d, *J* = 16.0 Hz, 1H α), 6.42 (d, *J* = 15.9 Hz, 1H β), 6.37 − 6.34 (m, 1H α + 1H β), 6.22 (dt, *J* = 16.0, 5.8 Hz, 1H α), 6.08 (dt, *J* = 15.7, 6.8 Hz, 1H β), 5.42 − 5.33 (m, 1H β), 5.27 − 5.19 (m, 1H α), 4.88 − 4.77 (m, 1H α + 1H β), 3.82 (s, 3H β), 3.82 (s, 3H α), 3.79 (s, 3H α + 3H β), 2.40 − 2.08 (m, 2H α + 2H β), 2.03 (s, 3H α), 2.03 (s, 3H β), 1.84 − 1.38 (m, 10H α + 10H β), 1.35 (d, *J* = 6.3 Hz, 3H α), 1.31 (d, *J* = 6.4 Hz, 3H β);

¹³C{¹H} NMR (126 MHz, CDCl$_3$) δ 171.0 (β), 170.9 (α), 168.3 (α), 167.9 (β), 161.3 (β), 161.3 (α), 157.8 (α), 157.6 (β), 137.2 (α), 136.9 (β), 133.4 (β), 133.3 (α), 128.1 (β), 126.7 (α), 116.8 (β), 116.6 (α), 101.5 (α), 101.2 (β), 97.7 (β), 97.7 (α), 73.8 (α), 72.1 (β), 70.8 (β), 70.6 (α), 56.1 (α), 56.1 (β), 55.6 (β), 55.6 (α), 35.4 (α), 34.8 (β), 33.1 (β), 31.0 (α), 30.4 (β), 30.2 (α), 29.7 (β), 29.1 (α), 23.0 (α+β), 21.5 (β), 21.5 (α), 20.6 (α), 20.2 (α), 19.7 (β), 19.6 (β).

HRMS (ESI) m/z calcd. for C$_{22}$H$_{31}$O$_6$ ([M+H]⁺): 391.2115; found: 391.2115 (α) & 391.2114 (β).

2.4.4.2. Preparation and characterization of boryl donors

6b,9a-dimethyl-8-vinyl-6b,9a-dihydroacenaphtho[1,2-d][1,3,2]dioxaborole 2b
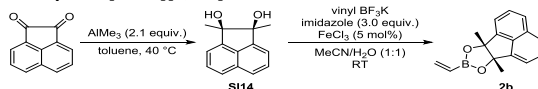
The compound was prepared according to a modified literature procedure.[131]

First step (1,2-dimethyl-1,2-dihydroacenaphthylene-1,2-diol, SI14):

Under a nitrogen atmosphere, a solution of acenaphthoquinone (911 mg, 5.0 mmol, 1.0 equiv) in dry toluene (5 mL) was allowed to stir at 40 °C for 30 min. Trimethyl aluminum (5.3 mL, 2.0 M in toluene, 10.5 mmol, 2.1 equiv) was added dropwise with the aid of a syringe. Upon completion of the addition, the reaction mixture was allowed to stir at 40 °C for 1 h. The mixture was cooled to 0 °C, and the reaction was quenched with H$_2$O (2 mL) and HCl (1 M, 1 mL). The resulting mixture was passed through a plug of celite. Upon washing with brine, the organic fraction was dried over Na$_2$SO$_4$. After filtration, the volatiles of the filtrate were removed under reduced pressure. The crude product was recrystallized from ethyl acetate to afford the title product as an off-white solid (304 mg, 1.4 mmol, 28%). The NMR data match previously reported data for the title product.[131]

¹H NMR (500 MHz, CDCl$_3$) δ 7.75 (d, *J* = 8.1 Hz, 2H), 7.61 − 7.55 (m, 2H), 7.50 (d, *J* = 6.9 Hz, 2H), 2.96 (s, 2H), 1.64 (s, 6H).

Second step:

To a solution of vinyl potassium trifluoroborate (190 mg, 1.4 mmol, 1.0 equiv) in acetonitrile/H$_2$O (1:1, 4 mL) at room temperature, 1,2-dimethylacenaphthylene-1,2-diol (304 mg, 1.4 mmol, 1.0 equiv), imidazole (290 mg, 4.3 mmol, 3.0 equiv), and FeCl$_3$ (19.2 mg, 0.07 mmol, 5 mol%) were added. The reaction mixture was allowed to stir for 50 min. The mixture was filtered through a plug of celite (eluent: diethyl ether). The volatiles were removed under reduced pressure. The residue was subjected to column chromatography (silica gel, 0 − 10% EtOAc in petroleum ether) to isolate the title product **2b** as a white solid (284 mg, 1.14 mmol, 81%). The NMR data match previously reported data for the title product.[132]

¹H NMR (400 MHz, CDCl$_3$) δ 7.79 (dd, *J* = 7.8, 1.1 Hz, 2H), 7.67 − 7.52 (m, 4H), 6.12 (dd, *J* = 19.6, 4.2 Hz, 1H), 5.96 (dd, *J* = 13.7, 4.2 Hz, 1H), 5.79 (dd, *J* = 19.5, 13.8 Hz, 1H), 1.81 (s, 6H).

(3a*S*,4*R*,6*R*,7a*R*)-3a,5,5-trimethyl-2-vinylhexahydro-4,6-methanobenzo[*d*][1,3,2]dioxaborole 2c
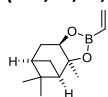
The compound was prepared in accordance to a literature procedure.[133] A solution of vinylboronic acid dibutyl ester (300 mg, 359 µL, 1.63 mmol, 1.0 equiv) and (+)-pinane diol (277 mg, 1.63 mmol, 1.0 equiv) in *n*-pentane (4.8 mL) and Et$_2$O (0.54 mL) was allowed to stir at room temperature for 19.5 h under a nitrogen atmosphere. The volatiles were removed under reduced pressure and the residue was subjected to column chromatography (silica gel, 0-100% EtOAc in petroleum ether) to isolate the title compound (328 mg, 1.59 mmol, 98%) as a colorless oil. The NMR data match previously reported data for the title product.[133]

¹H NMR (500 MHz, CDCl$_3$) δ 6.16 (dd, *J* = 19.6, 4.1 Hz, 1H), 6.03 (dd, *J* = 13.7, 4.1 Hz, 1H), 5.89 (dd, *J* = 19.6, 13.7 Hz, 1H), 4.32 (dd, *J* = 8.7, 1.9 Hz, 1H), 2.39 − 2.31 (m, 1H), 2.27 − 2.17 (m, 1H), 2.07 (t, *J* = 5.5 Hz, 1H), 1.95 − 1.86 (m, 2H), 1.41 (s, 3H), 1.29 (s, 3H), 1.15 (d, *J* = 10.8 Hz, 1H), 0.85 (s, 3H);

13C{1H} NMR (126 MHz, CDCl₃) δ 137.2, 85.9, 77.9, 51.5, 39.6, 38.3, 35.6, 28.8, 27.2, 26.6, 24.2.

(*E*)-1,2-bis(4,4,5,5-tetramethyl-1,3,2-dioxaborolan-2-yl)ethene 4
The compound was prepared in accordance to a modified literature procedure.[134] In a nitrogen-filled glove box, a 20 mL scintillation vial was charged sequentially with Grubbs II catalyst (84.9 mg, 0.1 mmol, 0.02 equiv), toluene (5 mL), and vinyl Bpin (846.3 µL, 770.1 mg, 5.0 mmol, 1.0 equiv). The vial was sealed with a Teflon-lined screw cap, placed in a pre-heated aluminum block, and allowed to stir at 110 °C. The reaction progress was monitored with GC/MS analysis. When GC/MS analysis indicated no further conversion of vinyl Bpin, 1 mol% of Grubbs II was added. For full conversion of vinyl Bpin, a total of 5 mol% Grubbs II catalyst and 24 h reaction time were required. After completion of the reaction, the vial was removed from the glove box and the reaction mixture was filtered through a pad of celite. The volatiles of the filtrate were removed under reduced pressure. The residue was subjected to column chromatography (silica gel, 0 - 5% EtOAc in petroleum ether) to isolate the title product as a white solid (235 mg, 0.84 mmol, 34%). The NMR data match previously reported data for the title product.[134]
**1H NMR** (400 MHz, CDCl₃) δ 6.64 (s, 2H), 1.25 (s, 24H).

(*E*)-2-(3,3-dimethylbut-1-en-1-yl)-4,4,5,5-tetramethyl-1,3,2-dioxaborolane 3ab
The compound was prepared in accordance to a literature procedure.[135] A mixture of 3,3-dimethyl-1-butyne (1.50 g, 2.25 mL, 18.3 mmol, 1.0 equiv), HBpin (2.57 g, 2.91 mL, 20.1 mmol, 1.1 equiv), and Schwartz's reagent (471 mg, 1.83 mmol, 0.10 equiv) was allowed to stir at room temperature for 17.5 h under a nitrogen atmosphere. The reaction was quenched by filtration over a short plug of silica. The silica plug was washed with CH₂Cl₂ (300 mL). The filtrate was concentrated under reduced pressure to furnish the title compound (2.94 g, 14.0 mmol, 77%) as a colorless solid. The NMR data match previously reported data for the title product.[136]
1H NMR (500 MHz, CDCl₃) δ 6.64 (d, *J* = 18.2 Hz, 1H), 5.35 (d, *J* = 18.3 Hz, 1H), 1.27 (s, 12H), 1.02 (s, 9H).

2.4.5. General procedures for Rh-catalyzed C-H borylation of alkenes

General procedure 1
In a nitrogen-filled glove box, a 10 mL screw-cap vial equipped with a Teflon-coated magnetic stirring bar was charged with [Rh(COD)OMe]₂ (1.9 mg, 4 µmol, 2 mol%), xantphos (4.6 mg, 8 µmol, 4 mol%), dioxane (200 µL), boryl group donor reagent (300 µmol, 1.5 equiv), and alkene (200 µmol). The vial was sealed with a cap, removed from the glove box, placed in a pre-heated aluminum block and allowed to stir (800 rpm) at 90 °C for 16 h. Upon cooling to room temperature, the reaction mixture was filtered through a plug of celite (eluent: ethyl acetate). The volatiles of the filtrate were removed under reduced pressure and the residue was subjected to column chromatography to isolate the corresponding product.

General procedure 2
In a nitrogen-filled glove box, a 10 mL screw-cap vial equipped with a Teflon-coated magnetic stirring bar was charged with [Rh(COD)OMe]₂ (3.9 mg, 8 µmol, 4 mol%), xantphos (9.3 mg, 16 µmol, 8 mol%), dioxane (200 µL), boryl group donor reagent (600 µmol, 3.0 equiv), and alkene (200 µmol). The vial was sealed with a cap, removed from the glove box, placed in a pre-heated aluminum block and allowed to stir (800 rpm) at 90 °C for 16 h. Upon cooling to room temperature, the reaction mixture was filtered through a plug of celite (eluent: ethyl acetate). The volatiles of the filtrate were removed under reduced pressure and the residue was subjected to column chromatography to isolate the corresponding product.

General procedure 3
In a nitrogen-filled glove box, a 10 mL screw-cap vial equipped with a Teflon-coated magnetic stirring bar was charged with [Rh(COD)OMe]₂ (3.9 mg, 8 µmol, 4 mol%), xantphos (9.3 mg, 16 µmol, 8 mol%), dioxane (200 µL), boryl group donor reagent (600 µmol, 3.0 equiv), and alkene (200 µmol). The vial was sealed with a cap, removed from the glove box, placed in a pre-heated aluminum block and allowed to stir (800 rpm) at 90 °C for 48 h. Upon cooling to room temperature, the reaction mixture was filtered through a plug of celite (eluent: ethyl acetate). The volatiles of the filtrate were removed under reduced pressure and the residue was subjected to column chromatography to isolate the corresponding product.

General procedure for the determination of the crude yield by 1H NMR spectroscopy
For the determination of the analytical yields of the reaction, the same general procedure was used as for the determination of the isolated yields (scale: 200 µmol). Upon cooling to room temperature, a solution of the standard (100 µL of 0.5 M 1,3,5-trimethoxybenzene in chloroform) and CDCl₃ (400 µL) were added to the reaction mixture. The yield was determined based on the integrals of the signals of the aromatic protons of the internal standard and the signals of the product that did not overlap with any other signals, typically vinylic protons, in a 1H NMR experiment.

2.4.6. Overview of synthetic capacity

Substrate	Catalyst loading [mol%]	B₂pin₂ loading [mol%]	Boron donor [donor, equiv.]	Tempera-ture [°C]	Time [h]	NMR yield [%]ᵃ	Isolated yield [%]ᵃ
1a	2	-	**2**, 1.5	90	16	92	81
1b	4	-	**2**, 2.0	90	16	80	25
1c	4	-	**2**, 3.0	90	16	69	65
1d	4	-	**2**, 3.0	90	16	80	73
1e	4	-	**2**, 3.0	90	16	58	45
1f	4	-	**2**, 3.0	90	16	87	55
1g	2	-	**2**, 1.5	90	16	82	65
1h	4	-	**2**, 3.0	90	16	83	51
1i	2	-	**2**, 1.5	90	16	n.d.	76
1j	4	-	**2**, 3.0	90	16	74	53
1k	4	-	**2**, 3.0	90	16	70	47
1l	4	-	**2**, 3.0	90	16	92	89
1m	2	-	**2**, 1.5	90	16	n.d.	66
1n	2	-	**2**, 1.5	90	16	90	75
1o	4	-	**2**, 3.0	90	16	86	79
1p	4	-	**4**, 1.0	90	48	53	22
1q	4	-	**4**, 1.0	90	48	42	17
1r	4	-	**2**, 3.0	90	16	76	43
1s	2	-	**2**, 1.5	90	16	80	n.d.
1t	4	-	**2**, 3.0	90	16	88	75
1u	4	-	**2**, 3.0	90	16	98	63
1v	2	-	**2**, 1.5	90	16	55	52
1w	4	-	**2**, 3.0	90	16	54	n.d.
1x	4	-	**2**, 3.0	90	16	80	80
1y	2	5	**2**, 1.5	90	16	97	n.d.
1z	2	5	**2**, 1.5	90	16	93	n.d.
1aa	2	5	**2**, 1.5	90	16	85	n.d.
1ab	4	10	**2**, 2.0	90	16	52	23
1ac	4	10	**2**, 3.0	150	16	81	27
1ad	4	10	**2**, 3.0	150	48	77	53
1ae	4	10	**2**, 3.0	150	16	50	29
1af	4	10	**3z**, 2.0	150	16	94	68
1af	4	10	**2**, 2.0	150	16	88	n.d.

Table 2.11. Concise overview for conditions of reactions of all substrates. ᵃ Because vinylboronic esters tend to partially decompose during chromatography on silica gel[137–139], depending on the relative stability of the products, the yields of isolated material in some cases are substantially lower than the analytical yields determined by ¹H NMR analysis.

82
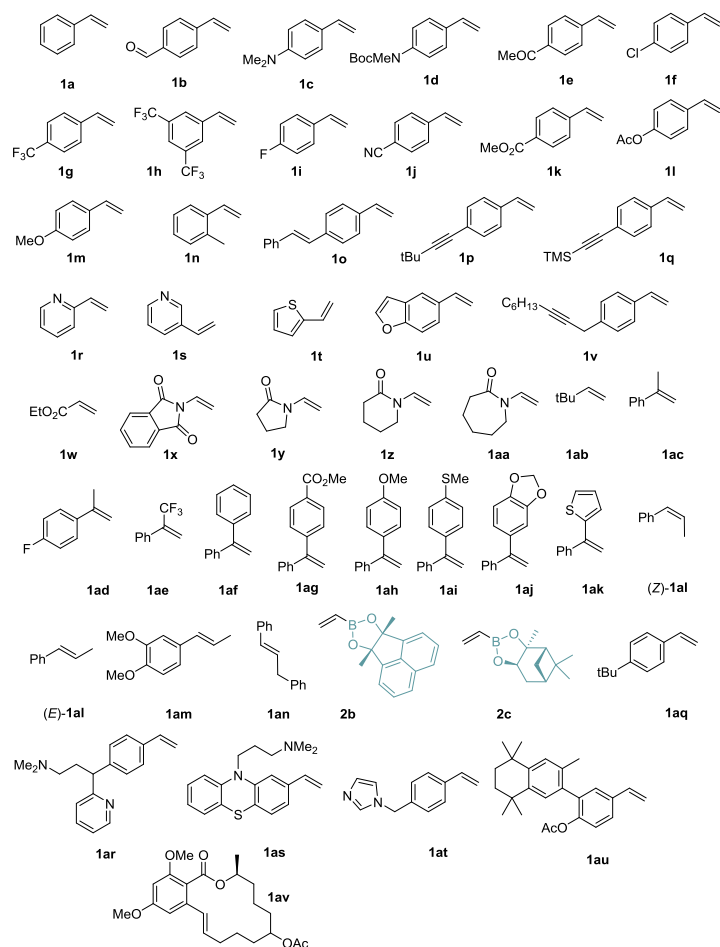
Figure 2.46: Overview of successful substrates
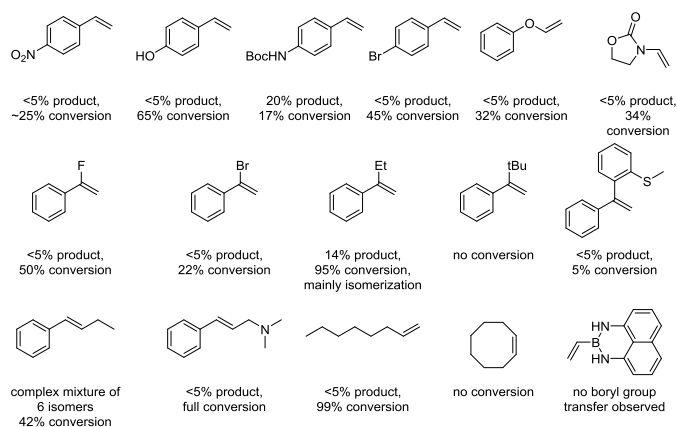
Figure 2.47: Overview of unsuccessful substrates.

2.4.7. Characterization of products
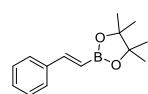
(E)-4,4,5,5-tetramethyl-2-styryl-1,3,2-dioxaborolane 3a

The compound was prepared according to general procedure 1 by reaction of styrene (20.8 mg, 200 µmol) and vinyl Bpin (46.2 mg, 300 µmol) and was isolated by column chromatography (silica gel, 0 – 5.5% MTBE in petroleum ether) to give a colorless oil (37.1 mg, 161 µmol, 81%). The NMR data match previously reported data for the title product.[140] The crude yield of the reaction was found to be 92% as determined in an analogous experiment using ^{1}H NMR spectroscopy and 1,3,5-trimethoxybenzene as an internal standard.

^{1}H NMR (500 MHz, CDCl₃) δ 7.51 – 7.47 (m, 2H), 7.40 (d, J = 18.4 Hz, 1H), 7.37 – 7.25 (m, 3H), 6.17 (d, J = 18.4 Hz, 1H), 1.32 (s, 12H);

^{13}C{^{1}H} NMR (126 MHz, CDCl₃) δ 149.6, 137.6, 129.0, 128.7, 127.2, 83.5, 24.9 [Note: the carbon atom attached to the boron atom was not observed due to quadrupole broadening or relaxation delay caused by the [11]B nucleus[141]];

^{11}B NMR (160 MHz, CDCl₃) δ 30.3.

(*E*)-4-(2-(4,4,5,5-tetramethyl-1,3,2-dioxaborolan-2-yl)vinyl)benzaldehyde 3b
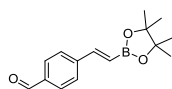
In a nitrogen-filled glove box, a 10 mL screw-cap vial equipped with a Teflon-coated magnetic stirring bar was charged with [Rh(COD)OMe]$_2$ (3.9 mg, 8 µmol, 4 mol%), xantphos (9.3 mg, 16 µmol, 8 mol%), dioxane (200 µL), vinyl boronate pinacol ester (**2**, 61.6 mg, 400 µmol, 2.0 equiv) and 4-vinylbenzaldehyde (26.4 mg, 200 µmol, 1.0 equiv). The vial was sealed with a cap, removed from the glove box, placed in a pre-heated aluminum block and allowed to stir (800 rpm) at 90 °C for 16 h. Upon cooling to room temperature, the reaction mixture was filtered through a plug of celite (eluent: ethyl acetate), the filtrate was concentrated under reduced pressure and the residue was subjected to column chromatography (silica gel, 0-10% MTBE in petroleum ether) to give the title compound (13.2 mg, 51.0 µmol, 25%) alongside with (*E*)-1,2-bis(4,4,5,5-tetramethyl-1,3,2-dioxaborolan-2-yl)ethene (**4**, 0.5 mg, 1.78 µmol) and 2,2'-(ethene-1,1-diyl)bis(4,4,5,5-tetramethyl-1,3,2-dioxaborolane) (3.6 mg, 13.0 µmol) as a yellow oil. The NMR data match previously reported data for the title product.[142] The crude yield of the reaction was found to be 80% as determined in an analogous experiment using ^{1}H NMR spectroscopy and isochroman as an internal standard.

^{1}H NMR (400 MHz, CDCl$_3$) δ 9.99 (s, 1H), 7.90 – 7.82 (m, 2H), 7.65 – 7.58 (m, 2H), 7.42 (d, *J* = 18.4 Hz, 1H), 6.32 (d, *J* = 18.5 Hz, 1H), 1.32 (s, 12H);

^{13}C{^{1}H} NMR (126 MHz, CDCl$_3$) δ 191.9, 147.9, 143.3, 136.4, 130.2, 127.6, 83.8, 24.9 [Note: the carbon atom attached to the boron atom was not observed due to quadrupole broadening or relaxation delay caused by the ^{11}B nucleus[141]];

^{11}B NMR (160 MHz, CDCl$_3$) δ 30.7.

(*E*)-*N*,*N*-dimethyl-4-(2-(4,4,5,5-tetramethyl-1,3,2-dioxaborolan-2-yl)vinyl)aniline 3c
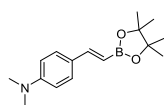
The compound was prepared according to general procedure 2 by reaction of *N*,*N*-dimethyl-4-vinylaniline (29.4 mg, 200 µmol) and vinyl Bpin (92.4 mg, 600 µmol) and was isolated by column chromatography (silica gel, 0 – 4% MTBE in petroleum ether) to give a pale yellow solid (53.7 mg, mixture of product and vinyl Bpin dimer (2/1), calculated amount of product: 35.5 mg, 130 µmol, 65%). The isolated material contained a mixture of **3c** (67%) and vinyl Bpin dimer (33%). The NMR data match previously reported data for the title product.[140] The crude yield of the reaction was found to be 69% as determined in an analogous experiment using ^{1}H NMR spectroscopy and 1,3,5-trimethoxybenzene as an internal standard.

^{1}H NMR (500 MHz, CDCl$_3$) δ 7.39 (d, *J* = 8.8 Hz, 2H), 7.33 (d, *J* = 18.4 Hz, 1H), 6.66 (d, *J* = 8.6 Hz, 2H), 5.92 (d, *J* = 18.4 Hz, 1H), 2.98 (s, 6H), 1.30 (s, 12H).

tert-butyl (*E*)-methyl(4-(2-(4,4,5,5-tetramethyl-1,3,2-dioxaborolan-2-yl)vinyl)phenyl)carbamate 3d
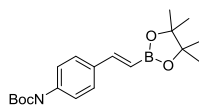
The compound was prepared according to the general procedure 2 by reaction of *tert*-butyl methyl(4-vinylphenyl)carbamate (**1d**, 46.7 mg, 200 µmol, 1.0 equiv) and vinyl Bpin (92.4 mg, 102 µL, 600 µmol, 3.0 equiv), and was isolated by column chromatography (silica gel, 0-10% MTBE in petroleum ether) to give the title compound (52.5 mg, 146 µmol, 73%) as a colorless solid. The crude yield of the reaction was found to be 80% as determined in an analogous experiment using ^{1}H NMR spectroscopy and 1,3,5-trimethoxybenzeneas an internal standard.

^{1}H NMR (500 MHz, CDCl$_3$) δ 7.46 – 7.40 (m, 2H), 7.36 (d, *J* = 18.5 Hz, 1H), 7.23 – 7.18 (m, 2H), 6.10 (d, *J* = 18.5 Hz, 1H), 3.25 (s, 3H), 1.44 (s, 9H), 1.31 (s, 12H);

^{13}C{^{1}H} NMR (126 MHz, CDCl$_3$) δ 154.7, 148.9, 144.4, 134.5, 127.3, 125.3, 83.5, 80.6, 37.2, 28.4, 24.9 [Note: the carbon atom attached to the boron atom was not observed due to quadrupole broadening or relaxation delay caused by the ^{11}B nucleus[141]];

^{11}B NMR (160 MHz, CDCl$_3$) δ 29.2;

HRMS (ESI) m/z calcd. for C$_{20}$H$_{31}$BNO$_4$ ([M+H]$^+$): 360.2341; found: 360.2330.

(*E*)-1-(4-(2-(4,4,5,5-tetramethyl-1,3,2-dioxaborolan-2-yl)vinyl)phenyl)ethan-1-one 3e
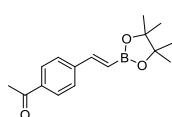
The compound was prepared according to general procedure 2 by reaction of 1-(4-vinylphenyl)ethanone (29.2 mg, 200 µmol) and vinyl Bpin (92.4 mg, 600 µmol) and was isolated by column chromatography (silica gel, 0 – 8% MTBE in petroleum ether) to give a yellow oil (24.2 mg, 89 µmol, 45%). The NMR data match previously reported data for the title product.[115] The crude yield of the reaction was found to be 58% as determined in an analogous experiment using ^{1}H NMR spectroscopy and 1,3,5-trimethoxybenzene as an internal standard.

^{1}H NMR (500 MHz, CDCl$_3$) δ 7.95 – 7.89 (m, 2H), 7.55 (d, *J* = 8.2 Hz, 2H), 7.44 – 7.36 (m, 1H), 6.28 (d, *J* = 18.4 Hz, 1H), 2.59 (s, 3H), 1.31 (s, 12H);

^{13}C{^{1}H} NMR (126 MHz, CDCl$_3$) δ 197.7, 148.1, 141.9, 137.1, 128.9, 127.2, 83.7, 26.8, 25.0 [Note: the carbon atom attached to the boron atom was not observed due to quadrupole broadening or relaxation delay caused by the ^{11}B nucleus[141]];

^{11}B NMR (160 MHz, CDCl$_3$) δ 29.8.

**(*E*)-2-(4-chlorostyryl)-4,4,5,5-tetramethyl-1,3,2-dioxaborolane 3f**
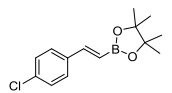
The compound was prepared according to general procedure 2 by reaction of 4-chlorostyrene (27.7 mg, 200 µmol) and vinyl Bpin (92.4 mg, 600 µmol) and was isolated by column chromatography (silica gel, 0 – 6% MTBE in petroleum ether) to give a white solid (29.2 mg, 110 µmol, 55%). The NMR data match previously reported data for the title product.[140] The crude yield of the reaction was found to be 87% as determined in an analogous experiment using ^{1}H NMR spectroscopy and 1,3,5-trimethoxybenzene as an internal standard.

^{1}H NMR (500 MHz, CDCl$_3$) δ 7.44 – 7.38 (m, 2H), 7.38 – 7.20 (m, 3H), 6.13 (d, *J* = 18.4 Hz, 1H), 1.31 (s, 12H);

^{13}C{^{1}H} NMR (126 MHz, CDCl$_3$) δ 148.1, 136.1, 134.7, 128.9, 128.4, 83.6, 24.9 [Note: the carbon atom attached to the boron atom was not observed due to quadrupole broadening or relaxation delay caused by the ^{11}B nucleus[141]];

^{11}B NMR (160 MHz, CDCl$_3$) δ 30.3.

(*E*)-4,4,5,5-tetramethyl-2-(4-(trifluoromethyl)styryl)-1,3,2-dioxaborolane 3g

The compound was prepared according to the general procedure 1 by reaction of 4-(trifluoromethyl)styrene (34.4 mg, 29.6 µL, 200 µmol, 1.0 equiv) and vinyl Bpin (46.2 mg, 50.9 µL, 300 µmol, 1.5 equiv), and was isolated by column chromatography (silica gel, 0-10% Et$_2$O in petroleum ether) to give the title compound (38.7 mg, 130 µmol, 65%) as a colorless solid. The NMR data match previously reported data for the title product.[143] The crude yield of the reaction was found to be 82% as determined in an analogous experiment using ^{1}H NMR spectroscopy and 1,3,5-trimethoxybenzene as an internal standard.

^{1}H NMR (500 MHz, CDCl$_3$) δ 7.61 – 7.54 (m, 4H), 7.40 (d, *J* = 18.5 Hz, 1H), 6.26 (d, *J* = 18.5 Hz, 1H), 1.32 (s, 12H);

13C{1H} NMR (126 MHz, CDCl₃) δ 147.8, 140.9, 130.6 (q, *J* = 32.3 Hz), 127.3, 125.7 (q, *J* = 3.8 Hz), 124.2 (q, *J* = 272.0 Hz), 83.8, 25.0 [Note: the carbon atom attached to the boron atom was not observed due to quadrupole broadening or relaxation delay caused by the ¹¹B nucleus[141]];
11B NMR (160 MHz, CDCl₃) δ 30.3;
19F NMR (471 MHz, CDCl₃) δ −62.6.

(*E*)-2-(3,5-bis(trifluoromethyl)styryl)-4,4,5,5-tetramethyl-1,3,2-dioxaborolane 3h

The compound was prepared according to the general procedure 2 by reaction of 3,5-bis(trifluoromethyl)styrene (48.0 mg, 200 µmol, 1.0 equiv) and vinyl Bpin (92.4 mg, 102 µL, 600 µmol, 3.0 equiv), and was isolated by column chromatography (silica gel, 0-5% MTBE in petroleum ether) to give the title compound (37.4 mg, 102 µmol, 51%) as a colorless oil. The NMR data match previously reported data for the title product.[144] The crude yield of the reaction was found to be 83% as determined in an analogous experiment using ¹H NMR spectroscopy and 1,3,5-trimethoxybenzene as an internal standard.

1H NMR (500 MHz, CDCl₃) δ 7.88 (s, 2H), 7.78 (s, 1H), 7.41 (d, *J* = 18.5 Hz, 1H), 6.32 (d, *J* = 18.3 Hz, 1H), 1.32 (s, 12H);
13C{1H} NMR (126 MHz, CDCl₃) δ 146.0, 139.60, 132.14 (q, *J* = 33.3 Hz), 126.88 (qq, *J* = 3.7, 1.0 Hz), 123.38 (q, *J* = 272.7 Hz), 122.18 (sept, *J* = 8.2, 4.1 Hz), 84.0, 24.9 [Note: the carbon atom attached to the boron atom was not observed due to quadrupole broadening or relaxation delay caused by the ¹¹B nucleus[141]];
11B NMR (160 MHz, CDCl₃) δ 30.1;
19F NMR (471 MHz, CDCl3) δ −63.1.

(*E*)-2-(4-fluorostyryl)-4,4,5,5-tetramethyl-1,3,2-dioxaborolane 3i

The compound was prepared according to the general procedure 1 by reaction of 4-fluorostyrene (24.4 mg, 23.9 µL, 200 µmol, 1.0 equiv) and vinyl Bpin (46.2 mg, 50.9 µL, 300 µmol, 1.5 equiv), and was isolated by column chromatography (silica gel, 0-10% MTBE in petroleum ether) to give the title compound (37.5 mg, 151 µmol, 76%) as a colorless solid. The NMR data match previously reported data for the title product.[145]

1H NMR (500 MHz, CDCl₃) δ 7.49 – 7.41 (m, 2H), 7.35 (d, *J* = 18.4 Hz, 1H), 7.06 – 6.96 (m, 2H), 6.07 (d, *J* = 18.5 Hz, 1H), 1.31 (s, 12H);
13C{1H} NMR (126 MHz, CDCl₃) δ 163.3 (d, *J* = 248.6 Hz), 148.3, 133.9 (d, *J* = 3.3 Hz), 128.8 (d, *J* = 8.3 Hz), 115.7 (d, *J* = 21.7 Hz), 83.5, 24.9 [Note: the carbon atom attached to the boron atom was not observed due to quadrupole broadening or relaxation delay caused by the ¹¹B nucleus[141]];
11B NMR (160 MHz, CDCl₃) δ 30.3;
19F NMR (471 MHz, CDCl₃) δ −112.4.

(*E*)-4-(2-(4,4,5,5-tetramethyl-1,3,2-dioxaborolan-2-yl)vinyl)benzonitrile 3j

The compound was prepared according to the general procedure 2 by reaction of 4-cyanostyrene (25.8 mg, 200 µmol, 1.0 equiv) and vinyl Bpin (92.4 mg, 102 µL, 600 µmol, 3.0 equiv), and was isolated by column chromatography (silica gel, 0-10% MTBE in petroleum ether) to give the title compound (26.8 mg, 105 µmol, 53%) as a colorless solid. The NMR data match previously reported data for the title product.[146] The crude yield of the reaction was found to be 74% as determined in an analogous experiment using ¹H NMR spectroscopy and 1,3,5-trimethoxybenzene as an internal standard.

1H NMR (500 MHz, CDCl₃) δ 7.67 – 7.59 (m, 2H), 7.59 – 7.51 (m, 2H), 7.36 (d, *J* = 18.3 Hz, 1H), 6.28 (d, *J* = 18.5 Hz, 1H), 1.32 (s, 12H);
13C{1H} NMR (126 MHz, CDCl₃) δ 147.1, 141.7, 132.5, 127.4, 118.8, 112.0, 83.8, 24.8 [Note: the carbon atom attached to the boron atom was not observed due to quadrupole broadening or relaxation delay caused by the ¹¹B nucleus[141]];
11B NMR (160 MHz, CDCl₃) *δ* = 30.4.

methyl (*E*)-4-(2-(4,4,5,5-tetramethyl-1,3,2-dioxaborolan-2-yl)vinyl)benzoate 3k
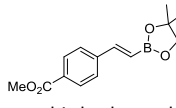
The compound was prepared according to the general procedure 2 by reaction of methyl 4-vinylbenzoate (32.4 mg, 200 µmol, 1.0 equiv) and vinyl Bpin (92.4 mg, 102 µL, 600 µmol, 3.0 equiv), and was isolated by two column chromatographies (silica gel, 0-10% MTBE in petroleum ether) to give a mixture of the title compound (27.0 mg, 93.8 µmol, 47%) and vinyl Bpin dimer (4.7 mg, 16.9 µmol) as a colorless solid. An analytical sample was subjected to a third column chromatography (silica, 0-5% MeOH in CH₂Cl₂). The NMR data match previously reported data for the title product.[145] The crude yield of the reaction was found to be 70% as determined in an analogous experiment using ¹H NMR spectroscopy and 1,3,5-trimethoxybenzene as an internal standard.

1H NMR (500 MHz, CDCl₃) δ 8.05 – 7.95 (m, 2H), 7.57 – 7.47 (m, 2H), 7.40 (d, *J* = 18.5 Hz, 1H), 6.27 (d, *J* = 18.5 Hz, 1H), 3.90 (s, 3H), 1.31 (s, 12H);
13C{1H} NMR (126 MHz, CDCl₃) δ 166.9, 148.3, 141.8, 130.3, 130.0, 127.0, 83.7, 52.3, 24.9 [Note: the carbon atom attached to the boron atom was not observed due to quadrupole broadening or relaxation delay caused by the ¹¹B nucleus[141]];
11B NMR (160 MHz, CDCl₃) δ 30.3.

### (*E*)-4-(2-(4,4,5,5-tetramethyl-1,3,2-dioxaborolan-2-yl)vinyl)phenyl acetate 3l
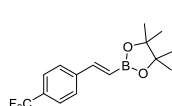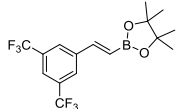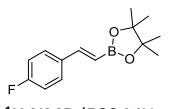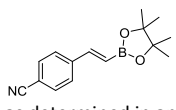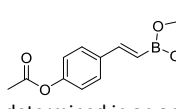
The compound was prepared according to general procedure 2 by reaction of 4-acetoxystyrene (32.4 mg, 200 µmol) and vinyl Bpin (92.4 mg, 600 µmol) and was isolated by column chromatography (silica gel, 0 – 10% MTBE in petroleum ether, 30% EtOAc in petroleum ether) to give a white solid (51.3 mg, 178 µmol, 89%). The NMR data match previously reported data for the title product.[147] The crude yield of the reaction was found to be 92% as determined in an analogous experiment using ¹H NMR spectroscopy and 1,3,5-trimethoxybenzene as an internal standard.

1H NMR (500 MHz, CDCl₃) δ 7.51 – 7.46 (m, 2H), 7.36 (d, *J* = 18.4 Hz, 1H), 7.06 (d, *J* = 8.6 Hz, 2H), 6.11 (d, *J* = 18.4 Hz, 1H), 2.29 (s, 3H), 1.31 (s, 12H);
13C{1H} NMR (126 MHz, CDCl₃) δ 169.4, 151.1, 148.4, 135.4, 128.2, 121.8, 83.5, 24.9, 21.3 [Note: the carbon atom attached to the boron atom was not observed due to quadrupole broadening or relaxation delay caused by the ¹¹B nucleus[141]];
11B NMR (160 MHz, CDCl₃) δ 30.7.

### (*E*)-2-(4-methoxystyryl)-4,4,5,5-tetramethyl-1,3,2-dioxaborolane 3m
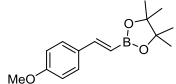
The compound was prepared according to the general procedure 1 by reaction of 4-methoxystyrene (26.8 mg, 26.9 µL, 200 µmol) and vinyl Bpin (46.2 mg, 50.9 µL, 300 µmol), and was subjected to column chromatography (silica gel, 0-10% MTBE in petroleum ether) to give 57.7 mg of a yellowish oil, which was isolated by column chromatography (silica

gel, 0-10% MTBE in petroleum ether) to give the title compound (34.1 mg, 131 μmol, 66%) as a colorless oil. The NMR data match previously reported data for the title product.[145]

¹H NMR (500 MHz, CDCl₃) δ 7.46 – 7.41 (m, 2H), 7.35 (d, *J* = 18.5 Hz, 1H), 6.88 – 6.84 (m, 2H), 6.01 (d, *J* = 18.3 Hz, 1H), 3.80 (s, 3H), 1.30 (s, 12H);

¹³C{¹H} NMR (126 MHz, CDCl₃) δ 160.4, 149.2, 130.5, 128.6, 114.1, 83.3, 55.4, 24.9 [Note: the carbon atom attached to the boron atom was not observed due to quadrupole broadening or relaxation delay caused by the ¹¹B nucleus[141]];

¹¹B NMR (160 MHz, CDCl₃) δ 30.7.

(*E*)-4,4,5,5-tetramethyl-2-(2-methylstyryl)-1,3,2-dioxaborolane 3n

The compound was prepared according to general procedure 1 by reaction of 2-methylstyrene (23.6 mg, 200 μmol) and vinyl Bpin (46.2 mg, 300 μmol) and was isolated by column chromatography (silica gel, 0 – 6% MTBE in petroleum ether) to give a colorless oil (36.6 mg, 150 μmol, 75%). The NMR data match previously reported data for the title product.[140] The crude yield of the reaction was found to be 90% as determined in an analogous experiment using ¹H NMR spectroscopy and 1,3,5-trimethoxybenzene as an internal standard.

¹H NMR (500 MHz, CDCl₃) δ 7.71 – 7.48 (m, 2H), 7.17 (m, 3H), 6.09 (d, *J* = 18.2 Hz, 1H), 2.43 (s, 3H), 1.32 (s, 12H);

¹³C{¹H} NMR (126 MHz, CDCl₃) δ 147.2, 136.8, 136.4, 130.5, 128.7, 126.2, 125.9, 83.4, 24.9, 20.0 [Note: the carbon atom attached to the boron atom was not observed due to quadrupole broadening or relaxation delay caused by the ¹¹B nucleus[141]];

¹¹B NMR (160 MHz, CDCl₃) δ 30.3.

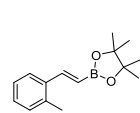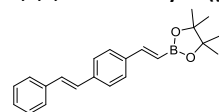### 4,4,5,5-tetramethyl-2-((*E*)-4-((*E*)-styryl)styryl)-1,3,2-dioxaborolane 3o

The compound was prepared according to general procedure 2 by reaction of (*E*)-1-styryl-4-vinylbenzene (41.3 mg, 200 μmol) and vinyl Bpin (92.4 mg, 600 μmol) and was isolated by column chromatography (silica gel, 0 – 5% MTBE in petroleum ether) to give a yellow solid (49.2 mg, 148 μmol, 79%). The crude yield of the reaction was found to be 86% as determined in an analogous experiment using ¹H NMR spectroscopy and 1,3,5-trimethoxybenzene as an internal standard.

¹H NMR (500 MHz, CDCl₃) δ 7.40 – 7.28 (m, 6H), 7.24 – 7.16 (m, 3H), 7.13 – 7.07 (m, 1H), 7.01 – 6.89 (m, 2H), 6.02 (d, *J* = 18.4 Hz, 1H), 1.16 (s, 12H);

¹³C{¹H} NMR (126 MHz, CDCl₃) δ 149.1, 138.1, 137.3, 136.9, 129.3, 128.8, 128.3, 127.9, 127.6, 126.8, 126.7, 83.5, 25.0 [Note: the carbon atom attached to the boron atom was not observed due to quadrupole broadening or relaxation delay caused by the ¹¹B nucleus[141]];

¹¹B NMR (160 MHz, CDCl₃) δ 30.7;

HRMS (ESI) m/z calcd. for C₂₂H₂₆BO₂ ([M+H]⁺): 333.2020; found: 333.2022.

(*E*)-2-(4-(3,3-dimethylbut-1-yn-1-yl)styryl)-4,4,5,5-tetramethyl-1,3,2-dioxaborolane 3p
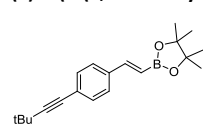
In a nitrogen-filled glove box, a 10 mL screw-cap vial equipped with a Teflon-coated magnetic stirring bar was charged with [Rh(COD)OMe]₂ (3.9 mg, 8 μmol, 4 mol%), xantphos (9.3 mg, 16 μmol, 8 mol), dioxane (300 μL), (*E*)-1,2-bis(4,4,5,5-tetramethyl-1,3,2-dioxaborolan-2-yl)ethene (**4**, 56.0 mg, 200 μmol, 1.0 equiv) and 1-(3,3-dimethylbut-1-yn-1-yl)-4-vinylbenzene (**1p**, 36.9 mg, 200 μmol, 1.0 equiv). The vial was sealed with a cap, removed from the glove box, placed in a pre-heated aluminum block and allowed to stir (800 rpm) at 90 °C for 48 h. Upon cooling to room temperature, as solution of 1,3,5-trimethoxybenzene (8.4 mg, 50 μmol, 0.25 equiv) in CHCl₃ (100 μL) was added and the crude yield was determined to be 53%. The mixture was concentrated under reduced pressure and the residue was subjected to column chromatography (silica gel, 0-2% MTBE in petroleum ether) to give the title compound (13.5 mg, 43.5 μmol, 22%) as a colorless solid alongside with the starting material (9.7 mg, 52.6 μmol, 26%) as a pale yellow oil. The crude yield of the reaction was found to be 53% as determined in an analogous experiment using ¹H NMR spectroscopy and 1,3,5-trimethoxybenzene as an internal standard.

¹H NMR (500 MHz, CDCl₃) δ 7.42 – 7.31 (m, 5H), 6.14 (d, *J* = 18.5 Hz, 1H), 1.31 (s, 9H)*, 1.31 (s, 12H)*;

* Signals overlap.

¹³C{¹H} NMR (126 MHz, CDCl₃) δ 149.0, 136.6, 131.9, 127.0, 124.7, 100.1, 83.5, 79.2, 31.2, 28.2, 25.0. [Note: the carbon atom attached to the boron atom was not observed due to quadrupole broadening or relaxation delay caused by the ¹¹B nucleus[141]];

¹¹B NMR (160 MHz, CDCl₃) δ 30.6;

HRMS (ESI) m/z calcd. for C₂₀H₂₈BO₂ ([M+H]⁺): 311.2177; found: 311.2772.

(*E*)-trimethyl((4-(2-(4,4,5,5-tetramethyl-1,3,2-dioxaborolan-2-yl)vinyl)phenyl)ethynyl)silane 3q
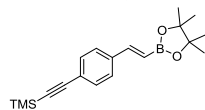
In a nitrogen-filled glove box, a 10 mL screw-cap vial equipped with a Teflon-coated magnetic stirring bar was charged with [Rh(COD)OMe]₂ (3.9 mg, 8 μmol, 4 mol%), xantphos (9.3 mg, 16 μmol, 8 mol), dioxane (300 μL), (*E*)-1,2-bis(4,4,5,5-tetramethyl-1,3,2-dioxaborolan-2-yl)ethene (**4**, 56.0 mg, 200 μmol, 1.0 equiv) and trimethyl((4-vinylphenyl)ethynyl)silane (**1q**, 40.1 mg, 200 μmol, 1.0 equiv). The vial was sealed with a cap, removed from the glove box, placed in a pre-heated aluminum block and allowed to stir (800 rpm) at 90 °C for 48 h. Upon cooling to room temperature, the reaction mixture was filtered through a plug of celite (eluent: ethyl acetate), the filtrate was concentrated under reduced pressure and the residue was isolated by column chromatography (silica gel, 0-2% MTBE in petroleum ether) to give the title compound (11.2 mg, 34.3 μmol, 17%) as pale yellow solid contaminated by traces of grease, alongside with starting material (15.4 mg, 76 .0 μmol, 38%) as a colorless oil. The crude yield of the reaction was found to be 42% as determined in an analogous experiment using ¹H NMR spectroscopy and 1,3,5-trimethoxybenzene as an internal standard.

¹H NMR (500 MHz, CDCl₃) δ 7.44 – 7.38 (m, 4H), 7.35 (d, *J* = 18.5 Hz, 1H), 6.17 (d, *J* = 18.4 Hz, 1H), 1.31 (s, 12H), 0.24 (s, 9H);

¹³C{¹H} NMR (126 MHz, CDCl₃) δ 148.7, 137.6, 132.3, 127.0, 123.6, 105.1, 95.7, 83.6, 24.9, 0.1 [Note: the carbon atom attached to the boron atom was not observed due to quadrupole broadening or relaxation delay caused by the ¹¹B nucleus[141]];

¹¹B NMR (160 MHz, CDCl₃) δ 30.5.

HRMS (ESI) m/z calcd. for C₁₉H₂₈BO₂Si ([M+H]⁺): 327.1946; found: 327.1942.

(*E*)-2-(2-(4,4,5,5-tetramethyl-1,3,2-dioxaborolan-2-yl)vinyl)pyridine 3r
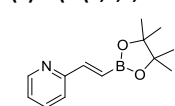
The compound was prepared according to general procedure 2 by reaction of 2-vinylpyridine (21.0 mg, 200 μmol) and vinyl Bpin (92.4 mg, 600 μmol) and was isolated by column chromatography (silica gel, 0 – 10% MTBE in petroleum ether, 30 – 80% EtOAc in petroleum ether) to give a red oil (20.0 mg, 87 μmol, 43%). The NMR data match previously reported data for the title product.[115] The crude yield of the reaction was found to be 76% as determined in an analogous experiment using ¹H NMR spectroscopy and 1,3,5-trimethoxybenzene as an internal standard.

¹H NMR (500 MHz, CDCl₃) δ 8.59 (d, *J* = 4.3 Hz, 1H), 7.65 (td, *J* = 7.7, 1.6 Hz, 1H), 7.52 – 7.33 (m, 2H), 7.22 – 7.12 (m, 1H), 6.61 (d, *J* = 18.3 Hz, 1H), 1.30 (s, 12H);
¹³C{¹H} NMR (126 MHz, CDCl₃) δ 155.5, 149.8, 148.8, 136.6, 123.2, 122.3, 83.6, 24.9 [Note: the carbon atom attached to the boron atom was not observed due to quadrupole broadening or relaxation delay caused by the ¹¹B nucleus[141]];
¹¹B NMR (160 MHz, CDCl₃) δ 30.3.

(*E*)-3-(2-(4,4,5,5-tetramethyl-1,3,2-dioxaborolan-2-yl)vinyl)pyridine 3s

The compound was prepared according to the general procedure 1 by reaction of 3-vinylpyridine (21.3 mg, 203 µmol, 1.0 equiv) and vinyl Bpin (46.2 mg, 50.9 µL, 300 µmol, 1.48 equiv). The crude yield of the reaction was found to be 80% as determined using ¹H NMR spectroscopy and 1,3,5-trimethoxybenzene as an internal standard. The mixture was subjected to two consecutive runs of column chromatography (silica gel, 0-10% MTBE, then 30-100% EtOAc in petroleum ether; silica gel 0-70% EtOAc in petroleum ether) to yield a yellow oil (21.0 mg). After addition of CH₂Cl₂ (10 mL), the organic fraction was washed with saturated CsF solution (10 mL). The aqueous fraction was washed with CH₂Cl₂ (2 × 10 mL) and the combined organic fractions were dried over Na₂SO₄. Filtration and removal of the solvent under reduced pressure gave an analytical sample of the title compound as a yellow resin. The NMR data match previously reported data for the title product.[148]
¹H NMR (500 MHz, CDCl₃) δ 8.68 (d, *J* = 2.3 Hz, 1H), 8.51 (dd, *J* = 5.0, 1.6 Hz, 1H), 7.81 (dt, *J* = 8.0, 2.1 Hz, 1H), 7.37 (d, *J* = 18.5 Hz, 1H), 7.29 (dd, *J* = 8.0, 4.8 Hz, 1H), 6.25 (d, *J* = 18.5 Hz, 1H), 1.31 (s, 12H);
¹³C{¹H} NMR (126 MHz, CDCl₃) δ 149.6, 149.0, 145.7, 133.5, 133.2, 123.8, 83.8, 25.0. [Note: the carbon atom attached to the boron atom was not observed due to quadrupole broadening or relaxation delay caused by the ¹¹B nucleus[141]];
¹¹B NMR (160 MHz, CDCl₃) δ 29.9.

(*E*)-4,4,5,5-tetramethyl-2-(2-(thiophen-2-yl)vinyl)-1,3,2-dioxaborolane 3t

The compound was prepared according to the general procedure 2 by reaction of 2-vinylthiophene (22.0 mg, 23.9 µL, 200 µmol, 1.0 equiv) and vinyl Bpin (92.4 mg, 102 µL, 600 µmol, 3.0 equiv), and was isolated by column chromatography (silica gel, 0-7.5% MTBE in petroleum ether) to give the title compound (35.2 mg, 149 µmol, 75%) as a pale yellow solid. The NMR data match previously reported data for the title product.[149] The crude yield of the reaction was found to be 88% as determined in an analogous experiment using ¹H NMR spectroscopy and 1,3,5-trimethoxybenzene as an internal standard.
¹H NMR (500 MHz, CDCl₃) δ 7.47 (d, *J* = 18.0 Hz, 1H), 7.24 (d, *J* = 5.0 Hz, 1H), 7.08 (d, *J* = 3.4 Hz, 1H), 6.98 (dd, *J* = 5.2, 3.5 Hz, 1H), 5.91 (d, *J* = 18.0 Hz, 1H), 1.30 (s, 12H);
¹³C{¹H} NMR (126 MHz, CDCl₃) δ 144.1, 141.9, 127.8, 127.8, 126.4, 83.5, 24.9 [Note: the carbon atom attached to the boron atom was not observed due to quadrupole broadening or relaxation delay caused by the ¹¹B nucleus[141]];
¹¹B NMR (160 MHz, CDCl₃) δ 30.2.

(*E*)-2-(2-(benzofuran-2-yl)vinyl)-4,4,5,5-tetramethyl-1,3,2-dioxaborolane 3u

The compound was prepared according to the general procedure 2 by reaction of 5-vinylbenzofuran (**1u**, 28.8 mg, 200 µmol, 1.0 equiv) and vinyl Bpin (92.4 mg, 102 µL, 600 µmol, 3.0 equiv), and was isolated by column chromatography (silica gel, 0-10% MTBE in petroleum ether) to give the title product (41.4 mg, 153 µmol) as a mixture with vinyl Bpin dimer (6.4 mg, 23.0 µmol). The title compound was isolated by column chromatography (silica gel, 0-10% MTBE in petroleum ether) as a colorless oil (33.9 mg, 125 µmol, 63%). The NMR data match previously reported data for the title product.[115] The crude yield of the reaction was found to be 98% as determined in an analogous experiment using ¹H NMR spectroscopy and 1,3,5-trimethoxybenzene as an internal standard.
¹H NMR (500 MHz, CDCl₃) δ 7.70 (d, *J* = 1.3 Hz, 1H), 7.61 (d, *J* = 2.3 Hz, 1H), 7.50 (d, *J* = 18.3 Hz, 1H), 7.49 (dd, *J* = 8.5, 1.8 Hz, 1H)*, 7.45 (d, *J* = 8.7 Hz, 1H)*, 6.76 (dd, *J* = 2.2, 0.8 Hz, 1H), 6.15 (d, *J* = 18.5 Hz, 1H), 1.32 (s, 12H);
* Signals overlap.
¹³C{¹H} NMR (126 MHz, CDCl₃) δ 155.6, 149.9, 145.7, 132.9, 127.9, 123.6, 120.3, 111.6, 107.0, 83.4, 25.0 [Note: the carbon atom attached to the boron atom was not observed due to quadrupole broadening or relaxation delay caused by the ¹¹B nucleus[141]];
¹¹B NMR (160 MHz, CDCl₃) δ 30.5.

4,4,5,5-tetramethyl-2-((*E*)-4-((1*E*,3*E*)-nona-1,3-dien-1-yl)styryl)-1,3,2-dioxaborolane 3v
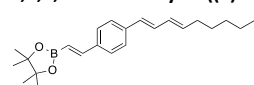
The compound was prepared according to general procedure 1 by reaction of 1-(non-2-yn-1-yl)-4-vinylbenzene (45.3 mg, 200 µmol) and vinyl Bpin (46.2 mg, 300 µmol, 1.5 equiv) and was isolated by column chromatography (silica gel, 0 – 6% MTBE in petroleum ether) to give a yellow solid (36.7 mg, 104 µmol, 52%). The crude yield of the reaction was found to be 55% as determined in an analogous experiment using ¹H NMR spectroscopy and 1,3,5-trimethoxybenzene as an internal standard.
¹H NMR (400 MHz, CDCl₃) δ 7.46 – 7.37 (m, 3H), 7.36 – 7.31 (m, 2H), 6.77 (dd, *J* = 15.5, 10.5 Hz, 1H), 6.42 (d, *J* = 15.7 Hz, 1H), 6.20 (dd, *J* = 14.3, 9.7 Hz, 1H), 6.14 (d, *J* = 18.5 Hz, 1H), 5.84 (dt, *J* = 14.8, 7.1 Hz, 1H), 2.21 – 2.06 (m, 2H), 1.43 (p, *J* = 6.8 Hz, 2H), 1.31 (s, 15H), 0.93 – 0.85 (m, 4H);
¹³C{¹H} NMR (126 MHz, CDCl₃) δ 149.2, 138.6, 136.8, 136.4, 130.6, 130.2, 129.6, 127.5, 126.4, 83.5, 33.0, 31.6, 29.1, 25.0, 22.7, 14.2 [Note: the carbon atom attached to the boron atom was not observed due to quadrupole broadening or relaxation delay caused by the ¹¹B nucleus[141]];
¹¹B NMR (160 MHz, CDCl₃) δ 28.6;
HRMS (ESI) m/z calcd. for C₂₃H₃₄BO₂ ([M+H]⁺): 353.2646; found: 353.2647.

(*E*)-2-(3,3-dimethylbut-1-en-1-yl)-4,4,5,5-tetramethyl-1,3,2-dioxaborolane 3w
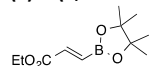
In a nitrogen-filled glove box, a 10 mL screw-cap vial equipped with a Teflon-coated magnetic stirring bar was charged with [Rh(COD)OMe]₂ (3.9 mg, 8 µmol, 4 mol%), xantphos (9.3 mg, 16 µmol, 8 mol%), toluene (200 µL), vinyl Bpin (92.4 mg, 600 µmol, 3.0 equiv) and ethyl acrylate (20.0 mg, 200 µmol). The vial was sealed with a cap, removed from the glove box, placed in a pre-heated aluminum block and allowed to stir (800 rpm) at 90 °C for 16 h. The crude yield of the reaction was found to be 54% as determined in an analogous experiment using ¹H NMR spectroscopy and 1,3,5-trimethoxybenzene as an internal standard.

(*E*)-2-(2-(4,4,5,5-tetramethyl-1,3,2-dioxaborolan-2-yl)vinyl)isoindoline-1,3-dione 3x
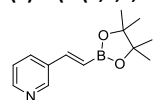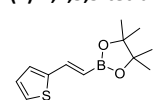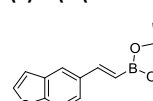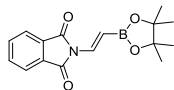
The compound was prepared according to general procedure 2 by reaction of *N*-vinylphthalimide (34.6 mg, 200 μmol) and vinyl Bpin (92.4 mg, 600 μmol) and was isolated by column chromatography (silica gel, 0 – 10% MTBE in petroleum ether, 30% EtOAc in petroleum ether) to give a beige solid (47.8 mg, 160 μmol, 80%). The NMR data match previously reported data for the title product.[150] The crude yield of the reaction was found to be 80% as determined in an analogous experiment using ¹H NMR spectroscopy and 1,3,5-trimethoxybenzene as an internal standard.

¹H NMR (500 MHz, CDCl₃) δ 7.89 (dt, *J* = 7.0, 3.5 Hz, 2H), 7.76 (dq, *J* = 6.7, 3.8 Hz, 2H), 7.47 (d, *J* = 17.0 Hz, 1H), 6.45 (d, *J* = 17.0 Hz, 1H), 1.29 (s, 12H);

¹³C{¹H} NMR (126 MHz, CDCl₃) δ 166.4, 134.8, 133.8, 131.7, 124.0, 83.6, 24.9 [Note: the carbon atom attached to the boron atom was not observed due to quadrupole broadening or relaxation delay caused by the ¹¹B nucleus[141]];

¹¹B NMR (160 MHz, CDCl₃) δ 30.7.

(*E*)-1-(2-(4,4,5,5-tetramethyl-1,3,2-dioxaborolan-2-yl)vinyl)pyrrolidin-2-one 3y
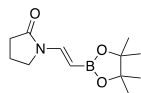
In a nitrogen-filled glove box, a 10 mL screw-cap vial equipped with a Teflon-coated magnetic stirring bar was charged with [Rh(COD)OMe]₂ (1.9 mg, 4 μmol, 2 mol%), xantphos (4.6 mg, 8 μmol, 4 mol%), dioxane (200 μL), vinyl Bpin (46.2 mg, 300 μmol), and **1y** (22.2 mg, 200 μmol). The vial was sealed with a cap, removed from the glove box, placed in a pre-heated aluminum block and allowed to stir (800 rpm) at 90 °C for 16 h. Upon cooling to room temperature, the reaction mixture was filtered through a plug of celite (eluent: ethyl acetate). The volatiles of the filtrate were removed under reduced pressure. The crude yield of the reaction was found to be 97% as determined using ¹H NMR spectroscopy and 1,3,5-trimethoxybenzene as an internal standard. The mixture was isolated by column chromatography (silica gel, 0 – 40% EtOAc in petroleum ether) to give the title compound as a yellow solid (41.3 mg) which was contaminated by an unknown Bpin-containing compound (Bpin-X), starting material and residual solvent. An analogous analytical sample was subjected to another column chromatography (silica, 0 – 40% EtOAc in petroleum ether).

¹H NMR (400 MHz, CDCl₃) δ 7.70 (d, *J* = 16.4 Hz, 1H), 4.57 (d, *J* = 16.4 Hz, 1H), 3.54 (t, *J* = 7.3 Hz, 2H), 2.51 (t, *J* = 8.1 Hz, 2H), 2.10 (quint, *J* = 7.9 Hz, 2H), 1.25 (s, 12H);

¹³C{¹H} NMR (101 MHz, CDCl₃) δ 173.7, 140.0, 83.3, 44.7, 31.6, 24.9, 17.5;

¹¹B NMR (128 MHz, CDCl₃) δ 32.9.

(*E*)-1-(2-(4,4,5,5-tetramethyl-1,3,2-dioxaborolan-2-yl)vinyl)piperidin-2-one 3z
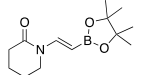
In a nitrogen-filled glove box, a 10 mL screw-cap vial equipped with a Teflon-coated magnetic stirring bar was charged with [Rh(COD)OMe]₂ (1.9 mg, 4 μmol, 2 mol%), xantphos (4.6 mg, 8 μmol, 4 mol%), B₂pin₂ (2.5 mg, 10 μmol, 5 mol%) dioxane (200 μL), vinyl Bpin (46.2 mg, 300 μmol, 1.5 equiv) and *N*-vinyl-d-valerolactam (25.0 mg, 200 μmol). The vial was sealed with a cap, removed from the glove box, placed in a pre-heated aluminum block and allowed to stir (800 rpm) at 90 °C for 16 h. Upon cooling to room temperature, the reaction mixture was filtered through a plug of celite (eluent: ethyl acetate), the filtrate was concentrated under reduced pressure and the residue was subjected to column chromatography (silica gel, 0 - 46% EtOAc in petroleum ether) to give an orange oil as an analytically pure sample. The crude yield of the reaction was found to be 93% as determined in an analogous experiment using ¹H NMR spectroscopy and 1,3,5-trimethoxybenzene as an internal standard.

¹H NMR (500 MHz, CDCl₃) δ 8.20 (d, *J* = 16.6 Hz, 1H), 4.66 (d, *J* = 16.7 Hz, 1H), 3.40 (t, *J* = 6.2 Hz, 2H), 2.50 (t, *J* = 6.6 Hz, 2H), 1.92 – 1.84 (m, 2H), 1.79 (m, 2H).1.25 (s, 12H);

¹³C{¹H} NMR (126 MHz, CDCl₃) δ 169.2, 143.1, 83.1, 44.6, 33.3, 24.9, 22.7, 20.5;

¹¹B NMR (160 MHz, CDCl₃) δ 30.8;

HRMS (ESI) m/z calcd. for C₁₃H₂₃BNO₃ ([M+H]⁺): 252.1765; found: 252.1779.

(*E*)-1-(2-(4,4,5,5-tetramethyl-1,3,2-dioxaborolan-2-yl)vinyl)azepan-2-one 3aa

In a nitrogen-filled glove box, a 10 mL screw-cap vial equipped with a Teflon-coated magnetic stirring bar was charged with [Rh(COD)OMe]₂ (1.9 mg, 4 μmol, 2 mol%), xantphos (4.6 mg, 8 μmol, 4 mol%), B₂pin₂ (2.5 mg, 10 μmol, 5 mol%) dioxane (200 μL), vinyl Bpin (46.2 mg, 300 μmol, 1.5 equiv) and *N*-vinyl-e-caprolactam (27.8 mg, 200 μmol). The vial was sealed with a cap, removed from the glove box, placed in a pre-heated aluminum block and allowed to stir (800 rpm) at 90 °C for 16 h. Upon cooling to room temperature, the reaction mixture was filtered through a plug of celite (eluent: ethyl acetate), the filtrate was concentrated under reduced pressure and the residue was subjected to column chromatography (silica gel, 0 – 35% EtOAc in petroleum ether) to give an orange oil as an analytically pure sample. The crude yield of the reaction was found to be 85% as determined in an analogous experiment using ¹H NMR spectroscopy and 1,3,5-trimethoxybenzene as an internal standard.

¹H NMR (400 MHz, C₆D₆) δ 8.73 (d, *J* = 16.6 Hz, 1H), 4.79 (d, *J* = 16.6 Hz, 1H), 2.94 (t, *J* = 4.5 Hz, 2H), 2.27 – 2.04 (m, 2H), 1.22 – 1.14 (m, 2H), 1.12 (s, 12H), 1.09 – 0.97 (m, 4H);

¹³C NMR (101 MHz, C₆D₆) δ 173.5, 143.6, 82.9, 43.3, 37.2, 29.2, 27.3, 24.9, 23.5;

¹¹B NMR (128 MHz, C₆D₆) δ 32.1;

HRMS (ESI) m/z calcd. for C₁₄H₂₅BNO₃ ([M+H]⁺): 266.1922; found: 266.1938.

(*E*)-2-(3,3-dimethylbut-1-en-1-yl)-4,5,5-tetramethyl-1,3,2-dioxaborolane 3ab
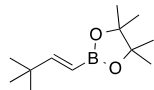
In a nitrogen-filled glove box, a 10 mL screw-cap vial equipped with a Teflon-coated magnetic stirring bar was charged with [Rh(COD)OMe]₂ (3.9 mg, 8 μmol, 4 mol%), xantphos (9.3 mg, 16 μmol, 8 mol%), B₂pin₂ (5.1 mg, 20 μmol, 10 mol%) dioxane (200 μL), vinyl Bpin (61.6 mg, 400 μmol, 2.0 equiv) and 3,3-dimethyl-1-butene (16.8 mg, 200 μmol). The vial was sealed with a cap, removed from the glove box, placed in a pre-heated aluminum block and allowed to stir (800 rpm) at 90 °C for 16 h. Upon cooling to room temperature, the reaction mixture was filtered through a plug of celite (eluent: ethyl acetate), the filtrate was concentrated under reduced pressure and the residue was subjected to column chromatography (silica gel, 0 – 3% MTBE in petroleum ether) to give a colourless oil (9.7 mg, 46 μmol, 23%). The NMR data match previously reported data for the title product.[136] The crude yield of the reaction was found to be 52% as determined in an analogous experiment using ¹H NMR spectroscopy and 1,3,5-trimethoxybenzene as an internal standard.

¹H NMR (500 MHz, CDCl₃) δ 6.64 (d, *J* = 18.2 Hz, 1H), 5.35 (d, *J* = 18.3 Hz, 1H), 1.27 (s, 12H), 1.02 (s, 9H);

¹³C{¹H} NMR (126 MHz, CDCl₃) δ 164.6, 83.2, 35.2, 28.9, 24.9 [Note: the carbon atom attached to the boron atom was not observed due to quadrupole broadening or relaxation delay caused by the ¹¹B nucleus[141]];

¹¹B NMR (128 MHz, CDCl3) δ 31.2.

(*E*)-4,4,5,5-tetramethyl-2-(2-phenylprop-1-en-1-yl)-1,3,2-dioxaborolane 3ac

In a nitrogen-filled glove box, a 10 mL screw-cap vial equipped with a Teflon-coated magnetic stirring bar was charged with [Rh(COD)OMe]$_2$ (3.9 mg, 8 µmol, 4 mol%), xantphos (9.3 mg, 16 µmol, 8 mol%), B$_2$pin$_2$ (5.1 mg, 20.0 µmol, 10 mol%), dioxane (200 µL), vinyl Bpin (92.4 mg, 102 µL, 600 µmol, 3.0 equiv) and α-methylstyrene (23.6 mg, 26.0 µL, 200 µmol, 1.0 equiv). The vial was sealed with a cap, removed from the glove box, placed in a pre-heated aluminum block and allowed to stir (800 rpm) at 150 °C for 16 h. Upon cooling to room temperature, the reaction mixture was filtered through a plug of celite (eluent: ethyl acetate), the filtrate was concentrated under reduced pressure and the residue was subjected to column chromatography (silica gel, 0-5% MTBE in petroleum ether) to give a fraction of the title compound (13.3 mg, 54.5 µmol, 27%) as a colorless oil, alongside with a fraction of a diastereomeric mixture (1.6 mg, 6.55 µmol, 3%, 54/46 = E/Z) as a colorless oil contaminated by traces of grease. The NMR data match previously reported data for the title product.[151] The crude yield of the reaction was found to be 81% (d.r. = 90/10) as determined in an analogous experiment using ^{1}H NMR spectroscopy and 1,3,5-trimethoxybenzene as an internal standard.

Major diastereoisomer (*E*)-**3ac**
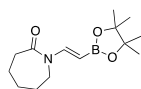**^{1}H NMR** (500 MHz, CDCl$_3$) δ 7.53 – 7.47 (m, 2H), 7.36 – 7.26 (m, 3H), 5.76 (s, 1H), 2.41 (s, 3H), 1.32 (s, 12H);
^{13}C{^{1}H} NMR (126 MHz, CDCl$_3$) δ 157.9, 143.9, 128.3, 128.1, 126.0, 83.1, 25.0, 20.2. [Note: the carbon atom attached to the boron atom was not observed due to quadrupole broadening or relaxation delay caused by the [11]B nucleus[141]];
^{11}B NMR (160 MHz, CDCl$_3$) δ 30.2.
Minor diastereoisomer (*Z*)-**3ac** (as a *E/Z* = 54/46 mixture)
^{1}H NMR (500 MHz, CDCl$_3$) δ 7.35 – 7.27 (m, 5H), 5.47 (q, *J* = 1.4 Hz, 1H), 2.21 (d, *J* = 1.4 Hz, 3H), 1.15 (s, 12H).

(E)-2-(2-(4-fluorophenyl)prop-1-en-1-yl)-4,4,5,5-tetramethyl-1,3,2-dioxaborolane 3ad

In a nitrogen-filled glove box, a 10 mL screw-cap vial equipped with a Teflon-coated magnetic stirring bar was charged with [Rh(COD)OMe]$_2$ (3.9 mg, 8 µmol, 4 mol%), xantphos (9.3 mg, 16 µmol, 8 mol%), B$_2$pin$_2$ (5.1 mg, 20.0 µmol, 10 mol%), dioxane (200 µL), vinyl Bpin (92.4 mg, 102 µL, 600 µmol, 3.0 equiv), and 4-fluoro-α-methylstyrene (27.2 mg, 26.9 µL, 200 µmol, 1.0 equiv). The vial was sealed with a cap, removed from the glove box, placed in a pre-heated aluminum block, and allowed to stir (800 rpm) at 150 °C for 48 h. Upon cooling to room temperature, the reaction mixture was filtered through a plug of celite (eluent: ethyl acetate), the filtrate was concentrated under reduced pressure and the residue was subjected to column chromatography (silica gel, 0-4% MTBE in petroleum ether). Upon evaporation of volatiles from the fraction containing the pure product, the title compound together with its (*Z*)-diastereoisomer (27.9 mg, 106 µmol, 53%, 86/14 = *E/Z*) was obtained as a colorless oil. The NMR data match previously reported data for the title product.[152] The crude yield of the reaction was found to be 77% 87/13 = *E/Z*) as determined in an analogous experiment using ^{1}H NMR spectroscopy and 1,3,5-trimethoxybenzene as an internal standard.

All NMR spectra correspond to a mixture of diastereoisomers (86/14 = E/Z):
^{1}H NMR (500 MHz, CDCl$_3$) δ 7.50 – 7.43 (m, 2H^E), 7.31 – 7.26 (m, 2H^Z), 7.04 – 6.93 (m, 2H^E, 2H^Z), 5.69 (s, 1H^E), 5.46 (q, *J* = 1.4 Hz, 1H^Z), 2.38 (d, *J* = 0.9 Hz, 3H^E), 2.19 (d, *J* = 1.4 Hz, 3H^Z), 1.31 (s, 12H^E), 1.15 (s, 12H^Z).
^{13}C{^{1}H} NMR (126 MHz, CDCl$_3$) δ 162.8 (d, J_{CF} = 247.1 Hz, *E*), 162.5 (d, J_{CF} = 247.1 Hz, *Z*), 156.9 (*Z*), 156.7 (*E*), 140.0 (d, J_{CF} = 3.2 Hz, *E*), 139.2 (d, J_{CF} = 3.2 Hz, *Z*), 129.4 (d, J_{CF} =8.0 Hz, *Z*), 127.65 (d, J_{CF} = 8.1 Hz, *E*), 115.1 (d, J_{CF} = 21.3 Hz, *E*), 114.5 (d, J_{CF} = 21.3 Hz, *Z*), 83.2 (*Z*), 83.1 (*E*), 28.0 (*Z*), 25.0 (*E*), 24.8 (*Z*), 20.3 (*E*). [Note: the carbon atom attached to the boron atom was not observed due to quadrupole broadening or relaxation delay caused by the [11]B nucleus[141]];
^{11}B NMR (160 MHz, CDCl$_3$) δ 30.4 (*E+Z*);
^{19}F NMR (471 MHz, CDCl$_3$) δ −114.6 (*E*), −115.3 (*Z*).

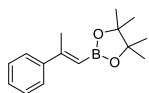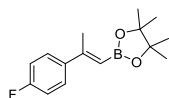## (Z)-4,4,5,5-tetramethyl-2-(3,3,3-trifluoro-2-phenylprop-1-en-1-yl)-1,3,2-dioxaborolane 3ae
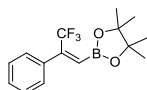
In a nitrogen-filled glove box, a 10 mL screw-cap vial equipped with a Teflon-coated magnetic stirring bar was charged with [Rh(COD)OMe]$_2$ (3.9 mg, 8 µmol, 4 mol%), xantphos (9.3 mg, 16 µmol, 8 mol%), B$_2$pin$_2$ (5.1 mg, 20.0 µmol, 10 mol%), dioxane (200 µL), vinyl Bpin (92.4 mg, 102 µL, 600 µmol, 3.0 equiv) and [1-(trifluoromethyl)vinyl]benzene (34.4 mg, 200 µmol, 1.0 equiv). The vial was sealed with a cap, removed from the glove box, placed in a pre-heated aluminum block and allowed to stir (800 rpm) at 150 °C for 16 h. Upon cooling to room temperature, the reaction mixture was filtered through a plug of celite (eluent: ethyl acetate), the filtrate was concentrated under reduced pressure and the residue was subjected to column chromatography (silica gel, 0-10% MTBE in petroleum ether) to give the title compound together with its (*E*)-diastereoisomer (17.2 mg, 57.8 µmol, 29%, 91/9 = *Z/E*) contaminated by starting material **1ae** (1.9 mg, 11.0 µmol, 5.5%), and **3a** (0.7 mg, 2.9 µmol) as a yellow oil. The NMR data match previously reported data for the title product.[153] The crude yield of the reaction was found to be 50% (90/10 = *Z/E*) as determined in an analogous experiment using ^{1}H and ^{19}F NMR spectroscopy and 1,3,5-trimethoxybenzene as an internal standard.

All NMR spectra correspond to a mixture of diastereoisomers (91/9 = Z/E):
^{1}H NMR (400 MHz, CDCl$_3$) δ 7.47 – 7.21 (m, 5H^Z + 5H^E), 6.35 (d, *J* = 1.4 Hz, 1H^Z), 6.12 (d, *J* = 1.3 Hz, 1H, H^E), 1.34 (s, 12H^E), 1.11 (s, 12H^Z).
^{13}C{^{1}H} NMR (101 MHz, CDCl$_3$) 146.1 (q, J_{CF} = 30.3 Hz), 134.5, 129.3, 128.9, 128.5, 128.0, 127.5, 123.0 (q, J_{CF} = 274.5 Hz), 84.2, 84.0, 24.9, 24.7. [Note: Only selected signals are given for the minor diastereoisomer; the carbon atom attached to the boron atom was not observed due to quadrupole broadening or relaxation delay caused by the [11]B nucleus[141]];
^{11}B NMR (160 MHz, CDCl$_3$) δ 30.0;
^{19}F NMR (377 MHz, CDCl$_3$) δ −61.2 (*E*), −67.1 (*Z*).

2-(2,2-diphenylvinyl)-4,4,5,5-tetramethyl-1,3,2-dioxaborolane 3af
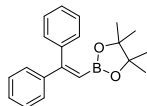
In a nitrogen-filled glove box, a 10 mL screw-cap vial equipped with a Teflon-coated magnetic stirring bar was charged with [Rh(COD)OMe]$_2$ (3.9 mg, 8 µmol, 4 mol%), xantphos (9.3 mg, 16 µmol, 8 mol%), B$_2$pin$_2$ (5.1 mg, 20.0 µmol, 10 mol%), dioxane (200 µL), (*E*)-2-(3,3-dimethylbut-1-en-1-yl)-4,4,5,5-tetramethyl-1,3,2-dioxaborolane (**3z**, 84.1 mg, 400 µmol, 2.0 equiv) and 1,1-diphenylethylene (36.1 mg, 35.3 µL, 200 µmol, 1.0 equiv). The vial was sealed with a cap, removed from the glove box, placed in a pre-heated aluminum block and allowed to stir (800 rpm) at 150 °C for 16 h. Upon cooling to room temperature, the reaction mixture was filtered through a plug of celite (eluent: ethyl acetate), the filtrate was concentrated under reduced pressure and the residue was subjected to column chromatography (silica gel, 0-6% MTBE in petroleum ether) to give the title compound (41.6 mg, 136 µmol, 68%) as a colorless oil. The NMR data match previously reported data for the title product.[154] The crude yield of the reaction was found to be 88% as determined in an analogous experiment with vinyl Bpin (**2**, 2.0 equiv) as the boryl group donor using ^{1}H NMR spectroscopy and 1,3,5-trimethoxybenzene as an internal standard.

^{1}H NMR (500 MHz, CDCl$_3$) δ 7.35 – 7.23 (m, 10H), 5.99 (s, 1H), 1.15 (s, 12H);
^{13}C{^{1}H} NMR (126 MHz, CDCl$_3$) δ 159.9, 143.2, 142.0, 130.0, 128.2, 128.1 (2 × C)[154], 127.7, 127.7, 83.3, 24.7 [Note: the carbon atom attached to the boron atom was not observed due to quadrupole broadening or relaxation delay caused by the [11]B nucleus[141]];
^{11}B NMR (160 MHz, CDCl$_3$) δ 30.4.

methyl 4-(1-phenyl-2-(4,4,5,5-tetramethyl-1,3,2-dioxaborolan-2-yl)vinyl)benzoate 3ag
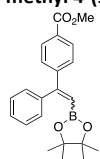
In a nitrogen-filled glove box, a 10 mL screw-cap vial equipped with a Teflon-coated magnetic stirring bar was charged with [Rh(COD)OMe]$_2$ (3.9 mg, 8 μmol, 4 mol%), xantphos (9.3 mg, 16 μmol, 8 mol%), B$_2$pin$_2$ (5.1 mg, 20.0 μmol, 10 mol%), dioxane (200 μL), vinyl Bpin (61.6 mg, 400 μmol, 2.0 equiv) and **1ag** (47.7 mg, 200 μmol, 1.0 equiv). The vial was sealed with a cap, removed from the glove box, placed in a pre-heated aluminum block and allowed to stir (800 rpm) at 150 °C for 16 h. Upon cooling to room temperature, the reaction mixture was filtered through a plug of celite (eluent: dichloromethane), the filtrate was concentrated under reduced pressure and the residue was subjected to column chromatography (silica gel, 0-9.4% MTBE in petroleum ether) to give the title compound (34.4 mg, 94.4 μmol, 47%, d.r. = 53/47)* contaminated with **4** (6.6 mg, 23.6 μmol) as light pink solid.

*The major diastereoisomer was not assigned.

All NMR spectra correspond to a mixture of diastereoisomers (d.r. = 53/47):

^{1}H NMR (400 MHz, CDCl$_3$) δ 7.99 – 7.97 (m, 2H^{d1}), 7.94 – 7.92 (m, 2H^{d2}), 7.41 – 7.07 (m, 7H^{d1} + 7H^{d2}), 6.05 (s, 1H^{d1} + 1H^{d2}), 3.92 (s, 3H^{d1}), 3.88 (s, 3H^{d2}), 1.14 (s, 12H^{d1}), 1.13 (s, 12H^{d2});

^{13}C{^{1}H} NMR (101 MHz, CDCl$_3$) δ 167.3, 167.0, 159.0, 158.6, 147.6, 146.8, 142.5, 141.3, 130.0, 129.9, 129.6, 129.5, 129.3, 129.0, 128.4, 128.3, 128.0, 128.0, 127.8 (2C), 83.5, 83.5, 52.2 (2C), 24.8, 24.7 [Note: the carbon atom attached to the boron atom was not observed due to quadrupole broadening or relaxation delay caused by the ^{11}B nucleus[141]];

^{11}B NMR (128 MHz, CDCl$_3$) δ 29.9;

HRMS (ESI) m/z calcd. for C$_{22}$H$_{26}$BO$_4$ ([M+H]$^+$): 365.1919; found: 365.1935.

2-(2-(4-methoxyphenyl)-2-phenylvinyl)-4,4,5,5-tetramethyl-1,3,2-dioxaborolane 3ah
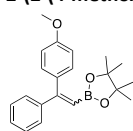
In a nitrogen-filled glove box, a 10 mL screw-cap vial equipped with a Teflon-coated magnetic stirring bar was charged with [Rh(COD)OMe]$_2$ (3.9 mg, 8 μmol, 4 mol%), xantphos (9.3 mg, 16 μmol, 8 mol%), B$_2$pin$_2$ (5.1 mg, 20.0 μmol, 10 mol%), dioxane (200 μL), vinyl Bpin (61.6 mg, 400 μmol, 2.0 equiv) and **1ah** (42.1 mg, 200 μmol, 1.0 equiv). The vial was sealed with a cap, removed from the glove box, placed in a pre-heated aluminum block and allowed to stir (800 rpm) at 150 °C for 16 h. Upon cooling to room temperature, the reaction mixture was filtered through a plug of celite (eluent: ethyl acetate), the filtrate was concentrated under reduced pressure and the residue was subjected to column chromatography (silica gel, 0-7% MTBE in petroleum ether) to give the title compound (25.1 mg, 74.7 μmol, 37%, d.r. = 57/43)* contaminated with starting material (4.6 mg, 22.0 μmol, 11%), DCM and BpinX as a red oil. The crude yield of the reaction was found to be 51% (d.r. = 55/45) as determined in an analogous experiment using ^{1}H NMR spectroscopy and 1,3,5-trimethoxybenzene as an internal standard. The NMR data match previously reported data for the title product.[155,156]

*The major diastereoisomer was not assigned.

All NMR spectra correspond to a mixture of diastereoisomers (57/43 = E/Z):

^{1}H NMR (400 MHz, CDCl$_3$) δ 7.37 – 7.18 (m, 7H^{d1} + 7H^{d2}), 6.91 – 6.79 (m, 2H^{d1} + 2H^{d2}), 5.93 (s, 1H^{d1}), 5.89 (s, 1H^{d2}), 3.85 (s, 3H^{d2}), 3.81 (s, 3H^{d1}), 1.20 (s, 12H^{d2}), 1.15 (s, 12H^{d1}).

^{13}C{^{1}H} NMR (101 MHz, CDCl$_3$) δ 159.8, 159.6, 159.5, 159.5, 143.9, 142.2, 135.8, 134.5, 131.4, 130.0, 129.4, 128.3, 128.1, 128.1, 127.7, 127.6, 113.5, 113.0, 83.3, 83.1, 55.4, 55.4, 24.8, 24.7. [Note: the carbon atom attached to the boron atom was not observed due to quadrupole broadening or relaxation delay caused by the ^{11}B nucleus[141]];

^{11}B NMR (128 MHz, CDCl$_3$) δ 31.2.

4,4,5,5-tetramethyl-2-(2-(4-(methylthio)phenyl)-2-phenylvinyl)-1,3,2-dioxaborolane 3ai
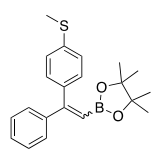
In a nitrogen-filled glove box, a 10 mL screw-cap vial equipped with a Teflon-coated magnetic stirring bar was charged with [Rh(COD)OMe]$_2$ (3.9 mg, 8 μmol, 4 mol%), xantphos (9.3 mg, 16 μmol, 8 mol%), B$_2$pin$_2$ (5.1 mg, 20.0 μmol, 10 mol%), dioxane (200 μL), vinyl Bpin (61.6 mg, 400 μmol, 2.0 equiv) and **1ai** (45.3 mg, 200 μmol, 1.0 equiv). The vial was sealed with a cap, removed from the glove box, placed in a pre-heated aluminum block and allowed to stir (800 rpm) at 150 °C for 16 h. Upon cooling to room temperature, the reaction mixture was filtered through a plug of celite (eluent: ethyl acetate), the filtrate was concentrated under reduced pressure and the residue was subjected to column chromatography (silica gel, 0-7% MTBE in petroleum ether) to give the title compound (26.7 mg, 75.8 μmol, 38%, d.r. = 53/47)* as a colorless oil. The crude yield of the reaction was found to be 47% (d.r. = 53/47) as determined in an analogous experiment using ^{1}H NMR spectroscopy and 1,3,5-trimethoxybenzene as an internal standard.

*The major diastereoisomer was not assigned.

*All NMR spectra correspond to a mixture of diastereoisomers (d.r. = 53/47):*

^{1}H NMR (400 MHz, CDCl$_3$) δ 7.42 – 7.17 (m, 9H^{d1} + 9H^{d2}), 6.04 (s, 1H^{d1}), 6.00 (s, 1H^{d2}), 2.57 (s, 3H^{d2}), 2.53 (s, 3H^{d1}), 1.24 (s, 12H^{d2}), 1.21 (s, 12H^{d1});

^{13}C NMR (101 MHz, CDCl$_3$) δ 159.5, 159.3, 143.3, 141.8, 139.9, 138.8, 138.7, 138.0, 130.5, 130.0, 128.5, 128.2, 128.2, 128.1, 127.8, 127.7, 125.9, 125.8, 83.3, 83.3, 24.8, 24.7, 16.1, 15.7 [Note: the carbon atom attached to the boron atom was not observed due to quadrupole broadening or relaxation delay caused by the ^{11}B nucleus[141]];

^{11}B NMR (128 MHz, CDCl$_3$) δ 31.3;

HRMS (ESI) m/z calcd. for C$_{21}$H$_{26}$BO$_2$S ([M+H]$^+$): 353.1741; found: 353.1757.

2-(2-(benzo[d][1,3]dioxol-5-yl)-2-phenylvinyl)-4,4,5,5-tetramethyl-1,3,2-dioxaborolane 3aj
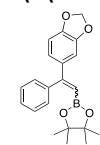
In a nitrogen-filled glove box, a 10 mL screw-cap vial equipped with a Teflon-coated magnetic stirring bar was charged with [Rh(COD)OMe]$_2$ (3.9 mg, 8 μmol, 4 mol%), xantphos (9.3 mg, 16 μmol, 8 mol%), B$_2$pin$_2$ (5.1 mg, 20.0 μmol, 10 mol%), dioxane (200 μL), vinyl Bpin (61.6 mg, 400 μmol, 2.0 equiv) and **1ak** (44.9 mg, 200 μmol, 1.0 equiv). The vial was sealed with a cap, removed from the glove box, placed in a pre-heated aluminum block and allowed to stir (800 rpm) at 150 °C for 16 h. Upon cooling to room temperature, the reaction mixture was filtered through a plug of celite (eluent: dichloromethane), the filtrate was concentrated under reduced pressure and the residue was subjected to column chromatography (silica gel, 0-5.5% MTBE in petroleum ether) to give the title compound (37.6 mg, 107 μmol, 54%, d.r. = 53/47)* as an orange oil. The crude yield of the reaction was found to be 81% (d.r. = 53/47) as determined in an analogous experiment using ^{1}H spectroscopy and 1,3,5-trimethoxybenzene as an internal standard.

*The major diastereoisomer was not assigned.

All NMR spectra correspond to a mixture of diastereoisomers (d.r. = 53/47):

1H NMR (400 MHz, CDCl3) δ 7.37 – 7.13 (m, 5H^{d1} + 5H^{d2}), 6.86 – 6.56 (m, 3H^{d1} + 3H^{d2}), 5.94 (s, 2H^{d1}), 5.91 (s, 2H^{d2}), 5.86 (s, 1H^{d1}), 5.86 (s, 1H^{d2}), 1.17 (s, 12H^{d1}), 1.11 (s, 12H^{d2});

13C{1H} NMR (101 MHz, CDCl3) δ 159.5 (2C), 147.8, 147.6, 147.4, 147.0, 143.4, 142.1, 137.7, 136.1, 129.9, 128.3, 128.2, 128.1, 127.7, 127.6, 123.8, 122.5, 110.6, 108.3, 107.8, 107.6, 101.2, 101.1, 83.3, 83.2, 24.8, 24.7 [Note: the carbon atom attached to the boron atom was not observed due to quadrupole broadening or relaxation delay caused by the ^{11}B nucleus[141]];

11B NMR (128 MHz, CDCl3) δ 31.3;

HRMS (ESI) m/z calcd. for $C_{21}H_{24}BO_4$ ([M+H]$^+$): 351.1762; found: 351.1783.

(E)-4,4,5,5-tetramethyl-2-(2-phenyl-2-(thiophen-2-yl)vinyl)-1,3,2-dioxaborolane 3ak
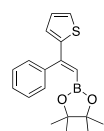
In a nitrogen-filled glove box, a 10 mL screw-cap vial equipped with a Teflon-coated magnetic stirring bar was charged with [Rh(COD)OMe]$_2$ (3.9 mg, 8 µmol, 4 mol%), xantphos (9.3 mg, 16 µmol, 8 mol%), B$_2$pin$_2$ (5.1 mg, 20.0 µmol, 10 mol%), dioxane (200 µL), vinyl Bpin (61.6 mg, 400 µmol, 2.0 equiv) and **1aj** (37.3 mg, 200 µmol, 1.0 equiv). The vial was sealed with a cap, removed from the glove box, placed in a pre-heated aluminum block and allowed to stir (800 rpm) at 150 °C for 16 h. Upon cooling to room temperature, the reaction mixture was filtered through a plug of celite (eluent: dichloromethane), the filtrate was concentrated under reduced pressure and the residue was subjected to column chromatography (silica gel, 0-6% MTBE in petroleum ether) to give the title compound together with its (Z)-diastereoisomer (15.3 mg, 49.0 µmol, 25%, E/Z =76/34) and a by-product resulting from an aromatic C–H borylation (6.0 mg, 19.2 µmol, 10%) as yellow oil. Indicated below are all NMR signals of the sample. The signals of the title compound match previously reported data.[156] The crude yield of the reaction was found to be 39% (77/23 = E/Z) as determined in an analogous experiment using ^{1}H spectroscopy and 1,3,5-trimethoxybenzene as an internal standard.

All NMR spectra correspond to a mixture of diastereoisomers (76/24 = E/Z):

1H NMR (500 MHz, CDCl3) δ 7.54 – 7.28 (m, 5H^E +6H^Z + 6H^{Ar}), 7.24 (dd, J = 5.0, 1.2 Hz, 1H^E), 7.12 (dd, J = 3.5, 1.2 Hz, 1H^Z), 7.03 – 6.96 (m, 1H^Z + 1H^{Ar}), 6.92 (dd, J = 5.1, 3.7 Hz, 1H^E), 6.76 (dd, J = 3.7, 1.2 Hz, 1H^E), 6.04 (s, 1H^E), 5.86 (s, 1H^Z), 5.68 – 5.65 (m, 1H^{Ar}), 5.30 – 5.29 (m, 1H^{Ar}), 1.35 (s, 12H^{Ar}), 1.25 (s, 12H^Z), 1.11 (s, 12H^E);

13C{1H} NMR (126 MHz, CDCl3) δ 153.2 (C^E), 151.8, 151.7, 147.9 (C^E), 143.8, 143.7, 143.4, 141.0, 141.0 (C^E), 137.5, 129.6 (C^E), 128.7, 128.4, 128.3, 128.2, 128.2, 128.1 (C^E), 127.9 (C^E), 127.8 (C^E), 127.7, 127.6 (C^E), 127.6, 126.7, 126.5 (C^E), 126.3, 114.8, 84.3, 83.5, 83.2 (C^E), 67.2, 24.9, 24.9, 24.7 (C^E) [Note: the carbon atom attached to the boron atom was not observed due to quadrupole broadening or relaxation delay caused by the ^{11}B nucleus[141]];

11B NMR (160 MHz, CDCl3) δ 30.2.

(Z)-4,4,5,5-tetramethyl-2-(1-phenylprop-1-en-2-yl)-1,3,2-dioxaborolane 3al
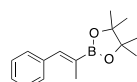
From trans-β-methylstyrene:

In a nitrogen-filled glove box, a 10 mL screw-cap vial equipped with a Teflon-coated magnetic stirring bar was charged with [Rh(COD)OMe]$_2$ (3.9 mg, 8 µmol, 4 mol%), xantphos (9.3 mg, 16 µmol, 8 mol%), B$_2$pin$_2$ (5.1 mg, 20 µmol, 10 mol%) dioxane (200 µL), vinyl Bpin (61.6 mg, 400 µmol, 2.0 equiv), and *trans*-β-methylstyrene (23.6 mg, 200 µmol). The vial was sealed with a cap, removed from the glove box, placed in a pre-heated aluminum block and allowed to stir (800 rpm) at 150 °C for 16 h. Upon cooling to room temperature, the reaction mixture was filtered through a plug of celite (eluent: ethyl acetate). The volatiles of the filtrate were removed under reduced pressure and the residue was subjected to column chromatography (silica gel, 0 – 5% MTBE in petroleum ether) to isolate the title product as a colorless oil (18.5 mg, 76 µmol, 38%). In agreement with the GC analysis of the initial reaction mixture, the NMR data indicated the formation of an 83:17 ratio of Z/E-product as well as traces of other isomers due to borylation of the benzylic position and isomerization of the double bond. The NMR data of the main compound match previously reported data for the (Z)-isomer of the product.[157]

*Major diastereoisomer, (Z)-**3al**:*

1H NMR (500 MHz, CDCl3) δ 7.34 – 7.23 (m, 4H), 7.20 – 7.14 (m, 2H), 1.92 (d, *J* = 1.8 Hz, 3H), 1.24 (s, 12H);

13C{1H} NMR (126 MHz, CDCl3) δ 142.5, 138.2, 129.6, 128.2, 127.2, 83.7, 25.0, 16.0 [Note: the carbon atom attached to the boron atom was not observed due to quadrupole broadening or relaxation delay caused by the ^{11}B nucleus[141]];

11B NMR (160 MHz, CDCl3) δ 31.1.

From cis-β-methylstyrene:
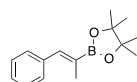
In a nitrogen-filled glove box, a 10 mL screw-cap vial equipped with a Teflon-coated magnetic stirring bar was charged with [Rh(COD)OMe]$_2$ (3.9 mg, 8 µmol, 4 mol%), xantphos (9.3 mg, 16 µmol, 8 mol%), B$_2$pin$_2$ (5.1 mg, 20 µmol, 10 mol%) dioxane (200 µL), vinyl Bpin (61.6 mg, 400 µmol, 2.0 equiv), and *cis*-β-methylstyrene (23.6 mg, 200 µmol). The vial was sealed with a cap, removed from the glove box, placed in a pre-heated aluminum block and allowed to stir (800 rpm) at 150 °C for 16 h. Upon cooling to room temperature, the reaction mixture was filtered through a plug of celite (eluent: ethyl acetate). The volatiles of the filtrate were removed under reduced pressure and the residue was subjected to column chromatography (silica gel, 0 – 5% MTBE in petroleum ether) to isolate the title product as a colorless oil (18.8 mg, 77 µmol, 39%). In agreement with the GC analysis of the initial reaction mixture, the NMR data indicated the formation of an 83:17 ratio of Z/E-product as well as traces of other isomers due to borylation of the benzylic position and isomerization of the double bond. The NMR data of the main compound match previously reported data for the (Z)-isomer of the product.[157]

*Major diastereoisomer, (Z)-**3al**:*

1H NMR (400 MHz, CDCl3) δ 7.42 – 7.30 (m, 4H), 7.30 – 7.17 (m, 2H), 2.00 (d, *J* = 1.7 Hz, 3H), 1.32 (s, 12H);

13C{1H} NMR (126 MHz, CDCl3) δ 142.5, 138.1, 129.6, 128.2, 127.2, 83.7, 25.0, 16.0 [Note: the carbon atom attached to the boron atom was not observed due to quadrupole broadening or relaxation delay caused by the ^{11}B nucleus[141]];

11B NMR (128 MHz, CDCl3) δ 31.0.

(Z)-2-(1-(3,4-dimethoxyphenyl)prop-1-en-2-yl)-4,4,5,5-tetramethyl-1,3,2-dioxaborolane 3am
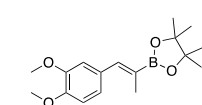
In a nitrogen-filled glove box, a 10 mL screw-cap vial equipped with a Teflon-coated magnetic stirring bar was charged with [Rh(COD)OMe]$_2$ (3.9 mg, 8 µmol, 4 mol%), xantphos (9.3 mg, 16 µmol, 8 mol%), B$_2$pin$_2$ (5.1 mg, 20 µmol, 10 mol%), dioxane (200 µL), vinyl Bpin (61.6 mg, 400 µmol, 2.0 equiv.), and methyl isoeugenol (35.6 mg, 200 µmol). The vial was sealed with a cap, removed from the glove box, placed in a pre-heated aluminum block and allowed to stir (800 rpm) at 150 °C for 16 h. Upon cooling to room temperature, the reaction mixture was filtered through a plug of celite (eluent: ethyl acetate). The volatiles of the filtrate were removed under reduced pressure and the residue was subjected to column chromatography (silica gel, 0 – 10% MTBE in petroleum ether) to isolate the title product as a yellow oil (25.5 mg, 84 µmol, 42%).

¹H NMR (500 MHz, C₆D₆) δ 7.88 – 7.56 (m, 1H), 7.04 (dd, J = 8.3, 2.0 Hz, 1H), 6.90 (d, J = 2.0 Hz, 1H), 6.53 (d, J = 8.3 Hz, 1H), 3.36 (d, J = 6.0 Hz, 6H), 2.31 (d, J = 1.8 Hz, 3H), 1.16 (s, 12H);
¹³C{¹H} NMR (126 MHz, C₆D₆) δ 149.8, 149.6, 143.8, 131.6, 122.9, 113.9, 111.9, 83.5, 55.5, 55.4, 25.1, 16.4 [Note: the carbon atom attached to the boron atom was not observed due to quadrupole broadening or relaxation delay caused by the ¹¹B nucleus[141]];
¹¹B NMR (160 MHz, C₆D₆) δ 31.4;
HRMS (ESI) m/z calcd. for $C_{17}H_{26}BO_4$ ([M+H]⁺): 305.1919; found: 305.1931.

(*Z*)-2-(1,3-diphenylprop-1-en-2-yl)-4,4,5,5-tetramethyl-1,3,2-dioxaborolane 3an
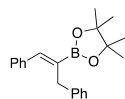
In a nitrogen-filled glove box, a 10 mL screw-cap vial equipped with a Teflon-coated magnetic stirring bar was charged with [Rh(COD)OMe]₂ (3.9 mg, 8 µmol, 4 mol%), xantphos (9.3 mg, 16 µmol, 8 mol%), B₂pin₂ (5.1 mg, 20 µmol, 10 mol%) dioxane (200 µL), vinyl Bpin (61.6 mg, 400 µmol, 2.0 equiv), and **1an** (38.9 mg, 200 µmol). The vial was sealed with a cap, removed from the glove box, placed in a pre-heated aluminum block and allowed to stir (800 rpm) at 150 °C for 16 h. Upon cooling to room temperature, the reaction mixture was filtered through a plug of celite (eluent: ethyl acetate). The volatiles of the filtrate were removed under reduced pressure and the residue was subjected to column chromatography (silica gel, 0 – 5% MTBE in petroleum ether) to isolate the title product as a colorless oil (23.7 mg, 74 µmol, 37%). The NMR data indicated the formation of a 77/23 ratio of two diastereoisomers. In analogy to a previous report,[158] the main diastereoisomer is most likely to be the *Z*-isomer. The NMR data of the main compound match previously reported data for the (*Z*)-isomer of the product.[159]
Major diastereoisomer, (Z)-3an:
**¹H NMR (400 MHz, CDCl₃)** δ 7.41 – 7.04 (m, 11H) 3.71 (s, 1H), 1.13 (s, 12H);
¹³C{¹H} NMR (101 MHz, CDCl₃) δ 143.1, 141.6, 137.7, 129.4, 129.1, 128.6, 128.4, 128.3, 128.3, 128.0, 127.5, 125.7, 83.7, 35.2, 24.7 [Note: the carbon atom attached to the boron atom was not observed due to quadrupole broadening or relaxation delay caused by the ¹¹B nucleus[141]];
¹¹B NMR (128 MHz, CDCl₃) δ 31.6.

(*E*)-6b,9a-dimethyl-8-styryl-6b,9a-dihydroacenaphtho[1,2-d][1,3,2]dioxaborole 3ao
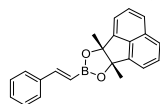
The compound was prepared according to general procedure 1 by reaction of styrene (20.8 mg, 200 µmol) and vinyl B(mac) (**2b**, 75.0 mg, 300 µmol) and was isolated by column chromatography (silica gel, 0 – 6% MTBE in petroleum ether) to give a white solid (45.0 mg, 138 µmol, 69%). The NMR data match previously reported data for the title product.[131] The crude yield of the reaction was found to be 86% as determined in an analogous experiment using ¹H NMR spectroscopy and 1,3,5-trimethoxybenzene as an internal standard.
¹H NMR (500 MHz, CDCl₃) δ 7.81 (dd, J = 6.7, 2.3 Hz, 2H), 7.66 – 7.55 (m, 4H), 7.45 – 7.40 (m, 2H), 7.36 (d, J = 18.4 Hz, 1H), 7.33 – 7.23 (m, 3H), 6.11 (d, J = 18.4 Hz, 1H), 1.86 (s, 6H);
¹³C{¹H} NMR (126 MHz, CDCl₃) δ 149.8, 144.8, 137.5, 134.8, 131.5, 129.0, 128.6, 128., 127.1, 125.4, 119.6, 92.1, 22.3 [Note: the carbon atom attached to the boron atom was not observed due to quadrupole broadening or relaxation delay caused by the ¹¹B nucleus[141]];
¹¹B NMR (160 MHz, CDCl₃) δ 30.5.

(3a*S*,4*R*,6*R*,7a*R*)-3a,5,5-trimethyl-2-((*E*)-styryl)hexahydro-4,6-methanobenzo[d][1,3,2]dioxaborole 3ap
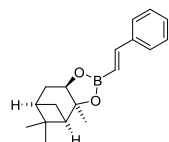
The compound was prepared according to general procedure 1 by reaction of styrene (20.8 mg, 200 µmol) and (3a*S*,4*R*,6*R*,7a*R*)-3a,5,5-trimethyl-2-vinylhexahydro-4,6-methanobenzo[d][1,3,2]dioxaborole (**2c**, 61.8 mg, 300 µmol) and was isolated by column chromatography (silica gel, 0 – 10% MTBE in petroleum ether) to give a colorless oil (47.7 mg, 169 µmol, 84%). The crude yield of the reaction was found to be 92% as determined in an analogous experiment using ¹H NMR spectroscopy and 1,3,5-trimethoxybenzene as an internal standard.
¹H NMR (500 MHz, CDCl₃) δ 7.47 – 7.39 (m, 2H), 7.33 (d, J = 18.4 Hz, 1H), 7.29 – 7.16 (m, 3H), 6.12 (d, J = 18.4 Hz, 1H), 4.29 (dd, J = 8.8, 1.9 Hz, 1H), 2.36 – 2.26 (m, 1H), 2.21 – 2.12 (m, 1H), 2.03 (t, J = 5.4 Hz, 1H), 1.91 – 1.82 (m, 2H), 1.38 (s, 3H), 1.23 (s, 3H), 1.13 (d, J = 10.9 Hz, 1H), 0.79 (s, 3H);
¹³C{¹H} NMR (126 MHz, CDCl₃) δ 149.6, 137.6, 129.0, 128.7, 127.2, 85.9, 78.0, 51.5, 39.6, 38.3, 35.7, 28.8, 27.2, 26.6, 24.2. [Note: the carbon atom attached to the boron atom was not observed due to quadrupole broadening or relaxation delay caused by the ¹¹B nucleus[141]];
¹¹B NMR (160 MHz, CDCl₃) δ 29.9.
HRMS (ESI) m/z calcd. for $C_{18}H_{24}BO_2$ ([M+H]⁺): 283.1864; found: 283.1860.

(*E*)-2-(4-(*tert*-butyl)styryl)-4,4,5,5-tetramethyl-1,3,2-dioxaborolane 3aq
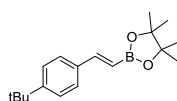
200 µmol scale
The title compound was prepared according to the general procedure 1 by reaction of 4-*tert*-butylstyrene (32.1 mg, 36.6 µL, 200 µmol, 1.0 equiv) and vinyl Bpin (46.2 mg, 50.9 µL, 300 µmol, 1.5 equiv), and was isolated by column chromatography (silica gel, 0-10% MTBE in petroleum ether) to give the title compound (53.2 mg, 186 µmol, 93%) as a colorless solid. The NMR data match previously reported data for the title product.[160] The crude yield of the reaction was found to be 96% as determined in an analogous experiment using ¹H NMR spectroscopy and 1,3,5-trimethoxybenzene as an internal standard.

5 mmol scale
In a nitrogen-filled glove box, 4-*tert*-butylstyrene (801 mg, 916 µL, 5.00 mmol, 1.0 equiv) was added to a mixture of xantphos (13.9 mg, 24.0 µmol, 0.48 mol%), [Rh(COD)OMe]₂ (5.8 mg, 12.0 µmol, 0.24 mol%), B₂pin₂ (15.2 mg, 59.9 µmol, 1.20 mol%), and vinyl Bpin (1.16 g, 1.27 mL, 7.50 mmol, 1.5 equiv) in dioxane (5.0 mL) in a high-pressure *Schlenk*-tube. The mixture was allowed to stir for 16 h at 90 °C, before it was cooled to room temperature, celite was added, and the volatiles were removed under reduced pressure. The crude product was subjected to column chromatography (40g gold cartridge, silica gel, 0-10% MTBE in petroleum ether) to give a clean fraction of the title compound as well as a fraction impure by resting starting material and vinyl Bpin dimer. The mixed fractions were subjected to column chromatography (40g gold cartridge, silica gel, 0-10% MTBE in petroleum ether) and the isolated product was combined with the isolated product of the first column chromatography, yielding the title compound (1.08 g, 3.78 mmol, 76%) as a colorless solid.
¹H NMR (500 MHz, CDCl₃) δ 7.47 – 7.42 (m, 2H), 7.42 – 7.34 (m, 3H), 6.14 (d, J = 18.4 Hz, 1H), 1.34 – 1.31 (m, 21H);
¹³C{¹H} NMR (126 MHz, CDCl₃) δ 152.2, 149.5, 134.9, 127.0, 125.6, 83.4, 34.8, 31.4, 25.0 [Note: the carbon atom attached to the boron atom was not observed due to quadrupole broadening or relaxation delay caused by the ¹¹B nucleus[141]];
¹¹B NMR (160 MHz, CDCl₃) δ 30.7.

(*E*)-*N*,*N*-dimethyl-3-(pyridin-2-yl)-3-(4-(2-(4,4,5,5-tetramethyl-1,3,2-dioxaborolan-2-yl)vinyl)phenyl)propan-1-amine 3ar
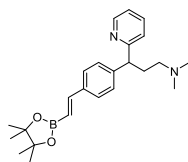
In a nitrogen-filled glove box, a 10 mL screw-cap vial equipped with a Teflon-coated magnetic stirring bar was charged with [Rh(COD)OMe]₂ (3.9 mg, 8.00 μmol, 4 mol%), xantphos (9.3 mg, 16.0 μmol, 8 mol%), B₂pin₂ (5.1 mg, 20.0 μmol, 0.10 equiv), dioxane (200 μL), vinyl Bpin (92.4 mg, 102 μL, 600 μmol, 3.0 equiv) and alkene **1ar** (53.3 mg, 200 μmol, 1.0 equiv). The vial was sealed with a cap, removed from the glove box, placed in a pre-heated aluminum block and allowed to stir (800 rpm) at 90 °C for 16 h. Upon cooling to room temperature, the reaction mixture was filtered through a plug of celite (eluent: ethyl acetate), the filtrate was concentrated under reduced pressure and the residue was subjected to column chromatography (silica, 0 – 9% NEt₃ in EtOAc) to afford the title compound (59.8 mg, 152 μmol, 76%) as a yellow oil which was contaminated by starting material **1ar** (3.2 mg, 12.2 μmol, 6%).

¹H NMR (400 MHz, CDCl₃) δ 8.54 (ddd, J = 4.9, 1.9, 0.9 Hz, 1H), 7.53 (td, J = 7.7, 1.9 Hz, 1H), 7.42 – 7.35 (m, 2H), 7.30 (d, J = 8.3 Hz, 3H), 7.14 (dt, J = 7.8, 1.1 Hz, 1H), 7.07 (ddd, J = 7.5, 4.9, 1.2 Hz, 1H), 6.09 (d, J = 18.4 Hz, 1H), 4.13 (t, J = 6.9 Hz, 1H), 2.50 – 2.36 (m, 1H), 2.26 – 2.15 (m, 9H), 1.29 (s, 12H);

¹³C{¹H} NMR (101 MHz, CDCl₃) δ 163.4, 149.4, 149.3, 144.6, 136.5, 135.9, 128.4, 127.4, 123.0, 121.5, 83.4, 57.8, 51.2, 45.5, 32.7, 24.9. [Note: the carbon atom attached to the boron atom was not observed due to quadrupole broadening or relaxation delay caused by the ¹¹B nucleus[141]];

¹¹B NMR (160 MHz, CDCl₃) δ 30.1;

HRMS (ESI) m/z calcd. for C₂₄H₃₄BN₂O₂ ([M+H]⁺): 393.2708; found: 393.2697.

### (*E*)-*N*,*N*-dimethyl-3-(2-(2-(4,4,5,5-tetramethyl-1,3,2-dioxaborolan-2-yl)vinyl)-10*H*-phenothiazin-10-yl)propan-1-amine 3as
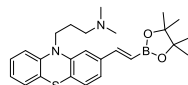
The compound was prepared according to general procedure 1 by reaction of **1as** (62.1 mg, 200 μmol) and vinyl Bpin (46.2 mg, 300 μmol) and was isolated by column chromatography (silica gel, EtOAc) to give a brown oil (55.7 mg, 128 μmol, 64%). The crude yield of the reaction was found to be 80% as determined in an analogous experiment using ¹H NMR spectroscopy and 1,3,5-trimethoxybenzene as an internal standard.

¹H NMR (500 MHz, CDCl₃) δ 7.32 (d, J = 18.4 Hz, 1H), 7.19 – 7.01 (m, 4H), 6.99 (d, J = 1.6 Hz, 1H), 6.94 – 6.82 (m, 2H), 6.10 (d, J = 18.4 Hz, 1H), 3.91 (t, J = 7.0 Hz, 2H), 2.40 (t, J = 7.1 Hz, 2H), 2.21 (s, 6H), 1.95 (p, J = 7.0 Hz, 2H), 1.31 (s, 12H);

¹³C{¹H} NMR (126 MHz, CDCl₃) δ 149.3, 145.5, 145.2, 137.0, 127.6, 127.5, 127.5, 124.9, 122.6, 121.6, 115.8, 114.0, 83.5, 57.3, 45.7, 45.5, 25.2, 25.0 [Note: the carbon atom attached to the boron atom was not observed due to quadrupole broadening or relaxation delay caused by the ¹¹B nucleus[141]];

¹¹B NMR (160 MHz, CDCl₃) δ 32.0;

HRMS (ESI) m/z calcd. for C₂₅H₃₄BN₂O₂S ([M+H]⁺): 437.2429; found: 437.2433.

(*E*)-1-(4-(2-(4,4,5,5-tetramethyl-1,3,2-dioxaborolan-2-yl)vinyl)benzyl)-1*H*-imidazole 3at
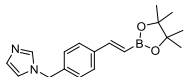
The compound was prepared according to general procedure 1 by reaction of **1at** (37.1 mg, 200 μmol) and vinyl Bpin (46.2 mg, 300 μmol) and was isolated by column chromatography (silica gel, 0 - 0.4% Et₃N in EtOAc) to give a yellow oil (48.2 mg, mixture of product and starting material (88/12), calculated amount of product: 46.4 mg, 150 μmol, 75%). The crude yield of the reaction was found to be 85% as determined in an analogous experiment using ¹H NMR spectroscopy and 1,3,5-trimethoxybenzene as an internal standard.

¹H NMR (500 MHz, CDCl₃) δ 7.57 (t, J = 1.1 Hz, 1H), 7.49 – 7.44 (m, 2H), 7.36 (d, J = 18.6 Hz, 1H), 7.15 – 7.06 (m, 3H), 6.90 (t, J = 1.4 Hz, 1H), 6.16 (d, J = 18.4 Hz, 1H), 5.11 (s, 2H), 1.31 (s, 12H);

¹³C{¹H} NMR (126 MHz, CDCl₃) δ 148.6, 137.7, 136.7, 129.8, 127.7, 127.6, 126.9, 119.4, 83.6, 50.7, 24.9 [Note: the carbon atom attached to the boron atom was not observed due to quadrupole broadening or relaxation delay caused by the ¹¹B nucleus[141]];

¹¹B NMR (160 MHz, CDCl₃) δ 30.5;

HRMS (ESI) m/z calcd. for C₁₈H₂₄BN₂O₂ ([M+H]⁺): 311.1925; found: 311.1926.

(*E*)-(4-((1*H*-imidazol-1-yl)methyl)styryl)boronic acid 5
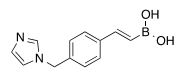
The compound was prepared according to a literature procedure.[88] A suspension of (*E*)-1-(4-(2-(4,4,5,5-tetramethyl-1,3,2-dioxaborolan-2-yl)vinyl)benzyl)-1*H*-imidazole (**3at**, 54.0 mg, 174 μmol, 1.0 equiv), NaIO₄ (111.7 mg, 522 μmol, 3.0 equiv), and NH₄OAc (40.2 mg, 522 μmol, 3.0 equiv) in acetone/water (1.5 mL, 2/1) was allowed to stir at room temperature for 24 h. Subsequently, acetone was removed under reduced pressure. Water was added (5 mL) and washed with ethyl acetate (3 x 3 mL). The combined organic phases were washed with brine (3 mL) and dried over Na₂SO₄. After filtration, the volatiles from the filtrate were removed under reduced pressure to obtain the crude product as a yellow viscous oil that was contaminated with the correspond terminal olefin (about 15% as judged by ¹H NMR spectroscopy; mixture: 31.0 mg; 27.0 mg product without contamination, 118 μmol, 68%). The crude product was subjected to preparative HPLC purification to obtain a spectroscopically pure sample.
Conditions of HPLC purification:

Solvent A : mQ H₂O (>18 MΩ) with 0.1% LCMS grade formic acid,

Solvent B : LCMS grade Acetonitrile (Honeywell Riedel-de Haën Chromasolv) with 0.1% LCMS grade formic acid,

Injection volume: 500 μL,

Method: Elution with a constant flow set to 20 mL/min : Isocratic for 1 min at 2% solvent B in 98% solvent A. Then increase of B to 42% in 20 min (2%/min gradient slope),Detection: Dual wavelength detection at 190 and 254 nm

Elution: peak of interest at 2.2 min.

¹H NMR (500 MHz, CD₃OD) δ 7.84 (s, 1H), 7.50 (d, J = 8.2 Hz, 2H), 7.36 – 7.25 (m, 1H), 7.22 (d, J = 8.4 Hz, 2H), 7.13 (s, 1H), 7.01 (s, 1H), 6.46 – 6.25 (m, 1H), 5.22 (s, 2H).

¹³C{¹H} NMR (126 MHz, CD₃OD) δ 139.4, 138.2, 137.5, 129.1, 128.6, 127.8, 121.4, 114.8, 51.7 [Note: the carbon atom attached to the boron atom was not observed due to quadrupole broadening or relaxation delay caused by the ¹¹B nucleus[141]];

¹¹B NMR (160 MHz, CD₃OD) δ 27.6;

HRMS (ESI) m/z calcd. for C₁₂H₁₄BN₂O₂ ([M+H]⁺): 229.1143; found: 229.1139.

(*E*)-2-(3,5,5,8,8-pentamethyl-5,6,7,8-tetrahydronaphthalen-2-yl)-4-(2-(4,4,5,5-tetramethyl-1,3,2-dioxaborolan-2-yl)vinyl)phenyl acetate 3au
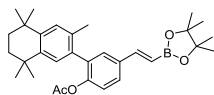
The compound was prepared according to general procedure 1 by reaction of alkene **1au** (18.1 mg, 50.0μmol) and vinyl Bpin (11.6 mg, 75.0μmol). The crude yield of the reaction was found to be 89% as determined using ¹H NMR spectroscopy and 1,3,5-trimethoxybenzene as an internal standard. The mixture was isolated by column chromatography (silica gel, 0 – 10% MTBE in petroleum ether) to give the title compound as a colorless oil (11.8 mg, 24.1 μmol, 48%) which was slightly contaminated by an unknown Bpin-containing compound (Bpin-X).

¹H NMR (400 MHz, CDCl₃) δ 7.48 (dd, *J* = 8.4, 2.2 Hz, 1H), 7.44 (d, *J* = 2.2 Hz, 1H), 7.39 (d, *J* = 18.4 Hz, 1H), 7.15 (s, 1H), 7.10 (d, *J* = 8.3 Hz, 1H), 7.04 (s, 1H), 6.12 (d, *J* = 18.4 Hz, 1H), 2.10 (s, 3H), 1.90 (s, 3H), 1.69 (s, 4H), 1.33 – 1.29 (m, 18H), 1.24 (s, 6H);

¹³C{¹H} NMR (126 MHz, CDCl₃) δ 169.5, 149.0, 148.6, 144.4, 141.9, 135.4, 135.3, 133.8, 133.1, 130.3, 128.2, 128.0, 126.9, 122.8, 83.5, 35.3, 35.3, 34.1, 34.0, 32.0 (2 × C)*, 24.9, 20.7, 19.8. [Note: the carbon atom attached to the boron atom was not observed due to quadrupole broadening or relaxation delay caused by the ¹¹B nucleus[141]];

* Assignment in analogy to compound **1au**.

¹¹B NMR (160 MHz, CDCl₃) δ 31.1.

HRMS (ESI) m/z calcd. for C₃₁H₄₂BO₄ ([M+H]⁺): 489.3171; found: 489.3164.

(*E*)-2,4-dimethoxy-2'-(4,4,5,5-tetramethyl-1,3,2-dioxaborolan-2-yl)-6'acetoxy α/β-zearanelol 3av
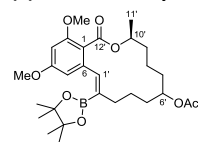
In a nitrogen-filled glove box, a 10 mL screw-cap vial equipped with a Teflon-coated magnetic stirring bar was charged with [Rh(COD)OMe]₂ (0.3 mg, 700 nmol, 1.75 mol%), xantphos (0.8 mg, 1.40 µmol, 3.50 mol%), B₂pin₂ (0.4 mg, 1.74 µmol, 4.36 mol%), dioxane (35 µL), vinyl Bpin (10.8 mg, 11.9 µL, 70.0 µmol, 1.75 equiv) and alkene **1av** (15.6 mg, 40.0 µmol, α/β = 34/66, 1.0 equiv). The vial was sealed with a cap, removed from the glove box, placed in a pre-heated aluminum block and allowed to stir (800 rpm) at 90 °C for 2 h. The vial was placed again in the glove box, opened, and a solution of Rh(COD)OMe]₂ (0.3 mg, 700 nmol, 1.75 mol%), xantphos (0.8 mg, 1.40 µmol, 3.50 mol%), and B₂pin₂ (0.4 mg, 1.74 µmol, 4.36 mol%) in dioxane (35 µL) was added. The vial was sealed with a cap, removed from the glove box, placed in a pre-heated aluminum block and allowed to stir (800 rpm) at 90 °C for additional 2 h. After this additional time, the procedure was repeated three times, while after the last cycle the solution was allowed to stir for 13 h. Therefore, a total amount of 8.75 mol% of [Rh(COD)OMe]₂ (and the other reagents accordingly) was used and the sample was allowed to stir for a total time period of 21 h.

This procedure was set up with five identical samples (each in a scale of 40.0 µmol of **1av**) in parallel which were combined at this point (giving a total scale of 200 µmol) and filtered over a small silica plug (in pasteur pipette). The filter residue was washed with EtOAc (20 mL) and the filtrate was concentrated under reduced pressure to afford a residue which was subjected to column chromatography (silica, 5 – 40% EtOAc in petroleum ether). To the residue isochroman (9.3 mg, 69.3 µmol, 0.347 equiv) as an internal standard and CDCl₃ (5 mL) were added and the crude yield was determined to be 11%. All volatiles were removed under reduced pressure and the residue was subjected to preparative HPLC purification to give reisolated starting material (26.4 mg, 67.5 µmol, α/β = 28/72, 34%) the title compound (11.8 mg) as a dark-yellow oil, which was subjected to column chromatography (silica 0-1% MeOH in CH₂Cl₂) to give the title compound (8.4 mg, 16.2 µmol, 8%) as a colorless oil contaminated by grease.

Conditions of HPLC purification:

Solvent A : mQ H₂O (>18 MΩ) with 0.1% LCMS grade formic acid,

Solvent B : LCMS grade Acetonitrile (Honeywell Riedel-de Haën Chromasolv) with 0.1% LCMS grade formic acid,

Injection volume: 1500 µL,

Method: Elution with a constant flow set to 10 mL/min: Isocratic for 2 min at 30% solvent B in 70% solvent A. Then increase of B to 70% in 50 min (0.8%/min gradient slope), Detection: Dual wavelength detection at 190 and 254 nm,

Elution: peaks of interest at 49.8 and 51.0 min.

¹H NMR (600 MHz, CDCl₃, 244 K) δ 7.39 – 7.29 (m, 1H, C-1'-H), 6.41 – 6.33 (m, 1H, C-3-H), 6.32 – 6.21 (m, 1H, C-5-H), 5.12 – 4.67 (m, 2H, C-6'-H, C-10'-H), 3.93 – 3.72 (m, 6H, OCH₃), 2.54 – 2.03 (m, 2H, CH₂), 1.98 (s, 3H, OCOCH₃), 1.72 – 0.93 (m, C-11'-H₃, 5 × CH₂);

¹³C{¹H} NMR (151 MHz, CDCl₃, 243 K) δ 171.2 (COCH₃), 171.2 (COCH₃), 168.1 (C-12'), 167.7 (C-12'), 161.3 (Cᵃʳ), 161.1 (Cᵃʳ), 160.9 (Cᵃʳ), 160.6 (Cᵃʳ), 159.7 (Cᵃʳ), 158.4 (Cᵃʳ), 157.8 (Cᵃʳ), 145.5 (C-1'), 144.6 (C-1'), 142.2 (C-1'), 141.7 (C-1'), 140.9 (Cᵃʳ), 140.1 (Cᵃʳ), 139.7 (Cᵃʳ), 138.4 (Cᵃʳ), 116.1 (Cᵃʳ), 115.6 (Cᵃʳ), 113.8 (Cᵃʳ), 112.7 (Cᵃʳ), 106.7 (C-5), 106.4 (C-5), 105.1 (C-5), 105.1 (C-5), 97.6 (C-3), 97.4 (C-3), 97.2 (C-3), 97.1 (C-3), 83.6 (BOC), 83.5 (BOC), 75.3 (C-6'/C-10'), 74.2 (C-6'/C-10'), 72.8 (C-6'/C-10'), 72.8 (C-6'/C-10'), 72.7 (C-6'/C-10'), 72.3 (C-6'/C-10'), 71.9 (C-6'/C-10'), 71.1 (C-6'/C-10'), 56.1 (OCH₃), 56.0 (OCH₃), 55.9 (OCH₃), 55.6 (OCH₃). [Note: The carbon atom attached to the boron atom was not observed due to quadrupole broadening or relaxation delay caused by the ¹¹B nucleus[141]. The assignment of signals was accomplished by analogy to compounds **SI12**, **SI13** and **1av**, but proved to be difficult: the isolated material consists of a mixture of diastereoisomers (diastereomeric mixture of **1av** was used as a starting material), which exist as slowly interconverting conformers in solution leading to signal broadening at room temperature. A change of solvent did not to have a considerable impact; however, the NMR experiments a lower temperature improved the resolution of signals of conformers, enabling their assignment. Nevertheless, an assignment of signals in the aliphatic region was not possible due to the complexity of the mixture. Only assigned signals are listed above for the ¹³C NMR spectrum. For the remaining aliphatic signals, see the accompanying document containing the copies of the spectrum];

¹¹B NMR (160 MHz, CDCl₃) δ 31.9;

HRMS (ESI) m/z calcd. for C₂₈H₄₂BO₈ ([M+H]⁺): 517.2967; found: 517.2967 (minor) and 517.2966 (major).

2.5. References

(1)   Hall, D. G. *Boronic Acids: Preparation and Applications in Organic Synthesis and Medicine*; Wiley-VCH Verlag: Weinheim, 2010.

(2)   Ban, H. S.; Nakamura, H. Boron-Based Drug Design: Boron-Based Drug Design. *Chem. Rec.* **2015**, *15* (3), 616–635. https://doi.org/10.1002/tcr.201402100.

(3)   Diaz, D. B.; Yudin, A. K. The Versatility of Boron in Biological Target Engagement. *Nat. Chem.* **2017**, *9* (8), 731–742. https://doi.org/10.1038/nchem.2814.

(4)   Miyaura, Norio.; Suzuki, Akira. Palladium-Catalyzed Cross-Coupling Reactions of Organoboron Compounds. *Chem. Rev.* **1995**, *95* (7), 2457–2483. https://doi.org/10.1021/cr00039a007.

(5)   Nicolaou, K. C.; Bulger, P. G.; Sarlah, D. Palladium-Catalyzed Cross-Coupling Reactions in Total Synthesis. *Angew. Chem. Int. Ed.* **2005**, *44* (29), 4442–4489. https://doi.org/10.1002/anie.200500368.

(6)   Lennox, A. J. J.; Lloyd-Jones, G. C. Selection of Boron Reagents for Suzuki–Miyaura Coupling. *Chem Soc Rev* **2014**, *43* (1), 412–443. https://doi.org/10.1039/C3CS60197H.

(7)   Xu, L.; Zhang, S.; Li, P. Boron-Selective Reactions as Powerful Tools for Modular Synthesis of Diverse Complex Molecules. *Chem. Soc. Rev.* **2015**, *44* (24), 8848–8858. https://doi.org/10.1039/C5CS00338E.

(8)   Hartwig, J. F.; Larsen, M. A. Undirected, Homogeneous C–H Bond Functionalization: Challenges and Opportunities. *ACS Cent. Sci.* **2016**, *2* (5), 281–292. https://doi.org/10.1021/acscentsci.6b00032.

(9)   Mkhalid, I. A. I.; Barnard, J. H.; Marder, T. B.; Murphy, J. M.; Hartwig, J. F. C–H Activation for the Construction of C–B Bonds. *Chem.*

Rev. **2010**, *110* (2), 890–931. https://doi.org/10.1021/cr900206p.

(10)   Hartwig, J. F. Regioselectivity of the Borylation of Alkanes and Arenes. *Chem. Soc. Rev.* **2011**, *40* (4), 1992. https://doi.org/10.1039/c0cs00156b.

(11)   Xu, L.; Wang, G.; Zhang, S.; Wang, H.; Wang, L.; Liu, L.; Jiao, J.; Li, P. Recent Advances in Catalytic C–H Borylation Reactions. *Tetrahedron* **2017**, *73* (51), 7123–7157. https://doi.org/10.1016/j.tet.2017.11.005.

(12)   Wright, J. S.; Scott, P. J. H.; Steel, P. G. Iridium-Catalysed C–H Borylation of Heteroarenes: Balancing Steric and Electronic Regiocontrol. *Angew. Chem. Int. Ed.* **2021**, *60* (6), 2796–2821. https://doi.org/10.1002/anie.202001520.

(13)   Reyes, R.; Sawamura, M. An Introductory Overview of C–H Bond Activation/ Functionalization Chemistry with Focus on Catalytic C(Sp3)–H Bond Borylation. *KIMIKA* **2021**, *32* (1), 70–109. https://doi.org/10.26534/kimika.v32i1.70-109.

(14)   Veth, L.; Grab, H.; Dydio, P. Recent Trends in Group 9–Catalyzed C–H Borylation Reactions: Different Strategies to Control Site-, Regio-, and Stereoselectivity. *Synthesis* **2022**, *54*, 3482 - 3498. https://doi.org/10.1055/a-1711-5889.

(15)   Carreras, J.; Caballero, A.; Pérez, P. J. Alkenyl Boronates: Synthesis and Applications. *Chem. – Asian J.* **2019**, *14* (3), 329–343. https://doi.org/10.1002/asia.201801559.

(16)   Wang, X.; Wang, Y.; Huang, W.; Xia, C.; Wu, L. Direct Synthesis of Multi(Boronate) Esters from Alkenes and Alkynes via Hydroboration and Boration Reactions. *ACS Catal.* **2021**, *11* (1), 1–18. https://doi.org/10.1021/acscatal.0c03418.

(17)   Flynn, A. B.; Ogilvie, W. W. Stereocontrolled Synthesis of Tetrasubstituted Olefins. *Chem. Rev.* **2007**, *107* (11), 4698–4745. https://doi.org/10.1021/cr050051k.

(18)   Blackwell, H. E.; O'Leary, D. J.; Chatterjee, A. K.; Washenfelder, R. A.; Bussmann, D. A.; Grubbs, R. H. New Approaches to Olefin Cross-Metathesis. *J. Am. Chem. Soc.* **2000**, *122* (1), 58–71. https://doi.org/10.1021/ja993063u.

(19)   Morrill, C.; Grubbs, R. H. Synthesis of Functionalized Vinyl Boronates via Ruthenium-Catalyzed Olefin Cross-Metathesis and Subsequent Conversion to Vinyl Halides. *J. Org. Chem.* **2003**, *68* (15), 6031–6034. https://doi.org/10.1021/jo0345345.

(20)   Morrill, C.; Funk, T. W.; Grubbs, R. H. Synthesis of Tri-Substituted Vinyl Boronates via Ruthenium-Catalyzed Olefin Cross-Metathesis. *Tetrahedron Lett.* **2004**, *45* (41), 7733–7736. https://doi.org/10.1016/j.tetlet.2004.08.069.

(21)   Kiesewetter, E. T.; O'Brien, R. V.; Yu, E. C.; Meek, S. J.; Schrock, R. R.; Hoveyda, A. H. Synthesis of Z-(Pinacolato)Allylboron and Z-(Pinacolato)Alkenylboron Compounds through Stereoselective Catalytic Cross-Metathesis. *J. Am. Chem. Soc.* **2013**, *135* (16), 6026–6029. https://doi.org/10.1021/ja403188t.

(22)   Hemelaere, R.; Carreaux, F.; Carboni, B. Cross-Metathesis/Isomerization/Allylboration Sequence for a Diastereoselective Synthesis of *Anti* -Homoallylic Alcohols from Allylbenzene Derivatives and Aldehydes. *Chem. - Eur. J.* **2014**, *20* (44), 14518–14523. https://doi.org/10.1002/chem.201403954.

(23)   Njardarson, J. T.; Biswas, K.; Danishefsky, S. J. Application of Hitherto Unexplored Macrocyclization Strategies in the Epothilone Series: Novel Epothilone Analogs by Total SynthesisElectronic Supplementary Information (ESI) Available: Experimental Details for the Synthesis of 14 and 32. See Http://Www.Rsc.Org/Suppdata/Cc/B2/B209941a/. *Chem. Commun.* **2002**, No. 23, 2759–2761. https://doi.org/10.1039/b209941a.

(24)   Nicolaou, K. C.; Tria, G. S.; Edmonds, D. J.; Kar, M. Total Syntheses of (±)-Platencin and (−)-Platencin. *J. Am. Chem. Soc.* **2009**, *131* (43), 15909–15917. https://doi.org/10.1021/ja906801g.

(25)   Speed, A. W. H.; Mann, T. J.; O'Brien, R. V.; Schrock, R. R.; Hoveyda, A. H. Catalytic Z-Selective Cross-Metathesis in Complex Molecule Synthesis: A Convergent Stereoselective Route to Disorazole C1. *J. Am. Chem. Soc.* **2014**, *136* (46), 16136–16139. https://doi.org/10.1021/ja509973r.

(26)   Williams, D. R.; Shah, A. A. Total Synthesis of (+)-Ileabethoxazole via an Iron-Mediated Pauson–Khand [2 + 2 + 1] Carbocyclization. *J. Am. Chem. Soc.* **2014**, *136* (24), 8829–8836. https://doi.org/10.1021/ja5043462.

(27)   Liao, L.; Zhou, J.; Xu, Z.; Ye, T. Concise Total Synthesis of Nannocystin A. *Angew. Chem. Int. Ed.* **2016**, *55* (42), 13263–13266. https://doi.org/10.1002/anie.201606679.

(28)   Reid, W. B.; Spillane, J. J.; Krause, S. B.; Watson, D. A. Direct Synthesis of Alkenyl Boronic Esters from Unfunctionalized Alkenes: A Boryl-Heck Reaction. *J. Am. Chem. Soc.* **2016**, *138* (17), 5539–5542. https://doi.org/10.1021/jacs.6b02914.

(29)   Reid, W. B.; Watson, D. A. Synthesis of Trisubstituted Alkenyl Boronic Esters from Alkenes Using the Boryl-Heck Reaction. *Org. Lett.* **2018**, *20* (21), 6832–6835. https://doi.org/10.1021/acs.orglett.8b02949.

(30)   Idowu, O. O.; Hayes, J. C.; Reid, W. B.; Watson, D. A. Synthesis of 1,1-Diboryl Alkenes Using the Boryl-Heck Reaction. *Org. Lett.* **2021**, acs.orglett.1c01567. https://doi.org/10.1021/acs.orglett.1c01567.

(31)   Coapes, R. B.; Souza, F. E. S.; Thomas, R. Ll.; Hall, J. J.; Marder, T. B. Rhodium Catalysed Dehydrogenative Borylation of Vinylarenes and 1,1-Disubstituted Alkenes without Sacrificial Hydrogenation—a Route to 1,1-Disubstituted Vinylboronates. *Chem. Commun.* **2003**, No. 5, 614–615. https://doi.org/10.1039/b211789d.

(32)   Brown, J. M.; Lloyd-Jones, G. C. Vinylborane Formation in Rhodium-Catalyzed Hydroboration of Vinylarenes. Mechanism versus Borane Structure and Relationship to Silation. *J. Am. Chem. Soc.* **1994**, *116* (3), 866–878. https://doi.org/10.1021/ja00082a006.

(33)   Mkhalid, I. A. I.; Coapes, R. B.; Edes, S. N.; Coventry, D. N.; Souza, F. E. S.; Thomas, R. Ll.; Hall, J. J.; Bi, S.-W.; Lin, Z.; Marder, T. B. Rhodium Catalysed Dehydrogenative Borylation of Alkenes: Vinylboronates via C–H Activation. *Dalton Trans* **2008**, No. 8, 1055–1064. https://doi.org/10.1039/B715584K.

(34)   Kondoh, A.; Jamison, T. F. Rhodium-Catalyzed Dehydrogenative Borylation of Cyclic Alkenes. *Chem. Commun.* **2010**, *46* (6), 907. https://doi.org/10.1039/b921387b.

(35)   Morimoto, M.; Miura, T.; Murakami, M. Rhodium-Catalyzed Dehydrogenative Borylation of Aliphatic Terminal Alkenes with Pinacolborane. *Angew. Chem. Int. Ed.* **2015**, *54* (43), 12659–12663. https://doi.org/10.1002/anie.201506328.

(36)   Selander, N.; Willy, B.; Szabó, K. J. Selective C H Borylation of Alkenes by Palladium Pincer Complex Catalyzed Oxidative Functionalization. *Angew. Chem. Int. Ed.* **2010**, *49* (24), 4051–4053. https://doi.org/10.1002/anie.201000690.

(37)   Kirai, N.; Iguchi, S.; Ito, T.; Takaya, J.; Iwasawa, N. PSiP-Pincer Type Palladium-Catalyzed Dehydrogenative Borylation of Alkenes and 1,3-Dienes. *Bull. Chem. Soc. Jpn.* **2013**, *86* (7), 784–799. https://doi.org/10.1246/bcsj.20130004.

(38)   Takaya, J.; Kirai, N.; Iwasawa, N. Efficient Synthesis of Diborylalkenes from Alkenes and Diboron by a New PSiP-Pincer Palladium-Catalyzed Dehydrogenative Borylation. *J. Am. Chem. Soc.* **2011**, *133* (33), 12980–12983. https://doi.org/10.1021/ja205186k.

(39)   Sasaki, I.; Doi, H.; Hashimoto, T.; Kikuchi, T.; Ito, H.; Ishiyama, T. Iridium(i)-Catalyzed Vinylic C–H Borylation of 1-Cycloalkenecarboxylates with Bis(Pinacolato)Diboron. *Chem. Commun.* **2013**, *49* (68), 7546. https://doi.org/10.1039/c3cc44149k.

(40)   Ohmura, T.; Takasaki, Y.; Furukawa, H.; Suginome, M. Stereoselective Synthesis of Cis-β-Methyl- and Phenyl-Substituted Alkenylboronates by Platinum-Catalyzed Dehydrogenative Borylation. *Angew. Chem. Int. Ed.* **2009**, *48* (13), 2372–2375. https://doi.org/10.1002/anie.200805406.

(41)   Wang, C.; Wu, C.; Ge, S. Iron-Catalyzed *E* -Selective Dehydrogenative Borylation of Vinylarenes with Pinacolborane. *ACS Catal.* **2016**, *6* (11), 7585–7589. https://doi.org/10.1021/acscatal.6b02654.

(42) Mazzacano, T. J.; Mankad, N. P. Dehydrogenative Borylation and Silylation of Styrenes Catalyzed by Copper-Carbenes. *ACS Catal.* **2017**, *7* (1), 146–149. https://doi.org/10.1021/acscatal.6b02594.

(43) Lu, W.; Shen, Z. Direct Synthesis of Alkenylboronates from Alkenes and Pinacol Diboron via Copper Catalysis. *Org. Lett.* **2019**, *21* (1), 142–146. https://doi.org/10.1021/acs.orglett.8b03599.

(44) Shi, X.; Li, S.; Wu, L. H $_2$ -Acceptorless Dehydrogenative Boration and Transfer Boration of Alkenes Enabled by Zirconium Catalyst. *Angew. Chem. Int. Ed.* **2019**, *58* (45), 16167–16171. https://doi.org/10.1002/anie.201908931.

(45) Bhawal, B. N.; Morandi, B. Catalytic Isofunctional Reactions—Expanding the Repertoire of Shuttle and Metathesis Reactions. *Angew. Chem. Int. Ed.* **2019**, *58* (30), 10074–10103. https://doi.org/10.1002/anie.201803797.

(46) Rochette, É.; Desrosiers, V.; Soltani, Y.; Fontaine, F.-G. Isodesmic C–H Borylation: Perspectives and Proof of Concept of Transfer Borylation Catalysis. *J. Am. Chem. Soc.* **2019**, *141* (31), 12305–12311. https://doi.org/10.1021/jacs.9b04305.

(47) Marciniec, B.; Jankowska, M.; Pietraszuk, C. New Catalytic Route to Functionalized Vinylboronates. *Chem. Commun.* **2005**, No. 5, 663. https://doi.org/10.1039/b414644a.

(48) Marciniec, B.; Dudziec, B.; Kownacki, I. A New Catalytic Route for the Activation of Sp-Hybridized Carbon–Hydrogen Bonds. *Angew. Chem. Int. Ed.* **2006**, *45* (48), 8180–8184. https://doi.org/10.1002/anie.200603582.

(49) Szyling, J.; Franczyk, A.; Pawluć, P.; Marciniec, B.; Walkowiak, J. A Stereoselective Synthesis of (*E*)- or (*Z*)-β-Arylvinyl Halides *via* a Borylative Coupling/Halodeborylation Protocol. *Org. Biomol. Chem.* **2017**, *15* (15), 3207–3215. https://doi.org/10.1039/C7OB00054E.

(50) Szyling, J.; Walkowiak, J.; Sokolnicki, T.; Franczyk, A.; Stefanowska, K.; Klarek, M. PEG-Mediated Recyclable Borylative Coupling of Vinyl Boronates with Olefins. *J. Catal.* **2019**, *376*, 219–227. https://doi.org/10.1016/j.jcat.2019.07.009.

(51) Szyling, J.; Sokolnicki, T.; Franczyk, A.; Walkowiak, J. Ru-Catalyzed Repetitive Batch Borylative Coupling of Olefins in Ionic Liquids or Ionic Liquids/ScCO2 Systems. *Catalysts* **2020**, *10* (7), 762. https://doi.org/10.3390/catal10070762.

(52) Lam, K. C.; Lin, Z.; Marder, T. B. DFT Studies of β-Boryl Elimination Processes: Potential Role in Catalyzed Borylation Reactions of Alkenes. *Organometallics* **2007**, *26* (13), 3149–3156. https://doi.org/10.1021/om0700314.

(53) Kalläne, S. I.; Braun, T.; Braun, B.; Mebs, S. Versatile Reactivity of a Rhodium(i) Boryl Complex towards Ketones and Imines. *Dalton Trans.* **2014**, *43* (18), 6786. https://doi.org/10.1039/c4dt00080c.

(54) Franke, R.; Selent, D.; Börner, A. Applied Hydroformylation. *Chem. Rev.* **2012**, *112* (11), 5675–5732. https://doi.org/10.1021/cr3001803.

(55) Murphy, S. K.; Park, J.-W.; Cruz, F. A.; Dong, V. M. Rh-Catalyzed C–C Bond Cleavage by Transfer Hydroformylation. *Science* **2015**, *347* (6217), 56–60. https://doi.org/10.1126/science.1261232.

(56) Wu, X.; Cruz, F. A.; Lu, A.; Dong, V. M. Tandem Catalysis: Transforming Alcohols to Alkenes by Oxidative Dehydroxymethylation. *J. Am. Chem. Soc.* **2018**, *140* (32), 10126–10130. https://doi.org/10.1021/jacs.8b06069.

(57) Tan, G.; Wu, Y.; Shi, Y.; You, J. Syngas-Free Highly Regioselective Rhodium-Catalyzed Transfer Hydroformylation of Alkynes to α,β-Unsaturated Aldehydes. *Angew. Chem. Int. Ed.* **2019**, *58* (22), 7440–7444. https://doi.org/10.1002/anie.201902553.

(58) Baker, R. T.; Calabrese, J. C.; Westcott, S. A.; Nguyen, P.; Marder, T. B. Insertion of Alkenes into Rhodium-Boron Bonds. *J. Am. Chem. Soc.* **1993**, *115* (10), 4367–4368. https://doi.org/10.1021/ja00063a067.

(59) *For Precedences of B-Boryl Elimination for Other Transition Metal Complexes, Implicated by the Results of Their Catalytic Activities, Including Zr, Ru, and Pd-Catalyzed Reactions, See Ref. 43, 46, 56, and 57.*

(60) Miyaura, N.; Suzuki, A. The Palladium-Catalyzed "Head-to-Tail" Cross-Coupling Reaction of 1-Alkenylboranes with Phenyl or 1-Alkenyl Iodides. A Novel Synthesis of 2-Phenyl-1-Alkenes or 2-Alkyl-1,3-Alkadienes via Organoboranes. *J. Organomet. Chem.* **1981**, *213* (2), C53–C56. https://doi.org/10.1016/S0022-328X(00)82970-8.

(61) Ohmura, T.; Oshima, K.; Taniguchi, H.; Suginome, M. Switch of Regioselectivity in Palladium-Catalyzed Silaboration of Terminal Alkynes by Ligand-Dependent Control of Reductive Elimination. *J. Am. Chem. Soc.* **2010**, *132* (35), 12194–12196. https://doi.org/10.1021/ja105096r.

(62) Teltewskoi, M.; Panetier, J. A.; Macgregor, S. A.; Braun, T. A Highly Reactive Rhodium(I)-Boryl Complex as a Useful Tool for C H Bond Activation and Catalytic C F Bond Borylation. *Angew. Chem. Int. Ed.* **2010**, *49* (23), 3947–3951. https://doi.org/10.1002/anie.201001070.

(63) Dai, C.; Stringer, G.; Marder, T. B.; Scott, A. J.; Clegg, W.; Norman, N. C. Synthesis and Characterization of Rhodium(I) Boryl and Rhodium(III) Tris(Boryl) Compounds: Molecular Structures of [(PMe $_3$) $_4$ Rh(B(Cat))] and *Fac* -[(PMe $_3$) $_3$ Rh(B(Cat)) $_3$] (Cat = 1,2-O $_2$ C $_6$ H $_4$). *Inorg. Chem.* **1997**, *36* (3), 272–273. https://doi.org/10.1021/ic9611047.

(64) Masuda, Y.; Hasegawa, M.; Yamashita, M.; Nozaki, K.; Ishida, N.; Murakami, M. Oxidative Addition of a Strained C–C Bond onto Electron-Rich Rhodium(I) at Room Temperature. *J. Am. Chem. Soc.* **2013**, *135* (19), 7142–7145. https://doi.org/10.1021/ja403461f.

(65) Irvine, G. J.; Lesley, M. J. G.; Marder, T. B.; Norman, N. C.; Rice, C. R.; Robins, E. G.; Roper, W. R.; Whittell, G. R.; Wright, L. J. Transition Metal–Boryl Compounds: Synthesis, Reactivity, and Structure. *Chem. Rev.* **1998**, *98* (8), 2685–2722. https://doi.org/10.1021/cr9500085.

(66) Braunschweig, H.; Colling, M. Transition Metal Complexes of Boron — Synthesis, Structure and Reactivity. *Coord. Chem. Rev.* **2001**, *223* (1), 1–51. https://doi.org/10.1016/S0010-8545(01)00378-2.

(67) Esteruelas, M. A.; Oliván, M.; Vélez, A. POP–Rhodium-Promoted C–H and B–H Bond Activation and C–B Bond Formation. *Organometallics* **2015**, *34* (10), 1911–1924. https://doi.org/10.1021/acs.organomet.5b00176.

(68) Zhao, P.; Incarvito, C. D.; Hartwig, J. F. Carbon–Oxygen Bond Formation between a Terminal Alkoxo Ligand and a Coordinated Olefin. Evidence for Olefin Insertion into a Rhodium Alkoxide. *J. Am. Chem. Soc.* **2006**, *128* (30), 9642–9643. https://doi.org/10.1021/ja063347w.

(69) Richers, C. P.; Roediger, S.; Laserna, V.; Hartwig, J. F. Effects of Ligands on the Migratory Insertion of Alkenes into Rhodium–Oxygen Bonds. *Chem. Sci.* **2020**, *11* (38), 10449–10456. https://doi.org/10.1039/D0SC04402D.

(70) *For Details, See the Supporting Information.*

(71) Uetake, Y.; Niwa, T.; Hosoya, T. Rhodium-Catalyzed *Ipso* -Borylation of Alkylthioarenes via C–S Bond Cleavage. *Org. Lett.* **2016**, *18* (11), 2758–2761. https://doi.org/10.1021/acs.orglett.6b01250.

(72) Lindhardt (neé Hansen), A. T.; Mantel, M. L. H.; Skrydstrup, T. Palladium-Catalyzed Intermolecular Ene–Yne Coupling: Development of an Atom-Efficient Mizoroki–Heck-Type Reaction. *Angew. Chem. Int. Ed.* **2008**, *47* (14), 2668–2672. https://doi.org/10.1002/anie.200705558.

(73) Kaminsky, L.; Wilson, R. J.; Clark, D. A. Stereo- and Regioselective Formation of Silyl-Dienyl Boronates. *Org. Lett.* **2015**, *17* (12), 3126–3129. https://doi.org/10.1021/acs.orglett.5b01434.

(74) Shintani, R.; Duan, W.-L.; Park, S.; Hayashi, T. Rhodium-Catalyzed Isomerization of Unactivated Alkynes to 1,3-Dienes. *Chem. Commun.* **2006**, No. 34, 3646. https://doi.org/10.1039/b605368h.

96

(75) Geier, M. J.; Vogels, C. M.; Decken, A.; Westcott, S. A. The Transition Metal Catalyzed Hydroboration of Enamines. *J. Organomet. Chem.* **2009**, *694* (19), 3154–3159. https://doi.org/10.1016/j.jorganchem.2009.05.016.

(76) Myhill, J. A.; Wilhelmsen, C. A.; Zhang, L.; Morken, J. P. Diastereoselective and Enantioselective Conjunctive Cross-Coupling Enabled by Boron Ligand Design. *J. Am. Chem. Soc.* **2018**, *140* (45), 15181–15185. https://doi.org/10.1021/jacs.8b09909.

(77) Hecker, S. J.; Reddy, K. R.; Lomovskaya, O.; Griffith, D. C.; Rubio-Aparicio, D.; Nelson, K.; Tsivkovski, R.; Sun, D.; Sabet, M.; Tarazi, Z.; Parkinson, J.; Totrov, M.; Boyer, S. H.; Glinka, T. W.; Pemberton, O. A.; Chen, Y.; Dudley, M. N. Discovery of Cyclic Boronic Acid QPX7728, an Ultrabroad-Spectrum Inhibitor of Serine and Metallo-β-Lactamases. *J. Med. Chem.* **2020**, *63* (14), 7491–7507. https://doi.org/10.1021/acs.jmedchem.9b01976.

(78) Matteson, D. S. Boronic Esters in Asymmetric Synthesis. *J. Org. Chem.* **2013**, *78* (20), 10009–10023. https://doi.org/10.1021/jo4013942.

(79) Andrés, P.; Ballano, G.; Calaza, M. I.; Cativiela, C. Synthesis of α-Aminoboronic Acids. *Chem. Soc. Rev.* **2016**, *45* (8), 2291–2307. https://doi.org/10.1039/C5CS00886G.

(80) Du, R.; Liu, L.; Xu, S. Iridium-Catalyzed Regio- and Enantioselective Borylation of Unbiased Methylene C(Sp^3)–H Bonds at the Position β to a Nitrogen Center. *Angew. Chem. Int. Ed.* **2021**, *60* (11), 5843–5847. https://doi.org/10.1002/anie.202016009.

(81) Hitosugi, S.; Tanimoto, D.; Nakanishi, W.; Isobe, H. A Facile Chromatographic Method for Purification of Pinacol Boronic Esters. *Chem. Lett.* **2012**, *41* (9), 972–973. https://doi.org/10.1246/cl.2012.972.

(82) Kloek, S. M.; Heinekey, D. M.; Goldberg, K. I. C H Bond Activation by Rhodium(I) Hydroxide and Phenoxide Complexes. *Angew. Chem. Int. Ed.* **2007**, *46* (25), 4736–4738. https://doi.org/10.1002/anie.200700270.

(83) Kegley, S. E.; Schaverien, C. J.; Freudenberger, J. H.; Bergman, R. G.; Nolan, S. P.; Hoff, C. D. Rhodium Alkoxide Complexes. Formation of an Unusually Strong Intermolecular Hydrogen Bond in (PMe3)3Rh-Otol(HOtol). *J. Am. Chem. Soc.* **1987**, *109* (21), 6563–6565. https://doi.org/10.1021/ja00255a080.

(84) Qi, X.; Li, Y.; Bai, R.; Lan, Y. Mechanism of Rhodium-Catalyzed C–H Functionalization: Advances in Theoretical Investigation. *Acc. Chem. Res.* **2017**, *50* (11), 2799–2808. https://doi.org/10.1021/acs.accounts.7b00400.

(85) Bhawal, B. N.; Reisenbauer, J. C.; Ehinger, C.; Morandi, B. Overcoming Selectivity Issues in Reversible Catalysis: A Transfer Hydrocyanation Exhibiting High Kinetic Control. *J. Am. Chem. Soc.* **2020**, *142* (25), 10914–10920. https://doi.org/10.1021/jacs.0c03184.

(86) Veth, L.; Grab, H. A.; Martínez, S.; Antheaume, C.; Dydio, P. Transfer C–H Borylation of Alkenes under Rh(I) Catalysis: Insight into the Synthetic Capacity, Mechanism, and Selectivity Control. *Chem Catal.* **2022**, *2* (4), 762–778. https://doi.org/10.1016/j.checat.2022.02.008.

(87) de Oliveira Dias, A.; Gutiérrez, M. G. P.; Villarreal, J. A. A.; Carmo, R. L. L.; Oliveira, K. C. B.; Santos, A. G.; dos Santos, E. N.; Gusevskaya, E. V. Sustainable Route to Biomass-Based Amines: Rhodium Catalyzed Hydroaminomethylation in Green Solvents. *Appl. Catal. Gen.* **2019**, *574* (November 2018), 97–104. https://doi.org/10.1016/j.apcata.2019.02.003.

(88) Boelke, A.; Caspers, L. D.; Nachtsheim, B. J. NH2-Directed C-H Alkenylation of 2-Vinylanilines with Vinylbenziodoxolones. *Org. Lett.* **2017**, *19* (19), 5344–5347. https://doi.org/10.1021/acs.orglett.7b02630.

(89) Lee, J.; Radomkit, S.; Torker, S.; Pozo, J.; Hoveyda, A. H. Mechanism-Based Enhancement of Scope and Enantioselectivity for Reactions Involving a Copper-Substituted Stereogenic Carbon Centre. *Nat. Chem.* **2018**, *10* (1), 99–108. https://doi.org/10.1038/NCHEM.2861.

(90) Ohmura, T.; Yamamoto, Y.; V, H. U.; January, R. V. Rhodium- or Iridium-Catalyzed Trans -Hydroboration of Terminal Alkynes , Giving (Z) -1-Alkenylboron Compounds Di V Ision of Molecular Chemistry Graduate School of Engineering of 1-Alkenylboron Compounds Which Are a Versatile Reagent for Reversing the Co. *J. Am. Chem. Soc.* **2000**, No. 11, 4990–4991.

(91) Polášek, J.; Paciorek, J.; Stošek, J.; Semrád, H.; Munzarová, M.; Mazal, C. Stereoselective Bromoboration of Acetylene with Boron Tribromide: Preparation and Cross-Coupling Reactions of (Z)-Bromovinylboronates. *J. Org. Chem.* **2020**, *85* (11), 6992–7000. https://doi.org/10.1021/acs.joc.0c00341.

(92) Fulmer, G. R.; Miller, A. J. M.; Sherden, N. H.; Gottlieb, H. E.; Nudelman, A.; Stoltz, B. M.; Bercaw, J. E.; Goldberg, K. I. NMR Chemical Shifts of Trace Impurities: Common Laboratory Solvents, Organics, and Gases in Deuterated Solvents Relevant to the Organometallic Chemist. *Organometallics* **2010**, *29* (9), 2176–2179. https://doi.org/10.1021/om100106e.

(93) Richers, C. P.; Roediger, S.; Laserna, V.; Hartwig, J. F. Effects of Ligands on the Migratory Insertion of Alkenes into Rhodium-Oxygen Bonds. *Chem. Sci.* **2020**, *11* (38), 10449–10456. https://doi.org/10.1039/d0sc04402d.

(94) Zhang, L.; An, K.; Wang, Y.; Wu, Y. D.; Zhang, X.; Yu, Z. X.; He, W. A Combined Computational and Experimental Study of Rh-Catalyzed C-H Silylation with Silacyclobutanes: Insights Leading to a More Efficient Catalyst System. *J. Am. Chem. Soc.* **2021**, *143* (9), 3571–3582. https://doi.org/10.1021/jacs.0c13335.

(95) Esteruelas, M. A.; Oliván, M.; Vélez, A. Xantphos-Type Complexes of Group 9: Rhodium versus Iridium. *Inorg. Chem.* **2013**, *52* (9), 5339–5349. https://doi.org/10.1021/ic4002658.

(96) Teltewskoi, M.; Panetier, J. A.; Macgregor, S. A.; Braun, T. A Highly Reactive Rhodium(I)-Boryl Complex as a Useful Tool for C-H Bond Activation and Catalytic C-F Bond Borylation. *Angew. Chem. - Int. Ed.* **2010**, *49* (23), 3947–3951. https://doi.org/10.1002/anie.201001070.

(97) Uetake, Y.; Niwa, T.; Hosoya, T. Rhodium-Catalyzed Ipso-Borylation of Alkylthioarenes via C-S Bond Cleavage. *Org. Lett.* **2016**, *18* (11), 2758–2761. https://doi.org/10.1021/acs.orglett.6b01250.

(98) Ren, P.; Pike, S. D.; Pernik, I.; Weller, A. S.; Willis, M. C. Rh-POP Pincer Xantphos Complexes for C-S and C-H Activation. Implications for Carbothiolation Catalysis. *Organometallics* **2015**, *34* (4), 711–723. https://doi.org/10.1021/om500984y.

(99) Pietsch, S.; Neeve, E. C.; Apperley, D. C.; Bertermann, R.; Mo, F.; Qiu, D.; Cheung, M. S.; Dang, L.; Wang, J.; Radius, U.; Lin, Z.; Kleeberg, C.; Marder, T. B. Synthesis, Structure, and Reactivity of Anionic Sp2-Sp3 Diboron Compounds: Readily Accessible Boryl Nucleophiles. *Chem. - Eur. J.* **2015**, *21* (19), 7082–7099. https://doi.org/10.1002/chem.201500235.

(100) Lee, B.; Chirik, P. J. Ketone Synthesis from Benzyldiboronates and Esters: Leveraging α-Boryl Carbanions for Carbon-Carbon Bond Formation. *J. Am. Chem. Soc.* **2020**, *142* (5), 2429–2437. https://doi.org/10.1021/jacs.9b11944.

(101) Esteruelas, M. A.; Oliván, M.; Vélez, A. POP-Rhodium-Promoted C-H and B-H Bond Activation and C-B Bond Formation. *Organometallics* **2015**, *34* (10), 1911–1924. https://doi.org/10.1021/acs.organomet.5b00176.

(102) Irvine, G. J.; Lesley, M. J. G.; Marder, T. B.; Norman, N. C.; Rice, C. R.; Robins, E. G.; Roper, W. R.; Whittell, G. R.; Wright, L. J. Transition Metal – Boryl Compounds : Synthesis , Reactivity , and Structure. *Chem Rev* **1998**, *98*, 2685–2722.

(103) Kays, D. L.; Aldridge, S. Transition Metal Boryl Complexes. In *Contemporary Metal Boron Chemistry I. Structure and Bonding, vol. 130.*; Marder, T. B., Lin, Z., Eds.; Springer: Berlin, Heidelberg, 2008; pp 29–122. https://doi.org/10.1007/430_2007_079.

(104) Wessendorf, F.; Grimm, B.; Guldi, D. M.; Hirsch, A. Pairing Fullerenes and Porphyrins: Supramolecular Wires That Exhibit Charge Transfer Activity. *J. Am. Chem. Soc.* **2010**, *132* (31), 10786–10795. https://doi.org/10.1021/ja101937w.

(105) Bhawal, B. N.; Reisenbauer, J. C.; Ehinger, C.; Morandi, B. Overcoming Selectivity Issues in Reversible Catalysis: A Transfer Hydrocyanation Exhibiting High Kinetic Control. *J. Am. Chem. Soc.* **2020**, *142* (25), 10914–10920. https://doi.org/10.1021/jacs.0c03184.

(106) Anai, T.; Nakata, E.; Koshi, Y.; Ojida, A.; Hamachi, I. Design of a Hybrid Biosensor for Enhanced Phosphopeptide Recognition Based on a Phosphoprotein Binding Domain Coupled with a Fluorescent Chemosensor. *J. Am. Chem. Soc.* **2007**, *129* (19), 6233–6239. https://doi.org/10.1021/ja0693284.

(107) Basel, Y.; Hassner, A. Imidazole and Trifluoroethanol as Efficient and Mild Reagents for Destruction of Excess Di-Tert-Butyl Dicarbonate [(BOC)2O]1. *Synthesis* **2001**, 550–552. https://doi.org/10.1055/s-2001-12350.

(108) Seo, H.; Liu, A.; Jamison, T. F. Direct β-Selective Hydrocarboxylation of Styrenes with CO2 Enabled by Continuous Flow Photoredox Catalysis. *J. Am. Chem. Soc.* **2017**, *139* (40), 13969–13972. https://doi.org/10.1021/jacs.7b05942.

(109) Zha, Z.; Choi, S. R.; Ploessl, K.; Lieberman, B. P.; Qu, W.; Hefti, F.; Mintun, M.; Skovronsky, D.; Kung, H. F. Multidentate 18F-Polypegylated Styrylpyridines As Imaging Agents for Aβ Plaques in Cerebral Amyloid Angiopathy (CAA). *J. Med. Chem.* **2011**, *54* (23), 8085–8098. https://doi.org/10.1021/jm2009106.

(110) Qu, W.; Kung, M. P.; Hou, C.; Benedum, T. E.; Kung, H. F. Novel Styrylpyridines as Probes for SPECT Imaging of Amyloid Plaques. *J. Med. Chem.* **2007**, *50* (9), 2157–2165. https://doi.org/10.1021/jm070025+.

(111) Molander, G. A.; Brown, A. R. Suzuki-Miyaura Cross-Coupling Reactions of Potassium Vinyltrifluoroborate with Aryl and Heteroaryl Electrophiles. *J. Org. Chem.* **2006**, *71* (26), 9681–9686. https://doi.org/10.1021/jo0617013.

(112) Denmark, S. E.; Butler, C. R. Vinylation of Aryl Bromides Using an Inexpensive Vinylpolysiloxane. *Org. Lett.* **2006**, *8* (1), 63–66. https://doi.org/10.1021/ol052517r.

(113) Shirakawa, E.; Zhang, X.; Hayashi, T. Mizoroki-Heck-Type Reaction Mediated by Potassium Tert-Butoxide. *Angew. Chem. - Int. Ed.* **2011**, *50* (20), 4671–4674. https://doi.org/10.1002/anie.201008220.

(114) Jiang, L.; Xu, Q. Observation of Anomalous C-O Bond Weakening on Discandium and Activation Process to CO Dissociation. *J. Am. Chem. Soc.* **2005**, *127* (1), 42–43. https://doi.org/10.1021/ja0442421.

(115) Lu, W.; Shen, Z. Direct Synthesis of Alkenylboronates from Alkenes and Pinacol Diboron via Copper Catalysis. *Org. Lett.* **2019**, *21* (1), 142–146. https://doi.org/10.1021/acs.orglett.8b03599.

(116) Fernández-Salas, J. A.; Eberhart, A. J.; Procter, D. J. Metal-Free CH-CH-Type Cross-Coupling of Arenes and Alkynes Directed by a Multifunctional Sulfoxide Group. *J. Am. Chem. Soc.* **2016**, *138* (3), 790–793. https://doi.org/10.1021/jacs.5b12579.

(117) Semina, E.; Tuzina, P.; Bienewald, F.; Hashmi, A. S. K.; Schaub, T. Ruthenium-Catalyzed Synthesis of Vinylamides at Low Acetylene Pressure. *Chem. Commun.* **2020**, *56* (44), 5977–5980. https://doi.org/10.1039/d0cc01533d.

(118) Lu, G.; Lin, B.; Gao, Y.; Ying, J.; Tang, G.; Zhao, Y. Mn(OAc)3-Mediated Synthesis of 3-Phosphonyldihydrofurans from β-Ketophosphonates and Alkenes. *Synlett* **2016**, *28* (06), 724–728. https://doi.org/10.1055/s-0036-1588112.

(119) Lei, C.; Yip, Y. J.; Zhou, J. S. Nickel-Catalyzed Direct Synthesis of Aryl Olefins from Ketones and Organoboron Reagents under Neutral Conditions. *J. Am. Chem. Soc.* **2017**, *139* (17), 6086–6089. https://doi.org/10.1021/jacs.7b02742.

(120) Tang, J.; Hackenberger, D.; Goossen, L. J. Branched Arylalkenes from Cinnamates: Selectivity Inversion in Heck Reactions by Carboxylates as Deciduous Directing Groups. *Angew. Chem. Int. Ed.* **2016**, *55* (37), 11296–11299. https://doi.org/10.1002/anie.201605744.

(121) Tsukamoto, H.; Uchiyama, T.; Suzuki, T.; Kondo, Y. Palladium(0)-Catalyzed Direct Cross-Coupling Reaction of Allylic Alcohols with Aryl- and Alkenylboronic Acids. *Org. Biomol. Chem.* **2008**, *6* (16), 3005. https://doi.org/10.1039/b804991b.

(122) Niu, D.; Buchwald, S. L. Design of Modified Amine Transfer Reagents Allows the Synthesis of α-Chiral Secondary Amines via CuH-Catalyzed Hydroamination. *J. Am. Chem. Soc.* **2015**, *137* (30), 9716–9721. https://doi.org/10.1021/jacs.5b05446.

(123) Valverde, D.; Porcar, R.; Izquierdo, D.; Burguete, M. I.; Garcia-Verdugo, E.; Luis, S. V. Rose Bengal Immobilized on Supported Ionic-Liquid-like Phases: An Efficient Photocatalyst for Batch and Flow Processes. *ChemSusChem* **2019**, *12*, 3996–4004. https://doi.org/10.1002/cssc.201901533.

(124) Seoane, A.; Casanova, N.; Quiñones, N.; Mascareñas, J. L.; Gulías, M. Straightforward Assembly of Benzoxepines by Means of a Rhodium(III)- Catalyzed C-H Functionalization of o-Vinylphenols. *J. Am. Chem. Soc.* **2014**, *136* (3), 834–837. https://doi.org/10.1021/ja410538w.

(125) Payer, S. E.; Pollak, H.; Schmidbauer, B.; Hamm, F.; Juričić, F.; Faber, K.; Glueck, S. M. Multienzyme One-Pot Cascade for the Stereoselective Hydroxyethyl Functionalization of Substituted Phenols. *Org. Lett.* **2018**, *20* (17), 5139–5143. https://doi.org/10.1021/acs.orglett.8b02058.

(126) Faul, M. M.; Ratz, A. M.; Sullivan, K. A.; Trankle, W. G.; Winneroski, L. L. Synthesis of Novel Retinoid X Receptor-Selective Retinoids. *J. Org. Chem.* **2001**, *66* (17), 5772–5782. https://doi.org/10.1021/jo0103064.

(127) Yamada, S.; Kawasaki, M.; Fujihara, M.; Watanabe, M.; Takamura, Y.; Takioku, M.; Nishioka, H.; Takeuchi, Y.; Makishima, M.; Motoyama, T.; Ito, S.; Tokiwa, H.; Nakano, S.; Kakuta, H. Competitive Binding Assay with an Umbelliferone-Based Fluorescent Rexinoid for Retinoid X Receptor Ligand Screening. *J. Med. Chem.* **2019**, *62* (19), 8809–8818. https://doi.org/10.1021/acs.jmedchem.9b00995.

(128) Kinzel, T.; Zhang, Y.; Buchwald, S. L. A New Palladium Precatalyst Allows for the Fast Suzuki-Miyaura Coupling Reactions of Unstable Polyfluorophenyl and 2-Heteroaryl Boronic Acids. *J. Am. Chem. Soc.* **2010**, *132* (40), 14073–14075. https://doi.org/10.1021/ja1073799.

(129) Tadpetch, K.; Kaewmee, B.; Chantakaew, K.; Kantee, K.; Rukachaisirikul, V.; Phongpaichit, S. Synthesis and Cytotoxic Activities of Semisynthetic Zearalenone Analogues. *Bioorg. Med. Chem. Lett.* **2016**, *26* (15), 3612–3616. https://doi.org/10.1016/j.bmcl.2016.06.007.

(130) Burckhardt, S.; Ley, S. V. The Use of π-Allyltricarbonyliron Lactone Complexes in the Synthesis of the Resorcylic Macrolides α- and β-Zearalenol. *J. Chem. Soc. Perkin 1* **2002**, *2* (7), 874–882. https://doi.org/10.1039/b201164f.

(131) Myhill, J. A.; Wilhelmsen, C. A.; Zhang, L.; Morken, J. P. Diastereoselective and Enantioselective Conjunctive Cross-Coupling Enabled by Boron Ligand Design. *J. Am. Chem. Soc.* **2018**, *140* (45), 15181–15185. https://doi.org/10.1021/jacs.8b09909.

(132) Koo, S. M.; Vendola, A. J.; Momm, S. N.; Morken, J. P. Alkyl Group Migration in Ni-Catalyzed Conjunctive Coupling with C(Sp3) Electrophiles: Reaction Development and Application to Targets of Interest. *Org. Lett.* **2020**, *22* (2), 666–669. https://doi.org/10.1021/acs.orglett.9b04453.

(133) Wallace, R. H.; Zong, K. K. The Preparation of Optically Active Boronic Ester Substituted Δ2-Isoxazolines. *J. Organomet. Chem.* **1999**, *581* (1–2), 87–91. https://doi.org/10.1016/S0022-328X(99)00055-8.

(134) Meng, Y.; Kong, Z.; Morken, J. P. Catalytic Enantioselective Synthesis of Anti -Vicinal Silylboronates by Conjunctive Cross-Coupling . *Angew. Chem.* **2020**, *132* (22), 8534–8537. https://doi.org/10.1002/ange.202000937.

(135) Wang, Y. D.; Kimball, G.; Prashad, A. S.; Wang, Y. Zr-Mediated Hydroboration: Stereoselective Synthesis of Vinyl Boronic Esters.

Tetrahedron Lett. **2005**, *46* (50), 8777–8780. https://doi.org/10.1016/j.tetlet.2005.10.031.

(136)   Bismuto, A.; Thomas, S. P.; Cowley, M. J. Aluminum Hydride Catalyzed Hydroboration of Alkynes. *Angew. Chem. - Int. Ed.* **2016**, *55* (49), 15356–15359. https://doi.org/10.1002/anie.201609690.

(137)   Reid, W. B.; Spillane, J. J.; Krause, S. B.; Watson, D. A. Direct Synthesis of Alkenyl Boronic Esters from Unfunctionalized Alkenes: A Boryl-Heck Reaction. *J. Am. Chem. Soc.* **2016**, *138* (17), 5539–5542. https://doi.org/10.1021/jacs.6b02914.

(138)   Du, R.; Liu, L.; Xu, S. Iridium-Catalyzed Regio- and Enantioselective Borylation of Unbiased Methylene C(Sp3)−H Bonds at the Position β to a Nitrogen Center. *Angew. Chem. - Int. Ed.* **2021**, *60* (11), 5843–5847. https://doi.org/10.1002/anie.202016009.

(139)   Hitosugi, S.; Tanimoto, D.; Nakanishi, W.; Isobe, H. A Facile Chromatographic Method for Purification of Pinacol Boronic Esters. *Chem. Lett.* **2012**, *41* (9), 972–973. https://doi.org/10.1246/cl.2012.972.

(140)   Shi, X.; Li, S.; Wu, L. H2-Acceptorless Dehydrogenative Boration and Transfer Boration of Alkenes Enabled by Zirconium Catalyst. *Angew. Chem. - Int. Ed.* **2019**, *58* (45), 16167–16171. https://doi.org/10.1002/anie.201908931.

(141)   Wrackmeyer, B. Organoboron Chemistry. In *Modern Magnetic Resonance*; Webb, G. A., Ed.; Springer: Dordrecht, The Netherlands, 2008; pp 455–457.

(142)   Chan, K. W. H.; Chourasia, A. H.; Erdman, P. E.; Fung, L.; Mercurio, F.; Sullivan, R. Fused Thiophene Compounds. U.S. Patent WO 2019/241271, 2019.

(143)   Nakajima, K.; Kato, T.; Nishibayashi, Y. Hydroboration of Alkynes Catalyzed by Pyrrolide-Based PNP Pincer-Iron Complexes. *Org. Lett.* **2017**, *19* (16), 4323–4326. https://doi.org/10.1021/acs.orglett.7b01995.

(144)   Rawat, V. S.; Sreedhar, B. Iron-Catalyzed Borylation Reactions of Alkynes: An Efficient Synthesis of e -Vinyl Boronates. *Synlett* **2014**, *25* (8), 1132–1136. https://doi.org/10.1055/s-0033-1341048.

(145)   Ho, H. E.; Asao, N.; Yamamoto, Y.; Jin, T. Carboxylic Acid-Catalyzed Highly Efficient and Selective Hydroboration of Alkynes with Pinacolborane. *Org. Lett.* **2014**, *16* (17), 4670–4673. https://doi.org/10.1021/ol502285s.

(146)   Mamidala, R.; Pandey, V. K.; Rit, A. AgSbF6-Catalyzed: Anti -Markovnikov Hydroboration of Terminal Alkynes. *Chem. Commun.* **2019**, *50*, 989–992. https://doi.org/10.1039/c8cc07499b.

(147)   Jang, W. J.; Kang, B. N.; Lee, J. H.; Choi, Y. M.; Kim, C. H.; Yun, J. NHC-Copper-Thiophene-2-Carboxylate Complex for the Hydroboration of Terminal Alkynes. *Org. Biomol. Chem.* **2019**, *17* (21), 5249–5252. https://doi.org/10.1039/c9ob00839j.

(148)   Mandal, S.; Verma, P. K.; Geetharani, K. Lewis Acid Catalysis: Regioselective Hydroboration of Alkynes and Alkenes Promoted by Scandium Triflate. *Chem. Commun.* **2018**, *54* (97), 13690–13693. https://doi.org/10.1039/c8cc08361d.

(149)   Zhao, J.; Niu, Z.; Fu, H.; Li, Y. Ligand-Free Hydroboration of Alkynes Catalyzed by Heterogeneous Copper Powder with High Efficiency. *Chem. Commun.* **2014**, *50*, 2058–2060. https://doi.org/10.1039/c3cc48670b.

(150)   Takaya, J.; Kirai, N.; Iwasawa, N. Efficient Synthesis of Diborylalkenes from Alkenes and Diboron by a New PSiP-Pincer Palladium-Catalyzed Dehydrogenative Borylation. *J. Am. Chem. Soc.* **2011**, *133* (33), 12980–12983. https://doi.org/10.1021/ja205186k.

(151)   Tai, C. C.; Yu, M. S.; Chen, Y. L.; Chuang, W. H.; Lin, T. H.; Yap, G. P. A.; Ong, T. G. Synthesis of a Guanidine NHC Complex and Its Application in Borylation Reactions. *Chem. Commun.* **2014**, *50* (33), 4344–4346. https://doi.org/10.1039/c4cc00550c.

(152)   Molloy, J. J.; Metternich, J. B.; Daniliuc, C. G.; Watson, A. J. B.; Gilmour, R. Contra-Thermodynamic, Photocatalytic *E → Z* Isomerization of Styrenyl Boron Species: Vectors to Facilitate Exploration of Two-Dimensional Chemical Space. *Angew. Chem. Int. Ed.* **2018**, *57* (12), 3168–3172. https://doi.org/10.1002/anie.201800286.

(153)   Kovalenko, M.; Yarmoliuk, D. V.; Serhiichuk, D.; Chernenko, D.; Smyrnov, V.; Breslavskyi, A.; Hryshchuk, O. V.; Kleban, I.; Rassukana, Y.; Tymtsunik, A. V.; Tolmachev, A. A.; Kuchkovska, Y. O.; Grygorenko, O. O. The Boron-Wittig Olefination of Aldehydes and Ketones with Bis[(Pinacolato)Boryl]Methane: An Extended Reaction Scope: The Boron-Wittig Olefination of Aldehydes and Ketones with Bis[(Pinacolato)Boryl]Methane: An Extended Reaction Scope. *Eur. J. Org. Chem.* **2019**, *2019* (33), 5624–5635. https://doi.org/10.1002/ejoc.201900648.

(154)   Hu, T. J.; Zhang, G.; Chen, Y. H.; Feng, C. G.; Lin, G. Q. Borylation of Olefin C-H Bond via Aryl to Vinyl Palladium 1,4-Migration. *J. Am. Chem. Soc.* **2016**, *138* (9), 2897–2900. https://doi.org/10.1021/jacs.5b11990.

(155)   Wang, C.; Xu, Z.; Tobrman, T.; Negishi, E. Arylethyne Bromoboration-Negishi Coupling Route to *E* - or *Z* -Aryl-Substituted Trisubstituted Alkenes of ≥98% Isomeric Purity. New Horizon in the Highly Selective Synthesis of Trisubstituted Alkenes. *Adv. Synth. Catal.* **2010**, *352* (4), 627–631. https://doi.org/10.1002/adsc.200900766.

(156)   Hu, T. J.; Zhang, G.; Chen, Y. H.; Feng, C. G.; Lin, G. Q. Borylation of Olefin C-H Bond via Aryl to Vinyl Palladium 1,4-Migration. *J. Am. Chem. Soc.* **2016**, *138* (9), 2897–2900. https://doi.org/10.1021/jacs.5b11990.

(157)   Meng, F.; Jung, B.; Haeffner, F.; Hoveyda, A. H. NHC-Cu-Catalyzed Protoboration of Monosubstituted Allenes. Ligand-Controlled Site Selectivity, Application to Synthesis and Mechanism. *Org. Lett.* **2013**, *15* (6), 1414–1417. https://doi.org/10.1021/ol4004178.

(158)   Ping, Y.; Wang, R.; Wang, Q.; Chang, T.; Huo, J.; Lei, M.; Wang, J. Synthesis of Alkenylboronates from N-Tosylhydrazones through Palladium-Catalyzed Carbene Migratory Insertion. *J. Am. Chem. Soc.* **2021**, *143* (26), 9769–9780. https://doi.org/10.1021/jacs.1c02331.

(159)   Hu, Y.; Sun, W.; Zhang, T.; Xu, N.; Xu, J.; Lan, Y.; Liu, C. Stereoselective Synthesis of Trisubstituted Vinylboronates from Ketone Enolates Triggered by 1,3-Metalate Rearrangement of Lithium Enolates. *Angew. Chem. Int. Ed.* **2019**, *58* (44), 15813–15818. https://doi.org/10.1002/anie.201909235.

(160)   Zhang, J.; Dai, W.; Liu, Q.; Cao, S. Cu-Catalyzed Stereoselective Borylation of Gem-Difluoroalkenes with B2pin2. *Org. Lett.* **2017**, *19* (12), 3283–3286. https://doi.org/10.1021/acs.orglett.7b01430.

CHAPTER 3

Selective Ir-Catalyzed Transfer C-H Borylation of Alkenes Compatible with Drug-Oriented Functional Groups

3.1 Introduction

The ability to selectively install a boronic acid derivative group at a specific C–H bond in existing molecules has the potential to streamline the discovery and development of new pharmaceuticals.[1–12] The resulting organoboron intermediates can be readily converted to families of derivatives through established divergent post-functionalization reactions (Figure 3.1a).[13–16] While the selective borylation of aromatic C–H bonds has been the subject of numerous studies,[11] selective borylation of vinylic C–H bonds remains underdeveloped, especially for fine chemicals bearing reactive or polar functional groups.[17–19] Recently, guided by mechanistic considerations, we have developed the Rh(I)-catalyzed transfer C–H borylation of alkenes (Figure 3.1b).[20] With a vinyl boronate ester being the source of the boronic group and the only stoichiometric reagent, in place of typical reactive reagents, such as, catBCl,[21–23] HBpin,[18,24,25] or B_2pin_2,[26,27] the method proved to be applicable to a broad range of alkenes bearing a range of functional groups, such as aldehydes, ketones, esters, and nitriles. However, due to the inherent reactivity of the catalytic Rh-species, the method remains incompatible with starting materials bearing many unprotected polar groups, especially those containing even moderately acidic protons, such as, NH or OH of carboxyamide, sulfonamide, urea, indole, carboxylic acid, phenol, alcohol, or amines, and similar motifs. Importantly, because these functional groups are predisposed to form specific interactions between drug molecules and their biologic targets,[28,29] they are present in the overwhelming majority of pharmaceuticals.[30] For instance, 191 of 200 top-selling small drug molecules contain at least one of these functional groups in their structures.[31]

In search of methods potentially suitable for the late-stage functionalization of pharmacophoric molecules, we hypothesized that a putative Ir-catalyzed transfer C–H borylation of alkenes would be appealing by being tolerant to otherwise incompatible polar protic and strongly coordinating functional groups. We considered that Ir-catalyzed borylation reactions of aromatic C–H bonds are tolerant to many functional groups,[6,7] including NH-amide,[32] urea,[33,34] free NH-amine[35,36] and NH-indole.[37,38] These reactions occur within a catalytic cycle operating through Ir-hydride and Ir-boryl intermediates.[6] Importantly, by analogy to the Rh-based method,[20] such Ir-intermediates would also partake in the catalytic cycle of the envisioned Ir-catalyzed transfer C–H borylation of alkenes. However, the question remained whether Ir-intermediates could undergo β-boryl elimination, a key elementary reaction that is unprecedented for Ir-complexes, and so far has been reported only for Ru[19,39] and Rh-complexes,[20] and presumed to occur for Zr[18] and Pd[40,41] catalysts.

This chapter describes the development of an Ir-catalyzed transfer C–H borylation of alkenes (Figure 3.1c). The method is compatible with starting materials bearing various previously incompatible functional groups, including those containing acidic N–H and O–H bonds and free NH-amines. Additionally, the Ir-catalyst tolerates a series of other formerly incompatible motifs, such as alkyl or aryl halides, vinyl or silyl ethers, and nitro or carbamate derivatives. The applicability of the protocol to the functionalization of pharmacophoric compounds was demonstrated with the transformations of indomethacin, rebamipide, and chlorpropamide

derivatives. The results of control experiments are consistent with the envisioned mechanism involving a series of alkene insertions, β-boryl and β-hydride elimination steps.

(a) Diverse post-functionalizations enabled by selective C–H borylation methods

(b) Our previous study on boryl group transfer under Rh-catalysis

(c) **This study:** boryl group transfer under Ir-catalysis

FG: -COOH, -(NH)CONH-, -SO₂NH₂, -OH, -NH₂, NH-indole, -NO₂, -PO(OR)₂, -Br ...
Such moieties are present in >95% of small molecule drugs

+ A range of previously incompatible key synthetic functional groups
+ Different boronic acid esters and amides (Bpin, Bmac, Baam, Bdan)
+ Drug derivatives (indomethacin, rebamipide, and chlorpropamide)

Figure 3.1. Context of this work.

3.2. Results and Discussion

3.2.1. Evaluation of reaction conditions

We commenced our studies by evaluating the feasibility of the Ir-catalyzed transfer C–H borylation of alkenes using a simple model reaction of styrene **1** with vinyl boronate pinacol ester **2** to form product **3**. To identify a suitable catalyst, we tested a series of Ir(I)-complexes as metal precursors, and common mono- and bidentate phosphine ligands. We also investigated the influence of co-catalytic amounts of B₂pin₂, which could assist the activation of the precatalyst by forming an Ir-boryl complex,[42,43] one intermediate of the putative catalytic cycle.

Upon evaluation of a range of precursors, ligands, and conditions (Table 3.1 and section 3.4.2.), we found that the model reaction of **1** with **2** formed product **3** quantitatively after 3 h at 90 °C in the presence of 2 mol% [Ir(cod)Cl]₂, with either 4 mol% *t*-Bu-xantphos (**L4**) or 8 mol% JohnPhos (**L6**) as a ligand, and 5 mol% B₂pin₂. The data presented in Table 3.1 show the influence of each element of the catalytic system on the yield of the model reaction. For instance, the backbone, the steric, and electronic features of the phosphine ligand are critical.

The reaction with xantphos (**L1**) formed product **3** in 23% yield (entry 1), while the one with dpfphos (**L2**), the analogue of **L1** with a wider bite-angle formed only traces of the product (<2% yield; entry 2), and the reaction with dpephos (**L3**), the flexible analogue of **L1** formed product **3** in 36% yield (entry 3). In turn, the reaction with *t*-Bu-xantphos (**L4**), a close analogue of **L1** bearing electron donating and sterically demanding bis(*tert*-butyl)phosphine groups formed product **3** quantitatively (entry 4). In that case, the reaction was nearly completed within 30 min (92% yield; entry 5), underscoring the strong impact of the ligand on the catalytic activity. Noteworthy, the reaction with structurally related dtbpx (**L5**) furnished **3** in only 25% yield (entry 6), further indicating the importance of the ligand backbone and its substitution pattern.

Table 3.1. Evaluation of reaction conditions.

Entry	Variation of conditions[a]	yield (%)[b]
1	[Ir(cod)Cl]₂, **L1**	23
2	[Ir(cod)Cl]₂, **L2**	<2
3	[Ir(cod)Cl]₂, **L3**	36
4	**[Ir(cod)Cl]₂, L4**	**>99[c] (74)[d]**
5	[Ir(cod)Cl]₂, **L4**, 30 min	92
6	[Ir(cod)Cl]₂, **L5**	25
7	**[Ir(cod)Cl]₂, L6 (8 mol%)**	**>99**
8	[Ir(cod)Cl]₂, no ligand	14
9	[Ir(cod)Cl]₂, **L4**, no B₂pin₂	96
10	[Ir(cod)Cl]₂, **L4**, 150 mol% B₂pin₂	66
11	[Ir(cod)Cl]₂, **L4**, 150 mol%, no **2**	2

[a] Conditions: 0.2 mmol scale, [Ir] (4 mol% Ir), ligand (4 mol% **L1**-**L5**, 8 mol% **L6**), B₂pin₂ (5 mol%), styrene (1.0 equiv), vinyl Bpin (1.5 equiv), 1,4-dioxane (0.2 mL), nitrogen atmosphere; [b] Yield determined by GC-FID analysis of the reaction mixture with dodecane as an internal standard; [c] thf can be used instead of 1,4-dioxane with no change of the yield; [d] Isolated yield. For evaluation of other ligands, see section 3.4.2.1.

During our investigation of ligands (section 3.4.2.1.), we found that monophosphine JohnPhos (**L6**) bearing the same bis(*tert*-butyl)phosphine moiety as **L4** also formed a highly active catalyst (entry 7). In turn, the evaluation of a series of Ir(I)-precursors bearing different

counterions showed that they form similarly active catalysts with [Ir(cod)Cl]$_2$ forming the most productive complex (section 3.4.2.2.). In the absence of any phosphine ligand, [Ir(cod)Cl]$_2$ retained residual catalytic activity (entry 8). Further, a co-catalytic amount of B$_2$pin$_2$ was not critical for the catalytic activity (entry 9), but its presence increased the reaction yield, most likely by increasing the efficacy of the precatalyst activation.[42,43] However, the presence of the stochiometric amounts of B$_2$pin$_2$ is detrimental for the reaction (entry 10). Also, nearly no product **3** was formed with stochiometric B$_2$pin$_2$ in the absence of **2** (entry 11), confirming the role of **2** as the sole donor of the boryl ester group.[44–53]

3.2.2. Scope of the reaction

Next, we evaluated the method with respect to its scope and functional group compatibility, focusing on starting materials bearing motifs that were previously problematic but would be of high importance in the context of synthesis and functionalization of bioactive molecules.[2] In case of many starting materials, we conducted experiments in parallel employing either *t*-Bu-xantphos (**L4**) or JohnPhos (**L6**) as a ligand. In many cases, catalysts with either ligand performed similarly well, albeit in some cases, one catalyst formed the product in substantially higher yield than the other, as summarized in Figure 3.2 and presented in detail in section 3.4.5.

The developed method is compatible with starting materials containing diverse groups with free N–H or O–H bonds (Figure 3.2). A series of borate pinacol ester derivatives bearing an acidic N–H bond in acetamide **4**, carbamate **5**, and sulfonamides **6-7**, as well as free NH-indole **8**, and unprotected NH$_2$-aniline **9** were formed in 50-88% yields, showing the compatibility of the catalyst with different types of NH motifs. Also, free phenol **10**, benzyl and aliphatic alcohols **11**-**13** were prepared in 39-79% yields, demonstrating the compatibility with O–H bonds. Remarkably, the method proved also compatible with carboxylic acids, as observed in reactions forming benzoic and phenylacetic acid derivatives **13-14** in 45-73% yields. However, the presence of strong sulfonic acid is detrimental for the reaction, as nearly no product **15** was formed.

Besides transferring the common borate pinacol ester group (Bpin), the catalyst proved also potent to transfer other borate ester and amide groups. Derivatives **16-18** containing dimethylacenaphthyl-1,2-diol, anthranilamide and 1,8-diaminonaphthalene-substituted organoboron moieties, that is, Bmac, Baam, and Bdan, respectively, were formed in 84-93% yields, when the corresponding vinyl derivative was used in place of vinyl Bpin **2** under otherwise standard conditions. Noteworthy, the method enabling the straightforward installation of the Baam and Bdan groups onto alkenes is particularly appealing due to their unique reactivity profiles, selectivity, and the outstanding stability toward air and moisture.[54,55] Although these derivatives have attracted increasing attention recently,[56–59] their synthesis from alkenes remained limited.[60–62]

The Ir-based protocol proved also tolerant to a range of other functional groups that tend to be incompatible with transition metal catalysis, including prior Rh catalysis,[20] due to either their strong coordination to a metal center or undergoing side reactions. For instance, the method is compatible with the readily reducible nitro group of derivative **19**, and strong

hydrogen bond acceptors of phosphonate **20** and sulfonate **21** esters, which were produced in 83-96% yields. Further, a series of otherwise reactive aryl and alkyl halides **22-23**, electron-rich vinyl heteroarenes **25-26**, and previously problematic vinyl carbamate **27** were formed in 85-99% yields. Silyl and vinyl ethers were problematic for Rh catalysis,[20] but here a range of structurally diversified products **28-33** were readily formed in 63-94% yields.
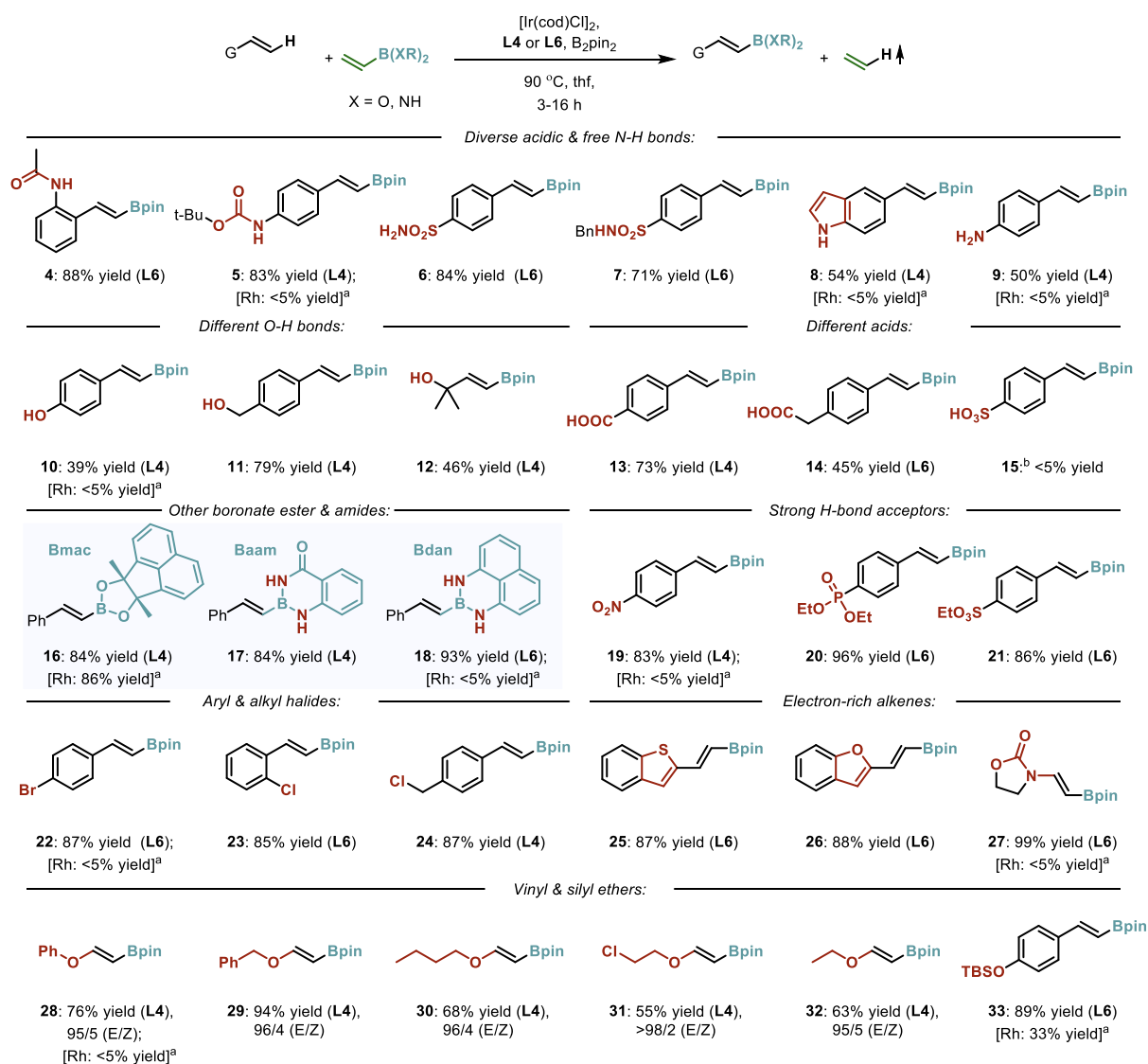
Figure 3.2. Scope of substrates. For the exact reaction conditions for each starting material, experimental details, product characterization, including the comparison between the yields of reactions for the same starting material with either **L4** and **L6** as a ligand, as well as the comparison of the analytical yields determined by ^{1}H NMR analysis of the reaction mixture with 1,3,5-trimethoxybenzene an internal standard and the yields of isolated materials, see section 3.4.5. and 3.5.6. Because vinylboronic esters tend to partially decompose during chromatography on silica gel,[21,63,64] the analytical yields are reported here to indicate the actual reaction performance. [a] For comparison, the reaction conducted in the presence of the previously reported Rh catalyst.[20] [b] Starting material was prepared *in situ* from its sodium salt and hydrogen chloride in diethyl ether.

Bolstered by the excellent functional group tolerance, we investigated the applicability of the protocol in vinyl C–H borylation of pharmacophoric molecules by preparing a series of derivatives of existing drug molecules (Figure 3.3). Specifically, boryl esters **34-36**, derivatives of nonsteroidal anti-inflammatory indomethacin, anti-diabetic chlorpropamide, and gastroprotective rebamipide drug molecules were formed readily in 67-72% yields under standard conditions.

Figure 3.3. Derivatives of market drug molecules.

3.2.3. Experimental mechanistic studies

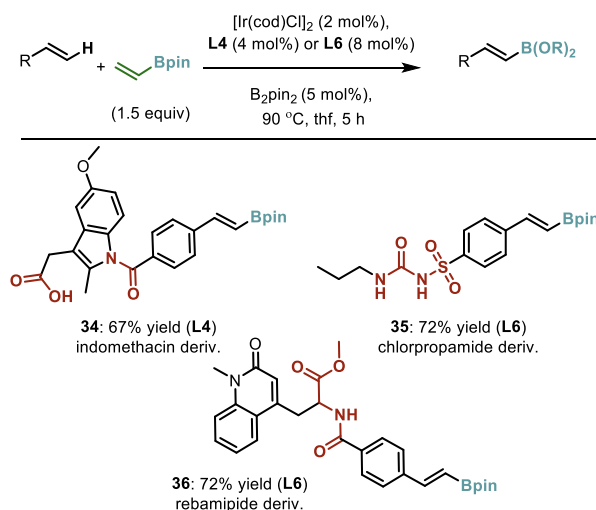Lastly, we performed a series of experiments to get some insight into the mechanism of the reaction (Figure 3.4). First, high-resolution mass analysis (ESI) of the reaction mixture showed a signal corresponding to the (**L4**)Ir(Bpin)(H)$^+$ species (819.3782 vs. calcd. 819.3821; section 3.4.3.3.), in line with the mechanism involving Ir-boryl intermediates (Figure 3.4a). Second, the reaction of styrene-d_8 **1**-d_8 and Bpin donor **2** revealed the extensive proton-deuterium scrambling throughout the different vinylic positions of reagents and products (Figure 3.4b, Figures S1-S4), in line with the presence of Ir-hydride intermediates that undergo fast and reversible alkene insertions (Figure 3.4a). Also, the reaction of 4-chlorostyrene **37** with styrylboronic acid derivative **3**, as a Bpin donor in place of **2**, led to formation 50% of styrene **1** and 50% of 4-chlorostyrylboronic acid derivative **38** (Figure 3.4c, Figure S3.9), showing that all steps of the reaction toward the product formation are reversible under the catalytic conditions. Further, we observed that the (*Z*)-isomer of the product could undergo fast interconversion to the thermodynamically more stable (*E*)-stereoisomer **3** under reaction conditions as established in the experiment with independently prepared isomer (*Z*)-**3** as an additive in the reaction of 4-cyanostyrene **39** and **2** (Figure 3.4d, Figure 3.10). Thus, the experiment indicated that the stereoselectivity of the transfer reaction might be under thermodynamic control, strongly favoring **3** over (*Z*)-**3**. In sharp contrast, the (β)-boryl regioisomer of the product does not undergo interconversion to the typical (β)-regioisomer under reaction conditions as observed in the experiment with independently prepared (α)-**3**

as an additive in the reaction of 4-cyanostyrene **39** and **2** (Figure 3.4e, Figure 3.11). Consequently, the experiment showed that the regioselectivity of the transfer reaction is under kinetic control.
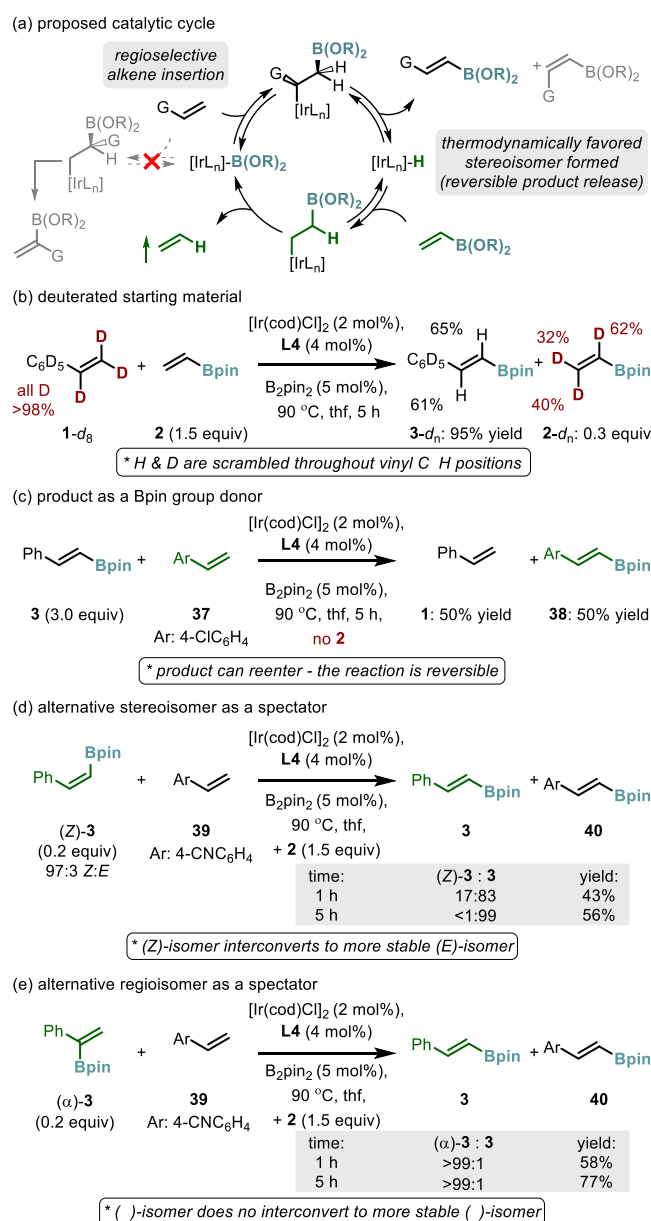
Figure 3.4. The proposed mechanism of the reaction and control experiments. For details, see section 3.4.3.

Overall, the experiments are consistent with the mechanism shown in Figure 3.4a that involves a series of reversible alkene insertions into Ir–H and Ir–B bonds, with the regioselectivity of the product being controlled by regioselective alkene insertion and the stereoselectivity being controlled by the thermodynamic stability of the products.

3.3. Conclusions

In summary, a broadly applicable Ir-catalyzed transfer C-H borylation of alkenes was developed. The method tolerates a number of functional groups, including many previously incompatible moieties bearing acidic N–H and O–H bonds, amines, alkyl or aryl halides, vinyl or silyl ethers, nitro or carbamate derivatives. The synthetic compatibility with

pharmacophoric molecules was demonstrated by preparing a series of vinyl boryl derivatives of commercial drug molecules. In greater perspective, the study underscores the exceptional potential of Ir catalysis in borylation of different types of C–H bonds occurring through distinct mechanistic pathways.

3.4. Experimental details

3.4.1. Experimental methods

Unless stated otherwise, all reactions and manipulations were conducted on the laboratory bench or in a well-ventilated fume hood in air with reagent grade solvents. Reactions under inert gas atmosphere were carried out in oven-dried glassware in a nitrogen-filled glove box or by standard Schlenk techniques under nitrogen. Unless noted otherwise, all reagents and solvents were purchased from commercial suppliers and used without further purification. For experiments under inert gas atmosphere, dried and degassed solvents were purchased from commercial suppliers, stored in a nitrogen-filled glove box and used as received. Column chromatography was carried out with the aid of a CombiFlash EZ Prep Chromatography System with integrated ELSD using the RediSep Rf (Bronze, Silver, or Gold) Silica Gel Disposable Flash columns. TLC was carried out on Merck Kieselgel F254 plates. TLC visualization was carried out with ultraviolet light (254 nm), followed by staining with a 1% aqueous $KMnO_4$ solution. NMR spectra were acquired on the 400 MHz (Bruker 400 MHz NMR UltraShield Magnet, Console Avance III, equipped by a standard probe BBFO ^{1}H-X inverse 5 mm (with ^{31}P < X < ^{15}N)) or 500 MHz (Bruker 500 MHz NMR Ascend Magnet, Console Avance Neo equipped by a Cryo-Probe Prodigy ^{1}H-X 5 mm (with ^{31}P < X < ^{15}N) with a 24-positions auto-sampler) instruments at the Institute of Science and Supramolecular Engineering (ISIS). NMR spectra were processed using the MestReNova 14.1 software. Chemical shifts are reported in parts per million (ppm) and referenced to residual solvent peaks or tetramethylsilane (TMS). Coupling constants are reported in hertz (Hz). GC-FID analysis was obtained on a Shimadzu GC-2010 Plus instrument equipped with a SH-Rxi-5MS column (25 m x 0.20 mm ID x 0.33 mm film) connected to a FID detector. GC-MS analysis was obtained on a Shimadzu QP2020 (EI) instrument equipped with a SH-Rxi-5MS column (25 m x 0.20 mm ID x 0.33 mm film). GC-FID and NMR yields were calculated using dodecane or 1,3,5-trimethoxybenzene, as the internal standards. GC-FID yields were corrected for response factors for all compounds. High-resolution electrospray ionization mass spectra (HR-ESI-MS) were obtained at the Analytical Facility of the Department of Chemistry, University of Strasbourg or at the Institute of Science and Supramolecular Engineering using a ThermoFisher Orbitrap Exactive Plus with Extend Mass Range (source HESI II) with a Vanquish PDA (VF-XX) detector.

3.4.2. Evaluation of reaction parameters

3.4.2.1. Evaluation of different ligands

Table 3.2.

Entry	Ligand	Yield [%]
1	xantphos **L1** (4 mol%)	23
2	dpfphos **L2** (4 mol%)	<2
3	dpephos **L3** (4 mol%)	36
4	tBu-xantphos **L4** (4 mol%)	>99
5	dtbpx **L5** (4 mol%)	25
6	JohnPhos **L6** (8 mol%)	>99
7	tribenzylphosphine (8 mol%)	39
8	rac-BI-DIME (8 mol%)	<2
9	P(OEt)3 (8 mol%)	64
10	BISBI (4 mol%)	<2
11	N-xantphos (4 mol%)	23
12	dppe (4 mol%)	11

13	BIPHEP (4 mol%)	<2
14	DPBP (4 mol%)	<2
15	DPEPhos (4 mol%)	36
16	DBFPhos (4 mol%)	<2
17	α,α'-Bis(di-t-butylphosphino)-o-xylene (4 mol%)	25
18	SEGPHOS (4 mol%)	23
19	(R,R)-DIOP (4 mol%)	87
20	dppb (4 mol%)	<2
21	BIPHEPHOS (4 mol%)	7
22	(R)-Monophos (8 mol%)	<2
23	triphenylphosphite (8 mol%)	<2
24	trimethylphosphite (8 mol%)	46
25	dppp (4 mol%)	31
26	TMEDA (2 mol%)	15
27	TEEDA (2 mol%)	31
28	Di-t-butylphenylphosphine (4 mol%)	5

Conditions: 0.2 mmol of styrene, 0.6 mmol vinyl Bpin, [Ir(COD)Cl]$_2$/xantphos (1:2 ratio), dioxane (200 µL, 1 M), 90 °C, 3 h. Yields were determined by GC-FID using dodecane as an internal standard.

3.4.2.2. Evaluation of other parameters
Table 3.3.

$$Ph\diagdown \xrightarrow[\substack{\text{vinyl Bpin (1.5 equiv.),} \\ \text{thf, 90 °C, 3 h}}]{\substack{[Ir]\ (4\ mol\%),\\ \text{ligand (4 mol\%)},\\ B_2pin_2\ (5\ mol\%)}} Ph\diagup \diagdown Bpin$$

Entry	Variation of conditions	Yield [%]
1	[Ir(cod)OMe]$_2$, **L4**, 30 min	91
2	[Ir(cod)acac]$_2$, **L4**, 30 min	80
3	[Ir(cod)$_2$OTf], **L4**, 30 min	72
4	[Ir(cod)Cl]$_2$, **L4**, no B$_2$pin$_2$, 30 min	94

Conditions: 0.2 mmol of styrene, 0.6 mmol vinyl Bpin, [Ir(COD)Cl]$_2$/xantphos (1:2 ratio), dioxane (200 µL, 1 M), 90 °C, 3 h. Yields were determined by GC-FID using dodecane as an internal standard.

3.4.3. Mechanistic experiments

3.4.3.1. Preparation of product (*Z*)-**3**

**(*Z*)-4,4,5,5-tetramethyl-2-styryl-1,3,2-dioxaborolane** (*Z*)-**3**

The compound was prepared according to a modified literature procedure.[65] A mixture of [Rh(cod)Cl]$_2$ (11.1 mg, 23 µmol, 1.5 mol%), triisopropylphosphine (17.2 µL, 14.4 mg, 90 µmol, 6 mol%), and HBpin (218 µL, 192 mg, 1.5 mmol, 1.0 equiv) in triethylamine (5 mL) and *n*-hexane (9 mL) was allowed to stir at room temperature for 30 minutes under a nitrogen atmosphere. Phenylacetylene (330 µL, 306 mg, 3.0 mmol, 2.0 equiv) was added, and the resulting mixture was allowed to stir for 2.5 h at room temperature. The reaction was quenched by addition of MeOH (3 mL). The reaction mixture was filtered over a plug of celite, which was washed with DCM (100 mL). The combined filtrate was concentrated under reduced pressure, and the residue was subjected to column chromatography (silica, 0 – 6.8% MTBE in petroleum ether) to isolate the title compound (*Z/E* ratio = 97/3, 253 mg, 1.1 mmol, 73%) as a yellow oil. The NMR data match previously reported data for the title product.[20]
¹H NMR (400 MHz, CDCl$_3$) δ 7.56 – 7.51 (m, 2H), 7.34 – 7.18 (m, 4H), 5.60 (d, *J* = 14.8 Hz, 1H), 1.29 (s, 12H).

3.4.3.2. Experiments with isotope-labeled starting materials or potential products

The experiments described below are shown in the manuscript in **Figure 3.4** in the main text.

(a)
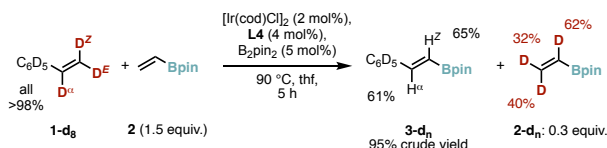
In a nitrogen-filled glove box, a 10 mL screw-cap vial equipped with a Teflon-coated magnetic stirring bar was charged with [Ir(cod)Cl]$_2$ (2.7 mg, 4.0 µmol, 2 mol%), t-Bu-xantphos (4.0 mg, 4.0 µmol, 4 mol%), B$_2$pin$_2$ (2.5 mg, 10.0 µmol, 5 mol%), thf (200 µL), vinyl Bpin (50.8 µL, 46.2 mg, 300 µmol, 1.5 equiv), and styrene-d_8 (22.4 mg, 200 µmol, 1.0 equiv). The vial was sealed with a cap, removed from the glove box, placed in a pre-heated aluminum block, and allowed to stir (800 rpm) at 90 °C for 5 h. The reaction mixture was concentrated under reduced pressure, and the residue was subjected to column chromatography (silica gel, 0-3.6% MTBE in petroleum ether) to give the title compound (25.5 mg, 108 µmol, 54%) as a red oil.

The ^{1}H NMR of the isolated product shows the deuterium incorporation in the olefinic protons.
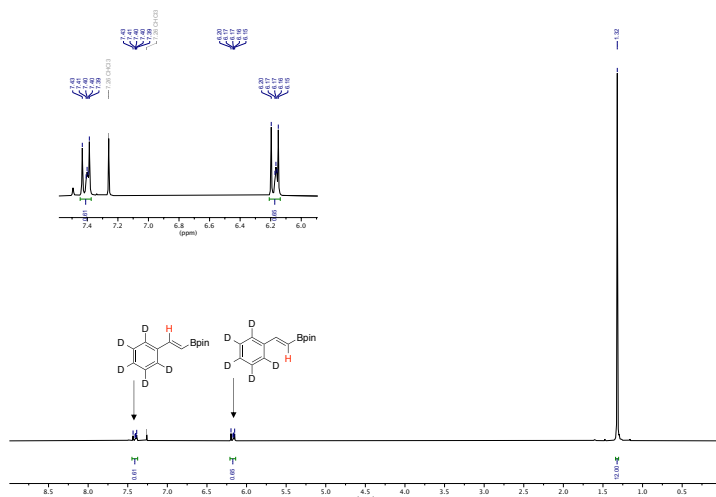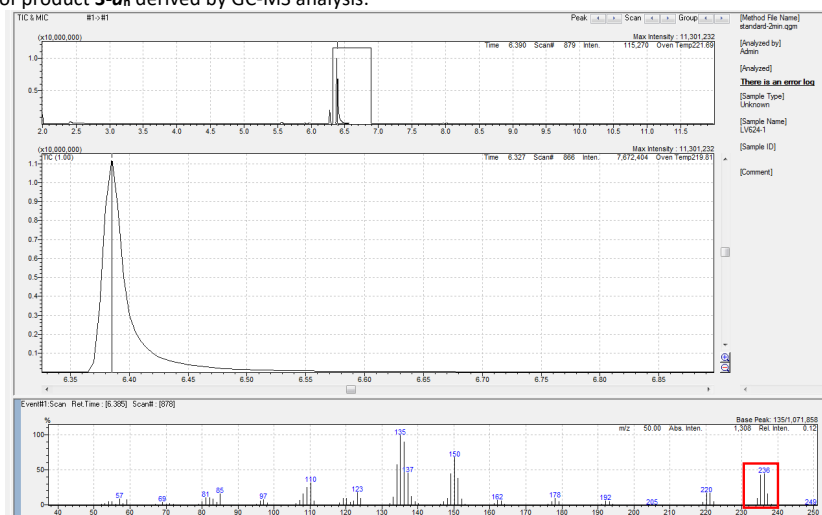**^{1}H NMR** (CDCl$_3$, 400 MHz):

Figure 3.5: Partial deuterium retaining in **3a** in the reaction of **1a**-d_8 detected by ^{1}H NMR spectroscopy.

Isotopomeric cluster of product **3-d_n** derived by GC-MS analysis:

Figure 3.6: Partial deuterium retaining in **3-d_n** in the reaction of **1**-d_8 detected by GC-MS analysis.
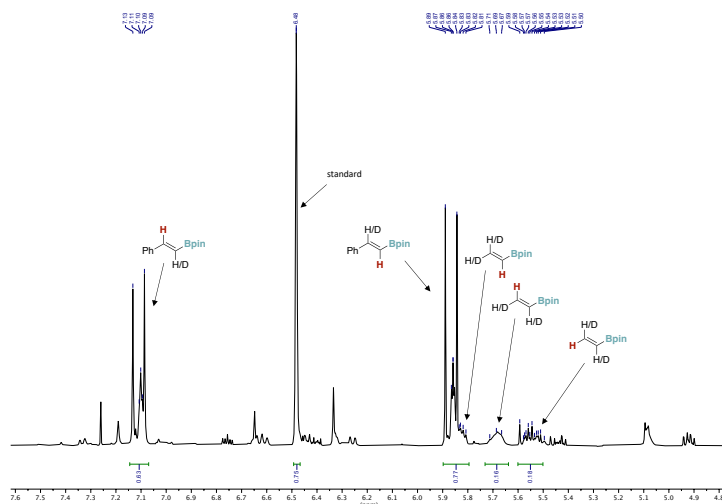
112

^{1}H NMR (CDCl$_3$, thf, 400 MHz):

Figure 3.7: Deuterium incorporation into **2** in the reaction of **1**-d_8 detected by ^{1}H NMR analysis.

The NMR yield of **3**-d_n (95%) and conversion of **2**-d_n (82%) were determined by GC-FID analysis of the reaction mixture using a calibration for styrene and vinyl Bpin with dodecane and mesitylene as an internal standard, respectively. Taking into account the values of ^{1}H content obtained from the ^{1}H NMR spectra of the isolated product **3**-d_n and the reaction mixture, the H/D ratios for the indicated positions was calculated.

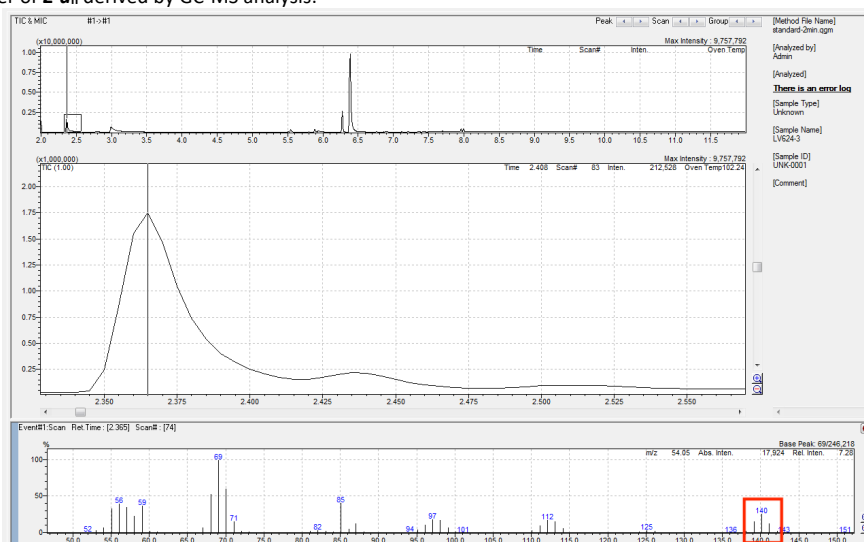Isotopomeric cluster of **2**-d_n derived by GC-MS analysis:

Figure 3.8: Partial deuterium incorporation into **2** in the reaction of **1**-d$_8$ detected by GC-MS analysis.

(b)
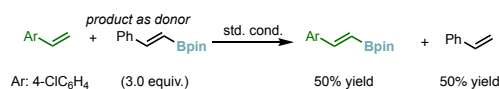
Ar: 4-ClC$_6$H$_4$ (3.0 equiv.)   50% yield   50% yield

In a nitrogen-filled glove box, a 10 mL screw-cap vial equipped with a Teflon-coated magnetic stirring bar was charged with [Ir(cod)Cl]$_2$ (2.7 mg, 4.0 μmol, 2 mol%), *t*-Bu-xantphos (4.0 mg, 4.0 μmol, 4 mol%), B$_2$pin$_2$ (2.5 mg, 10.0 μmol, 5 mol%), thf (200 μL), *trans*-2-phenylvinyl Bpin (**3**, 138.1 mg, 600 μmol, 3.0 equiv), and *p*-chlorostyrene (27.7 mg, 200 μmol, 1.0 equiv). The vial was sealed with a cap, removed from the glove box, placed in a pre-heated aluminum block, and allowed to stir (800 rpm) at 90 °C for 5 h. Upon cooling to room temperature, a standard solution (100 μL of 0.5 M 1,3,5-trimethoxybenzene in chloroform) and CDCl$_3$ (300 μL) were added to the reaction mixture. The yield was calculated based on the ratio between the integrals of the internal standard's aromatic signal and an isolated product's signal in the ^{1}H NMR spectrum of the reaction mixture (see below).

¹H NMR (CDCl₃, CHCl₃, 1,4-dioxane, 400 MHz):
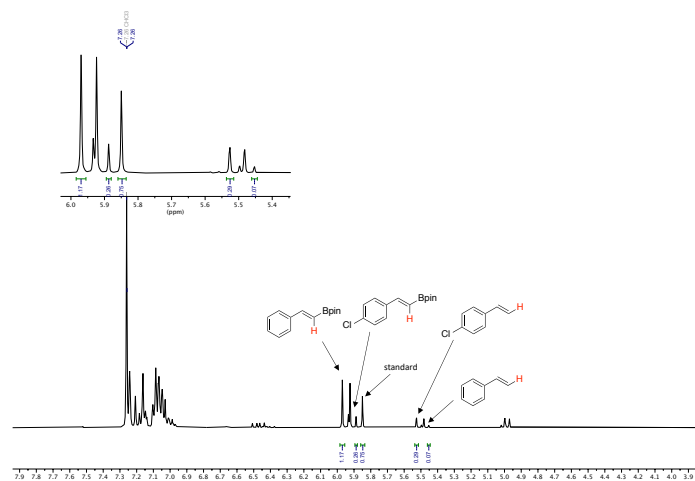
Figure 3.9: ¹H NMR of reaction (2) after 5 h.

(c)
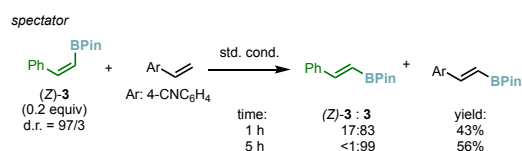
In a nitrogen-filled glove box, a 10 mL screw-cap vial equipped with a Teflon-coated magnetic stirring bar was charged with [Ir(cod)Cl]₂ (2.7 mg, 4.0 μmol, 2 mol%), t-Bu-xantphos (4.0 mg, 8.00 μmol, 4 mol%), B₂pin₂ (2.5 mg, 10.0 μmol, 5 mol%), thf (200 μL), vinyl Bpin (50.8 μL, 46.2 mg, 300 μmol, 1.5 equiv), 4-cyanostyrene (25.8 mg, 200 μmol, 1.0 equiv), and (Z)-4,4,5,5-tetramethyl-2-styryl-1,3,2-dioxaborolane ((Z)-**3**, 9.2 mg, 40.0 μmol, 0.20 equiv). The vial was sealed with a cap, removed from the glove box, placed in a pre-heated aluminum block, and allowed to stir (800 rpm) at 90 °C for 1 or 5 h. Upon cooling to room temperature, a solution of the standard (100 μL of 0.5 M 1,3,5-trimethoxybenzene in chloroform) and CDCl₃ (300 μL) were added to the reaction mixture. The yield was calculated based on the ratio of the integrals of a signal of the standard and a signal of the product in the ¹H NMR spectrum of the reaction mixture (see below).

After 1 h: **¹H NMR** (CDCl₃/CHCl₃/dioxane, 400 MHz):
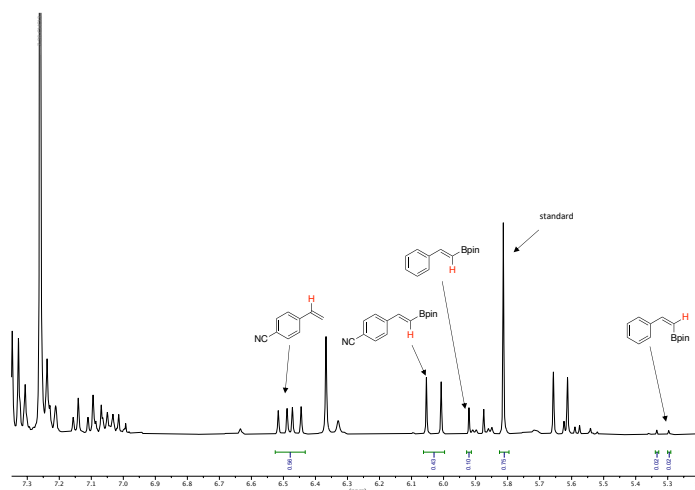
After 5 h: **¹H NMR** (CDCl₃/CHCl₃/dioxane, 400 MHz)
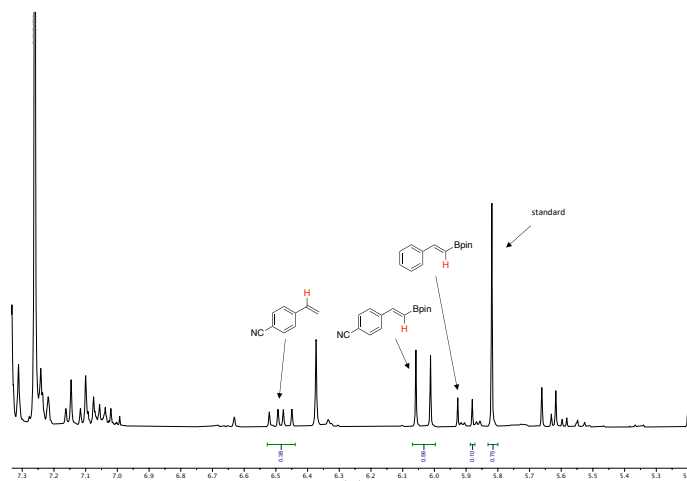
Figure 3.10: ¹H NMR of reaction (3) after 1 h (top) and 5 h (bottom).

(d)

(α)-**3**	Ar: 4-CNC₆H₄	time:	(α)-**3:3**	yield:	
(0.2 equiv)		1 h	>99:1	58%	
		5 h	>99:1	77%	

In a nitrogen-filled glove box, a 10 mL screw-cap vial equipped with a Teflon-coated magnetic stirring bar was charged with [Ir(cod)Cl]₂ (2.7 mg, 4.0 μmol, 2 mol%), t-Bu-xantphos (4.0 mg, 8.00 μmol, 4 mol%), B₂pin₂ (2.5 mg, 10.0 μmol, 5 mol%), thf (200 μL), vinyl Bpin (50.8 μL, 46.2 mg, 300 μmol, 1.5 equiv), 4-cyanostyrene (25.8 mg, 200 μmol, 1.0 equiv), and 1-phenylvinyl Bpin (9.2 mg, 40 μmol, 0.2 equiv). The vial was sealed with a cap, removed from the glove box, placed in a pre-heated aluminum block, and allowed to stir (800 rpm) at 90 °C for 1 or 5 h. Upon cooling to room temperature, a solution of the standard (100 μL of 0.5 M 1,3,5-trimethoxybenzene in chloroform) and CDCl₃ (300 μL) were added to the reaction mixture. The yield was calculated based on the ratio of the integrals of a signal of the standard and a signal of the product in the ¹H NMR spectrum of the reaction mixture (see below).

After 1 h: **¹H NMR** spectrum (CDCl₃/CHCl₃/1,4-dioxane, 500 MHz):
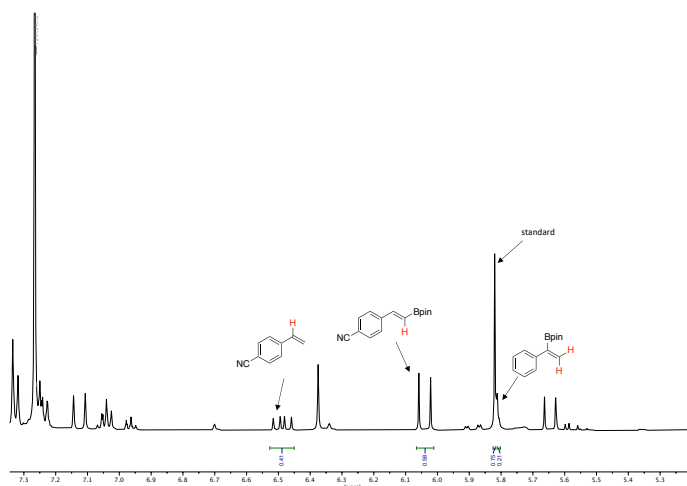
After 5 h: **¹H NMR** spectrum (CDCl₃/CHCl₃/1,4-dioxane, 500 MHz):
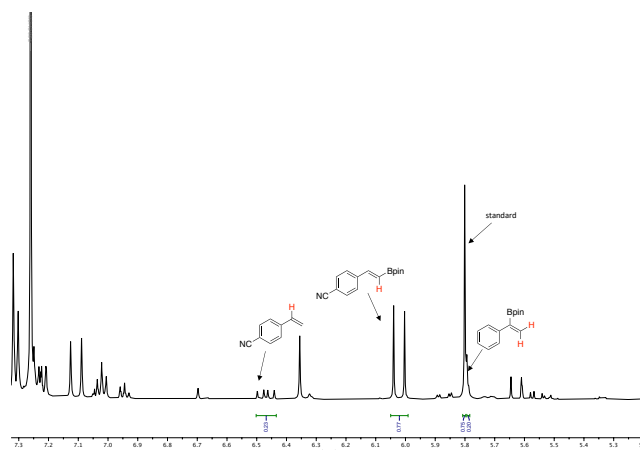
Figure 3.11: ^{1}H NMR spectrum of the reaction mixture (4) after 1 h (top) and 5 h (bottom).

3.4.3.2. HRMS experiments

HRMS analysis of catalytic reaction

In a nitrogen-filled glove box, a 10 mL screw-cap vial equipped with a Teflon-coated magnetic stirring bar was charged with [Ir(cod)Cl]$_2$ (2.7 mg, 4.0 μmol, 2 mol%), t-Bu-xantphos (4.0 mg, 8.00 μmol, 4 mol%), B$_2$pin$_2$ (2.5 mg, 10.0 μmol, 5 mol%), thf (200 μL), vinyl Bpin (50.8 μL, 46.2 mg, 300 μmol, 1.5 equiv), and styrene (20.8 mg, 200 μmol, 1.0 equiv). The vial was sealed with a cap, placed in a pre-heated aluminum block, and allowed to stir (800 rpm) at 90 °C for 1 h. Upon cooling to room temperature, an aliquot of the reaction mixture was diluted with MeCN and the sample was analyzed by high resolution ESI mass spectroscopy.

In this experiment, three Ir-species, namely [Ir(t-Bu-xantphos)]$^+$, {[Ir(t-Bu-xantphos)(Bpin)]H}$^+$, and [Ir(t-Buxantphos)(styrene)]$^+$, were detected in the mass spectrum (see below). The [Ir(t-Bu-xantphos)]$^+$ complex was also observed as a solvent adduct with one or two molecules of MeCN (the solvent used for the sample preparation).

Mass spectrum - zoom into the m/z = 550-825 region:
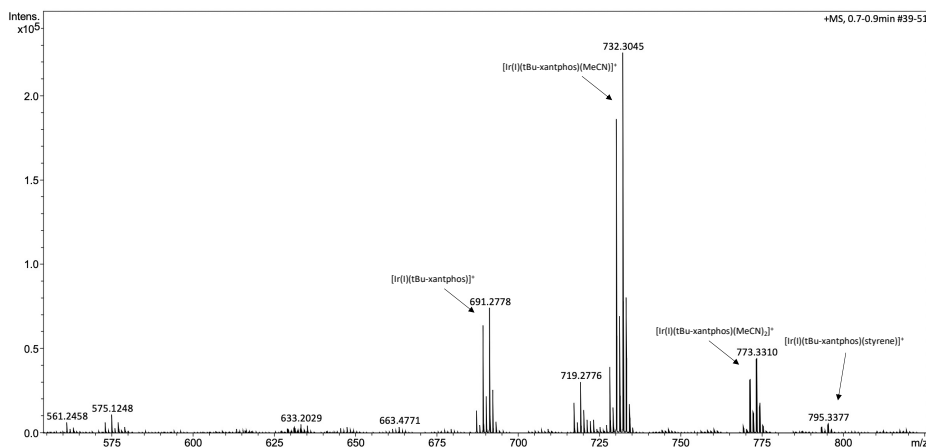
Mass spectrum - zoom into the m/z = 790-1025 region:
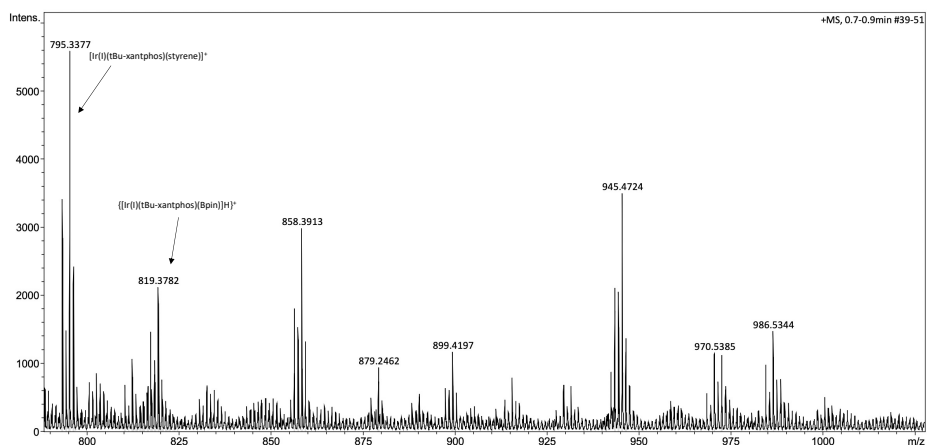
Found and simulated signals of isotopomeric cluster of the molecular ion [Ir(*t*-Bu-xantphos)]⁺:

Found and simulated signals of isotopomeric cluster of the molecular ion [Ir(*t*-Bu-xantphos)(MeCN)]⁺:

Found and simulated signals of isotopomeric cluster of the molecular ion [Ir(*t*-Bu-xantphos)(MeCN)₂]⁺:

Found and simulated signals of isotopomeric cluster of the molecular ion {[Ir(*t*-Bu-xantphos)(Bpin)]H}+:

Figure 3.12: HRMS data for the reaction mixture.

3.4.4. General procedures for Ir-catalyzed C–H borylation of alkenes

General procedure

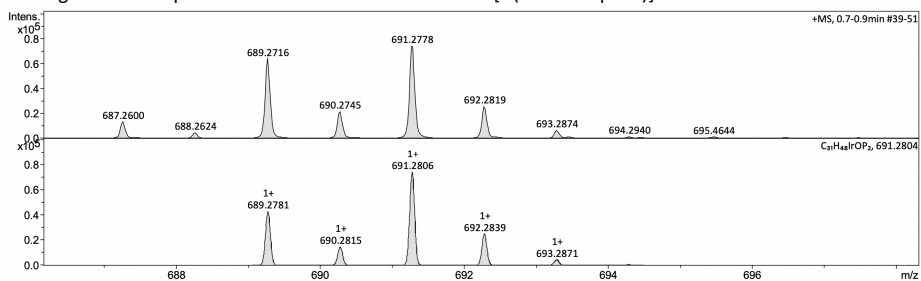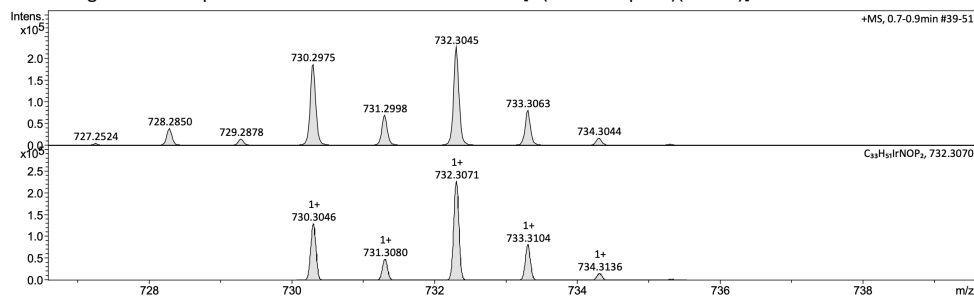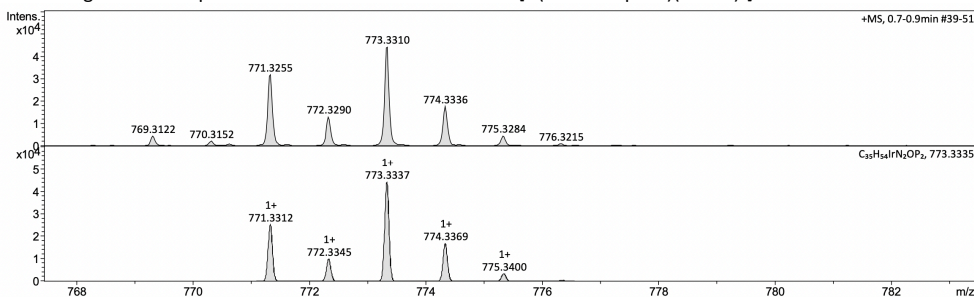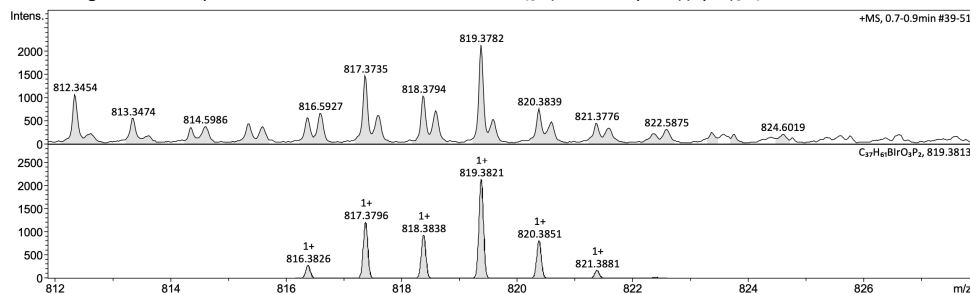In a nitrogen-filled glove box, a 10 mL screw-cap vial equipped with a Teflon-coated magnetic stirring bar was charged with [Ir(cod)Cl]$_2$ (2.7 mg, 4.0 μmol, 2 mol%), 9,9-dimethyl-4,5-bis(di-*tert*-butylphosphino)xanthene ("*t*-Bu-xantphos") (4.0 mg, 4.0 μmol, 4 mol%) or JohnPhos (4.8 mg, 16.0 μmol, 8 mol%), B$_2$pin$_2$ (2.5 mg, 10.0 μmol, 5 mol%), thf (200 μL), vinylboronic acid pinacol ester ("vinyl Bpin") (50.8 μL, 46.2 mg, 300 μL, 1.5 equiv), and an alkene starting material (200 μmol, 1.0 equiv). The vial was sealed with a cap, removed from the glove box, placed in a pre-heated aluminum block, and allowed to stir (800 rpm) at 90 °C for 5 h. The volatiles were removed under reduced pressure and the residue was subjected to flash column chromatography to isolate the target products.

For the determination of an analytical yield of a reaction, an aliquot of a solution of the standard (100 μL of 0.5 M 1,3,5-trimethoxybenzene in chloroform) and CDCl$_3$ (400 μL) were added to the reaction mixture. The analytical yield was calculated based on the integrals of the signals of the aromatic protons of the internal standard and the signals of the product that did not overlap with any other signals, typically vinylic protons, in the ^{1}H NMR spectrum of the reaction mixture. Typically, the same sample was used for the determination of the analytical yield and the isolation of the product; and hence the analytical yield is indicated before the isolation in the specific procedure. In some cases, however, the product and the standard were of similar retention factors (R$_f$'s), thereby hindering the isolation of the product. In such cases, two analogous reactions were run independently; one sample used for the isolation of the product, and the other sample used for the determination of the analytical yield by the NMR analysis. In such case, the experimental procedure indicates that the ^{1}H NMR yield of the product was determined in "an analogous experiment".

3.4.5. Overview of synthetic capacity
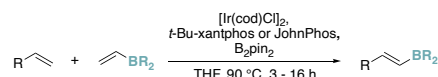
Boron donors:
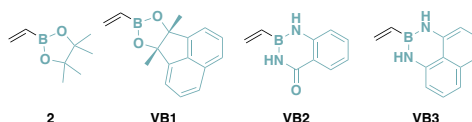
Table 3.4. Concise overview for conditions of reactions of all substrates

Product	Catalyst loading [mol%]	Ligand	Boron donor [donor, equiv]	Tempera-ture [°C]	Time [h]	NMR yield [%]ᵃ	Isolated yield [%]ᵃ
3	2	*t*-Bu-xantphos	**2**, 1.5	90	3	>99	74
3	2	JohnPhos	**2**, 1.5	90	3	>99	-
4	2	JohnPhos	**2**, 1.5	90	8	88	54
4	2	JohnPhos	**2**, 1.5	90	16	86	-
4	2	*t*-Bu-xantphos	**2**, 1.5	90	16	77	-
5	2	*t*-Bu-xantphos	**2**, 1.5	90	5	83	65
5	2	JohnPhos	**2**, 1.5	90	5	57	-
6	2	JohnPhos	**2**, 1.5	90	5	84	72
6	2	*t*-Bu-xantphos	**2**, 1.5	90	5	80	-
7	2	JohnPhos	**2**, 1.5	90	5	71	29

7	2	*t*-Bu-xantphos	**2**, 1.5	90	5	66	-
8	4	*t*-Bu-xantphos	**2**, 1.5	90	5	54	32
9	4	*t*-Bu-xantphos	**2**, 1.5	90	16	50	34
9	4	JohnPhos	**2**, 1.5	90	16	18	-
10	2	*t*-Bu-xantphos	**2**, 1.5	90	5	39	39
10	2	JohnPhos	**2**, 1.5	90	5	34	-
11	2	*t*-Bu-xantphos	**2**, 1.5	90	5	79	72
11	2	JohnPhos	**2**, 1.5	90	5	74	-
12	2	*t*-Bu-xantphos	**2**, 1.5	90	5	46	39
12	2	JohnPhos	**2**, 1.5	90	5	12	-
13	2	*t*-Bu-xantphos	**2**, 1.5	90	5	73	n.d.
13	2	*t*-Bu-xantphos	**2**, 1.5	90	19	73	-
13	2	JohnPhos	**2**, 1.5	90	19	72	-
14	2	JohnPhos	**2**, 1.5	90	3	45	36
14	2	JohnPhos	**2**, 1.5	90	5	21	-
14	2	*t*-Bu-xantphos	**2**, 1.5	90	5	19	-
16	2	*t*-Bu-xantphos	**VB1**, 1.5	90	5	84	60
17	2	*t*-Bu-xantphos	**VB2**, 1.5	90	5	84	75
17	2	JohnPhos	**VB2**, 1.5	90	5	65	-
18	2	JohnPhos	**VB3**, 1.5	90	5	93	76
18	2	*t*-Bu-xantphos	**VB3**, 1.5	90	5	<5	-
19	2	*t*-Bu-xantphos	**2**, 1.5	90	5	83	64
20	2	JohnPhos	**2**, 1.5	90	5	96	77
20	2	*t*-Bu-xantphos	**2**, 1.5	90	5	93	-
21	2	JohnPhos	**2**, 1.5	90	5	86	66
22	2	JohnPhos	**2**, 1.5	90	5	87	70
22	2	*t*-Bu-xantphos	**2**, 1.5	90	5	87	-
23	2	JohnPhos	**2**, 1.5	90	5	85	77
23	2	*t*-Bu-xantphos	**2**, 1.5	90	5	85	-
24	2	*t*-Bu-xantphos	**2**, 1.5	90	5	87	83
25	2	JohnPhos	**2**, 1.5	90	5	87	75
26	2	JohnPhos	**2**, 1.5	90	5	88	64
27	2	JohnPhos	**2**, 1.5	90	5	>99	71
28	2	*t*-Bu-xantphos	**2**, 1.5	90	3	76	72
28	2	JohnPhos	**2**, 1.5	90	3	54	-
29	2	*t*-Bu-xantphos	**2**, 1.5	90	3	94	54
30	2	*t*-Bu-xantphos	**2**, 1.5	90	3	68	30
31	2	*t*-Bu-xantphos	**2**, 1.5	90	3	55	29
32	2	*t*-Bu-xantphos	**2**, 1.5	90	3	63	42
33	2	JohnPhos	**2**, 1.5	90	5	89	71

34-Me	2	JohnPhos	**2**, 1.5	90	5	76	53
34-Me	2	*t*-Bu-xantphos	**2**, 1.5	90	5	74	-
34	2	*t*-Bu-xantphos	**2**, 1.5	90	5	67	21
35	2	JohnPhos	**2**, 1.5	90	5	72	41
36	2	JohnPhos	**2**, 1.5	90	5	72	39

[a] Because vinylboronic esters tend to partially decompose during chromatography on silica gel,[66–68] depending on the relative stability of the products, the yields of isolated material in some cases are substantially lower than the analytical yields determined by ^{1}H NMR analysis. n.d.: not determined.

3.4.6. Characterization of products

(*E*)-4,4,5,5-tetramethyl-2-styryl-1,3,2-dioxaborolane 3
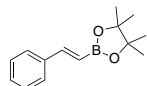
The title compound was prepared according to the general procedure using styrene (20.8 mg, 200 µmol, 1.0 equiv) as an alkene starting material, *t*-Bu-xantphos as a ligand, and thf as a solvent; the reaction mixture was allowed to stir for 3 h (instead of 5 h). The ^{1}H NMR yield of the title product was determined to be >99%. The reaction mixture was concentrated under reduced pressure, and the residue was subjected to column chromatography (silica gel, 0-5% MTBE in petroleum ether) to give the title compound (33.9 mg, 147 µmol, 74%) as a pale yellow oil. The NMR data match previously reported data for the title product.[20]

^{1}H NMR (400 MHz, CDCl$_3$) δ 7.52 – 7.46 (m, 2H), 7.41 (d, *J* = 18.4 Hz, 1H), 7.37 – 7.26 (m, 3H), 6.18 (d, *J* = 18.4 Hz, 1H), 1.32 (s, 12H).

(*E*)-*N*-(2-(2-(4,4,5,5-tetramethyl-1,3,2-dioxaborolan-2-yl)vinyl)phenyl)acetamide 4
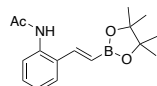
The title compound was prepared according to the general procedure using *N*-(2-vinylphenyl)acetamide (32.2 mg, 200 µmol, 1.0 equiv) as an alkene starting material, JohnPhos as a ligand, and thf as a solvent; the reaction mixture was allowed to stir for 8 h (instead of 5 h). The ^{1}H NMR yield of the title product was determined to be 88%. The reaction mixture was concentrated under reduced pressure, and the residue was subjected to column chromatography (silica gel, 0-50% EtOAc in petroleum ether) to give the title compound (31.1 mg, 108 µmol, 54%) as an off-white solid.

^{1}H NMR (500 MHz, CDCl$_3$) δ 7.82 (d, *J* = 8.1 Hz, 1H), 7.60 – 7.41 (m, 2H), 7.39 – 7.28 (m, 2H), 7.15 (t, *J* = 7.6 Hz, 1H), 6.12 (d, *J* = 18.1 Hz, 1H), 2.22 (s, 3H), 1.31 (s, 12H);

^{13}C{^{1}H} NMR (126 MHz, CDCl$_3$) δ 168.7, 143.9, 134.9, 130.1, 129.5, 127.1, 125.5, 124.3, 83.7, 24.9, 24.6 [Note: the carbon atom attached to the boron atom was not observed due to quadrupole broadening or relaxation delay caused by the [11]B nucleus[69]];

^{11}B NMR (160 MHz, CDCl$_3$) δ 30.4;

**HRMS** (ESI) m/z calcd. for C$_{16}$H$_{23}$BNO$_3$ ([M+H]$^+$): 288.1766; found: 288.1781.

tert-*t*-butyl (*E*)-(4-(2-(4,4,5,5-tetramethyl-1,3,2-dioxaborolan-2-yl)vinyl)phenyl)carbamate 5
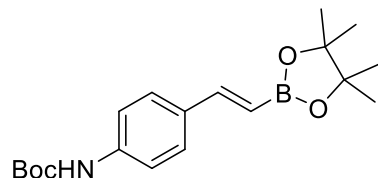
The title compound was prepared according to the general procedure using *tert*-butyl (4-vinylphenyl)carbamate (43.9 mg, 200 µmol, 1.0 equiv) as an alkene starting material, *t*-Bu-xantphos as a ligand, and thf as a solvent. The ^{1}H NMR yield of the title product was determined to be 83%. The mixture containing the title product and the standard was concentrated under reduced pressure, and the residue was subjected to column chromatography (silica gel, 0-10% MTBE in petroleum ether) to give the title compound (44.7 mg, 129 µmol, 65%) as a yellow solid. The NMR data match previously reported data for the title product.[70]

^{1}H NMR (500 MHz, CDCl$_3$) δ 7.45 – 7.39 (m, 2H), 7.37 – 7.29 (m, 3H), 6.50 (s, 1H), 6.05 (d, *J* = 18.4 Hz, 1H), 1.51 (s, 9H), 1.30 (s, 12H).

(*E*)-4-(2-(4,4,5,5-tetramethyl-1,3,2-dioxaborolan-2-yl)vinyl)benzenesulfonamide 6
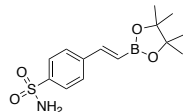
The title compound was prepared according to the general procedure using 4-vinylbenzenesulfonamide (36.6 mg, 200 µmol, 1.0 equiv) as an alkene starting material, JohnPhos as a ligand, and thf as a solvent. The ^{1}H NMR yield of the title product was determined to be 84%. The reaction mixture was filtered over silica upon cooling to room temperature, the filtrate was concentrated under reduced pressure, and the residue was subjected to column chromatography (silica gel, 10-42% EtOAc in petroleum ether) to give the title compound (44.7 mg, 145 µmol, 72%) as a beige solid.

^{1}H NMR (500 MHz, CDCl$_3$) δ 7.89 (d, *J* = 8.5 Hz, 2H), 7.58 (d, *J* = 8.5 Hz, 2H), 7.38 (d, *J* = 18.4 Hz, 1H), 6.27 (d, *J* = 18.4 Hz, 1H), 4.93 (s, 2H), 1.32 (s, 12H);

^{13}C{^{1}H} NMR (126 MHz, CDCl$_3$) δ 147.3, 141.9, 141.7, 127.7, 127.0, 83.9, 25.0 [Note: the carbon atom attached to the boron atom was not observed due to quadrupole broadening or relaxation delay caused by the [11]B nucleus[69]];

^{11}B NMR (160 MHz, CDCl$_3$) δ 30.4;

HRMS (ESI) m/z calcd. for C$_{14}$H$_{20}$BNO$_4$S ([M]$^+$): 309.1201; found: 309.1216.

(*E*)-*N*-benzyl-4-(2-(4,4,5,5-tetramethyl-1,3,2-dioxaborolan-2-yl)vinyl)benzenesulfonamide 7
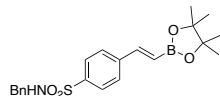
The title compound was prepared according to the general procedure using *N*-benzyl-4-vinylbenzenesulfonamide (54.7 mg, 200 µmol, 1.0 equiv) as an alkene starting material, JohnPhos as a ligand, and thf as a solvent. The reaction mixture was concentrated under reduced pressure, and the residue was subjected to column chromatography (silica gel, 0-20% EtOAc in petroleum ether) to give the title compound (23.2 mg, 58 µmol, 29%) as a white solid. The NMR yield of the title prodcut was found to be 71% as determined in an analogous experiment using ^{1}H NMR spectroscopy.

^{1}H NMR (500 MHz, CDCl$_3$) δ 7.83 (d, *J* = 8.1 Hz, 2H), 7.58 (d, *J* = 8.1 Hz, 2H), 7.40 (d, *J* = 18.4 Hz, 1H), 7.29 – 7.23 (m, 3H), 7.18 – 7.20 (m, 2H), 6.29 (d, *J* = 18.4 Hz, 1H), 4.92 (t, *J* = 6.2 Hz, 1H), 4.16 (d, *J* = 6.2 Hz, 2H), 1.34 (s, 12H);

¹³C{¹H} NMR (126 MHz, CDCl₃) δ 147.3, 141.6, 139.6, 136.1, 128.7, 128.0, 127.9, 127.5, 127.5, 83.7, 47.3, 24.8 [Note: the carbon atom attached to the boron atom was not observed due to quadrupole broadening or relaxation delay caused by the ¹¹B nucleus[69]];
¹¹B NMR (160 MHz, CDCl₃) δ 30.5;
HRMS (ESI) m/z calcd. for C₂₁H₂₇BNO₄S ([M+H]⁺): 400.1748; found: 400.1758.

(*E*)-5-(2-(4,4,5,5-tetramethyl-1,3,2-dioxaborolan-2-yl)vinyl)-1*H*-indole 8
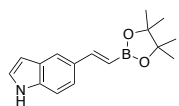
In a nitrogen-filled glove box, a 10 mL screw-cap vial equipped with a Teflon-coated magnetic stirring bar was charged with [Ir(cod)Cl]₂ (5.4 mg, 8.0 μmol, 4 mol%), *t*-Bu-xantphos (8.0 mg, 16.0 μmol, 8 mol%) B₂pin₂ (5.1 mg, 20.0 μmol, 10 mol%), thf (200 μL), vinyl Bpin (50.8 μL, 46.2 mg, 300 μmol, 1.5 equiv), and 5-vinyl-1*H*-indole (28.6 mg, 200 μmol, 1.0 equiv). The vial was sealed with a cap, removed from the glove box, placed in a pre-heated aluminum block and allowed to stir (800 rpm) at 90 °C for 5 h. Upon cooling to room temperature, the reaction mixture was concentrated under reduced pressure, and the residue was subjected to column chromatography (silica gel, 0-20% MTBE in petroleum ether) to give the title compound (17.1 mg, 65 μmol, 32%) as a dark oil. The NMR data match previously reported data for the title product.[70] The ¹H NMR yield of the title product was found to be 54% as determined in an analogous experiment using ¹H NMR spectroscopy.
¹H NMR (500 MHz, CDCl₃) δ 8.24 (s, 1H), 7.74 (s, 1H), 7.54 (d, *J* = 18.5 Hz, 1H), 7.43 (dd, *J* = 8.5, 1.6 Hz, 1H), 7.34 (d, *J* = 8.5 Hz, 1H), 7.19 (t, *J* = 2.8 Hz, 1H), 6.56 (t, *J* = 2.6 Hz, 1H), 6.12 (d, *J* = 18.4 Hz, 1H), 1.33 (s, 12H).

(*E*)-4-(2-(4,4,5,5-tetramethyl-1,3,2-dioxaborolan-2-yl)vinyl)aniline 9
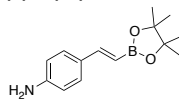
In a nitrogen-filled glove box, a 10 mL screw-cap vial equipped with a Teflon-coated magnetic stirring bar was charged with [Ir(cod)Cl]₂ (5.4 mg, 8.0 μmol, 4 mol%), *t*-Bu-xantphos (8.0 mg, 16.0 μmol, 8 mol%) B₂pin₂ (5.1 mg, 20.0 μmol, 10 mol%), thf (200 μL), vinyl Bpin (50.8 μL, 46.2 mg, 300 μmol, 1.5 equiv), and 4-vinylaniline (23.8 mg, 200 μmol, 1.0 equiv). The vial was sealed with a cap, removed from the glove box, placed in a pre-heated aluminum block and allowed to stir (800 rpm) at 90 °C for 16 h. Upon cooling to room temperature, the reaction mixture was concentrated under reduced pressure, and the residue was subjected to column chromatography (silica gel, 0-25% EtOAc in petroleum ether) to give the title compound (16.7 mg, 68 μmol, 34%) as a dark oil. The NMR data match previously reported data for the title product.[71] The ¹H NMR yield of the title product was found to be 50% as determined in an analogous experiment using ¹H NMR spectroscopy.
¹H NMR (500 MHz, CDCl₃) δ 7.33 – 7.27 (m, 3H), 6.62 (d, *J* = 8.0 Hz, 2H), 5.93 (d, *J* = 18.4 Hz, 1H), 3.80 (s, 2H), 1.30 (s, 12H).

(*E*)-4-(2-(4,4,5,5-tetramethyl-1,3,2-dioxaborolan-2-yl)vinyl)phenol 10

The title compound was prepared according to the general procedure using 4-vinylphenol (24.0 mg, 200 μmol, 1.0 equiv) as an alkene starting material, *t*-Bu-xantphos as a ligand, and thf as a solvent; the reaction mixture was filtered over silica upon cooling to room temperature. The filtrate was concentrated under reduced pressure, and the residue was subjected to column chromatography (silica gel, 0-20% EtOAc in petroleum ether) to give the title compound (19.3 mg, 78 μmol, 39%) as a brown solid. The NMR data match previously reported data for the title product.[72] The ¹H NMR yield of the title product was found to be 39% as determined in an analogous experiment using ¹H NMR spectroscopy.
¹H NMR (500 MHz, CDCl₃) δ 7.41 – 7.29 (m, 3H), 6.80 (d, *J* = 8.1 Hz, 2H), 5.98 (d, *J* = 18.5 Hz, 1H), 5.90 (s, 1H), 1.31 (s, 12H).

(*E*)-(4-(2-(4,4,5,5-tetramethyl-1,3,2-dioxaborolan-2-yl)vinyl)phenyl)methanol 11

The title compound was prepared according to the general procedure using (4-vinylphenyl)methanol (26.8 mg, 200 μmol, 1.0 equiv) as an alkene starting material, *t*-Bu-xantphos as a ligand, and thf as a solvent; the reaction mixture was filtered over silica upon cooling to room temperature. The reaction mixture was concentrated under reduced pressure, and the residue was subjected to column chromatography (silica gel, 0-20% EtOAc in petroleum ether) to give t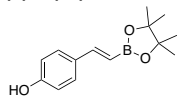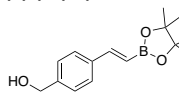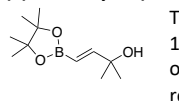he title compound (37.7 mg, 145 μmol, 72%) as a beige solid. The NMR data match previously reported data for the title product.[73] The ¹H NMR yield of the reaction was found to be 79% as determined in an analogous experiment using ¹H NMR spectroscopy.
¹H NMR (500 MHz, CDCl₃) δ 7.47 (d, *J* = 7.8 Hz, 2H), 7.38 (d, *J* = 18.5 Hz, 1H), 7.33 (d, *J* = 7.9 Hz, 2H), 6.15 (d, *J* = 18.4 Hz, 1H), 4.68 (s, 2H), 1.31 (s, 12H) [Note: the OH proton was not detected].

(*E*)-2-methyl-4-(4,4,5,5-tetramethyl-1,3,2-dioxaborolan-2-yl)but-3-en-2-ol 12

The title compound was prepared according to the general procedure using 2-methyl-3-buten-2-ol (17.2 mg, 200 μmol, 1.0 equiv) as an alkene starting material, *t*-Bu-xantphos as a ligand, and thf as a solvent; the reaction mixture was filtered over silica upon cooling to room temperature. The reaction mixture was concentrated under reduced pressure, and the residue was subjected to column chromatography (silica gel, 0-20% EtOAc in petroleum ether) to give the title compound (16.5 mg, 78 μmol, 39%) as a yellow oil. The NMR data match previously reported data for the title product.[74] The ¹H NMR yield of the title product was found to be 46% as determined in an analogous experiment using ¹H NMR spectroscopy.
¹H NMR (400 MHz, CDCl₃) δ 6.71 (d, *J* = 18.5 Hz, 1H), 5.61 (d, *J* = 18.5 Hz, 1H), 1.31 (s, 6H), 1.27 (s, 12H) [Note: the OH proton was not detected].

(*E*)-4-(2-(4,4,5,5-tetramethyl-1,3,2-dioxaborolan-2-yl)vinyl)benzoic acid 13
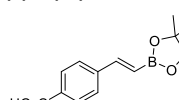
The title compound was prepared according to the general procedure using 4-vinylbenzoic acid (29.6 mg, 200 μmol, 1.0 equiv) as an alkene starting material, *t*-Bu-xantphos as a ligand, and thf as a solvent; the reaction mixture was filtered over silica upon cooling to room temperature. The ¹H NMR yield of the title product was determined to be 73%. The mixture containing the product and the standard was concentrated under reduced pressure, and the residue was subjected to column chromatography (silica gel, 0-10% MTBE in petroleum ether) to isolate an analytically pure sample of the title compound as a yellow solid.
¹H NMR (500 MHz, CDCl₃) δ 8.08 (d, *J* = 8.1 Hz, 2H), 7.57 (d, *J* = 8.0 Hz, 2H), 7.42 (d, *J* = 18.4 Hz, 1H), 6.31 (d, *J* = 18.4 Hz, 1H), 1.32 (s, 12H) [Note: the COOH proton was not detected];
¹³C{¹H} NMR (126 MHz, CDCl₃) δ 171.1, 148.1, 142.6, 130.7, 129.3, 127.1, 126.4, 83.8, 25.0;
¹¹B NMR (160 MHz, CDCl₃) δ 29.8;
HRMS (ESI) m/z calcd. for C₁₅H₂₀BO₄ ([M+H]⁺): 275.1449; found: 275.1432.

(*E*)-2-(4-(2-(4,4,5,5-tetramethyl-1,3,2-dioxaborolan-2-yl)vinyl)phenyl)acetic acid 14
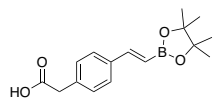
The title compound was prepared according to the general procedure using 2-(4-vinylphenyl)acetic acid (36.6 mg, 200 μmol, 1.0 equiv) as an alkene starting material, JohnPhos as a ligand, thf as a solvent; the reaction mixture was allowed to stir for 3 h (instead of 5 h). The reaction mixture was concentrated under reduced pressure, and the residue was subjected to column chromatography (silica gel, 0-25% EtOAc in petroleum ether + 0.5% AcOH) to give the title compound (20.9 mg, 73 μmol, 36%) as a yellow solid. The ^{1}H NMR yield of the title product was found to be 45% as determined in an analogous experiment using ^{1}H NMR spectroscopy.

^{1}H NMR (500 MHz, CDCl$_3$) δ 7.44 (d, *J* = 7.8 Hz, 2H), 7.37 (d, *J* = 18.3 Hz, 1H), 7.25 (d, *J* = 7.8 Hz, 2H), 6.14 (d, *J* = 18.3 Hz, 1H), 3.64 (s, 2H), 1.31 (s, 12H) [Note: the COOH proton was not detected];
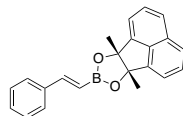
^{13}C{^{1}H} NMR (126 MHz, CDCl$_3$) δ 177.4, 149.1, 136.8, 134.0, 129.8, 127.5, 83.6, 40.9, 24.9 [Note: the carbon atom attached to the boron atom was not observed due to quadrupole broadening or relaxation delay caused by the ^{11}B nucleus[69]];

^{11}B NMR (160 MHz, CDCl$_3$) δ 30.4;

HRMS (ESI) m/z calcd. for C$_{16}$H$_{22}$BO$_4$ ([M+H]$^+$): 289.1606; found: 289.1622.

(*E*)-6b,9a-dimethyl-8-styryl-6b,9a-dihydroacenaphtho[1,2-d][1,3,2]dioxaborole 16

In a nitrogen-filled glove box, a 10 mL screw-cap vial equipped with a Teflon-coated magnetic stirring bar was charged with [Ir(cod)Cl]$_2$ (2.7 mg, 4.0 μmol, 2 mol%), *t*-Bu-xantphos (4.0 mg, 8.0 μmol, 4 mol%) B$_2$pin$_2$ (2.5 mg, 10.0 μmol, 5 mol%), thf (200 μL), 6b,9a-dimethyl-8-vinyl-6b,9a-dihydroacenaphtho[1,2-d][1,3,2]dioxaborole ("vinyl B(mac)") (75.0 mg, 300 μmol, 1.5 equiv), and styrene (20.8 mg, 22.9 μL, 200 μmol, 1.0 equiv). The vial was sealed with a cap, removed from the glove box, placed in a pre-heated aluminum block, and allowed to stir (800 rpm) at 90 °C for 5 h. The ^{1}H NMR yield of the title product was determined to be 84%. Upon cooling to room temperature, the reaction mixture was concentrated under reduced pressure, and the residue was subjected to column chromatography (silica gel, 0-5.5% MTBE in petroleum ether) to give the title compound (39.3 mg, 120 μmol, 60%) as a white solid. The NMR data match previously reported data for the title product.[20]

^{1}H NMR (400 MHz, CDCl$_3$) δ 7.79 (dt, *J* = 6.9, 3.4 Hz, 2H), 7.63 – 7.55 (m, 4H), 7.45 – 7.38 (m, 2H), 7.35 (d, *J* = 18.4 Hz, 1H), 7.31 – 7.21 (m, 3H), 6.09 (d, *J* = 18.4 Hz, 1H), 1.84 (s, 6H).

(*E*)-2-styryl-2,3-dihydrobenzo[*d*][1,3,2]diazaborinin-4(1*H*)-one 17

In a nitrogen-filled glove box, a 10 mL screw-cap vial equipped with a Teflon-coated magnetic stirring bar was charged with [Ir(cod)Cl]$_2$ (2.7 mg, 4.0 μmol, 2 mol%), *t*-Bu-xantphos (4.0 mg, 8.0 μmol, 4 mol%), B$_2$pin$_2$ (2.5 mg, 10.0 μmol, 5 mol%), thf (200 μL), 2-vinyl-2,3-dihydrobenzo[*d*][1,3,2]diazaborinin-4(1*H*)-one ("vinyl B(aam)") (51.6 mg, 300 μmol, 1.5 equiv), and styrene (20.8 mg, 22.9 μL, 200 μmol, 1.0 equiv). The vial was sealed with a cap, removed from the glove box, placed in a pre-heated aluminum block, and allowed to stir (800 rpm) at 90 °C for 5 h. Upon cooling to room temperature, the reaction mixture was concentrated under reduced pressure, and the residue was subjected to column chromatography (silica gel, 0-48% EtOAc in petroleum ether) to give the title compound (37.4 mg, 151 μmol, 75%) as a white solid. The NMR data match previously reported data for the title product.[75] The NMR yield of the title product was found to be 84% as determined in an analogous experiment using ^{1}H NMR spectroscopy.

^{1}H NMR (500 MHz, DMSO-d$_6$) δ 9.49 (s, 1H), 9.21 (s, 1H), 7.98 (d, *J* = 7.9 Hz, 1H), 7.64 (d, *J* = 18.8 Hz, 1H), 7.53 (d, *J* = 7.5 Hz, 3H), 7.43 (t, *J* = 7.5 Hz, 2H), 7.35 (d, *J* = 7.3 Hz, 1H), 7.28 (d, *J* = 8.2 Hz, 1H), 7.07 (t, *J* = 7.5 Hz, 1H), 6.48 (d, *J* = 18.7 Hz, 1H).

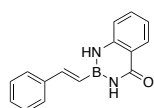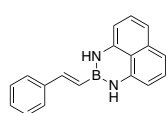**(*E*)-2-styryl-2,3-dihydro-1*H*-naphtho[1,8-*de*][1,3,2]diazaborinine 18**

In a nitrogen-filled glove box, a 10 mL screw-cap vial equipped with a Teflon-coated magnetic stirring bar was charged with [Ir(cod)Cl]$_2$ (2.7 mg, 4.0 μmol, 2 mol%), JohnPhos (4.8 mg, 16.0 μmol, 8 mol%), B$_2$pin$_2$ (2.5 mg, 10.0 μmol, 5 mol%), thf (200 μL), 2-vinyl-2,3-dihydro-1*H*-naphtho[1,8-*de*][1,3,2]diazaborinine ("vinyl B(dan)") (58.2 mg, 300 μmol, 1.5 equiv), and styrene (20.8 mg, 22.9 μL, 200 μmol, 1.0 equiv). The vial was sealed with a cap, removed from the glove box, placed in a pre-heated aluminum block, and allowed to stir (800 rpm) at 90 °C for 5 h. The ^{1}H NMR yield of the title product was determined to be 93%. Upon cooling to room temperature, the reaction mixture was concentrated under reduced pressure, and the residue was subjected to column chromatography (silica gel, 0-10% MTBE in petroleum ether) to give the title compound (41.3 mg, 153 μmol, 76%) as a dark blue solid. The NMR data match previously reported data for the title product.[76]

^{1}H NMR (400 MHz, CDCl$_3$) δ 7.52 (d, *J* = 7.2 Hz, 2H), 7.45 – 7.29 (m, 3H), 7.20 – 7.08 (m, 3H), 7.04 (d, *J* = 8.2 Hz, 2H), 6.48 – 6.23 (m, 3H), 5.85 (s, 2H).

(*E*)-4,4,5,5-tetramethyl-2-(4-nitrostyryl)-1,3,2-dioxaborolane 19
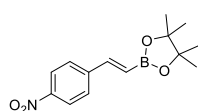
The title compound was prepared according to the general procedure using 1-nitro-4-vinylbenzene (29.8 mg, 200 μmol, 1.0 equiv) as an alkene starting material, *t*-Bu-xantphos as a ligand, and thf as a solvent. The reaction mixture was concentrated under reduced pressure, and the residue was subjected to column chromatography (silica gel, 0-10% MTBE in petroleum ether) to give the title compound (35.4 mg, 129 μmol, 64%) contaminated by vinyl Bpin dimer (1.4 mg) as a colorless solid. The NMR data match previously reported data for the title product.[77] The ^{1}H NMR yield of the title product was determined to be 83% in an analogous experiment.

^{1}H NMR (500 MHz, CDCl$_3$) δ 8.23 – 8.18 (m, 2H), 7.64 – 7.57 (m, 2H), 7.42 (d, *J* = 18.4 Hz, 1H), 6.33 (d, *J* = 18.4 Hz, 1H), 1.32 (s, 12H).

Diethyl (*E*)-(4-(2-(4,4,5,5-tetramethyl-1,3,2-dioxaborolan-2-yl)vinyl)phenyl)phosphonate 20
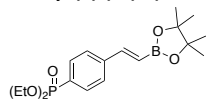
The title compound was prepared according to the general procedure using diethyl (4-vinylphenyl)phosphonate (48.0 mg, 200 μmol, 1.0 equiv) as an alkene starting material, JohnPhos as a ligand, and thf as a solvent. The ^{1}H NMR yield of the title product determined to be 96%. The reaction mixture was concentrated under reduced pressure, and the residue was subjected to column chromatography (silica gel, 0-77% EtOAc in petroleum ether) to give the title compound (56.5 mg, 154 μmol, 77%) as a brown oil.

^{1}H NMR (500 MHz, CDCl$_3$) δ 7.77 (dd, *J* = 13.0, 8.2 Hz, 2H), 7.58 – 7.48 (m, 2H), 7.38 (d, *J* = 18.5 Hz, 1H), 6.26 (d, *J* = 18.4 Hz, 1H), 4.20 – 4.00 (m, 4H), 1.35 – 1.27 (m, 18H);

^{13}C{^{1}H} NMR (126 MHz, CDCl$_3$) δ 148.2 (d, *J* = 1.6 Hz), 141.3 (d, *J* = 3.3 Hz), 132.2 (d, *J* = 10.1 Hz), 129.3, 127.8, 127.1 (d, *J* = 15.4 Hz), 83.7, 62.3 (d, *J* = 5.4 Hz), 24.9, 16.5 (d, *J* = 6.5 Hz);

^{11}B NMR (160 MHz, CDCl$_3$) δ 30.2;

^{31}P NMR (202 MHz, CDCl$_3$) δ 18.5;

HRMS (ESI) m/z calcd. for C$_{18}$H$_{29}$BO$_5$P ([M+H]$^+$): 367.1840; found: 367.1857.

122

Ethyl (*E*)-4-(2-(4,4,5,5-tetramethyl-1,3,2-dioxaborolan-2-yl)vinyl)benzenesulfonate 21
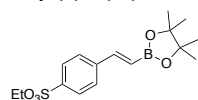
The title compound was prepared according to the general procedure using ethyl 4-vinylbenzenesulfonate (42.5 mg, 200 µmol, 1.0 equiv) as an alkene starting material, JohnPhos as a ligand, and thf as a solvent. The reaction mixture was concentrated under reduced pressure, and the residue was subjected to column chromatography (silica gel, 0-20% EtOAc in petroleum ether) to give the title compound (44.5 mg, 132 µmol, 66%) as a yellow oil. The ^{1}H NMR yield of the title product was found to be 86% as determined in an analogous experiment using ^{1}H NMR spectroscopy.

^{1}H NMR (400 MHz, CDCl$_3$) δ 7.86 (d, *J* = 8.4 Hz, 2H), 7.60 (d, *J* = 8.3 Hz, 2H), 7.38 (d, *J* = 18.5 Hz, 1H), 6.30 (d, *J* = 18.5 Hz, 1H), 4.11 (q, *J* = 7.1 Hz, 2H), 1.30 – 1.27 (m, 15H);

^{13}C{^{1}H} NMR (101 MHz, CDCl$_3$) δ 147.0, 142.7, 136.0, 128.3, 127.6, 83.9, 67.2, 24.9, 14.8 [Note: the carbon atom attached to the boron atom was not observed due to quadrupole broadening or relaxation delay caused by the ^{11}B nucleus[69]];

^{11}B NMR (128 MHz, CDCl$_3$) δ 31.1;

HRMS (ESI) m/z calcd. for C$_{16}$H$_{23}$BO$_5$S ([M]$^+$): 338.1354; found: 338.1361.

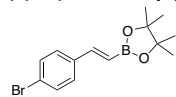**(*E*)-2-(4-bromostyryl)-4,4,5,5-tetramethyl-1,3,2-dioxaborolane 22**

The title compound was prepared according to the general procedure using 1-bromo-4-vinylbenzene (36.6 mg, 200 µmol, 1.0 equiv) as an alkene starting material, JohnPhos as a ligand, and thf as a solvent. The reaction mixture was concentrated under reduced pressure, and the residue was subjected to column chromatography (silica gel, 0-6% MTBE in petroleum ether) to give the title compound (43.5 mg, 141 µmol, 70%) as a white solid. The NMR data match previously reported data for the title product.[78] The ^{1}H NMR yield of the title product was found to be 87% as determined in an analogous experiment using ^{1}H NMR spectroscopy.

^{1}H NMR (500 MHz, CDCl$_3$) δ 7.49 – 7.39 (m, 2H), 7.39 – 7.26 (m, 3H), 6.15 (d, *J* = 18.6 Hz, 1H), 1.31 (s, 12H).
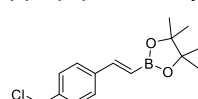
(*E*)-2-(2-chlorostyryl)-4,4,5,5-tetramethyl-1,3,2-dioxaborolane 23
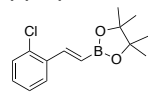
The title compound was prepared according to the general procedure using 1-chloro-2-vinylbenzene (27.7 mg, 200 µmol, 1.0 equiv) as an alkene, JohnPhos as a ligand, and thf as a solvent. The reaction mixture was concentrated under reduced pressure, and the residue was subjected to column chromatography (silica gel, 0-5% MTBE in petroleum ether) to give the title compound (41.0 mg, 155 µmol, 77%) as a yellow oil. The NMR data match previously reported data for the title product.[79] The ^{1}H NMR yield of the title product was found to be 85% as determined in an analogous experiment using ^{1}H NMR spectroscopy.

^{1}H NMR (500 MHz, CDCl$_3$) δ 7.82 (d, *J* = 18.5 Hz, 1H), 7.66 (dd, *J* = 7.2, 2.3 Hz, 1H), 7.39 (dd, *J* = 7.2, 2.0 Hz, 1H), 7.31 – 7.21 (m, 2H), 6.21 (d, *J* = 18.5 Hz, 1H), 1.35 (s, 12H).

(*E*)-2-(4-(chloromethyl)styryl)-4,4,5,5-tetramethyl-1,3,2-dioxaborolane 24

The title compound was prepared according to the general procedure using 1-(chloromethyl)-4-vinylbenzene (30.5 mg, 200 µmol, 1.0 equiv) as an alkene starting material, *t*-Bu-xantphos as a ligand, and thf as a solvent. The reaction mixture was concentrated under reduced pressure, and the residue was subjected to column chromatography (silica gel, 0-10% MTBE in petroleum ether) to give the title compound (46.5 mg, 167 µmol, 83%) as a pale-yellow solid. The ^{1}H NMR yield of the title product was found to be 87% as determined in an analogous experiment using ^{1}H NMR spectroscopy.

^{1}H NMR (500 MHz, CDCl$_3$) δ 7.50 – 7.44 (m, 2H), 7.43 – 7.31 (m, 3H), 6.18 (d, *J* = 18.5 Hz, 1H), 4.58 (s, 2H), 1.31 (s, 12H).

^{13}C{^{1}H} NMR (126 MHz, CDCl$_3$) δ 148.8, 138.1, 137.8, 129.0, 127.5, 83.6, 46.1, 25.0. [Note: the carbon atom attached to the boron atom was not observed due to quadrupole broadening or relaxation delay caused by the ^{11}B nucleus[69]];

^{11}B NMR (160 MHz, CDCl$_3$) δ 30.3;

HRMS (ESI) m/z calcd. for C$_{15}$H$_{21}$BClO$_2$ ([M+H]$^+$): 279.1318; found: 279.1327.

(*E*)-2-(2-(benzo[b]thiophen-2-yl)vinyl)-4,4,5,5-tetramethyl-1,3,2-dioxaborolane 25
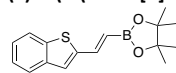
The title compound was prepared according to the general procedure using 2-vinylbenzo[b]thiophene (32.0 mg, 200 µmol, 1.0 equiv) as an alkene starting material, JohnPhos as a ligand, and thf as a solvent. The reaction mixture was concentrated under reduced pressure, and the residue was subjected to column chromatography (silica gel, 0-6% MTBE in petroleum ether) to give the title compound (43.1 mg, 151 µmol, 75%) as a yellow oil. The NMR data match previously reported data for the title product.[80] The ^{1}H NMR yield of the title product was found to be 87% as determined in an analogous experiment using ^{1}H NMR spectroscopy.

^{1}H NMR (400 MHz, CDCl$_3$) δ 7.78 – 7.74 (m, 1H), 7.73 – 7.69 (m, 1H), 7.57 (d, *J* = 18.0 Hz, 1H), 7.38 – 7.27 (m, 2H), 7.26 (s, 1H), 6.02 (d, *J* = 18.0 Hz, 1H), 1.32 (s, 12H).

(*E*)-2-(2-(benzofuran-2-yl)vinyl)-4,4,5,5-tetramethyl-1,3,2-dioxaborolane 26
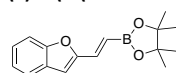
The title compound was prepared according to the general procedure using 2-vinylbenzofuran (28.8 mg, 200 µmol, 1.0 equiv) as an alkene starting material, JohnPhos as a ligand, and thf as a solvent. The reaction mixture was concentrated under reduced pressure, and the residue was subjected to column chromatography (silica gel, 0-6% MTBE in petroleum ether) to give the title compound (34.7 mg, 128 µmol, 64%) as a pale yellow solid. The ^{1}H NMR yield of the title product was found to be 88% as determined in an analogous experiment using ^{1}H NMR spectroscopy.

^{1}H NMR (400 MHz, CDCl$_3$) δ 7.51 (d, *J* = 7.2 Hz, 1H), 7.43 (d, *J* = 8.3 Hz, 1H), 7.25 (ddd, *J* = 16.5, 7.8, 2.3 Hz, 2H), 7.18 – 7.12 (m, 1H), 6.68 (s, 1H), 6.29 (d, *J* = 18.2 Hz, 1H), 1.28 (s, 12H);

^{13}C{^{1}H} NMR (101 MHz, CDCl$_3$) δ 155.3, 155.1, 136.6, 128.9, 125.4, 123.0, 121.5, 111.4, 107.3, 83.6, 25.0 [Note: the carbon atom attached to the boron atom was not observed due to quadrupole broadening or relaxation delay caused by the ^{11}B nucleus[69]];

^{11}B NMR (128 MHz, CDCl$_3$) δ 30.3;

HRMS (ESI) m/z calcd. for C$_{16}$H$_{20}$BO$_3$ ([M+H]$^+$): 271.1500; found: 271.1514.

(*E*)-3-(2-(4,4,5,5-tetramethyl-1,3,2-dioxaborolan-2-yl)vinyl)oxazolidin-2-one 27
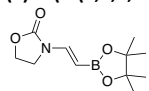
The title compound was prepared according to the general procedure using 3-vinyloxazolidin-2-one (22.6 mg, 200 μmol, 1.0 equiv) as an alkene starting material, JohnPhos as a ligand, and thf as a solvent. The reaction mixture was concentrated under reduced pressure, and the residue was subjected to column chromatography (silica gel, 0-30% EtOAc in petroleum ether) to give the title compound (33.9 mg, 142 μmol, 71%) as a brown solid. The ^{1}H NMR yield of the title product was found to be quantitative as determined in an analogous experiment using ^{1}H NMR spectroscopy. **^{1}H NMR** (500 MHz, CDCl$_3$) δ 7.48 (d, J = 16.2 Hz, 1H), 4.53 – 4.36 (m, 3H), 3.73 (dd, J = 9.1, 7.1 Hz, 2H), 1.24 (s, 12H);

^{13}C{^{1}H} NMR (126 MHz, CDCl$_3$) δ 155.9, 140.4, 83.3, 62.4, 41.9, 24.8 [Note: the carbon atom attached to the boron atom was not observed due to quadrupole broadening or relaxation delay caused by the ^{11}B nucleus[69]];

^{11}B NMR (160 MHz, CDCl$_3$) δ 30.8;

HRMS (ESI) m/z calcd. for C$_{11}$H$_{19}$BNO$_4$ ([M+H]$^+$): 240.1402; found: 240.1404.

(*E*)-4,4,5,5-tetramethyl-2-(2-phenoxyvinyl)-1,3,2-dioxaborolane 28
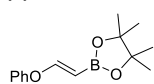
The title compound was prepared according to the general procedure using phenyl vinyl ether (24.0 mg, 200 μmol, 1.0 equiv) as an alkene starting material, *t*-Bu-xantphos as a ligand, thf as a solvent; the reaction mixture was allowed to stir for 3 h (instead of 5 h). The mixture containing the product was concentrated under reduced pressure, and the residue was subjected to column chromatography (silica gel, 0.4% NEt$_3$ in petroleum ether/10% MTBE in petroleum ether = 1/0 → 0/1) to give the title compound (35.4 mg, 144 μmol, 72%, E/Z = 98/2) as a red oil. The ^{1}H NMR yield of the title product was determined to be 76% (E/Z = 95/5)$^\#$ in an analogous experiment.

^{1}H NMR (400 MHz, CDCl$_3$)* δ 7.38 – 7.28 (m, 2H, H^E), 7.24 (d, J = 14.6 Hz, 1H, H^E)$^+$, 7.16 – 7.08 (m, 1H, H^E), 7.08 – 7.01 (m, 2H, H^E), 4.87 (d, J = 13.9 Hz, 1H, H^E), 4.56 (d, J = 8.0 Hz, 1H, H^Z), 1.27 (s, 12H, H^E);

$^\#$ Besides the major set of signals corresponding to the title product, a minor second set of signals is present in the ^{1}H NMR spectrum of the reaction mixture. Due to the overall similarity to the title compound in standard 2D NMR experiments, the similarity of the chemical shifts to the literature-known compound Z-**30**[81], and the coupling constant of 8.0 Hz of the doublet assigned to C*H*Bpin (versus the coupling constant of 13.9 Hz of the analogous proton in the title compound), this set of signals was assigned to the Z-isomer.

* NMR data corresponds to a E/Z = 98/2 mixture. Only not overlapping signals of the Z-isomer are listed.

$^+$ Signal overlaps partially with the CDCl$_3$ solvent peak.

^{13}C NMR (126 MHz, CDCl$_3$) δ 159.7, 156.2, 129.8, 124.2, 118.5, 83.1, 24.9 [Note: the carbon atom attached to the boron atom was not observed due to quadrupole broadening or relaxation delay caused by the ^{11}B nucleus[69]];

^{11}B NMR (160 MHz, CDCl$_3$) δ 31.0;

HRMS (ESI) m/z calcd. for C$_{14}$H$_{20}$BO$_3$ ([M+H]$^+$): 247.1500; found: 247.1498.

(*E*)-2-(2-(benzyloxy)vinyl)-4,4,5,5-tetramethyl-1,3,2-dioxaborolane 29
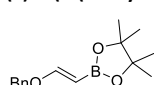
The title compound was prepared according to the general procedure using 2-(vinyloxy)ethan-1-ol (26.8 mg, 200 μmol, 1.0 equiv) as an alkene starting material, *t*-Bu-xantphos as a ligand, thf as a solvent; the reaction mixture was allowed to stir for 3 h (instead of 5 h). The reaction mixture was concentrated under reduced pressure, and the residue was subjected to column chromatography (silica gel, 0.4% NEt$_3$ in petroleum ether/10% MTBE in petroleum ether = 1/0 → 0/1) to give the title compound (28.3 mg, 109 μmol, 54%) as a yellow oil. The NMR data match previously reported data for the title product.[82] The ^{1}H NMR yield of the title product was found to be 94% (E/Z = 96/4)$^\#$ as determined in an analogous experiment using ^{1}H NMR spectroscopy.

^{1}H NMR (500 MHz, CDCl$_3$) δ 7.38 – 7.29 (m, 5H), 7.15 (d, J = 14.4 Hz, 1H), 4.84 (s, 2H), 4.56 (d, J = 14.4 Hz, 1H), 1.26 (s, 12H).

$^\#$ Besides the major set of signals corresponding to the title product, a minor second set of signals is present in the ^{1}H NMR spectrum of the reaction mixture. Due to the overall similarity to the title compound in standard 2D NMR experiments, the similarity of the chemical shifts to the literature-known compound Z-**30**[81], and the coupling constant of 8.3 Hz of the doublet assigned to C*H*Bpin (versus the coupling constant of 14.4 Hz of the analogous proton in the title compound), this set of signals was assigned to the Z-isomer.

(*E*)-2-(2-butoxyvinyl)-4,4,5,5-tetramethyl-1,3,2-dioxaborolane 30
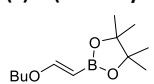
The title compound was prepared according to the general procedure using butyl vinyl ether (20.0 mg, 200 μmol, 1.0 equiv) as an alkene starting material, *t*-Bu-xantphos as a ligand, thf as a solvent; the reaction mixture was allowed to stir for 3 h (instead of 5 h). The reaction mixture was concentrated under reduced pressure, and the residue was subjected to column chromatography (silica gel, 0.4% NEt$_3$ in petroleum ether/10% MTBE in petroleum ether = 1/0 → 0/1) to give the title compound (13.4 mg, 59 μmol, 30%) as a brown solid. The chemical shift and coupling constant used for the determination of the stereoselectivity of the reaction in the reaction mixture match previously reported data for the Z-isomer of the title product.[81] The ^{1}H NMR yield of the title product was found to be 68% (E/Z = 96/4) as determined in an analogous experiment using ^{1}H NMR spectroscopy.

^{1}H NMR (500 MHz, CDCl$_3$) δ 7.05 (d, J = 14.4 Hz, 1H), 4.43 (d, J = 14.4 Hz, 1H), 3.77 (t, J = 6.6 Hz, 2H), 1.68 – 1.59 (m, 2H), 1.44 – 1.34 (m, 2H), 1.25 (s, 12H), 0.92 (t, J = 7.4 Hz, 3H);

^{13}C{^{1}H} NMR (101 MHz, CDCl$_3$) δ 163.5, 82.8, 68.8, 31.1, 24.9, 19.3, 13.9 [Note: the carbon atom attached to the boron atom was not observed due to quadrupole broadening or relaxation delay caused by the ^{11}B nucleus[69]];

^{11}B NMR (128 MHz, CDCl$_3$) δ 31.9;

HRMS (ESI) m/z calcd. for C$_{12}$H$_{24}$BO$_3$ ([M+H]$^+$): 227.1813; found: 227.1810.

(*E*)-2-(2-(2-chloroethoxy)vinyl)-4,4,5,5-tetramethyl-1,3,2-dioxaborolane 31
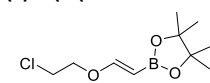
The title compound was prepared according to the general procedure using (2-chloroethoxy)ethene (21.3 mg, 200 μmol, 1.0 equiv) as an alkene starting material, *t*-Bu-xantphos as a ligand, thf as a solvent; the reaction mixture was allowed to stir for 3 h (instead of 5 h). The reaction mixture was concentrated under reduced pressure, and the residue was subjected to column chromatography (silica gel, 0.4% NEt$_3$ in petroleum ether/10% MTBE in petroleum ether = 1/0 → 0/1) to give the title compound (13:6 mg, 58.5 μmol, 29%) as a pale-yellow solid. The ^{1}H NMR yield of the title product was found to be 55% as determined in an analogous experiment using ^{1}H NMR spectroscopy.

^{1}H NMR (500 MHz, CDCl$_3$) δ δ 7.04 (d, J = 14.3 Hz, 1H), 4.47 (d, J = 14.5 Hz, 1H), 4.03 (t, J = 5.8 Hz, 2H), 3.70 (t, J = 5.8 Hz, 2H), 1.25 (s, 12H),

^{13}C{^{1}H} NMR (126 MHz, CDCl$_3$) δ 162.2, 83.0, 68.5, 41.7, 24.9. [Note: the carbon atom attached to the boron atom was not observed due to quadrupole broadening or relaxation delay caused by the ^{11}B nucleus[69]];

^{11}B NMR (160 MHz, CDCl$_3$) δ 30.9;

HRMS (ESI) m/z calcd. for C$_{10}$H$_{19}$BClO$_3$ ([M+H]$^+$): 233.1110; found: 233.1118.

124

(*E*)-2-(2-ethoxyvinyl)-4,4,5,5-tetramethyl-1,3,2-dioxaborolane 32
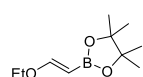
The title compound was prepared according to the general procedure using ethyl vinyl ether (14.4 mg, 200 µmol, 1.0 equiv) as an alkene starting material, *t*-Bu-xantphos as a ligand, and thf as a solvent; the reaction mixture was allowed to stir for 3 h (instead of 5 h). The reaction mixture was concentrated under reduced pressure, and the residue was subjected to column chromatography (silica gel, 0.4% NEt$_3$ in petroleum ether/10% MTBE in petroleum ether = 1/0 → 0/1) to give the title compound (16.4 mg, 83 µmol, 42%) as a yellow solid. The NMR data match previously reported data for the title product.[83] The ^{1}H NMR yield of the title product was found to be 63% (*E/Z* ≥ 95/5) as determined in an analogous experiment using ^{1}H NMR spectroscopy and TMB as an internal standard.

^{1}H NMR (400 MHz, CDCl$_3$) δ 7.04 (d, *J* = 14.5 Hz, 1H), 4.43 (d, *J* = 14.4 Hz, 1H), 3.84 (q, *J* = 7.0 Hz, 2H), 1.33 – 1.21 (m, 15H).

(*E*)-tert-butyldimethyl(4-(2-(4,4,5,5-tetramethyl-1,3,2-dioxaborolan-2-yl)vinyl)phenoxy)silane 33
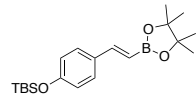
The title compound was prepared according to the general procedure using *tert*-butyldimethyl(4-vinylphenoxy)silane (46.9 mg, 200 µmol, 1.0 equiv), as an alkene starting material, JohnPhos as a ligand, and thf as a solvent. The reaction mixture was concentrated under reduced pressure, and the residue was subjected to column chromatography (silica gel, 0-6.5% MTBE in petroleum ether) to give the title compound (51.0 mg, 142 µmol, 71%) as a white solid. The NMR data match previously reported data for the title product.[84] The ^{1}H NMR yield of the title product was found to be 89% as determined in an analogous experiment using ^{1}H NMR spectroscopy.

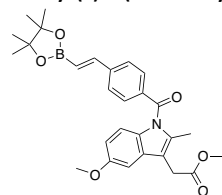**^{1}H NMR** (400 MHz, CDCl$_3$) δ 7.40 – 7.29 (m, 3H), 6.80 (d, *J* = 8.6 Hz, 2H), 6.00 (d, *J* = 18.4 Hz, 1H), 1.30 (s, 12H), 0.98 (s, 9H), 0.20 (s, 6H).

Methyl (*E*)-2-(5-methoxy-2-methyl-1-(4-(2-(4,4,5,5-tetramethyl-1,3,2-dioxaborolan-2-yl)vinyl)ben-zoyl)-1*H*-indol-3-yl)acetate 34-Me

The title compound was prepared according to the general procedure using methyl 2-(5-methoxy-2-methyl-1-(4-vinylbenzoyl)-1*H*-indol-3-yl)acetate (72.7 mg, 200 µmol, 1.0 equiv) as an alkene starting material, JohnPhos as a ligand, and thf as a solvent; the reaction mixture was not filtered over silica upon cooling to room temperature. The ^{1}H NMR yield was determined to be 76%. The reaction mixture was concentrated under reduced pressure, and the residue was subjected to column chromatography (silica gel, 0-25% EtOAc in petroleum ether) to give the title compound (52.0 mg, 106 µmol, 53%) as a yellow solid.

^{1}H NMR (500 MHz, CDCl$_3$) δ 7.69 (d, *J* = 8.3 Hz, 2H), 7.58 (d, *J* = 8.3 Hz, 2H), 7.44 (d, *J* = 18.5 Hz, 1H), 6.95 (d, *J* = 2.6 Hz, 1H), 6.87 (d, *J* = 9.0 Hz, 1H), 6.64 (dd, *J* = 9.0, 2.5 Hz, 1H), 6.32 (d, *J* = 18.5 Hz, 1H), 3.83 (s, 3H), 3.70 (s, 3H), 3.67 (s, 2H), 2.38 (s, 3H), 1.32 (s, 12H);

^{13}C{^{1}H} NMR (126 MHz, CDCl$_3$) δ 171.6, 169.2, 156.0, 148.0, 141.8, 136.2, 135.5, 131.0, 130.7, 130.3, 127.4, 115.2, 112.3, 111.6, 101.3, 83.8, 55.8, 52.3, 30.3, 24.9, 13.4 [Note: the carbon atom attached to the boron atom was not observed due to quadrupole broadening or relaxation delay caused by the ^{11}B nucleus[69]];

^{11}B NMR (160 MHz, CDCl$_3$) δ 30.8;

HRMS (ESI) m/z calcd. for C$_{28}$H$_{33}$BNO$_6$ ([M+H]$^+$): 490.2395; found: 490.2388.

(*E*)-2-(5-methoxy-2-methyl-1-(4-(2-(4,4,5,5-tetramethyl-1,3,2-dioxaborolan-2-yl)vinyl)benzoyl)-1*H*-indol-3-yl)acetic acid 34
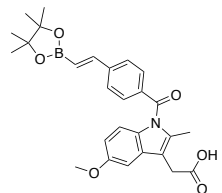
The title compound was prepared according to the general procedure using 2-(5-methoxy-2-methyl-1-(4-vinylbenzoyl)-1*H*-indol-3-yl)acetic acid (69.9 mg, 200 µmol, 1.0 equiv) as an alkene starting material, *t*-Bu-xantphos as a ligand, and thf as a solvent.. The ^{1}H NMR yield of the title product was determined to be 67%. The reaction mixture was concentrated under reduced pressure, and the residue was subjected to column chromatography (two columns, silica gel, 0-45% EtOAc in petroleum ether + 0.5% AcOH) to give the title compound (19.9 mg, 42 µmol, 21%) as a yellow oil [Note: the low yield of isolated material results from the limited separation of the product from the unreacted starting material during the chromatographic purification].

^{1}H NMR (500 MHz, CDCl$_3$) δ 7.68 (d, *J* = 8.4 Hz, 2H), 7.57 (d, *J* = 8.3 Hz, 2H), 7.44 (d, *J* = 18.4 Hz, 1H), 6.95 (d, *J* = 2.6 Hz, 1H), 6.87 (d, *J* = 9.0 Hz, 1H), 6.64 (dd, *J* = 9.0, 2.6 Hz, 1H), 6.31 (d, *J* = 18.5 Hz, 1H), 3.82 (s, 3H), 3.69 (s, 2H), 2.38 (s, 3H), 1.32 (s, 12H);

^{13}C{^{1}H} NMR (126 MHz, CDCl$_3$) δ 176.7, 169.2, 156.1, 148.0, 141.9, 136.4, 135.5, 131.1, 130.6, 130.3, 127.4, 115.2, 111.8, 111.8, 101.3, 83.8, 55.9, 25.0, 20.8, 13.4 [Note: the carbon atom attached to the boron atom was not observed due to quadrupole broadening or relaxation delay caused by the ^{11}B nucleus[69]];

^{11}B NMR (160 MHz, CDCl$_3$) δ 30.1;

HRMS (ESI) m/z calcd. for C$_{27}$H$_{29}$BNO$_6$ ([M-H]$^-$): 474.2082; found: 474.2093.

Methyl (*E*)-3-(1-methyl-2-oxo-1,2-dihydroquinolin-4-yl)-2-(4-(2-(4,4,5,5-tetramethyl-1,3,2-dioxaborolan-2-yl)vinyl)benzamido)propano-ate 35
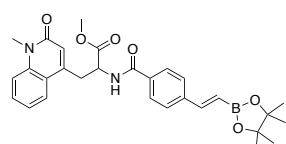
The title compound was prepared according to the general procedure using methyl 3-(1-methyl-2-oxo-1,2-dihydro-quinolin-4-yl)-2-(4-vinylbenzamido)propanoate (78.1 mg, 200 µmol, 1.0 equiv) as an alkene starting material, JohnPhos as a ligand, and thf as a solvent; the reaction mixture was not filtered over silica upon cooling to room temperature. The ^{1}H NMR yield of the title product was determined to be 72%. The reaction mixture was concentrated under reduced pressure, and the residue was subjected to column chromatography (silica gel, 0-3.5% MeOH in DCM) to give the title compound alongside starting material (71/29, 42.1 mg, 82 µmol, 41% of title compound) as an off-white solid.

^{1}H NMR (400 MHz, CDCl$_3$) δ 7.93 – 7.86 (m, 1H), 7.61 (dd, *J* = 8.4, 2.7 Hz, 2H), 7.50 (ddt, *J* = 8.8, 7.2, 1.9 Hz, 1H), 7.45 – 7.40 (m, 2H), 7.37 – 7.27 (m, 2H), 7.22 – 7.13 (m, 1H), 6.80 (d, *J* = 7.4 Hz, 1H), 6.50 (s, 1H), 6.16 (d, *J* = 18.5 Hz, 1H), 5.09 (qd, *J* = 6.5, 1.9 Hz, 1H), 3.67 (s, 3H), 3.62 (s, 3H), 3.36 (dd, *J* = 6.5, 3.0 Hz, 2H), 1.24 (s, 12H);

^{13}C{^{1}H} NMR (101 MHz, CDCl$_3$) δ 171.6, 166.8, 161.6, 148.0, 145.0, 140.1, 135.9, 133.3, 130.9, 127.5, 127.2, 125.2, 122.4, 122.2, 120.4, 114.8, 83.6, 52.8, 52.7, 34.9, 29.4, 24.8 [Note: the carbon atom attached to the boron atom was not observed due to quadrupole broadening or relaxation delay caused by the ^{11}B nucleus[69]];

^{11}B NMR (160 MHz, CDCl$_3$) δ 29.9;

HRMS (ESI) m/z calcd. for C$_{29}$H$_{34}$BN$_2$O$_6$ ([M+H]$^+$): 517.2504; found: 517.2528.

(*E*)-*N*-(propylcarbamoyl)-4-(2-(4,4,5,5-tetramethyl-1,3,2-dioxaborolan-2-yl)vinyl)benzenesulfonamide 36
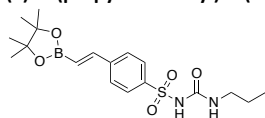
The title compound was prepared according to the general procedure using *N*-(propylcarbamoyl)-4-vinylbenzenesulfon-amide (53.7 mg, 200 μmol, 1.0 equiv) as an alkene starting material, JohnPhos as a ligand, and thf as a solvent; the reaction mixture was not filtered over silica upon cooling to room temperature. The ¹H NMR yield of the title prodcut was determined to be 72%. The reaction mixture was concentrated under reduced pressure, and the residue was subjected to column chromatography (silica gel, 0-50% EtOAc in petroleum ether) to give the title compound (30.4 mg, 77 μmol, 39%) as a white solid.

¹H NMR (400 MHz, CDCl₃) δ 8.47 (s, 1H), 7.85 (d, *J* = 8.3 Hz, 2H), 7.58 (d, *J* = 8.2 Hz, 2H), 7.38 (d, *J* = 18.5 Hz, 1H), 6.57 (t, *J* = 5.9 Hz, 1H), 6.29 (d, *J* = 18.5 Hz, 1H), 3.19 (q, *J* = 6.6 Hz, 2H), 1.50 (h, *J* = 7.3 Hz, 2H), 1.32 (s, 12H), 0.87 (t, *J* = 7.4 Hz, 3H);

¹³C{¹H} NMR (101 MHz, CDCl₃) δ 151.3, 146.6, 142.5, 138.9, 127.4, 127.1, 83.6, 41.9, 24.6, 22.6, 11.0
[Note: the carbon atom attached to the boron atom was not observed due to quadrupole broadening or relaxation delay caused by the ¹¹B nucleus[69]];

¹¹B NMR (160 MHz, CDCl₃) δ 30.6;

HRMS (ESI) m/z calcd. for C₁₈H₂₆BN₂O₅S ([M-H]⁻): 393.1650; found: 393.1664.

3.4.7. Synthesis of starting materials

6b,9a-dimethyl-8-vinyl-6b,9a-dihydroacenaphtho[1,2-d][1,3,2]dioxaborole VB1
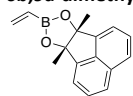
The compound was prepared according to a modified literature procedure.[85] To a solution of vinyl potassium trifluoroborate (190 mg, 1.4 mmol, 1.0 equiv) in acetonitrile/H₂O (1:1, 4 mL) at room temperature, 1,2-dimethylacenaphthylene-1,2-diol (304 mg, 1.4 mmol, 1.0 equiv), imidazole (290 mg, 4.3 mmol, 3.0 equiv), and FeCl₃ (19.2 mg, 0.07 mmol, 5 mol%) were added. The reaction mixture was allowed to stir for 50 min. The mixture was filtered through a plug of celite (eluent: diethyl ether). The volatiles from the filtrate were removed under reduced pressure. The residue was subjected to column chromatography (silica gel, 0 – 10% EtOAc in petroleum ether) to isolate the title product as a white solid (284 mg, 1.14 mmol, 81%). The NMR data match previously reported data for the title product.[86]

¹H NMR (400 MHz, CDCl₃) δ 7.79 (dd, *J* = 7.8, 1.1 Hz, 2H), 7.67 – 7.52 (m, 4H), 6.12 (dd, *J* = 19.6, 4.2 Hz, 1H), 5.96 (dd, *J* = 13.7, 4.2 Hz, 1H), 5.79 (dd, *J* = 19.5, 13.8 Hz, 1H), 1.81 (s, 6H).

2-vinyl-2,3-dihydrobenzo[*d*][1,3,2]diazaborinin-4(1*H*)-one VB2
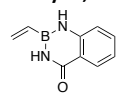
The compound was prepared according to a modified literature procedure.[87] Under a nitrogen atmosphere, a screw-cap vial was charged with anthranilamide (545 mg, 4.0 mmol, 1.0 equiv), potassium vinyltrifluoroborate (563 mg, 4.2 mmol, 1.05 equiv), oven-dried SiO₂ (400 mg), and CPME/toluene (1/1, 12 mL). The vial was sealed with a screw-cap, and the reaction mixture was allowed to stir at 60 °C for 17 h. The reaction mixture was filtered through a pad of celite, which was washed with diethyl ether, and the volatiles from the filtrate were removed under reduced pressure. The residue was subjected to column chromatography (silica gel, 0 – 40% EtOAc in petroleum ether) to give the title product (343 mg, 2.0 mmol, 50%) as a white solid.

¹H NMR (500 MHz, DMSO-d₆) δ 9.43 (s, 1H), 9.10 (s, 1H), 7.96 (dd, *J* = 8.0, 1.6 Hz, 1H), 7.52 (ddd, *J* = 8.6, 7.2, 1.7 Hz, 1H), 7.25 (dd, *J* = 8.2, 1.1 Hz, 1H), 7.06 (ddd, *J* = 8.1, 7.1, 1.1 Hz, 1H), 6.42 – 6.29 (m, 1H), 6.19 – 6.07 (m, 1H), 6.00 (dd, *J* = 13.8, 3.5 Hz, 1H);

**¹³C{¹H} NMR** (126 MHz, DMSO-d₆) δ 166.1, 145.3, 134.2, 133.3, 128.0, 120.7, 118.9, 117.9 [Note: the carbon atom attached to the boron atom was not observed due to quadrupole broadening or relaxation delay caused by the ¹¹B nucleus[69]];

¹¹B NMR (160 MHz, DMSO-d₆) δ 28.4;

HRMS (ESI) m/z calcd. for C₉H₁₀BN₂O ([M+H]⁺): 173.0881; found: 173.0891.

2-vinyl-2,3-dihydro-1H-naphtho[1,8-de][1,3,2]diazaborinine VB3
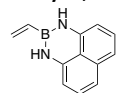
The compound was prepared according to a modified literature procedure.[88] Under a nitrogen atmosphere, to a mixture of vinyl Bpin (592 μL, 539 mg, 3.5 mmol, 1.0 equiv) and FeCl₃ (47.3 mg, 0.18 mmol, 5 mol%) in acetonitrile/water (14/1, 15 mL), imidazole (715 mg, 10.5 mmol, 3.0 equiv) and 1,8-diaminonaphthalene (554 mg, 3.5 mmol, 1.0 equiv) were added. The mixture was allowed to stir at room temperature for 2 h, diluted with EtOAc (20 mL), and filtered through a pad of celite, which was washed with EtOAc. The organic phase was separated, then washed with water (2 x 30 mL), and brine (1 x 30 mL), dried over sodium sulfate, and filtered. The volatiles of the filtrate were removed under reduced pressure. The residue was subjected to column chromatography (silica gel, 0 – 15% EtOAc in petroleum ether) to give the title product (530 mg, 2.7 mmol, 78%) as a dark blue oil. The NMR data match previously reported data for the title product.[88]

¹H NMR (400 MHz, CDCl₃) δ 7.11 (dd, *J* = 8.4, 7.2 Hz, 2H), 7.02 (dd, *J* = 8.3, 1.0 Hz, 2H), 6.34 (dd, *J* = 7.3, 1.0 Hz, 2H), 6.09 – 5.99 (m, 1H), 5.95 – 5.87 (m, 2H), 5.75 (br s, 2H).

N-(2-vinylphenyl)acetamide SM4

The compound was prepared according to a modified literature procedure.[89] In a sealed vial under a nitrogen atmosphere, a mixture of *N*-(2-bromophenyl)acetamide (642 mg, 3.0 mmol, 1.0 equiv), PdCl₂ (10.6 mg, 0.06 mmol, 2 mol%), PPh₃ (47.2 mg, 0.12 mmol, 6 mol%), Cs₂CO₃ (2.93 g, 9.0 mmol, 3.0 equiv), potassium vinyltrifluoroborate (402 mg, 3.0 mmol, 1.0 equiv), and thf/H₂O (9:1, 6 mL) was allowed to stir at 85 °C for 22 h. The reaction mixture was allowed to cool to room temperature, diluted with water (10 mL), and then washed with DCM (3 x 20 mL). The combined organic layers were dried over sodium sulfate and filtered. The volatiles of the filtrate were removed under reduced pressure and the residue was subjected to column chromatography (silica gel, 0 – 50% EtOAc in petroleum ether) to give the title product (340 mg, 2.1 mmol, 70%) as a white solid. The NMR data match previously reported data for the title product.[90]

¹H NMR (500 MHz, CDCl₃) δ 7.80 (d, *J* = 8.1 Hz, 1H), 7.42 (dd, *J* = 7.7, 1.6 Hz, 1H), 7.31 – 7.26 (m, 1H), 7.19 – 7.10 (m, 2H), 6.79 (dd, *J* = 17.4, 11.0 Hz, 1H), 5.68 (dd, *J* = 17.5, 1.3 Hz, 1H), 5.41 (dd, *J* = 11.0, 1.3 Hz, 1H), 2.20 (s, 3H).

tert-butyl (4-vinylphenyl)carbamate SM5
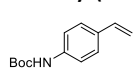
The compound was prepared in accordance to a literature procedure.[91] A solution of 4-aminostyrene (596 mg, 5.00 mmol, 1.0 equiv) and di-*tert*-butyl dicarbonate (2.18 g, 10.0 mmol, 2.0 equiv) in CH₂Cl₂ (3.6 mL) was allowed to stir at room temperature for 17 h under a nitrogen atmosphere. Imidazole (1.02 g, 15.0 mmol, 3.0 equiv) was added, and the resulting solution was allowed to stir for 2 h at room temperature. The subsequent work-up was performed according to a literature procedure:[92] The

volatiles were removed under reduced pressure. CH_2Cl_2 (20 mL) was added. The organic phase was washed with 1% aqueous HCl (3 × 40 mL) with back-washing (CH_2Cl_2, 5 mL). The combined organic phases were washed with brine (20 mL), dried over Na_2SO_4, and filtrated. The volatiles of the filtrate were removed under reduced pressure to isolate the title product (936 mg, 4.27 mmol, 85%) as a colorless solid. The NMR data match previously reported data for the title product.[20]

^{1}H NMR (500 MHz, $CDCl_3$) δ 7.38 – 7.28 (m, 4H), 6.65 (dd, J = 17.6, 10.9 Hz, 1H), 6.48 (s, 1H), 5.65 (dd, J = 17.6, 0.9 Hz, 1H), 5.16 (dd, J = 10.8, 1.0 Hz, 1H), 1.52 (s, 9H).

4-vinylbenzenesulfonamide SM6
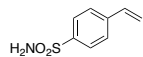
The title compound was prepared according to a literature procedure.[93] *p*-Styrene sulfonyl chloride[94] (1.01 g, 5.0 mmol, 1.0 equiv) was added dropwise to an aqueous ammonia solution (30%, 15 mL) at room temperature. The reaction mixture was allowed to stir for 3 h and washed with diethyl ether (3 x 15 mL). The combined organic layers were dried over sodium sulfate, and filtered. The volatiles were removed under reduced pressure to give the title compound (755 mg, 4.1 mmol, 82%) as a white solid. The NMR data match previously reported data for the title product.[93]

^{1}H NMR (400 MHz, $CDCl_3$) δ 7.88 (d, J = 8.4 Hz, 2H), 7.53 (d, J = 8.5 Hz, 2H), 6.75 (dd, J = 17.6, 10.9 Hz, 1H), 5.88 (d, J = 17.6 Hz, 1H), 5.44 (d, J = 10.9 Hz, 1H), 4.84 (s, 2H).

N-benzyl-4-vinylbenzenesulfonamide SM7

The title compound was prepared according to a literature procedure.[95] *p*-Styrene sulfonyl chloride[94] (1.01 g, 5.0 mmol, 1.0 equiv) was added dropwise to a solution of benzyl amine (589 mg, 5.5 mmol, 1.1 equiv) and triethylamine (1.11 g, 1.52 mL, 11.0 mmol, 2.2 equiv) in DCM (10 mL) at 0 °C under a nitrogen atmosphere. The reaction mixture was allowed to stir for 15 h at room temperature and the volatiles were removed under reduced pressure. The residue was subjected to column chromatography (silica gel, 0-20% EtOAc in petroleum ether) to give the title compound (957 mg, 3.5 mmol, 70%) as a yellow solid. The NMR data match previously reported data for the title product.[96]

^{1}H NMR (400 MHz, $CDCl_3$) δ 7.82 (d, J = 8.5 Hz, 2H), 7.52 (d, J = 8.4 Hz, 2H), 7.31 – 7.24 (m, 3H), 7.22 – 7.17 (m, 2H), 6.76 (dd, J = 17.6, 10.9 Hz, 1H), 5.89 (d, J = 17.6 Hz, 1H), 5.44 (d, J = 10.9 Hz, 1H), 4.67 (t, J = 6.2 Hz, 1H), 4.15 (d, J = 6.2 Hz, 2H).

5-vinyl-1*H*-indole SM8

The compound was prepared according to a modified literature procedure.[89] In a sealed vial under a nitrogen atmosphere, a mixture of 5-bromoindole (588 mg, 3.0 mmol, 1.0 equiv), $PdCl_2$ (10.6 mg, 0.06 mmol, 2 mol%), PPh_3 (47.2 mg, 0.12 mmol, 6 mol%), Cs_2CO_3 (2.93 g, 9.0 mmol, 3.0 equiv), potassium vinyltrifluoroborate (402 mg, 3.0 mmol, 1.0 equiv), and thf/H_2O (9:1, 6 mL) was allowed to stir at 85 °C for 22 h. The reaction mixture was allowed to cool to room temperature, diluted with water (10 mL), and then washed with DCM (3 x 20 mL). The combined organic layers were dried over sodium sulfate and filtered. The volatiles of the filtrate were removed under reduced pressure and the residue was subjected to column chromatography (silica gel, 0 – 20% EtOAc in petroleum ether) to give the title product (168 mg, 1.2 mmol, 39%) as an off-white solid. The NMR data match previously reported data for the title product.[97]

^{1}H NMR (500 MHz, $CDCl_3$) δ 8.12 (s, 1H), 7.65 (s, 1H), 7.36 – 7.33 (m, 2H), 7.19 (t, J = 2.8 Hz, 1H), 6.84 (dd, J = 17.6, 10.8 Hz, 1H), 6.56 – 6.50 (m, 1H), 5.70 (dd, J = 17.5, 1.1 Hz, 1H), 5.15 (dd, J = 10.9, 1.0 Hz, 1H).

4-vinylphenol SM10

The title compound was prepared according to a literature procedure.[98] Sodium hydroxide (500 mg, 12.5 mmol, 2.5 equiv) in water (5 mL) was slowly added to a solution of 4-acetoxystyrene (811 mg, 5.0 mmol, 1.0 equiv) in thf (8 mL) at 0 °C. The reaction mixture was allowed to stir for 16 h at room temperature, cooled down to 0 °C and 1.5 M HCl (5 mL, until acidic) was added. After addition of water (20 mL), the mixture was washed with diethyl ether (3 x 45 mL). The combined organic layers were dried over sodium sulfate and filtered. The volatiles were removed under reduced pressure and the residue was subjected to column chromatography (silica gel, 0 – 10% EtOAc in petroleum ether) to give the title compound (492 mg, 4.1 mmol, 82%) as a yellow oil. The NMR data match previously reported data for the title product.[98]

^{1}H NMR (500 MHz, $CDCl_3$) δ 7.30 (d, J = 8.5 Hz, 2H), 6.82 (d, J = 8.6 Hz, 2H), 6.66 (dd, J = 17.6, 10.9 Hz, 1H), 5.99 (s, 1H), 5.61 (dd, J = 17.6, 0.9 Hz, 1H), 5.13 (dd, J = 11.0, 0.9 Hz, 1H).

(4-vinylphenyl)methanol SM11
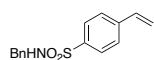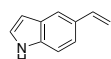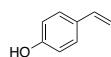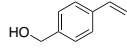
The compound was prepared according to a literature procedure.[99] To sodium hydroxide (200 mg, 5.0 mmol, 1.0 equiv) and tetrabutylammonium bromide (1.61 g, 5.0 mmol, 1.0 equiv) in water (10 mL), 4-vinylbenzylchloride (763 mg, 707 µL, 5.0 mmol, 1.0 equiv) was added. The reaction mixture was allowed to stir at 125 °C for 20 min, allowed to cool down to room temperature, and washed with EtOAc (3 x 10 mL). The combined organic layers were dried over sodium sulfate and filtered. The volatiles of the filtrate were removed under reduced pressure and the residue was subjected to column chromatography (silica gel, 0 – 20% EtOAc in petroleum ether) to give the title product (299 mg, 2.2 mmol, 45%) as a yellow oil. The NMR data match previously reported data for the title product.[99]

^{1}H NMR (500 MHz, $CDCl_3$) δ 7.41 (d, J = 8.1 Hz, 2H), 7.33 (d, J = 8.1 Hz, 2H), 6.72 (dd, J = 17.6, 10.9 Hz, 1H), 5.76 (d, J = 17.6 Hz, 1H), 5.25 (d, J = 10.9 Hz, 1H), 4.68 (s, 2H) [Note: the OH proton was not detected].

2-(4-vinylphenyl)acetic acid SM14
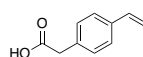
The compound was prepared according to a modified literature procedure.[100] A mixture of 4-vinylphenylacetonitrile (358 mg, 2.5 mmol, 1.0 equiv), hydroquinone (5.5 mg, 50 µmol, 2 mol%), and KOH (982 mg, 17.5 mmol, 7.0 equiv) in ethanol (6 mL) was heated to 90 °C for 3 h under a nitrogen atmosphere. After cooling down to room temperature, water (20 mL) was added, and the mixture was washed with diethyl ether (2 x 30 mL). The aqueous solution was treated with aqueous 1 M HCl (until pH = 1) and washed with DCM (3 x 30 mL). The combined organic layers were dried over sodium sulfate and filtered. The volatiles were removed under reduced pressure to give the title product (320 mg, 1.98 mmol, 79%) as a red solid. The NMR data match previously reported data for the title product.[100]

^{1}H NMR (500 MHz, $CDCl_3$) δ 7.38 (d, J = 8.2 Hz, 2H), 7.24 (d, J = 8.1 Hz, 2H), 6.70 (dd, J = 17.6, 10.9 Hz, 1H), 5.74 (dd, J = 17.5, 0.9 Hz, 1H), 5.24 (dd, J = 10.8, 0.9 Hz, 1H), 3.64 (s, 2H) [Note: the COOH proton was not detected].

diethyl (4-vinylphenyl)phosphonate SM20
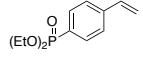
The compound was prepared according to a modified literature procedure.[101] A mixture of diethylphosphite (323 µL, 345 mg, 2.5 mmol, 1.0 equiv), 4-vinylphenylboronic acid (740 mg, 5.0 mmol, 2.0 equiv), Cu_2O (22.5 mg, 125 µmol,

5 mol%), 1,10-phenanthroline (56.1 mg, 0.25 mmol, 10 mol%), and DIPEA (1.28 mL, 969 mg, 7.5 mmol, 3.0 equiv) in acetonitrile (10 mL) was allowed to stir under air at room temperature for 14 h. The reaction mixture was then filtered through a pad of celite, the volatiles were removed under reduced pressure, and the residue was subjected to column chromatography (silica gel, 0 – 100% EtOAc in petroleum ether) to give the title product (353 mg, 1.47 mmol, 59%) as a colorless oil. The NMR data match previously reported data for the title product.[101]

¹H NMR (500 MHz, CDCl₃) δ 7.86 – 7.65 (m, 2H), 7.57 – 7.45 (m, 2H), 6.72 (dd, J = 17.6, 10.9 Hz, 1H), 5.85 (d, J = 17.6 Hz, 1H), 5.37 (d, J = 10.9 Hz, 1H), 4.23 – 3.95 (m, 4H), 1.31 (t, J = 7.1 Hz, 6H).

ethyl 4-vinylbenzenesulfonate SM21
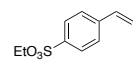
The title compound was prepared according to a literature procedure.[102] *p*-Styrene sulfonyl chloride[94] (1.01 g, 5.0 mmol, 1.0 equiv) was added dropwise to a solution of DABCO (673 mg, 6.0 mmol, 1.2 equiv) and ethanol (240 mg, 304 µL, 7.5 mmol, 1.5 equiv) in DCM (10 mL) at 0 °C under a nitrogen atmosphere. The reaction mixture was allowed to warm up to room temperature and allowed to stir for 16 h. Water (10 mL) was added, and the layers were separated. The organic layer was washed with water (3 x 10 mL) and brine (1 x 10 mL), and dried over sodium sulfate. After filtration, the volatiles were removed under reduced pressure to give the title compound (662 mg, 3.1 mmol, 62%) as a light yellow oil. The NMR data match previously reported data for the title product.[103]

¹H NMR (400 MHz, CDCl₃) δ 7.86 (d, J = 8.5 Hz, 2H), 7.55 (d, J = 8.5 Hz, 2H), 6.76 (dd, J = 17.6, 10.9 Hz, 1H), 5.91 (d, J = 17.6 Hz, 1H), 5.47 (d, J = 10.9 Hz, 1H), 4.13 (q, J = 7.1 Hz, 2H), 1.31 (t, J = 7.1 Hz, 3H).

2-vinylbenzo[*b*]thiophene SM25
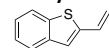
The title compound was prepared according to a modified literature procedure.[104] To a solution of methyltriphenylphosphonium bromide (4.40 g, 12.3 mmol, 1.1 equiv) in anhydrous thf (40 mL), *n*-BuLi (7.7 mL, 1.6 M in hexanes, 12.3 mmol, 1.1 equiv) was added dropwise at 0 °C under a nitrogen atmosphere. The solution was allowed to stir at room temperature for 1 h. Then, a solution of benzo[*b*]thiophene-2-carbaldehyde (1.82 g, 11.2 mmol, 1.0 equiv) in anhydrous thf (5 mL) was added dropwise to the mixture kept at 0 °C. The reaction mixture was allowed to stir for 26 h at room temperature. The reaction was quenched by addition of saturated aqueous NH₄Cl (25 mL) solution. The organic layer was separated. The aqueous layer was washed with EtOAc (3 x 25 mL). The combined organic layers were washed with brine (25 mL) and dried over sodium sulfate. After filtration, the volatiles of the filtrate were removed under reduced pressure and the residue was subjected to column chromatography (silica gel, 100% petroleum ether) to give the title compound (1.22 g, 7.6 mmol, 68%) as a white solid. The NMR data match previously reported data for the title product.[105]

¹H NMR (500 MHz, CDCl₃) δ 7.82 – 7.75 (m, 1H), 7.74 – 7.64 (m, 1H), 7.36 – 7.27 (m, 2H), 7.17 (s, 1H), 6.93 (dd, J = 17.3, 10.8 Hz, 1H), 5.67 (d, J = 17.3 Hz, 1H), 5.31 (d, J = 10.8 Hz, 1H).

2-vinylbenzofuran SM26
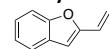
The title compound was prepared according to a literature procedure.[104] To a solution of methyltriphenylphosphonium bromide (3.14 g, 8.8 mmol, 1.1 equiv) in anhydrous thf (250 mL), *n*-BuLi (5.5 mL, 1.6 M in hexanes, 8.8 mmol, 1.1 equiv) was added dropwise at 0 °C under a nitrogen atmosphere. The solution was allowed to stir at room temperature for 1 h. Then, a solution of benzofuran-2-carbaldehyde (1.17 g, 8.0 mmol, 1.0 equiv) in anhydrous thf (5 mL) was added dropwise to the mixture kept at 0 °C. The reaction mixture was allowed to stir for 26 h at room temperature. The reaction was quenched by addition of saturated aqueous NH₄Cl (25 mL) solution. The organic layer was separated. The aqueous layer was washed with EtOAc (3 x 25 mL). The combined organic layers were washed with brine (25 mL) and dried over sodium sulfate. After filtration, the volatiles of the filtrate were removed under reduced pressure and the residue was subjected to column chromatography (silica gel, 100% petroleum ether) to give the title compound (545 mg, 3.8 mmol, 47%) as a colorless oil. The NMR data match previously reported data for the title product.[106]

¹H NMR (500 MHz, CDCl₃) δ 7.57 – 7.50 (m, 1H), 7.46 (dt, J = 8.2, 1.0 Hz, 1H), 7.31 – 7.26 (m, 1H), 7.20 (td, J = 7.5, 1.1 Hz, 1H), 6.65 (dd, J = 17.4, 11.2 Hz, 1H), 6.60 (s, 1H), 5.97 (dd, J = 17.4, 1.2 Hz, 1H), 5.39 (dd, J = 11.2, 1.3 Hz, 1H).

3-vinyloxazolidin-2-one SM27

The compound was prepared according to a literature procedure.[107] Under a nitrogen atmosphere, a screw-cap vial was charged with 2-oxazolidinone (261 mg, 3.0 mmol, 1.0 equiv), CuI (28.6 mg, 0.15 mmol, 5 mol%), DMEDA (26.4 mg, 32.3 µL, 0.30 mmol, 10 mol%), potassium carbonate (829 mg, 6.0 mmol, 2.0 equiv), and vinyl bromide (6 mL, 1 M in thf, 6.0 mmol, 2.0 mmol). The vial was sealed with a screw-cap and allowed to stir at 80 °C for 22 h. The reaction mixture was filtered through a pad of celite, and the volatiles of the filtrate were removed under reduced pressure. The residue was subjected to column chromatography (silica gel, 10 – 30% EtOAc in petroleum ether) to give the title product (339 mg, 3.0 mmol, 100%) as a yellow oil. The NMR data match previously reported data for the title product.[108]

¹H NMR (400 MHz, CDCl₃) δ 6.88 (dd, J = 15.8, 8.9 Hz, 1H), 4.48 – 4.40 (m, 3H), 4.29 (dd, J = 15.8, 1.2 Hz, 1H), 3.76 – 3.64 (m, 2H).

tert-butyldimethyl(4-vinylphenoxy)silane SM33
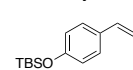
The title compound was prepared according to a literature procedure.[109] To a solution of 4-vinylphenol (240 mg, 2.0 mmol, 1.0 equiv) in DCM/DMF (8 mL, 9/1), triethylamine (405 mg, 4.0 mmol, 2.0 equiv) and TBSCl (603 mg, 4.0 mmol, 2.0 equiv) were added at room temperature under a nitrogen atmosphere. The reaction was allowed to stir for 3 h. Water (5 mL) and brine (5 mL) were added. The organic phase was separated, and the aqueous phase was washed with DCM (3 x 40 mL). The combined organic layers were dried over sodium sulfate and filtered. The volatiles from the filtrate were removed under reduced pressure and the residue was subjected to column chromatography (silica gel, 0-10% EtOAc in petroleum ether) to give the title compound (380 mg, 1.6 mmol, 81%) as a colorless oil. The NMR data match previously reported data for the title product.[109]

¹H NMR (500 MHz, CDCl₃) δ 7.28 (d, J = 8.5 Hz, 2H), 6.79 (d, J = 8.6 Hz, 2H), 6.65 (dd, J = 17.6, 10.9 Hz, 1H), 5.60 (dd, J = 17.6, 1.0 Hz, 1H), 5.12 (dd, J = 10.9, 1.0 Hz, 1H), 0.98 (s, 9H), 0.20 (s, 6H).

Synthesis of drug derivatives

General procedure for Suzuki-Miyaura coupling of aryl chlorides
The procedure was adapted from the literature.[110] In a nitrogen-filled glove box, a 25 mL screw-cap vial equipped with a Teflon-coated magnetic stirring bar was charged with aryl chloride (1.0 equiv), $Pd(OAc)_2$ (7.5 mol%), SPhos (15 mol%), K_2CO_3 (4.0 equiv), vinyl BF_3K (2.0 equiv), and dioxane/water (6/1, 0.2M). The vial was sealed with a cap, removed from the glove box, placed in a pre-heated aluminum block, and allowed to stir (800 rpm) at 90 °C for 16 h. Upon cooling to room temperature, the reaction mixture was filtered through a short pad of celite and concentrated under reduced pressure. The residue was subjected to column chromatography to give the title compound.

methyl 2-(5-methoxy-2-methyl-1-(4-vinylbenzoyl)-1*H*-indol-3-yl)acetate SM34-Me
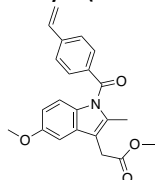
The title compound was prepared according to the general procedure for the Suzuki-Miyaura coupling of aryl chlorides using indomethacin methyl ester[111] (558 mg, 1.5 mmol). The residue obtained after filtration was subjected to column chromatography (silica gel, 0-30% EtOAc in petroleum ether) to give the title compound (440 mg, 1.21 mmol, 81%) as a yellow oil.

¹H NMR (400 MHz, CDCl₃) δ 7.69 (d, *J* = 8.4 Hz, 2H), 7.51 (d, *J* = 8.3 Hz, 2H), 6.96 (d, *J* = 2.5 Hz, 1H), 6.91 (d, *J* = 9.0 Hz, 1H), 6.79 (dd, *J* = 17.6, 10.9 Hz, 1H), 6.66 (dd, *J* = 9.0, 2.5 Hz, 1H), 5.91 (d, *J* = 17.6 Hz, 1H), 5.43 (d, *J* = 10.9 Hz, 1H), 3.84 (s, 3H), 3.71 (s, 3H), 3.68 (s, 2H), 2.40 (s, 3H);
¹³C{¹H} NMR (101 MHz, CDCl₃) δ 171.6, 169.2, 156.1, 142.1, 136.2, 136.0, 134.7, 131.1, 130.7, 130.4, 126.6, 117.1, 115.2, 112.2, 111.6, 101.3, 55.9, 52.3, 30.3, 13.4;
HRMS (ESI) m/z calcd. for $C_{22}H_{22}NO_4$ ([M+H]⁺): 364.1543; found: 364.1561.

2-(5-methoxy-2-methyl-1-(4-vinylbenzoyl)-1*H*-indol-3-yl)acetic acid SM34
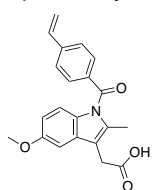
The title compound was prepared according to modified literature procedure.[112] To a mixture of methyl 2-(5-methoxy-2-methyl-1-(4-vinylben-zoyl)-1H-indol-3-yl)acetate (218 mg, 0.60 mmol, 1.0 equiv) and lithium bromide (521 mg, 6.0 mmol, 3.0 equiv) in MeCN/H₂O (2 mL, 98/2), NEt₃ (250 μL, 182 mg, 1.8 mmol, 3.0 equiv) was added at room temperature. The reaction mixture was allowed to stir for 16 h after which it was diluted with water and treated with aqueous 1 M HCl (until pH 6). The mixture was then washed with EtOAc (3 x 10 mL). The combined organic layers dried over Na₂SO₄ and filtered. The volatiles of the filtrate were removed under reduced pressure and the residue was subjected to column chromatography (silica gel, 0 – 36% EtOAc in petroleum ether + 0.5% AcOH) to give the title product (70.1 mg, 0.2 mmol, 33%) as an off-white solid.

¹H NMR (400 MHz, CDCl₃) δ 7.68 (d, *J* = 8.2 Hz, 2H), 7.50 (d, *J* = 8.1 Hz, 2H), 6.95 (d, *J* = 2.5 Hz, 1H), 6.90 (d, *J* = 9.0 Hz, 1H), 6.78 (dd, *J* = 17.6, 10.9 Hz, 1H), 6.66 (dd, *J* = 9.0, 2.5 Hz, 1H), 5.91 (d, *J* = 17.6 Hz, 1H), 5.43 (d, *J* = 10.9 Hz, 1H), 3.83 (s, 3H), 3.70 (s, 2H), 2.39 (s, 3H) [Note: the COOH proton was not detected];
¹³C{¹H} NMR (101 MHz, CDCl₃) δ 176.6, 169.2, 156.1, 142.2, 136.5, 136.90, 134.6, 131.1, 130.5, 130.4, 126.6, 117.1, 115.2, 111.8, 111.5, 101.2, 55.9, 30.1, 13.4;
HRMS (ESI) m/z calcd. for $C_{21}H_{20}NO_4$ ([M+H]⁺): 350.1387; found: 350.1382.

methyl 2-(4-chlorobenzamido)-3-(1-methyl-2-oxo-1,2-dihydroquinolin-4-yl)propanoate SM35a
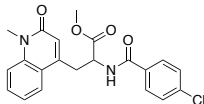
Methyl iodide (280 μL, 639 mg, 4.5 mmol, 3.0 equiv) was added to a suspension of rebamipide (556 mg, 1.5 mmol, 1.0 equiv) in DMF (3.8 mmol). The reaction mixture was allowed to stir at room temperature for 5 h after which the starting material was fully consumed as indicated by TLC. Ethyl acetate (30 mL) and water (30 mL) were added. The aqueous layer was washed with EtOAc (2 x 30 mL). The combined organic layers were washed with brine (2 x 30 mL), dried over sodium sulfate, and filtered. The volatiles were removed under reduced pressure and the residue was subjected to column chromatography (silica gel, 10% MeOH in DCM) to give the title product (320 mg, 0.83 mmol, 55%) as a white solid.

¹H NMR (500 MHz, CDCl₃) δ 7.94 (dd, *J* = 8.1, 1.4 Hz, 1H), 7.71 – 7.61 (m, 2H), 7.58 (ddd, *J* = 8.5, 7.1, 1.4 Hz, 1H), 7.44 – 7.31 (m, 3H), 7.29 – 7.14 (m, 1H), 6.83 (d, *J* = 7.4 Hz, 1H), 6.55 (s, 1H), 5.15 (q, *J* = 6.6 Hz, 1H), 3.75 (s, 3H), 3.69 (s, 3H), 3.43 (qd, *J* = 14.1, 6.4 Hz, 2H);
¹³C{¹H} NMR (126 MHz, CDCl₃) δ 171.6, 166.2, 161.6, 144.8, 140.1, 138.3, 131.8, 131.0, 129.0, 128.5, 125.1, 122.4, 122.3, 120.3, 114.8, 52.9, 52.7, 34.8, 29.4;
HRMS (ESI) m/z calcd. for $C_{21}H_{20}ClN_2O_4$ ([M+H]⁺): 399.1106; found: 399.1123.

methyl 3-(1-methyl-2-oxo-1,2-dihydroquinolin-4-yl)-2-(4-vinylbenzamido)propanoate SM35b
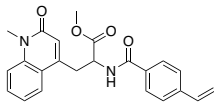
The title compound was prepared according to the general procedure for the Suzuki-Miyaura coupling of aryl chlorides using methyl 2-(4-chlorobenzamido)-3-(1-methyl-2-oxo-1,2-dihydroquinolin-4-yl)propanoate (271 mg, 0.68 mmol). The residue obtained after filtration was subjected to column chromatography (silica gel, 0-8% MeOH in DCM) to give the title compound (219 mg, 0.54 mmol, 79%) as an off-white solid.

¹H NMR (400 MHz, CDCl₃) δ 7.98 (dd, *J* = 8.1, 1.4 Hz, 1H), 7.73 – 7.64 (m, 2H), 7.57 (td, *J* = 7.7, 1.4 Hz, 1H), 7.45 – 7.34 (m, 3H), 7.30 – 7.21 (m, 1H), 6.86 (d, *J* = 7.4 Hz, 1H), 6.71 (dd, *J* = 17.6, 10.9 Hz, 1H), 6.57 (s, 1H), 5.82 (d, *J* = 17.4 Hz, 1H), 5.35 (d, *J* = 10.9 Hz, 1H), 5.16 (q, *J* = 6.7 Hz, 1H), 3.74 (s, 3H), 3.69 (s, 3H), 3.43 (d, *J* = 6.4 Hz, 2H);
¹³C{¹H} NMR (101 MHz, CDCl₃) δ 171.8, 167.0, 161.7, 145.1, 141.3, 140.2, 136.0, 132.6, 131.0, 127.5, 126.5, 125.4, 122.5, 122.4, 120.5, 116.4, 114.9, 52.9, 52.8, 35.1, 29.5;
HRMS (ESI) m/z calcd. For $C_{23}H_{23}N_2O_4$ ([M+H]⁺): 391.1652; found: 391.1669.

N-(propylcarbamoyl)-4-vinylbenzenesulfonamide SM36
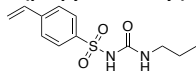
The title compound was prepared according to a modified literature procedure.[113] To a mixture of 4-vinylsulfonamide (367 mg, 2.0 mmol, 1.0 equiv) and phenyl propylcarbamate (394 mg, 2.2 mmol, 1.1 equiv) in MeCN (10 mL), DBU (448 μL, 457 mg, 3.0 mmol, 1.5 equiv) was added. The reaction mixture was allowed to stir at 80 °C for 16 h. After allowing to cool to room temperature, the volatiles were removed under reduced pressure and EtOAc (20 mL) was added. The mixture was washed with water, aqueous 1 M HCl, and water (20 mL each), dried over Na₂SO₄, and filtered. The volatiles of the filtrate were removed under reduced pressure and the residue was subjected to column chromatography (silica gel, 0 – 46% EtOAc in petroleum ether) to give the title product (349 mg, 1.27 mmol, 63%) as an off-white solid.

¹H NMR (500 MHz, CDCl₃) δ 8.54 (s, 1H), 7.83 (d, *J* = 8.6 Hz, 2H), 7.52 (d, *J* = 8.5 Hz, 2H), 6.74 (dd, *J* = 17.6, 10.9 Hz, 1H), 6.59 (s, 1H), 5.89 (d, *J* = 17.6 Hz, 1H), 5.47 (d, *J* = 10.9 Hz, 1H), 3.19 (td, *J* = 7.1, 5.7 Hz, 2H), 1.51 (h, *J* = 7.3 Hz, 2H), 0.88 (t, *J* = 7.4 Hz, 3H);
¹³C{¹H} NMR (126 MHz, CDCl₃) δ 151.7, 143.1, 138.5, 135.3, 127.4, 127.0, 118.3, 42.2, 22.9, 11.3;
HRMS (ESI) m/z calcd. for $C_{12}H_{17}N_2O_3S$ ([M+H]⁺): 269.0954; found: 269.0952.

3.5. References

(1)   Cernak, T.; Dykstra, K. D.; Tyagarajan, S.; Vachal, P.; Krska, S. W. The Medicinal Chemist's Toolbox for Late Stage Functionalization of Drug-like Molecules. *Chem. Soc. Rev.* **2016**, *45* (3), 546–576. https://doi.org/10.1039/C5CS00628G.

(2)   Blakemore, D. C.; Castro, L.; Churcher, I.; Rees, D. C.; Thomas, A. W.; Wilson, D. M.; Wood, A. Organic Synthesis Provides Opportunities to Transform Drug Discovery. *Nat. Chem.* **2018**, *10* (4), 383–394. https://doi.org/10.1038/s41557-018-0021-z.

(3)   Hall, D. G. *Boronic Acids: Preparation and Applications in Organic Synthesis and Medicine*; Wiley-VCH Verlag: Weinheim, 2010.

(4)   Diaz, D. B.; Yudin, A. K. The Versatility of Boron in Biological Target Engagement. *Nat. Chem.* **2017**, *9* (8), 731–742. https://doi.org/10.1038/nchem.2814.

(5)   Hartwig, J. F.; Larsen, M. A. Undirected, Homogeneous C–H Bond Functionalization: Challenges and Opportunities. *ACS Cent. Sci.* **2016**, *2* (5), 281–292. https://doi.org/10.1021/acscentsci.6b00032.

(6)   Mkhalid, I. A. I.; Barnard, J. H.; Marder, T. B.; Murphy, J. M.; Hartwig, J. F. C–H Activation for the Construction of C–B Bonds. *Chem. Rev.* **2010**, *110* (2), 890–931. https://doi.org/10.1021/cr900206p.

(7)   Hartwig, J. F. Regioselectivity of the Borylation of Alkanes and Arenes. *Chem. Soc. Rev.* **2011**, *40* (4), 1992. https://doi.org/10.1039/c0cs00156b.

(8)   Xu, L.; Wang, G.; Zhang, S.; Wang, H.; Wang, L.; Liu, L.; Jiao, J.; Li, P. Recent Advances in Catalytic C–H Borylation Reactions. *Tetrahedron* **2017**, *73* (51), 7123–7157. https://doi.org/10.1016/j.tet.2017.11.005.

(9)   Wright, J. S.; Scott, P. J. H.; Steel, P. G. Iridium-Catalysed C–H Borylation of Heteroarenes: Balancing Steric and Electronic Regiocontrol. *Angew. Chem. Int. Ed.* **2021**, *60* (6), 2796–2821. https://doi.org/10.1002/anie.202001520.

(10)   Reyes, R.; Sawamura, M. An Introductory Overview of C–H Bond Activation/ Functionalization Chemistry with Focus on Catalytic C(Sp3)–H Bond Borylation. *KIMIKA* **2021**, *32* (1), 70–109. https://doi.org/10.26534/kimika.v32i1.70-109.

(11)   Veth, L.; Grab, H.; Dydio, P. Recent Trends in Group 9–Catalyzed C–H Borylation Reactions: Different Strategies to Control Site-, Regio-, and Stereoselectivity. *Synthesis* **2022**, *54*, 3482–3498. https://doi.org/10.1055/a-1711-5889.

(12)   Ban, H. S.; Nakamura, H. Boron-Based Drug Design: Boron-Based Drug Design. *Chem. Rec.* **2015**, *15* (3), 616–635. https://doi.org/10.1002/tcr.201402100.

(13)   Xu, L.; Zhang, S.; Li, P. Boron-Selective Reactions as Powerful Tools for Modular Synthesis of Diverse Complex Molecules. *Chem. Soc. Rev.* **2015**, *44* (24), 8848–8858. https://doi.org/10.1039/C5CS00338E.

(14)   Miyaura, Norio.; Suzuki, Akira. Palladium-Catalyzed Cross-Coupling Reactions of Organoboron Compounds. *Chem. Rev.* **1995**, *95* (7), 2457–2483. https://doi.org/10.1021/cr00039a007.

(15)   Nicolaou, K. C.; Bulger, P. G.; Sarlah, D. Palladium-Catalyzed Cross-Coupling Reactions in Total Synthesis. *Angew. Chem. Int. Ed.* **2005**, *44* (29), 4442–4489. https://doi.org/10.1002/anie.200500368.

(16)   Lennox, A. J. J.; Lloyd-Jones, G. C. Selection of Boron Reagents for Suzuki–Miyaura Coupling. *Chem Soc Rev* **2014**, *43* (1), 412–443. https://doi.org/10.1039/C3CS60197H.

(17)   Carreras, J.; Caballero, A.; Pérez, P. J. Alkenyl Boronates: Synthesis and Applications. *Chem. – Asian J.* **2019**, *14* (3), 329–343. https://doi.org/10.1002/asia.201801559.

(18)   Shi, X.; Li, S.; Wu, L. H₂-Acceptorless Dehydrogenative Boration and Transfer Boration of Alkenes Enabled by Zirconium Catalyst. *Angew. Chem. Int. Ed.* **2019**, *58* (45), 16167–16171. https://doi.org/10.1002/anie.201908931.

(19)   Marciniec, B.; Jankowska, M.; Pietraszuk, C. New Catalytic Route to Functionalized Vinylboronates. *Chem. Commun.* **2005**, No. 5, 663. https://doi.org/10.1039/b414644a.

(20)   Veth, L.; Grab, H. A.; Martínez, S.; Antheaume, C.; Dydio, P. Transfer C–H Borylation of Alkenes under Rh(I) Catalysis: Insight into the Synthetic Capacity, Mechanism, and Selectivity Control. *Chem Catal.* **2022**, *2* (4), 762–778. https://doi.org/10.1016/j.checat.2022.02.008.

(21)   Reid, W. B.; Spillane, J. J.; Krause, S. B.; Watson, D. A. Direct Synthesis of Alkenyl Boronic Esters from Unfunctionalized Alkenes: A Boryl-Heck Reaction. *J. Am. Chem. Soc.* **2016**, *138* (17), 5539–5542. https://doi.org/10.1021/jacs.6b02914.

(22)   Reid, W. B.; Watson, D. A. Synthesis of Trisubstituted Alkenyl Boronic Esters from Alkenes Using the Boryl-Heck Reaction. *Org. Lett.* **2018**, *20* (21), 6832–6835. https://doi.org/10.1021/acs.orglett.8b02949.

(23)   Idowu, O. O.; Hayes, J. C.; Reid, W. B.; Watson, D. A. Synthesis of 1,1-Diboryl Alkenes Using the Boryl-Heck Reaction. *Org. Lett.* **2021**, acs.orglett.1c01567. https://doi.org/10.1021/acs.orglett.1c01567.

(24)   Morimoto, M.; Miura, T.; Murakami, M. Rhodium-Catalyzed Dehydrogenative Borylation of Aliphatic Terminal Alkenes with Pinacolborane. *Angew. Chem. Int. Ed.* **2015**, *54* (43), 12659–12663. https://doi.org/10.1002/anie.201506328.

(25)   Murata, M.; Watanabe, S.; Masuda, Y. Rhodium-Catalyzed Dehydrogenative Coupling Reaction of Vinylarenes with Pinacolborane to Vinylboronates. *Tetrahedron Lett.* **1999**, *40* (13), 2585–2588. https://doi.org/10.1016/S0040-4039(99)00253-1.

(26)   Kondoh, A.; Jamison, T. F. Rhodium-Catalyzed Dehydrogenative Borylation of Cyclic Alkenes. *Chem. Commun.* **2010**, *46* (6), 907. https://doi.org/10.1039/b921387b.

(27)   Lu, W.; Shen, Z. Direct Synthesis of Alkenylboronates from Alkenes and Pinacol Diboron via Copper Catalysis. *Org. Lett.* **2019**, *21* (1), 142–146. https://doi.org/10.1021/acs.orglett.8b03599.

(28)   Andrews, P. R.; Craik, D. J.; Martin, J. L. Functional Group Contributions to Drug-Receptor Interactions. *J. Med. Chem.* **1984**, *27* (12), 1648–1657. https://doi.org/10.1021/jm00378a021.

(29)   Silverman, R. B.; Holladay, M. W. *The Organic Chemistry of Drug Design and Drug Action*, 3d edition.; Elsevier/AP, Academic Press, is an imprint of Elsevier: Amsterdam Boston, 2014.

(30)   Ertl, P.; Altmann, E.; McKenna, J. M. The Most Common Functional Groups in Bioactive Molecules and How Their Popularity Has Evolved over Time. *J. Med. Chem.* **2020**, *63* (15), 8408–8418. https://doi.org/10.1021/acs.jmedchem.0c00754.

(31)   McGrath, N. A.; Brichacek, M.; Njardarson, J. T. A Graphical Journey of Innovative Organic Architectures That Have Improved Our Lives. *J. Chem. Educ.* **2010**, *87* (12), 1348–1349. https://doi.org/10.1021/ed1003806.

(32)   Genov, G. R.; Douthwaite, J. L.; Lahdenperä, A. S. K.; Gibson, D. C.; Phipps, R. J. Enantioselective Remote C–H Activation Directed by a Chiral Cation. *Science* **2020**, *367* (6483), 1246–1251. https://doi.org/10.1126/science.aba1120.

(33) Kuninobu, Y.; Ida, H.; Nishi, M.; Kanai, M. A Meta-Selective C–H Borylation Directed by a Secondary Interaction between Ligand and Substrate. *Nat. Chem.* **2015**, *7* (9), 712–717. https://doi.org/10.1038/nchem.2322.

(34) Lu, X.; Yoshigoe, Y.; Ida, H.; Nishi, M.; Kanai, M.; Kuninobu, Y. Hydrogen Bond-Accelerated *Meta* -Selective C–H Borylation of Aromatic Compounds and Expression of Functional Group and Substrate Specificities. *ACS Catal.* **2019**, *9* (3), 1705–1709. https://doi.org/10.1021/acscatal.8b05005.

(35) Smith, M. R.; Bisht, R.; Haldar, C.; Pandey, G.; Dannatt, J. E.; Ghaffari, B.; Maleczka, R. E.; Chattopadhyay, B. Achieving High Ortho Selectivity in Aniline C–H Borylations by Modifying Boron Substituents. *ACS Catal.* **2018**, *8* (7), 6216–6223. https://doi.org/10.1021/acscatal.8b00641.

(36) Shahzadi, H. T.; Fatima, S.; Akhter, N.; Alazmi, M.; Nawaf, A.; Said, K. B.; AlGhadhban, A.; Sulieman, A. M. E.; Saleem, R. S. Z.; Chotana, G. A. Iridium-Catalyzed C–H Borylation of CF ₃ -Substituted Pyridines. *ACS Omega* **2022**, *7* (13), 11460–11472. https://doi.org/10.1021/acsomega.2c00773.

(37) Larsen, M. A.; Hartwig, J. F. Iridium-Catalyzed C–H Borylation of Heteroarenes: Scope, Regioselectivity, Application to Late-Stage Functionalization, and Mechanism. *J. Am. Chem. Soc.* **2014**, *136* (11), 4287–4299. https://doi.org/10.1021/ja412563e.

(38) Bai, S.; Bheeter, C. B.; Reek, J. N. H. Hydrogen Bond Directed *Ortho* -Selective C–H Borylation of Secondary Aromatic Amides. *Angew. Chem. Int. Ed.* **2019**, *58* (37), 13039–13043. https://doi.org/10.1002/anie.201907366.

(39) Lam, K. C.; Lin, Z.; Marder, T. B. DFT Studies of β-Boryl Elimination Processes: Potential Role in Catalyzed Borylation Reactions of Alkenes. *Organometallics* **2007**, *26* (13), 3149–3156. https://doi.org/10.1021/om0700314.

(40) Miyaura, N.; Suzuki, A. The Palladium-Catalyzed "Head-to-Tail" Cross-Coupling Reaction of 1-Alkenylboranes with Phenyl or 1-Alkenyl Iodides. A Novel Synthesis of 2-Phenyl-1-Alkenes or 2-Alkyl-1,3-Alkadienes via Organoboranes. *J. Organomet. Chem.* **1981**, *213* (2), C53–C56. https://doi.org/10.1016/S0022-328X(00)82970-8.

(41) Ohmura, T.; Oshima, K.; Taniguchi, H.; Suginome, M. Switch of Regioselectivity in Palladium-Catalyzed Silaboration of Terminal Alkynes by Ligand-Dependent Control of Reductive Elimination. *J. Am. Chem. Soc.* **2010**, *132* (35), 12194–12196. https://doi.org/10.1021/ja105096r.

(42) Irvine, G. J.; Lesley, M. J. G.; Marder, T. B.; Norman, N. C.; Rice, C. R.; Robins, E. G.; Roper, W. R.; Whittell, G. R.; Wright, L. J. Transition Metal–Boryl Compounds: Synthesis, Reactivity, and Structure. *Chem. Rev.* **1998**, *98* (8), 2685–2722. https://doi.org/10.1021/cr9500085.

(43) Esteruelas, M. A.; Fernández, I.; Martínez, A.; Oliván, M.; Oñate, E.; Vélez, A. Iridium-Promoted B–B Bond Activation: Preparation and X-Ray Diffraction Analysis of a *Mer* -Tris(Boryl) Complex. *Inorg. Chem.* **2019**, *58* (8), 4712–4717. https://doi.org/10.1021/acs.inorgchem.9b00339.

(44) Esteruelas, M. A.; Martínez, A.; Oliván, M.; Oñate, E. Direct C–H Borylation of Arenes Catalyzed by Saturated Hydride-Boryl-Iridium-POP Complexes: Kinetic Analysis of the Elemental Steps. *Chem. – Eur. J.* **2020**, *26* (55), 12632–12644. https://doi.org/10.1002/chem.202001838.

(45) Press, L. P.; Kosanovich, A. J.; McCulloch, B. J.; Ozerov, O. V. High-Turnover Aromatic C–H Borylation Catalyzed by POCOP-Type Pincer Complexes of Iridium. *J. Am. Chem. Soc.* **2016**, *138* (30), 9487–9497. https://doi.org/10.1021/jacs.6b03656.

(46) Esteruelas, M. A.; Martínez, A.; Oliván, M.; Oñate, E. Kinetic Analysis and Sequencing of Si–H and C–H Bond Activation Reactions: Direct Silylation of Arenes Catalyzed by an Iridium-Polyhydride. *J. Am. Chem. Soc.* **2020**, *142* (45), 19119–19131. https://doi.org/10.1021/jacs.0c07578.

(47) Sasaki, I.; Doi, H.; Hashimoto, T.; Kikuchi, T.; Ito, H.; Ishiyama, T. Iridium(i)-Catalyzed Vinylic C–H Borylation of 1-Cycloalkenecarboxylates with Bis(Pinacolato)Diboron. *Chem. Commun.* **2013**, *49* (68), 7546. https://doi.org/10.1039/c3cc44149k.

(48) Kikuchi, T.; Takagi, J.; Ishiyama, T.; Miyaura, N. Iridium-Catalyzed Vinylic C–H Borylation of Cyclic Vinyl Ethers by Bis(Pinacolato)Diboron. *Chem. Lett.* **2008**, *37* (6), 664–665. https://doi.org/10.1246/cl.2008.664.

(49) Wang, G.; Liang, X.; Chen, L.; Gao, Q.; Wang, J.; Zhang, P.; Peng, Q.; Xu, S. Iridium-Catalyzed Distal Hydroboration of Aliphatic Internal Alkenes. *Angew. Chem. Int. Ed.* **2019**, *58* (24), 8187–8191. https://doi.org/10.1002/anie.201902464.

(50) Fiorito, D.; Mazet, C. Ir-Catalyzed Selective Hydroboration of 2-Substituted 1,3-Dienes: A General Method to Access Homoallylic Boronates. *ACS Catal.* **2018**, *8* (10), 9382–9387. https://doi.org/10.1021/acscatal.8b02334.

(51) Hunter, N. M.; Vogels, C. M.; Decken, A.; Bell, A.; Westcott, S. A. [Cp*IrCl2]2 Catalyzed Hydroborations of Alkenes Using a Bulky Dioxaborocine. *Inorganica Chim. Acta* **2011**, *365* (1), 408–413. https://doi.org/10.1016/j.ica.2010.09.051.

(52) Yamamoto, Y.; Fujikawa, R.; Umemoto, T.; Miyaura, N. Iridium-Catalyzed Hydroboration of Alkenes with Pinacolborane. *Tetrahedron* **2004**, *60* (47), 10695–10700. https://doi.org/10.1016/j.tet.2004.09.014.

(53) Evans, D. A.; Fu, G. C.; Hoveyda, A. H. Rhodium(I)- and Iridium(I)-Catalyzed Hydroboration Reactions: Scope and Synthetic Applications. *J. Am. Chem. Soc.* **1992**, *114* (17), 6671–6679. https://doi.org/10.1021/ja00043a009.

(54) Kamio, S.; Yoshida, H. Synthetic Chemistry with Lewis Acidity-Diminished B(Aam) and B(Dan) Groups: Borylation Reactions and Direct Cross-Couplings. *Adv. Synth. Catal.* **2021**, *363* (9), 2310–2324. https://doi.org/10.1002/adsc.202001460.

(55) Yoshida, H.; Li, J. Recent Advances in Synthetic Transformations with Robust Yet Reactive B(Dan) Moiety. *HETEROCYCLES* **2021**, *102* (8), 1478. https://doi.org/10.3987/REV-20-949.

(56) Zhang, C.; Hu, W.; Lovinger, G. J.; Jin, J.; Chen, J.; Morken, J. P. Enantiomerically Enriched α-Borylzinc Reagents by Nickel-Catalyzed Carbozincation of Vinylboronic Esters. *J. Am. Chem. Soc.* **2021**, *143* (35), 14189–14195. https://doi.org/10.1021/jacs.1c05274.

(57) Wilhelmsen, C. A.; Zhang, X.; Myhill, J. A.; Morken, J. P. Enantioselective Synthesis of Tertiary B-Boryl Amides by Conjunctive Cross-Coupling of Alkenyl Boronates and Carbamoyl Chlorides. *Angew. Chem. Int. Ed.* **2022**, *61* (15). https://doi.org/10.1002/anie.202116784.

(58) Dorn, S. K.; Tharp, A. E.; Brown, M. K. Modular Synthesis of a Versatile Double-Allylation Reagent for Complex Diol Synthesis. *Angew. Chem. Int. Ed.* **2021**, *60* (29), 16027–16034. https://doi.org/10.1002/anie.202103435.

(59) Myhill, J. A.; Wilhelmsen, C. A.; Zhang, L.; Morken, J. P. Diastereoselective and Enantioselective Conjunctive Cross-Coupling Enabled by Boron Ligand Design. *J. Am. Chem. Soc.* **2018**, *140* (45), 15181–15185. https://doi.org/10.1021/jacs.8b09909.

(60) Iwadate, N.; Suginome, M. Rhodium-Catalyzed Dehydroborylation of Styrenes with Naphthalene-1,8-Diaminatoborane [(Dan)BH]: New Synthesis of Masked β-Borylstyrenes as New Phenylene–Vinylene Cross-Coupling Modules. *Chem. Lett.* **2010**, *39* (6), 558–560. https://doi.org/10.1246/cl.2010.558.

(61) Iwadate, N.; Suginome, M. Synthesis of B-Protected β-Styrylboronic Acids via Iridium-Catalyzed Hydroboration of Alkynes with 1,8-Naphthalenediaminatoborane Leading to Iterative Synthesis of Oligo(Phenylenevinylene)s. *Org. Lett.* **2009**, *11* (9), 1899–1902. https://doi.org/10.1021/ol9003096.

(62) Yoshida, H.; Kimura, M.; Tanaka, H.; Murashige, Y.; Kageyuki, I.; Osaka, I. An Anthranilamide-Substituted Borane [H–B(Aam)]: Its Stability and Application to Iridium-Catalyzed Stereoselective Hydroboration of Alkynes. *Chem. Commun.* **2019**, *55* (38), 5420–5422. https://doi.org/10.1039/C9CC02002K.

131

(63)   Du, R.; Liu, L.; Xu, S. Iridium-Catalyzed Regio- and Enantioselective Borylation of Unbiased Methylene C(Sp[3])–H Bonds at the Position β to a Nitrogen Center. *Angew. Chem. Int. Ed.* **2021**, *60* (11), 5843–5847. https://doi.org/10.1002/anie.202016009.

(64)   Hitosugi, S.; Tanimoto, D.; Nakanishi, W.; Isobe, H. A Facile Chromatographic Method for Purification of Pinacol Boronic Esters. *Chem. Lett.* **2012**, *41* (9), 972–973. https://doi.org/10.1246/cl.2012.972.

(65)   Chang, N.; Chen, X.; Nonobe, H.; Okuda, Y.; Mori, H.; Nakajima, K.; Nishihara, Y. Synthesis of Substituted Picenes through Pd-Catalyzed Cross-Coupling Reaction/Annulation Sequences and Their Physicochemical Properties. *Org. Lett.* **2013**, *15* (14), 3558–3561. https://doi.org/10.1021/ol401375n.

(66)   Reid, W. B.; Spillane, J. J.; Krause, S. B.; Watson, D. A. Direct Synthesis of Alkenyl Boronic Esters from Unfunctionalized Alkenes: A Boryl-Heck Reaction. *J. Am. Chem. Soc.* **2016**, *138* (17), 5539–5542. https://doi.org/10.1021/jacs.6b02914.

(67)   Du, R.; Liu, L.; Xu, S. Iridium-Catalyzed Regio- and Enantioselective Borylation of Unbiased Methylene C(Sp3)–H Bonds at the Position β to a Nitrogen Center. *Angew. Chem. - Int. Ed.* **2021**, *60* (11), 5843–5847. https://doi.org/10.1002/anie.202016009.

(68)   Hitosugi, S.; Tanimoto, D.; Nakanishi, W.; Isobe, H. A Facile Chromatographic Method for Purification of Pinacol Boronic Esters. *Chem. Lett.* **2012**, *41* (9), 972–973. https://doi.org/10.1246/cl.2012.972.

(69)   Wrackmeyer, B. Organoboron Chemistry. In *Modern Magnetic Resonance*; Webb, G. A., Ed.; Springer: Dordrecht, The Netherlands, 2008; pp 455–457.

(70)   Liu, Z.; Wei, W.; Xiong, L.; Feng, Q.; Shi, Y.; Wang, N.; Yu, L. Selective and Efficient Synthesis of Trans-Arylvinylboronates and Trans-Hetarylvinylboronates Using Palladium Catalyzed Cross-Coupling. *New J. Chem.* **2017**, *41* (8), 3172–3176. https://doi.org/10.1039/C6NJ03984G.

(71)   Shi, X.; Li, S.; Wu, L. H2-Acceptorless Dehydrogenative Boration and Transfer Boration of Alkenes Enabled by Zirconium Catalyst. *Angew. Chem. Int. Ed.* **2019**, *58* (45), 16167–16171. https://doi.org/10.1002/anie.201908931.

(72)   Jang, W. J.; Kang, B.-N.; Lee, J. H.; Choi, Y. M.; Kim, C.-H.; Yun, J. NHC-Copper-Thiophene-2-Carboxylate Complex for the Hydroboration of Terminal Alkynes. *Org. Biomol. Chem.* **2019**, *17* (21), 5249–5252. https://doi.org/10.1039/C9OB00839J.

(73)   Aelterman, M.; Sayes, M.; Jubault, P.; Poisson, T. Electrochemical Hydroboration of Alkynes. *Chem. – Eur. J.* **2021**, *27* (32), 8277–8282. https://doi.org/10.1002/chem.202101132.

(74)   Murray, S. A.; Luc, E. C. M.; Meek, S. J. Synthesis of Alkenyl Boronates from Epoxides with Di-[B(Pin)]-Methane via Pd-Catalyzed Dehydroboration. *Org. Lett.* **2018**, *20* (2), 469–472. https://doi.org/10.1021/acs.orglett.7b03853.

(75)   Yoshida, H.; Kimura, M.; Tanaka, H.; Murashige, Y.; Kageyuki, I.; Osaka, I. An Anthranilamide-Substituted Borane [H–B(Aam)]: Its Stability and Application to Iridium-Catalyzed Stereoselective Hydroboration of Alkynes. *Chem. Commun.* **2019**, *55* (38), 5420–5422. https://doi.org/10.1039/C9CC02002K.

(76)   Birepinte, M.; Liautard, V.; Chabaud, L.; Pucheault, M. Zirconium-Catalyzed Synthesis of Alkenylaminoboranes: From a Reliable Preparation of Alkenylboronates to a Direct Stereodivergent Access to Alkenyl Bromides. *Org. Lett.* **2020**, *22* (7), 2838–2843. https://doi.org/10.1021/acs.orglett.0c00908.

(77)   Lu, W.; Shen, Z. Direct Synthesis of Alkenylboronates from Alkenes and Pinacol Diboron via Copper Catalysis. *Org. Lett.* **2019**, *21* (1), 142–146. https://doi.org/10.1021/acs.orglett.8b03599.

(78)   González, M. J.; Bauer, F.; Breit, B. Cobalt-Catalyzed Hydroboration of Terminal and Internal Alkynes. *Org. Lett.* **2021**, *23* (21), 8199–8203. https://doi.org/10.1021/acs.orglett.1c02854.

(79)   Magre, M.; Maity, B.; Falconnet, A.; Cavallo, L.; Rueping, M. Magnesium-Catalyzed Hydroboration of Terminal and Internal Alkynes. *Angew. Chem. Int. Ed.* **2019**, *58* (21), 7025–7029. https://doi.org/10.1002/anie.201902188.

(80)   Blanchard, D. J. M.; Cservenyi, T. Z.; Manderville, R. A. Dual Fluorescent Deoxyguanosine Mimics for FRET Detection of G-Quadruplex Folding. *Chem. Commun.* **2015**, *51* (94), 16829–16831. https://doi.org/10.1039/C5CC07154B.

(81)   Kiesewetter, E. T.; O'Brien, R. V.; Yu, E. C.; Meek, S. J.; Schrock, R. R.; Hoveyda, A. H. Synthesis of *Z* -(Pinacolato)Allylboron and *Z* -(Pinacolato)Alkenylboron Compounds through Stereoselective Catalytic Cross-Metathesis. *J. Am. Chem. Soc.* **2013**, *135* (16), 6026–6029. https://doi.org/10.1021/ja403188t.

(82)   Barcan, G. A.; Patel, A.; Houk, K. N.; Kwon, O. A Torquoselective 6π Electrocyclization Approach to Reserpine Alkaloids. *Org. Lett.* **2012**, *14* (21), 5388–5391. https://doi.org/10.1021/ol302265z.

(83)   Crestey, F.; Hooyberghs, G.; Kristensen, J. L. Concise Synthesis of New Bridged-Nicotine Analogues. *Tetrahedron* **2012**, *68* (5), 1417–1421. https://doi.org/10.1016/j.tet.2011.12.029.

(84)   Li, S.; Li, J.; Xia, T.; Zhao, W. Stereoselective Synthesis of Vinylboronates by Rh-Catalyzed Borylation of Stereoisomeric Mixtures. *Chin. J. Chem.* **2019**, *37* (5), 462–468. https://doi.org/10.1002/cjoc.201800575.

(85)   Myhill, J. A.; Wilhelmsen, C. A.; Zhang, L.; Morken, J. P. Diastereoselective and Enantioselective Conjunctive Cross-Coupling Enabled by Boron Ligand Design. *J. Am. Chem. Soc.* **2018**, *140* (45), 15181–15185. https://doi.org/10.1021/jacs.8b09909.

(86)   Koo, S. M.; Vendola, A. J.; Momm, S. N.; Morken, J. P. Alkyl Group Migration in Ni-Catalyzed Conjunctive Coupling with C(Sp3) Electrophiles: Reaction Development and Application to Targets of Interest. *Org. Lett.* **2020**, *22* (2), 666–669. https://doi.org/10.1021/acs.orglett.9b04453.

(87)   Davies, G. H. M.; Mukhtar, A.; Saeednia, B.; Sherafat, F.; Kelly, C. B.; Molander, G. A. Azaborininones: Synthesis and Structural Analysis of a Carbonyl-Containing Class of Azaborines. *J. Org. Chem.* **2017**, *82* (10), 5380–5390. https://doi.org/10.1021/acs.joc.7b00747.

(88)   Cain, D.; McLaughlin, C.; Molloy, J.; Carpenter-Warren, C.; Anderson, N.; Watson, A. A Cascade Suzuki–Miyaura/Diels–Alder Protocol: Exploring the Bifunctional Utility of Vinyl Bpin. *Synlett* **2019**, *30* (07), 787–791. https://doi.org/10.1055/s-0037-1611228.

(89)   Molander, G. A.; Brown, A. R. Suzuki−Miyaura Cross-Coupling Reactions of Potassium Vinyltrifluoroborate with Aryl and Heteroaryl Electrophiles. *J. Org. Chem.* **2006**, *71* (26), 9681–9686. https://doi.org/10.1021/jo0617013.

(90)   Horino, H.; Inoue, N. Ortho Vinylation of Aromatic Amides via Cyclopalladation Complexes. *J. Org. Chem.* **1981**, *46* (22), 4416–4422. https://doi.org/10.1021/jo00335a019.

(91)   Anai, T.; Nakata, E.; Koshi, Y.; Ojida, A.; Hamachi, I. Design of a Hybrid Biosensor for Enhanced Phosphopeptide Recognition Based on a Phosphoprotein Binding Domain Coupled with a Fluorescent Chemosensor. *J. Am. Chem. Soc.* **2007**, *129* (19), 6233–6239. https://doi.org/10.1021/ja0693284.

(92)   Basel, Y.; Hassner, A. Imidazole and Trifluoroethanol as Efficient and Mild Reagents for Destruction of Excess Di-Tert-Butyl Dicarbonate [(BOC)2O]1. *Synthesis* **2001**, 550–552. https://doi.org/10.1055/s-2001-12350.

(93)   Carboni, D.; Flavin, K.; Servant, A.; Gouverneur, V.; Resmini, M. The First Example of Molecularly Imprinted Nanogels with Aldolase Type I Activity. *Chem. - Eur. J.* **2008**, NA-NA. https://doi.org/10.1002/chem.200800675.

(94)   Rusere, L. N.; Lockbaum, G. J.; Lee, S.-K.; Henes, M.; Kosovrasti, K.; Spielvogel, E.; Nalivaika, E. A.; Swanstrom, R.; Yilmaz, N. K.; Schiffer, C. A.; Ali, A. HIV-1 Protease Inhibitors Incorporating Stereochemically Defined P2′ Ligands To Optimize Hydrogen Bonding in the Substrate Envelope. *J. Med. Chem.* **2019**, *62* (17), 8062–8079. https://doi.org/10.1021/acs.jmedchem.9b00838.

(95)   Haraguchi, N.; Tsuru, K.; Arakawa, Y.; Itsuno, S. Asymmetric Transfer Hydrogenation of Imines Catalyzed by a Polymer-Immobilized Chiral Catalyst. *Org Biomol Chem* **2009**, *7* (1), 69–75. https://doi.org/10.1039/B815407B.

(96)   Reed-Berendt, B. G.; Morrill, L. C. Manganese-Catalyzed *N* -Alkylation of Sulfonamides Using Alcohols. *J. Org. Chem.* **2019**, *84* (6), 3715–3724. https://doi.org/10.1021/acs.joc.9b00203.

(97)   Ortiz, G. X.; Hemric, B. N.; Wang, Q. Direct and Selective 3-Amidation of Indoles Using Electrophilic *N* -[(Benzenesulfonyl)Oxy]Amides. *Org. Lett.* **2017**, *19* (6), 1314–1317. https://doi.org/10.1021/acs.orglett.7b00358.

(98)   Wu, F.; Zhu, S. A Strategy To Obtain *o* -Naphthoquinone Methides: Ag(I)-Catalyzed Cyclization of Enynones for the Synthesis of Benzo[*h*]Chromanes and Naphthopyryliums. *Org. Lett.* **2019**, *21* (5), 1488–1492. https://doi.org/10.1021/acs.orglett.9b00281.

(99)   He, R.; Toy, P. H.; Lam, Y. Polymer-Supported Hantzsch 1,4-Dihydropyridine Ester: An Efficient Biomimetic Hydrogen Source. *Adv. Synth. Catal.* **2008**, *350* (1), 54–60. https://doi.org/10.1002/adsc.200700344.

(100)   Zhang, L.; Dolbier, W. R.; Sheeller, B.; Ingold, K. U. Absolute Rate Constants of Alkene Addition Reactions of a Fluorinated Radical in Water. *J. Am. Chem. Soc.* **2002**, *124* (22), 6362–6366. https://doi.org/10.1021/ja0256010.

(101)   Zhuang, R.; Xu, J.; Cai, Z.; Tang, G.; Fang, M.; Zhao, Y. Copper-Catalyzed C–P Bond Construction via Direct Coupling of Phenylboronic Acids with H-Phosphonate Diesters. *Org. Lett.* **2011**, *13* (8), 2110–2113. https://doi.org/10.1021/ol200465z.

(102)   Kolomanska, J.; Johnston, P.; Gregori, A.; Fraga Domínguez, I.; Egelhaaf, H.-J.; Perrier, S.; Rivaton, A.; Dagron-Lartigau, C.; Topham, P. D. Design, Synthesis and Thermal Behaviour of a Series of Well-Defined Clickable and Triggerable Sulfonate Polymers. *RSC Adv.* **2015**, *5* (82), 66554–66562. https://doi.org/10.1039/C5RA13867A.

(103)   Sikkema, F. D.; Comellas-Aragonès, M.; Fokkink, R. G.; Verduin, B. J. M.; Cornelissen, J. J. L. M.; Nolte, R. J. M. Monodisperse Polymer–Virus Hybrid Nanoparticles. *Org Biomol Chem* **2007**, *5* (1), 54–57. https://doi.org/10.1039/B613890J.

(104)   Bhawal, B. N.; Reisenbauer, J. C.; Ehinger, C.; Morandi, B. Overcoming Selectivity Issues in Reversible Catalysis: A Transfer Hydrocyanation Exhibiting High Kinetic Control. *J. Am. Chem. Soc.* **2020**, *142* (25), 10914–10920. https://doi.org/10.1021/jacs.0c03184.

(105)   Zhou, M.-J.; Zhang, L.; Liu, G.; Xu, C.; Huang, Z. Site-Selective Acceptorless Dehydrogenation of Aliphatics Enabled by Organophotoredox/Cobalt Dual Catalysis. *J. Am. Chem. Soc.* **2021**, *143* (40), 16470–16485. https://doi.org/10.1021/jacs.1c05479.

(106)   Seo, H.; Liu, A.; Jamison, T. F. Direct β-Selective Hydrocarboxylation of Styrenes with CO_2 Enabled by Continuous Flow Photoredox Catalysis. *J. Am. Chem. Soc.* **2017**, *139* (40), 13969–13972. https://doi.org/10.1021/jacs.7b05942.

(107)   Feltenberger, J. B.; Hayashi, R.; Tang, Y.; Babiash, E. S. C.; Hsung, R. P. Enamide-Benzyne-[2 + 2] Cycloaddition: Stereoselective Tandem [2 + 2]–Pericyclic Ring-Opening–Intramolecular *N* -Tethered [4 + 2] Cycloadditions. *Org. Lett.* **2009**, *11* (16), 3666–3669. https://doi.org/10.1021/ol901434g.

(108)   Semina, E.; Tuzina, P.; Bienewald, F.; Hashmi, A. S. K.; Schaub, T. Ruthenium-Catalyzed Synthesis of Vinylamides at Low Acetylene Pressure. *Chem. Commun.* **2020**, *56* (44), 5977–5980. https://doi.org/10.1039/D0CC01533D.

(109)   Garcia-Barrantes, P. M.; Lindsley, C. W. Total Synthesis of Gombamide A. *Org. Lett.* **2016**, *18* (15), 3810–3813. https://doi.org/10.1021/acs.orglett.6b01825.

(110)   Niu, D.; Buchwald, S. L. Design of Modified Amine Transfer Reagents Allows the Synthesis of α-Chiral Secondary Amines via CuH-Catalyzed Hydroamination. *J. Am. Chem. Soc.* **2015**, *137* (30), 9716–9721. https://doi.org/10.1021/jacs.5b05446.

(111)   Zhao, D.; Xu, P.; Ritter, T. Palladium-Catalyzed Late-Stage Direct Arene Cyanation. *Chem* **2019**, *5* (1), 97–107. https://doi.org/10.1016/j.chempr.2018.09.027.

(112)   Mattsson, S.; Dahlström, M.; Karlsson, S. A Mild Hydrolysis of Esters Mediated by Lithium Salts. *Tetrahedron Lett.* **2007**, *48* (14), 2497–2499. https://doi.org/10.1016/j.tetlet.2007.02.029.

(113)   Tanwar, D. K.; Ratan, A.; Gill, M. S. A Facile Synthesis of Sulfonylureas via Water Assisted Preparation of Carbamates. *Org. Biomol. Chem.* **2017**, *15* (23), 4992–4999. https://doi.org/10.1039/C7OB00872D.

CHAPTER 4

Dehomologative Borylation of Aldehydes and Alcohols and Their Postfunctionalization Enabled by Multicatalysis

The work in this chapter was done by myself.

4.1 Introduction

Next to the C–H bond, the C–C bond is the most widespread and fundamental in organic synthesis. Its cleavage can be found in plenty of processes in nature, embedded in highly complex cascades for the fragmentation of biologically relevant structural motives.[1] Dehomologation methods, i.e., C–C cleavage reactions in which a one carbon unit is removed from the starting material, which operate directly on common functional groups, such as aldehydes and alcohols, are of high importance. Considering the unique synthetic potential of alkenyl boronate esters[2], a dehomologative borylation of broadly available[3] and versatile[4] aldehydes and alcohols would be an attractive synthetic transformation.

There are only a few examples for a direct conversion of aldehydes to alkenyl boronic esters, commonly coined as "boron-Wittig reaction"[5] (Figure 4.1). Early works, building on the well-established Takai olefination, utilized a chromium reagent to prepare vinyl boronates from dichloromethylboronic esters and aldehydes (Figure 4.1A). A more practical approach was pioneered by Matteson in the 1970s[6–8] and recently further developed by Morken, Pattison, and Grygorenko (Figure 4.1B).[9–11] This method makes use of geminal bis(pinacolboronates) that, upon deprotonation, undergo reaction with the respective aldehyde to deliver vinyl boronates with high E/Z selectivities. However, these transformations are homologative, i.e., a one carbon unit is introduced into the starting material. A direct conversion of allylic and aliphatic alcohols to alkenyl boronic esters remains elusive to date.

A)
Takai and Moriwake

B)
Matteson, Morken, Pattison, Grygorenko
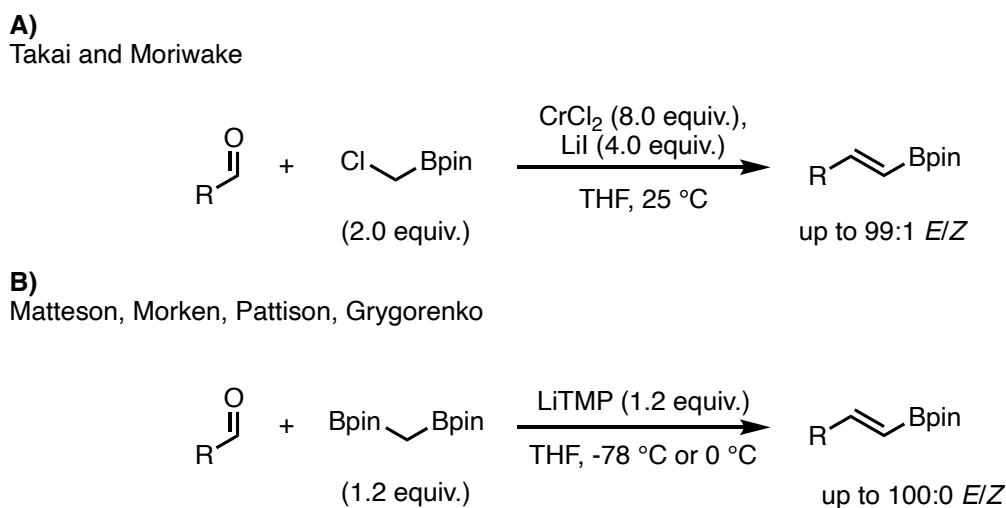
Figure 4.1. Literature precedences for reactions of aldehydes to vinyl boronate esters, **A)** Takai-type olefination; **B)** Boron-Wittig reaction.

To achieve an unprecedented dehomologative borylation of aldehydes and alcohols, I considered a multicatalytic approach utilizing the unique reactivity of Rh- and Ir-complexes. I envisioned a relay-type reaction in which the aldehyde or alcohol undergoes defunctionalization to form the corresponding dehomologated alkene, which can then undergo borylation to form the alkenyl boronate ester (Figure 4.2C). Ideally, the boronate ester can undergo postfunctionalization *in situ* to give access to a wide range of products in a one-pot process.

The dehomologation of aldehydes and alcohols using Rh-catalysis has been described by Dong.[12,13] The aldehyde undergoes dehydroformylation to the alkene with transfer of the formyl group and hydride to an acceptor, usually norbornadiene. The subsequently reported oxidative dehydroxymethylation features a Rh-catalyzed oxidation of the alcohol to the aldehyde with transfer of an equivalent of hydrogen to an acceptor (*N*,*N*-dimethylacryl amide), followed by dehydroformylation with transfer of another equivalent of hydrogen to the acceptor and release of carbon monoxide. In turn, the allylic alcohol undergoes isomerization to the aldehyde followed by dehydroformylation. The catalytic system for these three transformations, which consists of [Rh(cod)OMe]$_2$, xantphos, and 3-OMeBzOH, employs the same Rh-precursor and ligand as the Rh-catalyzed transfer C–H borylation described in this thesis (Figure 4.2B, cf. chapter 2). Further, the Ir-catalyzed transfer borylation (cf. chapter 3) represents a more robust catalytic system for the borylation of alkenes, showcased by a higher functional group tolerance (cf. chapter 3).
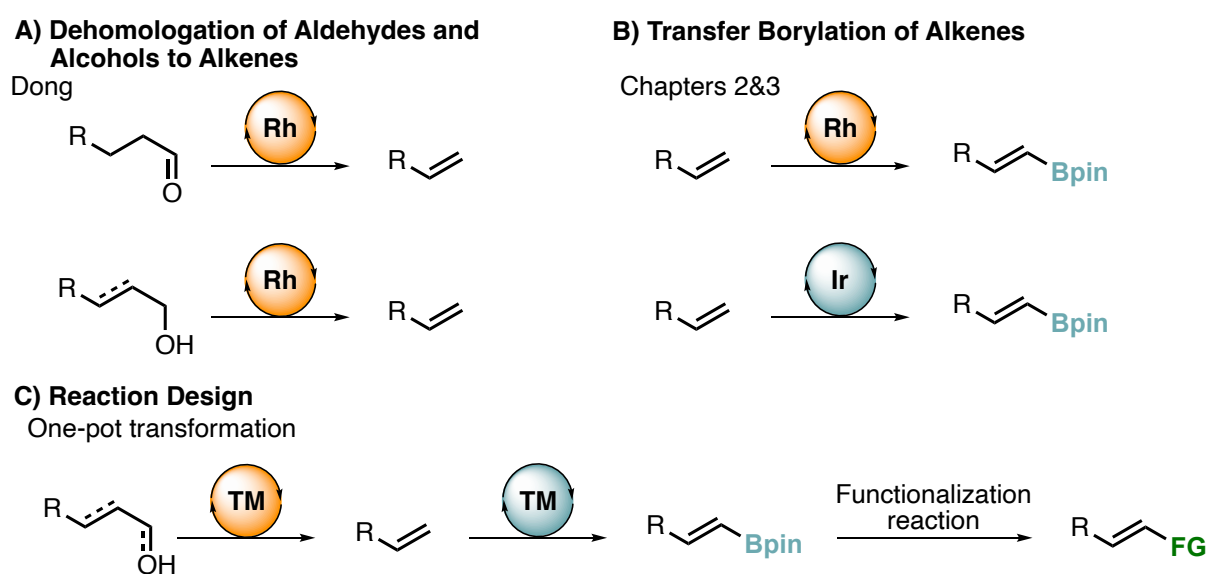
Figure 4.2. A) Methods for the dehomologation of aldehydes and (allylic) alcohols, B) methods for transfer borylation; C) reaction design.

This chapter describes studies toward the merger of Rh-catalyzed dehydroformylation and dehydroxymethylation and Rh- or Ir-catalyzed transfer borylation reactions in a multicatalytic process (Figure 4.1D). Different approaches to achieve such process were considered, which are discussed in detail below. A perspective discussing the different classes of multicatalysis, which are only briefly introduced in this chapter, and the challenges associated with each one of them in detail is presented in chapter 5.

4.2 Results and Discussion

In light of the extensive experience with styrene as the model substrate for transfer borylation reactions (cf. chapters 2 and 3), hydrocinnamaldehyde, cinnamic alcohol, and 3-phenylpropanol, were selected as model substrates for the dehomologative borylation reactions. All three are produced by the use of well-established selective hydrogenation reactions from the biomass-derived cinnamaldehyde.[11] The studies were started with

attempts to merge the dehydroformylation of aldehydes, the least complex of the three dehomologation reactions, with transfer borylation.

4.2.1. Orthogonal or Auto-Relay Catalysis

One-pot processes in which at least two catalytic transformations occur in the presence of one or more catalysts as a sequence of independent reactions are typically referred to as "relay catalysis".[14] Importantly, the catalytic cycles do not share any catalytic intermediates. From the viewpoint of operational simplicity, orthogonal and auto-relay catalysis are the most appealing strategies. Here, all reagents are present from the start and no further manipulation, i.e., addition of reagents or change of reaction conditions, is required. However, due to the possible incompatibility of the different reagents required for each transformation, they are also the most challenging to develop. The sole difference between orthogonal and auto-relay catalysis is the number of catalysts. Transformations that proceed through auto-relay catalysis make use of only one (pre)catalyst that mediates all transformations.

Considering the high resemblance of the catalytic systems for the dehydroformylation and transfer borylation (both utilize [Rh(cod)OMe]$_2$ as a catalyst precursor and xantphos as ligand), an approach utilizing auto-relay catalysis, appeared to be the most promising. The studies commenced with experiments to evaluate whether both transformations could be independently performed under similar reaction conditions (temperature, solvent, reaction time). If this was not the case, the reaction could not proceed under auto-relay catalysis. Both dehydroformylation of hydrocinnamaldehyde and transfer borylation of styrene could be performed under the same set of reaction conditions (Figure 4.3) - at 90 °C, 16 h reaction time, 1,4-dioxane as the solvent - with 91% and 92% yield, respectively. This set of conditions served as the basis for the following investigations. Dimethyl maleate was chosen as the acceptor over norbornadiene (as reported by Dong) because only one equivalent is required for the full conversion of the starting aldehyde to form the alkene in a nearly quantitative yield. Therefore, possible side reactions, such as the borylation of resting acceptor, are obliviated. It was further validated that the transfer borylation could occur in the presence of 3-methoxybenzoic acid, the co-catalyst required for dehydroformylation.

A) Dehydroformylation

Ph⌒⌒CHO
[Rh(cod)OMe]$_2$ (1 mol%), xantphos (2 mol%), 3-OMeBzOH (2 mol%) / dimethyl maleate (1.0 equiv.), 1,4-dioxane, 90 °C, 16 h → Ph⌒⫝ 91% yield

B) Transfer Borylation

Ph⫝
[Rh(cod)OMe]$_2$ (2 mol%), xantphos (4 mol%) / vinyl Bpin (1.5 equiv.), 1,4-dioxane, 90 °C, 16 h → Ph⌒⫝—Bpin 92% yield
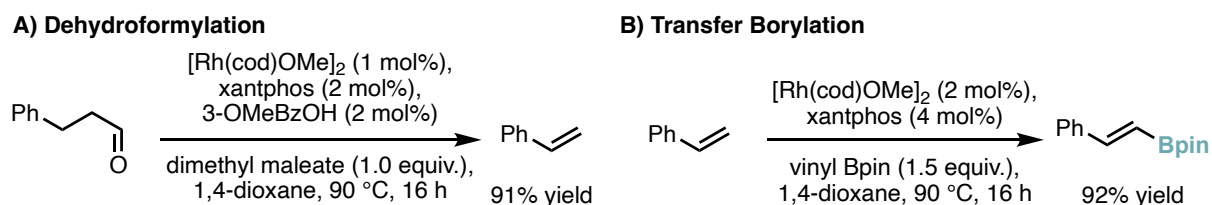
Figure 4.3: Dehydroformylation and transfer borylation under the same set of conditions.

Table 4.1 summarizes the efforts toward the target transformation. When combining all the reagents required for both reactions in a one-pot setup with the reaction conditions from Figure 4.3, no target product **3a** and 57% of intermediate **2a** were obtained (entry 1). At elevated temperatures 8% **3a** alongside 70% **2a** were formed (entry 2). In principle, this experiment confirmed the possibility to achieve such transformation in the auto-relay fashion. The dehydroformylation worked well (full conversion of **1a**); however, the transfer borylation

was inefficient. A control reaction revealed that dimethyl maleate is not compatible with the transfer borylation reaction therefore hindering the formation of **3a**. When using norbornadiene, a common hydrogen acceptor for the dehydroformylation reaction, was used instead of dimethyl maleate, no target product **3a** was formed alongside 65% **2a** (entry 3). The use of norbornene lead to only traces of **3a** and 64% of **2a** (entry 4). In both cases, **1a** was not fully converted (69% and 64%, respectively). I surmised that vinyl Bpin itself could act as the hydrogen acceptor. When using no additional acceptor, 5% of target product **3a** along with 76% intermediate **2a** were obtained (entry 5). The addition of catalytic amounts of B_2pin_2, which tends to promote the precatalyst activation, thereby improving the performance of the borylation catalyst, was not effective here (entry 6). Since there was no additional hydrogen acceptor added, 80% of "ethyl Bpin" – through hydrogenation of the double bond of vinyl Bpin, and 20% of ethylbenzene were formed. A higher loading of vinyl Bpin (2.0 – 3.0 equiv., entries 7 – 10), however, was detrimental for the reaction and led to the formation of lower amounts of **2a** and **3a**. Since **1a** was fully consumed, it is very likely that side-reactions consumed **2a** *in situ*. However, the nature of these side reactions could not be elucidated. The formation of common side-products, such as products of hydroboration or diborylation, were excluded by GC-MS and NMR analyses. A longer reaction time did not improve the outcome of the reaction (entries 11 and 12).

In order to improve the transfer borylation, the use of a mix of Rh- and Ir-catalysts, i.e., orthogonal relay catalysis, was tried. In contrast to the Rh-catalyst, under these conditions, the Ir-catalyst does not perform dehydroformylation but only transfer borylation. The reaction, however, turned out to be more complex (Table 4.1, entries 13 and 14). Under the reaction conditions of Figure 4.3 (Ir-catalyzed transfer borylation proceeds under the same conditions, cf. chapter 3), almost full conversion of **1a** was observed. However, only up to 5% of **2a** and no desired product **3a** could be obtained. The nature of the side reactions could not be elucidated. Again, the formation of expected side products, such as products of hydroboration or diborylation, was excluded by GC-MS and HRMS analyses.

In summary, the transformation utilizing orthogonal and auto-relay catalysis could not be realized. Although initial studies show the feasibility of the reaction in principle, the incompatibility of the reagents and the catalysts could not be overcome.

Table 4.1: Summary of the studies toward a dehomologative borylation of aldehydes under orthogonal or auto-relay catalysis.
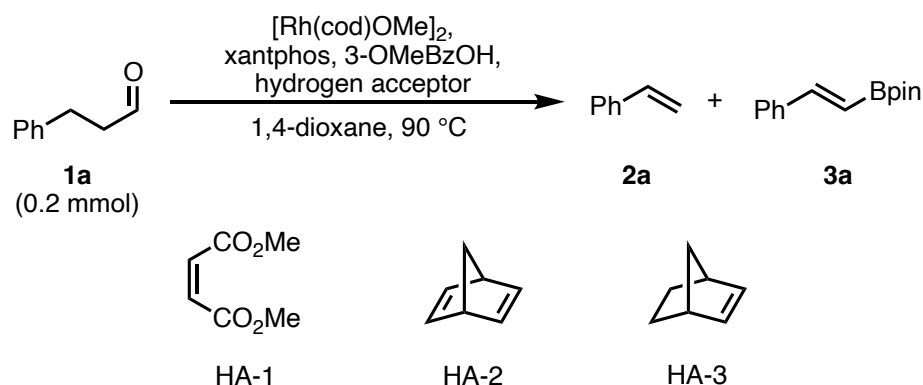
entry	[Rh][a]	time	hydrogen acceptor[b]	vBpin[b,c]	conv. **1a**	yield **2a**	yield **3a**
1	4	16 h	HA-1 (1.0)	1.5	100%	57%	-
2[d]	4	16 h	HA-1 (1.0)	1.5	100%	70%	8%
3	4	16 h	HA-2 (1.5)	1.5	69%	65%	-
4	4	16 h	HA-3 (1.5)	1.5	64%	64%	trace
5	4	16 h	-	1.5	100%	76%	5%
6[e]	4	16 h	-	1.5	100%	71%	6%
7	4	16 h	-	2.0	100%	78%	6%
8	4	16 h	-	2.5	100%	57%	4%
9	4	16 h	-	3.0	100%	54%	trace
10[e]	4	16 h	-	3.0	100%	44%	trace
11	4	48 h	-	3.0	100%	48%	trace
12[e]	4	48 h	-	3.0	100%	40%	trace
13[f]	2	16 h	-	2.0	85%	5%	-
14[g]	2	16 h	-	2.0	71%	4%	-

[a] [Rh] = [Rh(cod)OMe]$_2$/xantphos/3-OMeBzOH 1:2:2 ratio in mol% of [Rh(cod)OMe]$_2$; [b] in equiv.; [c] vBpin = vinyl Bpin; [d] at 120 °C; [e] with 4 mol% B$_2$pin$_2$; [f] with 1 mol% [Ir] = [Ir(cod)Cl]$_2$/ JohnPhos 1:4 ratio; [g] with 2 mol% [Ir] = [Ir(cod)Cl]$_2$/ JohnPhos 1:4 ratio.

4.2.2. Sequential Catalysis

As the transformation proved to be very challenging when all reagents are present from the start, using sequential catalysis was tested. In this approach, the catalysts and reagent required for each step are added sequentially. In general, this simplifies compatibility issues and the reaction optimization compared to orthogonal or auto-relay catalysis.

Initial studies showed that the dehydroformylation can be performed using 1 mol% of [Rh(cod)OMe]$_2$ (cf. Figure 4.3) and with 1.0 equiv. of dimethyl maleate as hydrogen acceptor. The latter is fully converted to dimethyl succinate, which does not interfere with the transfer borylation reaction.

Table 4.2 shows the evaluation of catalysts for the transfer borylation. Three different catalytic systems were evaluated: [Rh] consisting of [Rh(cod)OMe]$_2$ and xantphos, as described in chapter 2, [Ir] consisting of [Ir(cod)Cl]$_2$ and Johnphos, as described in chapter 3, and [Ir-2]

consisting of [Ir(cod)OMe]$_2$. During the studies of the Ir-catalyzed transfer borylation, [Ir(cod)OMe]$_2$ proved to be a suitable precursor for the borylation of styrene even without additional phosphine ligands, although with a much lower functional group compatibility.

Table 4.2: Evaluation of a suitable borylation catalyst for the sequential dehomologative borylation.

[Rh(cod)OMe]$_2$ (1 mol%),
xantphos (2 mol%),
3-OMeBzOH (2 mol%),
dimethyl maleate (1.0 equiv.)

Ph — CH$_2$CHO (O)
1a
(0.2 mmol)

1,4-dioxane, 90 °C, 16 h → Ph (2a) → [Rh] or [Ir] or [Ir-2], 1,4-dioxane, 90 °C, 16 h → Ph~Bpin (3a)

entry	[Rh][a]	[Ir][b]	[Ir-2][c]	B$_2$pin$_2$[d]	vBpin[e,f]	conv. **1a**	yield **2a**	yield **3a**
1	2	-	-	5	1.5	100%	46%	trace
2	-	2	-	5	1.5	100%	68%	6%
3	-	-	2	5	1.5	100%	85%	18%
4	-	4	-	10	1.5	100%	64%	39%
5	-	-	4	10	1.5	100%	83%	14%
6[g]	-	4	-	10	1.5	100%	49%	46%
7[h]	-	4	-	10	1.5	100%	74%	12%

[a] [Rh] = [Rh(cod)OMe]$_2$/xantphos 1:2 ratio in mol% of [Rh(cod)OMe]$_2$; [b] [Ir] = [Ir(cod)Cl]$_2$/ JohnPhos 1:4 ratio in mol% of [Ir(cod)Cl]$_2$; [c] [Ir(cod)Cl]$_2$ in mol%; [d] in mol%; [e] vBpin = vinyl Bpin; [f] in equiv.; [g] additional 1,4-dioxane (300 μL) for 2nd step; [h] additional 1,4-dioxane (750 μL) for 2nd step.

When using the Rh-catalyst, 46% of **2a** and only traces of **3a** were obtained in the model reaction. In turn, the reactions with Ir-based catalysts [Ir] and [Ir-2] formed target **3a** in 6% and 18% yield, respectively. Doubling the loading of [Ir] resulted in an increase of the yield of **3a** to 39%, (entry 4), while it had limited effect on the reaction with [Ir-2] (14% of **3a**, entry 5). Therefore, [Ir] was further evaluated. The yield of the reaction was improved by adding an extra portion of 1,4-dioxane (300 μL) for the borylation step (46%, entry 6), although further dilution was detrimental for the reaction (12%, entry 7).

To further increase the yield of **3a**, the effects of the ligand and vinyl Bpin loadings were evaluated (Table 4.3). I observed that reactions with an increased loading of vinyl Bpin occurred with higher yields of **3a** (up to 74%, entry 2); however, these results were poorly reproducible. In turn, the reactions with an increased loading of JohnPhos to 24 mol% formed **3a** in 62% yield (entry 3), but the further increase of ligand loading was detrimental for the reaction (22% yield with 32 mol% Johnphos, entry 4). A reaction with higher loadings of both vinyl Bpin and ligand furnished **3a** in 60% yield (entry 5). Higher loadings of vinyl Bpin lowered the yield. Using tBu-xantphos instead of JohnPhos (cf. chapter 3) did not yield any product **3a** (entry 7).

Table 4.3: Optimization of ligand and vinyl Bpin loading.

entry	Variation from reaction conditions	conv. **1a**	yield **2a**	yield **3a**
1	none	100%	49%	46%
2	2.0 equiv. vinyl Bpin	100%	23%	up to 74%[a]
3	24 mol% JohnPhos	100%	41%	62%
4	32 mol% JohnPhos	100%	67%	22%
5	2.0 equiv. vinyl Bpin and 24 mol% JohnPhos	100%	34%	60%
6	3.0 equiv. vinyl Bpin and 24 mol% JohnPhos	100%	74%	36%
7	2.0 equiv. vinyl Bpin and 8 mol% tBu-xantphos	100%	84%	n.d.

[a] result reproducible, yield of **3** ranged between 20% and 74%; n.d., not detected.

Further experimentation showed that the yield of the target product could be increased by varying the additional solvent and temperature of the borylation step. Specifically, when adding an extra portion of THF instead of 1,4-dioxane, **3a** was formed in 68% yield (Table 4.4, entry 2). When the second stop was conducted at an increased temperature (110 °C), the target product was formed in 80% yield (entry 3).

Table 4.4: Variation of solvent and temperature.

entry	Variation from reaction conditions	conv. **1a**	yield **2a**	yield **3a**
1	none	100%	34%	60%
2	+ 300 μL THF instead of 1,4-dioxane for 2nd step	100%	25%	68%[a]
3	like entry 2 and 110 °C	100%	7%	80%

[a] average of three runs.

4.2.3. Allylic and Aliphatic Alcohols

Having established a high-yielding method for the dehomologative borylation of aldehydes, the question arose whether the same protocol was also transferable to allylic and aliphatic alcohols. First, the reaction conditions for the dehomologation and formation of the alkene

were evaluated for the two model substrates cinnamic alcohol and 3-phenylpropanol and the optimal conditions are shown in Figure 4.4.

The allylic alcohol underwent dehomologation under the exact same conditions as the aldehyde and formed styrene in 79% yield (Figure 4.4A).
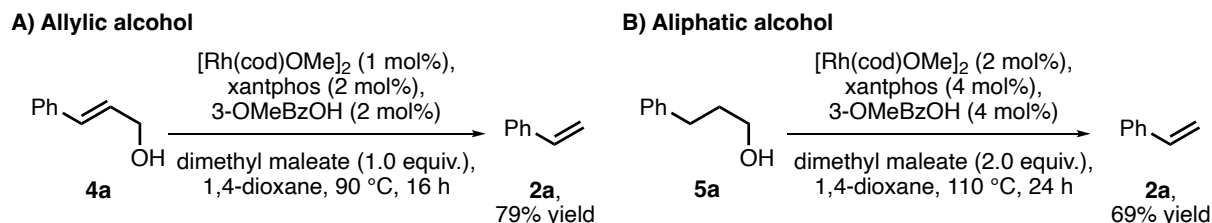

Figure 4.4: Dehomologation of cinnamic alcohol and 3-phenylpropanol.

Since the reaction for aliphatic alcohol is more complex (first oxidation to aldehyde, then dehydroformylation), the conditions were adjusted. Under optimized conditions, styrene is formed in 69 % yield. The optimized conditions consist of an increase of the catalyst loading, the use of an additional equivalent of the hydrogen acceptor (required for the oxidation step), and an increase of the reaction temperature and an extended reaction time.
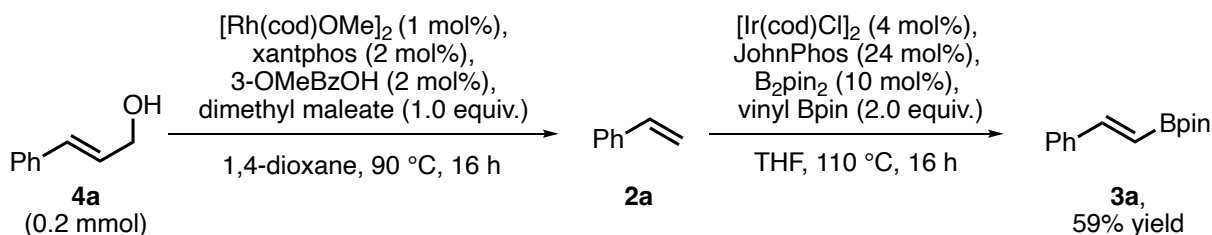
Figure 4.5: Full system for cinnamyl alcohol.

The evaluation of the reaction of **4a** in the full system with the same conditions as before furnished **3a** in 59% yield (Figure 4.5). Likewise, the transfer of the previously evaluated reaction conditions for the borylation was tried for aliphatic alcohol **4a**. However, only 28% of product **3a** were obtained. This is likely due to the higher catalyst loading for the conversion of **4a** to **2a** and the partial incompatibility of the two catalysts as discussed above (cf. 4.2.1).

Figure 4.6. Dehomologative borylation of aliphatic alcohol **5a**.

4.2.4. Hydroboration

To expand the utility of the strategy, the synthesis of alkyl boronate esters was further evaluated. I surmised that these target molecules can be accessed through hydroboration of alkene intermediates, as described in the literature under iridium catalysis using [Ir(cod)Cl]$_2$,

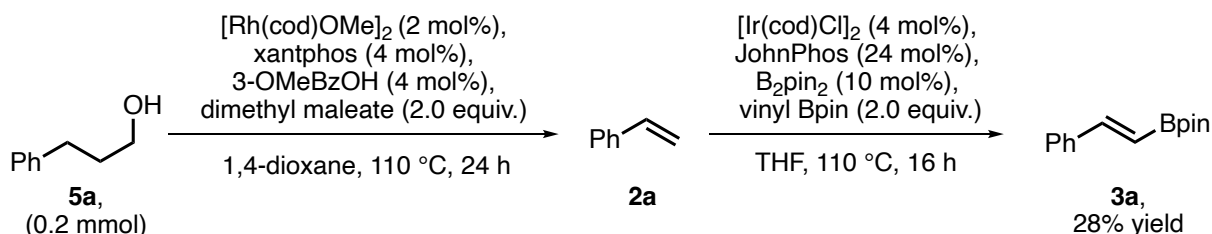dppb and pinacolborane (HBpin) as the borylation reagent.[15] When translating these reaction conditions to the multicatalytic protocol, **6a** was furnished in 89% yield (Figure 4.7A). Importantly, the reaction could be realized without the addition of Ir-catalyst in the second step, still furnishing **6a** in 85% yield and with excellent selectivity for the linear product. In this case, the Rh-catalyst from the first step catalyzes the hydroboration. This scenario is referred to as assisted-relay catalysis (cf. chapter 5).
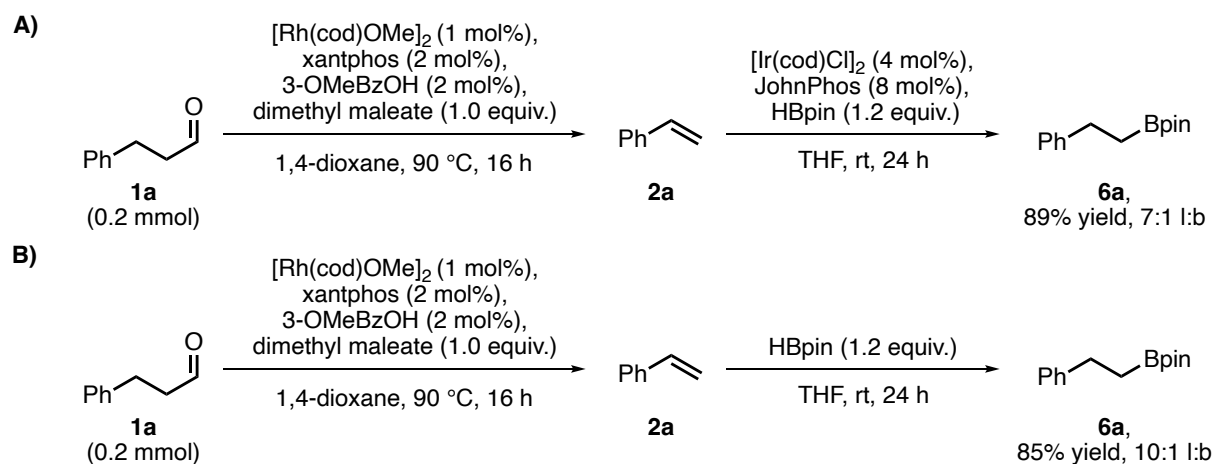
Figure 4.7. Access to alkyl boronates in one-pot reaction through sequential catalysis (A) and assisted-relay catalysis (B).

Further, the same reaction was also tried for allylic and aliphatic alcohols (Figure 4.8). In both cases, product **6a** was furnished in excellent yields of 81% and 76%, respectively.
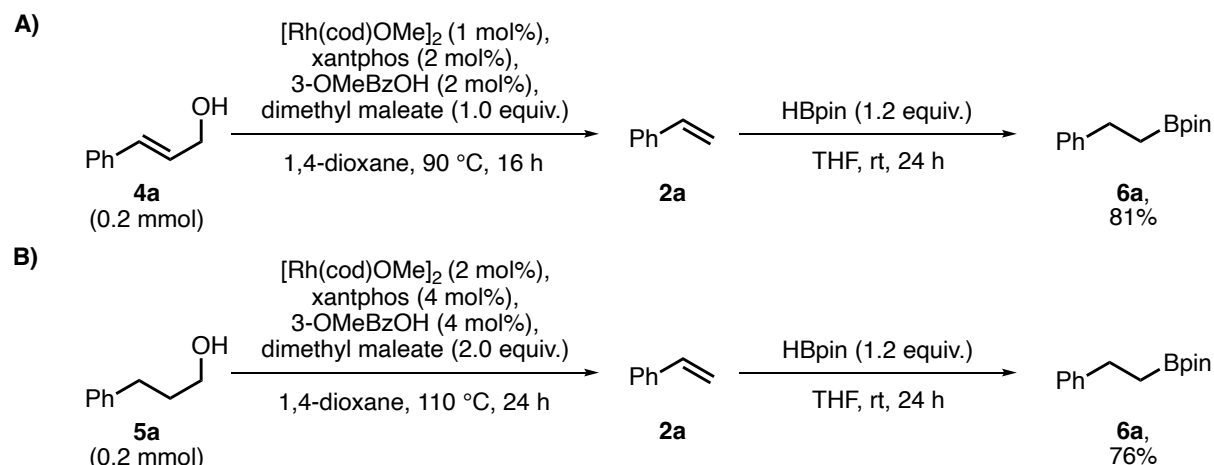
Figure 4.8. Access to alkyl boronate **6a** from allylic alcohol **4a** (A) and aliphatic alcohol **5a** (B).

4.2.5. Scope of substrates

To illustrate the applicability of the method to substrates bearing substituents other than phenyl, a preliminary scope was evaluated using the structurally and electronically varied substrates. shown in Figures 4.9 and 4.10.

145

Figure 4.9 shows the evaluation of aldehyde and allylic alcohol starting materials. The corresponding products after transfer borylation or hydroboration could be formed in moderate to excellent yields (41% - 88%). For **1c**, the lower yields compared to **1a** and **1b** can be explained by the higher reactivity of the intermediate alkene **2c** to act as the competing hydrogen acceptor. The corresponding hydrogenated by-product, *N*-ethyl phthalimide, was observed by GC-MS analysis of the reaction mixture. Unfortunately, phenyl ether substituted aldehyde **1d** did not undergo dehydroformylation and could therefore not be further functionalized, establishing a current limitation of the method.
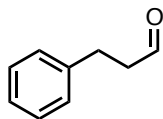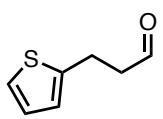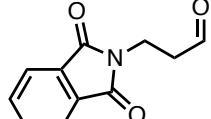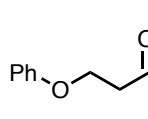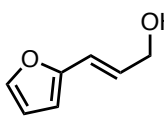

Dehomologative borylation to	**1a**	**1b**	**1c**	**1d**	**4f**
vinyl boronates:	**3a**: 80%	**3b**: 88%	**3c**: 40%	**3d**: <5%	**3f**: 38%
alkyl boronates:	**6a**: 85%	**6b**: 81%	**6c**: 31%[a]	**6d**: <5%	**6f**: 60%

Figure 4.9. Scope of the reaction starting from aldehyde starting materials; all crude yields under standard conditions (for details, see 4.2.2. and 4.4); [a] isolated yield.

The evaluation of the scope for transformations from aliphatic alcohols is shown in Figure 4.10. All alcohols underwent the dehomologation to the corresponding alkene smoothly (50 – 79% yield), including alcohol **5d** that is the analogue of **1d**. In the full system, all substrates underwent hydroboration to form the corresponding alkyl boronates **6b-6e** in good yields. Unfortunately, transfer borylation proved to be ineffective and the corresponding alkenyl boronates could not be formed in analogy to the discussion in 4.2.3.
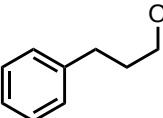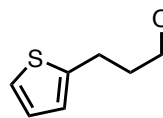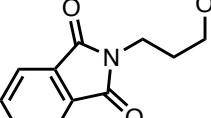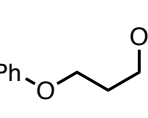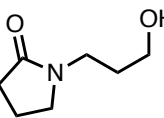
Dehomologative borylation to	**5a**	**5b**	**5c**	**5d**	**5e**
vinyl boronates:	**3a**: 28%	**3b**: <5%	**3c**: <5%	**3d**: <5%	**3e**: <5%
alkyl boronates:	**6a**: 79%	**6b**: 67%	**6c**: 37%[a]	**6d**: 31%[a]	**6e**: <5%

Figure 4.10. Scope of the reaction starting from aliphatic alcohols; all crude yields under standard conditions (for details, see 4.2.3. and 4.4); [a] isolated yield.

4.2.6. Postfunctionalization reactions

As discussed in the introduction, the combination of dehomologative borylation with postfunctionalization reactions to convert the boronic ester product *in situ* is desirable. It would expand the one-pot access to an even wider range of products and could therefore improve the utility of the transformation. To showcase this potential of the transformation, two examples of postfunctionalization reactions were chosen – a Suzuki-Miyaura cross coupling and an oxidation reaction.

Suzuki-Miyaura cross coupling

The arguably most known and most used reaction of boronic esters is the Suzuki-Miyaura cross coupling.[16] Therefore, the combination of the dehomologative borylation is of high utility and highly desirable. Figure 4.11 shows the combination of the standard reaction starting from **1a** to form **3a** and a subsequent Suzuki-Miyaura coupling with 3-methoxyphenylbromide. The final product **7** was obtained in 64% isolated overall yield showing the high efficiency of the overall process. Such transformation, i.e., a dehomolgative C_{sp2}–C_{sp2} coupling starting from aliphatic aldehydes has not been described in the literature.
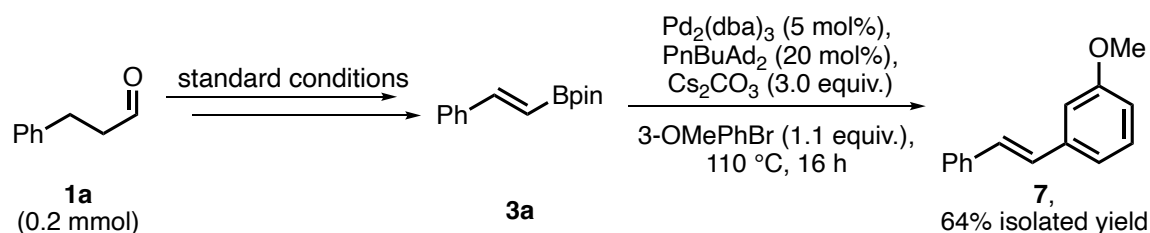
Figure 4.11. One-pot postfunctionalization by Suzuki-Miyaura cross coupling.

Oxidation

Alkyl boronic esters have been shown to be easily oxidized in the presence of a mixture of hydrogen peroxide and sodium hydroxide. This has been used to facilitate the isolation of the commonly unstable boronic ester products.[17] Figure 4.12 shows the combination of the standard reaction starting from **4a** or **4b** to form **5a** or **5b** and a subsequent oxidation. The final products **8a** and **8b** could be obtained in 41% and 29% isolated overall yield, respectively. Consequently, an overall dehomologation of aliphatic alcohols to alcohols is achieved that has not been reported in the literature.
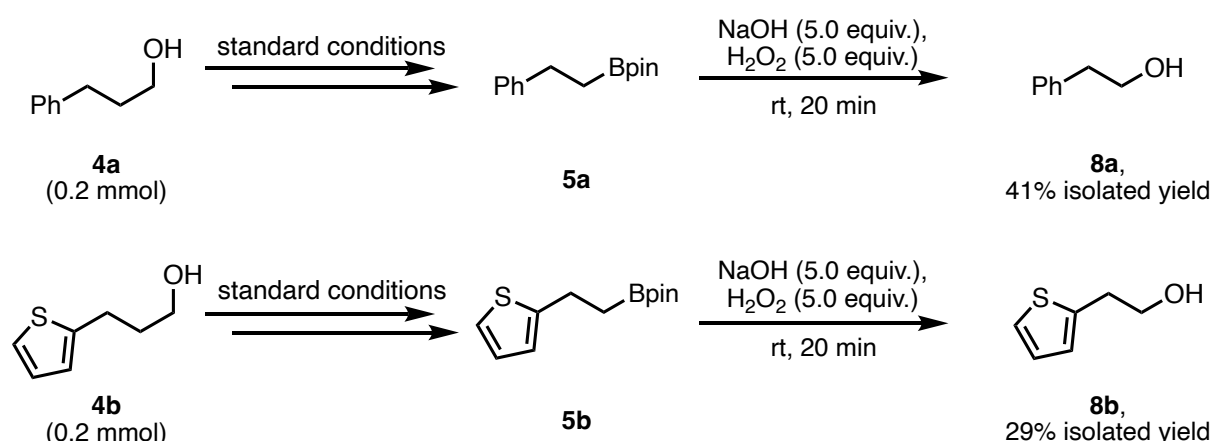
Figure 4.12. One-pot postfunctionalization by oxidation.

4.3 Conclusion and Outlook

In summary, the studies described in this chapter show the successful design of the unprecedented dehomologative borylation reactions of aldehydes and alcohols by using

multicatalysis. Although approaches using orthogonal relay or auto-relay catalysis failed, the transformation was achieved through sequential catalysis. The evaluation of the scope shows that the method has the potential to be broadly applicable. Further, the successful introduction of two different post-functionalization reactions – namely Suzuki-Miyaura cross coupling and oxidation – shows the further potential of the method. However, further work is required to reveal the full potential of the method. Specifically, a further evaluation of the substrate scope and the application of more post-functionalization reaction could broaden the applicability of the method for the future. Further, an application of the method to skeleton-editing can be envisioned.

4.4. Experimental details

4.4.1. Experimental methods

Unless stated otherwise, all reactions and manipulations were conducted on the laboratory bench or in a well-ventilated fume hood in air with reagent grade solvents. Reactions under inert gas atmosphere were carried out in oven-dried glassware in a nitrogen-filled glove box or by standard Schlenk techniques under nitrogen. Unless noted otherwise, all reagents and solvents were purchased from commercial suppliers and used without further purification. For experiments under inert gas atmosphere, dried and degassed solvents were purchased from commercial suppliers, stored in a nitrogen-filled glove box and used as received. Column chromatography was carried out with the aid of a CombiFlash EZ Prep Chromatography System with integrated ELSD using the RediSep Rf (Bronze, Silver, or Gold) Silica Gel Disposable Flash columns. TLC was carried out on Merck Kieselgel F254 plates. TLC visualization was carried out with ultraviolet light (254 nm), followed by staining with a 1% aqueous $KMnO_4$ solution. NMR spectra were acquired on the 400 MHz (Bruker 400 MHz NMR UltraShield Magnet, Console Avance III, equipped by a standard probe BBFO ^{1}H-X inverse 5 mm (with ^{31}P < X < ^{15}N)) or 500 MHz (Bruker 500 MHz NMR Ascend Magnet, Console Avance Neo equipped by a Cryo-Probe Prodigy ^{1}H-X 5 mm (with ^{31}P < X < ^{15}N) with a 24-positions auto-sampler) instruments at the Institute of Science and Supramolecular Engineering (ISIS). NMR spectra were processed using the MestReNova 14.2 software. Chemical shifts are reported in parts per million (ppm) and referenced to residual solvent peaks or tetramethylsilane (TMS). Coupling constants are reported in hertz (Hz). GC-FID analysis was obtained on a Shimadzu GC-2010 Plus instrument equipped with a SH-Rxi-5MS column (25 m x 0.20 mm ID x 0.33 mm film) connected to a FID detector. GC-MS analysis was obtained on a Shimadzu QP2020 (EI) instrument equipped with a SH-Rxi-5MS column (25 m x 0.20 mm ID x 0.33 mm film). GC-FID and NMR yields were calculated using 1,3,5-trimethoxybenzene, as the internal standards. GC-FID yields were corrected for response factors for all compounds. High-resolution electrospray ionization mass spectra (HR-ESI-MS) were obtained at the Analytical Facility of the Department of Chemistry, University of Strasbourg or at the Institute of Science and Supramolecular Engineering using a ThermoFisher Orbitrap Exactive Plus with Extend Mass Range (source HESI II) with a Vanquish PDA (VF-XX) detector.

4.4.2. Synthesis of substrates

3-(thiophen-2-yl)propan-1-ol 5b
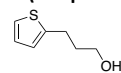
The reaction was performed according to a literature procedure.[18] To a solution of 3-(thiophen-2-yl)propanoic acid (1.95 g, 12.5 mmol, 1.0 equiv.) in THF (30 mL) was added borane dimethyl sulfide complex (2M in THF, 12.5 mL, 2.0 mmol, 2.0 equiv.) at 0 °C under a nitrogen atmosphere. The reaction was then allowed to warm up to room temperature, and allowed to stir for 3.5 h. The reaction mixture was quenched with sat. K_2CO_3 solution (15 mL) and washed with EtOAc (3 x 30 mL). The combined organic layers were dried over Na_2SO_4, filtered and the volatiles were removed under reduced pressure. The residue was subjected to flash column chromatography (silica gel, 0-45% EtOAC in petroleum ether) to obtain the product (1.77 g, 12.4 mmol, 99%) as a colorless oil. The NMR data match previously reported data for the title product.[18]

^{1}H NMR (400 MHz, CDCl$_3$) δ 7.12 (dd, J = 5.1, 1.2 Hz, 1H), 6.92 (dd, J = 5.1, 3.4 Hz, 1H), 6.83 − 6.80 (m, 1H), 3.71 (t, J = 6.3 Hz, 2H), 2.94 (ddd, J = 7.7, 7.1, 1.0 Hz, 2H), 2.00 − 1.90 (m, 2H), 1.47 (br s, 1H);
^{13}C{^{1}H} NMR (126 MHz, CDCl$_3$) δ 144.7, 126.9, 124.5, 123.2, 62.0, 34.6, 26.3.

General procedure for the oxidation of alcohols to aldehydes with Dess-Martin periodinane:
To a stirred suspension of Dess-Martin-Periodinane (1.15 equiv.) in DCM was added a solution of the respective aldehyde (1.0 equiv.) in DCM (40 mL). The mixture was allowed to stir at room temperature for the indicated time, filtered through celite (washed with DCM). After, the volatiles were removed under reduced and the residue was subjected to flash column chromatography to obtain the product.

3-(thiophen-2-yl)propanal 1b
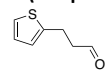
The title compound was prepared according to the general procedure using 3-(thiophen-2-yl)propan-1-ol (356 mg, 2.50 mmol) as the starting material and 16 h reaction time. After work-up, the volatiles were removed concentrated under reduced pressure, and the residue was subjected to column chromatography (silica gel, 0-38% EtOAc in petroleum ether) to give the title compound (239 mg, 1.70 mmol, 68%) as a yellow oil. The NMR data match previously reported data for the title product.[19]

¹H NMR (400 MHz, CDCl₃) δ 9.83 (t, *J* = 1.3 Hz, 1H), 7.14 (dd, *J* = 5.1, 1.2 Hz, 1H), 6.92 (dd, *J* = 5.2, 3.4 Hz, 1H), 6.82 (dq, *J* = 3.3, 1.1 Hz, 1H), 3.18 (td, *J* = 7.3, 0.9 Hz, 2H), 2.85 (ddd, *J* = 8.4, 7.1, 1.3 Hz, 2H);
¹³C{¹H} NMR (101 MHz, CDCl₃) δ 201.0, 143.1, 127.1, 124.9, 123.8, 45.5, 22.5.

3-(1,3-dioxoisoindolin-2-yl)propanal 1c
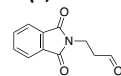
The title compound was prepared according to the general procedure using 2-(3-hydroxypropyl)isoindoline-1,3-dione (513 mg, 2.50 mmol) as the starting material. After work-up, the volatiles were removed concentrated under reduced pressure, and the residue was subjected to column chromatography (silica gel, 0-50% EtOAc in petroleum ether) to give the title compound (350 mg, 1.72 mmol, 69%) as a white solid. The NMR data match previously reported data for the title product.[20]

¹H NMR (400 MHz, CDCl₃) δ 9.82 (t, *J* = 1.4 Hz, 1H), 7.88 – 7.81 (m, 2H), 7.75 – 7.69 (m, 2H), 4.04 (t, *J* = 7.0 Hz, 2H), 2.87 (td, *J* = 7.0, 1.4 Hz, 2H);
¹³C{¹H} NMR (101 MHz, CDCl₃) δ 199.6, 168.2, 134.3, 132.1, 123.5, 42.5, 31.8.

3-phenoxypropanal 1d

The title compound was prepared according to the general procedure using 3-phenoxypropan-1-ol (381 mg, 2.5 mmol) as the starting material. After work-up, the volatiles were removed concentrated under reduced pressure, and the residue was subjected to column chromatography (silica gel, 0-30% EtOAc in petroleum ether) to give the title compound (120 mg, 0.80 mmol, 32%) as a colorless oil. The NMR data match previously reported data for the title product.[21]
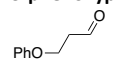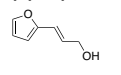
¹H NMR (400 MHz, CDCl₃) δ 9.88 (t, *J* = 1.6 Hz, 1H), 7.34 – 7.26 (m, 2H), 6.97 (tt, *J* = 7.3, 1.0 Hz, 1H), 6.93 – 6.86 (m, 2H), 4.32 (t, *J* = 6.1 Hz, 2H), 2.91 (td, *J* = 6.1, 1.6 Hz, 2H);
¹³C{¹H} NMR (101 MHz, CDCl₃) δ 200.4, 158.5, 129.7, 121.3, 114.7, 61.7, 43.4.

(*E*)-3-(furan-2-yl)prop-2-en-1-ol 4f

The compound was prepared according to modified literature procedures.[22,23] To a suspension of sodium hydride (440 mg, 11 mmol, 60% in mineral oil, 1.1 equiv.) in THF (40 mL) at 0 °C under argon was added triethyl phosphonoacetate (2.2 mL, 2.5 g, 11 mmol, 1.1 equiv.) dropwise. The reaction mixture was allowed to stir for 15 minutes at the same temperature. After, furfural (828 μL, 961 mg, 10 mmol, 1.0 equiv.) was added dropwise. The resulting mixture was stirred for 15 h at room temperature before quenching with sat. aqueous NH₄Cl (25 mL). The aqueous layer was washed with EtOAc (3 x 30 mL) and the combined organic layers were dried over anhydrous sodium sulfate. After filtration, the volatiles were removed under reduced pressure to obtain a brown oil. The crude product of the reaction was used in the next step without further purification.
To a stirred suspension of LiAlH₄ (304 mg, 8.0 mmol, 0.8 equiv.) in diethyl ether (40 mL) was added a solution of the crude product from above in diethyl ether (10 mL) dropwise at 0 °C. The reaction mixture was allowed to stir at room temperature for 1 h and then quenched using sat. aqueous NH₄Cl (10 mL). Upon filtration through celite (eluent: diethyl ether), the volatiles were removed. The residue was subjected to column chromatography (silica gel, 0-30% EtOAc in petroleum ether) to give the title compound (665 mg, 5.4 mmol, 54%) as a yellow oil. The NMR data match previously reported data for the title product.[23]

¹H NMR (400 MHz, CDCl₃) δ 7.35 (d, *J* = 1.8 Hz, 1H), 6.44 (dt, *J* = 15.9, 1.6 Hz, 1H), 6.37 (dd, *J* = 3.3, 1.8 Hz, 1H), 6.29 (dt, *J* = 15.9, 5.5 Hz, 1H), 6.24 (d, *J* = 3.3 Hz, 1H), 4.29 (dd, *J* = 5.6, 1.5 Hz, 2H), 1.63 (br s, 1H);
¹³C{¹H} NMR (126 MHz, CDCl₃) δ 152.5, 142.2, 127.3, 119.4, 111.4, 108.1, 63.4.

4.4.3. General procedures for the dehomologative borylation

General procedure 1: Dehydroformylation of aldehydes and allylic aldehydes
In a nitrogen-filled glove box, a 10 mL screw-cap vial equipped with a Teflon-coated magnetic stirring bar was charged with [Rh(cod)OMe]₂ (1.0 mg, 2.0 μmol, 1 mol%), xantphos (2.3 mg, 4.0 μmol, 2 mol%), 3-OMeBzOH (0.6 mg, 4.0 μmol, 2 mol%), 1,4-dioxane (200 μL), substrate (200 μmol, 1.0 equiv.), and dimethyl maleate (24.9 μL, 28.8 mg, 200 μmol, 1.0 equiv.). The vial was sealed with a cap, removed from the glove box, placed in a pre-heated aluminum block, and allowed to stir (800 rpm) at 90 °C for 16 h.

General procedure 2: Dehydromethoxylation of alcohols
In a nitrogen-filled glove box, a 10 mL screw-cap vial equipped with a Teflon-coated magnetic stirring bar was charged with [Rh(cod)OMe]₂ (1.9 mg, 4.0 μmol, 2 mol%), xantphos (4.6 mg, 8.0 μmol, 4 mol%), 3-OMeBzOH (1.2 mg, 8.0 μmol, 4 mol%), 1,4-dioxane (200 μL), substrate (200 μmol, 1.0 equiv.), and dimethyl maleate (49.7 μL, 57.7 mg, 400 μmol, 2.0 equiv.). The vial was sealed with a cap, removed from the glove box, placed in a pre-heated aluminum block, and allowed to stir (800 rpm) at 110 °C for 16 h.

General procedure 3: Transfer borylation of alkenes formed *in situ*
The vial from general procedure 1 or 2 was introduced into a nitrogen-filled glove box. The vial was further charged with THF (300 μL), [Ir(cod)Cl]₂ (5.4 mg, 8.0 μmol, 4 mol%), JohnPhos (14.3mg, 48.0 μmol, 24 mol%), B₂pin₂ (5.1 mg, 20.0 μmol, 10 mol%), and vinylboronic acid pinacol ester ("vinyl Bpin") (67.7 μL, 61.6 mg, 400 μmol, 2.0 equiv.). The vial was sealed with a cap, removed from the glove box, placed in a pre-heated aluminum block, and allowed to stir (800 rpm) at 110 °C for 16 h. The volatiles were removed under reduced pressure and the residue was subjected to flash column chromatography to isolate the target product.

General procedure 4: Hydroboration of alkenes formed *in situ*
The vial from general procedure 1 or 2 was introduced into a nitrogen-filled glove box. The vial was further charged with THF (300 μL) and HBpin (34.9 μL, 30.7 mg, 240 μmol, 1.2 equiv.). The vial was sealed with a cap, removed from the glove box, placed in a pre-heated aluminum block, and allowed to stir (800 rpm) at rt for 24 h. The volatiles were removed under reduced pressure and the residue was subjected to flash column chromatography to isolate the target product.

General procedure 5: Suzuki-Miyaura coupling of boronic esters formed *in situ*
The vial from general procedure 3 or 4 was introduced into a nitrogen-filled glove box. The vial was charged with Pd₂(dba)₃ (9.2 mg, 10 μmol, 5 mol%), PⁿBuAd₂ (14.3 mg, 40 μmol, 5 mol%), Cs₂CO₃ (196 mg, 0.6 mmol, 3.0 equiv.), H₂O (83.3 μL), and 3-methoxyphenylbromide (27.8 μL,

41.1 mg, 0.22 mmol, 1.1 equiv.). The vial was sealed with a cap, removed from the glove box, placed in a pre-heated aluminum block, and allowed to stir (800 rpm) at 110 °C for 16 h. The mixture was filtered through a short pad of celite (eluent: DCM) and the volatiles were removed under reduced pressure. The residue was subjected to flash column chromatography to isolate the target product.

General procedure 6: Oxidation of alkyl boronic esters
The vial from general procedure 3 or 4 was opened and NaOH (3M in water, 333μL, 1.0 mmol, 5.0 equiv.) and H_2O_2 (30% in water, 113.4 μL, 1.0 mmol, 5.0 equiv.) were added subsequently. The vial was sealed and allowed to stir at room temperature for 20 min. After, water (2 mL) was added and the mixture was washed with EtOAc (3 x 2 mL). The combined organic layers were dried over Na_2SO_4, filtered, and the volatiles were removed under reduced pressure. The residue was subjected to flash column chromatography to isolate the target product.

## 4.4.4. Characterization of products

(*E*)-4,4,5,5-tetramethyl-2-styryl-1,3,2-dioxaborolane 3a
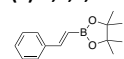
The title compound was prepared according to the general procedures 1 and 3 using cinnamyl alcohol (26.4 μL, 27.4 mg, 200 μmol, 1.0 equiv,) as the starting material. The reaction mixture was concentrated under reduced pressure, and the residue was subjected to column chromatography (silica gel, 0-3% MTBE in petroleum ether) to give the title compound (18.1 mg, 79 μmol, 39%) as a colorless oil. The crude yield of the title product was found to be 59% as determined using ^{1}H NMR spectroscopy. The NMR data match previously reported data for the title product.[24]

^{1}H NMR (400 MHz, CDCl₃) δ 7.53 – 7.46 (m, 2H), 7.40 (d, *J* = 18.5 Hz, 1H), 7.36 – 7.27 (m, 3H), 6.17 (d, *J* = 18.5 Hz, 1H), 1.32 (s, 12H).

(*E*)-4,4,5,5-tetramethyl-2-(2-(thiophen-2-yl)vinyl)-1,3,2-dioxaborolane 3b
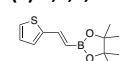
The title compound was prepared according to the general procedures 1 and 3 using 3-(thiophen-2-yl)propanal (28.0 mg, 200 μmol, 1.0 equiv,) as the aldehyde starting material. The reaction mixture was concentrated under reduced pressure, and the residue was subjected to column chromatography (silica gel, 0-6% MTBE in petroleum ether) to give the title compound (31.9 mg, 135 μmol, 68%) as a colorless oil. The crude yield of the title product was found to be 88% as determined using ^{1}H NMR spectroscopy. The NMR data match previously reported data for the title product.[24]

^{1}H NMR (500 MHz, CDCl₃) δ 7.47 (d, *J* = 18.1 Hz, 1H), 7.24 (dt, *J* = 5.0, 0.9 Hz, 1H), 7.08 (dd, *J* = 3.7, 1.1 Hz, 1H), 6.98 (dd, *J* = 5.1, 3.6 Hz, 1H), 5.91 (d, *J* = 18.1 Hz, 1H), 1.30 (s, 12H).

(*E*)-2-(2-(4,4,5,5-tetramethyl-1,3,2-dioxaborolan-2-yl)vinyl)isoindoline-1,3-dione 3c
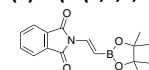
The title compound was prepared according to the general procedures 1 and 3 using 3-(1,3-dioxoisoindolin-2-yl)propanal (40.6 mg, 200 μmol, 1.0 equiv,) as the aldehyde starting material. The reaction mixture was concentrated under reduced pressure, and the residue was subjected to column chromatography (silica gel, 0-34% EtOAc in petroleum ether) to give the title compound (4.1 mg, 14 μmol, 7%) as a white solid. The crude yield of the title product was found to be 40% as determined using ^{1}H NMR spectroscopy. The NMR data match previously reported data for the title product.[24]

^{1}H NMR (400 MHz, CDCl₃) δ 7.90 (dd, *J* = 5.5, 3.0 Hz, 2H), 7.76 (dd, *J* = 5.5, 3.0 Hz, 2H), 7.48 (d, *J* = 16.9 Hz, 1H), 6.45 (d, *J* = 16.9 Hz, 1H), 1.30 (s, 12H).

(*E*)-2-(2-(furan-2-yl)vinyl)-4,4,5,5-tetramethyl-1,3,2-dioxaborolane 3f
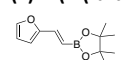
The title compound was prepared according to the general procedures 1 and 3 using (*E*)-3-(furan-2-yl)prop-2-en-1-ol (24.8 mg, 200 μmol, 1.0 equiv,) as the starting material. The reaction mixture was concentrated under reduced pressure, and the residue was subjected to column chromatography (silica gel, 0-50% MTBE in petroleum ether) to give the title compound (8.5 mg, 39 μmol, 19%) as a yellow oil. The crude yield of the title product was found to be 38% as determined using ^{1}H NMR spectroscopy.

^{1}H NMR (400 MHz, CDCl₃) δ 7.43 – 7.38 (m, 1H), 7.15 (d, *J* = 18.4 Hz, 1H), 6.39 (d, *J* = 1.3 Hz, 2H), 6.00 (d, *J* = 18.4 Hz, 1H), 1.29 (s, 12H);
^{13}C{^{1}H} NMR (101 MHz, CDCl₃) δ 153.8, 143.5, 136.5, 111.8, 110.9, 83.5, 24.9 [Note: the carbon atom attached to the boron atom was not observed due to quadrupole broadening or relaxation delay caused by the [11]B nucleus[6]];
^{11}B NMR (128 MHz, CDCl₃) δ 30.9;
HRMS (ESI) m/z calcd. for $C_{12}H_{18}BO_3$ ([M+H]⁺): 221.1344; found: 221.1341.

4,4,5,5-tetramethyl-2-phenethyl-1,3,2-dioxaborolane 6a
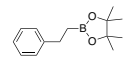
The title compound was prepared according to the general procedures 1 and 4 using cinnamyl alcohol (26.4 μL, 27.4 mg, 200 μmol, 1.0 equiv,) as the starting material. The reaction mixture was concentrated under reduced pressure, and the residue was subjected to column chromatography (silica gel, 0-5% MTBE in petroleum ether) to give the title compound (20.1 mg, 87 μmol, 44%) as a colorless oil. The title compound was isolated alongside **3a** (ratio **6a/3a** = 88/12). The crude yield of the title product was found to be 81% as determined using ^{1}H NMR spectroscopy. The NMR data match previously reported data for the title product.[25]

^{1}H NMR (400 MHz, CDCl₃) δ 7.41 – 7.23 (m, 4H), 7.23 – 7.14 (m, 1H), 2.79 (t, *J* = 8.2 Hz, 2H), 1.26 (s, 12H), 1.18 (t, *J* = 8.1 Hz, 2H).

4,4,5,5-tetramethyl-2-(2-(thiophen-2-yl)ethyl)-1,3,2-dioxaborolane 6b
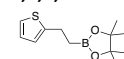
The title compound was prepared according to the general procedures 1 and 4 using 3-(thiophen-2-yl)propanal (28.0 mg, 200 μmol, 1.0 equiv,) as the aldehyde starting material. The reaction mixture was concentrated under reduced pressure, and the residue was subjected to column chromatography (silica gel, 0-4% MTBE in petroleum ether) to give the title compound (23.5 mg, 99 μmol, 49%) as a colorless oil. The title compound was isolated alongside **3b** (ratio **6b/3b** = 94/6). The crude yield of the title product was found to be 81% as determined using ^{1}H NMR spectroscopy. The NMR data match previously reported data for the title product.[25]

¹H NMR (500 MHz, CDCl₃) δ 7.08 (dd, *J* = 5.1, 1.2 Hz, 1H), 6.89 (dd, *J* = 5.1, 3.4 Hz, 1H), 6.81 – 6.77 (m, 1H), 2.96 (td, *J* = 7.9, 1.0 Hz, 2H), 1.25 – 1.19 (m, 14H).

2-(2-(4,4,5,5-tetramethyl-1,3,2-dioxaborolan-2-yl)ethyl)isoindoline-1,3-dione 6c
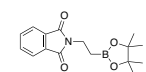
The title compound was prepared according to the general procedures 1 and 4 using 3-(1,3-dioxoisoindolin-2-yl)propanal (40.6 mg, 200 μmol, 1.0 equiv,) as the aldehyde starting material. The reaction mixture was concentrated under reduced pressure, and the residue was subjected to column chromatography (silica gel, 0-43% EtOAc in petroleum ether) to give the title compound (18.5 mg, 61 μmol, 31%) as a colorless oil. The reaction from 2-(3-hydroxypropyl)isoindoline-1,3-dione (41.0 mg, 200 μmol, 1.0 equiv.) gave the same compound (22.3 mg, 74 μmol, 37%).

¹H NMR (400 MHz, CDCl₃) δ 7.82 (dd, *J* = 5.4, 3.0 Hz, 2H), 7.68 (dd, *J* = 5.4, 3.0 Hz, 2H), 3.86 – 3.75 (m, 2H), 1.31 – 1.14 (m, 14H);
¹³C{¹H} NMR (101 MHz, CDCl₃) δ 168.3, 133.7, 132.4, 123.1, 83.4, 34.0, 24.8 [Note: the carbon atom attached to the boron atom was not observed due to quadrupole broadening or relaxation delay caused by the ¹¹B nucleus[6]];
¹¹B NMR (128 MHz, CDCl₃) δ 33.8;
HRMS (ESI) m/z calcd. for C₁₆H₂₁BNO₄ ([M+H]⁺): 302.1558; found: 302.1555.

4,4,5,5-tetramethyl-2-(3-phenoxypropyl)-1,3,2-dioxaborolane 6d

The title compound was prepared according to the general procedures 2 and 4 using 3-phenoxypropan-1-ol (30.4 mg, 200 μmol, 1.0 equiv.) as the alcohol starting material. The reaction mixture was concentrated under reduced pressure, and the residue was subjected to column chromatography (silica gel, 0-27% EtOAc in petroleum ether) to give the title compound (16.2 mg, 62 μmol, 31%) as a yellow oil. The NMR data match previously reported data for the title product.[26]

¹H NMR (400 MHz, CDCl₃) δ 7.35 – 7.20 (m, 2H), 6.97 – 6.85 (m, 3H), 4.11 (t, *J* = 7.8 Hz, 2H), 1.37 (t, *J* = 7.8 Hz, 2H), 1.27 (s, 12H).
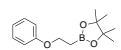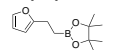
2-(2-(furan-2-yl)ethyl)-4,4,5,5-tetramethyl-1,3,2-dioxaborolane 6f

The title compound was prepared according to the general procedures 1 and 4 using (*E*)-3-(furan-2-yl)prop-2-en-1-ol (24.8 mg, 200 μmol, 1.0 equiv,) as the starting material. The reaction mixture was concentrated under reduced pressure, and the residue was subjected to column chromatography (silica gel, 0-40% MTBE in petroleum ether) to give the title compound (6.7 mg, 30 μmol, 15%) as a colorless oil. The title compound was isolated alongside **3f** (ratio **6f/3f** = 2/1). The crude yield of the title product was found to be 60% as determined using ¹H NMR spectroscopy.

¹H NMR (500 MHz, CDCl₃) δ 7.28 – 7.26 (m, 1H), 6.27 – 6.22 (m, 1H), 5.98 – 5.93 (m, 1H), 2.74 (t, *J* = 7.9 Hz, 2H), 1.23 (s, 12H), 1.14 (t, *J* = 7.9 Hz, 2H);
¹³C{¹H} NMR (126 MHz, CDCl₃) δ 158.1, 140.7, 110.1, 104.1, 83.3, 24.9, 22.6 [Note: the carbon atom attached to the boron atom was not observed due to quadrupole broadening or relaxation delay caused by the ¹¹B nucleus[6]];
¹¹B NMR (160 MHz, CDCl₃) δ 34.0;
HRMS (ESI) m/z calcd. for C₁₂H₂₀BO₃ ([M+H]⁺): 223.1500; found: 223.1498.

(*E*)-1-methoxy-3-styrylbenzene 7
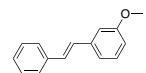
The title compound was prepared according to the general procedures 1, 3, and 5 using 3-phenylpropanal (26.8 mg, 200 μmol, 1.0 equiv.) as the aldehyde starting material. The reaction mixture was concentrated under reduced pressure, and the residue was subjected to column chromatography (silica gel, 100% petroleum ether) to give the title compound (27.1 mg, 129 μmol, 64%) as a yellow oil. The NMR data match previously reported data for the title product.[27]

¹H NMR (400 MHz, CDCl₃) δ 7.55 – 7.49 (m, 2H), 7.39 – 7.33 (m, 2H), 7.27 (td, *J* = 7.9, 6.3 Hz, 2H), 7.15 – 7.04 (m, 4H), 6.83 (ddd, *J* = 8.2, 2.5, 1.0 Hz, 1H), 3.85 (s, 3H).

2-phenylethan-1-ol 8a
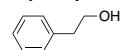
The title compound was prepared according to the general procedures 2, 4, and 6 using 3-phenylpropanol (27.2 mg, 200 μmol, 1.0 equiv.) as the starting material. The reaction mixture was concentrated under reduced pressure, and the residue was subjected to column chromatography (silica gel, 0-50% EtOAc in petroleum ether) to give the title compound (10.0 mg, 82 μmol, 41%) as a colorless oil. The NMR data match previously reported data for the title product.[28]

¹H NMR (400 MHz, CDCl₃) δ 7.36 – 7.29 (m, 2H), 7.26 – 7.20 (m, 3H), 3.87 (t, *J* = 6.6 Hz, 2H), 2.88 (t, *J* = 6.6 Hz, 2H), 1.56 (s, 1H).

2-(thiophen-2-yl)ethan-1-ol 8b
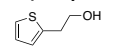
The title compound was prepared according to the general procedures 2, 4, and 6 using 3-(thiophen-2-yl)propan-1-ol (28.4 mg, 200 μmol, 1.0 equiv.) as the alcohol starting material. The reaction mixture was concentrated under reduced pressure, and the residue was subjected to column chromatography (silica gel, 0-38% EtOAc in petroleum ether) to give the title compound (7.3 mg, 57 μmol, 29%) as a colorless oil. The NMR data match previously reported data for the title product.[28]

¹H NMR (400 MHz, CDCl₃) δ 7.18 (dd, *J* = 5.1, 1.2 Hz, 1H), 6.96 (dd, *J* = 5.2, 3.4 Hz, 1H), 6.88 (dt, *J* = 3.5, 1.0 Hz, 1H), 3.87 (t, *J* = 6.3 Hz, 2H), 3.09 (td, *J* = 6.3, 0.9 Hz, 2H), 1.59 (br s, 1H).

4.5. References

(1)   Chen, F.; Wang, T.; Jiao, N. Recent Advances in Transition-Metal-Catalyzed Functionalization of Unstrained Carbon–Carbon Bonds. *Chem. Rev.* **2014**, *114* (17), 8613–8661. https://doi.org/10.1021/cr400628s.
(2)   Carreras, J.; Caballero, A.; Pérez, P. J. Alkenyl Boronates: Synthesis and Applications. *Chem. - Asian J.* **2019**, *14* (3), 329–343. https://doi.org/10.1002/asia.201801559.
(3)   Wu, L.; Moteki, T.; Gokhale, A. A.; Flaherty, D. W.; Toste, F. D. Production of Fuels and Chemicals from Biomass:

Condensation Reactions and Beyond. *Chem* **2016**, *1* (1), 32–58. https://doi.org/10.1016/j.chempr.2016.05.002.

(4)   Davison, R. T.; Kuker, E. L.; Dong, V. M. Teaching Aldehydes New Tricks Using Rhodium- and Cobalt-Hydride Catalysis. *Acc. Chem. Res.* **2021**, *54* (5), 1236–1250. https://doi.org/10.1021/acs.accounts.0c00771.

(5)   Cuenca, A. B.; Fernández, E. Boron-Wittig Olefination with *Gem* -Bis(Boryl)Alkanes. *Chem. Soc. Rev.* **2021**, *50* (1), 72–86. https://doi.org/10.1039/D0CS00953A.

(6)   Matteson, D. S.; Moody, R. J.; Jesthi, P. K. Reaction of Aldehydes and Ketones with a Boron-Substituted Carbanion, Bis(Ethylenedioxyboryl)Methide. Simple Aldehyde Homologation. *J. Am. Chem. Soc.* **1975**, *97* (19), 5608–5609. https://doi.org/10.1021/ja00852a062.

(7)   Matteson, D. S.; Moody, R. J. Carbanions from Deprotonation of Gem-Diboronic Esters. *J. Am. Chem. Soc.* **1977**, *99* (9), 3196–3197. https://doi.org/10.1021/ja00451a071.

(8)   Matteson, D. S.; Moody, R. J. Deprotonation of 1,1-Diboronic Esters and Reactions of the Carbanions with Alkyl Halides and Carbonyl Compounds. *Organometallics* **1982**, *1* (1), 20–28. https://doi.org/10.1021/om00061a005.

(9)   Coombs, J. R.; Zhang, L.; Morken, J. P. Synthesis of Vinyl Boronates from Aldehydes by a Practical Boron–Wittig Reaction. *Org. Lett.* **2015**, *17* (7), 1708–1711. https://doi.org/10.1021/acs.orglett.5b00480.

(10)   Kovalenko, M.; Yarmoliuk, D. V.; Serhiichuk, D.; Chernenko, D.; Smyrnov, V.; Breslavskyi, A.; Hryshchuk, O. V.; Kleban, I.; Rassukana, Y.; Tymtsunik, A. V.; Tolmachev, A. A.; Kuchkovska, Y. O.; Grygorenko, O. O. The Boron-Wittig Olefination of Aldehydes and Ketones with Bis[(Pinacolato)Boryl]Methane: An Extended Reaction Scope: The Boron-Wittig Olefination of Aldehydes and Ketones with Bis[(Pinacolato)Boryl]Methane: An Extended Reaction Scope. *Eur. J. Org. Chem.* **2019**, *2019* (33), 5624–5635. https://doi.org/10.1002/ejoc.201900648.

(11)   Stephens, T. C.; Pattison, G. Transition-Metal-Free Homologative Cross-Coupling of Aldehydes and Ketones with Geminal Bis(Boron) Compounds. *Org. Lett.* **2017**, *19* (13), 3498–3501. https://doi.org/10.1021/acs.orglett.7b01474.

(12)   Murphy, S. K.; Park, J.-W.; Cruz, F. A.; Dong, V. M. Rh-Catalyzed C–C Bond Cleavage by Transfer Hydroformylation. *Science* **2015**, *347*, 56–60. https://doi.org/10.1126/science.1261232.

(13)   Wu, X.; Cruz, F. A.; Lu, A.; Dong, V. M. Tandem Catalysis: Transforming Alcohols to Alkenes by Oxidative Dehydroxymethylation. *J. Am. Chem. Soc.* **2018**, *140* (32), 10126–10130. https://doi.org/10.1021/jacs.8b06069.

(14)   Martínez, S.; Veth, L.; Lainer, B.; Dydio, P. Challenges and Opportunities in Multicatalysis. *ACS Catal.* **2021**, *11* (7), 3891–3915. https://doi.org/10.1021/acscatal.0c05725.

(15)   Crudden, C. M.; Hleba, Y. B.; Chen, A. C. Regio- and Enantiocontrol in the Room-Temperature Hydroboration of Vinyl Arenes with Pinacol Borane. *J. Am. Chem. Soc.* **2004**, *126* (30), 9200–9201. https://doi.org/10.1021/ja049761i.

(16)   Kadu, B. S. Suzuki–Miyaura Cross Coupling Reaction: Recent Advancements in Catalysis and Organic Synthesis. *Catal. Sci. Technol.* **2021**, *11* (4), 1186–1221. https://doi.org/10.1039/D0CY02059A.

(17)   Yang, Y.; Chen, L.; Xu, S. Iridium-Catalyzed Enantioselective Unbiased Methylene C(Sp3)–H Borylation of Acyclic Amides. *Angew. Chem. Int. Ed.* **2021**, *60* (7), 3524–3528. https://doi.org/10.1002/anie.202013568.

(18)   Sandford, C.; Rasappan, R.; Aggarwal, V. K. Synthesis of Enantioenriched Alkylfluorides by the Fluorination of Boronate Complexes. *J. Am. Chem. Soc.* **2015**, *137* (32), 10100–10103. https://doi.org/10.1021/jacs.5b05848.

(19)   Huang, H.; Yu, C.; Zhang, Y.; Zhang, Y.; Mariano, P. S.; Wang, W. Chemo- and Regioselective Organo-Photoredox Catalyzed Hydroformylation of Styrenes via a Radical Pathway. *J. Am. Chem. Soc.* **2017**, *139* (29), 9799–9802. https://doi.org/10.1021/jacs.7b05082.

(20)   Zhang, Y.; Torker, S.; Sigrist, M.; Bregović, N.; Dydio, P. Binuclear Pd(I)–Pd(I) Catalysis Assisted by Iodide Ligands for Selective Hydroformylation of Alkenes and Alkynes. *J. Am. Chem. Soc.* **2020**, *142* (42), 18251–18265. https://doi.org/10.1021/jacs.0c09254.

(21)   Bi, H.; Zhou, Y.; Jiang, W.; Liu, J. Electrophotocatalytic C–H Hydroxyalkylation of Heteroaromatics with Aldehydes. *Adv. Synth. Catal.* **2022**, *364* (10), 1732–1737. https://doi.org/10.1002/adsc.202200055.

(22)   Chen, Y.; Song, X.; Gao, L.; Song, Z. Intramolecular Sakurai Allylation of Geminal Bis(Silyl) Enamide with Indolenine. A Diastereoselective Cyclization To Form Functionalized Hexahydropyrido[3,4- *b*]Indole. *Org. Lett.* **2021**, *23* (1), 124–128. https://doi.org/10.1021/acs.orglett.0c03806.

(23)   Takeuchi, M.; Taniguchi, T.; Ogasawara, K. Back to the Sugars: A New Enantio and Diastereocontrolled Route to Hexoses from Furfural. *Synthesis* **1999**, *1999* (02), 341–354. https://doi.org/10.1055/s-1999-3382.

(24)   Veth, L.; Grab, H. A.; Martínez, S.; Antheaume, C.; Dydio, P. Transfer C–H Borylation of Alkenes under Rh(I) Catalysis: Insight into the Synthetic Capacity, Mechanism, and Selectivity Control. *Chem Catal.* **2022**, *2* (4), 762–778. https://doi.org/10.1016/j.checat.2022.02.008.

(25)   Li, S.; Hu, C.; Cui, X.; Zhang, J.; Liu, L. L.; Wu, L. Site-Fixed Hydroboration of Terminal and Internal Alkenes Using BX $_3$ / ^{i} Pr $_2$ NEt**. *Angew. Chem. Int. Ed.* **2021**, *60* (50), 26238–26245. https://doi.org/10.1002/anie.202111978.

(26)   Verma, P. K.; Prasad, K. S.; Varghese, D.; Geetharani, K. Cobalt(I)-Catalyzed Borylation of Unactivated Alkyl Bromides and Chlorides. *Org. Lett.* **2020**, *22* (4), 1431–1436. https://doi.org/10.1021/acs.orglett.0c00038.

(27)   Wang, S.-M.; Song, H.-X.; Wang, X.-Y.; Liu, N.; Qin, H.-L.; Zhang, C.-P. Palladium-Catalyzed Mizoroki–Heck-Type Reactions of [Ph $_2$ SR $_{fn}$][OTf] with Alkenes at Room Temperature. *Chem. Commun.* **2016**, *52* (80), 11893–11896. https://doi.org/10.1039/C6CC06089G.

(28)   Kovalenko, O. O.; Adolfsson, H. Highly Efficient and Chemoselective Zinc-Catalyzed Hydrosilylation of Esters under Mild Conditions. *Chem. - Eur. J.* **2015**, *21* (7), 2785–2788. https://doi.org/10.1002/chem.201406176.

152

CHAPTER 5

Challenges and Opportunities in Multicatalysis

5.1 Introduction

The emergence of catalysis has had a transformative impact on various areas, including the production of chemicals, materials, and fuels, but also healthcare, agriculture, and the environment.[1] From a historical standpoint, first catalysts were developed to enhance the performance of known reactions, but later catalysis started enabling new transformations to address new challenges of the time. Catalytic transformations are typically constrained to one catalyst enabling a single reaction. However, the field continues evolving in complexity to further increase its potential.[2-19] Recently, there has been growing interest in developing multi-catalytic systems, which are inspired by the complexity of catalytic reactions occurring in nature.[2,3] Such efforts are further driven by remarkable characteristics of biosynthesis, that is, excellent selectivity, high yields, and material efficiency when producing complex molecules directly without any isolation of intermediates. However, to develop such multi-catalytic systems, major challenges need to be addressed, including incompatibility between multiple catalysts or reagents, precise ordering of all individual processes, and operation of all reactions under a single set of conditions.

To shed light on different approaches that address the challenges and take advantage of the opportunities of multi-catalysis, i analyze the field and provide insights into its three main categories: cooperative, domino, and relay catalysis. Each type of multi-catalysis is illustrated with a selection of representative reports that highlight their different features. Special emphasis is paid to relay catalysis, sub-categories of which are discussed and further portrayed with corresponding examples. Lastly, more complex systems, consisting of combinations of main multi-catalytic categories, are reviewed. The overall goal of this chapter is to emphasize the vast potential of multi-catalytic 'one-pot' processes to further inspire development and promote applications of such processes across molecular sciences.

Noteworthy, domino catalysis that uses a single catalyst to execute a series of reactions within one catalytic cycle lays at the edge of multi-catalysis, and as such, it might be considered to be outside of the field. However, we included domino catalysis into the scope of this chapter purposefully, in the efforts of portraying the full picture of synthetic systems that execute multiple catalytic events in one-pot.

Because multi-catalytic systems based solely on enzymatic catalysis encounter distinct challenges than the multi-catalytic systems incorporating 'small-molecule' catalysts, they stay beyond the scope of this chapter. I refer the readers to the corresponding reviews.[4–7]

5.2 Definitions and classification

The classification of different types of the multi-catalytic one-pot processes is somewhat inconsistent in the chemical literature. The herein proposed classification is inspired by the efforts of Fogg and Santos,[8] and Patil[9] and aims to provide a systematic analysis that includes all current approaches in this field. All systems with either multiple catalysts or multiple catalytic reactions taking place in the same reaction vessel are accounted for, irrespectively if

all reagents or catalysts are present from the start or are added during the reaction along with the possible change of reaction conditions.

Our primary classification of multi-catalytic systems takes into account (i) how the catalysts operate, i.e., the number of catalytic cycles that are involved and if the catalytic cycles are intertwined, and (ii) the number of independent catalytic reactions, i.e., number of bonds being formed, modified, or broken in the overall process, leading to the three categories of "cooperative catalysis", "domino catalysis", and "relay catalysis". Because relay catalysis encompasses a range of distinct systems bearing different challenges and opportunities, the further division into sub-categories is proposed. Here, the distinction is based on whether one or multiple pre-catalysts are used, i.e., whether each pre-catalyst operates in single or multiple independent catalytic cycles, and whether a change in reaction conditions or an addition of components throughout the process takes place. The general features for each category and sub-category are summarized in Figure 5.1.

a. Cooperative Catalysis

Cat 1   Cat 2

Key features:
Number of **catalytic reactions**[a] in the process: **1**
Number of **catalysts** in the process: **= 2**
Number of **catalytic cycles** in the process: **= 2**
Shared intermediates between catalytic cycles: **yes**

b. Domino Catalysis

Cat

Key features:
Number of **catalytic reactions**[a] in the process: **= 2**
Number of **catalysts** in the process: **1**
Number of **catalytic cycles** in the process: **1**
Shared intermediates between catalytic cycles: **not applicable**

c. Relay Catalysis

Cat 1   Cat 2

Key features:
Number of **catalytic reactions**[a] in the process: **= 2**
Number of **catalysts** in the process: **= 1**
Number of **catalytic cycles** in the process: **= 2**
Shared intermediates between catalytic cycles: **No**

Subcategories of Relay Catalysis:

orthogonal relay   Reactions **can be cooperative**   **autorelay**

No   No

Change of conditions?   ←— No — Cat 1 **?** **=** Cat 2 — Yes —→   **Change of conditions?**

Yes   Yes

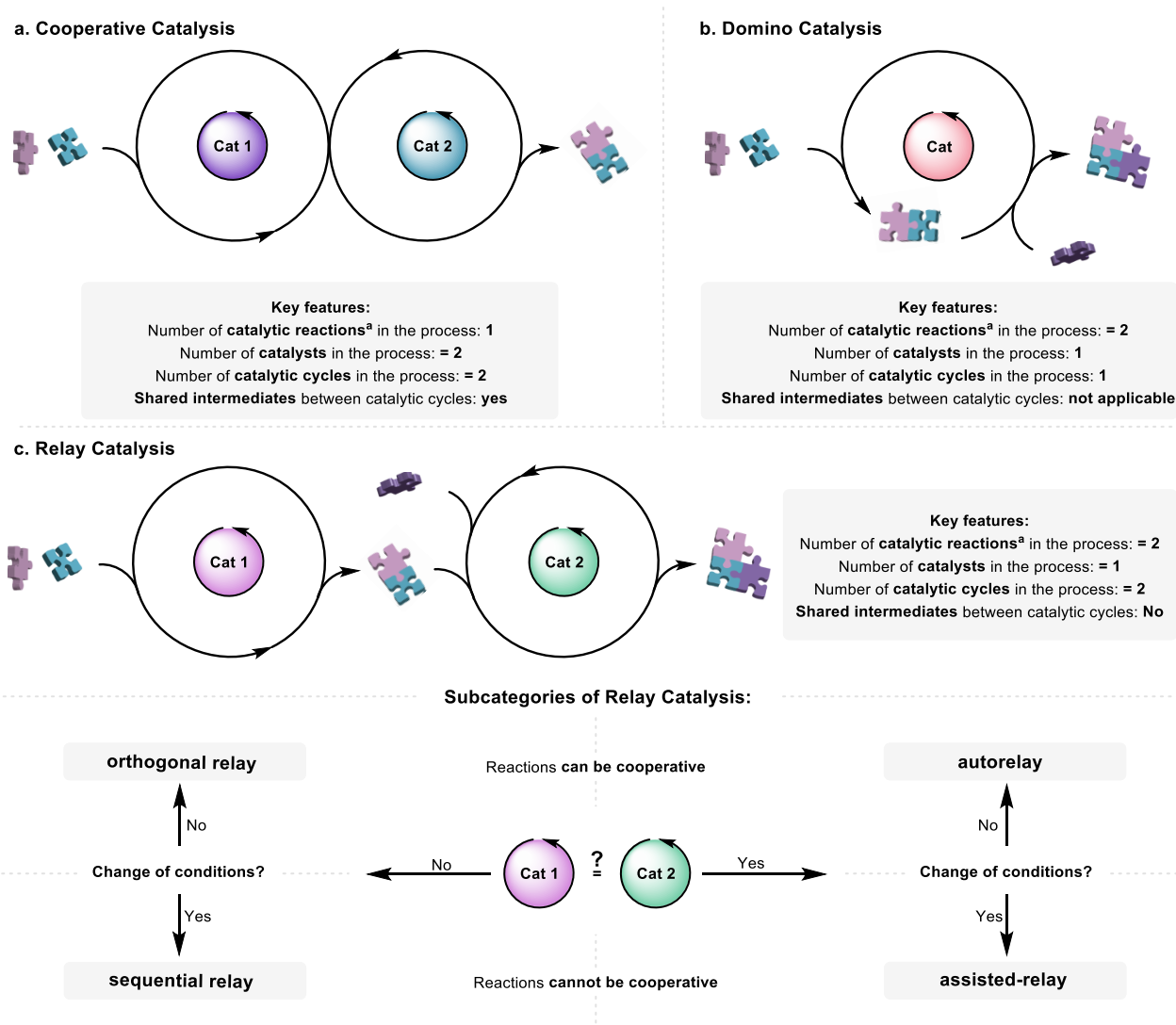**sequential relay**   Reactions **cannot be cooperative**   **assisted-relay**

Figure 5.1. General characteristics of different categories and subcategories of multi-catalytic one-pot processes discussed in the chapter. [a] A single catalytic reaction is understood as a distinct event of making, modifying, or breaking a bond occurring without any noncatalytic reaction intermediates.

It is noteworthy that the literature often refers to some multi-catalytic processes as "cascade catalysis". Because of its wide-spread use in different independent contexts, we propose the term "cascade catalysis" to be avoided in the future, as previously also suggested by Tietze.[10]

We also need to note that for the sake of simplicity in this chapter, we use the term 'catalyst' rather liberally to indicate a molecule that is either catalytically active or itself forms a catalytically active species under reaction conditions. When necessary for clarity, we differentiate between a 'pre-catalyst' and an actual 'catalyst' or 'catalytic species'.

5.3. Cooperative catalysis

Cooperative catalysis, often referred to as *synergistic catalysis*,[11] refers to catalytic systems in which multiple catalysts operate in concert by sharing their individual catalytic cycles in a single reaction to create, modify, or break a single bond. Consequently, the accumulation of reaction intermediates is not possible. The field of research has been extensively reviewed recently.[12–15] Therefore, below we only discuss representative examples that indicate the key features enabled by cooperative catalysis, noting all possible combinations regarding the different types of catalysts, such as organo/organo, organo/metal, and metal/metal, found in dual-catalytic systems. It is worth noting that in a recent perspective article on enantioselective synthesis with the aid of cooperative dual-catalytic systems,[16] Hoveyda and co-workers pointed out that the two catalysts are not necessarily acting cooperatively in such reactions. Therefore, the term *cooperative catalysis* might be somewhat misleading.

Enabling precise stereocontrol

In stereoselective synthesis, the synergistic action of two catalysts enables the enhancement of stereoselectivity control through the formation of highly organized transition states. For instance, Carreira[17] and co-workers developed a metal/organo dual-catalytic system for the enantio- and diastereodivergent α-allylation of branched aldehydes **1.1** to form γ,δ-unsaturated aldehydes **1.3** from a pair of racemic starting materials (Scheme 5.1).
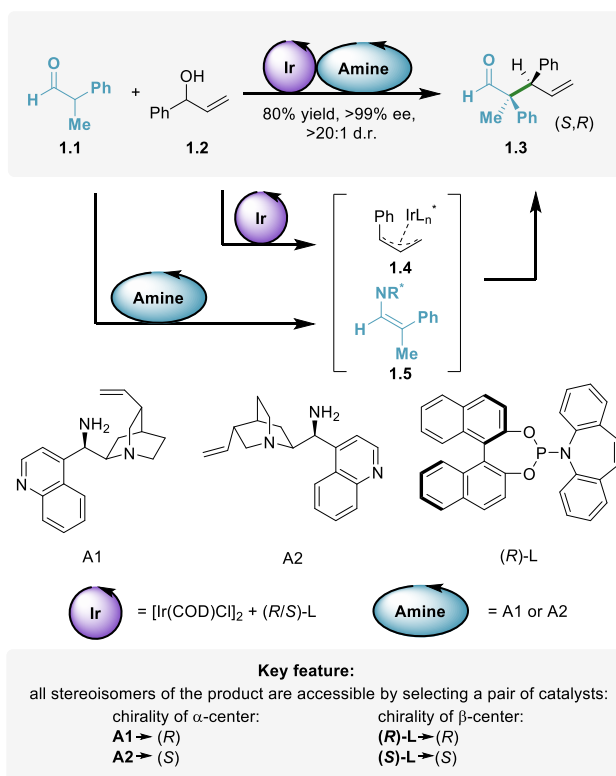
Scheme 5.1. Ir-/chiral amine-catalyzed cooperative enantio- and diastereodivergent α-allylation of α-branched aldehydes.

The reaction occurs in the presence of a chiral Ir-phosphoramidite complex that activates allylic alcohol **1.2** to form allyliridium intermediate **1.4** and chiral cinchona alkaloid A1 or A2 that activates aldehyde **1.1** through the formation of an iminium intermediate **1.5**. Because each catalyst controls the selectivity of each new stereogenic center independently, each of all four possible stereoisomers of **1.3** can be prepared selectively by selecting a pair of suitable enantiomers of both catalysts. By adapting the strategy, the same group subsequently reported two similar systems for the α-allylation of linear aldehydes,[18] and protected α-amino or α-hydroxyacetaldehydes.[19] The strategy was also utilized in a number of other studies with metal/metal[20–26], metal/organo,[27–29] and organo/organo[30] dual-catalytic systems, which demonstrated that multi-catalysis provides powerful tools for stereodivergent asymmetric synthesis.
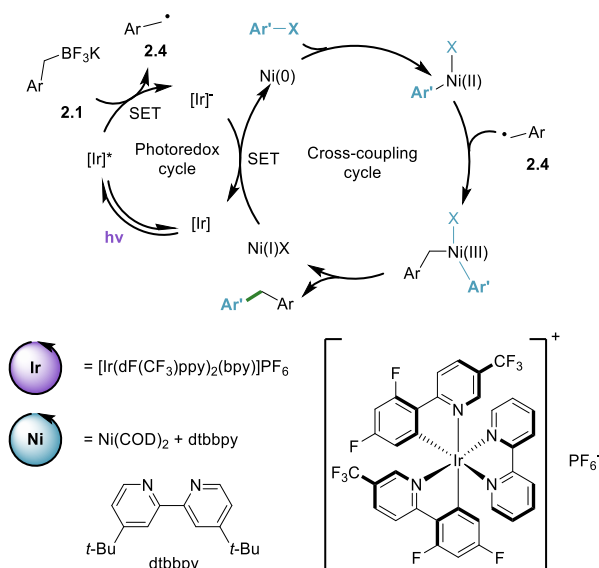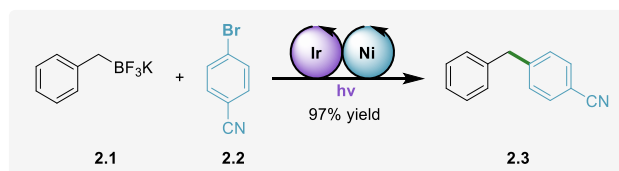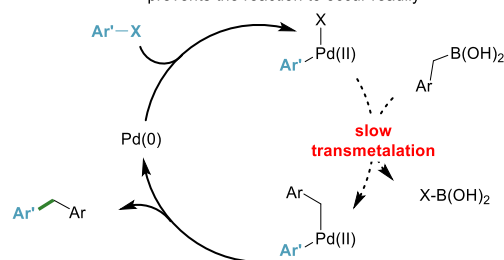
Scheme 5.2. Ir-/Ni-catalyzed cooperative cross-coupling of sp³-nucleophiles with aryl bromides assisted by a single-electron transmetalation step.

Enabling new reaction pathways

Thanks to the interactions between multiple catalytic cycles, multi-catalysis can create new reaction pathways, enabling transformations that are otherwise either kinetically or thermodynamically unfeasible. For instance, cross-coupling reactions involving alkyl boronic acids occurring in the presence of a single catalyst are typically sluggish, because transmetalation involving sp³-hybridized organoboronic acid **2.1** is rather slow and requires harsh reaction conditions, limiting the overall applicability.

To address these issues, Molander[31] and co-workers developed a metal/metal dual-catalytic system that combines a classical Ni-catalyst with an Ir-photoredox catalyst (Scheme 5.2).[32] The latter mediates a single-electron transfer (SET) to readily form benzyl radicals **2.4** from **2.1**, which undergo fast single electron transmetalation with the Ni-catalyst. Overall, incorporation of a SET enables efficient cross-coupling between sp³-centered potassium alkoxyalkyl- or

159

benzyltrifluoroborates **2.1** and aryl bromides **2.2** under mild conditions and consequently for a broad range of substrates. In turn, the merger of photoredox catalysis and transition metal catalysis was examined by MacMillan and Doyle to execute cross-coupling reactions with alkyl carboxylic acids as coupling partners.[33] The versatility of the approach was further indicated in other studies, including the report of Molander[34] on using alkyl silicon derivatives as coupling partners and the work of Nishibayashi[35] on using alkyl dihydropyridines as coupling partners. The field of cross-coupling reactions exploiting the combination of photo- and transition metal-catalysts was recently reviewed.[36]

The latter undergoes sequential oxidative addition of aryl halide **3.2** to furnish a Ni^{III}(aryl)(alkyl) species followed by subsequent reductive elimination affording the cross-coupled product **3.3**. Lastly, a series of electron transfer events regenerates catalytic species, closing both catalytic cycles. Other reports on functionalization of unactivated C-H bonds occurring in the presence of analogous metal/metal dual-catalytic systems further underscored the efficacy of the strategy.[43–45]
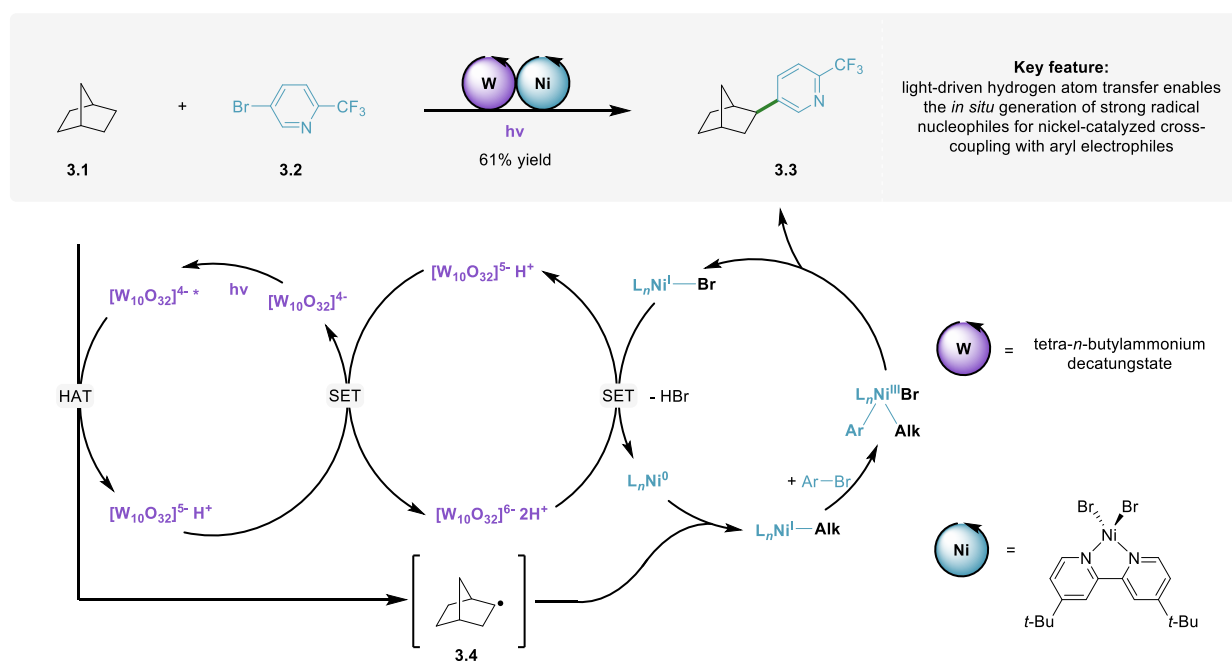
Scheme 5.3. W-/Ni-catalyzed arylation of strong sp^3-C-H bonds with aryl bromides enabled by light-driven hydrogen atom transfer (HAT).

Cooperation between a photocatalyst (PC) and a hydrogen atom transfer (HAT) catalyst provided new opportunities for free radical organic chemistry.[46] In general, open-shell radical intermediates can be readily generated by an electron transfer process between PCs and organic starting materials. Such radicals can be engaged in transformations that are inaccessible for the closed-shell starting materials. Upon completing the target reactions, the radical intermediates are converted back to the closed-shell products by reacting with the HAT catalysts.[47] For instance, Nicewicz and coworkers[48] recently established anti-Markovnikov hydrohalogenation of styrenyl alkenes occurring selectively in the presence of a organo/organo dual-catalytic system built of an acridinium salt acting as a PC and a thiophenol derivative acting as a HAT catalyst (Scheme 5.4). Initially, the visible light-excited photoredox

160

catalyst reacts with alkene **4.1** through photoinduced electron-transfer (PET) to form alkene radical cation **4.4**. The latter reacts with a chloride anion through the nucleophilic addition to produce benzylic carbon-centered radical **4.5**. Upon a HAT from the redox-active thiol, the anti-Markovnikov hydrohalogenation product **4.3** is formed. Lastly, a source of acidic protons converts thiolate to the active hydrogen atom donor, allowing turnover of the HAT catalyst. Notably, several halogen, phosphate, and sulfonate anions can be used as nucleophiles, when a well-paired combination of PC and HAT catalysts is used.
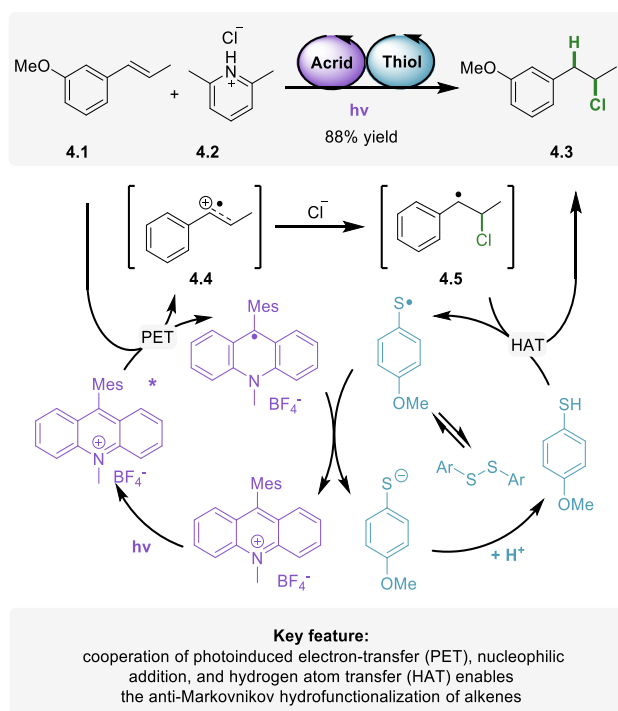
Scheme 5.4. Merging two organocatalysts enables the light-driven anti-Markovnikov hydrohalogentaion of styrenyl alkenes.

The abovementioned photocatalytic strategy using organocatalysts has been extensively studied to afford a range of new reactions, including recent studies on generation and trapping of alkene radical cations[49] in other transformations such as hydroacetoxylation,[50] intra-[51] and intermolecular[52] hydroamination, a range of novel polar radical crossover cycloadditions,[53–55] synthesis of polysubstituted aldehydes,[56] as well as a site-selective arene C-H amination[57] and direct arene C–H fluorination.[58] HAT organocatalysts, such as zwitterionic triazolium amidates, proved also effective in the organo/metal dual-catalytic systems enabling C–H bond alkylation reactions.[59]

Enabling thermodynamically unfeasible transformations

The ability to directly convert a racemic mixture of a compound into its enantiomerically pure form would be attractive from a synthetic standpoint. However, such transformations are thermodynamically unfeasible, due to the prospective increase in entropy (DG = +0.42 kcal/mol).[60] To overcome the intrinsic challenges of unfavorable thermodynamics, Miller,

Knowles,[60] and co-workers developed an elegant protocol of a light-driven direct deracemization of cyclic ureas **5.1** by the cooperative action of three catalysts namely an (achiral) Ir-photocatalyst, a chiral phosphate catalyst, and a chiral peptide thiol catalyst. The reaction proceeds through the excited-state redox events enabling a kinetic enrichment of one enantiomer (Scheme 5.5).
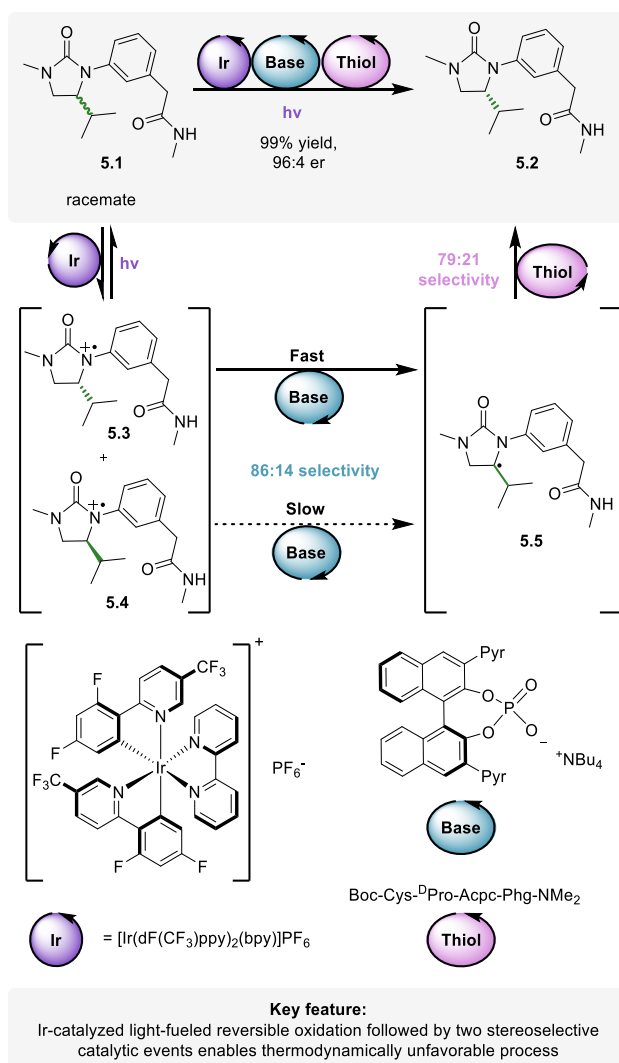
Scheme 5.5. Ir-/phosphate-/peptide thiol-catalyzed light-driven cooperative deracemization of ureas through stereoselective excited-state processes.

First, both enantiomers of cyclic urea **5.1** undergo continuous reversible oxidation by the excited state of the Ir-photocatalyst to form a pair of transient chiral radical cations **5.3** and **5.4**. Then, one enantiomer of the transiently formed **5.3** or **5.4** is preferentially deprotonated by the chiral phosphate catalyst with 86:14 selectivity. In turn, thus-formed α-amino radical **5.5** undergoes enantioselective hydrogen atom transfer (HAT) in the presence of the chiral thiol catalyst, recovering preferentially the opposite enantiomer of the starting material with 79:21 selectivity. Upon reaching the steady-state level of optical enrichment, the effective overall deracemization is achieved with 96:4 er through the composition of selectivities of chiral oxidation (86:14 er) and chiral hydrogen atom transfer (79:21 er) steps. Overall, the

multi-catalytic strategy enables to create the out-of-equilibrium state at the expense of light energy as the fuel.

Cooperation between a series of light-driven organocatalytic processes furnished a kinetically controlled site-selective epimerization of natural sugars to afford rare sugar isomers, as recently reported by Wendlandt[61] and co-workers (Scheme 5.6). Within the reaction, four organo-catalysts operate in concert, namely a photocatalyst (4-CzIPN), a hydrogen-atom abstraction catalyst (quinuclidine), a HAT catalyst (1-adamantane thiol), and a base (tetrabutylammonium *p*-chlorobenzoate). First, the blue LED light-excited photocatalyst is quenched by quinuclidine to generate a quinuclidinium radical cation. The latter mediates an irreversible hydrogen-atom abstraction from substrate **6.1** to form sugar radical **6.3**, followed by a diastereoselective HAT from the thiol catalyst to afford the epimerized sugar product **6.2** and the thiyl radical. A series of proton, electron, and hydrogen-atom transfers regenerates catalysts, closing the catalytic cycles.
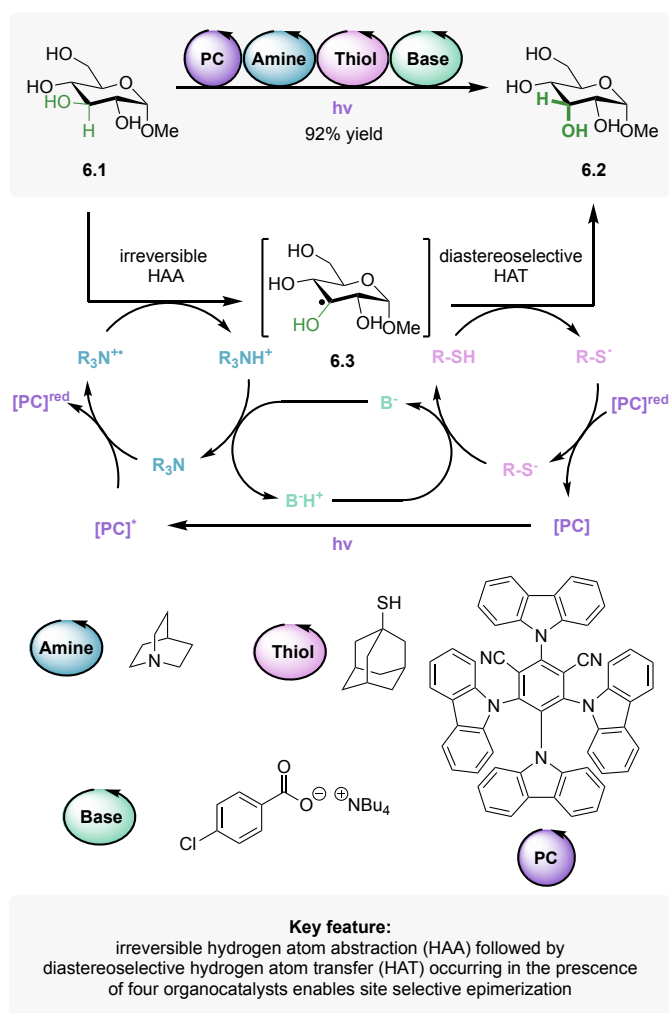
Scheme 5.6. Cooperative metal-free quadruple-catalytic catalysis enables site-selective epimerization of sugars to form rare sugar isomers.

5.4. Domino catalysis

Domino catalysis refers to catalytic systems with typically one catalyst operating in one catalytic cycle to form, modify, or break multiple bonds, i.e., multiple distinct reactions take place within the same catalytic cycle. Considering that a catalyst typically remains bound to the intermediates until the sequence is completed, the ac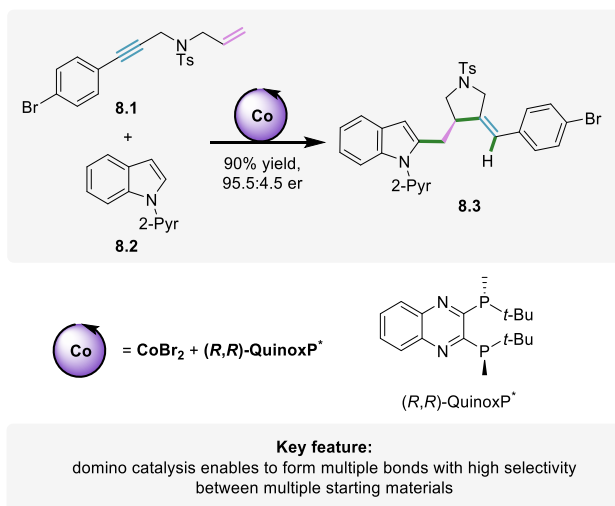cumulation of reaction intermediates is not possible. Because domino reactions have been extensively reviewed in journal articles[62–67] and books,[10,68] below we only discuss representative examples and we further refer the reader to the review literature. However, it is worth noting that some of the reviews do not strictly follow the same definition, sometimes using the term *domino catalysis* in a much broader sense.

It should be noted that *domino catalysis*, featuring only one catalyst that operates in one catalytic cycle, might not belong strictly to the field multi-catalysis. However, the approach represents a stepping stone towards the development of time- and resource-efficient processes with multiple catalytic bond-forming events occurring in one pot. Therefore, we consider its inclusion and a discussion of selected examples as pertinent for this chapter.

Creating multiple bonds within a single linear substrate

Domino reactions were shown to be particularly attractive for natural product synthesis, directly converting relatively simple linear starting materials into complex molecules with high diastereo- and enantioselectivity. The substrates for such processes usually require a high level of design and preorganization for a transformation to be successful; however, the reported examples demonstrate the impressive increase of molecular complexity within a single synthetic step.

For instance, Trost and co-workers[69] employed an intramolecular Pd-catalyzed polyenyne cycloisomerization as the centerpiece of the total synthesis of tremulanes, a group of sesquiterpenes. A linear polyenyne starting material **7.1** containing all the carbon and oxygen atoms in the targeted places undergowent a sequence of reactions through a series of sequential hydropalladation, carbopalladation, and β-hydride elimination steps (Scheme 5.7). Overall, the Pd-catalyzed domino process resulted in the formation of **7.2** with three new stereocenters, one 5-membered, and one 7-membered ring with high diastereoselectivity and yield in a single synthetic step. In an earlier work from the same group,[70] a Pd-catalyzed polyenyne cycloisomerization led to the formation of six new C-C bonds and seven 5-membered rings, highlighting the synthetic capacity of domino catalysis.

Scheme 5.7. Pd-catalyzed intramolecular domino polyenyne cycloisomerization for the synthesis of terpene derivatives.

Creating several bonds between multiple substrates

Multiple building blocks can undergo intermolecular reactions to build up molecular complexity under domino catalysis protocols. For instance, Lautens and co-workers[71] recently reported a Co-catalyzed domino transformation, which most likely occurs through a C-H activation of pyridylindole **8.2** followed by a series of insertion steps involving 1,6-enyne **8.1** as the second starting material (Scheme 5.5). Overall, a pair of simple achiral starting materials are directly converted into pyrrolidine derivatives **8.3** with high regio- and diastereoselectivities and in high yields.

Scheme 5.8. Co-catalyzed enantioselective hydroarylation of 1,6-enynes through an intermolecular domino reaction.

5.5. Relay catalysis

Relay catalysis refers to catalytic transformations occurring in the presence of catalysts, which operate in multiple functionally distinct, non-interfering catalytic cycles to execute a sequence of independent reactions. Importantly, unlike for cooperative catalysis, here catalytic cycles do not share any catalytic intermediates. Therefore, the accumulation of intermediates of the sequence might be possible. It is worth noting that relay catalysis involving two catalysts is often referred to as *tandem catalysis*.

As discussed above, *relay catalysis* covers a range of distinct systems, which we further divided into sub-categories, depending on the number of catalysts and the reaction conditions. In the following chapters, we discuss different types of *relay catalysis*, exemplified by selected examples. Special emphasis is placed on the potential and challenges related to each of the sub-categories.

5.5.1. Orthogonal relay catalysis

Orthogonal relay catalysis refers to catalytic systems exploiting at least two catalysts, which are present and active from the start, with each catalyst mediating only one of multiple consecutive reactions. The strategy requires to address all the common challenges of multi-catalysis, which include (i) the compatibility between all catalysts and reagents, i.e., catalysts and reagents must not inhibit each other or undergo non-productive side reactions; (ii) common conditions, i.e., all reactions need to occur under the same set of reaction conditions; and (iii) reaction ordering, i.e., each catalyst is designed to undergo a selective reaction only with one specific intermediate of the reaction sequence. Despite all the requirements associated, orthogonal relay catalysis represents arguably an ideal case of relay catalysis, providing numerous features inaccessible in other cases. The representative examples that highlight such features are discussed below.

Among typical advantages of orthogonal relay processes are reduction of the reaction time, the amount of work, and resources needed for the overall transformation when compared to the corresponding two-step process.
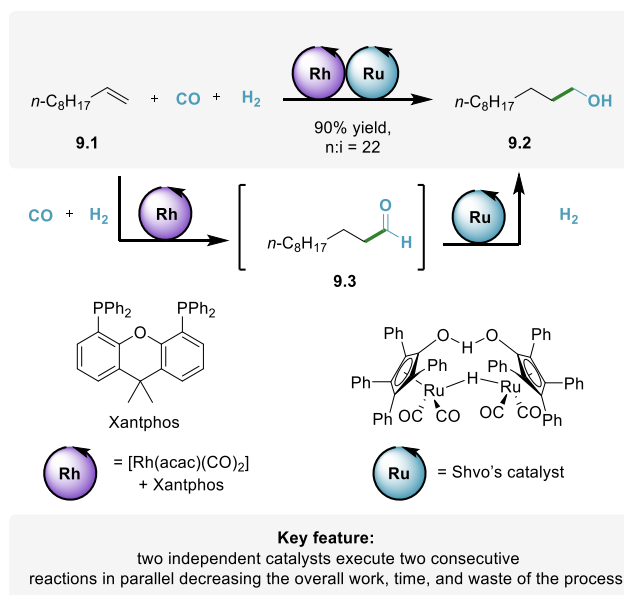
Scheme 5.9. Rh-/Ru-catalyzed orthogonal relay of hydroformylation-hydrogenation of terminal alkenes to form terminal alcohols.

For instance, a large volume of linear aliphatic alcohols in the industry is prepared by a two-step sequence involving hydroformylation of alkenes **9.1** to form aldehydes **9.3**, which are later hydrogenated to the target alcohol products **9.2**. To improve the economy of the process by limiting the overall reaction time of the process, Nozaki and co-workers[72,73] developed the orthogonal relay of hydroformylation and hydrogenation steps occurring in parallel in the same vessel in the presence of a dual-catalytic Rh-/Ru-system (Scheme 5.9). The control experiments confirmed that both reactions are fully independent of each other. The overall yield remains the same, irrespectively whether the process is conducted in a one-step or two-step fashion, with the catalysts added sequentially.

Enabling selective sequences under mild conditions

Hydroaminomethylation, a formal combination of hydroformylation of alkenes with reductive amination of aldehyde intermediates, represents an attractive strategy to convert abundant alkenes into value-added aliphatic amines.
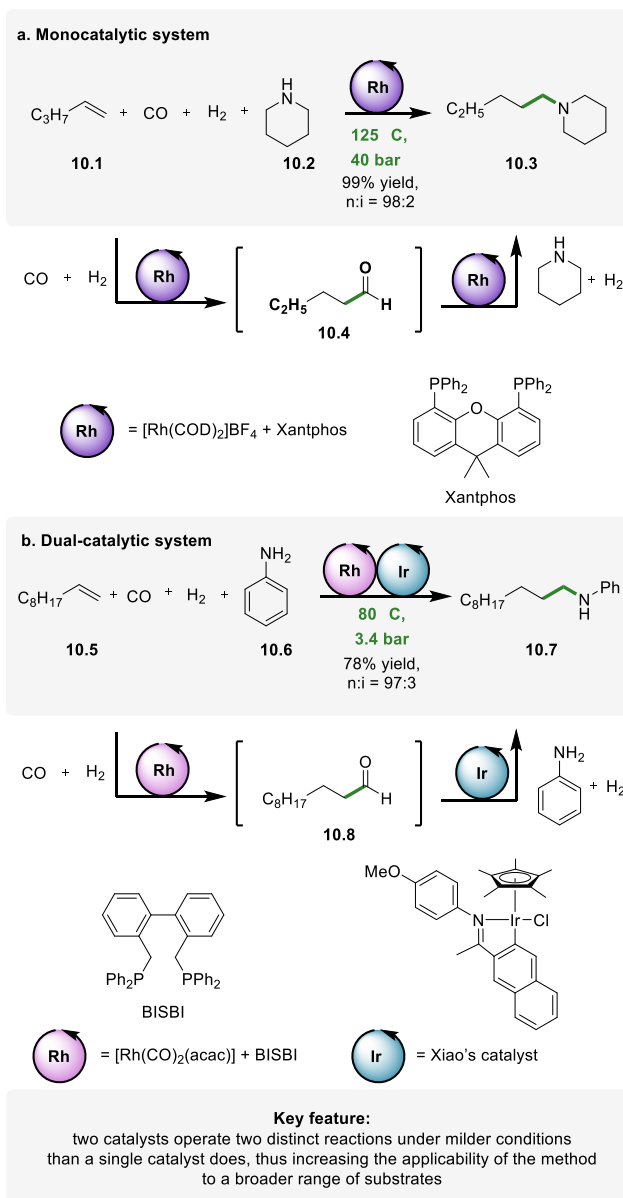
Scheme 5.10. Comparison of mono-catalytic Rh-catalyzed auto-relay protocol (a) and the bi-catalytic Rh-/Ir-catalyzed orthogonal relay protocol (b) for direct hydroaminomethylation of terminal alkenes to form amines.

Beller and co-workers[74] reported that the full sequence can be executed in the presence of a single Rh-complex (auto-relay catalysis, *vide infra*); however, harsh conditions (>120 °C, 40 bar) are required, which limit the prospective scope of the transformation (Scheme 5.10a). Because orthogonal relay catalysis enables to select each catalyst for each function independently, the dual-catalytic strategy might facilitate the optimization of the overall activity and selectivity. In that context, Hartwig and co-workers[75] reported an orthogonal relay protocol for hydroaminomethylation of alkenes, which connects Rh-catalyzed hydroformylation of alkenes **10.5** with *in situ* Ir-catalyzed reductive amination of aldehyde intermediates **10.8** to form amines **10.7** (Scheme 5.10b).
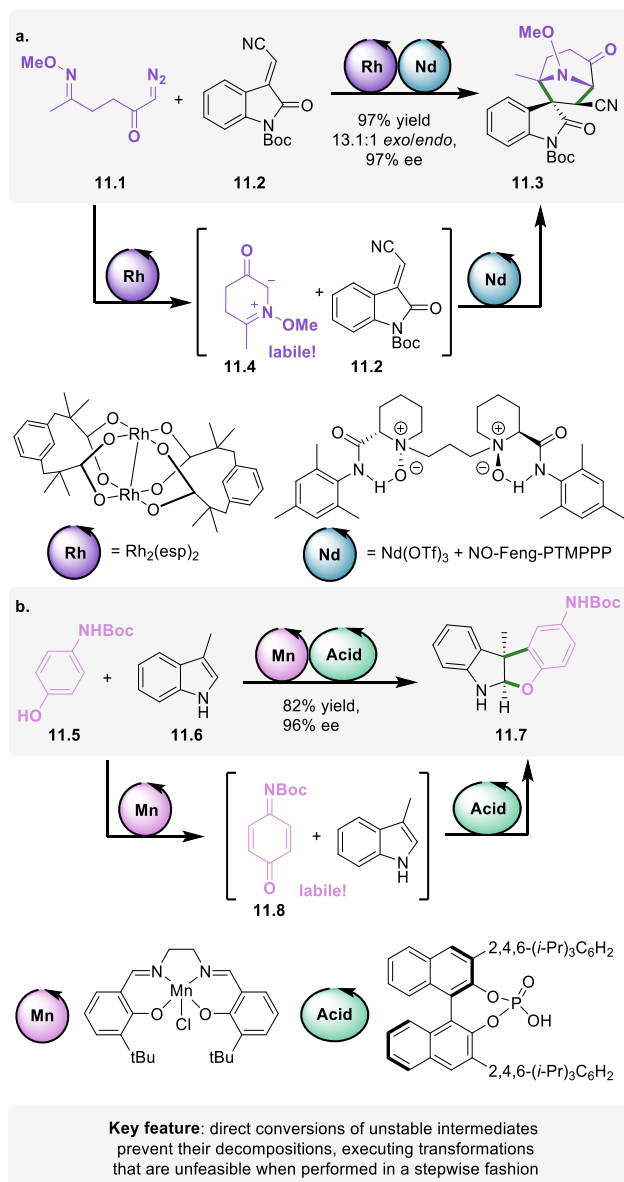
Scheme 5.11. Orthogonal relay processes occurring through unstable reaction intermediates: (a) Rh-catalyzed formation of labile azomethine ylides followed by Nd-catalyzed enantioselective 1,3-dipolar cycloaddition, and (b) Mn-catalyzed oxidation of phenol to labile N-boc quinone imines followed by CPA-catalyzed enantioselective 1,3-dipolar cycloaddition.

Although the approach requires two precious metal catalysts, the full sequence occurs under milder conditions (80 °C, 3.4 bar) with superior regioselectivity, and a broader functional group tolerance, when compared with the sequence in the presence of a single catalyst. The comparison of both protocols underscores the advantages of orthogonal relay catalysis.

Including unstable intermediates

  Under orthogonal relay catalysis, an intermediate can be converted further as soon as it is formed, leading to its short residence time in the reaction mixture.

Therefore, such pathways of reactions can include unstable intermediates, which would be otherwise unfeasible for a stepwise approach. Waldmann and co-workers[76] developed the

enantioselective synthesis of the spirotropanyl oxindole scaffold **11.3** proceeding through the Rh-catalyzed reaction of (*E*)-oximino α-diazo ketone **11.1** to form transient azomethine ylide **11.4** that subsequently underwent Nd-catalyzed intermolecular 1,3-dipolar cycloaddition with 3-alkenyl oxindoles **11.2** (Scheme 5.11a). That one-pot relay approach provides straightforward access to a class of complex biologically active compounds. The synthetic sequence could not be executed in a stepwise manner, due to the instability of the ylide intermediate.

Zhong and co-workers[77] reported a direct synthesis of benzofuroindolines **11.7**. The sequence occurs thorough Mn-catalyzed oxidation of *N*-Boc aminophenols **11.5** to unstable *N*-Boc quinone imines **11.8**, which subsequently undergo a phosphoric acid-catalyzed enantioselective 1,3-dipolar cycloaddition with indoles **11.6** (Scheme 5.11b). The strategy was inspired by related phenol oxidation processes occurring in nature, with the Mn-salen complex mimicking natural metalloenzymes.

Preventing secondary reactions of intermediates

In many cases, a primary product of a catalytic reaction remains reactive under catalytic conditions, undergoing secondary side reactions that lower the yield of the target transformation. Because under orthogonal relay catalysis, intermediates might be quickly converted in subsequent reactions, such secondary side reactions can be minimized, increasing the yield of the overall transformation.
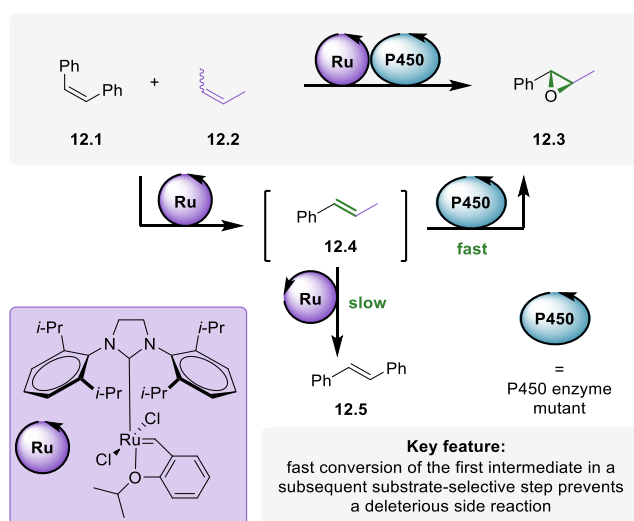
Scheme 5.12. Ru-/P450-catalyzed orthogonal relay of olefin cross-metathesis and substrate-selective epoxidation of heterocoupling olefin product.

To demonstrate the principle, Hartwig, Zhao, and co-workers[78] reported a dual-catalytic system that connects a Ru-catalyzed cross-metathesis of (*Z*)-stilbene **12.1** with 2-butene **12.2** that forms heterocoupling alkene intermediate **12.4** with a subsequent P450-catalyzed substrate-selective epoxidation of intermediate **12.4** to form selectively arylalkyl epoxide **12.3** (Scheme 5.12). The fast conversion of alkene intermediate **12.4** outcompetes its slow

conversion to (*E*)-stilbene **12.5** in a secondary reaction of the Ru-catalyzed cross-metathesis, leading to higher yields than a corresponding two-step procedure.

Enabling inaccessible transformations through hydrogen borrowing

Hydrogen borrowing catalysis[79] refers to the process exploiting transition metal-catalyzed reversible oxidation of alcohols, amines or alkanes to form transient aldehydes/ketones, imines or alkenes that can undergo a series of new reactions, including typically alkylation or amination, leading directly to value-added compounds.

Key feature:
cooperation of reversible dehydrogenation of alkanes with cross-metathesis of
transient alkenes enables challenging formal cross-metathesis of alkanes
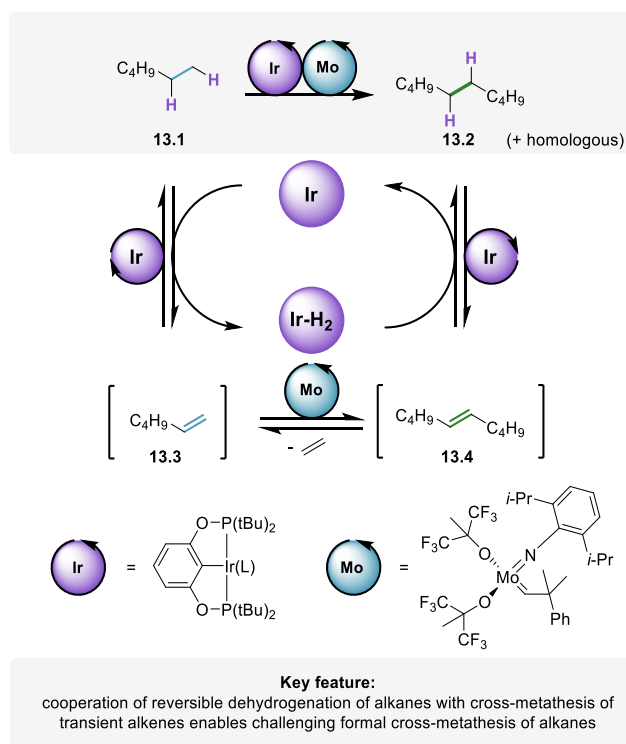
Scheme 5.13. Ir-/Mo-catalyzed orthogonal relay of alkane dehydrogenation-alkene metathesis-alkene hydrogenation for formal alkane cross-metathesis.

Attractively, the process eliminates any stochiometric redox reactions required otherwise in a stepwise approach. However, by combining the hydrogen borrowing catalysis with catalytic functionalization reactions into dual-catalytic systems, a broad chemical space of new transformations can be envisioned. In that context, Goldman, Brookhart, and co-workers[80] reported a remarkable dual-catalytic system for the elusive cross-metathesis of linear alkanes (Scheme 5.13). The sequence involves an Ir-catalyzed reversible dehydrogenation of starting alkane **13.1** to form a transient terminal alkene **13.3**, followed by Mo-catalyzed cross-metathesis to yield new larger alkenes **13.4** (and ethylene), which are lastly hydrogenated back to larger alkanes **13.2** by the initial Ir-catalyst. Although, the system suffers from isomerization reactions and harsh reaction conditions, forming a broad distribution of products, the study underscores the unique potential of cooperating reactions under orthogonal dual catalysis.

Following similar design principles, we devised dual-catalytic transition metal systems for functionalization of unreactive sites.[81] For instance, a relay of reversible oxidation of alcohols and arylation of transient aldehydes enables a general method for direct β-arylation of alcohols.
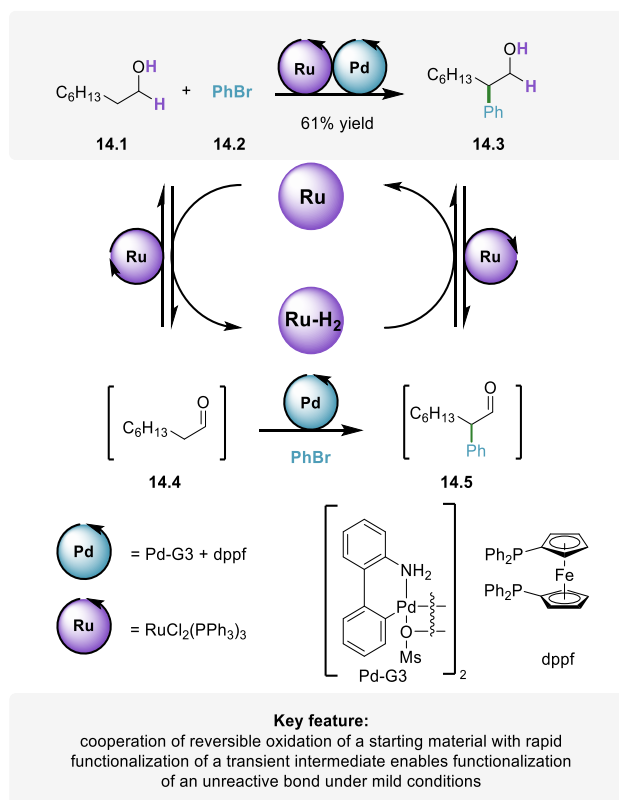
Scheme 5.14. Ru-/Pd-catalyzed orthogonal relay of alcohol dehydrogenation-aldehyde arylation-aldehyde hydrogenation for direct β-arylation of alcohols.

Specifically, in the system, primary alkyl alcohol **14.1** undergoes reversible oxidation by a Ru-catalyst to form transient aldehyde **14.4**. The latter undergoes Pd-catalyzed arylation to form aryl aldehyde **14.5** prior to reduction to the β-aryl alcohol **14.3** by the same hydrogen borrowing Ru-catalyst (Scheme 5.14). In the same vein, the combination of Fe-catalyzed hydrogen borrowing equilibrium with Rh-catalyzed enantioselective hydroarylation of an α,β-unsaturated aldehydes enables a method for direct enantioselective γ-hydroarylation of allylic alcohols. Importantly, because both reactions building such dual-catalytic systems occur under mild conditions, the overall functionalizations of unreactive sites occur also under mild conditions, enabling the application of such methods to a broad range of starting materials with a high functional group tolerance. Noteworthy, a combination of hydrogen-borrowing catalysis with organocatalysis was reported to enable the control of enantioselectivity of reactions[82,83] that are otherwise racemic under sole hydrogen-borrowing catalysis.[84]

Correcting selectivity of unselective reactions

Sequences of unselective but reversible reactions cooperating *in situ* with other selective reactions can increase the selectivity of the overall transformations. For instance, cross-metathesis of two olefins typically leads to the formation of a statistical mixture of a heterocoupling product and undesired homocoupling products, lowering the process efficiency. To address this issue, Hartwig, Zhao, and co-workers[85] showed that a combination of an unselective but reversible Ru-catalyzed cross-metathesis of alkenes **15.1** and **15.2** with a substrate-selective P450-catalyzed epoxidation of olefin **15.4** enables to increase the overall efficiency of the sequence (Scheme 5.15). Specifically, the selective conversion of heterocoupling alkene **15.4** to epoxide **15.3** drives the reversible metathesis reaction to continuously form a new portion of alkene **15.4** at the expense of homocoupling product **15.5** and starting alkene **15.2**. The authors showed that in the dual-catalytic system, the overall yield of the target epoxide product **15.3** was 1.5 times higher, while the end-concentration of the self-metathesis product **15.5** was 40% lower, and the remaining concentration of the starting material **15.2** was 20% lower, than in the stepwise transformation.
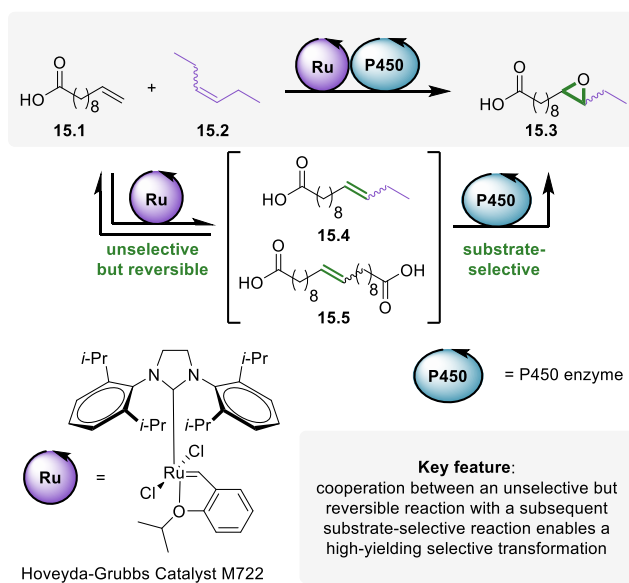
Scheme 5.15. Ru-/P450-catalyzed orthogonal relay of reversible olefin cross-metathesis and substrate-selective epoxidation of alkenes.

The design principles of the above-described system of cooperating reversible olefin metathesis with selective olefin epoxidation resemble the working principles of dynamic kinetic resolution reactions (DKR).[86–89] In the latter, a dynamic equilibrium between two enantiomers of a substrate is maintained, but one enantiomer undergoes a subsequent reaction selectively. For instance, a secondary alcohol continues to be reversibly oxidized-reduced to maintain the racemic composition of the mixture in the presence of a hydrogen-borrowing catalyst, but one enantiomer of the alcohol continuous to undergo a selective acylation in the presence of a lipase, leading in the end to a quantitative conversion of a racemic alcohol to an enantiomerically pure ester. This strategy has been extensively studied

for deracemization of alcohols, amines, aldehydes, and ketones. Recently, a combination of photo- and enzymatic catalysis has been reported, opening up the chemical space of DKR to the elusive stereoselective reduction of mixtures of (*E*)- and (*Z*)-alkenes.[90]

Exploiting thermodynamic leveraging

By exploiting the concept of *thermodynamic leveraging,* orthogonal relay catalysis bears the potential to execute reactions in sequence that are thermodynamically unfeasible. In such case, an endothermic reaction is coupled with a subsequent exothermic reaction to create an overall thermodynamically favorable sequence. For instance, Marks and co-workers[91] reported a dual-catalytic method for the etheric C-O bond hydrogenolysis through a combination of Ln(OTf)$_3$-catalyzed endothermic reversible C-O bond scission with a subsequent Pd-catalyzed exothermic C=C bond hydrogenation to generate an overall favorable process (Scheme 5.16). Such transformations can be used to convert biomass-based materials to alkanes,[92] providing a sustainable alternative to fossil fuels.
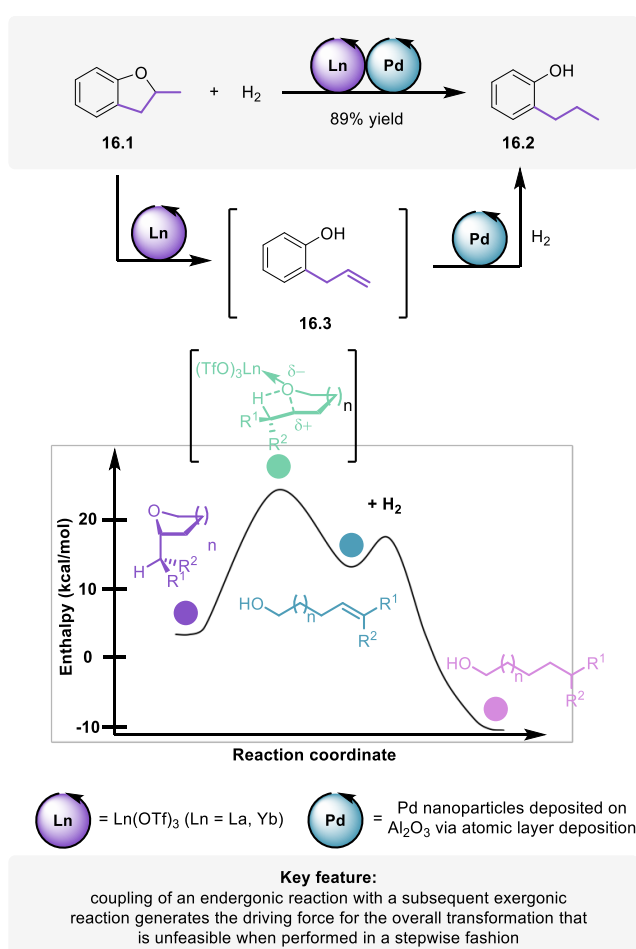
Scheme 5.16. Thermodynamic leveraging in Ln-/Pd-catalyzed orthogonal relay of retro-hydroalkoxylation of ethers and alkene hydrogenation drives the etheric C-O bond hydrogenolysis.

Preventing compatibility issues

One of the major challenges in the development of orthogonal relay-catalyzed transformations is the prospective incompatibility of catalysts that leads to inhibition of catalytic activity, preventing the overall process to occur. One of the common issues in case of transition metal-catalysis is the prospective ligand scrambling. For instance, in the synthesis of dihydroquinolines **17.3** through a combination of binap-Rh-catalyzed hydroarylation of alkyne **17.1** (with aryl boronic acid **17.2**) followed with Xphos-Pd-catalyzed *N*-arylation (Scheme 5.17).
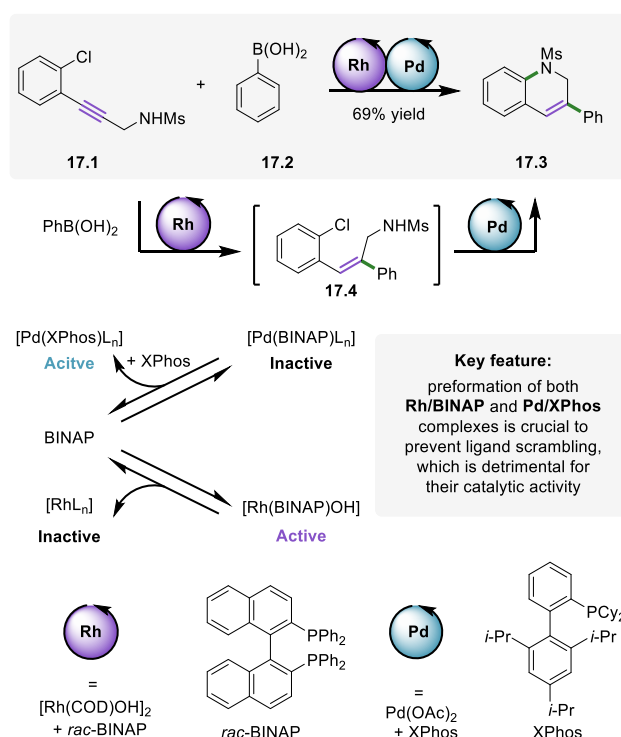
Scheme 5.17. Synthesis of dihydroquinolines in the orthogonal relay of Rh-catalyzed alkyne hydroarylation followed with Pd-catalyzed intramolecular N-arylation.

Lautens and co-workers[93] noted that the formation of mixed ligand complexes is detrimental to the catalytic process. However, the ligand exchange between complexes does not occur under the catalytic conditions (or occurs slowly). Therefore, when suitable complexes are formed prior to adding to the reaction mixture, their catalytic activities are maintained, enabling the formation of product **17.3** in 69% overall yield. Furthermore, this strategy proved effective to prevent premature ligand scrambling in asymmetric variants of orthogonal-relay catalytic reactions in which two metals and two ligands, one chiral and one achiral, are used.[94,95] Although effective, the approach is not general. Therefore, there have been many other strategies studied to address the incompatibility issues with the physical separation of catalysts.[96] In such a case, not only prospective ligand exchange processes are hindered but also any cross-reactivity is prevented. For instance, the physical separation of catalysts within the same vessel can be realized by catalysts immobilization on a solid support.[97]

The incompatibility between reagents of one step with the reagents or catalysts of other steps of the sequence might also be encountered in multi-catalytic systems. Strategies to address such incompatibility issues mainly focus on compartmentalization of different reactions, i.e., the catalysts and reagents for different steps are located in different 'compartments' of the reactor.[2] The compartments can be constructed by phases that are either immiscible,[98] separated by semi-permeable membrane,[99] or physically separated with the volatile intermediates being exchanged through the gas-phase.[100] An elegant example of reaction isolation was reported by Weck and co-workers in a sequence of a Co-catalyzed hydration of alkyne **18.1** to form ketone **18.3** and its subsequent Rh-catalyzed enantioselective transfer hydrogenation to form enantioenriched secondary alcohol **18.2** (Scheme 5.18).[101]
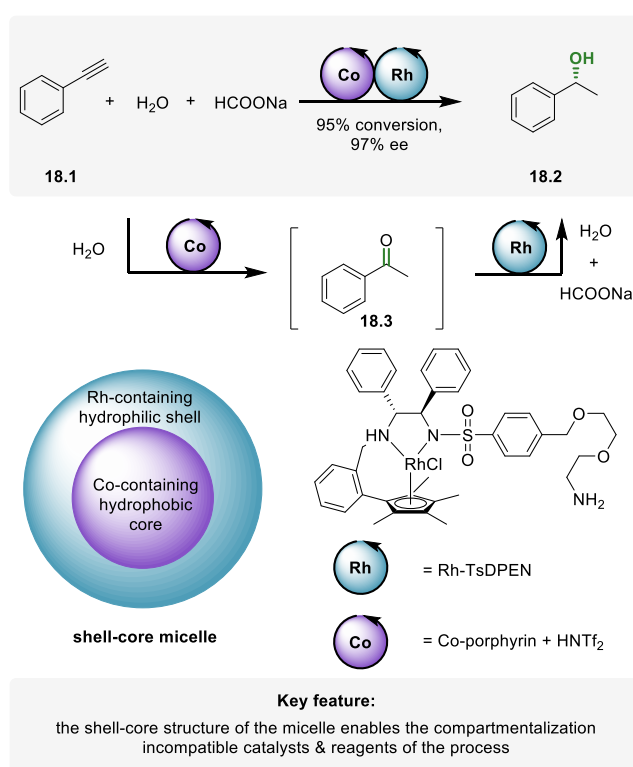
Scheme 5.18. Co-/Rh-catalyzed orthogonal relay for the enantioselective conversion of terminal alkynes to secondary alcohols enabled by the compartmentalization of incompatible reactions.

The reactions are not compatible with each other because HCOONa, that is, the hydrogen source for the Rh-catalyzed transfer hydrogenation, is not compatible with the Co-catalyst. Therefore, the authors designed a core-shell micellar support constructed in an aqueous environment. The Co-catalyzed hydration takes place in the hydrophobic core, which expels detrimental HCOONa, while the Rh-catalyzed hydrogenation takes place in the hydrophilic shell of the micelle. Notably, the fast diffusion of the ketone intermediate within the core-shell micelle containing both catalysts leads to increased yields, when compared to the control reactions in the presence of a mixture of micelles containing one or the other catalyst. Such spatial organization of catalysts mimics the substrate channeling operating in nature.[102]

Noteworthy, when biocatalysis and chemocatalysis are both employed, the sequences are typically executed with the aid of multi-phase systems with catalysts operating in different, non-mixable phases, between which the intermediates are exchanged. For instance, the sequence of Ru-catalyzed olefin metathesis and subsequent P450-catalyzed epoxidation (Scheme 5.15)[85] was executed in a biphasic system consisting of a dioctylphthalate-phase for the metathetic reaction and an aqueous-phase for the epoxidation reaction. Generally, the strategies for the separation of bio- and chemocatalysts are well-developed, and have been reviewed previously.[2] Also, the use of artificial biocatalysts, including artificial metalloenzymes, has been reviewed.[103,104]

5.5.2. Sequential catalysis

Sequential catalysis refers to catalytic transformations in which the catalysts or reagents for each step are added sequentially. The approach simplifies the way to address the issues of compatibility of catalysts and reagents, optimization of conditions for each step, or synchronization of reactions of the sequence, which are often encountered in orthogonal relay catalysis. However, such an approach prevents exploiting the cooperativity of the reactions, i.e., the enabling feature of relay catalysis that was discussed above. Nevertheless, the main advantage remains in the possibility of performing a target sequence of transformations in one-pot, without the need for costly and tedious isolations and purifications of potentially unstable intermediates.

Preventing side-reactions

The sequential addition of catalysts helps to eliminate side reactions. For instance, Reek[105] and co-workers reported a dual-catalytic transition metal system for branch-selective hydroformylation of terminal alkenes, in which two catalysts are added sequentially and the conditions are adapted for each step. The approach prevents secondary reactivity of the first catalyst and eliminates premature reactivity of the second catalyst over the initial substrate. In the first step of the sequence, terminal alkene **19.1** undergoes a Pd-catalyze mono-isomerization to sub-terminal alkene **19.3** (Scheme 5.19). Upon completion of the first step, a base is added to stop any further isomerization processes, which would lead to a mixture of internal alkenes, i.e., the secondary products of the isomerization reaction. The Rh-catalyst is added, and the reaction mixture is subjected to a syngas atmosphere (CO/H_2) to undergo the regioselective hydroformylation of the sub-terminal alkene intermediate **19.3**, yielding α-methyl-branched aldehyde **19.2** selectively in high yield.
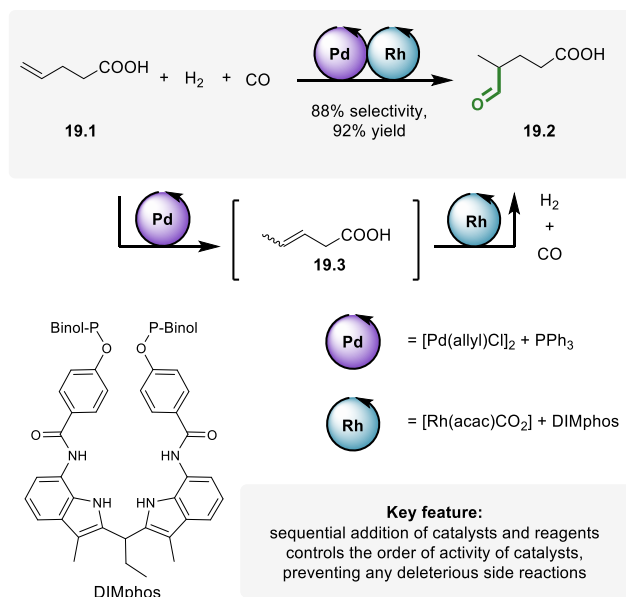
Scheme 5.19. Pd-/Rh-catalyzed sequential olefin isomerization – hydroformylation for α-branch-selective hydroformylation of terminal alkenes.

Eliminating incompatibility issues

The sequential addition of catalysts assists to mitigate the inherent incompatibility between catalysts, such as incompatibility between Brønsted acid and Brønsted base catalysts. For instance, Zhou and co-workers[106] executed a one-pot three-step enantioselective synthesis of spirocyclic indolines **20.3** employing the acid- and base-catalyzed reactions (Scheme 5.20). The sequence starts with a Pd-catalyzed hydrogenation of nitroarene **20.1** to form aryl amine **20.4**, which is then subjected to a Brønsted acid catalyzed coupling with isatin derivative **20.2** to form ketimine **20.5**. Subsequently, a chiral Brønsted base is added to promote the asymmetric 6π electrocyclization, yielding chiral product **20.3** in 85% yield and 92% ee. Sequential catalysis represents a particular advantage when the stability of intermediates with respect to purification procedures limits the yield of a synthetic route. The authors showed that stepwise synthesis yields the product in only 34% overall yield (with 97% ee), illustrating both the practicality and the increased efficiency of the one-pot procedure over the classic stepwise approach.
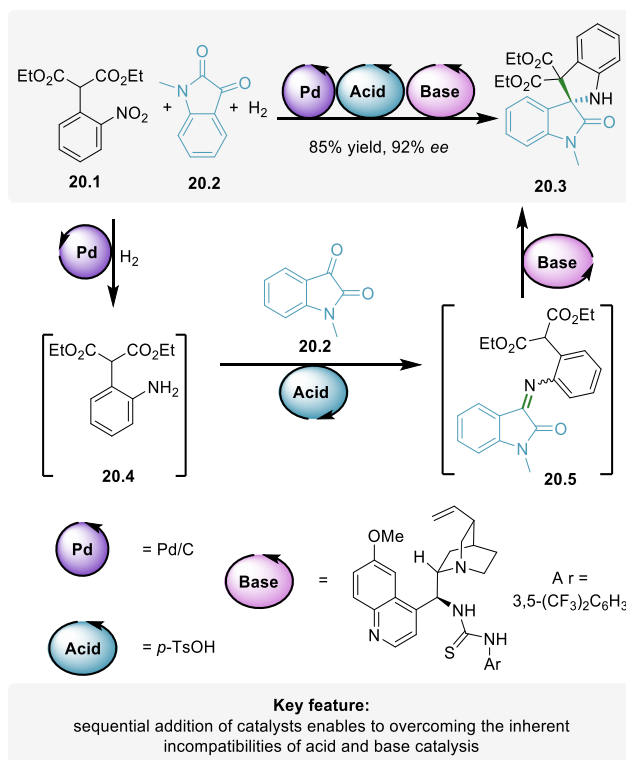
Scheme 5.20. Pd-/Brønsted acid-/ Brønsted base-catalyzed three step sequence involving reduction, coupling, and asymmetric 6π electrocyclization for the formation of spirocyclic indolines.

Exploiting multiple transition metal-catalysts

Although a number of examples of ternary catalytic systems combining transition metal- and organocatalysts operating in a sequential fashion has been reported,[107] three-step sequences occurring in the presence of three transition metal-catalysts remain rare. The main challenges are driven by both the compatibility requirements between all metal complexes and reagents, and the prospective ligand exchanges between the catalysts that are likely to deteriorate their catalytic activities. However, the potential of such multi-catalytic transformations stimulates the development of the ternary transition-metal systems. Ramasatry and co-workers reported one of the first examples of multi-catalytic protocols with three transition metal-catalysts for the 3-step synthesis of β-carbolines **21.2** (Scheme 5.21).[108]
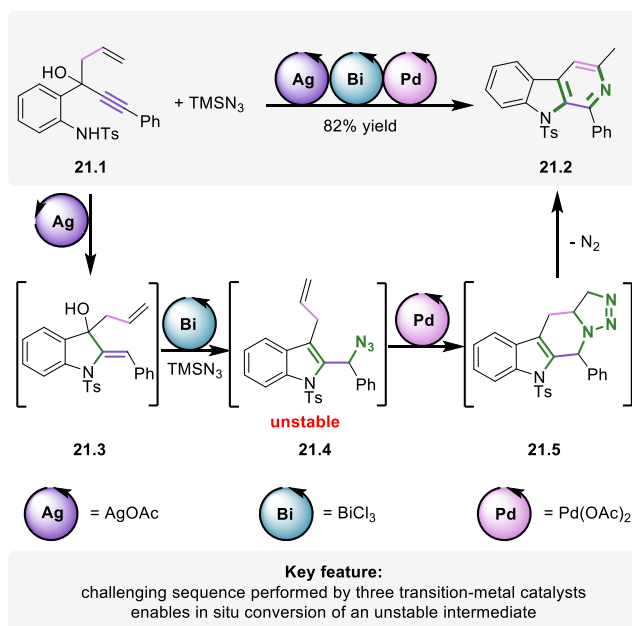
Scheme 5.21. Ag-/Bi-/Pd-catalyzed three step sequence involving hydroamination, 1,3-allylic alcohol isomerization (AAI), and [3+2] cycloaddition for the formation of β-carbolines.

Within the process, starting material **21.1** undergoes first Ag-catalyzed intramolecular hydroamination to form allylic alcohol **21.3**, which is followed by Bi-catalyzed 1,3-allylic alcohol isomerization (AAI) and the Friedel–Crafts-type dehydrative azidation to afford azide intermediate **21.4**. Lastly, the latter undergoes the Pd-catalyzed [3+2]-cycloaddition to form **21.5** followed by nitrogen extrusion to yield β-carbolines **21.2** in overall 82% yield. Noteworthy, azide intermediate **21.4** is unstable and potentially explosive. Hence *in situ* conversion of **21.4**, without the need for potentially dangerous isolation, is the key factor for the formation of the final product both in high yield and in a safe manner.

Multiple transition metal-catalysts in stereoselective synthesis

Compatibility issues aside, the prospective ligand exchange between multiple transition metal catalysts is particularly problematic in case of stereoselective reactions, because any ligand exchange is likely to deteriorate the stereocontrol of the overall transformation. However, because the efficient preparation of chiral molecules is the key in fine-chemical synthesis, stereoselective multi-catalytic systems remain of high interest. We have recently developed multi-catalytic transition-metal protocols that convert alkenes, unsaturated aliphatic alcohols, and aryl boronic acids to form secondary benzylic alcohols, a prevalent moiety in biologically active molecules and valuable building blocks in organic synthesis, with high stereoselectivities, within one-pot sequences of reactions by integrating transition-metal catalyzed alkene cross-metathesis, isomerization, and nucleophilic addition reactions (Scheme 5.22a).[109] Because each reaction of the sequence is executed by an independent catalyst, allylic alcohols bearing a prochiral double bond **22.8** can be converted to any stereoisomer of the product **22.9** with high stereoselectivity (>98:2 er and >20:1 dr, for 1,3-syn and 1,3-anti selective synthesis; Scheme 5.22b). Overall, with the aid of up to four catalysts

operating in a single vessel, the protocols directly convert simple starting materials into a range of valuable products with high stereocontrol. Not only the one-pot protocols are operationally simpler and up to ~3-fold resources more efficient than the stepwise syntheses, but also the overall yield of the product is increased thanks to preventing cumulative losses of materials during subsequent isolations and purifications of the intermediates. Overall, the approach simplifies the synthesis of target motives, increases material efficiency, and limits cost, time, and waste associated with the multi-step procedures.
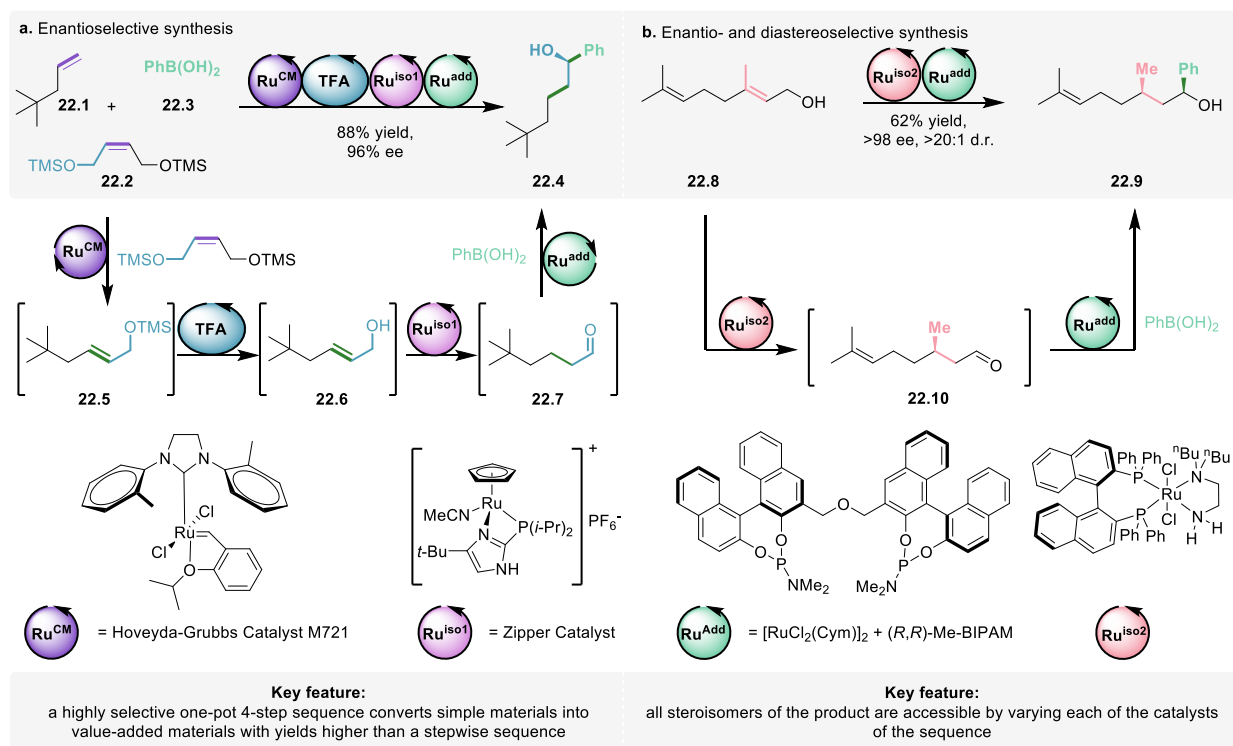
Scheme 5.22. Multi-catalytic sequences for stereoselective synthesis of secondary benzylic alcohols with up to four catalysts working in the same reaction mixture.

5.5.3. Auto-relay catalysis

Auto-relay catalysis, referred to as *auto-tandem catalysis* when two transformations take place, refers to catalytic systems in which a single (pre)-catalyst catalyzes multiple, independent reactions within mechanistically distinct catalytic cycles under the same reaction conditions with all reagents present from the start. The approach faces different challenges than orthogonal relay catalysis. Because a single catalyst is used, incompatibility issues concerning the catalysts are obsolete. The main challenge relates to designing a pre-catalyst that can catalyze two reactions of different catalytic mechanisms in a well-defined manner under the same conditions. The rates of each step are interrelated, and the starting materials and intermediates need to be reactive only in a specific step. Because catalytic activities are promoted by the same pre-catalyst, optimization of each step is challenging with a change of a single parameter affecting all reactions within the sequence. The field has been a subject of a micro-review[110] and conceptual article.[111] Selected examples are discussed below.
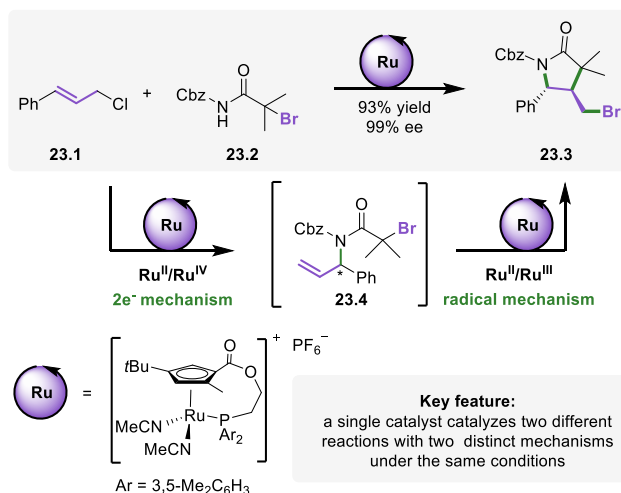
Scheme 5.23. Ru-catalyzed auto-relay of asymmetric allylic substitution (AAS) and atom transfer radical cyclization (ATRC) for enantioselective synthesis of γ-lactams.

The study by Onitsuka and co-workers[112] for the synthesis of enantiomerically enriched γ-lactams **23.3** constitutes an elegant example illustrating the development of auto-relay catalytic systems. The authors envisioned a sequence connecting previously established asymmetric allylic substitution (AAS)[113] of chloroalkene **23.1** with N-nucleophile **23.2** to form bromoalkene intermediate **23.4** with its subsequent atom transfer radical cyclization (ATRC) to yield the final product **23.3** (Scheme 5.23). Both reactions are catalyzed exclusively by a cyclopentadienylruthenium (Cp'Ru) complex through two different mechanisms. While the AAS reaction occurs through the 2-electron Ru^{II}/Ru^{IV} mechanism, the ATRC cyclization reaction occurs through the radical Ru^{II}/Ru^{III} mechanism. Overall, the protocol directly yields the target γ-lactams **23.3** in excellent yields and enantioselectivities.

The field of auto-relay catalysis is dominated by transition metal-based catalytic systems, including recent elegant studies on Ni-catalyzed direct transformations of dienyl allylic alcohols into chiral 1,3-dinitriles by Fang[114] and Rh-catalyzed dehomologation of alcohols into alkenes by Dong[115]; however, organocatalytic auto-relay catalytic systems have been developed as well. Radosevich[116] and co-workers reported a system based on a single redox-active organophosphorus catalyst, which operates two complementary cycles in the P^{III}/P^{V} couple, to execute a condensation-cyclodehydration sequence for amines **24.1** and carboxylic acids **24.2** as starting materials (Scheme 5.24).

The key common intermediate, bromophosponium cation **24.5**, is generated upon reduction of phosphine oxide pre-catalyst **R₃P=O** by phenylsilane and subsequent halophilic reaction with the oxidant DEBM (diethyl bromomalonate). Condensation involves the activation of acid **24.2** with cation **24.5** to form activated onium intermediated **24.6**, which in turn reacts with amine **24.1** to form amide intermediate **24.4** within the C-N bond forming cycle. Then, amide **24.4** reacts again with catalytic cation **24.5** to form the final product **24.3** through activated onium intermediate **24.7** within the C-C bond forming cycle.
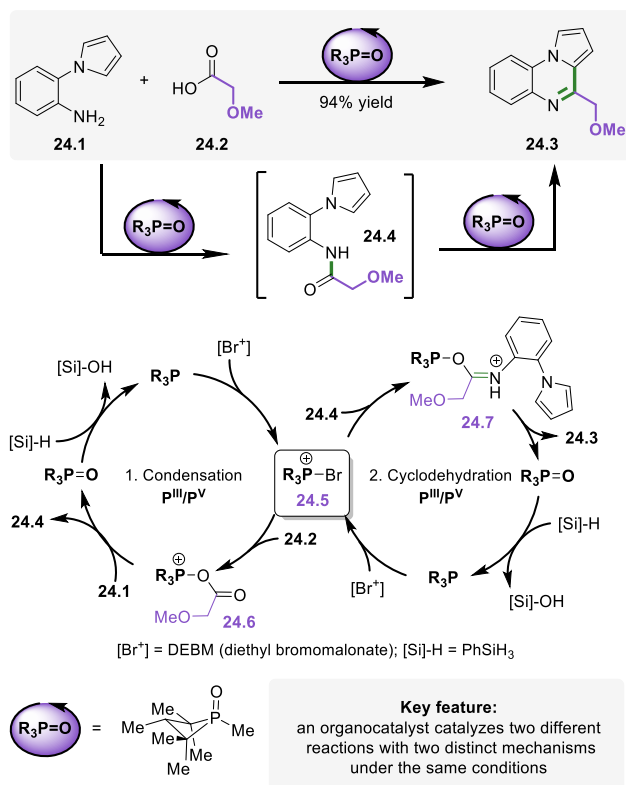
Scheme 5.24. Condensation-cyclodehydration sequence occurring in the presence of a single organocatalyst that operates two complementary and functionally distinct catalytic cycles.

Reaction ordering by 'delay loop'

A major challenge in auto-relay catalysis is to establish kinetic hierarchy for each catalytic cycle involved when the intrinsic reactivity order does not match the required sequence and leads to detrimental side reactions. With the aim to provide an easy access to enantioenriched unprotected homoallylic amines, a valuable building block in organic synthesis, Hoveyda[117] and co-workers studied a single copper-based catalytic system to promote reductive coupling of allenes and nitriles (Scheme 5.25). Two functionally different catalytic cycles operate simultaneously to catalyze allene **25.1** addition to a nitrile **25.2**, enabled by Cu-B(pin) species, and ketimine **25.5** reduction enabled by Cu−H species. However, premature addition of Cu-H to allene lead to side-products, lowering the efficiency of the overall process. To address this issue, the authors introduced a non-productive 'delay loop' by adding a sacrificial reagent, which reacts with Cu-H faster than the allene does, and hence holds the reduction step just until the ketimine intermediate is formed; the latter reacting with Cu-H faster than the sacrificial reagent. Overall, the delay loop ensures the required order of the catalytic events is kept, albeit at the price of non-productive consumption of sacrificial reagents.
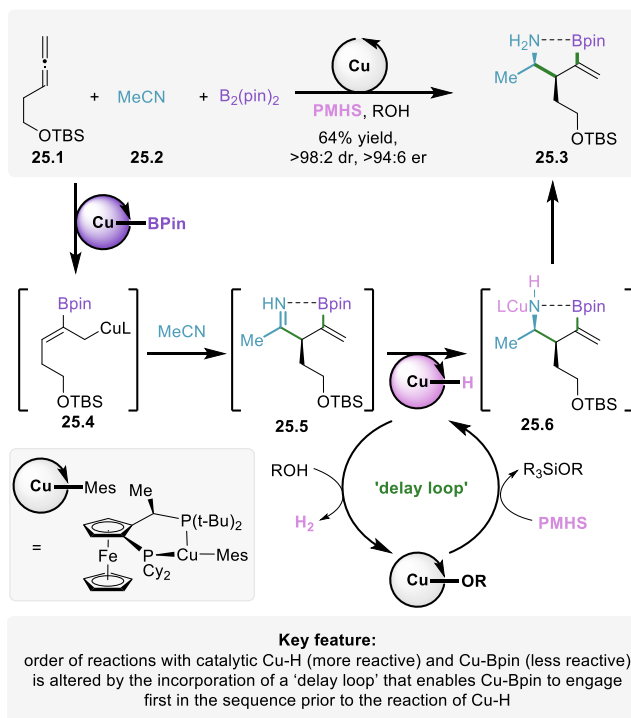
Scheme 5.25. Cu-catalyzed auto-relay of reductive coupling of allenes and nitriles for the preparation of NH$_2$-amines.

Pseudo-allosteric regulation of catalytic activity

Another strategy to ensure precise ordering of catalytic activities is to separate the operation of different catalytic cycles in the time domain through a pseudo-allosteric control. Herzon[118] and co-workers reported an example in which two catalytic functions of a Ru-complex - hydration and reduction - are separated in time (Scheme 5.26). The key aspect of this system is that the resting states of the catalyst in each catalytic cycle are metal–substrate complexes. Therefore, the substrate that binds the strongest to the Ru-resting state dominates its catalytic activity until this substrate is consumed. Within the sequence, first a strongly binding alkyne **26.1** undergoes anti-Markovnikov hydration to the corresponding aldehyde **26.4**, which in turn undergoes uncatalyzed Wittig olefination to form 1,4-enone intermediate **26.6**. Because the reduction activity of the catalyst remains latent in the presence of alkyne **26.1**, the side-reduction of the aldehyde **26.4** to the alcohol **26.5** is inhibited, so the intermediate is selectively converted to 1,4-enone **26.6**. When conversion of alkyne **26.1** is finished, 1,4-enone **26.6** can bind to the catalyst to be reduced to the ketone **26.3** through transfer-hydrogenation, forming the product in high yield (up to 75%). The overall control of activity resembles the allosteric mechanism controlling activity of enzymes, that is, one of the key features enabling biosynthetic pathways to be executed through well-orchestrated enzymatic reactions.
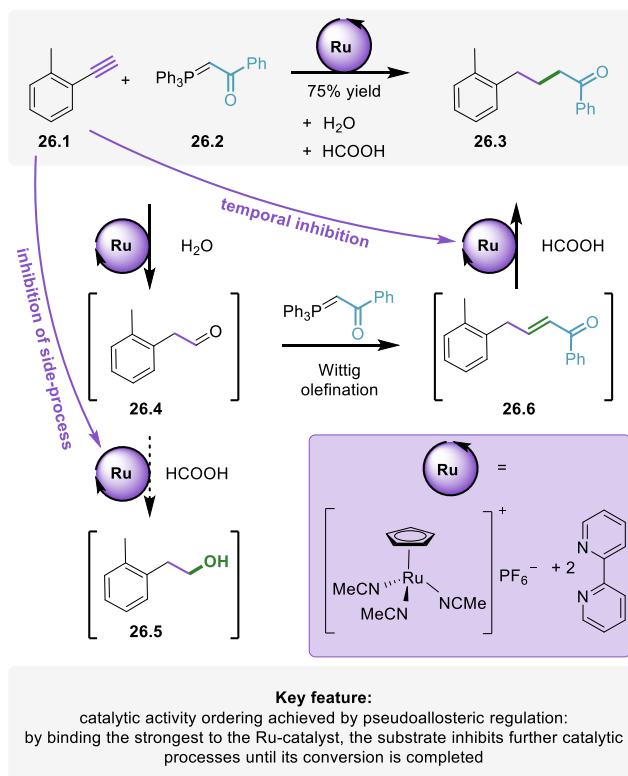
Scheme 5.26. Ru-catalyzed auto-relay of alkyne hydration, Wittig olefination, and transfer-hydrogenation with a pseudo-allosteric regulation of catalytic activity.

5.5.4. Assisted-relay catalysis

Assisted-relay catalysis refers to catalytic systems in which a single catalyst operates multiple reactions within different catalytic cycles, but the subsequent reactions are triggered by the addition of reagents or change in the reaction conditions. Because optimal conditions for each step can be easily adjusted, the order of steps can be controlled. However, because of the time separation of the different catalytic cycles, cooperation between reactions remains excluded.

<u>Temperature trigger</u>

Temperature changes are often used to change the activity of the catalyst. Recently, Ackermann[119] and co-workers reported sequential *meta*-C–H alkylation and *ortho*-C–H arylation of aryloxazoline **27.1** occurring in the presence of a single ruthenium(II) complex (Scheme 5.27). First, the starting material undergoes *meta*-selective C-H-alkylation with alkyl bromide **27.2** through the radical Ru^{II}/Ru^{III} mechanism. After completion of the first step, aryl bromide **27.3** is added, and the reaction temperature is increased to trigger Ru-catalyzed *ortho*-selective C–H-arylation through the two-electron Ru^{II}/Ru^{IV} mechanism to form the double C–H functionalized product **27.4** in one-pot in 73% overall yields.
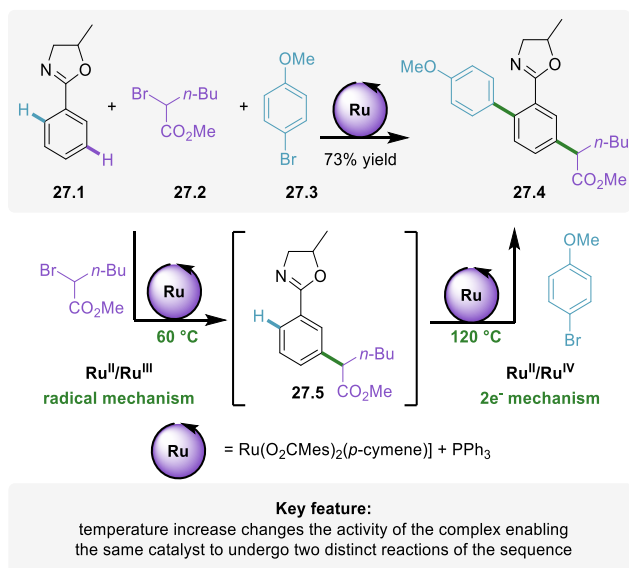
Scheme 5.27. Ru-catalyzed temperature-controlled assisted-relay of sequential C−H alkylation via radical mechanism and *ortho*-C−H arylation via Ru^{II}/Ru^{IV} mechanism.

Chemical trigger

Chemical triggers can be used to trigger the activity change of a catalyst in assisted-relay catalysis. Choudhury[120] and co-workers reported a Ru(II)-complex, which is able to adopt two different states for different catalytic functions: the first state for dehydrogenative coupling of amines, and the second state for hydrogenation of imines (Scheme 5.28). Both states of the catalyst are switched by the addition of an acid or a base. In a model experiment, 4-methylbenzylamine **28.1** undergoes dehydrogenative coupling to form the corresponding imine intermediate **28.3** in the presence of the catalyst in the first state. Upon addition of a base, the Ru-catalyst adapts the second state, which undergoes hydrogenation of the imine intermediate **28.3** in the presence of hydrogen gas, furnishing the dibenzylamine product **28.2** in 70% yield.
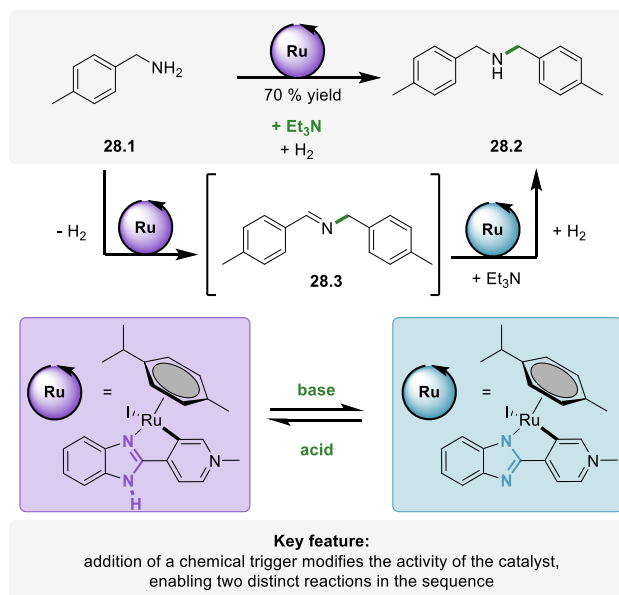
Scheme 5.28. Ru-catalyzed pH-controlled assisted-relay of sequential dehydrogenative coupling of amines followed with hydrogenation of the imine intermediate.

5.6. Complex systems

While most multi-catalytic systems involve just two reactions or two catalysts and can be assigned to a single class of cooperative, domino, or relay catalysis, a higher level of complexity becomes increasingly more common. Although the development of such systems is particularly challenging, due to increasing demand for the precise ordering of the catalytic events and preventing any incompatibility issues or side-reactions between multiple catalysts and reagents, enormous potential for achieving highly efficient synthetic transformations motivates the research in the field. Within this chapter, we discuss selected examples that illustrate various combinations of cooperative, domino, and different types of relay catalysis. The selected studies highlight both increasing complexity and synthetic potential of such multi-catalytic approaches to access increasingly complex architectures from simple starting materials within sequences of precisely orchestrated catalytic events.

We classified the studies of complex systems into two main categories: (a) unassisted complex systems, in which all reactions of the sequence occur without any change to the conditions or any additions of reagents or catalysts, and (b) assisted complex systems, in which the sequence requires the conditions to be modified or reagents/catalysts to be added in the course of the process to trigger subsequent transformations.

5.6.1. Unassisted complex systems

Unassisted complex systems that contain all reagents and catalysts from the start are particularly challenging to design, due to the requirement of compatibility between multiple reagents and catalysts, precise ordering of the catalytic events, and preventing any side-reactions. However, such systems offer the broadest realm of opportunities by merging the advantages of cooperativity between catalysts (i.e., cooperative catalysis) and cooperativity

between reactions (i.e., relay catalysis). Below we discuss selected examples of complex systems exploiting either orthogonal- or auto-relay catalysis together with cooperative catalysis.

Orthogonal relay catalysis with the 2nd step involving cooperative catalysis (4 catalysts):

Gong[121] and co-workers reported a protocol exploiting four catalysts to combine hydroformylation of alkenes and asymmetric allylation of aldehydes. The sequence directly converts styrene derivatives, allylic alcohols, and syngas (i.e., CO and H_2) to form α-quaternary aldehydes enantioselectively (Scheme 5.29). First, styrene **29.1** undergoes hydroformylation with H_2 and CO to form α-branched aldehyde **29.4** in the presence of a Rh-catalyst. In the meantime, the reaction of allylic alcohol **29.2**, a Pd(0)-complex, and a chiral phosphoric acid forms a chiral π-allyl Pd species. The aldehyde intermediate **29.4** reacts with an amine catalyst to form an enamine species **29.5**, which undergoes asymmetric allylation with the π-allyl Pd species, exploiting triple-catalytic cooperative catalysis to form quaternary imine enantioselectively. Upon imine hydrolysis **29.6**, the final α-quaternary chiral aldehyde **29.3** is released. Overall, two C-C bonds are created to form all-carbon quaternary center in a stereoselective fashion with the aid of four catalysts.
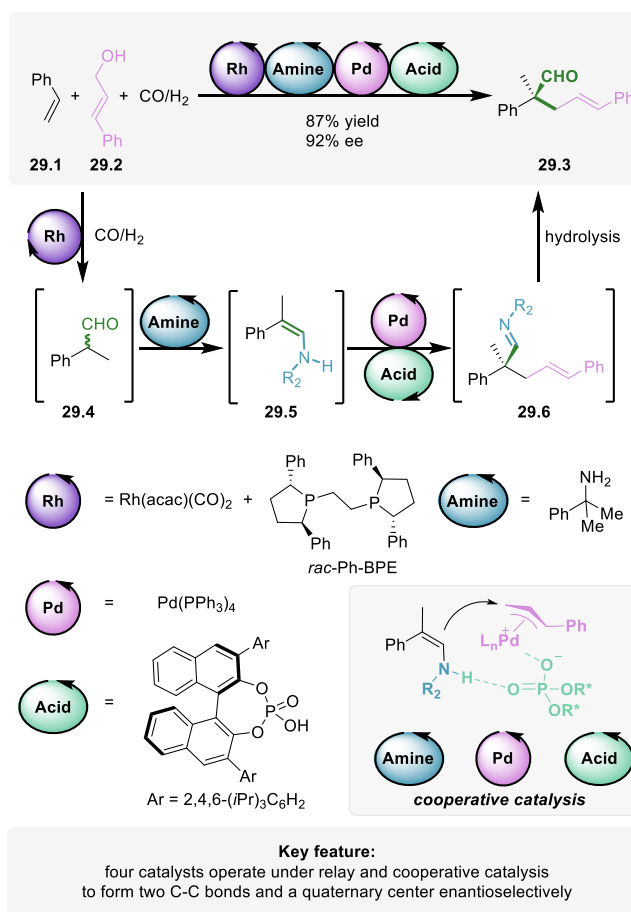
Scheme 5.29. Rh-/Pd-/Brønsted acid-/amine-catalyzed relay involving hydroformylation and cooperative asymmetric allylation to convert vinyl arenes, allylic alcohols, and syngas to form α-quaternary chiral aldehydes.

Gong[122] and co-workers reported a sequence of hydroamination and allylic alkylation reactions occurring in the presence of three catalysts operating under orthogonal relay- and cooperative catalysis (Scheme 5.30). The sequence starts with an Au-catalyst triggering intramolecular hydroamination of secondary amine-bridged enyne **30.1** to form N-allylic enamine intermediate **30.3**. Then, the N-allylic enamine undergoes intramolecular allylic alkylation under cooperative catalysis of a Pd-complex and a Brønsted acid to yield final pyrrolidine derivative **30.2**.
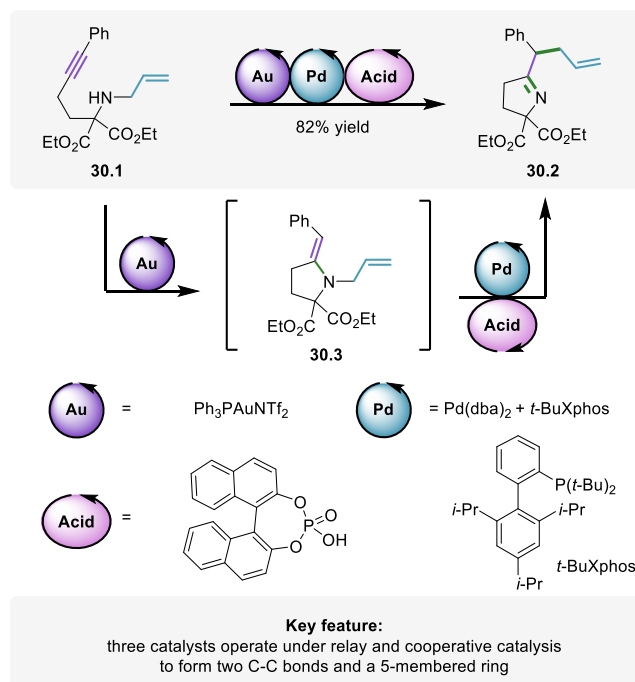
Scheme 5.30. Au-/Pd-/Brønsted acid-catalyzed relay of intramolecular hydroamination and cooperative allylic alkylation for transforming secondary amine-bridged enynes into pyrrolidine derivatives.

Auto-relay catalysis with the 2nd step involving cooperative catalysis (one catalyst acts both cooperatively and non-cooperatively):

Gong[123] and co-workers reported enantioselective one-pot synthesis of julolidine derivatives, exploiting two catalysts that operate under auto-relay and cooperative catalysis (Scheme 5.31). The synthesis embarks with phosphoric acid-catalyzed enantioselective [4+2] cycloaddition of the aryl imine formed *in situ* (from **31.1** + **31.2**) and enamine **31.3** to form tetrahydroquinoline intermediate **31.5** bearing an alkyne moiety. Subsequently, the latter undergoes intramolecular hydroamination to form dehydrojulolidine product **31.6** in the presence of cooperative gold phosphate and phosphoric acid catalysts. The synthesis is completed by the stochiometric reduction with a borohydride reagent to form julolidine derivative **31.4** in overall high yield and enantioselectivity.

Cooperative and orthogonal relay catalysis (two independent cooperative systems, consisting of three and two catalysts, respectively, work in relay,):

Merging racemic photoredox/organo dual-catalytic reactions[124] with enzymatic kinetic resolution can serve as a platform for executing elusive stereoselective functionalization reactions at remote, unactivated sites of starting materials. In that context, MacMillan, Hyster, and co-workers[125] recently reported an approach in which a racemic mixture of β-substituted ketone, (S)-**32.1** and (R)-**32.2**, is converted to nearly enantiopure γ-substituted alcohol **32.3** by merging a substrate-selective reduction process operated by two enzymes with a racemization sequence enabled by three cooperative catalysts (Scheme 5.32). In the system, (R)-**32.2** is reduced stereoselectively to alcohol **32.3** by substrate-selective NADPH-dependent ketoreductase working in combination with glucose dehydrogenase.
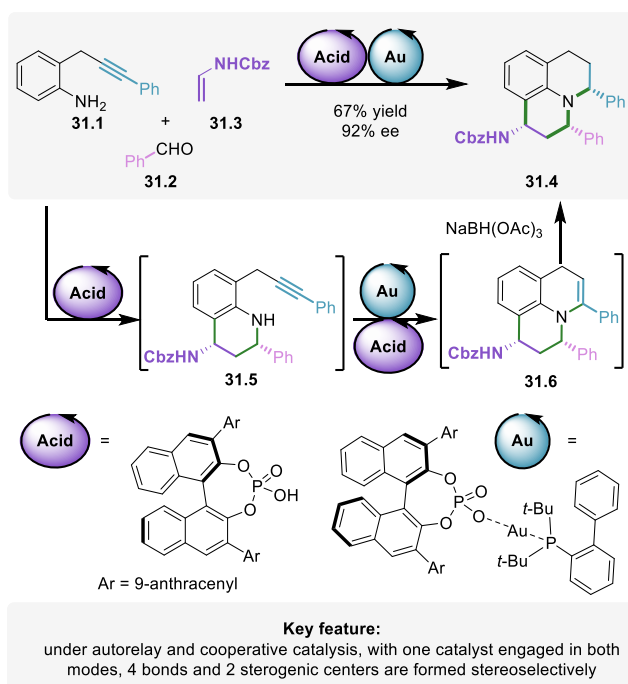
Scheme 5.31. Brønsted acid-/Au-catalyzed auto-relay of enantioselective [4+2] cycloaddition and cooperative intramolecular hydroamination for the synthesis of julolidine derivatives.
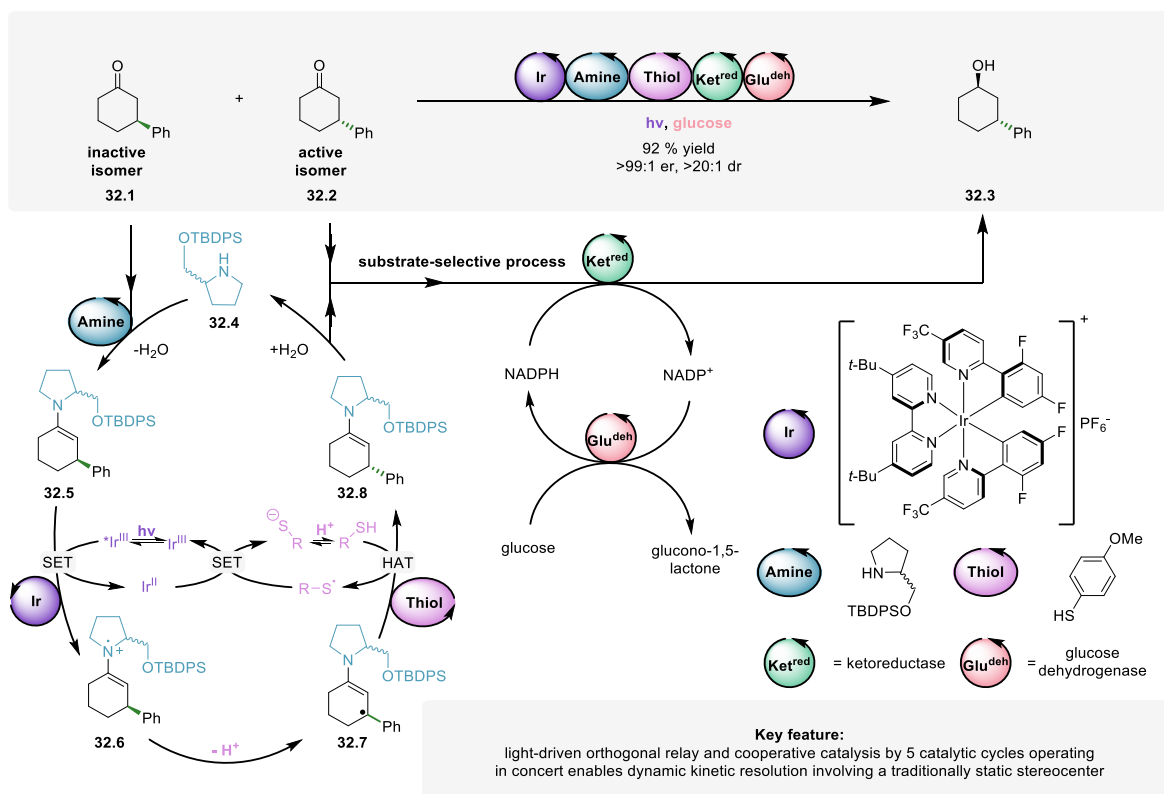
Scheme 5.32. Merging photocatalysis with enzymatic reactions enables stereoselective reactions at traditionally static stereocentres of racemic starting materials.

Importantly, (*S*)-**32.1** remains unreactive to the enzyme. However, (*S*)-**32.1** undergoes continuous racemization in the system with the aid of three cooperating catalysts under light irradiation. First, (*S*)-**32.1** undergoes condensation with amine **32.4** to form enamine (*S*)-**32.5**, which is oxidized to enaminyl radical cation (*S*)-**32.6** by the excited iridium photocatalyst. Upon subsequent deprotonation of (*S*)-**32.6** at its allylic site, the stereochemical information is lost and prochiral radical intermediate **32.7** is formed. An unselective HAT between **32.7** and the thiol catalyst forms a racemic mixture of (*S*)-**32.5** and (*R*)-**32.8**. Upon hydrolysis, (*R*)-**32.2** is formed, which undergoes selective reduction to product **32.3**, and (*S*)-**32.1**, which enters again the racemization cycle. This unique protocol that exploits five catalysts operating in parallel demonstrates the feasibility of catalytic systems of increasing complexity to execute attractive transformations that remain beyond the capabilities of standard systems.

5.6.2. Assisted complex systems

The possibility to modify the conditions of reaction sequence occurring under multi-catalysis expedites the development of such complex systems, however, at the price of preventing the cooperativity between reactions taking place in different phases of the process. Nevertheless, such 'assisted' systems can substantially simplify synthetic processes, increasing their overall efficiency. Bellow we discuss selected examples of assisted complex systems exploiting either sequential or assisted-relay catalysis along with cooperative, auto- or orthogonal-relay catalysis.

Beller[126] and co-workers developed a triple catalytic system that exploits sequential and cooperative catalysis to directly convert aryl alkynes, anilines, and molecular hydrogen into enantioenriched secondary benzylic amines (Scheme 5.33). Initially, an Au-catalyst triggers hydroamination of alkyne **33.1** with aniline **33.2** to form an imine, which is subsequently isomerized to ketimine intermediate **33.4**. Upon completion, the inert atmosphere is exchanged for hydrogen, Knölker's complex and a chiral phosphoric acid are added, which catalyze cooperative enantioselective reduction of the ketimine intermediate **33.4** to form the benzylamine **33.3** in high yield and enantioselectivity. Notably, the authors showed that the sequence occurs when all reagents and catalysts are present from the start (i.e., under orthogonal-relay and cooperative catalysis). However, in the latter case, the product was formed in lower yield and selectivity than for the sequential approach (42% yield and 49% ee, versus 80% yield, and 94% ee, respectively), indicating that sequential addition prevents the detrimental side reactions.
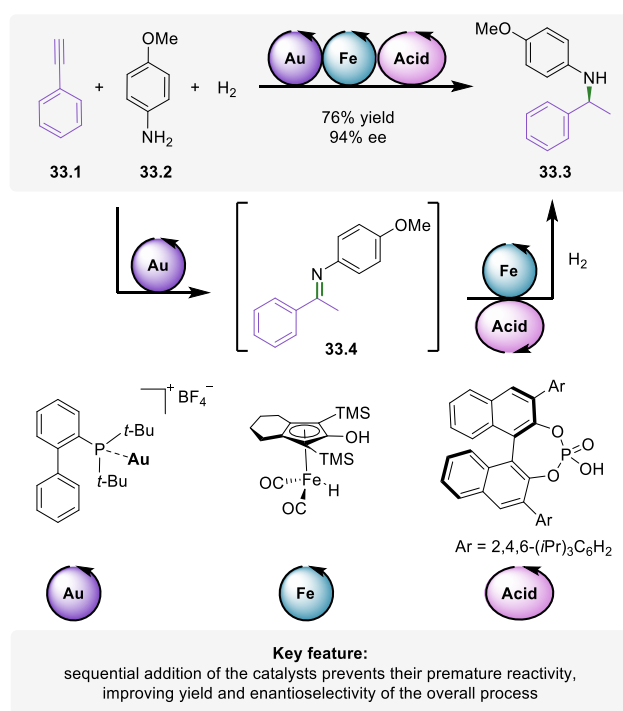
Scheme 5.33. Au-/ Fe-/Brønsted acid-catalyzed sequential hydroamination of alkynes with primary amines followed by cooperative enantioselective hydrogenation.

Sequential catalysis with the 2nd step involving both auto-relay and orthogonal relay catalysis (4 reactions with 3 catalysts)

Combining multiple catalytic activities of several catalysts can ideally provide synthetic sequences that transform abundant chemical commodities into value-added building blocks with high atom- and material-efficiency. Huang[127] and co-workers reported recently a

compelling example, where linear alkanes are converted directly into linear alcohols with theoretical 100% atom efficiency within a triple-catalytic, two-step sequence (Scheme 5.34). In the first step, alkane **34.1** undergoes acceptorless dehydrogenation to form a mixture of alkenes **34.3** and **34.4** in the presence of an Ir-catalyst. In the second step, the alkene intermediates undergo Rh-catalyzed auto-relay isomerization-hydroformylation sequence to form selectively linear aldehyde **34.5**, which in turn directly undergoes Ru-catalyzed hydrogenation to form the linear alcohol product **34.2**. In principle, dihydrogen, the sole by-product of the first step, could be incorporated in the subsequent step, demonstrating the concept of material leveraging in the reaction sequence to improve atom-economy of the synthesis.
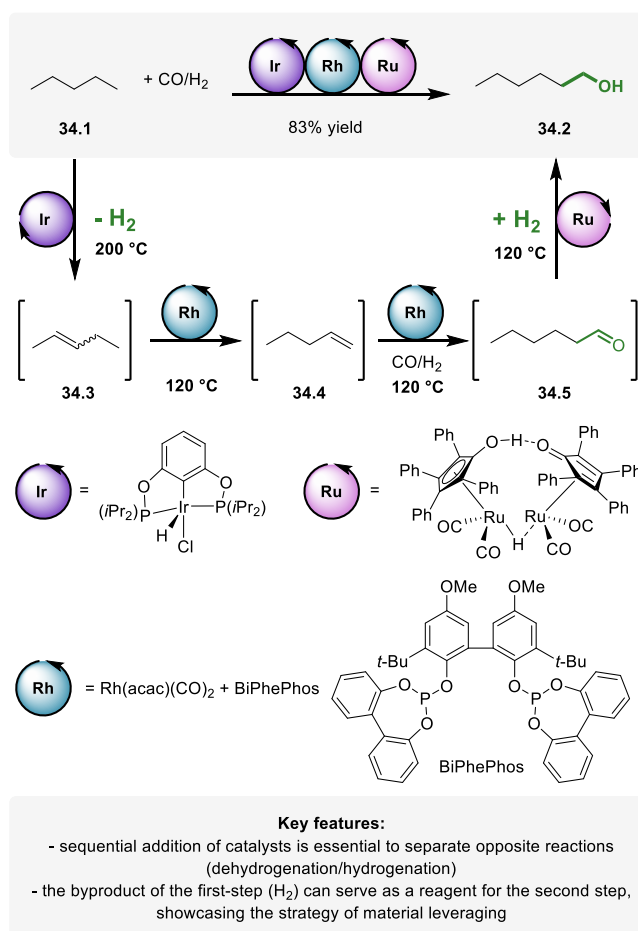
Scheme 5.34. Ir-/Rh-/Ru-catalyzed sequential dehydrogenation of alkanes followed with orthogonal and auto-relay of olefin isomerization, hydroformylation, and hydrogenation to transform *n*-alkanes to *n*-alcohols.

It is worth to underscore that all reactions of isomerization-hydroformylation-hydrogenation relay occur in parallel under the same conditions with suitable rates and high chemoselectivity, being the key to form the product in high yield.

Assisted-relay catalysis with the first step involving orthogonal relay catalysis (3 reactions with 2 catalysts)

Chaładaj[128] and co-workers reported a four-component Pd-catalyzed perfluoroalkylative arylation of alkynes, which operates through three functionally distinct catalytic cycles, exploiting relay catalysis and temperature-triggered assisted-relay catalysis (Scheme 5.35).
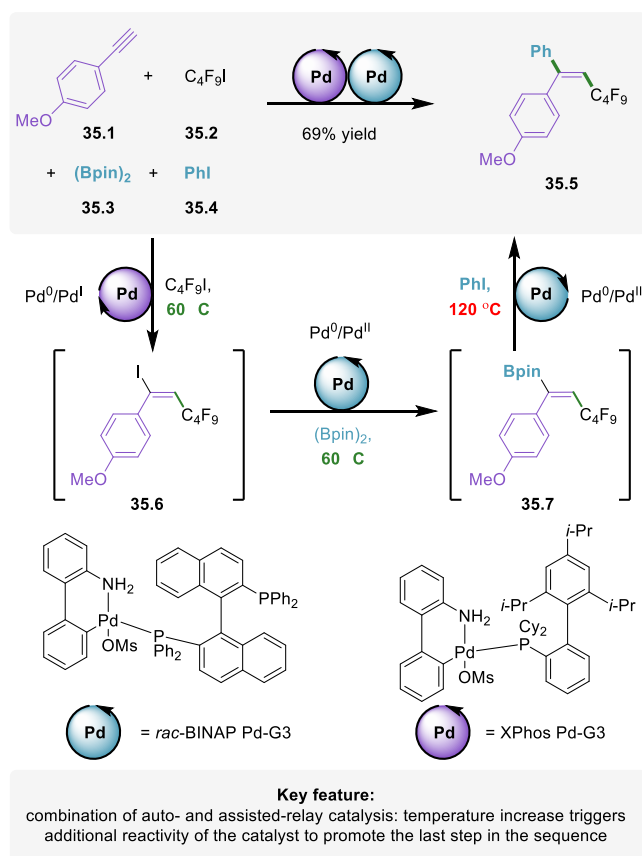
Scheme 5.35. A four-substrate orthogonal relay of perfluoroalkylative iodination of alkynes and borylation merged with assisted-relay of temperature-triggered Suzuki cross coupling. Two Pd-catalysts operate three functionally distinct catalytic cycles, merging auto-relay and assisted-relay catalysis.

Initially, alkyne **35.1** reacts with perfluoroalkyl iodide **35.2** to form vinyl iodide **35.6** through radical Pd^0/Pd^I mechanism involving binap-Pd catalyst. The vinyl iodide **35.6** undergoes directly borylation with $(Bpin)_2$ to form vinyl boronate ester **35.7** within the orthogonal relay through the Pd^0/Pd^{II} mechanism by Xphos-Pd catalyst. Upon completion, the reaction temperature is increased to trigger the Suzuki coupling of the vinyl boronate ester **35.7** with aryl iodide **35.4** to deliver the final product **35.5**.

Assisted-relay catalysis with the 2nd step involving cooperative catalysis (one catalyst acts both cooperatively and non-cooperatively):

Lautens[129] and co-workers reported a three-component synthesis of fully substituted triazoles in the presence of two catalysts operating under assisted-relay and cooperative

catalysis (Scheme 5.36). The sequence starts with a substrate-selective Cu-catalyzed cycloaddition of organic azide **36.1** with iodoalkyne **36.2** to form iodotriazole **36.5**, in the presence of another alkyne **36.3** that remains unreactive under the initial conditions.
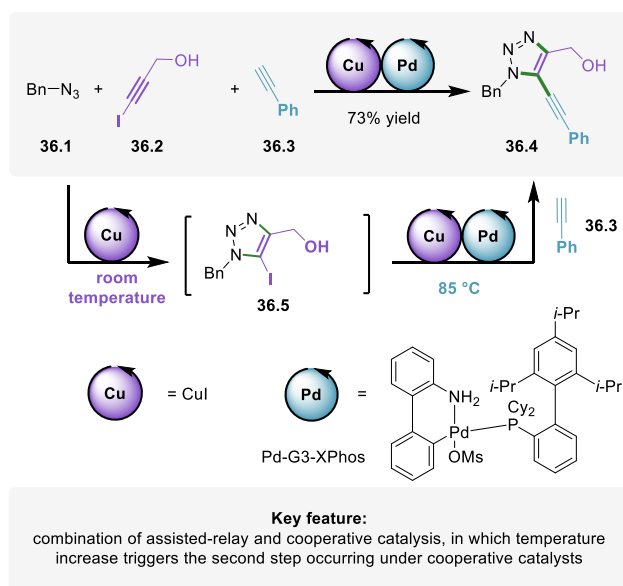
Scheme 5.36. Cu-/Pd-catalyzed temperature-controlled assisted-relay involving cycloaddition and cooperative Sonogashira coupling to obtain fully substituted triazoles.

Upon completion, the temperature is increased from room temperature to 85 °C to trigger the Pd-/Cu-catalyzed Sonogashira reaction of iodotriazole intermediate **36.5** with terminal alkyne **36.3**, yielding fully substituted triazole **36.4** in high overall yield. Although the complete sequence can also be executed directly at 85 °C, the product is formed in significantly lower yield (30% vs. 73%). Careful optimization of the Pd-precatalyst, base, and the temperature program was essential to prevent premature side reactions and ordering the catalytic activity.

Assisted-relay catalysis with the 1st step involving cooperative catalysis and the 2nd step involving divergent catalysis (one catalyst acts both cooperatively and non-cooperatively):

Catalysts with complementary selectivities, such as stereodivergent selectivity, are attractive in the context of diversity-oriented synthesis. The ability to control the activity of complementary catalysts within a sequence represents an appealing strategy for the divergent synthesis. Lalic[130] and co-workers recently reported an elegant dual-catalytic system to perform either (*Z*)- or (*E*)-selective synthesis of vinyl arenes, with the selectivity being controlled by the reaction conditions (Scheme 5.37). First, a Sonogashira cross-coupling reaction between terminal alkyl alkyne **37.1** and aryl halide **37.2** takes place under cooperative Pd/Cu-catalysis. Then, alkyne intermediate **37.5** undergoes semireduction under assisted-relay catalysis by either Cu- or Pd-complex. While the (*Z*)-selective semi-reduction to furnish **37.3** is promoted by the Cu-complex in the presences of close to stoichiometric amount of methanol as a reductant, the (*E*)-selective semi-reduction to yield **37.4** selectively is conducted by the Pd-complex in the presence of excess methanol. Overall, the possibility to suppress the

activity of the Cu-catalyst by excess methanol provides a convenient handle to direct the overall reaction to form either diastereomer of the product in high selectivity and yield.
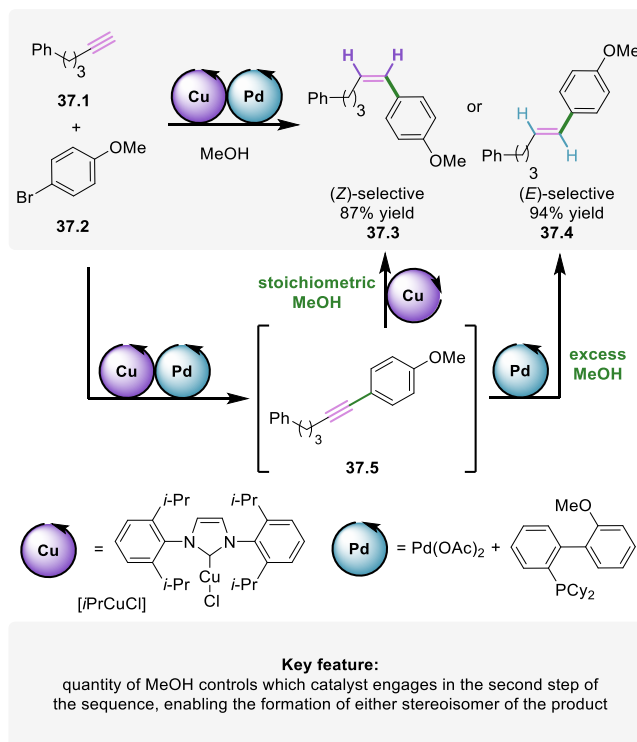
Scheme 5.37. Cu-/Pd-catalyzed reagent-triggered stereo-divergent assisted-relay of cooperative Sonogashira coupling and semireduction to form either the (Z)-alkenes under Cu-catalysis or the (E)-alkenes under Pd-catalysis: amount of methanol can divert the activity from Cu- to Pd-catalyst.

5.7. Conclusions and perspective of the chapter

Driven by the demand for more efficient and sustainable chemical processes, the field of catalysis continues its rapid development. As illustrated in this chapter, multi-catalysis emerges not only to outcompete the current synthetic protocols, but most importantly also to bring new 'one-pot' transformations that exhibit outstanding resource efficiency. Remarkably, multi-catalytic sequences can undergo through otherwise unfeasible pathways thanks to, for instance, prospectively unstable intermediates being converted as soon as formed. Exemplarily, dual-catalytic systems can enable the direct functionalization of inherently unreactive sites of molecules, thanks to cooperation between reversible catalytic reactions and orthogonal functionalization reactions, opening new valuable short-cuts to the synthetic practitioner.

Despite major challenges that need to be addressed with respect to compatibility issues and catalyst reactivity ordering, recent studies show many competent strategies to address these. For instance, sequential additions of reagents or catalysts, reaction compartmentalization or catalyst encapsulation, proved to be feasible solutions to overcome such incompatibility issues. Likewise, the use of chemical triggers able to induce a change of catalytic activity or stepwise temperature programming of the sequence of reactions, are practical solutions to deliver the correct order of reactions within the targeted sequence. However, these strategies

eliminate the advantage of cooperativity between reactions in the sequence, limiting the full potential of multi-catalytic systems. Therefore, novel strategies that address these challenges *in situ* need to be developed. Recent examples in the literature show that mimicking the features of enzymes, that is, (i) allosteric regulation, (ii) substrate-selective catalysis, or (iii) substrate channeling between consecutive catalytic sites, are plausible ways to solve those issues while maintaining the cooperativity between reactions.

In addition, a fundamental change in approach has to be made in order to improve the development of such complex multi-catalytic systems and to study its emergent properties. In this context, suitable catalysts able to perform with excellent chemo- and reaction-selectivity within a complex mixture are most likely to be different than those performing best in single reaction environments. Linear screening of different parameters for such multivariate systems is rather impractical. Therefore, new strategies to design, analyze and validate the development of such systems are required. Overall, although many challenges remain open, the prospects of multi-catalysis are vast. We envision that future studies will enable the rational design of processes, in which multiple catalysts are orchestrated precisely to transform simple starting materials into valuable products within complex systems of interconnected reactions.

5.8. References

(1) Bartholomew, C. H.; Farrauto, R. J. *Fundamentals of Industrial Catalytic Processes*; John Wiley & Sons, Inc.: Hoboken, NJ, USA, 2005.

(2) Rudroff, F.; Mihovilovic, M. D.; Gröger, H.; Snajdrova, R.; Iding, H.; Bornscheuer, U. T. Opportunities and Challenges for Combining Chemo- and Biocatalysis. *Nat. Catal.* **2018**, *1* (1), 12–22.

(3) Galván, A.; Fañanás, F. J.; Rodríguez, F. Multicomponent and Multicatalytic Reactions - A Synthetic Strategy Inspired by Nature. *Eur. J. Inorg. Chem.* **2016**.

(4) Hwang, E. T.; Lee, S. Multienzymatic Cascade Reactions via Enzyme Complex by Immobilization. *ACS Catal.* **2019**, *9* (5), 4402–4425.

(5) Ji, Q.; Wang, B.; Tan, J.; Zhu, L.; Li, L. Immobilized Multienzymatic Systems for Catalysis of Cascade Reactions. *Process Biochem.* **2016**, *51* (9), 1193–1203.

(6) Sperl, J. M.; Sieber, V. Multienzyme Cascade Reactions—Status and Recent Advances. *ACS Catal.* **2018**, *8* (3), 2385–2396.

(7) Ricca, E.; Brucher, B.; Schrittwieser, J. H. Multi-Enzymatic Cascade Reactions: Overview and Perspectives. *Adv. Synth. Catal.* **2011**, *353* (13), 2239–2262.

(8) Fogg, D. E.; dos Santos, E. N. Tandem Catalysis: A Taxonomy and Illustrative Review. *Coord. Chem. Rev.* **2004**, *248* (21–24), 2365–2379.

(9) Patil, N. T.; Shinde, V. S.; Gajula, B. A One-Pot Catalysis: The Strategic Classification with Some Recent Examples. *Org. Biomol. Chem.* **2012**, *10* (2), 211–224.

(10) Tietze, L. F.; Brasche, G.; Gericke, K. M. Domino Reactions in Organic Synthesis. In *Domino Reactions in Organic Synthesis*; Wiley: Weinheim, 2006; pp 1–541.

(11) Allen, A. E.; MacMillan, D. W. C. Synergistic Catalysis: A Powerful Synthetic Strategy for New Reaction Development. *Chem. Sci.* **2012**, *3* (3), 633.

(12) Inamdar, S. M.; Shinde, V. S.; Patil, N. T. Enantioselective Cooperative Catalysis. *Org. Biomol. Chem.* **2015**, *13* (30), 8116–8162.

(13) Kim, D.-S.; Park, W.-J.; Jun, C.-H. Metal–Organic Cooperative Catalysis in C–H and C–C Bond Activation. *Chem. Rev.* **2017**, *117* (13), 8977–9015.

(14) Afewerki, S.; Córdova, A. Combinations of Aminocatalysts and Metal Catalysts: A Powerful Cooperative Approach in Selective Organic Synthesis. *Chem. Rev.* **2016**, *116* (22), 13512–13570.

(15) Peters, R. *Cooperative Catalysis*; Peters, R., Ed.; Wiley: Weinheim, 2015.

(16) Romiti, F.; del Pozo, J.; Paioti, P. H. S.; Gonsales, S. A.; Li, X.; Hartrampf, F. W. W.; Hoveyda, A. H. Different Strategies for Designing Dual-Catalytic Enantioselective Processes: From Fully Cooperative to Non-Cooperative Systems. *J. Am. Chem. Soc.* **2019**, *141* (45), 17952–17961.

(17) Krautwald, S.; Sarlah, D.; Schafroth, M. A.; Carreira, E. M. Enantio- and Diastereodivergent Dual Catalysis: -Allylation of Branched Aldehydes. *Science* **2013**, *340* (6136), 1065–1068.

(18) Krautwald, S.; Schafroth, M. A.; Sarlah, D.; Carreira, E. M. Stereodivergent α-Allylation of Linear Aldehydes with Dual Iridium and Amine Catalysis. *J. Am. Chem. Soc.* **2014**, *136* (8), 3020–3023.

(19) Sandmeier, T.; Krautwald, S.; Zipfel, H. F.; Carreira, E. M. Stereodivergent Dual Catalytic α-Allylation of Protected α-Amino- and α-Hydroxyacetaldehydes. *Angew. Chemie Int. Ed.* **2015**, *54* (48), 14363–14367.

(20) He, R.; Huo, X.; Zhao, L.; Wang, F.; Jiang, L.; Liao, J.; Zhang, W. Stereodivergent Pd/Cu Catalysis for the Dynamic Kinetic Asymmetric Transformation of Racemic Unsymmetrical 1,3-Disubstituted Allyl Acetates. *J. Am. Chem. Soc.* **2020**, *142* (18), 8097–8103.

(21) Huo, X.; Zhang, J.; Fu, J.; He, R.; Zhang, W. Ir/Cu Dual Catalysis: Enantio- and Diastereodivergent Access to α,α-Disubstituted α-Amino Acids Bearing Vicinal Stereocenters. *J. Am. Chem. Soc.* **2018**, *140* (6), 2080–2084.

(22) Jiang, X.; Boehm, P.; Hartwig, J. F. Stereodivergent Allylation of Azaaryl Acetamides and Acetates by Synergistic Iridium and Copper Catalysis. *J. Am. Chem. Soc.* **2018**, *140* (4), 1239–1242.

(23) Wei, L.; Zhu, Q.; Xu, S.-M.; Chang, X.; Wang, C.-J. Stereodivergent Synthesis of α,α-Disubstituted α-Amino Acids via Synergistic Cu/Ir Catalysis. *J. Am. Chem. Soc.* **2018**, *140* (4), 1508–1513.

(24) He, Z.-T.; Jiang, X.; Hartwig, J. F. Stereodivergent Construction of Tertiary Fluorides in Vicinal Stereogenic Pairs by Allylic Substitution with Iridium and Copper Catalysts. *J. Am. Chem. Soc.* **2019**, *141* (33), 13066–13073.

(25) Xu, S.-M.; Wei, L.; Shen, C.; Xiao, L.; Tao, H.-Y.; Wang, C.-J. Stereodivergent Assembly of Tetrahydro-γ-Carbolines via Synergistic Catalytic Asymmetric Cascade Reaction. *Nat. Commun.* **2019**, *10* (1), 5553.

(26) Zhang, Q.; Yu, H.; Shen, L.; Tang, T.; Dong, D.; Chai, W.; Zi, W. Stereodivergent Coupling of 1,3-Dienes with Aldimine Esters Enabled by Synergistic Pd and Cu Catalysis. *J. Am. Chem. Soc.* **2019**, *141* (37), 14554–14559.

(27) Sandmeier, T.; Carreira, E. M. Enantioselective Iridium-Catalyzed α-Allylation with Aqueous Solutions of Acetaldehyde. *Org. Lett.* **2020**, *22* (3), 1135–1138.

(28) Singha, S.; Serrano, E.; Mondal, S.; Daniliuc, C. G.; Glorius, F. Diastereodivergent Synthesis of Enantioenriched α,β-Disubstituted γ-Butyrolactones via Cooperative N-Heterocyclic Carbene and Ir Catalysis. *Nat. Catal.* **2020**, *3* (1), 48–54.

(29) Zhang, M.-M.; Wang, Y.-N.; Wang, B.-C.; Chen, X.-W.; Lu, L.-Q.; Xiao, W.-J. Synergetic Iridium and Amine Catalysis Enables Asymmetric [4+2] Cycloadditions of Vinyl Aminoalcohols with Carbonyls. *Nat. Commun.* **2019**, *10* (1), 2716.

(30) Kim, B.; Kim, Y.; Lee, S. Y. Stereodivergent Carbon–Carbon Bond Formation between Iminium and Enolate Intermediates by Synergistic Organocatalysis. *J. Am. Chem. Soc.* **2021**, *143* (1), 73–79.

(31) Tellis, J. C.; Primer, D. N.; Molander, G. A. Single-Electron Transmetalation in Organoboron Cross-Coupling by Photoredox/Nickel Dual Catalysis. *Science* **2014**, *345* (6195), 433–436.

(32) Twilton, J.; Le, C.; Zhang, P.; Shaw, M. H.; Evans, R. W.; MacMillan, D. W. C. The Merger of Transition Metal and Photocatalysis. *Nat. Rev. Chem.* **2017**, *1* (7), 0052.

(33) Zuo, Z.; Ahneman, D. T.; Chu, L.; Terrett, J. A.; Doyle, A. G.; MacMillan, D. W. C. Merging Photoredox with Nickel Catalysis: Coupling of -Carboxyl Sp3-Carbons with Aryl Halides. *Science* **2014**, *345* (6195), 437–440.

(34) Jouffroy, M.; Primer, D. N.; Molander, G. A. Base-Free Photoredox/Nickel Dual-Catalytic Cross-Coupling of Ammonium Alkylsilicates. *J. Am. Chem. Soc.* **2016**, *138* (2), 475–478.

(35) Nakajima, K.; Nojima, S.; Nishibayashi, Y. Nickel- and Photoredox-Catalyzed Cross-Coupling Reactions of Aryl Halides with 4-Alkyl-1,4-Dihydropyridines as Formal Nucleophilic Alkylation Reagents. *Angew. Chemie Int. Ed.* **2016**, *55* (45), 14106–14110.

(36) Milligan, J. A.; Phelan, J. P.; Badir, S. O.; Molander, G. A. Alkyl Carbon–Carbon Bond Formation by Nickel/Photoredox Cross-Coupling. *Angew. Chemie Int. Ed.* **2019**, *58* (19), 6152–6163.

(37) Shaw, M. H.; Shurtleff, V. W.; Terrett, J. A.; Cuthbertson, J. D.; MacMillan, D. W. C. Native Functionality in Triple Catalytic Cross-Coupling: Sp3 C-H Bonds as Latent Nucleophiles. *Science* **2016**, *352* (6291), 1304–1308.

(38) Le, C.; Liang, Y.; Evans, R. W.; Li, X.; MacMillan, D. W. C. Selective Sp3 C–H Alkylation via Polarity-Match-Based Cross-Coupling. *Nature* **2017**, *547* (7661), 79–83.

(39) Zhang, X.; MacMillan, D. W. C. Direct Aldehyde C–H Arylation and Alkylation via the Combination of Nickel, Hydrogen Atom Transfer, and Photoredox Catalysis. *J. Am. Chem. Soc.* **2017**, *139* (33), 11353–11356.

(40) Heitz, D. R.; Tellis, J. C.; Molander, G. A. Photochemical Nickel-Catalyzed C–H Arylation: Synthetic Scope and Mechanistic Investigations. *J. Am. Chem. Soc.* **2016**, *138* (39), 12715–12718.

(41) Shields, B. J.; Doyle, A. G. Direct C(Sp 3)–H Cross Coupling Enabled by Catalytic Generation of Chlorine Radicals. *J. Am. Chem. Soc.* **2016**, *138* (39), 12719–12722.

(42) Perry, I. B.; Brewer, T. F.; Sarver, P. J.; Schultz, D. M.; DiRocco, D. A.; MacMillan, D. W. C. Direct Arylation of Strong Aliphatic C–H Bonds. *Nature* **2018**, *560* (7716), 70–75.

(43) Lee, G. S.; Won, J.; Choi, S.; Baik, M.-H.; Hong, S. H. Synergistic Activation of Amides and Hydrocarbons for Direct C(Sp 3)–H Acylation Enabled by Metallaphotoredox Catalysis. *Angew. Chemie Int. Ed.* **2020**, *59* (39), 16933–16942.

(44) Thullen, S. M.; Treacy, S. M.; Rovis, T. Regioselective Alkylative Cross-Coupling of Remote Unactivated C(Sp 3)–H Bonds. *J. Am. Chem. Soc.* **2019**, *141* (36), 14062–14067.

(45) Cao, H.; Kuang, Y.; Shi, X.; Wong, K. L.; Tan, B. B.; Kwan, J. M. C.; Liu, X.; Wu, J. Photoinduced Site-Selective Alkenylation of Alkanes and Aldehydes with Aryl Alkenes. *Nat. Commun.* **2020**, *11* (1), 1956.

(46) Shaw, M. H.; Twilton, J.; MacMillan, D. W. C. Photoredox Catalysis in Organic Chemistry. *J. Org. Chem.* **2016**, *81* (16), 6898–6926.

(47) Hamilton, D. S.; Nicewicz, D. A. Direct Catalytic Anti-Markovnikov Hydroetherification of Alkenols. *J. Am. Chem. Soc.* **2012**, *134* (45), 18577–18580.

(48) Wilger, D. J.; Grandjean, J.-M. M.; Lammert, T. R.; Nicewicz, D. A. The Direct Anti-Markovnikov Addition of Mineral Acids to Styrenes. *Nat. Chem.* **2014**, *6* (8), 720–726.

(49) Margrey, K. A.; Nicewicz, D. A. A General Approach to Catalytic Alkene Anti-Markovnikov Hydrofunctionalization Reactions via Acridinium Photoredox Catalysis. *Acc. Chem. Res.* **2016**, *49* (9), 1997–2006.

(50) Perkowski, A. J.; Nicewicz, D. A. Direct Catalytic Anti-Markovnikov Addition of Carboxylic Acids to Alkenes. *J. Am. Chem. Soc.* **2013**, *135* (28), 10334–10337.

(51) Nguyen, T. M.; Nicewicz, D. A. Anti-Markovnikov Hydroamination of Alkenes Catalyzed by an Organic Photoredox System. *J. Am. Chem. Soc.* **2013**, *135* (26), 9588–9591.

(52) Nguyen, T. M.; Manohar, N.; Nicewicz, D. A. Anti -Markovnikov Hydroamination of Alkenes Catalyzed by a Two-Component Organic Photoredox System: Direct Access to Phenethylamine Derivatives. *Angew. Chemie Int. Ed.* **2014**, *53* (24), 6198–6201.

(53) Zeller, M. A.; Riener, M.; Nicewicz, D. A. Butyrolactone Synthesis via Polar Radical Crossover Cycloaddition Reactions: Diastereoselective Syntheses of Methylenolactocin and Protolichesterinic Acid. *Org. Lett.* **2014**, *16* (18), 4810–4813.

(54) Cavanaugh, C. L.; Nicewicz, D. A. Synthesis of α-Benzyloxyamino-γ-Butyrolactones via a Polar Radical Crossover Cycloaddition Reaction. *Org. Lett.* **2015**, *17* (24), 6082–6085.

(55) Gesmundo, N. J.; Grandjean, J.-M. M.; Nicewicz, D. A. Amide and Amine Nucleophiles in Polar Radical Crossover Cycloadditions: Synthesis of γ-Lactams and Pyrrolidines. *Org. Lett.* **2015**, *17* (5), 1316–1319.

(56) Wu, F.; Wang, L.; Chen, J.; Nicewicz, D. A.; Huang, Y. Direct Synthesis of Polysubstituted Aldehydes via Visible-Light Catalysis. *Angew. Chemie Int. Ed.* **2018**, *57* (8), 2174–2178.

(57) Romero, N. A.; Margrey, K. A.; Tay, N. E.; Nicewicz, D. A. Site-Selective Arene C-H Amination via Photoredox Catalysis. *Science* **2015**, *349* (6254), 1326–1330.

(58) Chen, W.; Huang, Z.; Tay, N. E. S.; Giglio, B.; Wang, M.; Wang, H.; Wu, Z.; Nicewicz, D. A.; Li, Z. Direct Arene C–H Fluorination with 18 F − via Organic Photoredox Catalysis. *Science* **2019**, *364* (6446), 1170–1174.

(59) Ohmatsu, K.; Suzuki, R.; Furukawa, Y.; Sato, M.; Ooi, T. Zwitterionic 1,2,3-Triazolium Amidate as a Catalyst for Photoinduced Hydrogen-Atom Transfer Radical Alkylation. *ACS Catal.* **2020**, *10* (4), 2627–2632.

(60) Shin, N. Y.; Ryss, J. M.; Zhang, X.; Miller, S. J.; Knowles, R. R. Light-Driven Deracemization Enabled by Excited-State Electron Transfer. *Science* **2019**, *366* (6463), 364–369.

(61) Wang, Y.; Carder, H. M.; Wendlandt, A. E. Synthesis of Rare Sugar Isomers through Site-Selective Epimerization. *Nature* **2020**, *578* (7795), 403–408.

(62) Pellissier, H. Stereocontrolled Domino Reactions. *Chem. Rev.* **2013**, *113* (1), 442–524.

(63) Grossmann, A.; Enders, D. N-Heterocyclic Carbene Catalyzed Domino Reactions. *Angew. Chemie Int. Ed.* **2012**, *51* (2), 314–325.

(64) Pellissier, H. Recent Developments in Enantioselective Metal-Catalyzed Domino Reactions. *Advanced Synthesis and Catalysis*. 2016, pp 2194–2259.

(65) Clavier, H.; Pellissier, H. Recent Developments in Enantioselective Metal-Catalyzed Domino Reactions. *Adv. Synth. Catal.* **2012**, *354* (18), 3347–3403.

(66) Pellissier, H. Recent Developments in Enantioselective Metal-Catalyzed Domino Reactions. *Adv. Synth. Catal.* **2019**, *361* (8), 1733–1755.

(67) Chanda, T.; Zhao, J. C. G. Recent Progress in Organocatalytic Asymmetric Domino Transformations. *Adv. Synth. Catal.* **2018**, *360* (1), 2–79.

(68) Tietze, L. F. Domino Reactions. In *Domino Reactions: Concepts for Efficient Organic Synthesis*; Tietze, L. F., Ed.; Wiley-VCH Verlag GmbH & Co. KGaA: Weinheim, Germany, 2014; pp 1–621.

(69) Trost, B. M.; Min, C. Total Synthesis of Terpenes via Palladium-Catalysed Cyclization Strategy. *Nat. Chem.* **2020**, *12* (6), 568–573.

(70) Trost, B. M.; Shi, Y. Palladium-Catalyzed Cyclizations of Polyenynes. A Palladium Zipper. *J. Am. Chem. Soc.* **1993**, *115* (21), 9421–9438.

(71) Whyte, A.; Torelli, A.; Mirabi, B.; Prieto, L.; Rodríguez, J. F.; Lautens, M. Cobalt-Catalyzed Enantioselective Hydroarylation of 1,6-Enynes. *J. Am. Chem. Soc.* **2020**, *142* (20), 9510–9517.

(72) Takahashi, K.; Yamashita, M.; Nozaki, K. Tandem Hydroformylation/Hydrogenation of Alkenes to Normal Alcohols Using Rh/Ru Dual Catalyst or Ru Single Component Catalyst. *J. Am. Chem. Soc.* **2012**, *134* (45), 18746–18757.

(73) Takahashi, K.; Yamashita, M.; Ichihara, T.; Nakano, K.; Nozaki, K. High-Yielding Tandem Hydroformylation/Hydrogenation of a Terminal Olefin to Produce a Linear Alcohol Using a Rh/Ru Dual Catalyst System. *Angew. Chemie Int. Ed.* **2010**, *49* (26), 4488–4490.

(74) Ahmed, M.; Seayad, A. M.; Jackstell, R.; Beller, M. Amines Made Easily: A Highly Selective Hydroaminomethylation of Olefins. *J. Am. Chem. Soc.* **2003**, *125* (34), 10311–10318.

(75) Hanna, S.; Holder, J. C.; Hartwig, J. F. A Multicatalytic Approach to the Hydroaminomethylation of A-Olefins. *Angew. Chemie Int. Ed.* **2019**, *58* (11), 3368–3372.

(76) Jia, Z.-J.; Shan, G.; Daniliuc, C. G.; Antonchick, A. P.; Waldmann, H. Enantioselective Synthesis of the Spirotropanyl Oxindole Scaffold through Bimetallic Relay Catalysis. *Angew. Chemie Int. Ed.* **2018**, *57* (44), 14493–14497.

(77) Yu, Q.; Fu, Y.; Huang, J.; Qin, J.; Zuo, H.; Wu, Y.; Zhong, F. Enantioselective Oxidative Phenol-Indole [3 + 2] Coupling Enabled by Biomimetic Mn(Iii)/Brønsted Acid Relay Catalysis. *ACS Catal.* **2019**, *9* (8), 7285–7291.

(78) Denard, C. A.; Bartlett, M. J.; Wang, Y.; Lu, L.; Hartwig, J. F.; Zhao, H. Development of a One-Pot Tandem Reaction Combining Ruthenium-Catalyzed Alkene Metathesis and Enantioselective Enzymatic Oxidation to Produce Aryl Epoxides. *ACS Catal.* **2015**, *5* (6), 3817–3822.

(79) Corma, A.; Navas, J.; Sabater, M. J. Advances in One-Pot Synthesis through Borrowing Hydrogen Catalysis. *Chem. Rev.* **2018**, *118* (4), 1410–1459.

(80) Goldman, A. S. Catalytic Alkane Metathesis by Tandem Alkane Dehydrogenation-Olefin Metathesis. *Science* **2006**, *312* (5771), 257–261.

(81) Lichosyt, D.; Zhang, Y.; Hurej, K.; Dydio, P. Dual-Catalytic Transition Metal Systems for Functionalization of Unreactive Sites of Molecules. *Nat. Catal.* **2019**, *2* (2), 114–122.

(82) Quintard, A.; Constantieux, T.; Rodriguez, J. An Iron/Amine-Catalyzed Cascade Process for the Enantioselective Functionalization of Allylic Alcohols. *Angew. Chemie Int. Ed.* **2013**, *52* (49), 12883–12887.

(83) Roudier, M.; Constantieux, T.; Quintard, A.; Rodriguez, J. Triple Iron/Copper/Iminium Activation for the Efficient Redox Neutral Catalytic Enantioselective Functionalization of Allylic Alcohols. *ACS Catal.* **2016**, *6* (8), 5236–5244.

(84) Black, P. J.; Harris, W.; Williams, J. M. J. Catalytic Electronic Activation: Indirect Addition of Nucleophiles to an Allylic Alcohol This Work Was Supported by the University of Bath and Roche Discovery (P.J.B.). *Angew. Chemie Int. Ed.* **2001**, *40* (23), 4475.

(85) Denard, C. A.; Huang, H.; Bartlett, M. J.; Lu, L.; Tan, Y.; Zhao, H.; Hartwig, J. F. Cooperative Tandem Catalysis by an Organometallic Complex and a Metalloenzyme. *Angew. Chemie Int. Ed.* **2014**, *53* (2), 465–469.

(86) Bhat, V.; Welin, E. R.; Guo, X.; Stoltz, B. M. Advances in Stereoconvergent Catalysis from 2005 to 2015: Transition-Metal-Mediated Stereoablative Reactions, Dynamic Kinetic Resolutions, and Dynamic Kinetic Asymmetric Transformations. *Chem. Rev.* **2017**, *117* (5), 4528–4561.

(87) Verho, O.; Bäckvall, J. E. Chemoenzymatic Dynamic Kinetic Resolution: A Powerful Tool for the Preparation of Enantiomerically Pure Alcohols and Amines. *J. Am. Chem. Soc.* **2015**, *137* (12), 3996–4009.

(88) Pàmies, O.; Bäckvall, J. E. Combination of Enzymes and Metal Catalysts. A Powerful Approach in Asymmetric Catalysis. *Chem. Rev.* **2003**, *103* (8), 3247–3261.

(89) Chen, Z.; Aota, Y.; Nguyen, H. M. H.; Dong, V. M. Dynamic Kinetic Resolution of Aldehydes by Hydroacylation. *Angew. Chemie Int. Ed.* **2019**, *58* (14), 4705–4709.

(90) Litman, Z. C.; Wang, Y.; Zhao, H.; Hartwig, J. F. Cooperative Asymmetric Reactions Combining Photocatalysis and Enzymatic Catalysis. *Nature* **2018**, *560* (7718), 355–359.

(91) Atesin, A. C.; Ray, N. A.; Stair, P. C.; Marks, T. J. Etheric C–O Bond Hydrogenolysis Using a Tandem Lanthanide Triflate/Supported Palladium Nanoparticle Catalyst System. *J. Am. Chem. Soc.* **2012**, *134* (36), 14682–14685.

(92) Lohr, T. L.; Li, Z.; Marks, T. J. Thermodynamic Strategies for C–O Bond Formation and Cleavage via Tandem Catalysis. *Acc. Chem. Res.* **2016**, *49* (5), 824–834.

(93) Panteleev, J.; Zhang, L.; Lautens, M. Domino Rhodium-Catalyzed Alkyne Arylation/Palladium-Catalyzed N Arylation: A Mechanistic Investigation. *Angew. Chemie Int. Ed.* **2011**, *50* (39), 9089–9092.

(94) Friedman, A. A.; Panteleev, J.; Tsoung, J.; Huynh, V.; Lautens, M. Rh/Pd Catalysis with Chiral and Achiral Ligands: Domino Synthesis of Aza-Dihydrodibenzoxepines. *Angew. Chemie Int. Ed.* **2013**, *52* (37), 9755–9758.

200

(95) Zhang, L.; Qureshi, Z.; Sonaglia, L.; Lautens, M. Sequential Rhodium/Palladium Catalysis: Enantioselective Formation of Dihydroquinolinones in the Presence of Achiral and Chiral Ligands. *Angew. Chemie Int. Ed.* **2014**, *53* (50), 13850–13853.

(96) Lohr, T. L.; Marks, T. J. Orthogonal Tandem Catalysis. *Nat. Chem.* **2015**, *7* (6), 477–482.

(97) Huang, H.; Denard, C. A.; Alamillo, R.; Crisci, A. J.; Miao, Y.; Dumesic, J. A.; Scott, S. L.; Zhao, H. Tandem Catalytic Conversion of Glucose to 5-Hydroxymethylfurfural with an Immobilized Enzyme and a Solid Acid. *ACS Catal.* **2014**, *4* (7), 2165–2168.

(98) Cybulski, O.; Dygas, M.; Mikulak-Klucznik, B.; Siek, M.; Klucznik, T.; Choi, S. Y.; Mitchell, R. J.; Sobolev, Y. I.; Grzybowski, B. A. Concentric Liquid Reactors for Chemical Synthesis and Separation. *Nature* **2020**, *586* (7827), 57–63.

(99) Sato, H.; Hummel, W.; Gröger, H. Cooperative Catalysis of Noncompatible Catalysts through Compartmentalization: Wacker Oxidation and Enzymatic Reduction in a One-Pot Process in Aqueous Media. *Angew. Chemie Int. Ed.* **2015**, *54* (15), 4488–4492.

(100) Huff, C. A.; Sanford, M. S. Cascade Catalysis for the Homogeneous Hydrogenation of CO 2 to Methanol. *J. Am. Chem. Soc.* **2011**, *133* (45), 18122–18125.

(101) Lu, J.; Dimroth, J.; Weck, M. Compartmentalization of Incompatible Catalytic Transformations for Tandem Catalysis. *J. Am. Chem. Soc.* **2015**, *137* (40), 12984–12989.

(102) Wheeldon, I.; Minteer, S. D.; Banta, S.; Barton, S. C.; Atanassov, P.; Sigman, M. Substrate Channelling as an Approach to Cascade Reactions. *Nat. Chem.* **2016**, *8* (4), 299–309.

(103) Bornscheuer, U. T.; Huisman, G. W.; Kazlauskas, R. J.; Lutz, S.; Moore, J. C.; Robins, K. Engineering the Third Wave of Biocatalysis. *Nature* **2012**, *485* (7397), 185–194.

(104) Hyster, T. K.; Ward, T. R. Genetic Optimization of Metalloenzymes: Enhancing Enzymes for Non-Natural Reactions. *Angew. Chemie Int. Ed.* **2016**, *55* (26), 7344–7357.

(105) Dydio, P.; Ploeger, M.; Reek, J. N. H. Selective Isomerization–Hydroformylation Sequence: A Strategy to Valuable α-Methyl-Branched Aldehydes from Terminal Olefins. *ACS Catal.* **2013**, *3* (12), 2939–2942.

(106) Yin, X.-P.; Zeng, X.-P.; Liu, Y.-L.; Liao, F.-M.; Yu, J.-S.; Zhou, F.; Zhou, J. Asymmetric Triple Relay Catalysis: Enantioselective Synthesis of Spirocyclic Indolines through a One-Pot Process Featuring an Asymmetric 6π Electrocyclization. *Angew. Chemie Int. Ed.* **2014**, *53* (50), 13740–13745.

(107) Sancheti, S. P.; Urvashi; Shah, M. P.; Patil, N. T. Ternary Catalysis: A Stepping Stone toward Multicatalysis. *ACS Catal.* **2020**, *10* (5), 3462–3489.

(108) Dhiman, S.; Mishra, U. K.; Ramasastry, S. S. V. One-Pot Trimetallic Relay Catalysis: A Unified Approach for the Synthesis of β-Carbolines and Other [c]-Fused Pyridines. *Angew. Chemie Int. Ed.* **2016**, *55* (27), 7737–7741.

(109) Casnati, A.; Lichosyt, D.; Lainer, B.; Veth, L.; Dydio, P. Multicatalytic Approach to One-Pot Stereoselective Synthesis of Secondary Benzylic Alcohols. *Org. Lett.* **2021**, *23* (9), 3502–3506.

(110) Camp, J. E. Auto-Tandem Catalysis: Activation of Multiple, Mechanistically Distinct Process by a Single Catalyst. *European J. Org. Chem.* **2017**, *2017* (3), 425–433.

(111) Shindoh, N.; Takemoto, Y.; Takasu, K. Auto-Tandem Catalysis: A Single Catalyst Activating Mechanistically Distinct Reactions in a Single Reactor. *Chem. - A Eur. J.* **2009**, *15* (45), 12168–12179.

(112) Kanbayashi, N.; Takenaka, K.; Okamura, T.; Onitsuka, K. Asymmetric Auto-Tandem Catalysis with a Planar-Chiral Ruthenium Complex: Sequential Allylic Amidation and Atom-Transfer Radical Cyclization. *Angew. Chemie Int. Ed.* **2013**, *52* (18), 4897–4901.

(113) Matsushima, Y.; Onitsuka, K.; Kondo, T.; Mitsudo, T.; Takahashi, S. Asymmetric Catalysis of Planar-Chiral Cyclopentadienylruthenium Complexes in Allylic Amination and Alkylation. *J. Am. Chem. Soc.* **2001**, *123* (42), 10405–10406.

(114) Long, J.; Yu, R.; Gao, J.; Fang, X. Access to 1,3-Dinitriles by Enantioselective Auto-tandem Catalysis: Merging Allylic Cyanation with Asymmetric Hydrocyanation. *Angew. Chemie Int. Ed.* **2020**, *59* (17), 6785–6789.

(115) Wu, X.; Cruz, F. A.; Lu, A.; Dong, V. M. Tandem Catalysis: Transforming Alcohols to Alkenes by Oxidative Dehydroxymethylation. *J. Am. Chem. Soc.* **2018**, *140* (32), 10126–10130.

(116) Lecomte, M.; Lipshultz, J. M.; Kim-Lee, S.-H.; Li, G.; Radosevich, A. T. Driving Recursive Dehydration by P III /P V Catalysis: Annulation of Amines and Carboxylic Acids by Sequential C–N and C–C Bond Formation. *J. Am. Chem. Soc.* **2019**, *141* (32), 12507–12512.

(117) Zhang, S.; del Pozo, J.; Romiti, F.; Mu, Y.; Torker, S.; Hoveyda, A. H. Delayed Catalyst Function Enables Direct Enantioselective Conversion of Nitriles to NH 2 -Amines. *Science* **2019**, *364* (6435), 45–51.

(118) Li, L.; Herzon, S. B. Temporal Separation of Catalytic Activities Allows Anti-Markovnikov Reductive Functionalization of Terminal Alkynes. *Nat. Chem.* **2014**, *6* (1), 22–27.

(119) Korvorapun, K.; Kaplaneris, N.; Rogge, T.; Warratz, S.; Stückl, A. C.; Ackermann, L. Sequential Meta-/Ortho-C–H Functionalizations by One-Pot Ruthenium(II/III) Catalysis. *ACS Catal.* **2018**, *8* (2), 886–892.

(120) Semwal, S.; Choudhury, J. Switch in Catalyst State: Single Bifunctional Bi-State Catalyst for Two Different Reactions. *Angew. Chemie Int. Ed.* **2017**, *56* (20), 5556–5560.

(121) Meng, J.; Fan, L.-F.; Han, Z.-Y.; Gong, L.-Z. α-Quaternary Chiral Aldehydes from Styrenes, Allylic Alcohols, and Syngas via Multi-Catalyst Relay Catalysis. *Chem* **2018**, *4* (5), 1047–1058.

(122) Wu, H.; He, Y.-P.; Gong, L.-Z. The Combination of Relay and Cooperative Catalysis with a Gold/Palladium/Brønsted Acid Ternary System for the Cascade Hydroamination/Allylic Alkylation Reaction. *Adv. Synth. Catal.* **2012**, *354* (6), 975–980.

(123) Wang, C.; Han, Z.-Y.; Luo, H.-W.; Gong, L.-Z. Highly Enantioselective Relay Catalysis in the Three-Component Reaction for Direct Construction of Structurally Complex Heterocycles. *Org. Lett.* **2010**, *12* (10), 2266–2269.

(124) Pirnot, M. T.; Rankic, D. A.; Martin, D. B. C.; MacMillan, D. W. C. Photoredox Activation for the Direct -Arylation of Ketones and Aldehydes. *Science* **2013**, *339* (6127), 1593–1596.

(125) DeHovitz, J. S.; Loh, Y. Y.; Kautzky, J. A.; Nagao, K.; Meichan, A. J.; Yamauchi, M.; MacMillan, D. W. C.; Hyster, T. K. Static to Inducibly Dynamic Stereocontrol: The Convergent Use of Racemic β-Substituted Ketones. *Science* **2020**, *369* (6507), 1113–1118.

(126)   Fleischer, S.; Werkmeister, S.; Zhou, S.; Junge, K.; Beller, M. Consecutive Intermolecular Reductive Hydroamination: Cooperative Transition-Metal and Chiral Brønsted Acid Catalysis. *Chem. - A Eur. J.* **2012**, *18* (29), 9005–9010.

(127)   Tang, X.; Gan, L.; Zhang, X.; Huang, Z. N-Alkanes to n -Alcohols: Formal Primary C–H Bond Hydroxymethylation via Quadruple Relay Catalysis. *Sci. Adv.* **2020**, *6* (47), eabc6688.

(128)   Domański, S.; Gatlik, B.; Chaładaj, W. Pd-Catalyzed Boroperfluoroalkylation of Alkynes Opens a Route to One-Pot Reductive Carboperfluoroalkylation of Alkynes with Perfluoroalkyl and Aryl Iodides. *Org. Lett.* **2019**, *21* (13), 5021–5025.

(129)   Yamamoto, K.; Bruun, T.; Kim, J. Y.; Zhang, L.; Lautens, M. A New Multicomponent Multicatalyst Reaction (MC) 2 R: Chemoselective Cycloaddition and Latent Catalyst Activation for the Synthesis of Fully Substituted 1,2,3-Triazoles. *Org. Lett.* **2016**, *18* (11), 2644–2647.

(130)   Armstrong, M. K.; Goodstein, M. B.; Lalic, G. Diastereodivergent Reductive Cross Coupling of Alkynes through Tandem Catalysis: Z - and E -Selective Hydroarylation of Terminal Alkynes. *J. Am. Chem. Soc.* **2018**, *140* (32), 10233–10241.

Lukas Rainer Veth

Transfer C–H Borylation of Alkenes

Résumé

Cette thèse décrit les études de la borylation C-H de transfert d'alcènes sous catalyse Rh- et Ir conçue par des considérations mécanistiques. Bien que plusieurs méthodes aient été précédemment établies pour la borylation C-H des alcènes, aucun protocole général applicable à la fois aux alcènes terminaux et internes et présentant une excellente tolérance aux groupes fonctionnels n'était disponible jusqu'à présent. Dans ce contexte, la borylation C-H par transfert présente un grand potentiel. Cependant, son faible nombre d'antécédents et sa compréhension mécanistique limitée ont entravé le développement de protocoles pratiques. Les méthodes décrites ici débloquent des transformations efficaces et largement applicables qui sont attrayantes pour la synthèse et la dérivatisation tardive de molécules complexes, tandis que les études mécanistiques approfondies fournissent leur compréhension détaillée. Dans un contexte plus large, cette thèse prépare le terrain pour le développement d'une série d'autres réactions d'échange d'hydrogène contre des groupes fonctionnels suivant des voies similaires.

Mots-clés : borylation, fonctionnalisation C-H, alcène, catalyse de transfert, oléfine, shuttle catalysis, rhodium, iridium, multicatalyse

Abstract

This thesis describes the studies of transfer C–H borylation of alkenes under Rh- and Ir-catalysis designed by mechanistic considerations. Although several methods were previously established for the C–H borylation of alkenes, no general protocols applicable to both terminal and internal alkenes and with an excellent functional group tolerance were available thus far. In that context, transfer C–H borylation bears great potential. However, its scarce precedence and previously limited mechanistic understanding hindered the development of practical protocols. The methods described here unlock efficient and widely applicable transformations that are attractive for the synthesis and late-stage derivatization of complex molecules, while the thorough mechanistic studies provide their detailed understanding. In a broader context, this thesis sets the stage for the development of a range of other hydrogen-for-functional group exchange reactions undergoing similar pathways.

Keywords : borylation, C–H functionalization, alkene, transfer catalysis, olefin, shuttle catalysis, rhodium, iridium, multicatalysis